UNIVERSITY OF TASMANIA

Aging and Recovery of Listeria monocytogenes ScottA

by

Mona Alharbi

Master of

A thesis submitted in fulfilment of the requirements for the Degree of Doctor of Philosophy

University of Tasmania

August 2017

APPROVALS:

Doctor of Philosophy Dissertation

Aging and Recovery of *Listeria monocytogenes* ScottA

By

Mona Alharbi

Supervisor:

_____

Associate Professor John P Bowman

Head of School:

_____

Dr Alistair Gracie

Declaration of Originality

The thesis contains no material which has been accepted for a degree or diploma by the University or any other institution, except by way of background information and duly acknowledge in the thesis, and to the best of my knowledge and belief no material previously published or written by another person except where due acknowledgement is made in the text of the thesis, nor does the thesis contain any material that infringes copyright.

Signature:

Mona Alharbi - December 2016

Statement on Access to the Thesis

The authority of access statement should reflect any agreement which exists between the University and an external organisation (such as a sponsor of the research) regarding the work. This thesis may be made available for loan and limited copying and communication in accordance with the *Copyright Act 1968*, with the exception of material as described in the following Statement on Published Work.

Signature:

Mona Alharbi- December 2016

Statement of Co-Authorship

This thesis includes research, which has yet to be published or to be submitted to a peer-review journal. The following people and institutions contributed to the publication of work undertaken as part of this thesis:

Mona Alharbi: School of Land and Food, University of Tasmania (Candidate)

Tom Ross: School of Land and Food, University of Tasmania (Co-supervisor)

John P Bowman: School of Land and Food, University of Tasmania (Primary supervisor):

Richard Wilson: Central Science Laboratory, University of Tasmania (Collaborator)

Details of the Author Roles

The distribution of roles and efforts reflects all content in this thesis

Mona Alharbi (70%) did all laboratory work, analysed the data and wrote the thesis chapters. John Bowman (20%) and Tom Ross (10%) aided in data analysis, interpretation and writing. Richard Wilson performed peptide/protein identifications.

Contents

Acknowledgements

I would like to express my sincere gratitude to my supervisor, Assoc. Prof. John P. Bowman and Assoc. Prof. Tom Ross, without their extensive knowledge and leadership this work would not have occurred. Their constant guidance, support and patience have provided me with the courage to complete the project. Thank you for giving me the opportunity and believing in me.

Special thanks to Dr Richard Wilson from Central Science Laboratory, the University of Tasmania for highly expert assistance in the proteomics analysis. My sincere appreciation goes to staff within Food Safety Centre and the Tasmanian Institute of Agriculture, in particular, Dr Shane M. Powell, Dr Jay Kocharunchitt, Ms Michelle Williams, Mr Andrew Measham, Mrs Lauri Parkinson, Ms Bianca Porteus, Adam Smolenski and Prof. David Ratkowsky.

I would also to thank my friends Peipei Zhang, Tuflikha Putri, Ali Al-Naseri, Kevin Feng, Reham Mohammed and Syed Shah for their wonderful support and care.

I am very grateful to my family in Australia and in Saudi Arabia for their love, encouragement and support during my journey. Special thanks to my husband and my kids for their patience, continuous support and love. Thank you for sharing this long journey with me and being a big part of my life.

Thesis Summary

The bacterial growth curve is considered to involve four phases: lag, exponential, stationary and death/decline phase. The lag phase is the time that bacteria use to recover and adapt to a new environment before shifting to exponential growth at a rate determined by the environmental conditions and available resources. Aging, on the other hand, is the process in which the inheritance of “new” and “old” cell poles by bacterial cells during cell division as well as putative accumulation of protein aggregates. Stress has been shown to be needed to make aging inevitable, and aging leads to cells that lose fitness thus providing a finite duration to a stressed population. Significant knowledge gaps still exist about the lag phase and bacterial aging, in particular, mechanistic details of the processes and whether broad scale principals apply. The thesis study aims to describe the microbiological, biochemical and regulatory-level mechanisms of the effect of cell aging and lag phase recovery in *Listeria monocytogenes* (strain Scott A). *L. monocytogenes* was utilised in the study due to its comparatively streamlined genome, high level of genetic and protein-level characterisation and the fact it is an important food pathogen that causes the disease listeriosis. The species is adept at switching its lifestyle from an environmental saprophyte to a human parasite and thus has a capacity to respond and adapt to relatively hostile environments. In the environment, it can survive due to this high degree of adaptability, and this has resulted in a ubiquitous distribution. How it adapts in the scenarios of enforced aging and subsequent recovery was approached by mainly using quantitative proteomics, allowing assessment of most essential cell functions.

To enable understanding of the effect of culture-based aging on *L. monocytogenes* ScottA growth and survival behaviour, morphological and metabolic changes,

virulence potential, and ATP levels during aging processes were assessed. Aging was enforced by holding cells at 37°C deep into the stationary growth phase for up to 21 days. The temperature used represents the optimal temperature for growth rate (T_{opt}). In older cultures (aged ≥7 d) lag phase was proceeded by possible short, rapid recovery of a small segment (0.5-1.5 log units) of the population. The duration of the lag phase increased with the length of time the cells were initially incubated. The generation time of outgrowth increased with the duration of initial incubation suggesting more aged cells lost fitness. Extended incubation resulted in increasingly poor growth on agar. Aged cultures lose the ability to retain crystal violet, indicative of a thinner, less networked peptidoglycan layer. They also demonstrated cell elongation (2-10 fold increase), evidence of failed septation completion, and autolysis. After 7 d incubation, ATP levels in the cells collapsed to $<10^{-17}$ moles/cell from approximately 10^{-15} moles/cell. Catabolic enzymes associated with protein, lipid, phosphate, and carbohydrate metabolism though readily detected in young cultures become inactive in populations incubated ≥7 d. Haemolysis assays revealed no detectable listeriolysin activity was present in the bacterial supernatant fluid after ≥7 d, possibly suggesting reduced protein export**.** Overall, the results indicate that cell aging at the T_{opt} is associated with extensive loss of cell viability and results in lag phase extension and loss of fitness. Fitness loss may be attributable to depletion of ATP and reduced metabolism affecting protein secretion, cytokinetic and cell wall biogenic processes in the cell population.

Integrated global proteomic responses of *L. monocytogenes* ScottA incubated for 1 to 21 days at 37°C was performed to understand the metabolic mechanisms behind the loss of fitness and culturability in populations after extended incubation. The continued lack of availability of carbohydrates leads to an overall decrease in cellular

metabolism, loss of culturability on agar, elongated multi-septated cells, autolysis, and non-detectable haemolysis. Protein samples were analysed by nano-LC-MS/MS using an LTQ-Orbitrap XL instrument with 686 proteins assessed. Metabolism reduction observed for aged cells is linked to empty ATP and precursor pools; there was no evidence of a harsh response. The process is demonstrated by a decline in phosphotransferase system protein abundances and associated compensatory adjustments to enzyme abundances within the glycolysis pathway, amongst mixed fermentation enzymes, and a possible shift in F_1F_0 ATPase complex to a synthesis mode. The observed greatly enhanced abundances of glutamate dehydrogenase RocG in aged cells could suggest the use of oxidative deamination for resupply of pyruvate and NADH. Many central processes of the cell linked to growth such as the translational apparatus, ribosomal proteins and DNA methods showed a significant reduction. There is a greater emphasis on proteins involved in cytoplasmic homoeostasis, proteostasis, substrate scavenging, and amino acid/nucleic acid salvage processes in aged cells. Internalin A and B abundances were elevated in aged cells but were accompanied by reduced levels of wall teichoic acid synthesis enzymes. The abundances of several autolysins (including Spl, Iap, Auto, Ami) were substantially elevated, explaining aged induced autolysis. The increase in autolysins is potentially linked to cytokinetic dysfunction associated with the septal ring. The increase would likely explain the reason why the bulk of the cell population loses culturability though apparently, a subpopulation survives. The proteome data provides a perspective of *L. monocytogenes* in a state of decline deep in its stationary growth phase.

The proteome dynamics of *L. monocytogenes* ScottA recovering during the lag phase was investigated. A quantitative analysis of ScottA proteome was based on cells first being grown at 37°C over an extended stationary growth phases (1, 7, 14 and 21 days) and then allowed to recover in new TSYE media over 0.5 to 4 hours. A total 459 proteins were estimated for abundance for all treatments. During lag phase *L. monocytogenes* ScottA rapidly altered its proteome (within 0.5 h) partially rebounding from the aged state but not completely reattaining the original exponential phase state; this was evident at all time points. The length of initial incubation had no substantial effect on lag phase responses at the protein level. Proteins associated with carbohydrate catabolism became relatively abundant in the lag phase. Recovery of the intermediary metabolism based on protein abundance data revealed a shift to mixed acid fermentation occurs. The data also points to activation of initial stages of biosynthetic pathways for cell components including peptidoglycan, fatty acids, and menaquinone, but not broad-scale increased abundance of whole pathways. The molecular chaperone Hsp70 complex, detoxification-associated proteins, compatible solute uptake transporters, and metal ion homoeostasis transporters were detected at higher abundances relative to aged cells, potentially indicating processes are involved in remediation of the cytoplasmic contents. Overall, lag phase cells adjustments cover a wide range number of anabolic and remedial processes; however, the activation responses collectively do not represent a “full steam ahead” approach but is constrained possibly to ensure precursor and energy resources can be accumulated before the exponential growth phase.

Utilising proteomic data an original insight into the global regulation of protein production by *L. monocytogenes* ScottA during aging and lag phase processes at

37°C was performed. The data suggest that in lag phase SigB, SigH, CtsR, HrcA and AgrA regulons are more activated relative to old and exponential cells while the PrfA and SigC regulons were instead strongly repressed. CodY levels were highly elevated in lag phase resulting in intense repression and derepression of its previously defined regulon. The activation responses collectively link to increased fermentation and anabolic processes, protein folding and rescue, remediation of the cytoplasm from toxic compounds, and buffering of cytosolic proteins. At the same time the combined increased abundance of CodY and catabolite control protein CcpA seems to lead to constraints on the levels of enzymes that rely on expenditure ATP possibly allowing build-up of the precursor, ATP and reducing equivalent pools prior to exponential growth. The data support the observation that lag phase responses are rapid and that the proteomes do not rebound back to the previous exponential phase state. The data also suggest that the extent of aged incubation results in largely homogenous responses throughout the lag phase though subtle differences were observed in the degree of activation of regulons. This incomplete rebound effect creates the possibility that inputted cell recovery in lag phase manifests various outcomes for outgrowth in the exponential phase depending on the physiological nature of the coded cells.

Collectively, the results of this research provide an insight into the mechanisms engaged by *L. monocytogenes* ScottA during aging and recovery. The mechanism includes overviews if the morphological, metabolic and cell energetic changes during aging and the associated underlying mechanisms as revealed by proteomic assessments. Renewal of cells in lag phase showed the critical role of CodY and SigB in these processes as master regulators as well as providing some initial information of possible protein responses that could be linked to adaptation.

List of Abbreviations

μg	Microgram
μl	Microlitre
μM	Micromolar
2DS	Two-Dimensional Electrophoresis
CFU	Colony Forming Unit
DNA	Deoxyribonucleic Acid
mg	Milligram
min	Minute
nano-LC-MS/MS	Nanoscale liquid chromatography coupled to tandem mass spectrometry
OD	Optical Density
rpm	Revolutions per minute
SDS	Sodium Dodecyl Sulphate
SDS-PAGE	Polyacrylamide gel electrophoresis
TEMED	N,N,N',N'-Tetramethylethylenediamine
TRIS	2-Amino-2-hydroxymethyl-propane-1,3-diol
a_w	Water Activity
RLT	Relative Lag Times
NaCl	Sodium Chloride
LR	Log Ratio
TSYE	Tryptone Soya Broth plus 0.6% Yeast Extract

1. Literature Review

1.1 Introduction

The bacterial growth curve is considered to involve four phases: lag, exponential, stationary and death/decline phase. The lag phase is the earliest stage in the bacterial population growth cycle. It is the time that bacteria use to recover (recover) and adapt to a new environment (Rolfe et al., 2012). This process involves changes in the cell biochemistry (Monod, 1949). During the exponential phase, bacterial cells divide, and the biomass increases exponentially at definable rates over a specified period of time. In a non-continuous culture system, the exponential phase transitions to the stationary phase where bacterial metabolic activity decreases, cell numbers no longer increase while a general stress is manifested. Eventually, as a result of the accumulation of inhibitory products and cell component damage cells starts to inactivate and even lysis thus the population is considered to decline until cells are able to move to a new environment to start a new cell cycle.

Cells in the each of these phases have been studied, and combined transcriptome and proteome analysis and analysis of intracellular metabolites have been carried out, especially in the stationary growth phase. However, large knowledge gaps still exist about the lag phase and there and a comprehensive picture of the biochemical and molecular genetic activity of bacteria is needed for this significant period.

This review provides an overview of the lag phase in bacteria including the effect of environmental parameters on lag phase such as osmolality, pH, temperature, cell history and inoculum size. Predicting the lag phase duration is very important in performing a risk assessment or for generating process models as food safety is a concern in modern society. Therefore this review we include discussion of models

that have been reported as suitable for predicting the lag time. Finally, a compilation of State-of–the art of the physiology of stationary phase as a starvation period will be addressed, focusing on stationary phase regulon and cell morphology.

1.2 Lag Phase: A Definition

Buchanan and Solberg (2006) defined lag phase as the time in which the initial population density is increased by twofold of its initial value. Pirt (1975) on the other hand described lag phase as the transition period during which the specific growth rate increases to its maximum characteristic value for the culture environment. He recognised the causes of lag as (i) change in nutrition, (ii) change in the physical environment, (iii) presence of an inhibitor, (iv) spore germination, and (v) state of the inoculum. Baranyi and Roberts (1994) proposed in their logistic growth model that lag phase was the time required for a critical substance in a cell to accumulate to a threshold amount allowing initiation of growth. Lag time can also be identified as a delayed response of the microbial growth kinetics to a (sudden) change in the environment conditions (Dens et al., 2005). According to Dens et al. (2005) this natural phenomenon commonly immediately follows inoculation of a medium with cells growing under optimal condition. This lag period before exponential growth, which can be very short, has been referred to as the initial lag phase (Figure 1). However, a sudden change in the environment also can result in a temporary period called an intermediate lag phase where the cell metabolism becomes out of balance as a result of the environmental change causing delayed responses in the microbial population. There are many factors influencing bacterial lag time i.e., the history of the cells, initial cell counts, the current environmental conditions, the past and present environment (denoted as ENV^- and ENV+, respectively), the magnitude

(ΔENV) and the rate (ΔENV/Δ*t*) of the change between the past and present environments (Dens et al., 2005; Koseki & Nonaka 2012).

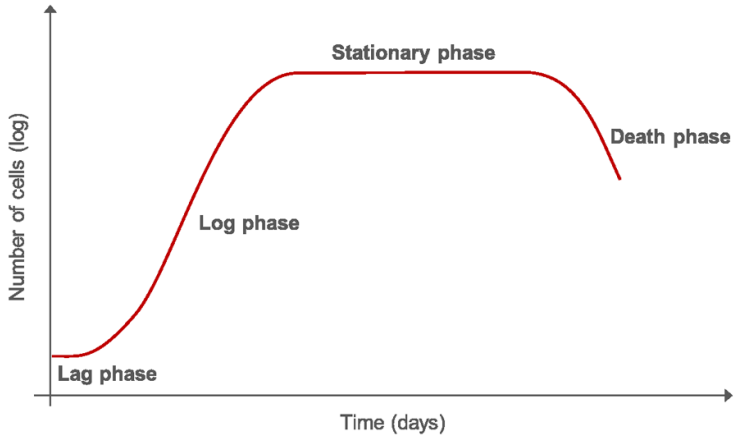

Figure 1. Growth curve of bacterial cells showing the phases of growth.

1.3 Theories to Explain Lag Phase

There are some theories that account for the occurrence of lag phases. One theory is the toxic theory which considers the latent (lag) period as the time necessary for the organisms to recover from an injury sustained in the previous culture environment (Chesney, 1916). It assumed that the termination of growth in a culture is due to the accumulation of toxic products of metabolism. It is well known that the acidic metabolic end-products inhibit streptococci and various other fermentative bacteria that they produce. Chesney performed his experiments on pneumococci (*Streptococcus pneumoniae*), which he showed produced hydrogen peroxide in quantities sufficient to inhibit growth. However, strains continued to grow rapidly for an appreciable time after inoculation into a new culture medium. A second theory that has been advanced is the metabolic theory, which assumes that the bacterial cell can reach a maximum growth only when an individual product has been

elaborated by the organisms and has accumulated to an optimum concentration. Sherman and Albus (1924) reported no lag phase when bacterial cells were transferred from a culture in the maximal growth rate period to a medium of the same formulation. Another theory is that of Buchanan (1918) who suggested that at the end of growth bacteria go into a resting state, and when transferred to a new medium they must undergo a process similar to germination before they can start to grow. A better understanding of lag phase in foodborne pathogens would help in defining accurate predictive growth models, which may suggest ways in which the lag phase can be extended to reduce the probability and extent of unwanted microbial growth in foods (Mellefont & Ross, 2003).

1.4 Effect of Environmental Parameters on Lag Phase Duration

The lag phase duration is much harder to predict than the specific growth rate, as it does not only depend on current conditions, but also on the physiological and environmental history of the cell. The duration of the lag phase is also influenced by : the identification and phenotype of the bacterium (Buchanan & Cygnarowicz, 1990; Mellefont & Ross, 2003), the physiological history of the population, inoculum size (Baranyi & Roberts, 1994) and changes in the physicochemical environment such as temperature, pH, water activity (a_w) and nutrient availability (Buchanan & Cygnarowicz, 1990). A metabolically active inoculum, i.e., exponential phase, has a shorter lag phase compared to a low active inoculum, i.e., stationary phase (Mellefont & Ross, 2003).

Most of the studies that have been published investigate the lag phase on population level using high inoculum size. However, foods are mostly initially contaminated with low numbers of food pathogens, for example, the initial contamination level of *L.*

monocytogenes on cooked meat products and poultry products are mostly between 0.1 to 10 CFU g^{-1} (Francois et al., 2005a). The variability of detection times of *L. monocytogenes* increased when a lower inoculum level was applied, and, when dealing with constant inoculum levels, an increase in variation was observed when more salt stress was applied (Robinson et al., 2001)

1.4.1 Effect of Osmolality

Abrupt osmotic shifts have an effect on the relative lag times (RLT) of foodborne bacteria (Mellefont & Ross, 2003). The RLT is the ratio of lag time to generation time that was used to differentiate the effects of the shift from the outgrowth environment. In their study, Mellefont & Ross (2003) focused on the effect of water activity shifts on the lag phase duration. They found that the (RLT) of tested Gram-negative organisms was extended when the conditions became less favourable, while in Gram-positive organisms the RLT remained the same. An upshift from a_w 0.960 resulted in RLTs increasing approximately in proportion to increasing a_w in *E. coli* SB1 (Figure 2). Downshift from a_w 0.999 results in increasing RLTs in proportion to decreasing a_w for shifts of −0.015 a_w units or less. For larger changes, the RLT response then increased up to an RLT of 4.5, which corresponded to a change of −0.034 a_w units and at downshifts >0.034 a_w units, RLT then decreased. In Gram-positive organisms, osmotic downshifts had little effect on RLTs. The RLTs of *S. aureus* remained <0.35 over the range of a_w tested. RLTs of <0.5 were also obtained over most of *L. monocytogenes* a_w growth range; however close to the a_w limits for growth, RLT increased up to 1.6.

Mellefont & Ross (2003) interpreted the lag time regarding the amount of work required to be done by bacterial cells to adapt to a new environment and the rate at which this work could be completed. They hypothesised that as the RLT increased:

‘*the amount of work required increases and the rate of work done decreases as conditions in a new environment deviate further from those under which an inoculum is grown*’.

Francois et al., (2006) examined the effect of individual environmental parameters such as temperature (2–30 °C), pH (4.4–7.4) and a_w (0.947–0.995) and their combinations on individual cell lag phases and generation times of *Listeria monocytogenes*. Their results suggested that the mean individual cell lag phase duration is increased when stress levels are increased, which led to broader histograms and distributions shifted towards the right. On the other hand, when the stress levels were decreased the individual cells showed no lag phase. Robinson et al. (1998) found that controlling the growth of *L. monocytogenes* by a combination of pH, NaCl concentration and temperature affected lag time as well as generation time, while the effect of individual factors was rather weak. The growth rate of *L. monocytogenes* was influenced more by the osmolality than the solute type, and there was a negative linear relationship between the growth rate of *L. monocytogenes* and osmolality of the medium adjusted with NaCl and glycerol. Glycerol had no effect on the lag phase, while an increase in NaCl concentration resulted in an increased the lag phase. Also, salt affects the lag phase more than the growth rate. The necessary work (as mentioned previously) seems to include repair of cell injury and accumulation of compatible solutes by the cells to adjust to the environment. The level of work required can increase beyond a critical concentration threshold (Robinson et al., 1998), which results in the cell not resolving lag.

1.4.2 Effect of pH

Robinson et al., (1998) revealed that pH has little effect on the lag time of

L. monocytogenes, which is in disagreement with Duffy at al., (1994) who found that acidic conditions increase lag time. The effect of pH (6.1, 5.5, 5.0, 4.7 and 4.3) at 30°C on the individual cell lag phase and the generation time of *L.monocytogenes* were investigated by Francois et al. (2005a). They found that at lowest pH (4.7) the growth was very limited and the maximum OD level decreased compared to the moderate pH stress levels. Cell death occurred at pH 4.3. They analysed the data of individual lag and generation time using histograms.At low-stress levels (pH 6.10), the distribution is skewed to the left side, containing many short individual lag phases. When the pH stress increases, the distribution shifts to the right side (Figure 3). The distribution has significant consequences for risk assessment as the chance of having fast growers decreases significantly. Metris et al., (2008) examined the effect of pH (7.0, 5.5, 5.0 and 4.5) on the individual cell lag phase of Listeria inocula at 30 °C. At a pH level of 5.5. They observed that when stress factors increase, the mean lag time is higher and the distribution becomes broader (increasing variability).

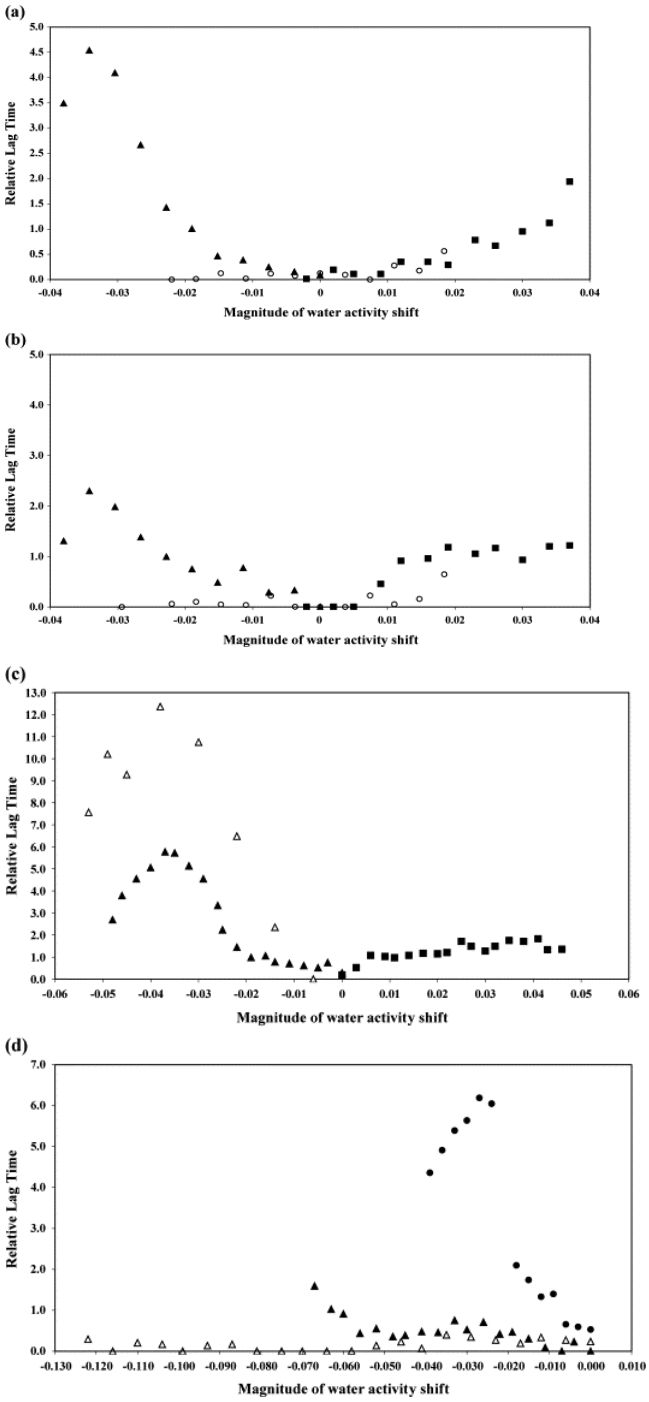

Figure 2 **:** Effect of osmotic shifts on the relative lag time response of (a) *E. coli* SB1 and (b) *E. coli* R31 in nutrient broth, where inoculum a_w is: ▲=0.999, ○=0.980 and ■=0.960. (c) *K. oxytoca* in brain heart infusion broth, where inoculum a_w is: ▲=0.996, ■=a_w 0.949 and △=0.998 (viable count). (d) *Salmonella typhimurium* in brain heart infusion broth, inoculum a_w=0.993 (●); *S. aureus* in nutrient broth, inoculum a_w=0.998 (△); and *L. monocytogenes* in tryptone soy broth with 0.6% yeast extract added, inoculum a_w=0.996 (▲) Data from (Mellefont & Ross, 2003).

1.5 Other Effects on Lag Phase

1.5.1 Effect of Temperature

Several researchers (Augustin et al., 2000; Buchanan & Klawitter, 1991; Dufrenne et al., 1997; Gay et al., 1996; Hudson, 1993; Wang & Shelef, 1992) reported that the temperature history of an inoculum had a significant influence on the lag phase duration. They found that the lag phase duration before regrowth at low temperature is shorter with lower than with higher pre-incubation temperatures. The process indicates that the temperature history of the inoculum can significantly influence the lag phase time. Francois et al investigated the effect of temperature (30, 10, 7, 4 and 2°C) at pH 7.4 on the individual cell lag phase and the generation time of Listeria monocytogenes., (2005b). The individual cell lag time and the growth rate of 100 replicates were calculated using optical density (OD) measurements (600nm). They found that lag times rise exponentially with increasing temperature stress, especially in the region between 7 and 2°C. At temperatures 10 and 7°C, the adjustments to the new environment for a high proportion of cells was shorter. It seems the cells occur in a physiological state which permits multiplication without any significant adaptation period, so there is more “work to be done”. Studying the effect of temperature on lag time of *L. monocytogenes* at three different salt concentrations, Robinson et al. (1998) found an increase in lag time with a decrease in temperature from to 37ºC to 25ºC. The lag time occurred down to a minimum of 15ºC. Further decreases in temperature below 5ºC resulted in sharp increases in lag time.

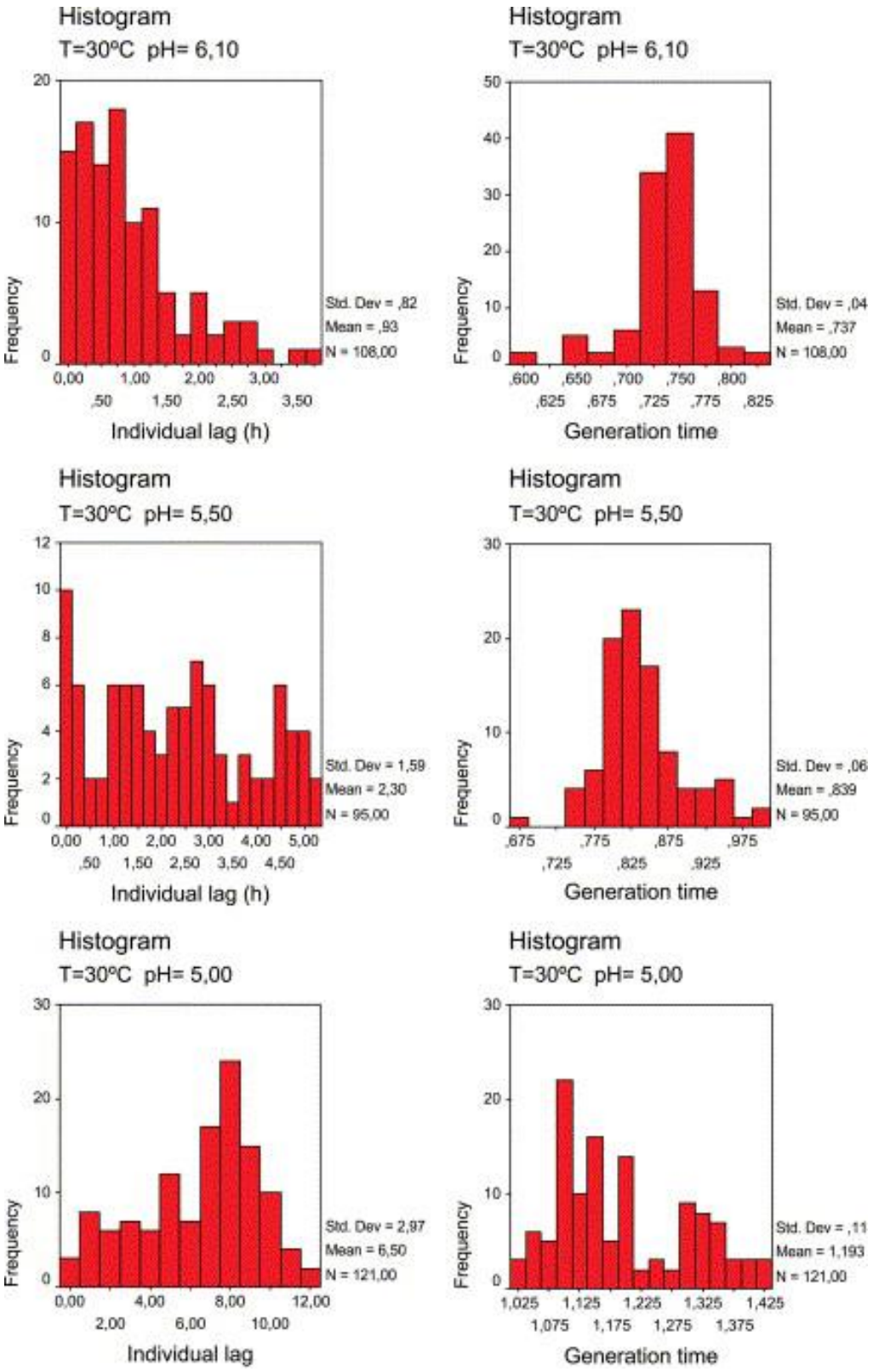

Figure 3:Histograms of the individual cell lag phase and the generation time of *L. monocytogenes* cells grown in BHI at different pH values at 30 °C Data from (Francois et al., 2005b).

1.5.2 Other Environmental Factors Effecting Lag Phase

Numerous factors affect lag including the presence of many exogenous substances. An example of this can be seen with the effect of cadmium sulphide quantum dots (CdSQDs) on the lag phase of *E. coli*, which was studied by Jaiganesh et al. (2012). The study showed an increase in the lag time when the cell was treated with CdSQDs. There was a positive relationship between the lag time and the CdSQDs size. The study used three different sizes of CdSQDs and measured the lag phase time of cells treated with each size. The difference between the control and the largest size of CdSQD was 1.2 h. It suggests the possibility of lack of some essential materials for the cells or some to some inhibitory effect due to foreseen influence of CdSQDs.

1.6 Effect of Cell History on Lag Phase

The cell history can affect the physiological state of the cells in lag phase. For example, if the cell was exposed to heat, freezing and drying injuries the lag time duration and its variability was found to extend considerably (Robinson et al., 2001). The length of lag phase varies according to the severity of the damage (Stephens et al., 2003). Under suitable conditions, heat injured cells recover by synthesis of phospholipids, re-synthesis of ribosomal RNA and ribosomes accompanied by protein synthesis (Stephens et al., 2003). Mackey and Derrick (1982) studied the effect of sub-lethal injury by heating, freezing, drying and gamma radiation on the duration of the lag phase of *Salmonella* Typhimurium. The study showed that bacteria sub-lethally injured by heat and freezing needed a longer period to repair than those injured by drying or gamma-radiation. Additionally, heat-injured *Salmonella* cells at 52 ˚C in phosphate buffer had a 9 hours lag time when measurement of cell repair on the membrane filter was taken, while some individual

cells needed up to 14 hours to recover after exposure to 3% of NaCl. Heat injured *Ps. fluorescens* had a lag time of 9 hours before regaining resistance to selective agents (Stephens et al., 2003; McCoy & Ordal, 1979).Gram-negative bacterial cells have longer lag times after heat treatment (Hershey, 1939; McCoy & Ordal, 1979; Mackey & Derrick, 1982). According to Van Schothorst and Van Leusden (1975), the population of injured cells are heterogeneous, and the level of injury is different among individual cells. Therefore, the lag time for the severely injured individuals in a cell population will be extended. Cells with the least injury will be the to complete repairs and begin multiplication (Mackey & Derrick, 1982). This concept was justified by Dupont and Augustin (2009) who examined the impact of stress on single-cell lag times and growth probability of *L. monocytogenes* in 12 typical food industry stresses (acetic acid, starvation, nitrite, lactic acid, freezing, HCl, phenol, osmotic stress, NaOH, BAC, heat, and peracetic acid stress) in Fraser broth, the primary enrichment broth of the International Organisation for Standardization detection method for Listeria. The study revealed that the cell history controls the ability of the cell to initiate growth. Additionally, when the cells were injured the single-cell lag time was extended on average and regarding variability. Also the greater the cell injury, the lower the single-cell growth probability. The study highlighted the importance of considering the physiological state of the cells when detecting the presence of food-borne pathogens.

D'Arrigo et al., (2006) studied the distribution of lag times of single cells of *L. monocytogenes* in a liquid dairy product and liver paté after different heat treatments using the log count distribution. The dairy product samples were inoculated and heated at 55˚C for 45 min, 62˚C for 2 min and the unheated samples were incubated at 4˚C. The results showed that unheated samples had shorter lag time than other

samples which showed the effect of previous cell history on the distribution of single-cell lag time. The paté samples were heated at 55˚C for 25 minutes, 62˚C for 81seconds and 65˚C for 20 seconds and incubated at 15˚C. The lag time of samples treated at 62˚C and 65˚C was longer and showed greater mean and variance than the lag time for samples treated at 55˚C.

Dufrenne et al., (1997) examined the effect of previous growth conditions on the lag phase duration of *Bacillus cereus*, *Salmonella* spp. and *Listeria*. The organisms were pre-cultured at different temperatures for various periods of time and then inoculated into fresh media. The lag phase durations were strongly influenced by the pre-incubation temperatures. The lag phase for *Bacillus* strains pre-incubated in 7˚C was 1.5 days, while the strains that pre-incubated at 37˚C showed a lag phase of one week. The effect of pre-incubation temperature was not significant for *Salmonella* strains, and the effect was less with *Listeria* strains. Pre-incubation of *Salmonella* strains in the presence of increased NaCl salt concentration led to a decrease in growth rate and an increase in lag phase duration.

1.7 Effect of Inoculum Size on Lag Phase

Several researchers reported that under optimum conditions, the lag and growth rate of *Escherichia col*i were unaffected by inoculum size (Robinson et al., 2001; Jason, 1983). According to (Robinson et al., 2001), a single cell of *L. monocytogenes* was able to initiate growth under optimum conditions. However, in the presence of high salt concentrations, they found that an increase in the inocula size was required. This study is in agreement with that of Razavilar and Genigeorgis (1998), who found that increasing the NaCl concentrations in the media required an increase in the inoculum size of *L. monocytogenes* in BHI broth. They found the number of cells

needed to initiate growth under the most stressful condition was 10^6. In a similar study, Pascual et al. (2001) found that the growth of *L. monocytogenes* in Tryptic Soy Broth (TSB) at 37 °C with different levels of sodium chloride and pH is a function of the inoculum size. They examined the effects of inoculum in media with a high salt concentration (1.7 M NaCl) and found that growth occurred from single cells at this level. A larger initial inoculum was however needed above this concentration. The inoculum effect for decreasing pH shows a similar trend but occurs only very close to the growth/no-growth boundary. A similar result was obtained by McKellar et al. (2002a, 2002b). Augustin et al. (2000) studied the growth of *L. monocytogenes* in a poor medium under suboptimal conditions and found that starvation and small size inoculum resulted in an increased lag time duration. Duffy et al. (1994) studied the effect of aeration, inoculum level and meat microbiota on the growth rate of *L. monocytogenes* and found that aeration and different levels of inocula had no effect on lag times or growth rates suggesting that the lag time was independent of inoculum size. However, according to Gay et al. (1996) storage conditions, pre-incubation temperature and inoculum concentration have an effect on the duration of the lag phase of *L. monocytogenes.* The study showed that cold storage (4˚C for weeks) and inoculum level (10^3 CFU ml^{-1}) of two strains of *L. monocytogenes* (Scott A serotype 4b and V7: serotype 1) and one strain of *Listeria* inocula (Lin 11) and pre-incubation temperatures (30˚C and 14˚C) did not influence the growth curve and the lag time was less than 21 hours. However, when the inoculum size was at a lower concentration 10^1 (CFU ml^{-1}) and the pre-incubation temperature was 30˚C a significant change in the growth curve was detected with lag phase as much as 7.7 d. At low inoculum concentration with a pre-incubation temperature of 14˚C resulted in a lag time measured at about 1 d. A lag time of 2.3 d was observed without cold

storage and a pre-incubation temperature of 30°C. Gay et al. (1996) concluded that there are two distinct values of the exponential growth rate (k): the initial portion of the growth curve described by a low value of k and the subsequent part of a consistently and significantly greater value for cultures from inocula, pre-incubated at either 30°C or 14°C.

Pascual et al., (2001) and McKellar et al., (2002b) also showed for *L. monocytogenes* that the inoculum size effect is more distinct near the growth/no growth interface.

The inoculum size effect can be explained by an increase in the variability of the individual cells' lag time when cells are damaged by stress (Swinnen et al., 2004)

Koutsoumanis and Sofos (2005) believe that the growth limits of *L. monocytogenes* are affected by the inoculum size. They examined four different levels of inoculum (0.90, 2.58, 4.20 and 6.81 log CFU/well; 300 µl medium/well) under various combinations of temperature (4 to 30 ºC), pH (3.76 to 6.44) and a_w (0.888 to 0.997) for 60 days. From the experiments, they found that the effect of inoculum size is greater in environments where a single inhibitory factor (pH or a_w) was present than in environments where combined stresses were applied. For example, at 25°C, the difference between minimum pH values that permitted growth at the higher and the lower inoculum levels decreased from 0.51 pH units at the optimum a_w of 0.997 to 0 pH units at a_w 0.960. A similar result was found at 25 °C where the difference of the minimum a_w values that permitted growth between the higher and the lower inoculum level decreased from 0.028 a_w units at the optimum pH of 6.44 to 0 a_w units at pH 4.96.

1.8 Gene Expression during the Lag Phase

McKellar (2007a) studied the effect of starvation of *Pseudomonas fluoresces* cells on

the duration of the lag phase. The examined strain contained a Tn7-*lux*CDABE gene cassette regulated by the rRNA promoter *rrnB P2*. The optical density of the growth was measured at 600 nm (OD_{600}) and fitted with a two-phase linear model to calculate the rate of increase (R_{OD}) and lag phase duration (LPD_{OD}). The results showed an exponential increase in RNA *rrnBP2* expression- indicating rRNA expression is a major step in preparing the cell for growth. The bioluminescence level increased rapidly after the cell was inoculated in fresh media; the increase was associated with early exponential phase cells. McKellar (2007b) studied the influence of sublethal heating at 47ºC and growth temperature on RNA *rrnBP2* expression on lag phase. The study showed that when the heating time increased the R_{OD} decreased by 50% with an increase in LPD_{OD} by 5-fold, while *rrnBP2* (LPD_{Exp}), increasing rrnB P(2) lag phase duration exponentially, increased 20-fold to 2.3 hours and the R_{Exp} decreased to 22% of the control rate. In the starvation treatment, the value of R_{OD} was reduced to 77% of the control and LPD_{OD} increased 3 to 4 fold, while R_{Exp} was decreased by 50% and LPD_{Exp} increased 2.5 and seven fold. Both studies showed that the heat treatment has a great impact on LPD_{OD} compared to the starvation treatment leading to the suggestion that sub-lethal injury has a significant effect on increasing *rrnBP2* activity.

Rolfe et al., (2012) described the physiological and transcriptional events in the lag phase of *Salmonella* Typhimurium over 2.09 hours duration at six-time points (4, 20, 40, 60, 90 and 120 minutes). The study revealed that 2675 genes changed significantly in expression between the stationary phase inoculum and at least one lag phase time point. Within 4 minutes 1119 genes changed, and the main change occurred during 20 minutes of inoculation as 1741 genes changed. The change in the 4 minute period was distinguished from other terms as it did not share as much

similarity with other changes across the assessed lag time. Transcription analysis showed that nucleotide metabolism, transcription, LPS biosynthesis and fatty acid biosynthesis were up-regulated. Up-regulation occurred for genes encoding aminoacyl-tRNA synthetases, and ribosomal proteins were observed reaching the exponential phase expression level within 20 minutes. Identification of lag phase signature genes showed that 20 genes were specifically up- regulated during lag phase and 19 genes were down-regulated. The up-regulated lag phase signature genes included nine genes associated with iron uptake or storage, four genes involved in Fe-S cluster synthesis and two genes implicated in manganese uptake. Therefore, the study suggested that accumulation of metals and assembly of iron-sulfur clusters, a cofactor for various metalloenzymes, may be necessary during lag phase. The research identified 346 *S.* Typhimurium essential genes induced during lag phase with 55% being up-regulated at 20 minutes and 5% at 60 minutes. A rapid induction of *phoBR* and *pstSCAB* suggested that phosphate uptake likely plays an essential role in lag phase duration.

Stasiewicz et al., (2011) investigated the synergistic transcriptional response of two strains of *L. monocytogenes* (F6854 and H7858) during adaption to growth on lactate and diacetate. Early stationary phase cells were used to inoculate BHI with 4.65% water-phase (w/v) NaCl at pH 6.1 with: (i) 2% w/v potassium lactate, (ii) 0.14% w./v sodium diacetate, (iii) the combination of both at the same levels, or (iv) no organic acids as a control and incubated at 7 ºC for 8 hours follow by cells harvesting for RNA extraction. Two ANOVA models were used to analyse full-genome microarrays that showed a significant difference in gene transcript level. Model A tested one pair of the four treatments and Model B tested the effect of combined treatment of lactate and diacetate. The results showed that 1041 genes

were transcribed in H7858 and 640 genes in F6854; among these genes, 265 were differentially transcribed in both strains. Combining those models revealed that H7858 transcript 474 genes and, in F6854, 209 were transcribed. Testing the gene transcription between each treatment showed that 983 and 662 genes were transcribed differentially in H7858 and F6854, respectively. The effect of combined treatments on gene transcription was different than the effect of diacetate where acetate is not present alone. The gene expression patterns suggest that the genes involved in the transcriptional response of F6854 to diacetate treatment alone are the same genes that are affected by the interaction of acetate and lactate. The combination of treatments showed a decrease in transcription of genes encoding a protein for production of organic acid to fermentative production of acetate and lactate to acetoin and away from aerobic respiration. They observed that H7858 shows further induction of CodY regulated genes, as well as decreased transcript levels of *codY*, in response to organic acid treatment. In addition, the PrfA virulence regulon was induced in F6854 in response to organic acid treatment.

1.9 Lag Phase, Generation Time and Cell Age

Pin and Baranyi (2008) examined how cell age (calculated as the incubation time in the pre-inoculation culture) affects the distribution of the generation (i.e., intradivision) times of single *Escherichia coli* K-12 cells. The researchers inoculated LB media with 2 % glucose with *ca.* 10^3 *E. coli* K-12 and incubated the cultures at 25°C for 53, 77, 83, 144, 151, 193, 218, 360, and 602 h. After the incubation period, the cells were removed from the culture and inoculated in the flow chamber. The average first division time (FDT), quantified as the sum of the lag time and the first generation time was found to increase with increase cell age. However, the second-

generation time (the time interval between the first and second division) was not affected by cell age (Figure 4). The effects of cell age on the lag period occurred before the first division, and the cells do divide before they adjust themselves to the new environment altogether.

Analysis of the transcriptional pattern of young and old cells of *Escherichia coli* during lag has been examined (Pin et al., 2009). The study showed a difference in the intracellular activity in both young and old cells during lag phase. In mature cells the number of genes differentially expressed (186 genes) was smaller than in young cells (467 genes). Also, down-regulated transcription of genes related to osmotolerance, acid resistance, oxidative stress and adaptation to other stresses was observed in both young and old cells. Transcription of genes related to the citrate cycle was up-regulated in immature cells while old cells up-regulated the Entner Doudoroff and gluconate oxidation pathways and down-regulated the (non-oxidative) pentose phosphate pathway. Anaerobic respiration and fermentation pathways were also down-regulated in both cells. DNA maintenance and replication, translation, ribosomal biosynthesis and RNA processing as well as biosynthesis of the cell envelope and flagellum and several components of the chemotaxis signal transduction complex were up-regulated only in young cells.

1.10Lag Phase Duration

Lin and Crowley (2001) starved *Pseudomonas fluoresces* 2-79RL in isolation or in non-sterile cultures with other soil bacteria to determine the length of lag phase. The results showed that the cells that were maintained in sterile soil extract had a shorter lag phase duration than those retained in non-sterile soil. A further examination was carried out to determine whether a longer lag phase might result in decreased ability

of the cell to compete for carbon inputs. Whiting and Bagi (2002) grew *L. monocytogenes* in BHI broth at different temperatures, from 4 to 37˚C, to the exponential phase and stationary phase. After that, the cells were frozen, desiccated and diluted in broth then transferred to BHI broth at different temperatures from 4 to 37˚C to determine the lag duration. They revealed that cells growing at higher temperatures had a longer lag phase when they were transferred to low temperature. Also cells in exponential phase had the shortest lag phase, while cells in the stationary phase and starved cells had longer lag periods. Frozen cells had a slightly longer lag phase. Desiccated cells had overall most extended lag phases indicating a greater effort to regain an active growth state.

The effect of sodium chloride and heating on individual –cell lag times of *E. coli* were examined by Niven et al., (2008) using digital image analysis. The research also determined the relative division time (RDT), which is a measure of the "work to be done" during lag, from direct observation of single cells. Also, the time to the first division of individual *E. coli* cells was determined by using box area ratio methods. The results showed that the first group time increased as the stress level increased. For unstressed cells, the RDT was estimated to be 1.8 h, and for cells that were stressed by heating to 50ºC for 80 minutes, the RDT was increased to 4.3 h. On the other hand, stressed cells exposed to various concentrations of salt (0.5%, 2.5%, 3%, and 4% NaCl (w/v) showed only a slight increase in RDT compared to heated cells.

It has been observed that no lag time occurs when *L. monocytogenes* is pre-incubated at 4° C and 7° C for 4 and six days and then transferred to fresh medium at 7° C (Membré et al., 2002). However, in the same study, a lag period of ~31 hours was observed when the cells were pre-incubated at 37° C for 20 hours and then

incubated at7° C. This result is consistent with Buchanan and Klawitter (1991) who found an increase in lag phase duration with increasing pre- incubation temperature. In addition, George and Lund (1992) found that there was no lag phase when *L. monocytogenes* cells in the exponential phase at 20°C were transferred to fresh medium at the same temperature.

1.11Modeling Lag Phase

Predicting the lag phase duration is very important in performing a risk assessment or for generating process models. Accurate predictions are difficult to achieve as there are many factors influencing lag phase behaviour (Swinnen et al., 2004). In addition, because the mechanisms leading lag time are not entirely understood (Baranyi & Roberts, 1994; Koseki & Nonaka, 2012) modelling requires some significant assumptions. Robinson et al., (1998) generated important hypotheses to model the lag phase: (i) the amount of work that cell has to perform to adopt to a new environment, and (ii) the rate at which it can perform that work:

$$< lag > . < rate > = < work >$$

In general to develop a predictive model to measure the lag time primary models and secondary models have been conceived. The primary model establishes the change in cell numbers in a constant environment over time. On the other hand, the secondary model determines how the environmental factors affect the measured lag time (λ). In this section there is separate focus on primary and secondary models developed to estimate lag time.

1.11.1 Primary Models

According to Swinnen et al., (2004), most primary models are either deterministic or

stochastic population models. In a deterministic model one single set of model parameters are used to describe the change in the total cell number of a population. The model parameters in the stochastic model are distributed over the total population randomly. In fact, the stochastic approach to bacterial growth is essential as the contamination of foods with pathogen bacteria occurs with very few cells.

An early primary model was a deterministic population model proposed by Baranyi and Roberts (1994) which evaluated the total cell number of a population by one single (deterministic) set of model parameters, e.g., N0, k, μ_{max}, N_{max} (Swinnen et al., 2004). In this model the work to be done changes at the same rate to the rate at which the work is performed.

$$\frac{dN}{dt} = \frac{Q(t)}{1+Q(t)} \cdot \mu_{max} \cdot [1- \frac{N(t)}{N_{max}}] \cdot N(t)$$

In this model *N* is the cell density (CFU ml^{-1}), μ_{max} the maximum specific growth rate (1/h), N_{max} , the maximum cell density (CFU ml^{-1}) and Q a measure of the physiological state of the cells. $Q(0)$ introduces a mechanistic meaning to the model. The model describes the transition phase (from the lag phase the exponential phase) which is the adjustment factor $\alpha(t)$ i.e., Q (t)/(1 + Q (t)). The decreasing effect of previous environment can be inserted in $Q(0)$, which describes the initial physiological state of the inocula. The model is depicted in Figure 4.

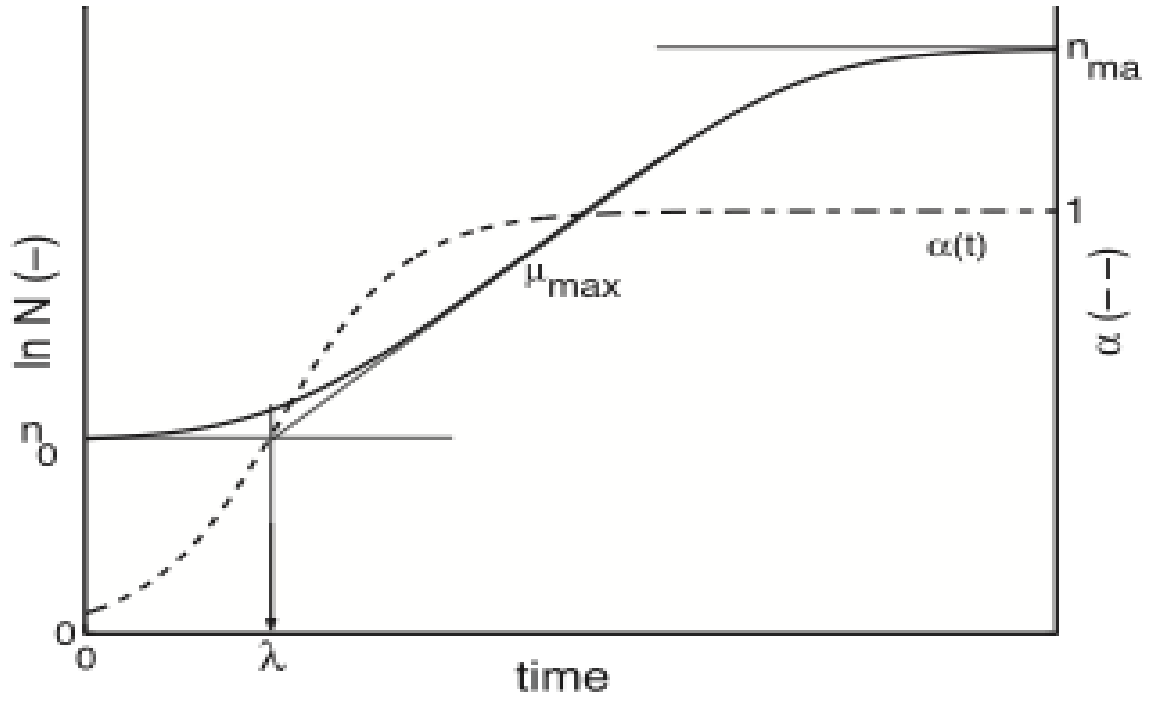

Figure **4:** Representation of the Baranyi and Robert (1994) D logistic growth model overlayed by an adjustment factor of Swinnen et al., (2004). The solid line represents the evolution of cell number, and the adjustment factor (∝) is represented by the dashed line. From (Swinnen et al., 2004).

$Q(0)$ starts at low value and when cells grow to the exponential phase the $Q(0)$ value starts to increase and results in $\alpha(t)$ changing from a low value (<1) to a value of 1. The disadvantage of this model is that it does not consider the stochastic variability of lag time (Koseki & Nonaka, 2012).

A stochastic model was developed by Robinson et al. (1998) to relate the distribution of individual cell physiology states or lag time (τ) to population lag time (λ). In this model a relationship between individual lag (τ_i) time and population lag time (λ) described as mathematical relationship depends on the factor h = t/(1/m), which is the ratio of the mean lag and generation time of the individual cells. As a result the relationship can be derived from the following equation:

$\lambda \cdot \mu_{max} = \mathrm{In}(1 + \mu_{max}\,\tau)$

However, one of the limitations with this is the assumptions made, and the associated mechanistic interpretations have not been experimentally proven (Swinnen et al., 2004)

A model based on the Baranyi and Roberts (1994) models was developed by Metris et al., (2005) (Figure 5). The model includes deterministic and stochastic parts to estimate the growth and division of single cells. The deterministic element models the gradual adaptation of the cell to the new environment. The stochastic component models the variability of individual generation times by measuring the threshold size for the division of a single cell. The deterministic primary model involved a structured cell kinetic bacterial metabolism model incorporating reaction-diffusion equations characterising the growth medium by Hills and Wright (1994). In their model, they introduced the total biomass per cell (s^*) and its minimum value (s_{min}), in which the cells are no longer viable. The excess amount of biomass per cell indicated by s, where $s^* = (s_{min}+s)$, includes the increased amount of DNA and RNA. The following equation shows the total biomass in culture (M) in term of s^*:

$M = Ns^* = N\ (s_{min}+s)$

Where N is the viable cell number in culture. Since the biomass grows exponentially in a constant environment, Hill and Wright assumed that minimum biomass per cell (s_{min}) is constant as well and restructured the equation as:

$M = Ns^* = N(\ 1 + s)$

As the biomass total grows in balance exponentially and since no lag time was observed in set-up experiment Hill and Wright assumed that, at any time,

$\frac{dM}{dt} = \mu_{max}\ .\ M\ (t)$

The increase in cell number (N) is synchronised to the cell DNA content as cells only divide after their DNA replicated. Therefore, they proposed:

$\frac{dN}{dt} = k_n$. *s*(t) . *N* (t)

when k_n is proportional to the rate constant related with the DNA synthesis per cell. The excess biomass *s* with time can be derived from this equation:

$\frac{ds}{dt} = (\mu_{\max}$ - $k_n\, s)\ (1 + s)$

In this model, the lag phase is defined by an increasing fraction s(*t*), which increases to a constant value (k_n) and once the constant value is reached the cells enters the exponential phase (Swinnen et al., 2004). The ability to change the acquired value of s(*t*) as the environmental condition change is one of the advantages of the Hill and Wright model.

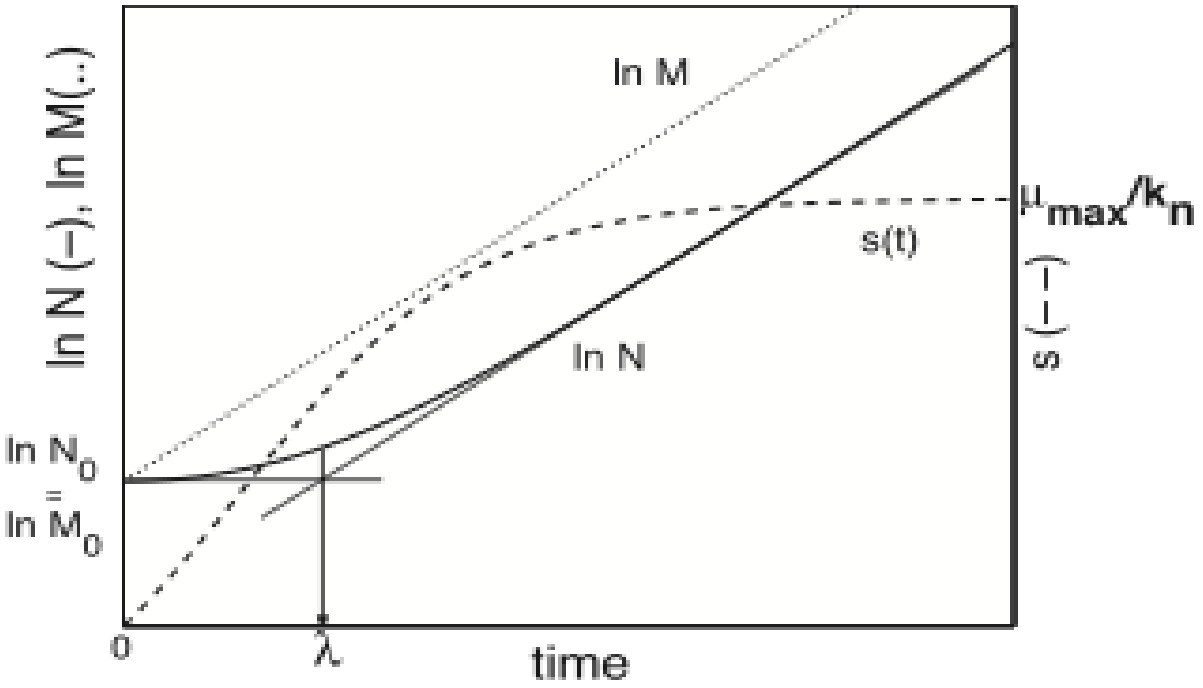

Figure 5**:** Representation of the Baranyi and Robert (1994) developed by Metris et al., (2005).

The impact of nine food industry stresses on the distribution of individual lag times of *L. monocytogenes* were investigated by Guillier at al., (2005). The particular lag

times were measured through the times of turbidity detection (T_d), which showed a significant difference in responses to given stress by *L. monocytogenes*. The mean of standard exposure time T_{ds} was used to compare the effect of the nine stresses (HCl, cold, lactic acid, chlorine, NaOH, NaCl, starvation, benzalkonium chloride and heat). The greatest impact on the lag phase duration was by BAC (the mean of T_{ds} was multiplied by 1.65) and heat stress (the mean of T_{ds} was increased by 1.78) in comparison with the average of T_{ds} values of cells in exponential phase. However, the observed difference observed for cold and acid stress in this study was not significant. An observation of the variance of T_{ds} for the nine strains revealed that acidification via HCl has the weakest impact on the total variance of T_{ds} followed by alkalinization via NaOH and cold stresses in which their variance was 30 times more important than the difference of cells in exponential phase. The factor of multiplication of the difference of T_{ds} for starvation, NaCl, and chlorine stresses was 140 times greater than the difference in cells in exponential phase. For BAC and heat emphasizes the variance of T_{ds} were 180 and 355-fold greater, respectively, in comparison to the variance of T_{ds} for cells in the exponential growth phase. The researchers pointed out the impact of the stress undergone by the cell on lag time distribution, which resulted in increases in variability of lag time.

The probabilistic model that was introduced by Koseki and Nonaka (2012) to predict the end of lag time (λ) has both deterministic and probabilistic aspects. The model was based on the growth of *Bacillus cereus* as a function of temperature, pH and salt concentration using logistic regressions. Koseki and Nonaka (2012) describe the probabilistic aspect of lag time deterministically as a function of environmental factors. The data in this study were gained by determining the beginning and the end of lag time (λ) by measuring the OD in culture media at different pH (5.5~7.0) and

salt concentrations (0.5~2.0%) at a static temperature (10~20°C) at each time point during the growth kinetics. At each OD measurement point, the probability of the end of (λ) was modelled using dichotomous judgments concerning whether a significant change had been observed. The model introduced the idea of *p*(t) which is the probability of the end of lag time at each time point and $f(t)$ is a function of time, which was modeled using logistic regressions as a function of time and other environmental parameters:

$$p(t) = \frac{1}{1+\exp[-f(t)]}$$

However, the disadvantage of this model is that the assumptions are empirical and have not been experimentally verified.

The lag phase duration and exponential growth of *L. monocytogenes* under different temperatures and water activity values were modelled by Muñoz-Cuevas et al., (2010) using Baranyi and Roberts (1994) primary model. The results showed that a decrease in a_w for cells growing as an exponentially will results in an increase in the perceived amount of work to be done in lag phase compared to a_w in the previous environment. The same was observed for decreasing the temperature.

Le Marc et al., (2010) developed a model to describe the effect of acid and abrupt osmotic shift on the growth of *L. monocytogenes* and the possibility to induce intermediate lag time within the growth region and across the growth region. The data were modelled through the dependence of the parameter h_0 to evaluate the work to be done when shifts are applied during the initial and intermediate lag time. The results showed again that the amount of work to be done within the growth region is related to the magnitude of the shift and the environmental condition after

the shift. For changes across the growth region the lag phase duration was affected by the length of time for which the microorganism was spent under inhibiting conditions. Also, within the growth region osmotic shift induces a greater amount of work before regrowth than acidic shift does. Moreover, acidic shifts do not induce long or intermediate lag times within the growth region unless the previous and current conditions are similar to the growth limits.

McKellar and Hawke (2006) (Figure 6) assessed a variety of continuous distributions to develop mathematical models for fitting lag times of individual cells in *E. coli* O157: H7. The study utilised the Bioscreen instrument as a tool to study single cell behaviour of six strains of *E. coli* O157: H7 which were subjected to 25 trials and 100 replicates wells per trial. The lag times for individual bacteria cells (τ) were calculated using the following equations:

$$\tau = t_d - \frac{\mathrm{In}N_d}{\mu}$$

$$\rho_{0=\tau\cdot\mu}$$

Where t_d is the detection limit for a well containing a nominal single cell and N_d is the number of cells per well at the Bioscreen limit. Six different types of statistical distributions were fitted to τ data and ranked according to Anderson–Darling statistics. Using BestFit, the tested distributions were in order (of greatest fit): Pearson V>Pearson VI>Extreme Value>Lognormal>Lognormal2>Inverse Gaussian showed the highest rank. Distributions Pearson V and Pearson VI were the two highest ranked. The distributions Pearson V, Pearson VI and Extreme Value showed the best fit when the number of sample points was few. The study ranked six distributions model in which can be selected to fit τ values.

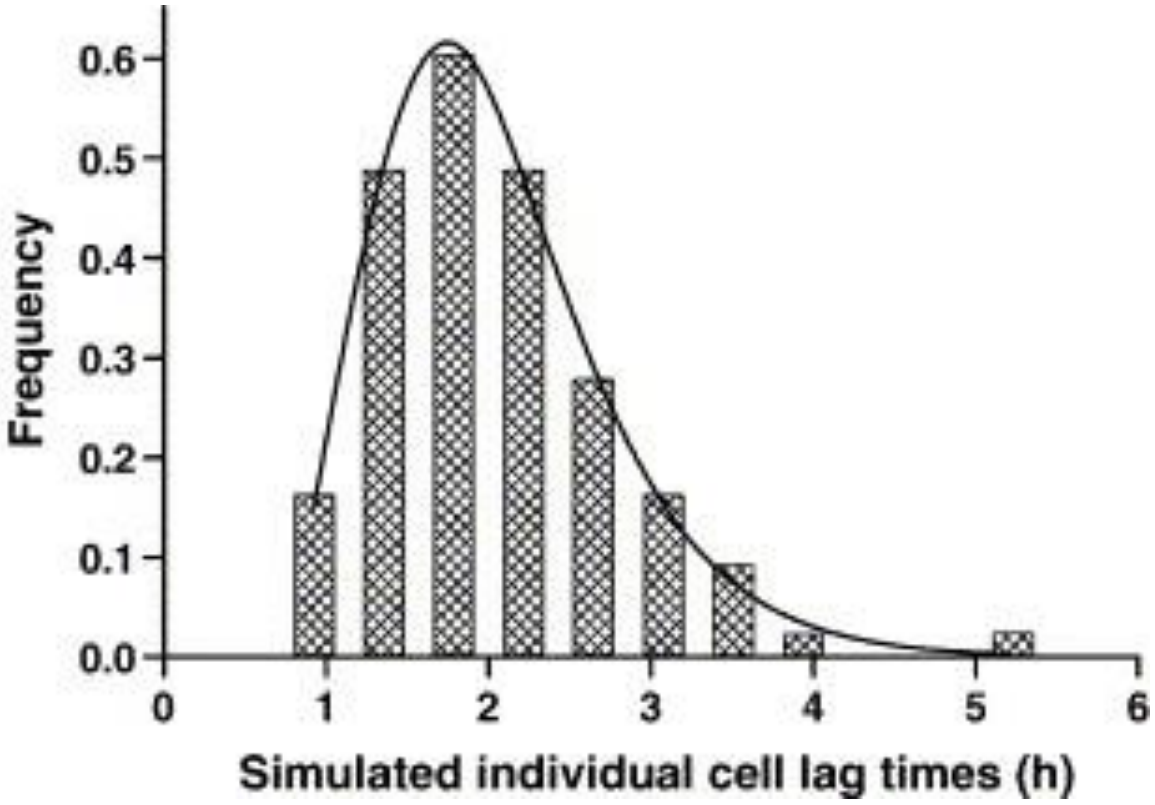

Figure 6: Example of lognormal fitting to simulate lag time values. Parameters A and B values used in the simulation were 2.25 and 0.72, respectively. From (McKellar & Hawke, 2006).

1.11.2 Secondary Models

Secondary models describe the relationship between lag time parameters such as λ and the environmental factors such as incubation environment and pre- incubation conditions. A mechanistically based model was proposed by Augustin et al. (2000) to describe the effect of temperature history and the duration of pre-incubation period on lag times for *L. monocytogenes.* The model assumes that the growth (increase in cell number) is controlled by an exponential accumulation of a critical substance before cell division occurs and this factor is assumed to be associated with the cell biomass. The cells were pre-incubated at temperature *Ti* for a duration *ti*, then

cultured in the actual conditions at constant temperature T (°C). The growth curves of regrown *L. monocytogenes* at low temperature were fitted using the Logistic growth model with delay. The pre- incubation duration (*ti*) is different resulting in different stage of cell growth (lag phase, exponential phase or stationary phase), which enabled the researchers to develop their model without influencing pre-incubation conditions on the duration of lag time. The model was developed depending on the product of $\lambda \cdot \mu_{max}$ and the results showed that:

- When the cells are in the lag phase ($t_i \leq \lambda_i$) with pre-inoculation temperature T_i inoculated at time t_i, the product of $\lambda \cdot \mu_{max}$ decrease to 0

  $\lambda \cdot \mu_{max} = \mu_{max} \cdot (\lambda - t_i)$
- When the inoculated cells were in the exponential phase ($t_i > \lambda_i$) there was no lag phase observed:

  $\lambda \cdot \mu_{max} = 0$
- A linear increase in the $\lambda \cdot \mu_{max}$ product was observed when the inoculum enters the stationary phase as the biomass decrease at time t_i.

One of the disadvantages of the proposed model is that it is only valid for situations where growth is instantaneously adjusted to environmental change (Dens et al., 2005). In contrast to this model is a model proposed by Zwietering et al., (1994) which indicated an additional lag phase for temperature shifts within the lag phase as well as within the exponential phase.

Working with *E. coli* O157: H7 (Li et al., 2006) studied the effect of starvation, heat or acid stress on the duration of cell lag time,τ, and standard deviation (SD) of τ. The cells were exposure to acid (pH 3.5), heat (50 ºC) or starvation in either glucose-free

mineral medium (MOPS), tryptic soy broth (TSB) or Luria broth (LB). The τ data were then fitted to Lognormal, Gamma, ExtremeValue and Weibull distributions using BestFit. The results showed that the cells treated with acid for 21 days and 2 days starvation in either TSB or LB has a significant increase in SD. In addition, heat treated cells had the longest lag time durations and τ increased more than 2-fold from 2.5 to 5.6 h. The researchers also observed that MOPS starvation was more harmful for the cells than acid treatment for the same period of time. The research found that lognormal best described the τ data from both stressed and unstressed cells.

1.12Methods for Measuring Lag Time

1.12.1 Population Lag Time

The commonly used methods for monitoring the bacterial population lag times are viable count and optical density (OD). The viable count method has been criticised as a very labour intensive and expensive method. As well, the quantity and the quality of the observations play an important role inaccurate estimations of the growth. A comparison between the fitting of three models on either datasets with only a few or a great number of data points has been made by Delignette-Muller et al. (2005). It was found that the uncertainty in the parameter estimates is correlated with the amount of data used.

The main problem with OD is the requirement for bacterial densities in the range of 10^6–10^7 bacteria/ml, which can lead to incorrect estimates of lag phase when based on mainly late-exponential growth phase (Swinnen et al., 2004). However, the estimation of the lag time not only depends on the technique but also on the model used to fit the growth data (Baty et al., 2002).

1.12.2 Individual Cell Lag Time

Studying individual cell lag time distributions requires techniques to isolate single cells and also relies on a lot of replicate measurements. The most common methods include indirect methods such as optical density (based on time to detection) (Métris et al., 2003; Francois et al., 2005b; Guillier et al., 2005) as well as direct observations of immobilized or attached cells (Wu et al., 2000, Elfwing et al., 2004; Kutalik et al., 2005b).

Serial two-fold dilutions of the inoculum were used by McKellar and Knight (2000) to obtain single cells. They used Bioscreen measurements to calculate mean individual cell lag time estimates for *Listeria monocytogenes* populations using the time to detection method. They define the detection time (t_d) as the time required for an initial measurable increase in optical density. A serial dilution was performed from the original inoculum to obtain plots of t_d against the initial cell density [*ln*(CFU ml^{-1})] which showed a straight line, and they calculated μ_{max} from the slope using the equation:

$$\mu_{max} = -1/slope$$

The difference between the predicted t_d values using μ_{max} and the observed t_d values were used to calculate the mean individual lag time τ. A disadvantage of the proposed approach is that the initial cell density of each (replicate) serial dilution needs to be known (Swinnen et al., 2004).

Francois et al., (2003) determined the individual lag time using a protocol to isolate the single cells and measure growth using a microplate reader. The means of OD were measured and a calibration curve obtained for the upper part of the standard growth curve. A linear extrapolation of the exponential phase was made and

individual lag phase times were calculated from the linear part of the exponential phase and the horizontal line of the inoculum level.

Flow cytometry is another method that has been used by (Smelt et al., 2002) to calculate the individual lag time encapsulated by the following equation:

$\lambda = t_d - [(\text{number of generations}) * (\text{generation time})]$.

Métris et al., (2003) measured the distribution of individual lag times using a Bioscreen instrument and found that if the initial number of cells is low, the source of variability of the detection times is close to the variability of individual lag times.

1.13 Stationary Phase in Bacteria

1.13.1 Definition

The stationary phase is defined as the transition period that begins in the exponential phase when all the cellular parameters such as DNA, protein and cell mass decrease at equal rates and continue to decrease until the time when no further increase in cell number can be detected. Stationary phase does not describe a particular physiological state, and it is effectively an operational definition. Cells in stationary phase culture can differ over time and are affected by the changing composition of the growth medium. Experimentally cells can enter stationary phase in many ways and means

Table 1: *Major changes observed during stationary phase in E. coli (Llorens et al., 2010)*

Cellular change in stationary phase	
Morphology	Smaller and spherical cells More resistance and rigid cell envelope
Nucleoid	Condensation of the nucleoid as certain histone-like proteins increase their concentration
Metabolic	Stringent response Repression of aerobic metabolism Increase fermentation enzymes expression Production of RMF (ribosome modulating factor) Drop in protein synthesis while increase peptidase/protease synthesis
Transcriptional	Changes of sigma factors affinity σ^S, σ^E Adjustments of global regulators: Lrp IHF sRNAs
Translation	100S ribosome dimers (inactive) Decrease protein synthesis Increase protease and peptidase synthesis
Others	Increase resistance to physical and chemical stresses Synthesis of quorum sensing molecules Production of secondary metabolites Programmed cell death (PCD) GASP phenotype Mutator phenotype Viable cut nonculturable (VBNC) state Stationary phase contact-dependent inhibition (SCDI)

cells entering stationary phase due to carbon exhaustion are physiologically different from cells that cease growth due to phosphate starvation.

Bacterial cells have the ability to live for long periods in non-growing stationary states. Forming spores is the mechanism of survival in some bacteria but non-spore-forming bacteria, including *Escherichia coli*, can survive in the stationary phase (Ishihama, 1997). Changes in the cell morphology and physiology occur in the stationary-phase to form cells resilient to various stresses (Table 1).

1.13.2 Stationary Phase Morphology

The size of bacterial cells entering the stationary phase is considered to be reduced. The reduction in the size is a result of two reductive process division and dwarfing (Nystrom, 2004). In some bacteria when the cell enters stationary phase, a new round of DNA replication is initiated and cell division cycles are completed in the absence of further growth resulting in the reductive division. As a result, the surface/volume ratio increases producing spherical cells (Nystrom, 2004; Llorens et al., 2010). Dwarfing is a starvation-induce activity observed after the completion of reductive division. This form of self-digestion is the result of degradation of endogenous cell material, especially from the cytoplasmic and the outer membranes (Nystrom, 2004). An enlarged periplasm has been reported. In some Gram-negative bacteria, such as *E. coli* the outer membrane is not digested and does not shrink within the stationary phase (Reeve et al., 1984). Other Gram-negative bacilli, for example, *Pseudomonas* and *Enterobacter* spp. produce and release outer membrane vesicles during dwarfism, and the outer membrane and cytoplasmic membrane are cut to the same extent. Therefore, the size and integrity of the periplasm are maintained in these bacterial species (Reeve et al., 1984).

Production of the cell envelope is a mechanism utilised by cells upon entering the stationary phase. This transformation is to protect the cells against different kind of stresses and including changes in the outer membrane, periplasm, peptidoglycan and inner membrane (Huisman et al., 1996; Llorens et al., 2010). The outer membrane undergoes multiple changes. The concentration of lipopolysaccharides increases and the amount of protein in the outer membrane reduced during the stationary phase (Huisman et al., 1996). As well, increasing the thickness of peptidoglycan layer. The cells synthesize D-amino acids during the stationary phase that modifies the peptidoglycan layer, by establishing the peptidoglycan polymer and inhibiting further peptidoglycan synthesis (Lam et al., 2009).

In the inner membrane, there is a reduction in monounsaturated fatty acids associated with an increase in polyunsaturated fatty acids (Huisman et al., 1996). In *E. coli* the unsaturated fatty acids are converted into cyclopropyl derivatives, and the ratio between phosphatidylglycerol and phosphatidylethanolamine increases as cells approach stationary phase (Llorens et al., 2010). During the starvation of the surface of many marine bacteria becomes increasingly hydrophobic, and the cells become more adhesive. Starvation in *E. coli* induces aggregates that appear as a result of self-generated and secreted attractant that is sensed by the chemotaxis machinery (Budrene & Berg, 1991). starvation of *Vibrio* sp. strain S14 results in new fibre-like structures and cellular aggregates or clumps (Siegele & Kolter, 1992).

Amino acid starvation causes the cells to synthesise a cell wall with a different structure from the cell wall synthesised during growth by increasing the amount of D-alanine. It assumed this change give the cells protection against autolysis induced by penicillin or chaotropic agents (Siegele & Kolter, 1992).

1.13.3 The Stationary Phase Regulon

Bacterial cells have evolved signalling cascades to regulate gene expression to survive under changing conditions. It includes genetic switches to control many metabolic variations in the cell. Sigma factor and many other regulators involved in regulation the entrance to the stationary phase. In Gram-negative bacteria entering the stationary phase, there are two sigma factors responsible for survival and damage protection σ^S (the product of *rpoS* gene) and σ^{32} (Llorens, 2010) (Table 2). Cross protection that results from secondary stress in cells entering stationary phase also relays on sigma factor σ^S (Nystrom, 2004). A study of RpoS regulation showed that σ^S plays a crucial role: it accumulates, binds and direct RNA polymerase to over 50 starvation and stress genes (Hengge-Aronis, 2002). During growth arrest, σ^{32} plays an important role in inducing the heat shock regulon, which increases chaperone production. Other regulons including the heat shock sigma factors σ^H and σ^E and the oxidative stress response regulators OxyR and SoxRS are activated when stationary growth phase commences.

Small noncoding RNAs (sRNAs) have been found to be involved in regulation during the stationary phase. They modify translation activity and stability of specific target mRNAs. In *E. coli* there are more than 60 species of sRNAs have been identified involved in regulation of stress response such as *hfq* and *dsrA.* The length of sRNAs ranges from 80 to 100 nucleotides. Hfq has an inhibitory effect on either its translation or in the stability of the target mRNA by binding to AU-rich single-stranded transcripts.

Table 2: *Variation of different sigma factors in stationary phase (Llorens, 2010)*

Sigma factor	Main function	Variation in stationary phase	References
RpoD(σ^{70})	Housekeeping	No variation in Ec	Yuste et al., (2006)
RpoF(σ^{28})	Synthesis of Flagella and chemotaxis	No variation in Ps and Ec	Yuste et al., (2006)
RpoN(σ^{54})	Nitrogen metabolism motility	No variation in Ps or Ec	Yuste et al., (2006)
RopH(σ^{32})	Heat shock	No variation in Ps or Ec	Yuste et al., (2006)
RopE(σ^{24})	Extracytoplasmic stress	Fivefold increase in Ec	Costanzo and Ades (2006)
RopS(σ^{38})	Stationary phase and stress resistance	Three- to fourfold increase in Ps and Ec	Yuste et al., (2006)
ECF sigma factor	Extracellular functions	Decrease in Ec	Maeda et al., (2000)

Ec, *Escherichia coli*; Ps, *Pseudomonas putida*; ECF, extracytoplasmic function.

Small RNAs *dsrA* and *rprA* stimulate RpoS translation by binding to the 5'-leader region and unfolding the mRNA making it inaccessible for the ribosomes. Other sRNA regulators are *micA* and *rybB* and are involved with *hfq* in regulating outer membrane permeability during the stationary phase by controlling the production of OmpC and OmpW (OMP, outer membrane proteins).

In Gram-positive bacteria the CodY regulon is required when cells experience starvation. The regulator CodY is a sensor of branched chain amino acids and GTP and effectively monitors the cell's physiological state. It is induced when cell energy is redirected via the stringent response, which typically occurs during starvation

(Sonenshein, 2005). In *Listeria monocytogenes* CodY plays an important indirect role in the regulation of various virulence genes and inactivation of CodY by mutation could lead to loss of virulence (Sonenshein, 2005). A major transcriptional regulator in *L. monocytogenes* is PrfA, a member of the Crp/Fnr family of transcription regulators which controls major virulence genes such as *hly* (listeriolysin) and *actA* (actin mobilisation protein) (Cossart & Archambaud, 2009). Starvation conditions induce the PrfA regulon while the presence of unphosphorylated sugars, such as glucose inhibit the expression of PrfA (Park & Kroll, 1993). As well, the Sigma B Regulon, one of the five RNA polymerase sigma factors in *L. monocytogenes* is responsible for control of approximately 100 genes, including virulence and stress response genes (Cossart & Archambaud, 2009), and overlaps several other stress adaptive regulons (Kazmierczak et al., 2003). Sigma (L) regulatory pathways as well play a significant role in facilitating resistance of *L. monocytogenes* against stress conditions such as low storage temperatures, exposure to organic acid, and elevated NaCl salt concentrations (Raimann et al., 2009).

1.14Bacterial Aging (Senescence)

Aging is manifested as a decline in growth rate and the ability to survive, mostly a loss of fitness (Rose, 1991). In bacteria, it has been conceived that since reproduction leads to two apparently identical cells that they are effectively immortal (Rose, 1991). However, it was shown in a bacterial species that has asymmetric cell division, *Calulobacter crescentus*, aging is evident (Ackermann et al., 2003). *C. crescentus* life starts as a free-living, rapidly moving swarmer cell. These cells do not divide until after they have settled onto a surface after differentiating and producing an adhesive stalk. The sessile stalked cell then continually divides to form daughter

swarmer cells, which swim away (Figure 7). It was hypothesised that the stalked "mother'" cell would over time deteriorate after many generations but since only a few cells would be aged at any given time natural selection, leading to immortality, would not significantly oppose aging. Ackermann and colleagues (2003) observed the production of progeny declined over time for *C. crescentus* cells under constant nutrient conditions in a flow chamber as time progressed this slowdown accelerated until division completely stopped. As two systematically different cells emerge during reproduction but only one seems to naturally age it was conceived that the aging was linked to cell division since bacteria, even those that divide entirely symmetrically, localise subcellular structures in the poles of the cell (Shapiro et al., 2002, 2009). In the case of C. *crescentus,* this is quite obvious as the stalked end of the cell is the "old pole", where aging could be an

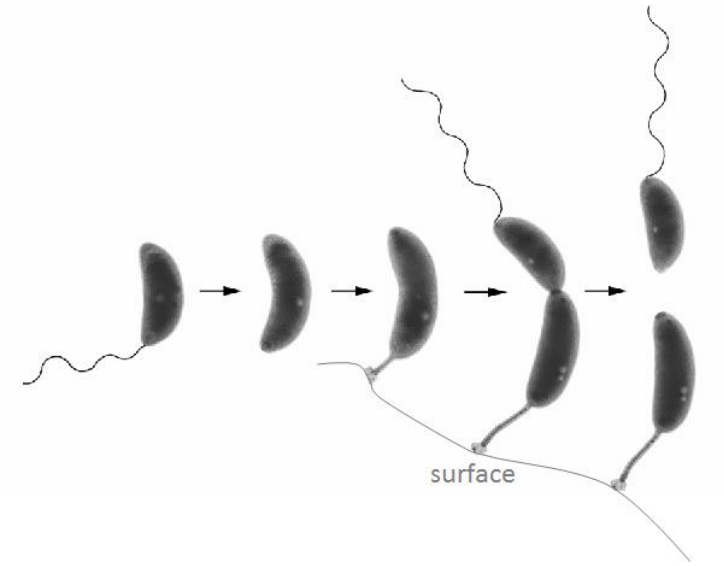

Figure 7**:** Life cycle of *Caulobacter crescentus* showing a motile swarmer cell differentiating into a stalked sessile cell that then continually dwells on a surface. The stalked cell then continuously reproduces new swarmer cell progeny. Based on Ackermann et al. (2003) bacterial aging was considered to be linked to the "old cell pole" (stalked end of the cell) while the reproducing cell end, the "new cell pole" was less associated with aging. The image is reproduced from Prof. Yves Brun (University of Indiana).

Accumulative inevitability, while the reproducing end of the cell is the “new pole” that is less subject to aging. Subsequently, it was shown that though *E. coli* is substantially symmetrical, subtle cell asymmetry of progeny cells contributes to aging as found for *C. crescentus*. Stewart and colleagues (2005) followed the division of lineages of *E. coli* cells and observed lineages that accumulated more old poles had less fitness and slower growth rates than those that maintained a high proportion of new poles (Figure 8). Based on the concept that fitness is naturally selected it was hypothesised bacterial cells when they divide deliberately sequester damaged, unwanted components into the old cell pole (Kirkwood, 2005; Watve et al., 2006; Ackermann et al., 2007).

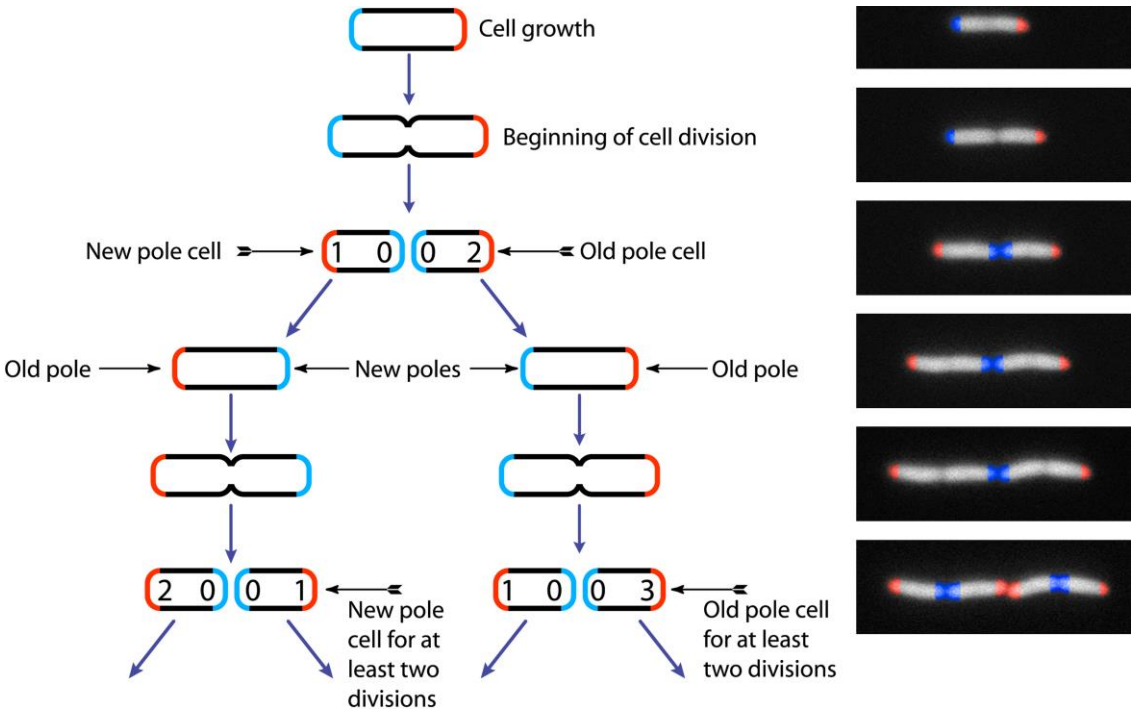

Figure 8**:** During the growth of *E. coli* the cell divisions daughter cells that emerge possess two poles, one from the mother cell – the old pole (shown in red) while the newly manufactured pole is the new pole (shown in blue). By tracking lineages of *E. coli* cells through their divisions Stewart and colleagues (2005) found that cells that inherited the old poles were inherently less fit, which was interpreted as the emergence of aging (senescence). Image reproduced from Stewart et al. (2005).

Subsequently, it was discovered a factor linked to aging was an accumulation of aggregated proteins at old cell poles (Lindner et al., 2008). Lindner and colleagues observed that by following a lineage of *E. coli* protein inclusion bodies tended to localise to one pole of cells (Figure 9). it was done by tracking inclusion bodies in *E. coli* in which the small heat shock chaperone (Hsp20-like) IbpA was combined with yellow fluorescent protein (YFP). IbpA-YFP was used as it accumulates in inclusion bodies and does not associate with cell division machinery (Figure 9).

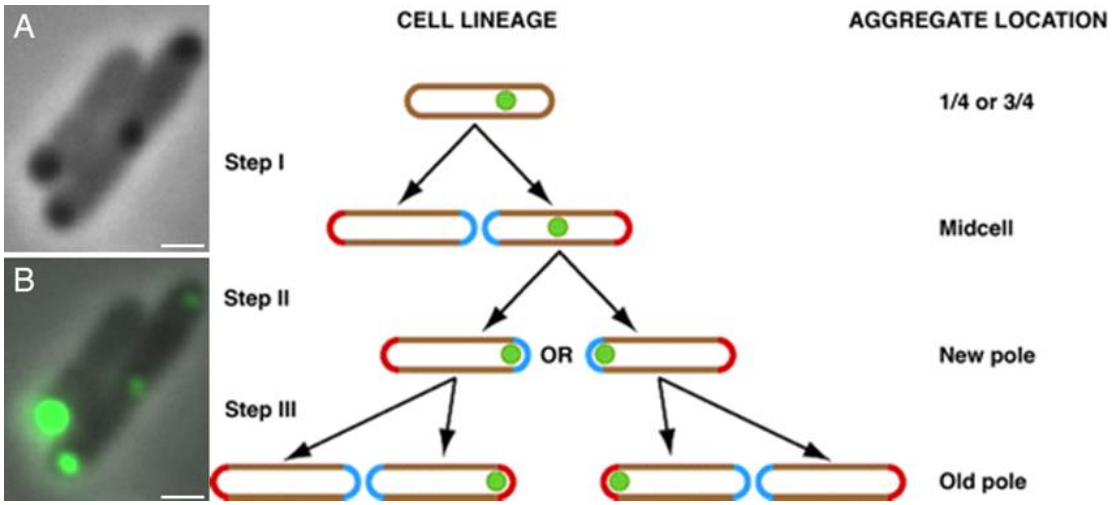

Figure 9**:** Accumulation of protein inclusions at the cell poles of *E. coli*. Left-hand photos show *E. coli* with in-vivo localised IbpA-YFP, which accumulates in insoluble protein inclusions. A) Cells treated with streptomycin showing protein concentrated at cell poles and the septal ring. B) Overlay of IbpA-YFP fluorescence showing a greater concentration of IfpA-YFP at one cell pole. Scale bar equals 1 µm. To the right is a proposed schematic model showing how inclusion bodies (green spot) progress to the old pole through successive cell division cell cycles. The old cell pole is shown in red and the new pole in blue. Images reproduced from Lindner et al. (2008).

These aggregates consist of misfolded, insoluble proteins termed inclusion bodies. Excessive levels of inclusions are toxic to the cell as they interfere with the natural homeostatic process of protein synthesis, folding and turnover – termed proteostasis (reviewed by Bednarska et al., 2013). To retrieve proteins from these inclusions, the proteins must be solubilized and refolded (Singh & Panda, 2005), which require substantial input of cell resources and energy (Rothman & Schekman, 2010). Enzyme systems associated with protein disaggregation in bacteria include heat shock proteins (ClpB - Hsp104, DnaK/DnaJ -Hsp70; IpbA/IpbB - Hsp20) and AAA-proteases (Clp-system proteases) (Tyedmers et al., 2010).

Highly symmetrical unicellular organism seem to evade aging for extended periods especially if maintained under non-stressful conditions (Wang et al., 2010; Coelho et al., 2013, Moseley, 2013). Wang and colleagues found that *E. coli* in a microfluidic device (which they termed the “Mother Machine”), when sustained by a constant flow of nutrients, could reproduce hundreds of times without any visible aging via protein aggregation at poles instead cells tended to become stochastically filamentous and suffer DNA damage. Thus the concept has developed that as long as cells are not stressed aging is not inevitable and that aging manifestation is likely a consequence of circumstances that the cells encounter. It is possibly less control of essential maintenance, and homeostatic processes accelerate aging. It is still unknown where aging fits in with bacterial cell death processes. It can be surmised aging could interrupt processes that help ensure survival. In the natural environment and that nutrient patchiness and rapid physical chemical fluctuations likely enforce aging and ensures that bacterial cells, by and large, have a finite existence regardless how efficient their survival systems are.

1.15 Conclusion and Thesis Objectives

The purpose of this review was to view the effect of environmental conditions on the lag phase and also understand what factors influence lag phase recovery. There have been many studies regarding this subject but significant knowledge gaps still exist in relation to the lag phase, and there is no comprehensive picture of the biochemical and molecular genetic activity of bacteria during this crucial period. A complete overview of the processes occurring during lag phase will help in preventing the growth of bacteria such as *Salmonella and E. coli*, leading to new ways to prevent diseases such as food poisoning. It could be possibly achieved by adding bacterial-specific inhibitors to certain foods that prevent some pathways from functioning. Because the mechanisms leading to induction and resolution of lag time are not entirely understood, accurate predictions of the lag phase period are difficult to achieve. The review also considered mathematical models that have been developed to predict the lag time. One of the disadvantages of these models is that they have not been experimentally proved. The state in which cells enter the lag phase was consistently seen as hugely influential on the success and the duration of lag phase recovery. Stationary growth phase was considered to be a time in which the heterogeneous physiological deterioration of the cell population could lead differently to subpopulations that behave if given a “new chance” so to speak. Aged cells, for example, being less fit would be expected to have less chance to recover than those that are less affected in that way. Much remains to be learnt on how aging influences bacterial survival as well as the underlying mechanisms of the processes.

This PhD thesis seeks to unveil knowledge in the area of lag phase and cell aging. The model organism that is used is *L. monocytogenes* strain Scott A. *L. monocytogenes* was used as it is well characterised genetically and physiologically and has an unusual and often unwanted propensity to persist in the environment. *L. monocytogenes* can survive in two major ways – first by being virulent it can invade host cells (theoretically most forms of life – from amoeba to humans) and dwell intracellularly (Freitag et al., 2009). It is the cell-to-cell spread that manifests as listeriosis. The second form of survival mode is that it is able to adjust its physiology such that it conserves energy but retains viability. As long as cells have some slim form of nutrient supply (carbohydrates, some amino acids and some vitamins), it can survive for extremely long periods, especially at low temperatures (Cole et al., 1990). Prior research performed in the labs of Ross and Bowman suggests that temperature dictates the survival of bacteria. increase in temperature resulting an increase rates of cell death, even if growth is not possible through the entropy (Ross et al., 2008). The rate is linearly related to temperature; thus at 25°C *L. monocytogenes* when in a non-growth permissive environment (for example low water activity and low pH) it is inactivated at approximately 10- and 100-fold slower than at 37°C and 45°C, respectively (Zhang et al., 2010). Despite these higher temperatures being growth or almost growth permissive (45°C is the T_{max} for *L. monocytogenes*). The increased rates of death are due to failure of defence mechanisms, but the failure is greatest in a proportion of the cell population that conceivably include aged cells. A robust subpopulation can still survive within the temperature time frame; it is likely age factors less burden this population.

Based on this concept the stability of *L. monocytogenes'* physiology is temperature dependent. The premise of this thesis is that aging and subsequent death is a

consequence of not dealing with stress and that death from aging is due to lethal cell damage caused by cells losing the means to counter age-based deterioration. In experiments performed therein the destabilisation is enforced and accelerated by growing cells in static broths that become nutrient depleted and by using a heightened temperature, 37°C, the T_{opt} of *L. monocxytogenes* Scott A. At this temperature the growth rate is high due to rapid enzyme reactions, consistent with Arrhenius kinetics, but advantages are offset by the need for the cell to invest energy and resources into continual cell maintenance. it is expected that the cells without nutrients will resulted in age-induced deterioration and rapid cell death will inevitably ensue.

In the thesis, the experiments performed thus examine cell survival and death in relation to aging and subsequent recovery. The renewal processes that occur within the lag phase are explored in the context that aged cells could recover differently to cell populations that are essentially younger. A hypothesis is presented that larger RLT values are associated with cell populations with more aged, deteriorated members but that the lag phase recovery process is completely fixed and as a result, the work needed that leads to an exponential outgrowth is overall larger when more aged cells are present. The work considers the proportion of cells with accumulated age factors can differ significantly. In the same context cellular regulatory elements, relatively well defined in *L. monocytogenes*, will be investigated to determine how the stress of aging and the subsequent recovery process is handled. The hypothesis is that through *L. monocytogenes* is adept at adjusting to environmental conditions which is inherently constrained with aging. Evolution may not create a particular system for countering aging as such. Thus the lag phase renewal and aging processes could be impacted by a degree of stochasticity in which subpopulations

emerge with different survival capacities since survival mechanisms are non-targeted.

Quantitative proteomics will be used to capture process related information and to provide a perspective on underlying mechanisms associated with aging and the lag phase at least on a preliminary level. The reasons for this are a matter of capability and cost, but the approach has proven to be useful in giving global and specific insights into cell biology generating new questions.

Overall, the thesis presents for the first time an in-depth investigation of *L. monocytogenes* death and renewal processes from a global view that could lead to further research relevant to bacterial survival and environmental persistence.

The thesis consists of the following experimental chapters:

Chapter 2. Phenotypes associated with aging *Listeria monocytogenes* ScottA. In this chapter phenotypes associated with aging, *L. monocytogenes* are investigated including the effect on growth and the lag phase duration, cell morphology, cell integrity, metabolism, energy levels and the ability to secrete proteins.

Chapter 3. Proteomic analysis of aging *Listeria monocytogenes* ScottA. Cultures from Chapter 2 are also examined in depth by quantitative proteomics revealing proteins and pathways associated with the associated stress conditions as well as embedded aging responses.

Chapter 4. Proteomic analysis of aged *Listeria monocytogenes* ScottA within the lag phase. Cultures from Chapter 3 were examined in the lag phase after being transferred to fresh broth media. The proteome level responses are observed over a temporary period depending on the extent of age-induced lag phase extension.

Chapter 5. Regulation of gene responses in lag phase recoverd and aged *Listeria monocytogenes* cells. The proteome data is interrogated to determine regulatory processes in aging and lag phase cells.

A final concluding chapter (Chapter 6) sums up the findings of the thesis and examines future research options.

2. Phenotypes associated with aging Listeria monocytogenes ScottA

2.1 Abstract

To allow understanding of the effect of culture-based aging on *L. monocytogenes* ScottA growth and survival behaviour, morphological and metabolic changes, virulence potential, and ATP levels during aging processes were assessed. Aging was enforced by holding cells at 37°C deep into the stationary growth phase for up to 21 days. The temperature used represents the optimal temperature for growth rate (T_{opt}). In older cultures (aged ≥7 d) lag phase was proceeded by possible short, rapid recovery of a small segment (0.5-1.5 log units) of the population. The duration of the lag phase increased with the length of time the cells were initially incubated. The generation time of outgrowth increased with the duration of initial incubation suggesting more aged cells lost fitness. Extended incubation resulted in increasingly poor growth on agar. Aged cultures lose the ability to retain crystal violet, indicative of a thinner, less networked peptidoglycan layer. They also demonstrated cell elongation (2-10 fold increase), evidence of failed septation completion, and autolysis. After 7 d of incubation, ATP levels in the cells collapsed to $<10^{-17}$ moles/cell from approximately 10^{-15} moles/cell. Catabolic enzymes associated with

protein, lipid, phosphate, and carbohydrate metabolism though readily detected in young cultures become inactive in populations incubated ≥7 d. Haemolysis assays revealed no detectable listeriolysin activity was present in the bacterial supernatant fluid after ≥7 d, possibly suggesting reduced protein export**.** Overall, the results indicate that cell aging at the T_{opt} is associated with extensive loss of cell viability and results in lag phase extension and loss of fitness. Fitness loss may be attributable to depletion of ATP and reduced metabolism affecting protein secretion, cytokinetic and cell wall biogenic processes in the cell population.

2.2 Introduction

Most bacteria reproduce by binary fission into two seemingly identical cells. It is assumed that both cells are "born" equally young and that these organisms do not, therefore, show differential age-related variations. However, a study by Stewart et al., (2005) suggested that *E. coli* cells are susceptible to aging by inheriting the old pole of cell division in successive generations. Old poles accumulate protein inclusion bodies that if large enough seem to be able to impact fitness (Lindner et al., 2008). Further experiments suggest stress appears to be a necessary ingredient to result in an identifiable age-related loss of fitness (Coelho et al., 2013). The fundamental molecular mechanisms underlying bacterial aging are not yet understood (Nyström, 2007; Gomez, 2010). At this stage aged bacterial cells exhibit "conditional senescence", which is conceived as a decline in cellular viability due to accumulated damage not overcome by cell maintenance processes (Gomez, 2010). A Recent analysis of the physiology and molecular biology of stationary phase *E. coli* cells has revealed aging processes share some fundamental similarities to that of higher organisms (Nyström, 2007). The similarities included increased oxidation of cellular constituents and associated target specificity. It is still unknown the role of

antioxidants and oxygen tension in determining bacterial cellular life span, and whether aging in an apparent trade-off between activities related to reproduction and survival (Nyström, 2004).

In this study, *L. monocytogenes* ScottA cells were examined in what is defined as an "aging process". This is essentially where the cells were kept at 37°C and sampled during stationary growth phase for an extended period, up to 21 days. Stationary growth phase adaptations occurring in *L. monocytogenes* lead to a physiological state that aid survival during limited nutrient conditions, which in the end provide a considerable growth advantage over "young, naive" cells, held under the same stress conditions. This phenotype is referred to as GASP ("Growth Advantage in Stationary Phase") and has been shown to occur readily in *L. monocytogenes* (Bruno & Freitag, 2010, who studied strain 10403S). The cells once achieving the GASP state are able to survive stably for extended incubation times under nutrient stress. An unpublished study by Liu (2012) showed that another strain FW04/0025 (Bowman et al., 2010) also behaved similarly but also indicated that its lag phase significantly increased with extended incubation to a roughly proportional degree. By extending the incubation time deep into the stationary growth phase and well within the "decline/death" phase it is expected there is a continual accumulation of the deleterious effects of the associated stress conditions, offset by responses related to the GASP phenotype. This results in longer lag phase durations due to the need to overcome accumulated damage before exponential growth can be enacted. Little is known about the phenotypes of these age-linked phenomena and the underlying associated functional aspects. The study of Bruno & Freutag (2012) shows cells in the GASP state have normal virulence in mice. Though somewhat removed from the

original “old” and “new” cell pole age theory the situation is ecologically relevant for bacteria, which regularly experience nutrient scarcity in the environment.

In the experiments here cell age-linked responses are studied in strain ScottA over a period of 21 days at 37°C. The goal of the research was to learn how progressively accumulated stress-induced damage, possibly relevant to aging of bacteria in general, manifests in terms of acquired phenotypes, ranging from growth properties, cell morphology, metabolism to the ability to secrete listeriolysin O. It was found ScottA is actively and deleteriously affected by extended incubation unlike other *L. monocytogenes* strains studied to date and that it exhibits autolysis amongst a number of phenotypic changes that could be linked to age attributes.

2.3 Methods

2.3.1 Preparation of Inocula

L. monocytogenes cultures (Scott A [clinical isolate, serotype 4b, originally obtained from improperly pasteurised milk associated with a listeriosis outbreak in 1983 in Massachusetts USA (Fleming et al., 1985)] was used in this study.

The culture was maintained in a cryovial at −80°C, from which plates of tryptic soy agar (Oxoid) with 0.6% yeast extract (Oxoid; TSAYE) were prepared on a weekly basis. The broth subcultures were prepared by inoculating a test tube containing 200 mL of sterile tryptic soy broth (Oxoid) and 0.6% yeast extract (TSYE) with one single colony from a plate."

The broth subcultures were prepared by inoculating a test tube containing 200 mL of sterile tryptic soy broth (Oxoid) and 0.6% yeast extract (TSYE) with one single colony from a plate. After inoculation, the tubes were incubated overnight at 25˚C, 30˚C, 37˚C, and 42˚C. 250 mL-flasks containing 50 mL of TSYE were inoculated with

the resulting subcultures to a final concentration of 10^{-5} CFU ml^{-1}. These flasks were incubated under agitation (130 rpm; Thermo Scientific™) at 25˚C, 30˚C, 37˚C, and 42˚C for 1, 4, 7, 14 and 21 days.

2.3.2 **Assessment of Viability and Relative Lag Phase Duration**

The total viable count (TVC) was used to measure the effect of culture age on the lag phase duration of *L. monocytogenes* ScottA. This was done by spreading 100 µl of the inocula (prepared as described in S.2.3.1 “Preparation of Inocula”) onto TSYE agar following incubation using standard serial dilution. Inocula was prespared from ScottA cultures grown at 37 C for 0.5 to 21 d. TVC analysis was performed every 10 to 30 minutes for the day 1 and 7^{th} time point cultures to assess lag phase duration. For cultures that had extended incubations of 14 d and 21 d TVCs were performed every 30-60 minutes. The plates were incubated at 37°C for 48 h before being counted. Growth curve data were fitted to an adaptation of the logistic-based model ("D-model") of Baranyi and Roberts (1994) using the Solver routine of Microsoft Excel 2016. The spreadsheet model was developed and provided by Associate Professor Tom Ross. When using the D-model to measure lag phase, the stationary phase and dead phase timepoints were excluded since these stages were not measured.

2.3.3 ATP Content Analysis

A single colony of ScottA has transferred aseptically into 10 ml of TSYE and then incubated at 25˚C, 30˚C, 37˚C, and 42˚C for 1, 4, 7, 14, 21 days. After incubation, the OD for each sample was adjusted to 2 at A_{600} nm. For cellular ATP analysis, the BacTiter-Glo Microbial Cell Viability Assay Kit (Promega) was used following the manufacturer’s instructions. ATP generated bioluminescence was detected using a

FluoStar Omega fluorometer (BMG Labtech, Ortenberg, Germany). Data was reported ar relative fluoresence units (RLU).

2.3.4 Cell Size and Medium pH Determination

For cell size and motility experiments, microscopic observation of a wet drop preparation from cultures at each time point was investigated using a Leica DAS microscope fitted with a Leitz DMR digital camera and oil-immersion objective (Leica Microsystems, Wetzler, Germany). A Gram stain was also performed for each time point and investigated using the same microscope. The pH of the medium at each of the timepoints was defined by using a pH electrode (ORION, model 250A). 500 µl aliquots of the cultures were centrifuged at 4000 × *g* for 10 min at 4 °C (Microcentrifuge 5417R, Eppendorf, Germany) to detect the level of the DNA in the culture supernatant as an indication of cell autolysis. A 10-20 µl aliquot of the supernatant was loaded onto a 1% agarose gel and electrophoresis was performed at 80V for 1 h. Gels were stained with 0.5 µg/100 mL acridine orange, observed by UV transillumination and a digital image obtained of the gel (Gel Doc XR Imaging system, BioRad).

2.3.5 Enzymatic Activity Analysis

The enzymatic activity of *L. monocytogenes* at each of the time points was determined using the API ZYM (BioMerieux, Marcy-l'Étoile, France) system following the manufacturer's instructions. After adjusting the OD for the cultures to 0.1, the API strips were inoculated with 1, 7, 14 and 21 days cultures grown in TSYE plus 0.6 yeast extract at 37ºC. The strips were incubated at 37ºC for 4 hours and evaluated for activity by applying the manufacturer's protocol and 5-grade categorical assessment scale, which is based on the intensity of coloration of the associated reaction.

2.3.6 Haemolysis Assay

Aliquots of 100 µl of defibrinated horse blood (Oxoid) were centrifuged at 600 × g for 10 min at 4ºC. Pellets were resuspended in 600 µl PBS at pH 7.4 and washed, stirred gently. The washing step was repeated until a distinct pellet, and clear supernatant was obtained. One mL of *L. monocytogenes* ScottA culture of the 1, 7, 14 and 21 days culture were centrifuged at 600 × g for 10 min at 4 º C, and the supernatant was used for the assay. Serial 4-fold dilutions were prepared by mixing 100 µl of the culture supernatant with 1 % NaCl solution in a microplate. Followed by addition of 100 µl of blood solution and mixed well by repeated pipetting and incubated for 30 min at 37 ºC.

2.4 Results

2.4.1 Lag Phase Durations of L. monocytogenes ScottA

TVC was estimated for ScottA in extended culture at four different temperatures. A linear decline in loss of TVC occurred with the rate increasing with increasing incubation temperature (r^2=0.86, Figure 10a). The estimated lag times were also affected by culture age and temperature (Figure 10b and 10c). It must be noted that the inoculum was prepassaged to attempt to keep RLT as short as possible by minimising physiological heterogeneity. Without doing so resulted in lag phase variability with lag often not resolving before 9 h for extended incubation cultures (>4 d in age). The estimated lag phase durations of ScottA showed an approximately linear increase in the lag phase period for the 1 to 14 d (80-200 to 250-450 min) at 25°C and 37°C. The lag phase duration for 21 d old cultures was not substantially increased (300-480 min). This compares with 90, 120, 210 and 240 min for the same

initial incubation times determined for *L. monocytogenes* strain FW04/0025 at 37°C (Liu, 2012). Thus the result showed that the Scott A lag time is extended from approximately 3 generation equivalents (assuming an average 30 min generation time at 37°C) to approximately 11-12 generation time equivalents after 14-21 days. RLT measurements were not performed for 25°C since high cultural viability is retain though it was observed in some initial experiments RLT was also extended at 14 and 21 d relative to shorter initial incubation times. Generation times of the outgrowth of cells from lag phase at 37°C were found to be slightly slower for 21 d culture inocula (41.5 min) than 1 d inocula (27.7 min) with 7 d and 14 d inocula doubling times were similar (~33 min) (Figure 10c).

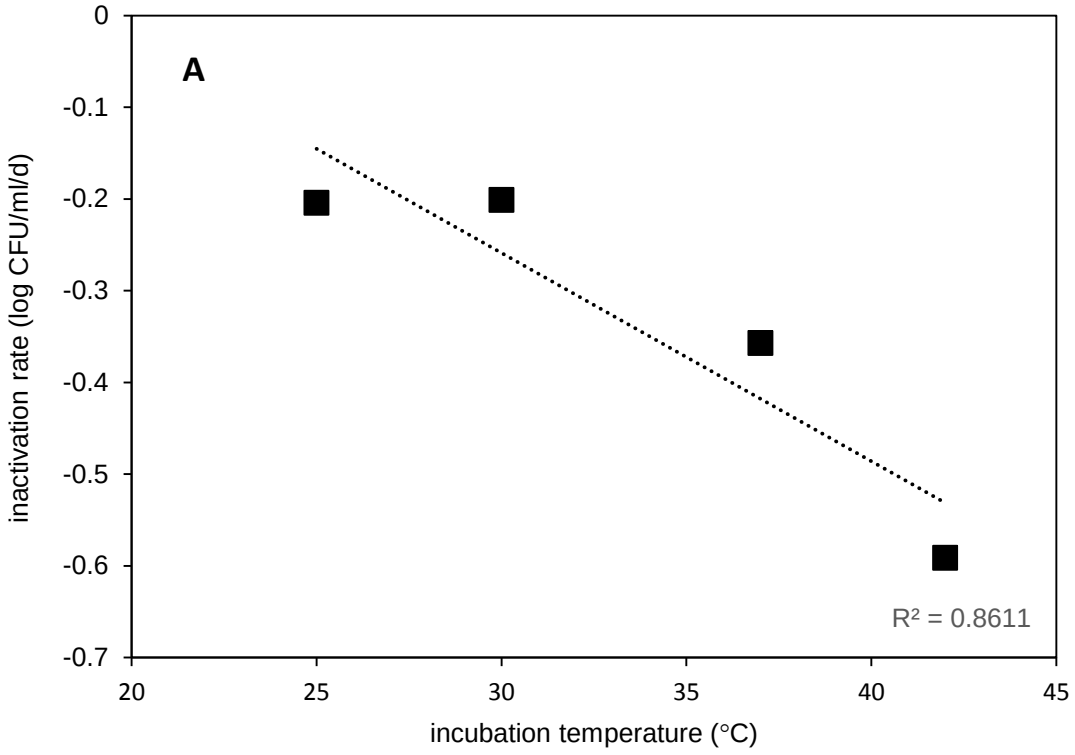

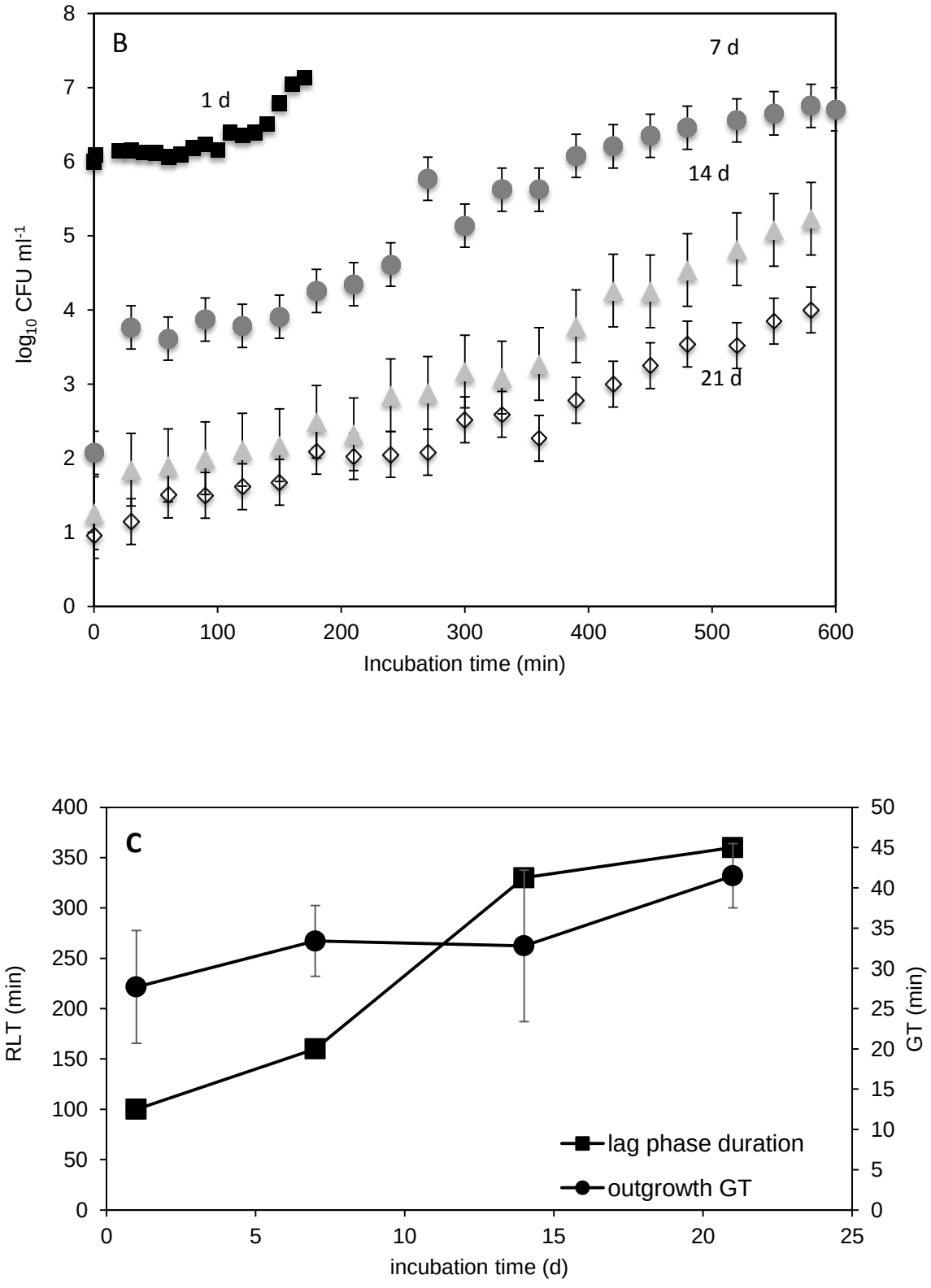

Figure 10**:** Effect of temperature on the viability and lag phase of *L. monocytogenes* ScottA. A) Decline in culturability in relation to incubation temperature. B) Growth responses of ScottA when transferred to fresh TSYE after initial incubation (1, 7, 14

and 21 d) at 37°C. Data based on plate count data (error bars represent standard error). C) Average estimated lag phase durations relative to temperature (blue circles) and estimates of growth rate of ScottA emerging after lag phase (red circles, determined using the D-model, see Methods section).

2.4.2 Cell Motility, Morphology, Size and Integrity

Some cellular motility was microscopically detected when the cells were young (up to day 1), despite the growth temperature of 37°C at which flagella protein secretion is repressed through the interactions of regulators DegU, MogR and GmaR (Shen et al., 2006). This motile subpopulation disappeared with time, with 7 d cultures having less observed motility, and after 21 d there was completely no evidence of motility present. Observations via phase contrast microscopy also showed that cells elongated (2-10 fold) in older cultures and seem to become possibly multi-septated, where cell separation has failed (Figure 11 A-C). Cell elongation was most visible at 7 d. By 21 d most cells became coccoidal in shape.It was was also observed cells lost the ability to retain crystal violet, indicative of a thinner less networked peptidoglycan layer. Rounded cells in Gram stain preparations had the appeearance of sphaeroplasts. Losing the capacity to retain crystal violet is indicative of loss of control of cell wall permeability consistent with occurrence of cell wall damaged. In this respect cell autolysis was evident based on the appearance of DNA in the culture supernatant, esepcially at 14d and 21 d (Figure 11 D). Such events would lead to eventual cell death and thus explain why a large portion of the cells lose culturability when transferred to agar media, which imposes a mild osmotic stress on the cells.

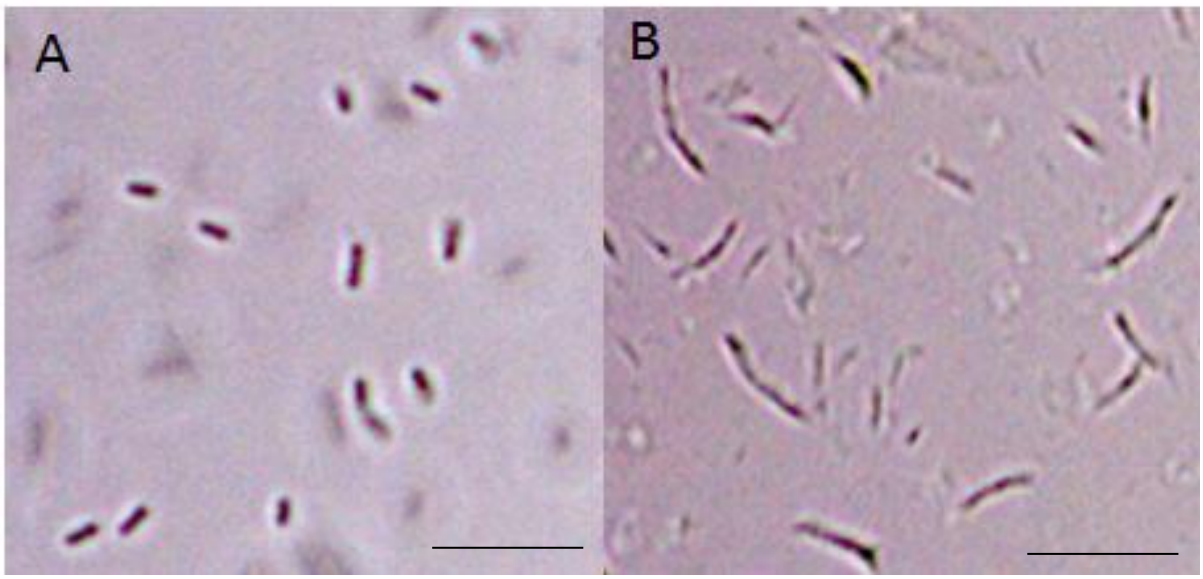
A
B

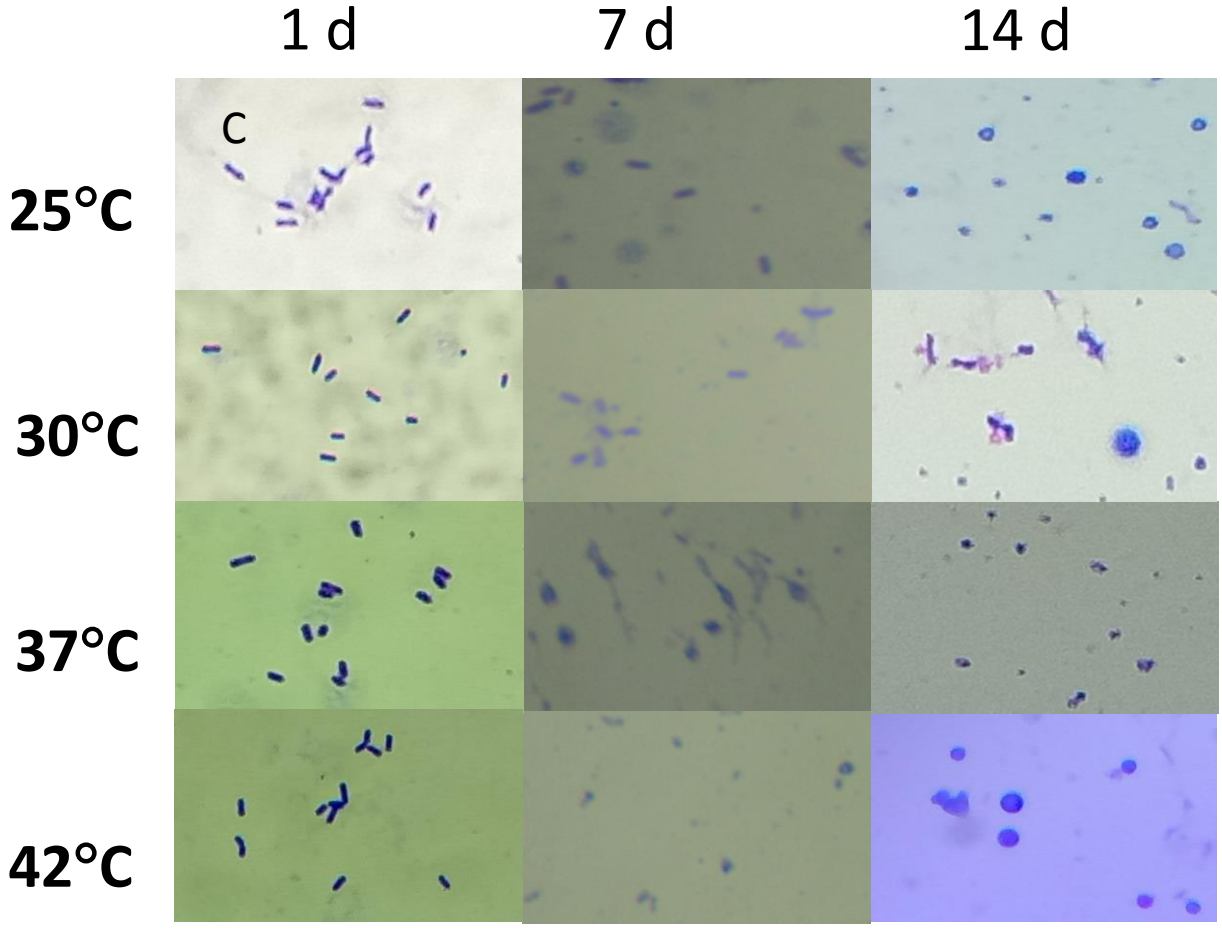
1 d
7 d
14 d
C
25°C
30°C
37°C
42°C

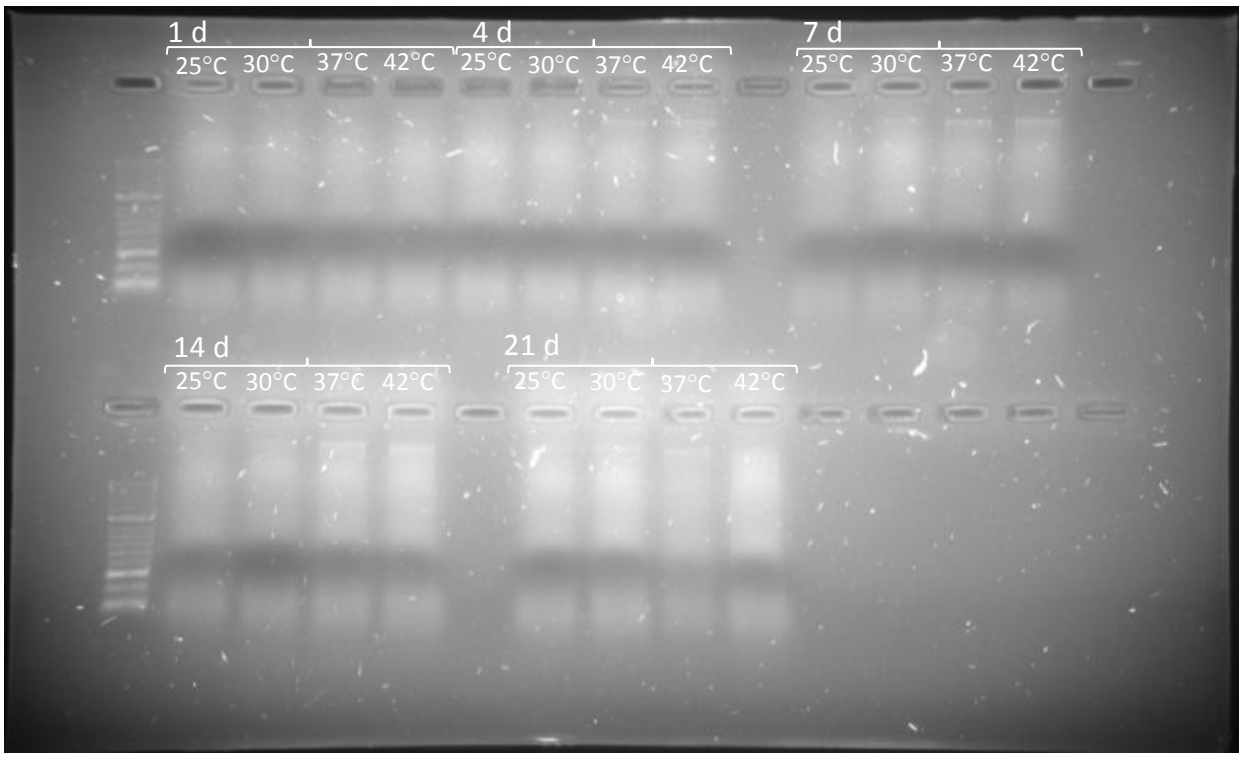

Figure 11. See caption next page.

Figure 11**:** *L. monocytogenes* Scott A cellular morphology in cultures after incubation for (A) 1 day and (B) 7 days in TSYE broth at 37°C as revealed by phase contrast microscopy (bar equals a length of 10 µm); C) Gram strains of cells grown at indicated times and temperatures showing shift in morphology from regular rods irregular coccoids inlcuding transitional elongated forms (7 d, 37°C panel) as shown in Fig11B; D) autolysis of cells at indicated times and temperatures indicated by free DNA in the supernatant as shown by gel electrophoresis.

2.4.3 Enzymatic Activity, ATP Content and Haemolysis Activity

L. monocytogenes grows mainly by fermenting sugars to organic acids (Romick et al., 1996). Acidification of TSYE broth medium was observed with pH decreasing from an initial pH of 6.9 to pH 5.3 after 1 d. However the pH stayed at this value from thereon. This suggested metabolic activity declines before 7 d. This was confirmed by testing the activity of several enzymes using the API ZYM test strip system with activities assessed on a categorical scoring scale. Seven enzymes associated with

protein, lipid, phosphate, and carbohydrate metabolism were readily detected (Figure 12) in 1 d cultures. Alkaline phosphatase and naphthol-AS-BI-phosphydrolase were detected under all temperature and incubation conditions. Butyrate (C4) esterase, leucine arylamidase, and β-glucosidase activity was very high in 1 d cells, but for cells incubated at 37°C or 42°C was mostly not detectable after 4 d incubation (Fig. 12). Cells incubated at 25°C and 30°C for 1 day also possessed N-acetyl-β-glucosaminidase and α-glucosidase activity but this activity declined by 4 d. (Figure 12). The results indicate a temperature and growth age interaction that could be regulatory but also indicates the narrower metabolism at 37 C and 42 C in the less viable cell populations. The decline in enzyme activity was accompanied by a reduction in the cellular ATP pool. ATP levels decline more rapidly as the culture temperature ages. After 4 d cell ATP levels decline at 25°C and 30°C by approximately 2-fold, however at 37 C and 42C the decline was approximately 20-fold. The decline appears log linear after this 4 d for 30, 37 C and 42 Cwhile at 25 C the rate is somewhat slower (Figure 13). After 7 d incubation ATP levels in cellsgrown at 37°C collapses to approximately 10^{-17} moles/cell from approximately 10^{-15} moles/cell in late exponential cell growth (Figure 13). The decline in ATP also correlates well with the loss of viability within the cell populations (about 1 log per 3 d for 37°C). Based on data from Zhang et al. (2010) ATP levels of ~10^{-18} moles per cell was indicative of an irreversibly inactivated cell population (equivalent to 1 RLU in Figure 13).

To further assess bacterial activity and protein export blood cell haemolysis was also carried out. Positive detection would indicate active secretion of listeriolysin O. The haemolysis assays performed at 37°C revealed detectable listeriolysin O production

for 1 d old cells, however activity was weak in 4 d cells and not evident for cells incubated 7 d or longer (data not shown)**.**

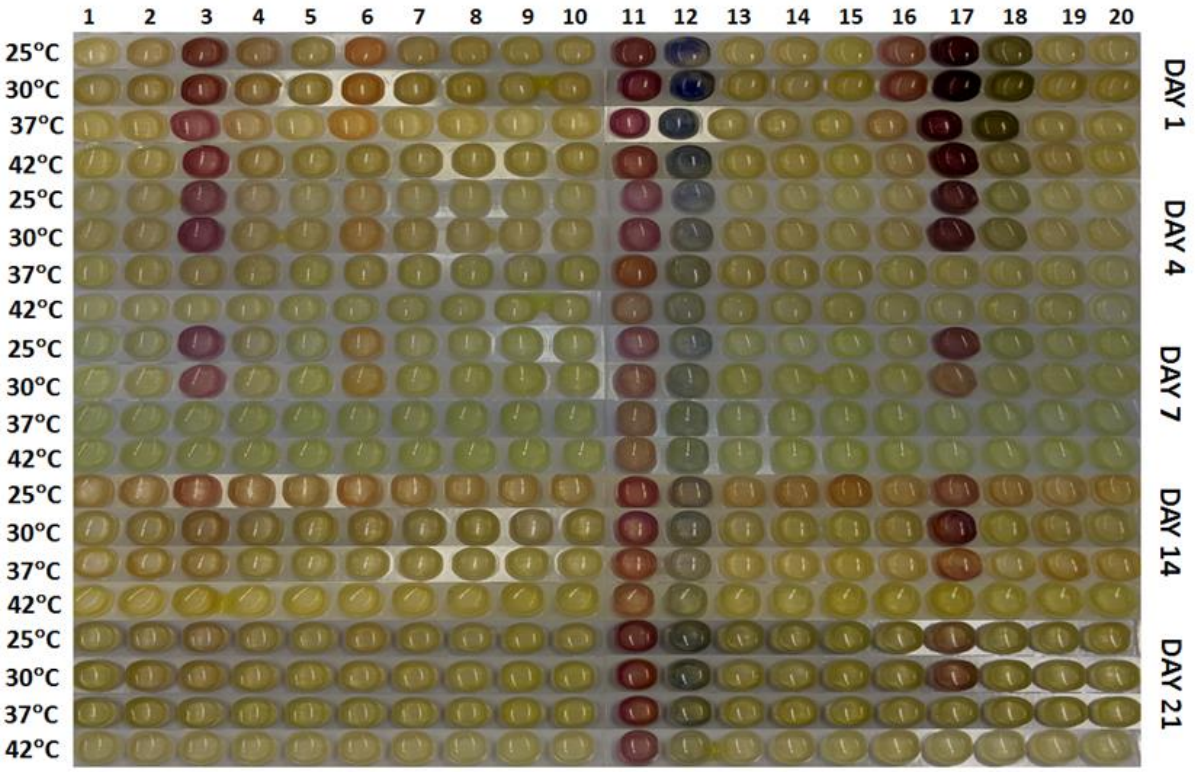

Figure 12 – also see next page.

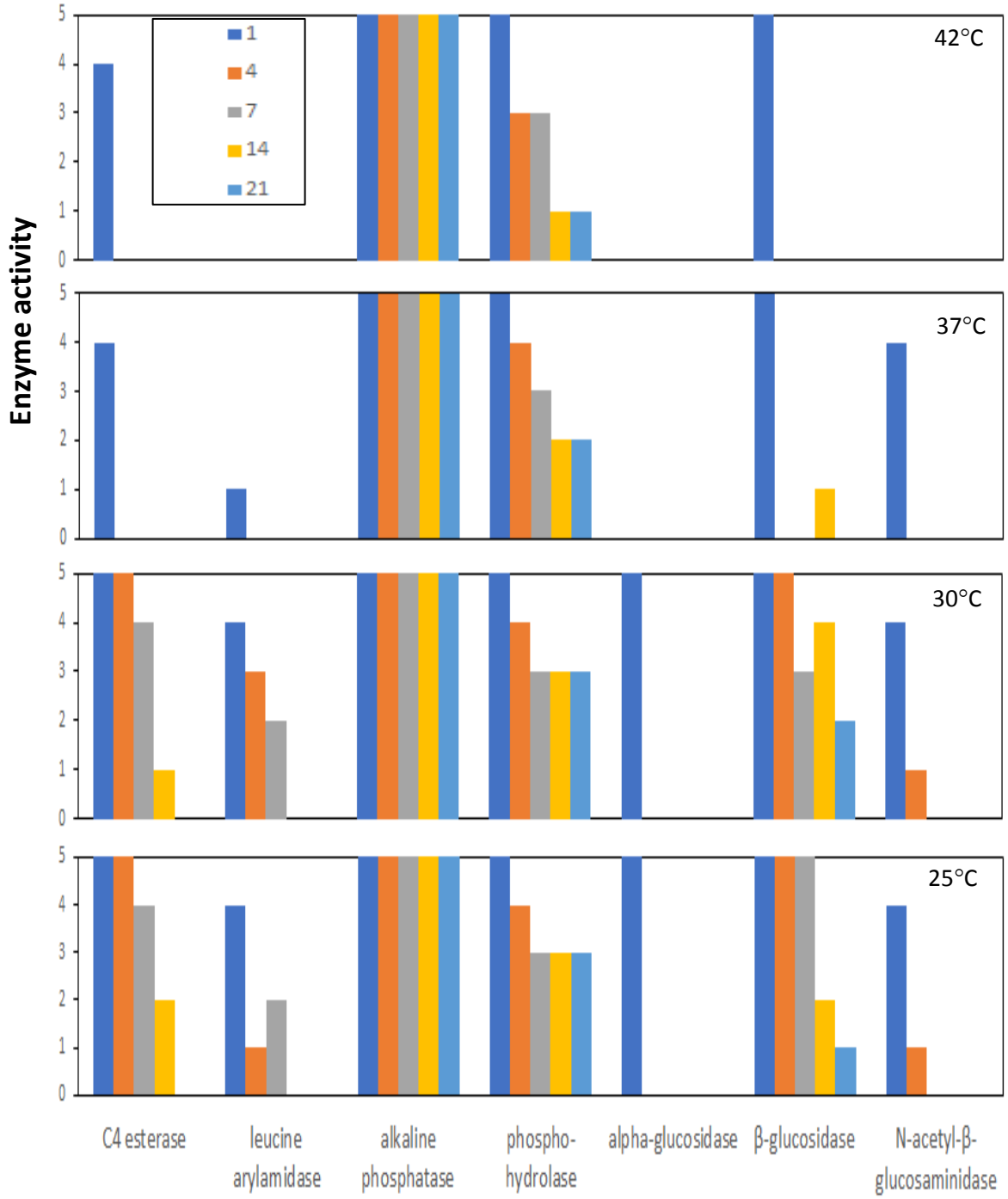

Figure 12**:** Enzymatic activity for *L. monocytogenes* Scott A during aging grown in TSYE. Enzyme activity is indicated on a categorical scale. Top image shows the API ZYM colour levels, which are interpreted as enzyme levels in the graph above.

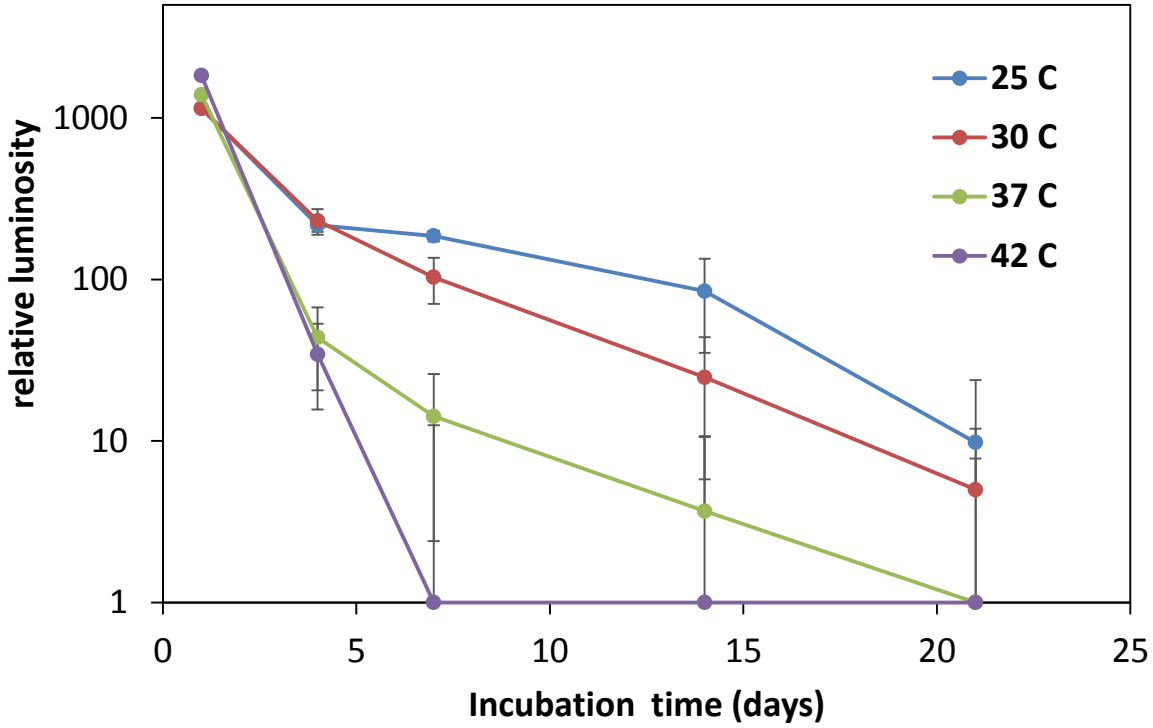

Figure 13**:** ATP levels in *L. monocytogenes* ScottA grown in TSYE broth over a period of 21 days. ATP levels are indicated as a relative luminosity (100 RLU equates approximately to 10^{-16} mol ATP per cell). Error bars are standard deviations.

2.5 Discussion

For the purposes of this study, we focused on readily assessable phenotypes in order to determine the transition of normal "youngster" to aged cells in a static system. Aged cells as explained in the literature review (chapter 1) previously accumulate damage from prior generations. Such damage accumulating passing a critical threshold could result in toxicity and death of the cell. GASP and starvation survival responses (SSR) characteristically leads to cell dwarfing and stable viability. For *L. monocytogenes* this seems best achieved when the temperature is relatively low, other stresses are minimal, and the cells have been stress pre-adapted, which leads to stress cross-protection (Herbert & Foster, 2001; Chan & Weidman, 2009).

However, in the experiments performed here at elevated growth permissive temperatures, cells became transiently elongated, possibly became multi-septated and then beaome coccoidal by which point lost culturability and/or fitness had occurred, also dwarfing was not very evident. Even after only 7 d Scott A viability declined as much as 3-log units. When supraoptimal thermal stress is applied to cells during starvation cells the die-off accelerates. This rapid die-off in late stationary growth phase is characteristic of the growth curve “death phase”(Postgate & Hunter, 1962). How bacteria cope within this phase and achieve more stable survivor subpopulations is less well known. It can be conceived by applying mild growth permissive thermal stress destabilisation of processes that lead to stable GASP/SSR states is disrupted. This is significant when considering environmental and host systems where besides temperature other stresses could also be present that would influence persistence and survival.

ScottA is comparatively susceptible to loss of agar-based culturability, as shown by the TVC estimates (Figure 10a, 10b) with 4 log units of culturability lost between 1 d and 14 d incubation at 37°C. By comparison for lineage II strains 10403S and FW04/0025 only exhibited approximately 1 log reduction in inoculum viability after 10 d (Bruno & Freitag, 2011; Liu, 2012), increasing to 2 log reduction by 21 d for strain FW04/0025 (Liu, 2012). Jarvis et al. (2017) found ScottA viability was lost slightly more rapidly after starving cells at 4°C in pure water than other strains, though after 6 weeks the results between did not differ greatly. This difference could reflect the fastidiousness of ScottA, and possibly a reduced ability to maintain cell integrity. ScottA requires branched chain amino acids. L-histidine, L-lysine and L-arginine (Premaratne et al., 1991) in addition to the typical growth factors most *L. monocytogenes* strains require (Tsai & Hodgson, 2003; Premaratne et al., 1991).

Furthermore, the resumption of exponential growth seems subject to heterogeneity in terms of growth levels and rates (Figure 10b). The increase in RLT and outgrowth growth rates suggests that the prior inoculum physiological state has an impact on fitness on the outgrowth population but the fitness loss does not seem to be large suggesting that lag phase recovery is at least partially successful in restoring normalcy to the cellular physiology of cells that still possessed or that had re-acquired culturability. Transferring the original 21 d cultures once or twice more to fresh media lead to outgrowth populations growing at the faster rates with short lag phases (data not shown). This suggests normal fitness is eventually restored and injured and non-viable cells incapable of growth diluted out of the population.

Based on the data obtained here the lag phase duration changes exhibited by aged *L. monocytogenes* Scott A cells is consistent with the parameters that would typically influence lag phase; that is cells require recovery before achieving the ability to initiate cytokinesis successfully. It must be noted that extended incubation performed here has the consequence of significant cell inactivation and that this seems logical to be due to general forms of cell damage and degeneration. It is assumed that a substantial proportion of the population that cannot recover have or will die due to the lethal accumulation of cell damage such as excessive levels of protein inclusions, leaky cell walls and loss of cytoplasmic homoeostasis. Thus the investigation also takes into account whether sub-populations are able to manifest restorative responses in the lag phase in the time limits applied within the experiment, which is effectively constrained to a finite number (12 or less) of generation time equivalents. The activities of cells that can recover need to restore ATP pools achieve cytoplasmic homeostasis, maintain cell wall and cytokinetic integrity. These are fundamental and substantial tasks and thus presumably

incorporates long evolved aspects of the cell biology. Lag time durations also relate to the harshness of the environment where the recovery takes place. In this experiment, the TSYE broth medium would be considered minimally stressful in regards to both physicochemical parameters and nutrient availability. However, based on the experiments here the incubation temperature of 37°C is at or has gone past a tipping point in which loss of culturability accelerates in a temperature dependent manner. Earlier studies performed on strain ScottA and *E. coli* suggests that at the T_{opt} the increased kinetic rate of enzyme activity is partly offset by an increase in maintenance energy costs (Ross et al., 2008; Zhang et al., 2010). This results in faster growth rates but presumably less stability when proteostasis and other processes are challenged by a lack of resources and energy. Higher incubation temperatures still within the biokinetic growth domain (42°C) would further reduce overall viable cell populations due to this system destabilisation as shown here. Evidence that inactivation rates directly correlate to temperature when growth is not occurring (Ross et al., 2008) suggests the means to repair the damage is likely subject to temperature conditions, even if that temperature is still growth permissive. As a result of the 37°C and 42°C environment applied to ScottA is inherently and increasingly destabilising, which would be explained by an increased rate of cell inactivation since when cells lose energy and then integrity, metabolism subsequently shuts down and a point of no return is not far away. It is also possible ScottA is more sensitive to temperature than other strains, such as FW04/0025 and 10403S. This is suggested in studies by Zhang et al. (2010) where non-thermal non-growth permissive stresses were applied to both ScottA and FW04/0025, and the effect of temperature was greater on ScottA though both were affected the same way overall. The reasons for this are unclear and it is uncertain if they are linked to

nutritional fastidiousness possessed by ScottA and other lineage I strains (such as ATCC 19115; Premaratne et al., 1991). In a minimal medium Premaratne et al. found that ScottA died off even more rapidly if D-glucose (at 55 mM) was present; equally as fast as the phosphate-buffered saline control that completely lacked nutrients. This was also faster than when alternative substrates were used including chitin and peptidoglycan. In the presence of glucose (or just PBS) 0 survivors were detected after 14 d at 37°C. In minimal medium lacking D-glucose log 4-5 CFU ml^{-1} survivors occurred after 21 d, which was similar to what was observed here while when chitin was present survivors were at log 7 CFU ml^{-1}. These results suggests loss of culturability is a combination of lack of glucose and the capacity of cells to retain culturability in the medium. The slow degradation rate of chitin via production of chitinase-like enzymes (Paspaliari et al., 2015) would explain the improved survival rate. In the presence of glucose of high concentration *L. monocytogenes* shows less growth in planktonic cultures (Friedman and Alm, 1962) and within biofilms (Kyoui et al., 2016). Though the exact reaon still has not be defined it is seems likley this is due to the combination of production of toxic metabolic by-products, increased acidity of the culture, and accumulated unprotonated organic acids that can enter the cell at (such as formate, lactate, acetate). TSYE used in this study by comparison has only 14 mM D-glucose and would likely be entirely consumed after 1-2 d. Other utilisable carbohydrates are present in the yeast extract (~0.13 g glucose l^{-1} TSYE, Plata et al. 2013) and soytone components that could also add to the glucose freely available. Thus it seems the loss of culturability is inherent to the medium (and availability of substrate) while temperature governs the rate of which viability decline occurs.

Aged cultures clearly have poor fitness and the data points to damage to the cell envelope and lack of ATP for that reason. This is consistent with selective elimination of ATP synthesis via proton translocation and glycolysis (by inhibiting glyceraldehyde-3-phosphate dehydrogenase) using metabolic inhibitors completely abolishing survival of Scott A (Jarvis et al. 2017). ScottA cells at around 7 d transiently go from rods to spindle shaped elongated cells that degenerate into smaller coccoids. This indicates loss of cell division control that logically seems related to the observed loss of cell wall integerity and subsequent autolysis. Cell autolysis also occurs in 4°C starved cells of *L. monocytogenes* but to what seems a somewhat lesser extent. The role, if any, of protein aggregation (Lindner et al., 2008), observed to occur during cell aging was not determined here. If the findings of Lindner and colleagues are however correct, the aged cells could have more aggregated protein. This accumulation passed a threshold becomes toxic (Vasquez et al., 2008) impedeing the efficiency of biochemical processes, for example, protein folding (van den Berg et al., 1999; Ellis & Minton, 2006; Bednarska et al., 2013). The lower activity of various enzymes in aged cultures held at elevated growth permissive temperatures may relate to this. The enzymes α-glucosidase and N-acetyl-β-glucosaminidase, however, could be controlled by substrate induction the regulation of which seems to be temperature and culture age dependent. Clear declines in activity were observed in leucine arylamidase, C4 esterase (similar to YvaK from *Bacillus subtilis*, Henke and Bornsheuer, 2002) and β-glucosidase show clear culture age dependent activity decline. These enzymes have roles in amino acquisition, lipid metabolism and sugar metabolism. This suggests impaired protein synthesis coupled to lack of transport may occur that reduces the presence of intact levels of these enzymes. The fate of these enzymes is unclear and several scenarios

are possible and requires follow up analysis. The declines seem logically linked in general to less ATP availability, required for proteostasis and transport of substrates. The maintained production of phosphatases in aged cells at all growth temperatures are required by kinases for ATP synthesis is interesting. The continual detection either means the enzymes are stable and not turned over rapidly or continue to be produced due to an increased emphasis on their production. This suggests some processes may persist in aged non-culturable ScottA cells despite the loss of cell culturability.

Overall, from the experiments, the amount of work to be done by aged cell populations represents a summed totality of cell populations that incorporates the biosynthetic and homeostatic responses needed to prepare for exponential growth in the new environment. This totality and its inherent complexity of underlying physiological capacity begin to explain why the inoculum physiological state essentially dictates lag duration when everything else is equal. The results for ScottA point to culture conditions and temperature being influential in viability and subsequently on the lag phase. A temperature of 37°C is at or near a tipping point where cell viability is rapidly lost as compared to 25-30°C where the rate of viability decline is approximately 3-times slower. Based on the data Scott A forms what appears to be starvation induced coccoidal cells with poor culturability and reduced fitness. The responses to culture age at 37°C by ScottA will be further explored utilising proteomics in the next chapter of this thesis. This temperature was chosen as it represents both the notional iooptimal tmepetrature for growth for Scott A, is the temperature at which it must be to be in a human host and where it clearly demonstrates relative instability. The goal is to determine the underlying metabolic

networks and other functional traits linked to death and decline of Scott A populations.

Acknowledgements: Some work performed in this chapter was performed by Ms Mary Joseph as part of her Masters of Applied Science research thesis in the centre for Food Safety and Innovation, Tasmanian Institute of Agriculture.

3. Proteomic analysis of aging Listeria monocytogenes ScottA

3.1 Abstract

Integrated global proteomic responses of *L. monocytogenes* ScottA incubated for 1 to 21 days at 37°C was performed to understand the metabolic mechanisms behind the loss of fitness and culturability in populations after extended incubation. Continued lack of availability of carbohydrates leads to an overall decrease in cellular metabolism, loss of culturability on agar, shift to a coccoidal morphology, autolysis, and non-detectable haemolysis. Protein samples were analysed by nano-LC-MS/MS using an LTQ-Orbitrap XL instrument. Metabolism reduction observed for aged cells is linked to empty ATP and precursor pools. This is demonstrated by a decline in phosphotransferase system protein abundances and associated compensatory adjustments to enzyme abundances within the glycolysis pathway, amongst mixed fermentation enzymes, and a possible shift in the F_1F_0 ATPase complex to a synthesis mode. The observed greatly enhanced abundances of glutamate dehydrogenase RocG in aged cells could suggest the use of oxidative deamination for resupply of pyruvate and NADH. Many central processes of the cell linked to growth such as the translational apparatus, ribosomal proteins and DNA processes showed a significant reduction. There is a greater emphasis on proteins involved in cytoplasmic homoeostasis, proteostasis, substrate scavenging, and amino acid/nucleic acid salvage processes in aged cells. Internalin A and B abundances were elevated in aged cells but were accompanied by reduced levels of wall teichoic acid synthesis enzymes. The abundances of several autolysins (Spl, Iap, Auto, Ami) were substantially elevated, explaining aged induced autolysis. The increase in autolysins is potentially linked to cytokinetic dysfunction associated with

the septal ring. This would likely explain the reason why the bulk of the cell population loses culturability though clearly, a subpopulation survives. The proteome data provides a perspective of *L. monocytogenes* in a state of decline deep into its stationary growth phase.

3.2 Introduction

Bacterial growth is constantly sustained as long as its environment remains supportive and is able to access required nutrients. Eventually, after rapid growth, the exhaustion of nutrients and/or increase in waste products, which may be toxic at high concentrations, will force the cells to enter the stationary growth phase. Bacterial cells have developed a starvation survival response (SSR) which involves a physiological adaption to enhance the acquisition of scarce nutrients and to cope with nutrient limitation,. This process is regulated in most bacteria by alternative RNA polymerase (RNAP) sigma factors, such as RpoS, which alters gene expression leading to more resilient cells able to survive in the stationary growth period. RpoS-like proteins are found in most bacteria but not all phyla.

L. monocytogenes can be found in a wide range of environments and thus likely regularly encounters conditions of starvation. A major transcriptional regulator in *L. monocytogenes* is PrfA, a member of the Crp/Fnr family of transcription regulators, which activates the major virulence genes for intracellular survival and cell-to-cell spread, such as *hly* and *actA* (Cossart & Archambaud, 2009). Starvation conditions induce the PrfA regulon while the presence of non-phosphorylated sugars, such as glucose inhibits the expression of PrfA (Park & Kroll, 1993).

The alternative RNAP Sigma B subunit protein SigB, one of the five sigma factors in *L. monocytogenes* is responsible for regulating ~100 genes including virulence and stress response genes (Cossart & Archambaud, 2009). Exposing *L. monocytogenes*

to heat leads to an increase in the expression of heat shock proteins, which includes GroEL, DnaK/DnaJ and other chaperone and Clp protease systems, required for protein folding, the rescue of misfolded proteins and driving protein turnover, processes collectively termed proteostasis. Loss of control of this process is believed to be toxic to cells (Bednarska et al., 2013). In *Bacillus subtilis,* there are four classes of heat-induced protein sets (HrcA repressor-dependent, SigB-dependent, CtsR-dependent and Class IV). ClpC, a member of the Clp ATPase stress protein family, is also known to have a role in stress resistance and virulence, with mutants found to be sensitive to iron limitation, increased osmolarity and heat stress, coupled with reduced virulence *in vivo* (Rouquette et al., 1996; Herbert & Foster, 2001). An extracellular catalase, which is produced through the growth, has been shown to contribute to H_2O_2 resistance. Oxidative damage has a major effect on cell inactivation rates and aging in starved cultures (Nyström, 1999). Sigma(L) regulatory pathways also play a significant role in facilitating resistance of *L. monocytogenes* against stress conditions such as low storage temperatures, exposure to organic acids, and elevated NaCl salt concentrations (Raimann et al., 2009).

As cells age and/or starve in the stationary growth phase, the cell morphology tends to change with cells often shrinking in size. The shrinkage is the result of two processes known as reductive division and dwarfing (Nyström, 2004). Aging (senescence) of bacteria is both separate to and underlies starvation responses. It can be considered the fate of cells that acquire the “older” cell pole during cell division. Cells that acquire the old pole over several generations of division also progressively receive inclusion bodies – masses of aggregated damaged or misfolded proteins (Agulaniu et al., 2003, Stewart et al., 2005; Watve et al., 2006; Nyström, 2007; Lindner et al., 2008). When faced with stress aged cells are likely the

first to inactivate in a cell population since they have to use a greater amount of energy and resources to maintain proteostasis at levels avoiding toxicity (Bednarska et al., 2013; Coelho et al., 2013). In terms of *L. monocytogenes,* it has been found that during the transition to long-term survival *L. monocytogenes* changes from bacilli to cocci (Wen et al., 2011) and a reduction in cell size is noticeable (Herbert & Foster, 2001). The improved cell symmetry likely slows the senescence process (Moseley, 2013) since the acquisition of inclusion bodies is likely both slower and more evenly distributed. Cell symmetry was found to be lost in *L. monocytogenes* Scott A when grown for prolonged periods at the T_{opt} (37°C) then shifts into a coccoidal form as shown in Chapter 2. The combination of stress at this temperature, which is akin to heat shock, and nutrient stress likely accelerates the aging process causing central cell processes to fail, such as complete cell wall biogenesis, demonstrated as morphological changes, cytoplasmic leakage and failed cytokinesis.

It has been found that most genes expressed during the stationary phase are required for starvation survival. The proteins encoded by these genes are involved in protecting the cells against oxidative stress, heat, osmotic challenge and exposure to toxic chemicals. In Gram-positive bacteria of the phylum *Firmicutes* such as *L. monocytogenes* the CodY regulon is required when cells experience starvation; CodY is a sensor of GTP and branched-chain amino acids (BCAA) and is linked to the stringent response and required for full virulence (Sonenshein, 2005; Bennett et al., 2007; Lobel et al., 2012, 2015). CodY is now recognised as a high level “master” regulator activating or repressing many genes associated with metabolism, motility and post-exponential phase survival. It does so by influencing several intertwined regulons including the SigB and PrfA regulons (Lobel & Herskovits, 2016). More

specifically a variety of regulators coordinates gene expression and subsequent phenotypes in *L. monocytogenes*. The species is able to rapidly respond to changes in its environment and when access to nutrient resources is diminished. Many of these regulators have been extensively studied and their associated regulons determined. These regulons overlap to varying degrees and thus play important roles in survival both in the host and in the outside environment (Abram et al., 2008). It is thus surmised CodY regulation along with strategies such as bet-hedging and persister cells (Garmyn et. al., 2011; Curtis et al., 2016) could allow for survival of a subpopulation of cells that are still able to recover during lag phase. The focus on regulons in relation to lag phase and cell aging in this thesis is detailed in Chapter 5. In this and the following chapter, the experimental focus is to understand the underlying cell phenotypes that are linked to aging and starvation and recovery therefrom.

The aim of this study is to provide an overview of the growth curve “death phase” which is equaletd to culture aging and attempts to identify the primary mechanisms involved in cell aging and subsequent loss of culturability. Another objective was to determine the mechanisms adopted by cells in response to starvation stress during the stationary phase, which acts to speed up aging and subsequent inactivation. A key feature of the experiment was that the temperature employed, 37°C, is the T_{opt} of *L. monocytogenes*. Based on prior research this temperature significantly increases the entropy in the system and based on concepts related to thermodynamics of growth rates could be a tipping point (Ross et al., 2008; Corkrey et al., 2014). This relates to enzyme rates being more rapid due to Arrhenius kinetics, but this is offset by a greater need to channel energy into maintenance processes in order to keep the system stable. Stress, especially stress that depletes cell energy, thus

endangers the stability of cellular processes with aged cells likely being especially vulnerable to this entropic state.

In this study, the well-studied strain *L. monocytogenes* ScottA was used and quantitative proteomics employed to investigate its responses to enforced aging and associated starvation. The bacterial cells were grown in tryptone soya broth plus 0.6% yeast extract (Oxoid) (TSYE) at 37°C for 1, 7, 14, and 21 days, during which changes to cellular phenotypes are already described in Chapter 2. These included partial loss of cell viability, morphological changes, cell wall leakage, metabolic decline, ATP depletion and presumed reduction in protein export, as suggested by lack of listeriolysin-induced haemolysis. Harvested cells were subjected to whole cell protein extraction using zirconia-silica beads for lysis such that primarily cytosolic proteins were obtained. The general principals of the proteomic analysis approach used here are described elsewhere (Bowman et al., 2012; see Methods). This study provides a unique view on bacterial cell decline and associated loss of culturability without deliberate application of external stress.

3.3 Methods

3.3.1 Preparation of Inocula

The strain used in this study was *Listeria monocytogenes* ScottA. This strain is of serotype 4b and is related to clonal cluster 2 within lineage I (Briers et al., 2011). A single colony of the organism was transferred aseptically into 100 ml of tryptone soya broth plus 0.6% yeast extract (Oxoid) (TSYE) and then incubated at 37˚C for 12 h. The same inoculum preparation approach was used as described in section 2.3.1 in Chapter 2. A 100 µl aliquot of this culture was used to inoculate fresh 100 ml

TSYE triplicate broths that were incubated for 1, 7, 14 and 21 d at 37˚C. Cells in exponential phase (8 h) was used as a control culture. This was done twice.

3.3.2 Proteomics Experiment

3.3.2.1 Protein Extraction

Cells were harvested on days 1, 7, 14 and 21 (100 mL each) using centrifugation at 4000 × *g* for 10 min at 4 °C (Microcentrifuge 5417R, Eppendorf, Germany). Cell pellets were washed twice using phosphate buffered saline (PBS; Oxoid, BR0014G). Whole cell protein was extracted using bead beating. For this process, 600 µL of the cell suspensions and 0.5 g of zirconia-silica beads (diameter 0.1 mm; Daintree Scientific, TAS, Australia) were mixed and bead beat using a TissueLyser III bead beater (Qiagen) at 30 cycles/s for 6 min. The samples were centrifuged to remove cellular debris at 14 000 rpm for 30 min at 4 °C. The protein concentration in the lysate was determined using a bicinchoninic acid (BCA) kit (Thermo Fisher Scientific, USA) with bovine serum albumin utilised as a standard. Cells in the exponential phase were harvested using the same approach. An aliquot of each supernatant containing ~50 µg of soluble protein, as determined with a BCA kit, was then lyophilized for 2 h using a Mini Ultra Cold freeze-drier (Dynavac Australia), according to the manufacturer's instructions then subjected to tryptic digestion.

3.3.2.2 SDS-PAGE

An aliquot of each of protein samples was diluted in an equal amount of sample buffer (Tris-HCl pH7.0) and heated at 80˚C for 10 min. SDS-PAGE was performed using a 10% resolving gel and a 4% stacking gel with approximately 3 µg of sample per well. The gel samples were electrophoresed at 25 mA for 1.5 h. After

electrophoresis, separated proteins were visualised by silver staining using the method of (Wilson et al., 2008).

3.3.2.3 Tryptic Digestion

Protein samples were reduced with a reducing agent (50 mM dithiothreitol, 100 mM ammonium bicarbonate; incubated for 1 h at RT), alkylated with an alkylating reagent (200 mM iodoacetamide, 100 mM ammonium bicarbonate; for 1 h at RT) and reduced again with the reducing agent (for 1 h at RT). After dithiothreitol reduction and iodoacetamide alkylation of cysteine residues, all solutions were diluted to a final volume of 220 µl of digestion buffer (50 mM ammonium bicarbonate, 1 mM $CaCl_2$ $2H_2O$) and digested with 0.1 µg/µl Sequencing grade modified trypsin (Promega, Madison, WI; USA) at a ratio of 1:50 (trypsin/protein). After incubation at 37 °C for 18-20 h, the digested reactions were quenched by acidification with 10 µl of 10% formic acid and stored at -80 °C for further analysis.

3.3.2.4 nanoLC-LTQ-Orbitrap Tandem Mass Spectrometry

Protein samples were analysed by nanoLC-MS/MS using an LTQ-Orbitrap XL (ThermoFisher Scientific). Aliquots of tryptic peptides equivalent to 50% of the in-solution digests were loaded at 0.05 mL/min onto a C18 capillary trapping column (Peptide CapTrap, Michrom Bio- Resources) controlled by an Alliance 2690 Separations Module (Waters). Peptides were then separated on an analytical nanoHPLC column packed with 5 µm C18 media (PicoFrit Column, 15 µm i.d. pulled tip, 10 cm, New Objective) controlled using a Surveyor MS Pump Plus (ThermoFisher Scientific) at 200 nL/min over a four-step gradient of 100% buffer A (5% acetonitrile in 0.2% formic acid) to 100% buffer B (90% acetonitrile in 0.2%

formic acid) using the following steps: 0− 10% B over 7.5 min; 10−25% B over 50 min; 25−55% B over 20 min; 55−100% B over 5 min; holding at 100% B for 15 min; and re-equilibration in 100% A for 15 min. The LTQ-Orbitrap XL was controlled using Xcalibur 2.0 software (ThermoFisher Scientific) and operated in data- dependent acquisition mode, where survey scans were acquired in the Orbitrap using a resolving power of 60 000 (at 400 m/z). MS/MS spectra were concurrently obtained in the LTQ mass analyser on the eight most intense ions from the FT survey scan. Charge state filtering, where unassigned and singly charged precursor ions were not selected for fragmentation, and dynamic exclusion (repeat count 1, repeat duration 30 s, exclusion list size 500) was used. Fragmentation conditions in the LTQ were: 35% normalised collision energy, activation q of 0.25, 30 ms activation time, and minimum ion selection intensity of 500 counts.

3.3.2.5 Peptide Identification

Centroid mode spectra acquired were converted from .RAW files into .mzXML peak list files using the msConvert command (Proteowizard). The extracted MS/MS data were searched against the Scott A proteome downloaded from the National Center for Biotechnology Information FTP server. Semi tryptic searches using parent ion and fragment ion mass tolerances of 10 ppm and 0.5 Da, respectively, were performed using X!Tandem (Craig & Beavis, 2004) running in the LabKey Server (LabKey Software Foundation), an open source bioinformatics resource for analysing large proteomics data sets (Rauch et al., 2006; Nelson et al., 2011). S-Carboxamido-methylation of cysteine residues was specified as a fixed modification, and oxidation of methionine was specified as a variable modification. The Peptide Prophet and Protein Prophet algorithms (Nesvizhskii et al., 2007) were applied to the X!Tandem

search results to assign probabilities to peptide and protein matches, respectively. Peptide−spectrum matches were accepted if the peptide was assigned a probability greater than 0.95, as specified by the Peptide Prophet algorithm. On the basis of the fit of the data to the predicted distributions of correct and incorrect matches, only peptide−spectrum matches for charge states +2 and +3 were accepted. Protein identifications were accepted if the protein contained two or more unique peptide sequences, and the protein was assigned a probability >0.95 by the Protein Prophet algorithm. This threshold constraints the protein false discovery rate (FDR) to <1%.

3.3.2.6 Proteome Data Analysis

The exponential phase control culture data was compared against the stationary growth phase culture data. The total spectral count normalisation was used to normalise the data (Gokce et al., 2011). Spectral counts from these samples were used to determine the fold-change in abundance between proteins across the time course experiment by using the approach developed by Old et al., (2005). A pseudospectral count of 0.5 was applied to each replicate (Zhang et al., 2006) to account for zero values. Validation of fold-change significance was performed using the beta-binomial distribution model (Pham et al., 2010) as implemented in R. Derived significance values were also assessed by false discovery rate analysis (Benjamini & Hochberg, 1995) with an α level of 0.05 considered significant for each individual time point compared to the control.

3.3.2.7 Functional Analysis

The proteomics responses were also examined at the functional level with identified proteins classified into functionally allied sets on the basis of gene ontology.(Bowman et al., 2012; Kocharunchitt et al., 2012). The T-Profiler method

was used to statistically test the significance of changes in overall protein abundance within the sets (Boorsma et al., 2005). A *t*-value of > +3 and −3 can be considered statistically significant for all sets, regardless of size ($p < 0.01$).

3.4 Results and Discussion

3.4.1 Overview of Proteome Response in Aged L. monocytogenes ScottA Cells

Protein profiles were determined for ScottA cultures collected after static incubation at 37°C for 12 h (exponential phase), 1 d, 7 d, 14 d and 21 d. Of 2953 predicted ORFs peptides for 2297 proteins were detected when all samples are considered together. Separately, on average 646 (428-806) proteins had abundance measures across all biological replicates. Details on the more abundant proteins identified, especially those exhibiting significant changes in abundance relative to the control are shown in Appendix I.

The entire proteomic experiment was repeated primarily to increase the depth of the protein sampling levels. However, subsequent visual analysis of the data revealed a degree divergence between the experiments. Multivariate analysis via nMDS and ANOSIM was used to reveal these differences in more concrete terms (Figure 14). Though exponential cultures between the experiments are statistically indistinguishable, the data sets seem to diverge with an increasing trend with the older treatments. Normalised protein profiles, however, still highly correlate (>0.8 Pearson correlation). Overall, ANOSIM indicates that exponential phase and 1 d cultures are relatively distinct from the older cultures. There was no difference between 14 d and 21 d in terms of the ANOSIM scores (R=-0.03, p=0.42). However, the greater divergence between replicates is notable, suggesting the cell

subpopulations present could become more heterogeneous, possibly due to initial differences in the inoculum and the different degrees of accumulated damage that occurs over time.

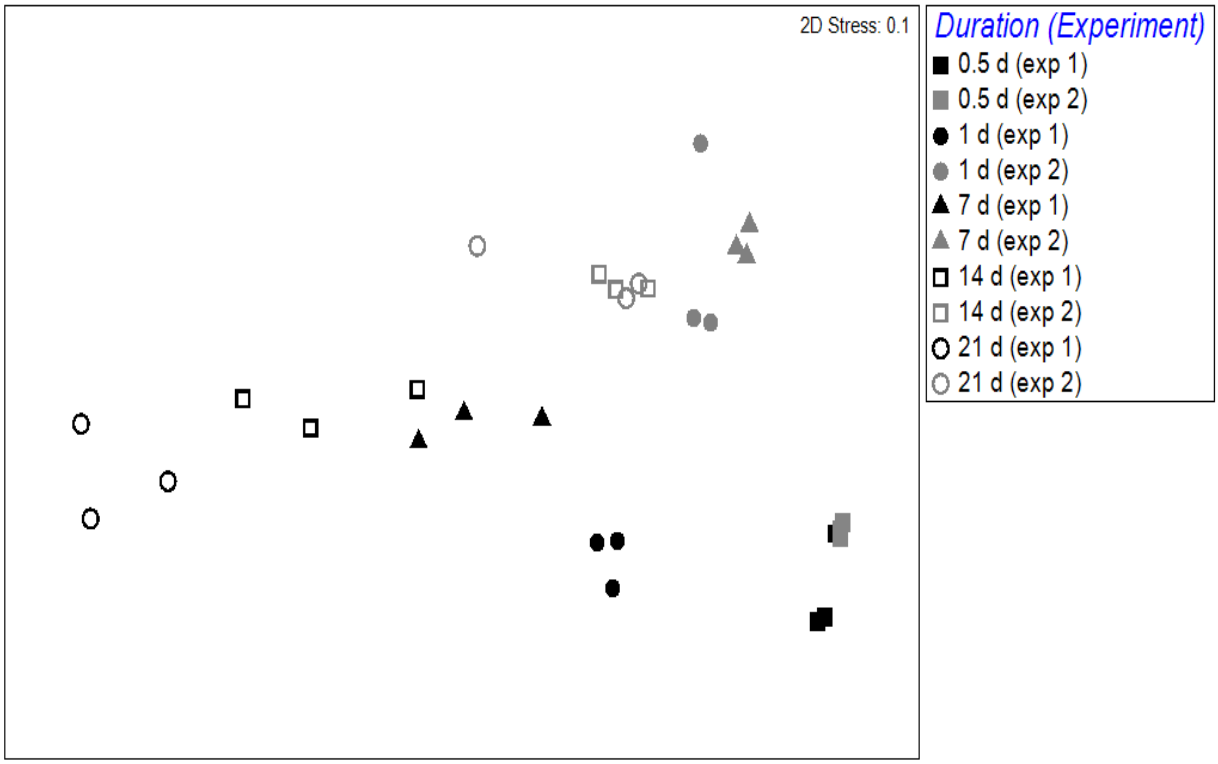

Figure 14**:** nMDS plot showing *L. monoctogenes* Scott A sample protein profile separateness. Scott A was cultured in TSYE broth statically 37°C for the duration indicated. The experiment was repeated twice. The 2D stress value is indicative of the goodness-of-fit when the multidimensional data is translated to a two-dimensional space.

To evaluate the relatively complex trends relative to the exponential phase cultures the two experimental datasets were combined since high correlations substantially outweighed any perceived divergence. Abundance change patterns of functionally allied classes of proteins were established statistically using the *T-value* scoring approach (Boorsma et al., 2005). The *T-value* scores across functionally allied sets or proteins are shown as a heat map in Figure 15. Distinct trends could be observed with the T-profile data. Growth related processes and cell components decline in

abundance on the onset of stationary phase and also as the cells subsequently age as would be expected since these include many resource and energy-dependent processes. The functional classes affected include DNA replication, RNA polymerase, transcription-associated proteins (involved in elongation, termination and of transcription and cold shock RNA chaperones), tRNA/ribosome assembly and processing proteins, ribosomal proteins, protein translation, transporters mainly dependent on a chemiosmotic gradient (given as “other transporters”), phosphotransferase systems, glycolysis, motility/chemotaxis and RNA degradation (Figure 15). The latter is interesting since high levels of stress and onset of inactivation lead to mRNA stabilisation in *L. monocytogenes* ScottA (Zhang et al., 2010).

Various functional sets promoted are those often seen to respond in the same way when *L. monocytogenes* is growth limited by stress including signal transduction, cell defence/detoxification, the SigB operon, DNA repair, and protein folding/turnover. These sets tend to strongly enriched during thermal and acidic stress in *L. monocytogenes* (van der Veen et al., 2007, 2010; Bowman et al., 2012). Since the medium became mildly acidic (pH 5.3) during the experiment and there was sustained, mild thermal pressure this result is not surprising. Some protein functional sets show increases not always seen with standard physicochemical stresses including protein export, cytokinesis, cell wall biogenesis, and cell surface proteins suggesting a strong response in relation to the cell envelope and other subcellular structures. This is consistent with what might be compensatory responses against the loss of cell integrity that occurs with extended incubation at 37°C as shown in Chapter 2.

To further interrogate the data CLUSTER 3.0 was used for k-means analysis producing 6 output groups that summarise distinct changes in relative abundance over time for functionally unrelated proteins (Figure 16). Appendices I includes the k-means group data. Particular features can be ascribed to the k-means groups when considering data from chapter 2. Group 0 proteins (Figure 16) shows a trend of

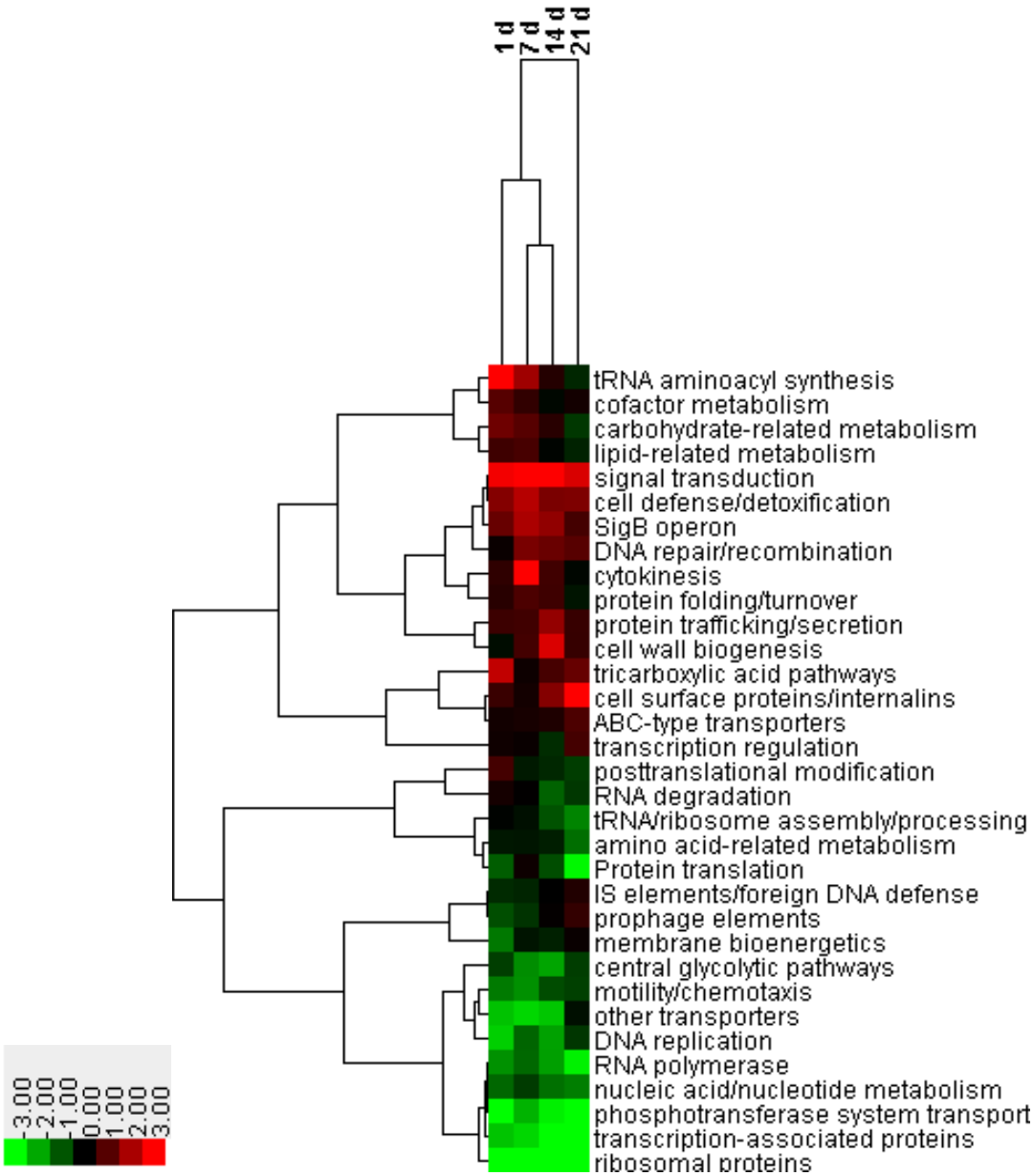

Figure 15: Functional responses of *L. monocytogenes* ScottA grown for up to 21 d at 37°C based on protein relative abundances. T-value scores for protein sets were determined using the approach of Boorsma et al. (2005) with independent experiments consolidated (n=6 biological replicates), non-detected proteins excluded from sets and with exponential phase cultures acting as the compared controls. The trends in overall abundance for the sets are shown in a colour coded format as denoted by the colour bar. Positive and negative T-values indicate a general trend of greater or lower abundance of proteins within each set relative to the overall measurable proteome.

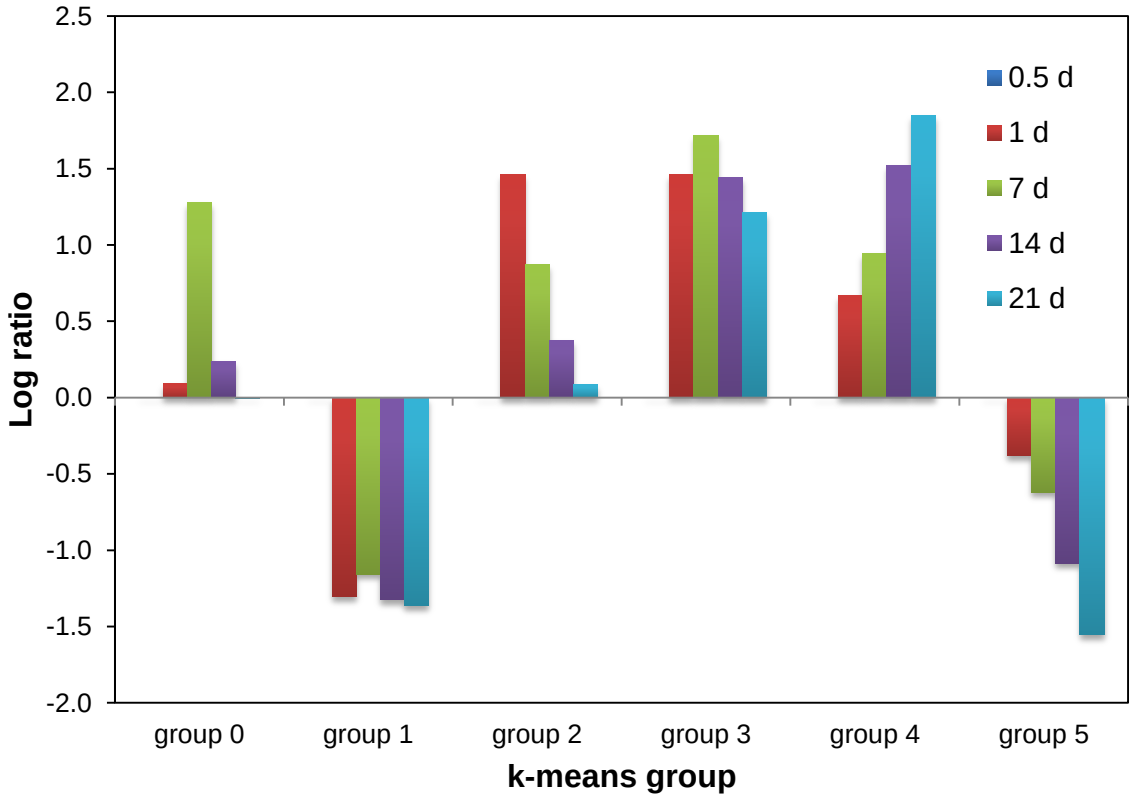

Figure 16: K-means based trend analysis of *L. monocytogenes* ScottA protein profiles grown in TSYE at 37°C for an extended period of time. Protein assignments to k-means groups are shown in Appendices I. Log ratios given are the average of log ratios (relative to the exponential growth control cultures) for the entire k-means group.

increased abundance for 39 proteins in 7 d samples the time at which ATP depletion and the metabolic decline was first clearly observed (see Chapter 2). These proteins have a broad cross-section of functions but amongst them are essential proteins that regulate sudden onsets of stress, promote protein translation, synthesise the starting precursors for fatty acids; and efflux or detoxify toxic metabolites. As examples, these proteins include a RelA ortholog (EGJ25157) that is likely linked to the stringent response; recombinase RecA (EGJ243934), which promotes the DNA repair SOS response; and peptide release factors RF1 (EGJ24491) and RF3

(EGJ26068) that together ensure correct translation of nascent peptides. Overall, the data suggest a transient protective response is activated, but this is not sustained suggesting the collective responses are not related to aging but instead to the cells being depleted of resources.

Group 1 proteins (n=105) have a lower abundance at all time points and seem to correspond to proteins associated with active growth as the group is rich in enzymes associated with catabolic and biosynthesis processes and is especially enriched in ribosomal proteins. Groups 2 and 5, on the other hand, include proteins that decline in abundance after stationary growth phase is invoked and thus could possibly have decreased as a consequence ofculture age. Group 2 proteins (n=95) include a proportion of proteins that are initially activated on the onset of the stationary growth phase, which includes many proteins in pathways that act to expand the acquisition and metabolism of nutrients but these decline suggesting as the medium depletes in nutrients these proteins become increasingly redundant. Group 5 proteins (n=67) decline from the outset of stationary growth phase and seem to have a similar spectrum of functionality as found in groups 1 and 2.

Groups 3 and 4 include proteins that have enhanced abundance either from the onset of stationary growth phase (group 3, n=219) or increase progressively (group 4, n=111). The key enzymes associated with protein disaggregation (see section 1.13 of Chapter 1) are concentrated in these groups, and thus culture age-related adaptations and compensations against cellular deterioration are likely embedded in these groups. Some of the most relevant proteins that could be connected to the aging process are discussed below in more detail.

3.4.2 Culture Age Promotes Cell Envelope Associated Proteins

Among cell wall biogenesis proteins that most obviously showed significant

abundance increases during aging were peptidoglycan (PG) turnover proteins CwlO (Spl/P45, EGJ26030), LytF (EGJ26216), LytG (Auto, EG24576), and AmiD (Ami, EGJ26082) (Figure 17). Furthermore the enzymes in the two final steps of PG synthesis were also mostly more abundant including MurG (EGJ25580), D-alanyl-D-alanine carboxypeptidase DacA (EGJ26280) and PpbB (EGJ25584). By comparison PpbA (EGJ24974) and an alternate D-alanyl-D-alanine carboxypeptidase (EGJ25391) were only barely detected in the protein profiles, and their abundance changes could not be measured. The PG turnover proteins are peptidoglycan hydrolases, a group of enzymes that are capable of cleaving bonds within mature PG. These proteins participate in bacterial cell wall growth and its regulation and act in different autolysis phenomena (Popowska, 2004). In addition, these hydrolases are responsible for the release of turnover products from PG during cell growth (Goodell & Schwarz, 1985). Turnover products can serve as signalling molecules for recognition of bacteria by other organisms and, in some bacteria, for the induction of β-lactamases (Jacobs et al., 1997).

The results showed CwlO/Spl/P45, which is secreted to the cell wall, increased in abundance by ≥ 13–fold ($P \geq 0.01$) after one day and by 21 days had increased to ≥90-fold ($P \geq .01$) (Figure 17). This enzyme had the greatest increase of all measured proteins when 21 d cultures are compared to exponential cultures. In one replicate the increase in CwlO abundance was estimated to be 474-fold. The Iap, Ami and Auto autolysins increased ~20-fold by 21 d. In Gram-positive bacteria, cell wall elongation requires redundant PG endopeptidases. In *B. subtilis* the CwlO protein is the primary DL-endopeptidase in vegetative cells, while LytF (also called LytE) becomes important when cells experience envelope stress (Meisner et al., 2013). The hydrolases are also responsible for autolysis induced under certain

conditions (Popowska, 2004). *L. monocytogenes* strains were found to autolyse at maximal rates at 37°C, pH 8.0 (Popowska et al., 1999) with an earlier study suggesting spontaneous autolysis is pH independent (Tyrrell, 1973). Our results indicate the significant increase in Ami, Auto and Iap abundance is also relevant to this process. These autolysins are required for full virulence by participating in adherence and invasion processes and in-vivo survival. Auto is needed by *L. monocytogenes* to enter nonphagocytic cells (Cabanes et al., 2004). Ami helps with adhesion of *L. monocytogenes* to eukaryotic cells as a prelude to subsequent invasion (Milohanic et al., 2001; Asano et al., 2012). Overall the increase in autolysins could be a response to morphological changes observed in Chapter 2. There is possibly lower teichoic acid levels in the cell walls since they are known to regulate the level of autolysins (Biswas et al., 2012).

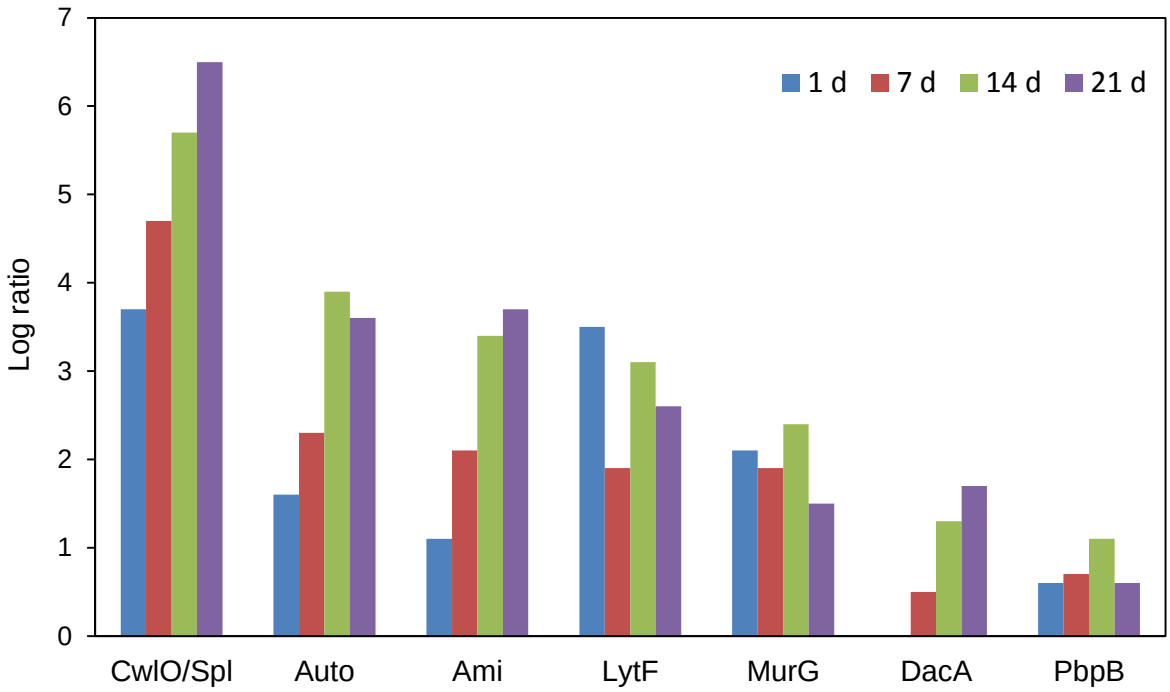

Figure 17**:** Changes in abundance (log ratio relative to exponential cells) of PG turnover and biosynthesis proteins in *L. monocytogenes* ScottA incubated at 37°C in

TSYE broth. See Appendices I and the text for more details.

Regulation of cell wall biosynthesis is controlled by the intermediate glucosamine-6-phosphate (Komatsuzawa et al., 2004) produced by NagA (α-N-acetylglucosaminidase, EGJ24458). A gradual increase in NagA abundance occurred during aging (3.0-5.3 fold). *Listeria monocytogenes* needs NagA for the deacetylation of *N*-acetyl-glucosamine-6 phosphate to glucosamine-6 phosphate and acetate which is a required step for cell wall peptidoglycan and teichoic acid (TA) biosynthesis (Barnhart et al., 2006; Popowska et al., 2012). The primary structure of the murein of *L. monocytogenes* is composed of glycan chains in which alternating N-acetylglucosamine (GlcNAc) and N-acetylmuramic acid (MurNAc) are β-1,4 linked. Deacetylation of N-acetylglucosamine is also important in cell wall recycling.This result in agreement with increased abundance of peptidoglycan turnover proteins. The cytoplasmic deacetylase (NagA) is also essential for both maintaining the shape of the bacterial envelope and for normal cell division (Popowska et al., 2012).

Hydroxymethylglutaryl-CoA synthase MvaS (EGJ24951), a key enzyme in the mevalonate pathway for the synthesis of isoprenoids. was found to be substantially more abundant in aged (14 d, 21 d) cells by 18-20 fold. In bacteria, isoprenoids are needed for the lipid carrier undecaprenyl diphosphate, which is required for cell wall biosynthesis and for biosynthesis of menaquinones (menaquinone-8 in the case of *L. monocytogenes*) involved in electron transport (Wilding, 2000). Expression of the heterologous mevalonate pathway can avoid unknown physiological control elements and thus result in a higher level of production of isoprenoid precursors. However, the remainder of the pathway enzymes through to UppS (EGJ24853) the final step in the synthesis of the lipid carrier were generally weakly abundant and had lower abundance in aged cells relative to the exponential phase. The reason for the

significant increase in MvaS could be related to its precursor, L-leucine, possibly being less available, as explained below in section 3.4.6. The lack of precursors leads to bottlenecks in pathways that may account for the compensatory expansion of individual proteins. It is uncertain if lipid carrier itself actually becomes less abundant but the data points in that direction.

L. monocytogenes possess cell wall teichoic acids (WTA) and lipoteichoic acids (LTA). LTA is a phosphodiester linked glycerol phosphate polymer which is anchored into the cell membrane. WTA consists of ribitol phosphate polymer anchored to PG. The decoration of WTA via glycosylation is primarily responsible for *L. monocytogenes* serotypes and immunogenicity. LTA and WTA also provide rigidity and influence surface charge of cell walls thus imparting important properties to the cell (Brown et al., 2013; Carvalho et al., 2015). Serotype 4b strains (like ScottA) when grown at 37°C to stationary growth phase have 10-fold more WTA than LTA (Fujii et al., 1985) so it is expected enzymes for WTA synthesis to be more abundant.

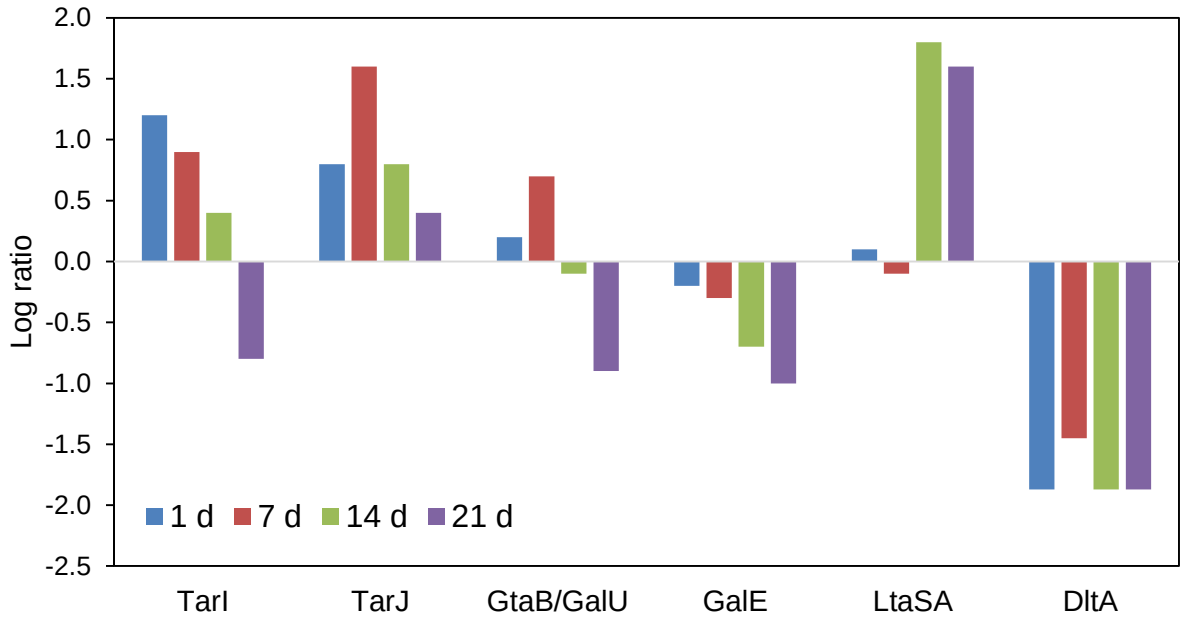

Figure 18**:** Changes in abundance (log ratio relative to exponential cells) of enzymes involved in the initial stages of WTA and LTA biosynthesis in *L. monocytogenes* ScottA incubated at 37°C in TSYE broth.

TarI (EGJ24583) and TarJ (EGJ24584) are involved in the synthesis of the CDP-ribitol precursor (from ribulose-5-phosphate) and subsequent polymerisation to form WTA were increased in abundance at the onset of stationary growth phase but decline after 7 d (Figure 18). Enzymes involved in the synthesis of UDP-activated sugars for WTA glycosylation also show the same pattern, including GalE (EGJ26002) and GtaB/GalU (EGJ24582). D-alanine-poly-(phosphoribitol) ligase DltA (EGJ24476), which D-alanylates WTA to PG significantly declined in abundance on the onset of the stationary growth phase. On the other hand, glycerol-phosphate lipoteichoic acid synthetase LtaSA (EGJ24430) increased in abundance as cells aged. The data suggests a decline in the synthesis of WTA possibly due to lower availability of PG and probably also a lack of phosphorylated carbohydrate precursors. On the other hand, the initial step in LTA synthesis utilising glycerol-3-phosphate as a precursor (see below section on intermediary metabolism changes with aging) could be promoted to bolster the integrity of the cell wall. It is unknown if LTA regulates autolysin levels in *L. monocytogenes* but has been shown to do so in *Staphylococcus aureus* (Fedtke et al., 2007) thus one could hypothesise that LTA synthesis stimulation is tied to greater abundance of autolysins.

Autolysins need to be targeted to the cell envelope and to do this requires secretion. *L. monocytogenes* has a number of secretion pathways including the general secretory system (Sec), twin arginine translocation (TAT) system and a functional type VII (ESX-1) secretion system (Pinheiro et al., 2016). From the proteomic data, only Sec system proteins were abundant enough to be measured. Individual protein abundance patterns revealed significant increased abundance of SecA (EGJ26035),

SecDF (EGJ25064), SecY (EGJ26137), YajC (EGJ25066), YidC (EGJ26378), Ffh (EGJ25337), and FtsY (EGJ25339) peaking after 7 d (1.9-7-fold increases) (Figure 19) and distinctly declining by 21 d. SecA2 (EGJ24099), and the SecE (EGJ23750) and SecG (EGJ25976) subunits of the export translocon along with SecY (Scott & Barnett, 2006) were not detected sufficiently to measure their abundance changes. The signal peptide hydrolase SppA (EGJ25122), which cleaves off signal peptides prior to export was not detectable after 21 d. The initial overall higher abundance of the Sec system proteins in stationary growth is consistent with stationary growth phase adjustments, but the system seems to decline in aged cells. Since there are only negligible levels of ATP in the cells, the peak increase in 7 d could be compensatory. The data suggest that the export process is probably increasingly impeded with culture age and lack of ATP. This would explain loss of haemolysis activity (see Chapter 2).

It has been reported that the SSR of *L. monocytogenes* is induced under glucose limitation. The cell dwarfing phenotype that emerges involves initially cell wall and protein biosynthesis (Herbert & Foster, 2001). SSR survival is an effective strategy for lower temperature survival (Chan & Weidmann, 2009) with hardly any loss of viability after 20 d. In this experiment,coccoid cells were observed though dwarfing was not obvious and they showed loss of viability and fitness. Thus the observed increased abundance of MurG, PpbB and DacA (Figure 17) seems to suggest a compensatory response instead. This is based on the observation many enzymes associated with PG synthesis did not significantly alter in abundance and indeed PG biosynthesis could be constrained since the enzymes conducting the first 6 steps of PG synthesis, GlmS (EGJ24245), GlmM (EGJ25668), GlmU (EGJ23704), MurAA (EGJ26051), and MurB (EGJ24956), all show reduced abundance (overall 60%

reduction, see Appendix I). The reduction could be a response to low rates of incoming carbohydrate precursors, i.e. fructose-6-phosphate, owing to slower phosphotransfer (as explained below in the section on PTS systems).

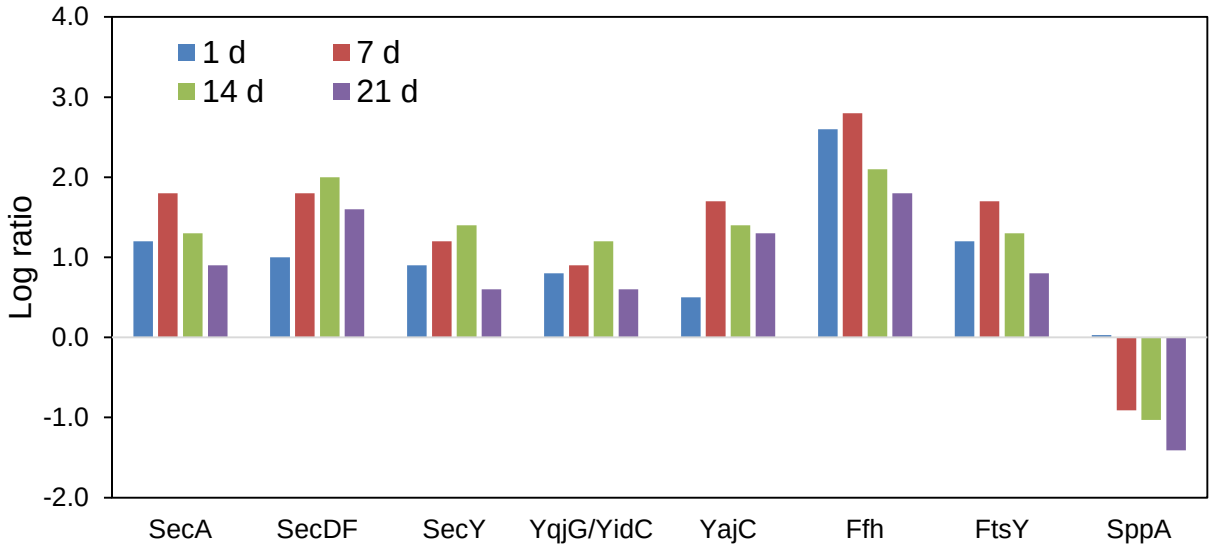

Figure 19: Changes in abundance (log ratio relative to exponential cells) of the Sec potein export system in *L. monocytogenes* ScottA incubated at 37°C in TSYE broth. See Appendices I and the text for more details.

The overall outcome of aging *L. monocytogenes* ScottA are cells that have thinner less-networked peptidoglycan and evidence of autolysis, as shown in Chapter 2. The results here indicate that greatly higher levels of several PG turnover proteins are a response to what is interpreted as lower PG synthesis that would typically replace and add to PG networks. Scavenging and active reworking of cell walls could be occurring causing cell autolysis and be linked to cell enlargement. Autolysins may still be able to add to cell walls and cause cell elongation by capturing and incorporating remnants of autolysed cell walls (involving the actions of MurG, DacA and PbpB). The increased abundance of protein export proteins could be needed to target more protein to the cell wall as cells expand in size but autolysin abundance increases could also be due to changes in teichoic acid levels. Chemical analysis of

proportions of PG, WTA and LTA are required to confirm the above suppositions. A side effect of the aged phenotype is lower cell wall rigidity and evidence of cell autolysis. Thus autolysins contribute to eventual cell death in aging cultures at 37°C.

3.4.3 Cytokinesis dysfunction in aging cultures

Aging is associated with slowed growth and eventual loss of viability. To get to the heart of this process proteomic analysis of cell division proteins may provide insight into what is behind this. Cytokinesis is the process bacteria use to divide into two cells and is possible due to a cytoskeletal array of proteins (the divisome) that acts as a scaffold for specific cytokinetic processes. The process of cytokinesis starts when the chromosome replicates and moves to opposite ends of the cell, a Z (septal) ring structure forms inside the plasma membrane in the middle cell region forming the septum at which the cell divides. FtsZ (EGJ25577), a GTPase homolog of tubulin is the major component of the Z-ring. During cytokinesis PG biosynthesis and autolysin proteins actively rework the cell wall allowing cell elongation and septation. As the cell elongates actin-like proteins (MreB, MreBH, MreC, Mbl) act as a scaffold coil-like structure through the cell resulting in the rod-shaped morphotype. Deletion mutants of various cytokinesis proteins and PG proteins (if not essential) lead to morphologically altered cells with reduced fitness, including minicells, filaments, multiseptate and L-forms (Dell'Era et al., 2009; Farley et al., 2016).

The proteomic data obtained here showed a significant number of proteins directly involved in cytokinesis had increased in abundance significantly at 1 to 7 d (Figure 19) but then decline. This includes proteins involved in initiation and regulation of Z-ring formation (DivIVA), FtsZ, and proteins recruited to the Z-ring involved with targeting other proteins to the Z-ring (FtsA, FtsK, FtsE, FtsX, EzrA) (Claessen et al., 2008; Arends et al., 2009; Chien et al. 2012). The 7 d point corresponds to ATP

dropping to below detectable levels, >100 –fold lower than exponential cells and with radical cell morphological change (Chapter 2).

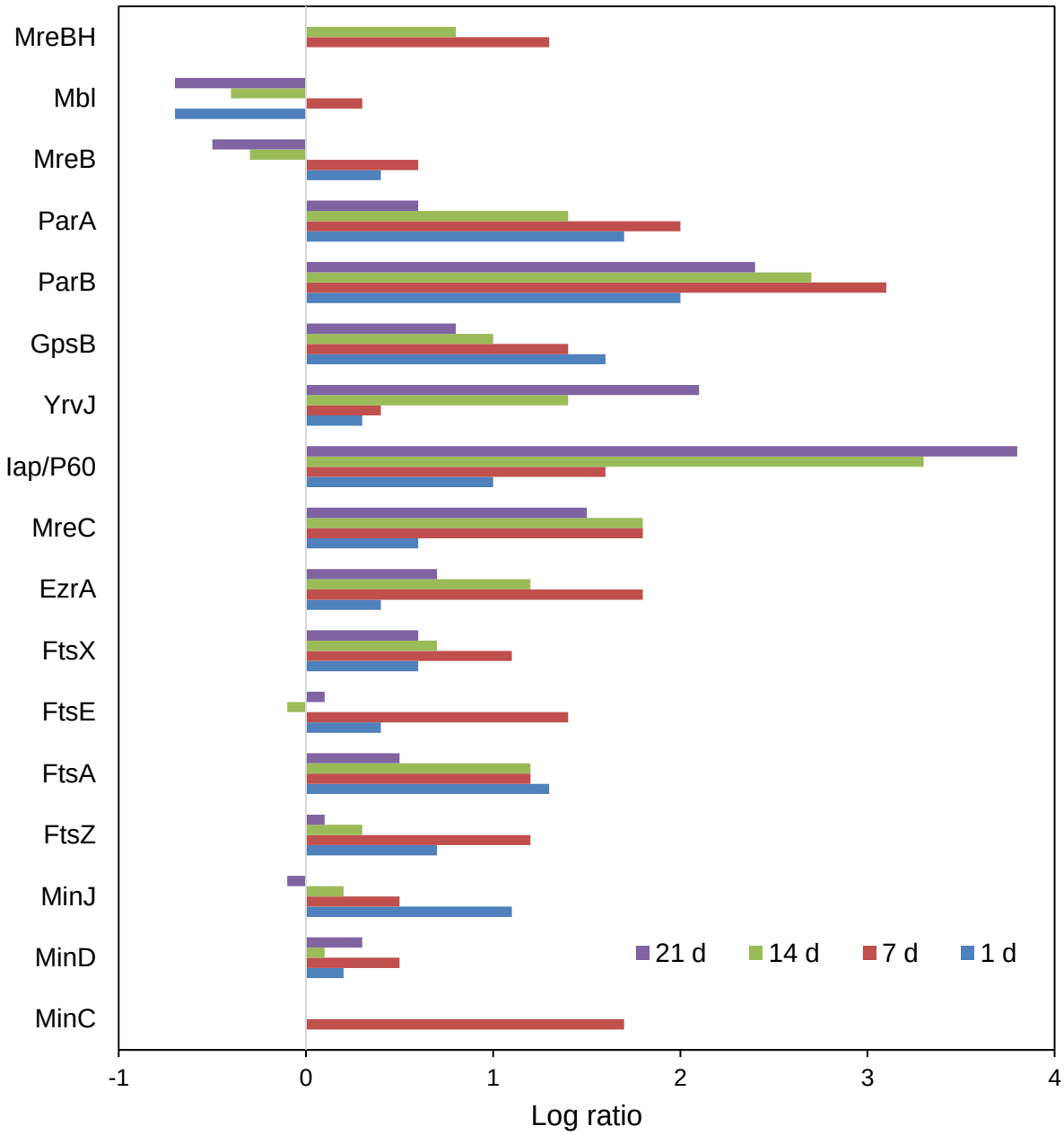

Figure 20**:** Changes in the abundance of proteins associated with cytokinesis during incubation of *L. monocytogenes* ScottA in TSYE broth at 37°C. MreBH, Mbl, MreB, MreC (cell shape determining actin-like proteins); ParA, ParB (chromosome partitioning proteins), GpsB (recruits PG synthesis proteins for cell elongation); EzrA (recruits PG synthesis proteins for Z-ring formation); Iap/60, YrvJ (muramidases that cleave the septum); FtsZ (Z-ring tubulin-like GTPase); FtsX, FtsE, FtsA (proteins that

target other proteins to the Z-ring e.g. FtsK, FtsW etc.); MinC, MinD, Min J (proteins that target the Z-ring to the mid-cell); FtsH (Z-ring targeted endopeptidase).

The results suggest an increase in the overall abundance of the cytokinetic cell machinery overall as a means to maintain the correct level to achieve cytokinesis. Chromosomal partitioning system proteins (ParA and ParB) (Lee & Grossman, 2006; Attaiech et al., 2015) were the most affected, which could suggest the expansion of the cell volume also affects the amount of cellular DNA, with potentially multiple chromosome copies present. It has been shown that inflating cells under nutrient stress at 37°C will accumulate extra DNA and protein (Basan et al., 2015). The possible expansion of DNA in aged cells is suggested by the greater abundance of the protein Hup (EGJ25469) and Fri/Dps (EGJ24445); these proteins become amongst the most abundant cytosolic proteins by 21 d with Hup doubling in abundance from 7 d to 21 d while Dps abundances increase 17-fold and 4-fold in relation to exponential and 1 d cultures. Both Hup and Dps bind to DNA and manage the integrity of the chromosome in entirely different ways. The ortholog of Hup in *E. coli* Hns plays a significant role in chromosome organisation and acts as a global gene silencer (affecting 250 genes) (Lim et al., 2012). The exact role has not been defined in *L. monocytogenes* but likely is analogous owing to its conserved sequence and high abundance. Dps, on the other hand, binds to DNA and protects it from iron and copper-induced oxidative damage, UV and gamma irradiation, thermal stress and acid and base shocks (Bellapradona et al., 2010). Dps bind iron and thus can also store it in the manner of a ferritin-like protein. The overall response suggests management of DNA either in a protective manner. Further work is needed to assess the exact nature of DNA expansion if any.

Clearly, the transient expansion of cell sizeand shift to coccoidal cells in aged cultures would implicate cytokinetic dysfunction. At 21 d levels of FtsZ and its associated partners are much lower than the peak at 7 d (Figure 20). At the same time, the membrane-bound Z-ring target endopeptidase FtsH (EGJ23724, Weiss, 2004) became non-detectable (data not shown). The specific substrates of this peptidase are thought to be septal ring proteins such as FtsZ in *E. coli* (Srinivisan et al., 2008). FtsH possibly functions as a "timer" for cell division (Fischer et al., 2002). However this will require more data since its function may vary between different groups of bacteria.

The data suggests the cytokinetic apparatus becomes somehow dysfunctional or is hindered in completing the process in aged cells. Could this be the result of the accumulation of proteins at the septal ring? Could the lack of available precursors, energy or some problem with enzyme activities in the late phase of septum separation (such as PG synthesis) hinder chromosome segregation and overall cell division? Considering these questions Iap/P60 (EGJ24098) and YrvJ (EGJ25058) murein hydrolases were clearly more abundant in aged cells. Iap/P60 is bacteriolytic and seems required for normal septum formation and daughter cell separation and seems essential for cell viability under certain conditions (Wuenscher et al., 1993; Machata et al., 2005). YrvJ, an AmiA ortholog may also contribute to the same process through specific studies are needed in *L. monocytogenes*. Other research suggests Iap also plays a role in intestinal invasion and in vivo survival (Pilgrim et al., 2003; Schmidt et al., 2011). In the study of Machata et al. Δ*iap,* Δ*iap*Δ*murA and* Δ*secA2* mutants produce rough colonies and multiseptate cells similar to cell morphotypes observed in Chapter 2. Wuenscher and colleagues found that purified Iap readily aggregated as a conglomerate of 4-6 copies and lost its cell wall

hydrolysis properties. An autolysin of *S. aureus*, E-amidase was found to be active only when aggregated when in the presence of choline, a typical compatible solute (Shinagawa & Seto, 1990). This could suggest Iap, and other murein hydrolases/endopeptidases may not be fully active or mistargeted, accumulating in the cytosol, not only at the Z-ring, leading to autolysis and failure of septate separation. Mistargeting could be due to loss or insufficient protein export. As mentioned above the exporter of Iap, SecA2 was not detected while SppA the signal peptide hydrolase was also not detected or with very low abundance in 14 d and 21 d cells. It could be speculated that Iap (and YvrJ) could contribute to cell dysfunction, but this requires further evidence, for example, a determination of their localisation in cells.

3.4.4 Aged cells show a shift to fermentation pathways and carbohydrate scavenging

Non-glucose carbohydrate enzyme activity and ATP levels were negligible in aged cultures as shown in Chapter 2. By 7 d no detectable activity of a number of enzymes was observed at 37°C but were still readily detcetd at 25°C and 30°C. The primary carbon source in TSYE broth is D-glucose (13.9 mM), while the soytone and yeast extract contain low levels of mono- and disaccharides (≤1 mM). Besides glycerol, only carbohydrate compounds support the growth of *L. monocytogenes* (Premaratne et al., 1991). The loss of enzyme activity and ATP was linked to metabolic decline and loss of cell culturability, possibly as a consequence of cell aging. The proteomic data was investigated to examine the basis of this decline in metabolism.

The first step of catabolism is the transport of carbohydrate units into the cell. This is carried out mainly by the phosphotransferase system (PTS), which phosphorylates sugars in the process. PTS permeases are multisubunit systems of *L. monocytogenes* strains typically have about 29 that have overlapping substrate specificity (Stoll & Goebel, 2010). In the analysis, the membrane-located subunit proteins of the permeases were poorly detected, however, exposed regions of subunits were readily detected (Appendices I). The most abundant of the detected PTS transporters in the exponential phase through to aged cells are shown in Figure 21. These included in order of abundance TreP (EGJ24796), LevE/MptA (EGJ23604), LevG/MptD (EGJ23606), BglP (EGJ23460), LicB (EGJ25892), FruA (EGJ25855), and LevE (EGJ24282). TreP and BglP transporters are of the PTS glucose family while the Mpt system (EGJ23604-06) is of the PTS Mannose family, and have been shown to efficiently transport both D-mannose and D-glucose in strain EGD-e (Stoll & Goebel, 2010). Thus it seems ScottA when grown in TSYE uses mainly TreP, to transport D-glucose from the medium with the BglP and the Mpt system assisting. The other transporters likely transport lower abundance sugars from the medium including β-glucosides, lactose or another disaccharide (LicB), D-fructose and/or D-mannitol (FruA, LevE). Based on the proteomic data MptA, MptD and FruA become 2.3-4.4-fold more abundant while TreP is 2.4-7.0 fold lower in aged cells (Figure 21). The other transporters do not significantly alter in abundance. The data suggests as D-glucose availability drops there is a shift to other transporters. The Mpt system could instead be working to transport D-mannose, which is present at low levels in the soytone and yeast extract in the medium. The key PTS proteins involved in phosphorylation showed reduced abundance after 14 d and 21 d. These include PTS system I protein PtsI (EGJ24506) which carries out the

sugar phosphorylation reaction; (PtsH, EGJ24505), which transfers the phosphate moiety from phosphoenolpyruvate (PEP) to PtsI, in cooperation with HprK (EGJ26008), a serine kinase. HprK was more abundant at the onset of stationary growth phase, but then declined with culture age (Figure 21). The cognate phosphatase HprP (EGJ26006) was at low abundance but was at maximal levels at 7 d. The results suggest that phosphorylation of sugars is likely lower with HprK increase being compensatory. This would most likely stem from a poor supply of PEP.

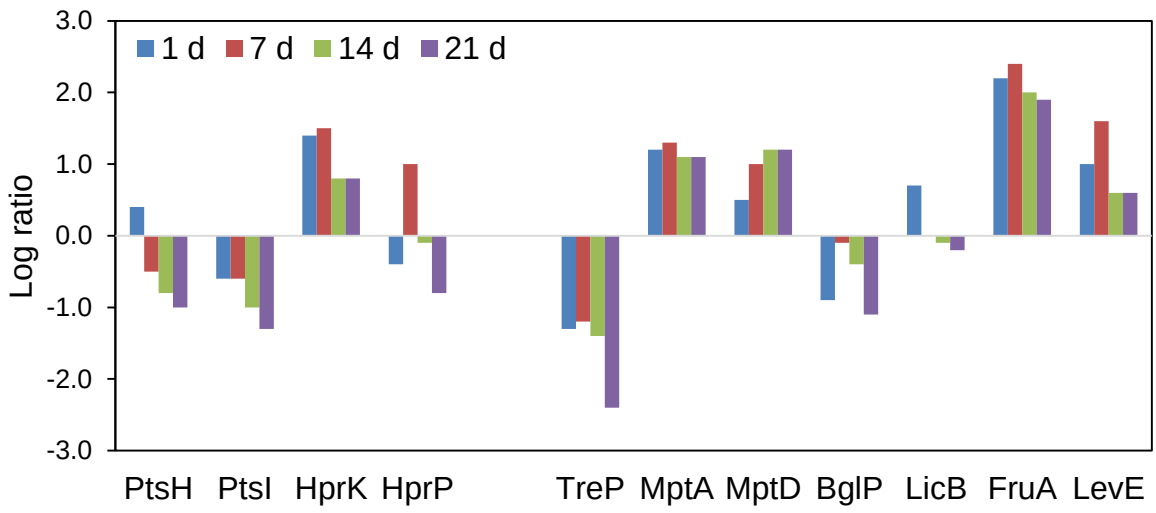

Figure 21**:** Changes in the abundance of proteins associated with PTS proteins and associated transporter subunits during incubation of *L. monocytogenes* ScottA in TSYE broth at 37°C. Primary components - PtsH (phosphocarrier HPr component); PtsI (phosphotransferase component), HprK (HPr protein serine kinase), HprP (HPr protein serine phosphatase); transporter subunits - TreP (Glucose/Glucoside family IIBC), MptA and MptD (Mannose/Fructose/Sorbose family IIAB and IID), BglP (Glucose/Glucoside family IIABC), LicB (Lactose/DACB/beta-glucoside family IIB), FruA (Fructose/Mannitol family IIB), LevE (Mannose/Fructose/Sorbose family IIB).

Other types of transporters for carbohydrates occur in *L. monocytogenes*. Of these only certain specific ABC-type transporters were detectable. Permeases that are

powered by the chemiosmotic gradient, such as glucose uptake (GlcU; EGD23676, EGJ23932) orthologs were not measurable. Putative dextrin/maltose (EGJ23685) and multi-carbohydrate (EGJ23791) ABC transporters were highly abundant and had slightly or significantly elevated abundance in aged cells (Appendix I). The lack of ATP in 7 d and older cells, however, would likely make these transporters somewhat ineffectual and could explain the abundance increase as being related to compensation for lower ATP levels. Overall, sugar transporter abundances seem to adjust to the lack of external (and internal) resources to maximise uptake.

Cells growing under stress have higher energy demands to produce and sustain ionic gradients across the cell membrane (Varela et al., 2004). As a result, the intracellular ATP content has been shown to increase under osmotic stress (Varela et al., 2004) assuming a plentiful supply of utilisable carbon. F_1F_0-ATPase is an essential enzyme complex for regulating intracellular pH and for maintaining a chemiosmotic gradient; these functions makes it indispensable for anaerobic growth (Müller-Herbst et al., 2014). Our results showed increases in abundance (2-11-fold) of all F_1F_0-ATPase subunits (EGJ26053-61) that could be detected (Figure 22). Membrane subunits AtpB and AtpE (subunits a and c) were too low in abundance to measure changes. The increased abundance of the complex could suggest an increased priority for ADP phosphorylation activity; a shift from being an ATPase to an ATP synthetase. Since ATP content is low in cells, this seems logical as the change in functionality attempts to compensate for this deficit. Another explanation is that the cells must maintain cytoplasmic pH homoeostasis and this would be achieved by consumption of ATP and extrusion of H^+. The medium does become mildly acidic (pH 5.3) due to the accumulation of organic acid end-products from fermentation (such as lactate and acetate). Significant abundance changes of the

two glutamate decarboxylase (GAD) paralogs (GadB1 EGJ25883, GadB2 EGJ25958) making up the GAD system (Cotter & Hill, 2003; Sleator & Hill, 2010) were observed. The GAD system buffers cytoplasmic pH the actual abundance of these enzymes (Appendix I), however the changes observed were not remarkable and furthermore the abundances decline as cells age when they would be expected to increase if cytoplasmic homeostasis is being compromised. Ten-fold or greater higher abundances of GAD proteins occur when the cells are placed under severe acid stress (Bowman et al., 2012), in particular, GadB2. Further evidence for the shift to ATP synthesis is that the ATPase beta subunit (AtpD, EGJ26054), which carries out the ADP phosphorylation reaction binding ADP and phosphate becomes highly abundant in old cells, 8-fold that of exponential cells (Figure 22). Mn-dependent pyrophosphatase PpaC which supplies pyrophosphate for the conversion of ADP to ATP has a stable abundance, which is also suggested by stable phosphatase and phosphohydrolase activity that would supply phosphate units (Chapter 2). The results thus suggest there is likely a priority for ADP phosphorylation to counter low ATP levels that manifest with culture aging, however, the process seems unable to counter the poor phosphor donor supply to central metabolism and transport.

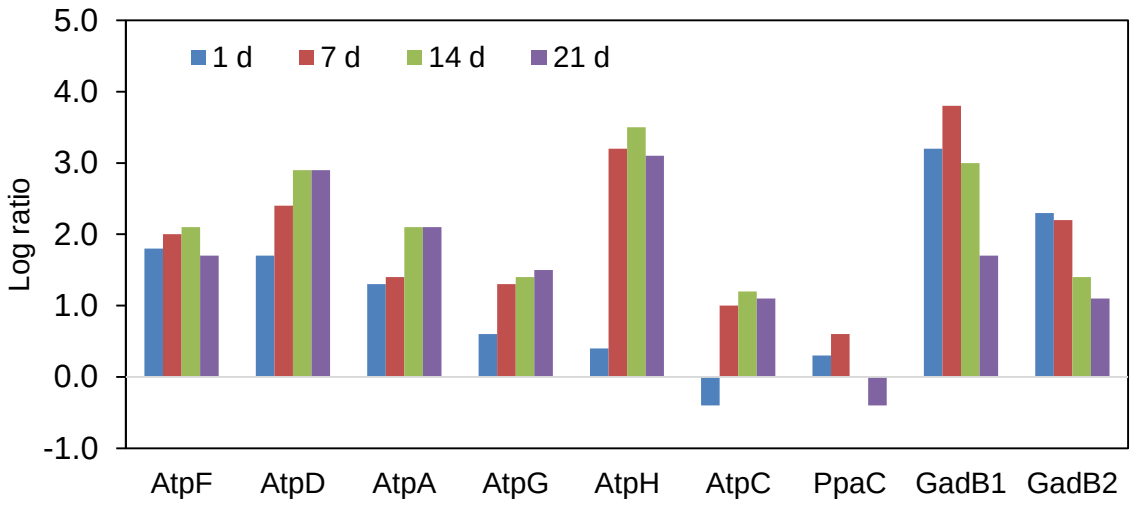

Figure 22**:** Changes in the abundance of proteins associated with oxidative phosphorylation and the GAD system during incubation of *L. monocytogenes* ScottA in TSYE broth at 37°C. F1Fo ATPase subunits – AtpF (subunit b), AtpD (β subunit), AtpA (α subunit), AtpG (γ subunit), AtpH (δ subunit), AtpC (ε subunit); PpaC –Mn-dependent inorganic pyrophosphatase; GadB1, GadB2 glutamate decarboxylase.

Assessment of the most abundant proteins associated with carbohydrate metabolism in aged cells in the aged cells indicates increased abundance of: i) enzymes in glycolysis that leads to the intermediate PEP and to pyruvate; ii) enzymes associated with mixed acid fermentation typically highly abundant in anaerobic conditions; iii) enzymes metabolising substrates besides D-glucose including glycerol, dihydroxyacetone, N-acetylglucosamine, galactitol (via tagatose-1,6-phosphate), possibly glycation products (such as glucose-lysine).

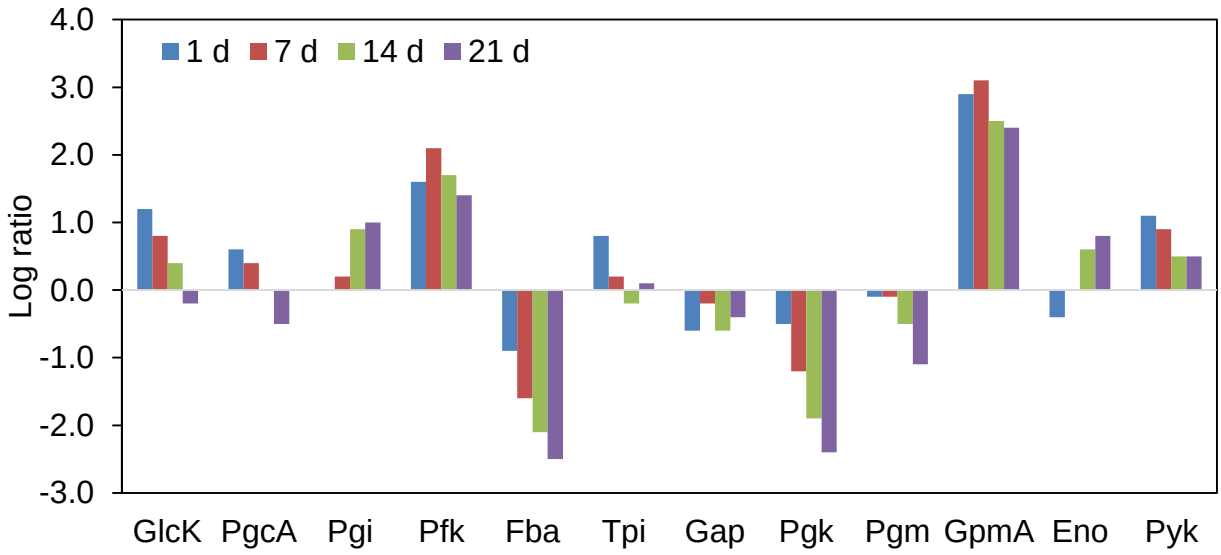

Figure 23**:** Changes in the abundance of proteins associated with glycolysis during incubation of *L. monocytogenes* ScottA in TSYE broth at 37°C. GlcK (glucokinase), PgcA (α-phosphoglucomutase), Pgi (glucose-6-phosphate isomerase), Pfk (6-phosphofructokinase), Fba (fructose 1,6-bisphosphate aldolase type II), Tpi (Triose-phosphate isomerase), Gap (glyceraldehyde-3-phosphate dehydrogenase), Pgk

(phosphoglycerate kinase), Pgm (phosphoglyceromutase), GpmA (phosphoglyceromutase I), Eno (enolase), Pyk (pyruvate kinase)

Glycolysis pathway proteins showed some specific changes in abundance in aged cells. Typically glycolysis remains relatively constant in *L. monocytogenes* cells (Bowman et al., 2012). Some enzymes were slightly more abundant in aged cultures (14 d, 21 d cells) namely Eno (EGJ25980) and Pgi (EGJ25886) (Figure 22 and 23). Enolase converts glyceraldehyde-2-phosphate to PEP. PEP is needed for phosphor donor reactions as this is the main source of energy and carbon; unsurprisingly enolase is the most abundant enzyme in aged cells (approximately 8-14% of total protein). Pgi converts glucose-6-phosphate to fructose-6-phosphate, and the increase suggests an emphasis on maintaining a flow of carbon units to PEP and fermentation so is likely compensating for reduced D-glucose availability as depicted in the metabolic map (Figure 24). Fba (EGJ26080) and Pgk (EGJ25983) decline (Figure 25) possibly reflecting the lower availability of ATP for phosphorylation reactions they carry out thus. The observed increase in GpmA (EGJ25752) after stationary phase onset likely makes up for reduced Pgm (EGJ25981) levels. The data suggests an emphasis on PEP synthesis (Figure 24) since the lack of phosphodonors effects all ensuing processes with the lower part of glycolysis increasingly derepressed for this purpose relative to 1 d cells (Figure 24).

The data suggests many enzymes involved in mixed fermentation are abundant in aged cells including PflB (EGJ25452), PflC (EGJ24943), YdaP (EGJ24241), Ldh (EGJ23714), MalS (EGJ25450) and PycA (EGJ 34571) while PflA (EGJ24942), Pta (EGJ5647), AckA1 (EGJ25118) and AdhE (EGJ5171) maintain high abundance levels though they become less abundant at 14 d and 21 d (Figure 25). The abundance of pyruvate-formate lyase PflB and the associated S-

adenosylmethionine-dependent PflB activase PflC increased 2.8-15-fold. These enzymes along with PflA convert pyruvate to acetyl-CoA and formate as part of mixed acid fermentation (Knappe & Sawers, 1990). Acetyl-CoA produced may be converted to acetyl phosphate and then to acetate via Pta and AckA1 to generate ATP. Observed increases in the abundance of pyruvate oxidase YdaP, which oxidises pyruvate to acetyl phosphate supports this activity. Another source of ATP, though likely quite limited, could be generated via succinate and malate as suggested in the metabolic map Figure 24). Malate generated in the split TCA cycle due to fumarate reductase FrdA (EGJ23868) and possibly via GABA (Feehily et al., 2013) can potentially be converted to pyruvate by reversal of malic enzyme MalS (EGJ25450) and pyruvate carboxylase Pyc (EGJ24571). The reaction is typically anaplerotic where carboxylic acids are generated to replenish the TCA cycle, however, ATP and HCO_3^- can be generated when this pathway is reversed (Sauer & Eikmanns, 2005).

Carbonic anhydrase, which concentrates CO_2 to HCO_3^-, declined with cell aging dropping to non-detectable levels (Appendices I, Cah, EGJ24310). The decline in Cah leads to the hypothesis that anaplerosis could be reversed in aged cells (and in the stationary growth phase). Further work would be needed to see if this interpretation is correct. The results suggest that fermentation is shifted to the direction of mixed acid fermentation typical of anaerobic conditions (Romick et al., 1996) based on the enzyme abundance patterns (Figure 24). The changes could also be more directed to maintaining reducing equivalent pools. Maintenance of high abundance of enzymes in the oxidative branch of the pentose phosphate pathway, however, still occurs in aged cells, including the enzymes Zwf (EGJ25507), Pgl (EGJ24074), Gnd (EGJ24913), Tkt (EGJ24844), and Rpe (EGJ25354) (see

Appendices I). These enzymes generate NAD(P)H+H^+ and D-ribulose 5-phosphate required for anabolic processes (Joseph et al., 2006). The abundance of pyruvate dehydrogenase complex proteins (PdhABCD, EGJ24556-9) was instead quite low; this complex converts pyruvate to acetyl-CoA and is important for survival in acidic conditions, such as during active fermentation when sugar levels are high (Bowman et al., 2012). The lack of carbohydrate availability likely leads to the overall scenario observed in aged cells. This is consistent with the inactive metabolism found in Chapter 2, and it is entirely possible end-product formation is negligible past 7 d.

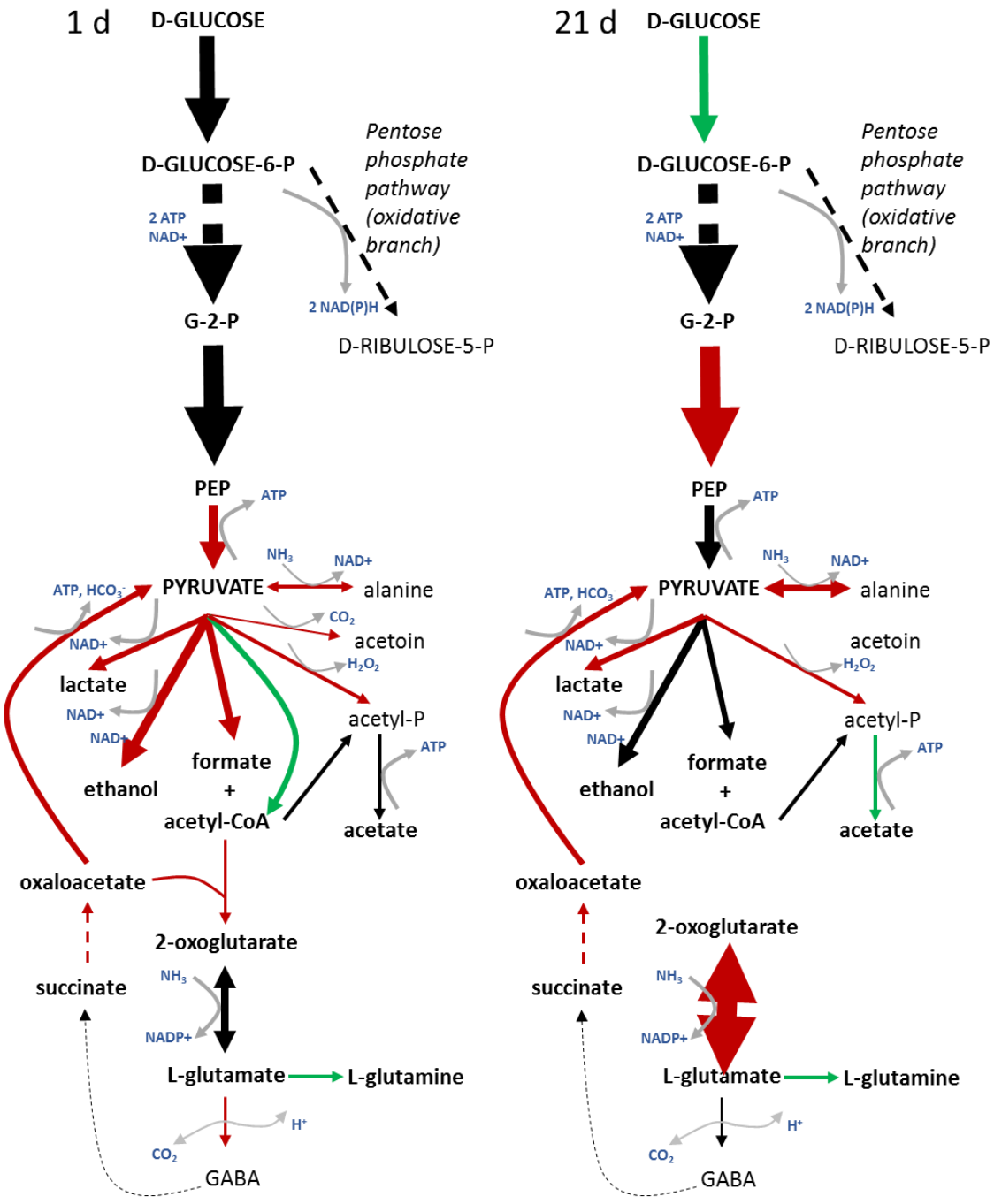

Figure 24: Metabolic map is showing central metabolism in *L. monocytogenes* ScottA grown statically in TSYE broth at 37°C for 1 d (left-hand map) and 21 d (right-hand map) in comparison to exponential phase cells. The thickness of lines denotes protein abundance while red lines indicate increased abundance and green indicates decreased abundance. For 1 d thism abundance change is relative to exponential phase cells while for 21 d the change is relative to 1 d cells (not exponential phase cells) thus indicates a progression of change. Product formation is shown where relevant. Dashed lines show a multi-enzyme pathway (the colour of the line is the general abundance trend).

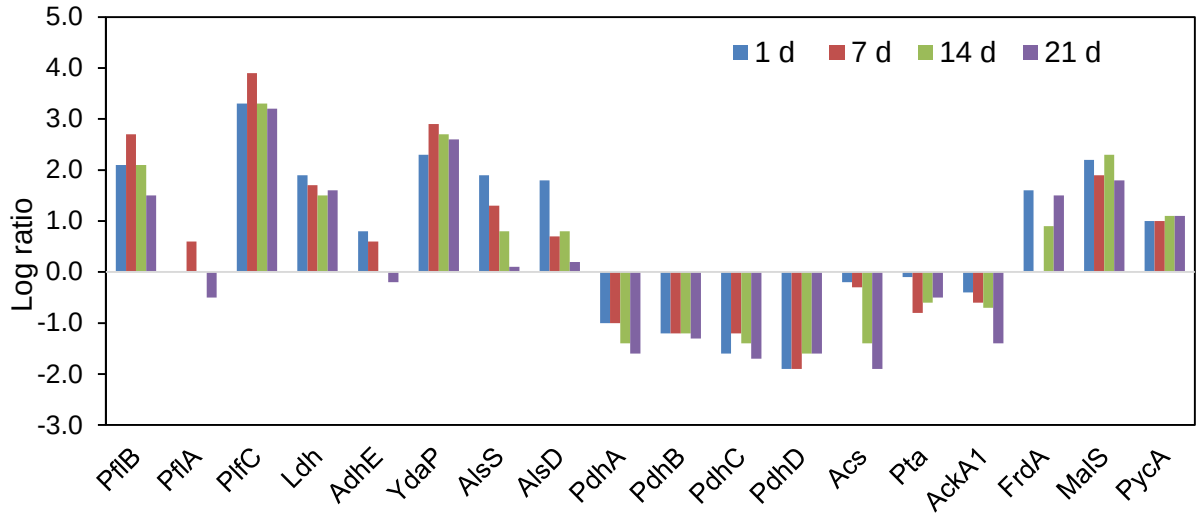

Figure 25**:** Changes in the abundance of proteins associated with mixed acid fermentation during incubation of *L. monocytogenes* ScottA in TSYE broth at 37°C. PflB (pyruvate formate-lyase), PflA (pyruvate formate-lyase), PflC (PflA/PflB activase), Ldh (lactate dehydrogenase), AdhE (acetaldehyde dehydrogenase), YdaP (pyruvate oxidase), AlsS (acetolactate synthase), AlsD (acetolactate decarboxylase), PdhABCD (pyruvate dehydrogenase complex), Acs (acetyl-CoA synthetase), Pta (phosphate acetyltransferase), AckA1 (acetate kinase), FrdA (fumarate reductase flavoprotein), MalS (malic enzyme), PycA (pyruvate decarboxylase).

Starvation likely leads to expansion of enzymes catabolising carbohydrates that may be present in the TSYE medium. This was observed for *Lactobacillus casei* starved of carbohydrates (Al-Naseri et al., 2013). Increased abundance of glycerol kinase GlpK (EGJ25075) and N-acetyl-D-glucosamine deacetylase NagA (EGJ24458), and the putative deglycation enzyme fructose lysine kinase FrlD (EGJ25527) was observed (Figure 26). The latter enzyme is unusual as it could allow the cells to catabolise Maillard reaction products (Monnier, 2005) formed in the medium after autoclaving. FrlD phosphorylates the glycated sugar, which could also be glucose lysine while FrlB (EGJ25526), which was relatively abundant (and quite constant between treatments) cleaves off the lysine residue, releasing glucose-6-phosphate. Overall, the metabolic pathway data suggests an energy starvation scenario that

seems to be a consequence of substrate depletion with all possible available substrates exploited.

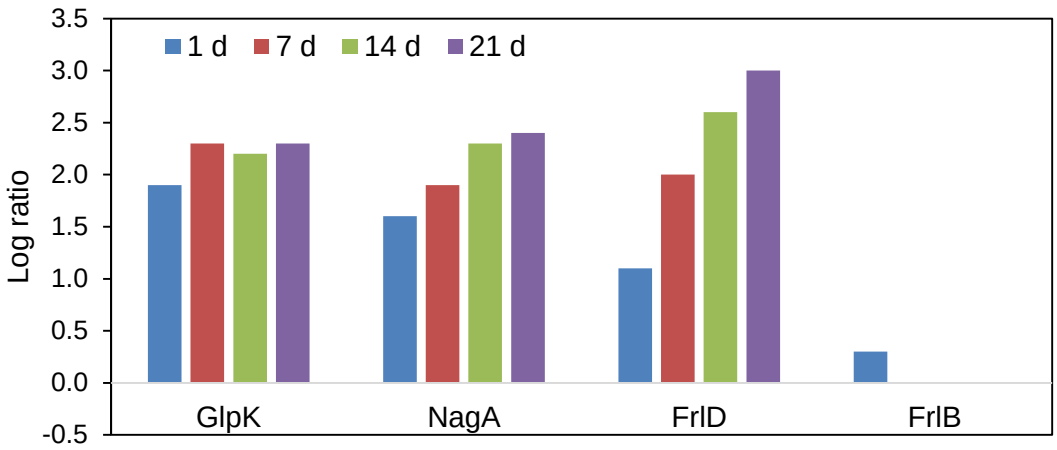

Figure 26: Changes in the abundance of proteins associated with particular carbohydrate associated catabolic enzymes during incubation of *L. monocytogenes* ScottA in TSYE broth at 37°C. GlpK (glycerol kinase), NagA (N-acetyl-D-glucosamine), FrlD (putative fructose lysine kinase), FrlB (putative fructose lysine deglycase).

3.4.5 Effect of Aging on amino acid metabolism and relation to protein translation and turnover

As mentioned in the previous chapter aging cultures could accumulate protein aggregates in cells. Protein resolubilization and refolding is the only avenue to restrict this accumulation otherwise the aggregates must be remediated. Protein proteolysis, rescue (via DnaK/J chaperone) and refolding by GroEL/ES systems is seen as the approach taken to do this remediationl (Tyedmers et al., 2010). If the cytoplasmic cell space becomes too crowded proteostasis can be hindered leading to cell toxicity. A supply of amino acids to protein translation is also required either through recycling, de novo synthesis or import. ScottA is fairly fastidious in terms of amino acid requirements for optimal growth, requiring Cys, Met, Leu, Val, Ile, Arg, His and Trp (Schneebeli and Egli, 2013). Leaving out any of the amino acids in

Schneebeli & Egli's minimal medium reduced growth yields by 4 log units and resulted in 5-fold slower growth rates. This fastidiousness appears to be due to bottlenecks in ScottA's metabolism. The proteomic data indicates many enzymes associated with the metabolism of several of these growth essential amino acids is reduced in abundance presumably due to Scott A not investing effort in de novo synthesis, which appears already inefficient due to aforementioned pathway lesions. The enzyme reduction seems most logically due to precursor limitations including PEP and pyruvate required for synthesis of aromatic and branched-chain amino acids.

Though *L. monocytogenes* cannot use amino acids directly for carbon and energy, it can exploit some for intermediary metabolism. Alanine can be converted to pyruvate via alanine dehydrogenase (Ald, EGJ25116). Ald was enhanced substantially in cells 6-20-fold, and the reaction has the advantage of also generating NH_3 which can help buffer cytoplasmic pH and provide reductant in the form of $NADPH/H^+$. An alternative explanation is that increasing usage of less energetically costly amino acids in abundant proteins such as Ala and Asp (Akashi & Gojobori, 2002) may offset energy costs in the cell. L-Ala also link the glycan strands of the cell wall, however as mentioned above it seems likely de novo PG and teichoic synthesis is lower thus would not explain a need for more L-Ala or D-Ala. This is also suggested by lower levels of D-alanine transaminase Dat. The catabolic explanation seems more likely since Ala would be relatively plentiful while pyruvate supply seems more likely a bottleneck, given it represents a critical metabolic "crossroads" of glycolysis and fermentation.

Glutamate, as mentioned above by being decarboxylated, can maintain cytoplasmic homoeostasis via GadB1 and GadB2. Glutamate dehydrogenase RocG (EGJ24076)

was also observed, interestingly, to become one of the most abundant enzymes in aged cultures, representing as much as 7% of the total protein (a 3.6-fold increase from exponential growth phase) (Figure 27). This enzyme interconverts 2-oxoglutarate and L-glutamate. What is the role of RocG in this scenario? One possibility is to maintain the proton gradient for ATP synthesis via conversion of glutamate to 2-oxoglutarate and $NADH+H^+$ and NH_3. The high levels of Ldh and AdhE would help resupply NAD^+ needed for the reaction while NH_3 accumulation could offset cytoplasmic acidification that would partly stem from increased ATPase complex activity. Going the opposite way seems less likely since enzymes leading to 2-oxoglurate in the partial TCA cycle have low and declining abundances in aged cells (i.e. CitB, CitC, Icd, Appendices I). Normally 2-oxoglutarate is the route through which anabolic reactions occur in *L. monocytogenes* (the anabolic direction of RocG) since the TCA cycle is split and as such does not supply NADH for oxidative phosphorylation (Joseph et al., 2006) as found in aerobic bacteria. Overall, this could result in L-glutamate being a bottleneck since it is a key component of many metabolic reactions. This is suggested by enzymes requiring L-glutamate as a substrate, such as a lysine (DapL), L-glutamine (GlnA) and D-alanine (Dat) synthesis since all the (initial) enzymatic steps require L-glutamate and all have reduced abundance in aged cultures. To truly understant this metabolomic analysis is necessary to investigate substrate fluxes in aged cultures.

Transport of amino acids would likely be hindered by a lack of ATP and possibly also by the weakness of the chemiosmotic gradient. This is consistent with the observation that though several amino acid/oligopeptide transporters were substantially more

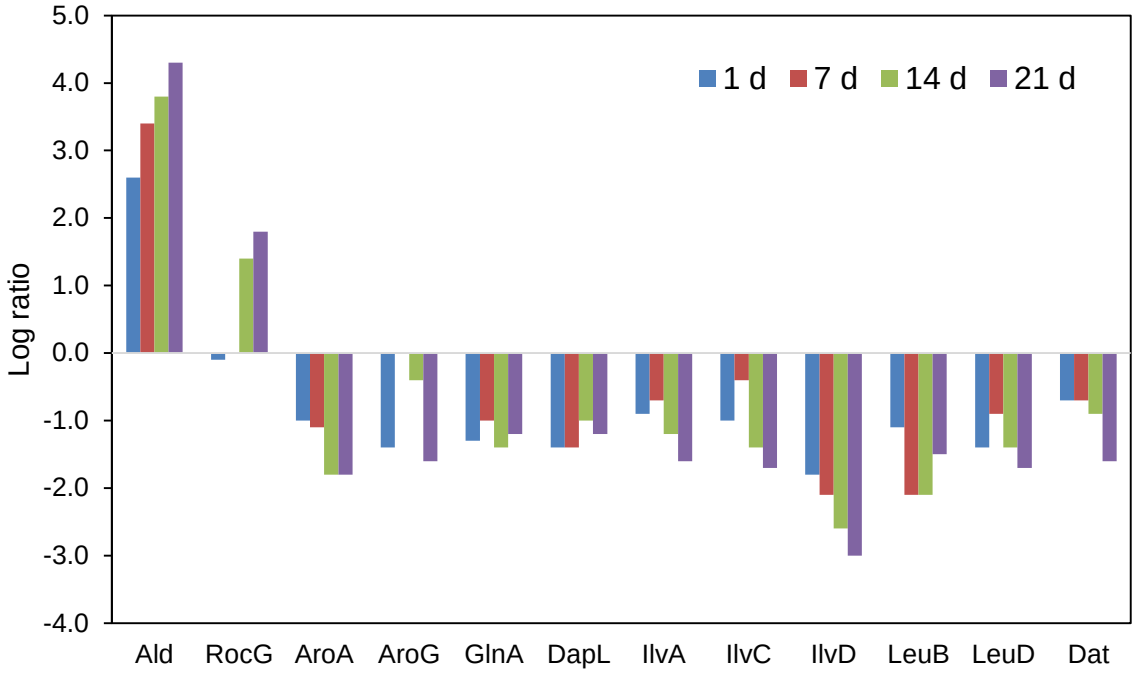

Figure 27 **:** Changes in the abundance of proteins associated with amino acid biosynthesis during incubation of *L. monocytogenes* ScottA in TSYE broth at 37°C. Ald (alanine dehydrogenase), RocG (glutamate dehydrogenase), AroA (5-enolpyruvyl-shikimate-3-phosphate synthase), AroG (phospho-2-dehydro-3-deoxyheptonate aldolase/ chorismate mutase), GlnA (glutamine synthetase), DapL (N-acetyl diaminopimelate deacetylase), IlvA (threonine dehydratase), IlvC (ketol-acid reductoisomerase), IlvD (dihydroxy-acid dehydratase), LeuB (3-isopropylmalate dehydrogenase), LeuD (3-isopropylmalate dehydratase), Dat (D-amino transaminase).

abundant at the onset of stationary growth phase; most become less abundant in aged cells dropping to levels equal to exponential growth phase (see Appendix I). This differs for the main oligopeptide ABC-type transporter substrate-binding OppA proteins (EGJ23644, EGJ25739-43), the most predominant proteins related to amino acid import show a 27-45% dip in abundance at 7 d but abundance increases as cells age (Figure 28). Several peptidases that cleave terminal amino acids from oligopeptides were alson relatively abundant in aged cells with some becoming more abundant with culture age (Figure 28). The most predominant of these include YtoP

(EGJ25147), a putative glutamyl aminopeptidase, seems to emphasise the importance L-glutamate has in supporting metabolism in ScottA, including in stress conditions. This response seems logical especially considering the fastidiousness of ScottA and the lack of metabolic pathway intermediates needed for de novo synthesis. However, findings from Chapter 2 highlighted that leucine arylamidase activity declines to below detectability in 7 d cultures. This could suggest the responses are largely futile as the lack of ATP (for protein export) may prevent deployment of these enzymes into the extracellular environment or periplasm. Further enzyme tests are warranted to determine if a wider range of substrates are not similarly affected.

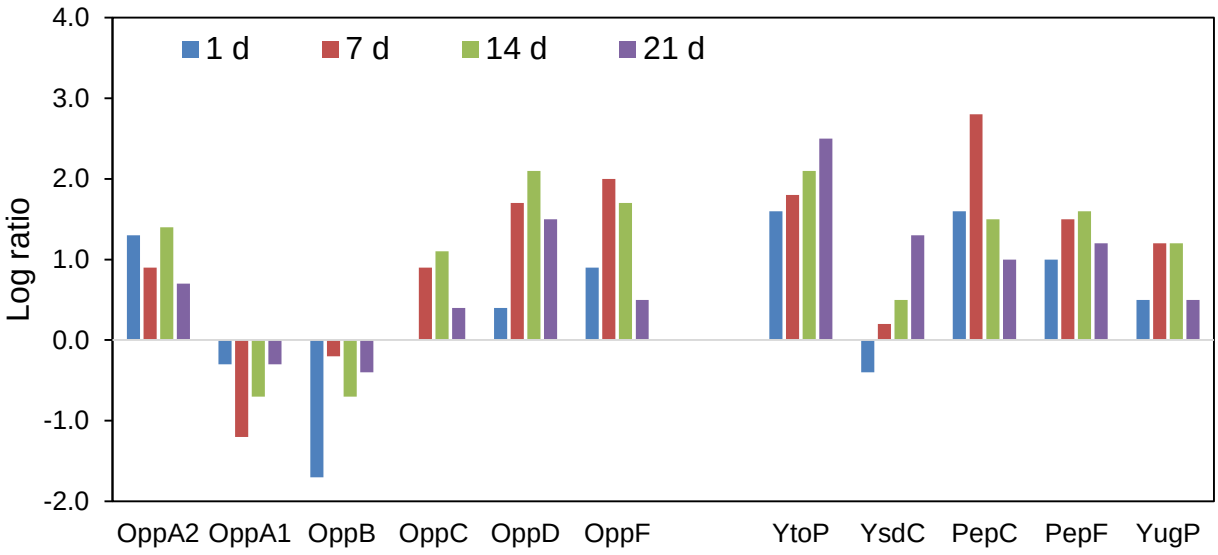

Figure 28**:** Changes in the abundance of proteins associated with ABC-type oligopeptide transporters and Proteolytic degradation during incubation of *L. monocytogenes* ScottA in TSYE broth at 37°C. ABC-type oligopeptide transporter subunits - OppA2, OppA (substrate binding subunits), OppB, oppC (permease subunits), OppD, OppF (ATP-binding subunits); peptidases (all putative) – YtoP, YsdC (glutamyl aminopeptidases), PepC (aminopeptidase C), PepF (aminopeptidase F), YugP (membrane-associated zinc metallopeptidase).

Another aspect of amino acid availability in aged cells can be potentially determined by examining the abundances of tRNA aminoacyl synthetases, which charge tRNA (Hausmann & Ibba, 2008) with amino acids for the creation of the peptide chains during translation. The following synthetases show enhanced abundance at the onset of stationary growth phase by 1.7-7.0 fold - CysS, LeuS, PheS, PheT, TrpS, TyrS, HisS, AlaS, GlyS, GlyR, and GltX (see Appendix I) and in general abundance of these enzymes is maintained in aged cells at about the same level. Several others (ValS, IleS, LysS, ArgS, MetS, ProS, ThrS, GatA), however, show lowered abundance in 21 d cells (Figure 29), with ProS having the greatest decline (10-fold). A decrease in these enzymes may presage a general decrease in protein synthesis in aged cells. Reduced levels could be brought about either by inadequate transport or synthesis (due to lack of precursors).

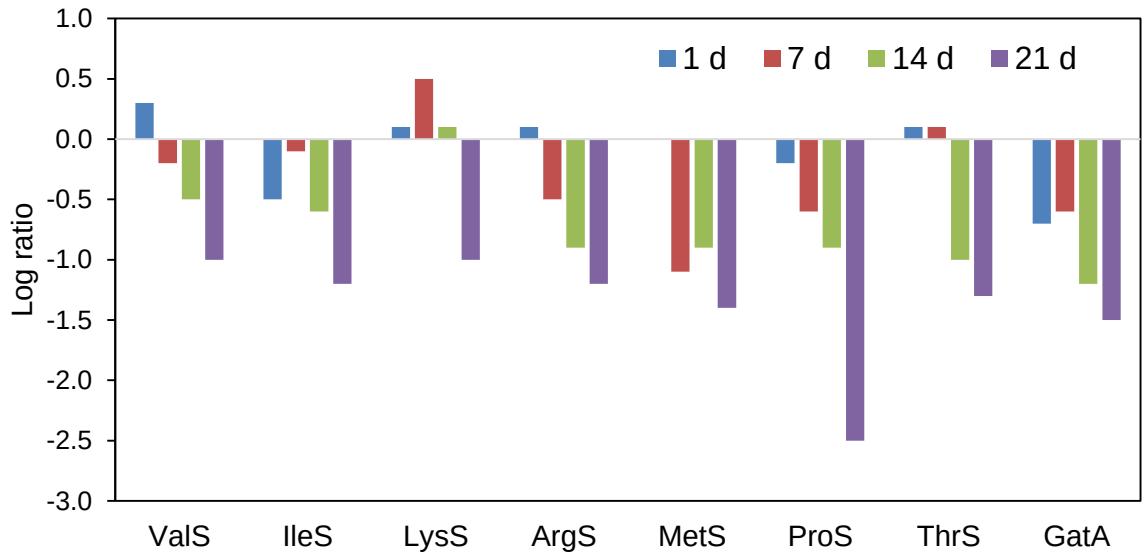

Figure 29**:** Changes in the abundance of tRNA aminoacyl synthetases during incubation of *L. monocytogenes* ScottA in TSYE broth at 37°C. GatA (aspartyl/glutamyl-tRNA amidotransferase subunit A).

The availability of precursors and available energy likely impacts the protein translation process. Based on the abundance of translation proteins the data suggest enzymes involved in translation initiation, including Fmt (EGJ25359), InfA (EGJ26135) and InfC (EGJ25320) are equally abundant in aged cells to that at the onset of stationary growth phase, however the three most important elongation factors Tuf (EGJ26177), Fus (EGJ26178) and Tsf (EGJ25192) are 1.9-4.6-fold less abundant in aged cells (Figure 30). Deformylase Def (EGJ24555) had increased abundance in 21 d cells. However methionyl aminopeptidase Map (EGJ25246) was reduced in abundance. The initiator proteins likely are acting in a compensatory fashion against the presumed lower elongation rates and lack of precursors, in particular methionine. Aging seems to strike at the heart of translation since the initiation of translation is a conserved process where tRNA-Met is formylated by Fmt to rRNA-fMet, which then acts as the N-terminal peptide residue in nascent peptide chains. At the end of translation, Def deformylase converts the N-terminal formylmethionine residue back to Met at which point Map cleaves it off the chain. These results suggest that translation could be slowed by lowered availability of loaded tRNA-Met . The reduction of elongation factors and Map over time between 1 d and 21 d suggests a global decline in the translation apparatus activity probably occurs due to the tRNA-Met shortage. This decrease also could correspond to the observed decline in ribosomal proteins proposed by the T-profiler results. In aged cells, 16 (14 d) and 19 (21 d) ribosome proteins showed substantial reductions in abundance (see Appendices I), which suggest most likely overall ribosome numbers have declined, and this is despite larger cell volumes. It was observed that Frr (EGJ24852), the ribosome recycling factor was more abundant, though did not increase with cell age (Figure 30). Frr recycles the ribosome upon translation

termination allowing it to commence a new round of peptide synthesis. It also stimulates translation and ensures correct initiation of translation. The increase in Frr likely compensates for a diminished capacity for conversion likely not sufficient to offset issues accumulated in aging cells.

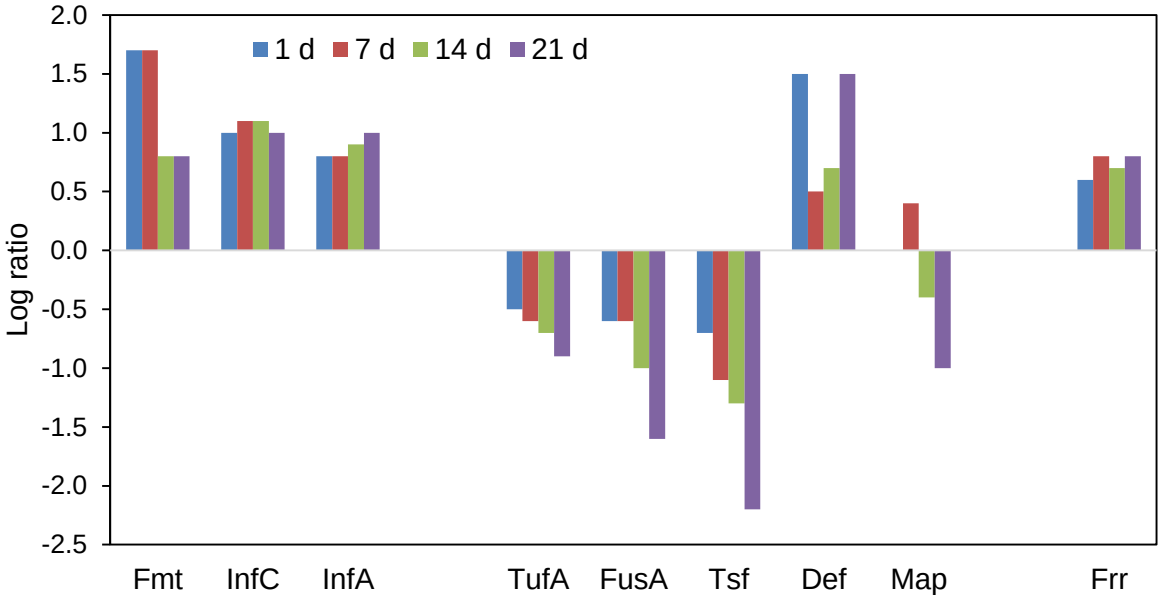

Figure 30**:** Changes in the abundance of proteins associated with translation during incubation of *L. monocytogenes* ScottA in TSYE broth at 37°C. Fmt (methionyl-tRNA formyltransferase), InfC, InfA (initiation factors), TufA (elongation factor Tu), FusA (elongation factor G), Tsf (elongation factor Ts), Def (N-formylmethionine deformylase), Map (methionyl aminopeptidase), Frr (ribosome recycling factor).

The subsequent process of protein folding and turnover would be theoretically similarly impeded including the fact they are rather an energy demanding processes. Rothman and Schekman (2011) indicated the energy of 14 ATP molecules (converted to ADP) is required to fold one protein through a single round of folding. In addition, aging associated aggregation and possibility of crowding of molecules in the cytoplasm as cells change in morphologuy (Banas et al., 2015) results in the scenario that folding and subsequent turnover is rendered less effective. If the key

proteins of folding are considered first, the proteomic data suggest an overall perturbation of the system relative to what is measured in the exponential growth phase. Trigger Factor Tig (EGJ24807), and chaperone DnaK (EGJ25010) show distinct and progressive reductions in abundance over time, at 21 d these proteins are only at about 33-40% of the abundance observed in the exponential growth phase. Co-chaperone DnaJ (EGJ25009) abundance stays relatively constant as does GrpE (EGJ25011), GroEL (EGJ25612) and GroES (EGJ25613). DnaK along with Tig have the important role of folding nascent and already formed proteins. Tig stabilises partly folded proteins as they are guided through folding transitions to the final native state (Mashaghi et al., 2013). DnaK catalyses the folding process, rescues misfolded proteins for a new round of folding and ensures exported proteins are in the correct native state after cleavage of the secretory signal peptide. Thus DnaK and its associated proteins (especially GroEL and GroES) are well known as heat shock proteins, e.g. Hsp60 since they act to rapidly repair the damage done by sudden thermal stress on protein conformations. Reduced levels of Tig and DnaK protein suggest folding and recovering of proteins is reduced in aged cells which are important in relation to protein aggregation.

Several enzymes of the proteasome ClpC1 (EGJ23738), ClpC2 (EGJ25753), ClpP1 (EGJ24620), ClpP2 (EGJ25993), and membrane-targeted protease HtrC/DegP (EGJ24465), which oversees generalised protein quality control and turnover show elevated abundance in aged cultures (Figure 31). This suggests that protein aggregate solubilization may be occurring but increase levels could be also due to protein folding stalling. The unfoldase complex subunits HslU and HslV (also called ClpY and ClpQ, EGJ24818-9) show an interesting response in that HslV, the peptidase (Ruiz-Gonzalez & Marin, 2006) has a substantially reduced abundance

possibly suggesting less available protein for folding. Abundance reduction of other enzymes associated with processes subsequent to protein folding and export, such as prolyl isomerase PpiB (EGJ25904) and signal peptide peptidase SppA (EGJ25122) could

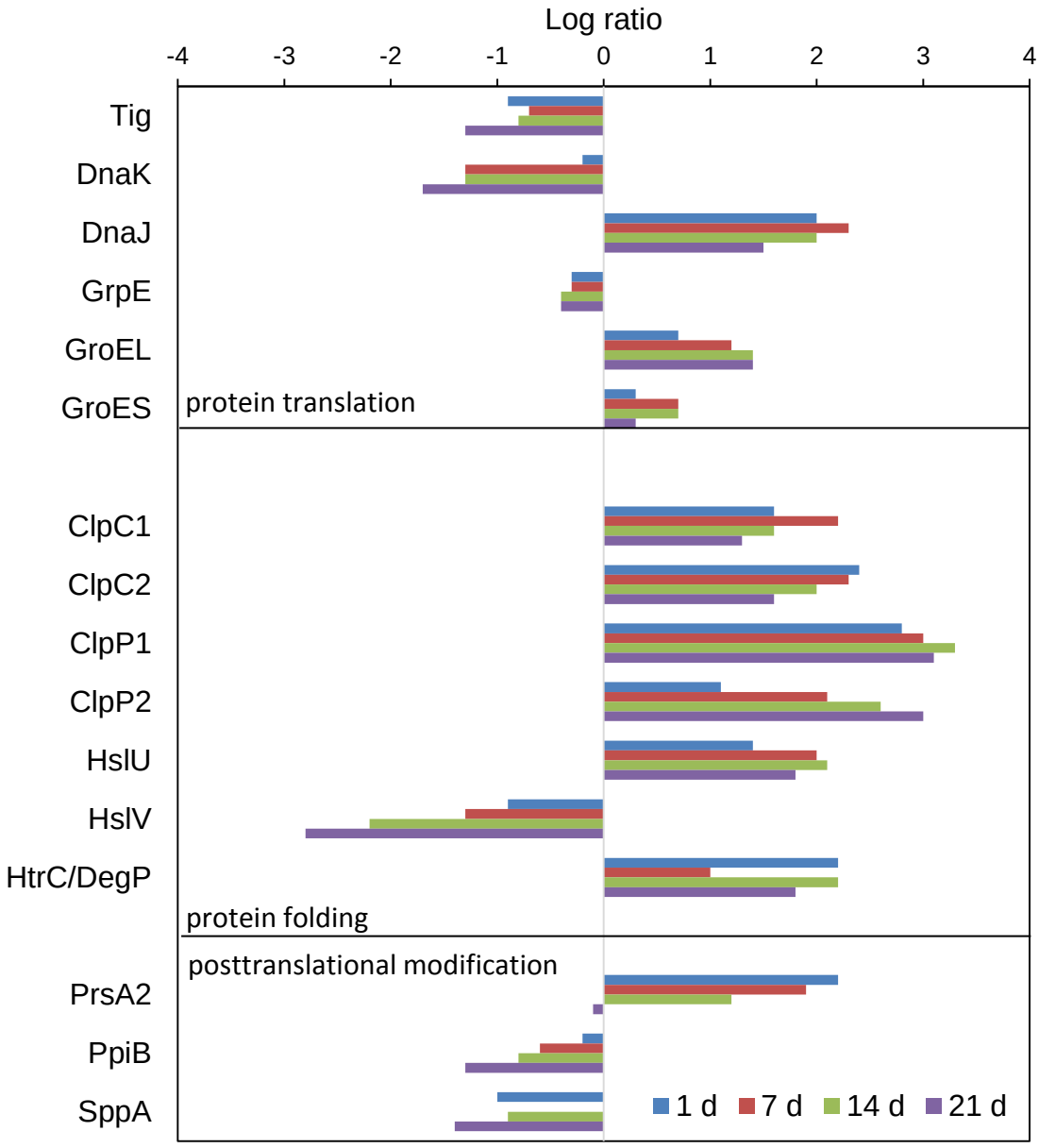

Figure 31**:** Changes in the abundance of proteins associated with protein folding, turnover and posttranslational modification during incubation of *L. monocytogenes* ScottA in TSYE broth at 37°C. Tig (trigger factor); DnaK/DnaJ/GrpE (Hsp70 molecular chaperone complex); GroEL/GroES (chaperonin complex); Clp

endopeptidase - ClpC1, ClpC2 (ATP-binding subunit), ClpP1, ClpP2 (protease subunit); HslV/HslU unfoldase complex; HtrC/DegP (serine endopeptidase); PrsA2 (post-translocation molecular chaperone/foldase), PpiB (prolyl isomerase); SppA (signal peptide peptidase).

also suggest lower protein outputs from translation. In this respect, prolyl isomerases are needed to ensure Pro residues are in the correct *trans* conformation; Tig may also perform this duty in *L. monocytogenes*. SppA cleaves signal peptides off proteins that need to be trafficked to the cell wall or beyond; its lower level could suggest fewer protein substrates are available. The lower abundance of FtsH, a membrane-anchored protease possibly associated with cytokinesis (Weiss, 2004) (see section 3.4.4) also suggest the same though its protein substrates still require elucidation. The overall observations thus suggest that limited resources in the cells permeates through to central processes of the cell and fundamentally impedes translation and folding and thus could be root source of the loss of culturability.

3.4.6 Effect of aging on DNA processes, stress defence mechanisms and possible promotion of aspects of virulence mechanisms

Damage to DNA has been indicated as being a factor in aging. Among DNA repair proteins (Appendices I) none were more abundant in aged cells (14 d, 21 d) while RecA abundance declined 17-fold between the 7 d and the 21 d samples (Figure 32). Since RecA activates the SOS response regulon in *L. monocytogenes* (van der Veen et al., 2010) the decline seems evidence that additional DNA repair is not invoked in aged cells. This could be due to lack of required precursor and/or energy needed for the processes involved. This is suggested by elevated abundance in aged cells of Dgt (EGJ26181), DeoD (EGJ25523), PupG (EGJ25489) and Upp (EGJ26063) (Figure 32) all of which are involved in nucleoside salvage. Dgt

salvages deoxyguanosine and guanosine from dGTp and GTP; DeoC and Ndk salvage purine and pyrimidine nucleosides; while Upp and PupG salvage pyrimidine and purine ribonucleosides, respectively. The data strongly points to a slowdown in de novo synthesis with start point enzymes showing lower abundance – the ATP-requiring enzyme homologs of phosphoribosylpyrophosphate synthetase (Prs1 – EGJ23703, Prs2 – EGJ24026) the first step of nucleic acid synthesis both decline in abundance in 14 d and 21 d cells relative to 1 d cells. Several enzymes that process nucleic acids to (deoxy)(ribo)nucleotides are also similarly reduced in abundance including GuaA, GuaB1, GuaB2, Ndk, PnpA, Pdp, NrdE, NrdF and Drm (Figure 32, see also Appendix I). Overall, DNA repair seems to be diminished or at a lower priority in aged cells likely because the system is no longer capable of enacting it, thus accumulation of DNA damage, if it is occurring, could continually accumulate, however, it is less likely a direct source of cell inactivation than autolysis, given the degree of inactivation and time frame, however, an interrelation cannot be excluded.

A diverse range of proteins maintains cell homoeostasis in terms of organic and non-organic chemicals that if excessive can lead to cell component damage and/or enzyme inhibition, for example, oxidative stress. The overall landscape of such proteins in aged cells seems dynamic, but there is no evidence of unusually specific responses. The compatible solute ABC-type carnitine uptake transporters OpuCA/OpuCC (EGJ24962-64) show 4-5-fold abundance increases at 7 d and 14 d but become less abundant at 21 d (Figure 33). Glycine betaine uptake declines (indicated by ATP-binding protein GbuA – EGJ24518) while ZnC/Cd/Cu exporter ZosA (EGJ24157) abundance is maintained in 21 d cultures at levels found in early stationary phase cells (Figure 33). From these results it might be surmised, there is

no systematic uptake of compatible solutes (besides what happens in the standard stationary growth phase) while toxic metal ion management is maintained.

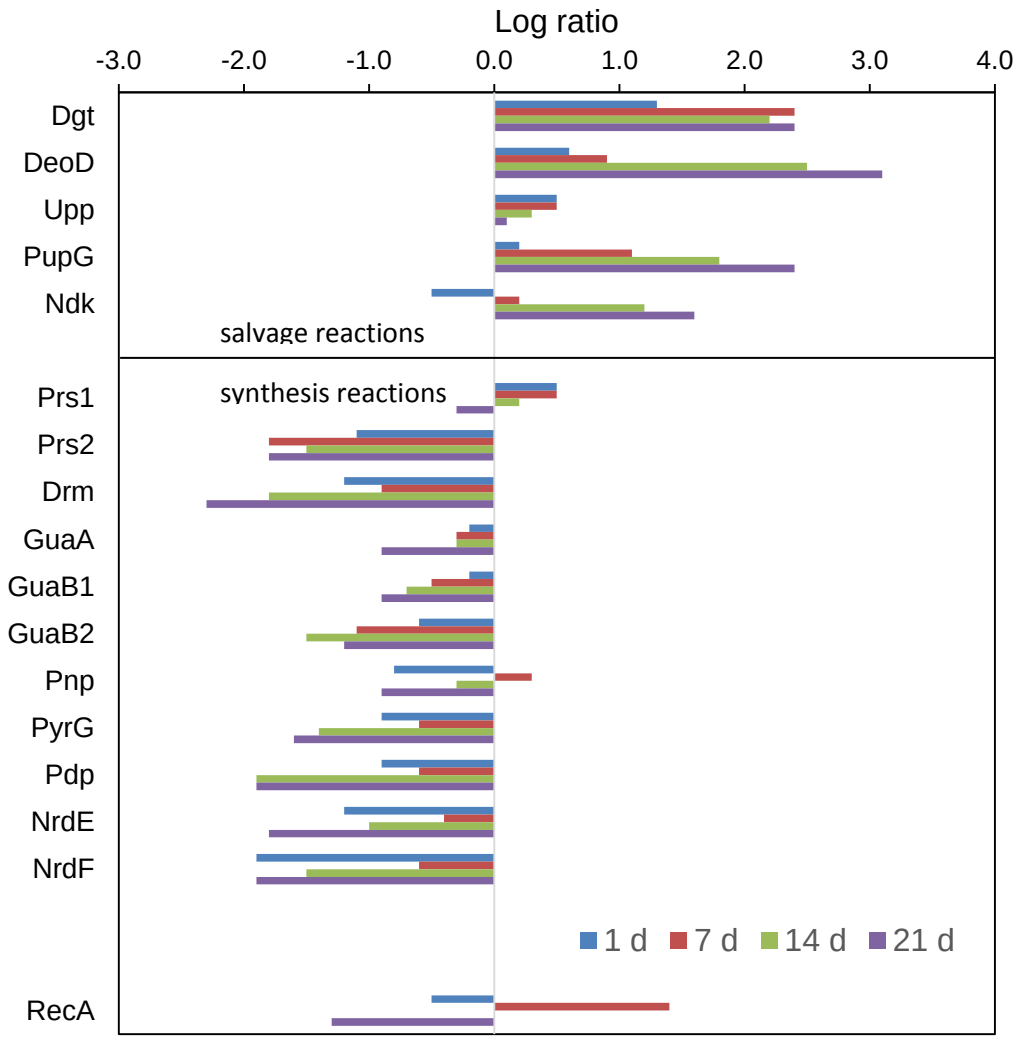

Figure 32**:** Changes in the abundance of proteins associated with nucleic/nucleotide salvage and synthesis during incubation of *L. monocytogenes* ScottA in TSYE broth at 37°C. Prs1, Prs2 (phosphoribosyl pyrophosphate synthetase); Drm (phosphopentomutase); GuaA (GMP synthase); GuaB1, GuaB2 (inosine monophosphate dehydrogenase), Pnp (polyribonucleotide nucleotidyltransferase), PyrG (CTP synthase), Pdp (pyrimidine-nucleoside phosphorylase), NrdE, NrdF (ribonucleoside reductase); RecA (DNA recombinase).

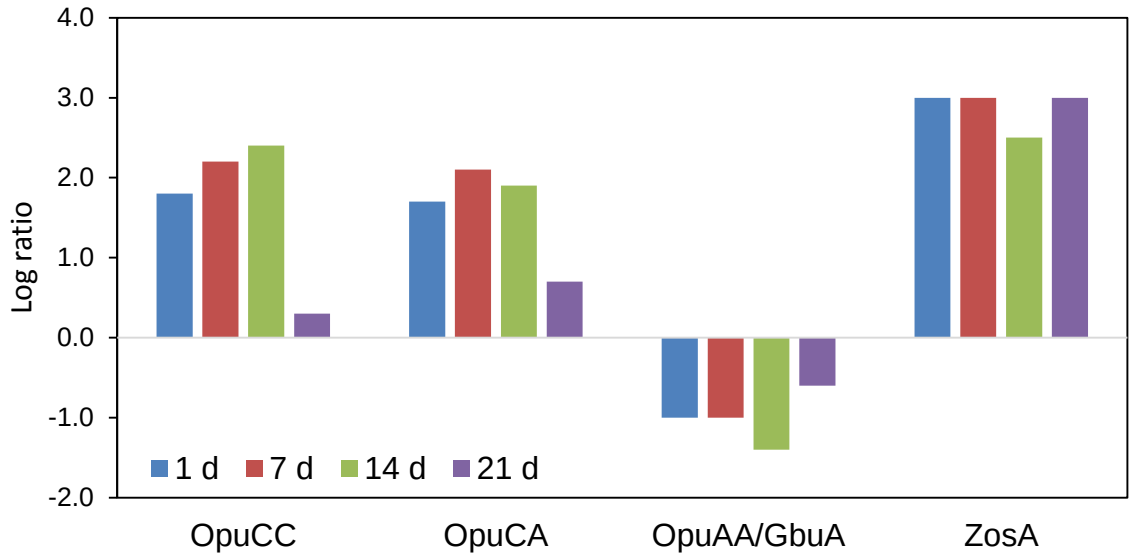

Figure 33**:** Changes in the abundance of proteins associated with nucleic/nucleotide salvage and synthesis during incubation of *L. monocytogenes* ScottA in TSYE broth at 37°C. OpuCC, OpuCA (carnitine uptake ABC-type transporter subunits); OpuAA/GbuA (glycine betaine uptake ABC-type transporter ATP-binding protein); ZosA (Zn/Cu/Cd exporting P-type ATPase).

The bile salt conjugate hydrolase Bsh (EGJ25611) was relatively abundant but also declines as cells age. The main enzymes of oxidative stress management are less abundant in aged cells compared to the onset of stationary growth phase where oxidative stress tolerance is bolstered. This is likely a response to a less active metabolism. Catalase KatX (EGJ26313) levels in aged cells are 9-10-fold lower than exponential phase cells while superoxide dismutase SodA (EGJ 24975) declines 2 to 3-fold in aged (14 d, 21 d) cells though it still remains relatively abundant (Figure 34). The levels are much lower than what is seen in acid stressed cells (Bowman et al., 2012).

There is some increased abundance of other proteins linked to oxidative stress management (such as OhrA – EGJ24407, YwfI – EGJ25658). OhrA, similar to *E. coli* OsmC, is a hydroperoxidase and possibly required for proper stationary growth survival (Lesniak et al., 2002). There is some suggestion methylglyoxal metabolism

is boosted in aged cells through the abundances of the enzymes involved are quite low. Methylglyoxal forms as a reactive byproduct of enzymatic phosphate elimination from glyceraldehyde phosphate and dihydroxyacetone phosphate; proteins subsequently suffer glycation damage. YraA (EGJ25839), very similar to *E. coli* protein YhbO, likely acts as an amino acid deglycase repairing glyoxal- and methylglyoxal-glycated proteins (Abdallah et al., 2016); its abundance was boosted >10-fold in aged cells (Figure 34). The removed (methyl)glyoxal groups are converted to lactate. Other glutathione–mediated enzymes YvgN (EGJ26117) and GloA-like protein YwbC (EGJ25714) (Figure 34), putatively degrade free methylglyoxal to lactate also preventing cell toxicity. Overall there are few signals of any systematic defence priorities in aged cells except for DNA-binding Dps, mentioned in section 3.4.3. Increased abundance of enzymes associated with S-adenosylhomocysteine detoxification, including Mtn (EGJ25031) and LuxS (EGJ24828) was evident (Figure 34). These enzymes help remove S-adenosylhomocysteine a toxic product which can form in cells during methyl transfer reactions via S-adenosylmethionine. LuxS converts the result of the response of Mtn S-ribosyl homo cysteine to homocysteine; there is no evidence LuxS has a role in quorum sensing via the autoinducer-2 pathway (Garmyn et al., 2009).

L. monocytogenes can survive stress by invading host eukaryote cells and does so by producing an elaborate array of virulence factors. The factors are activated at 37°C (Johansson et al., 2002; Leimeister-Wachter et al., 1992; Loh et al., 2009) when the cells experience low glucose and other utilisable carbohydrate levels (Chakraborty et al., 1992; Leimeister-Wachter et al., 1990). Virulence is under complex control at both the transcriptional and post-transcriptional level since it is a substantial commitment of cell resources.

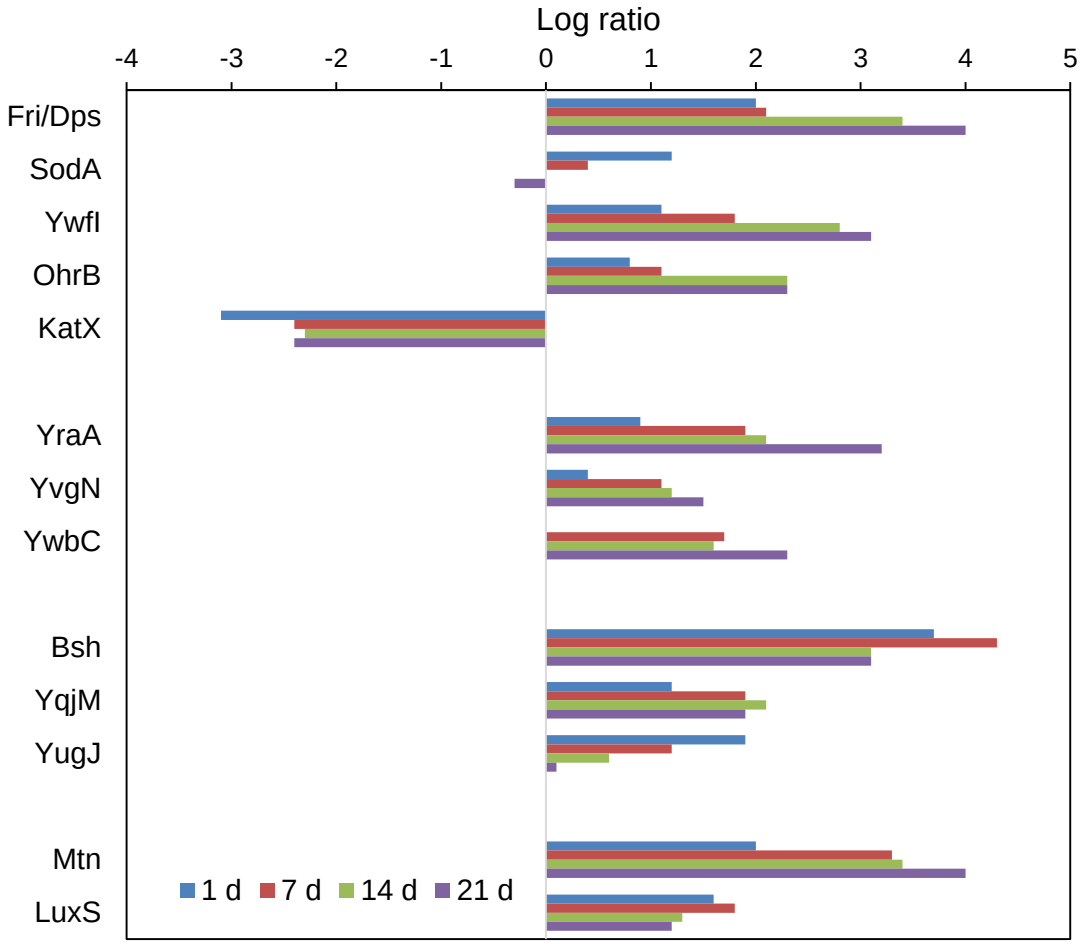

Figure 34**:** Changes in the abundance of proteins associated with detoxification reactions during incubation of *L. monocytogenes* ScottA in TSYE broth at 37°C. Fri/Dps (ferritin iron/DNA –binding protein), SodA (superoxide dismutase), YwfI (putative heme peroxidase/chlorite lyase), OhrB (organic hydroperoxides), KatX (catalase); YraA (amino acid deglycase), YvgN (multifunctional methylglyoxal reductase), YwbC (putative glyoxalase I); Bsh (conjugate bile hydrolase); YqjM (putative NemA like N-ethylmaleimide reductase), YugJ (putative butyraldehyde dehydrogenase); Mtn (S-adenosyl- homocysteine nucleosidase), LuxS (S-ribosyl homo cysteine lyase).

Virulence and the PrfA regulon in aged cells are investigated in Chapter 5. The results here showed that several virulence proteins are abundant in aged cells though the response is quite selective. Some have been mentioned above in section

3.4.2, including autolysins Auto, Iap and Ami, involved in invasion and initial adherence.

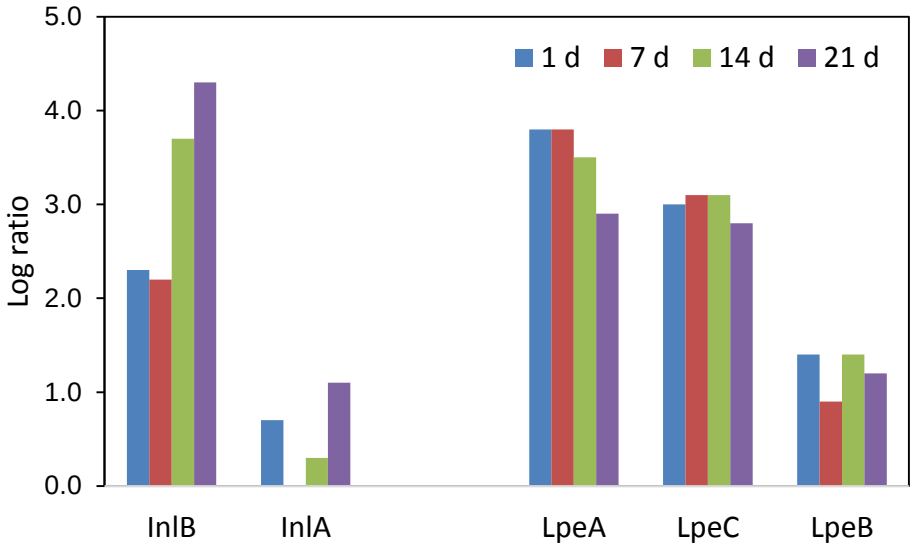

Figure 35**:** Changes in the abundance of proteins associated with virulence-related processes during incubation of *L. monocytogenes* ScottA in TSYE broth at 37°C. InlB (internalin B), InlA (internalin A), LpeABC (manganese/zinc uptake ABC-type transporter subunits).

Invasion internalins InlB (EGJ23959) and InlA (EGJ23958) are more abundant in aged cells. InlB allows generalised invasion of human cells via cell tight junctions. Its abundance was approximately 4-5-fold that of 1 d cells though quite variable between replicates (Figure 35). InlA, required for invasion of GI tract enterocytes though at low abundance was distinctly more abundant in 21 d cells (Figure 35). A further cell wall protein more abundant in aged cells is cell wall sorted surface protein (EGJ25726) not linked to virulence; this protein is located in an operon coding proteins involved with heme and/or iron scavenging (Malmirchegini et al, 2014). As mentioned above bile resistance protein (Bsh) was relatively abundant in aged cells (Figure 34). Increasing Bsh levels could be a result of low oxygen concentration in the medium (Dussurget et al., 2002) though Bsh enzyme abundance increases in

response to a range of stresses (Bowman et al., 2012). ABC-type manganese/zinc transporter subunits LpeABC (EGJ25383-5) were significantly increased in abundance. Lipoprotein LpeA, the substrate binding subunit of LpeABC is required for entry of *L. monocytogenes* into nonprofessional phagocytes but not needed for the invasion of macrophages (Réglier-Poupet et al., 2003).

A 7-fold decline from 1 d to 21 d cells was however observed for PrsA2 (EGJ25766), a critical post-translocation secretion chaperone required for virulence and contributes to the integrity of the *L. monocytogenes* cell wall. PrsA2 plays a unique and important role in *L. monocytogenes* pathogenesis by promoting the activity and stability of secreted virulence factors LLO, PldB, flagellin, and PG transpeptidases (Alonzo et al., 2011; Cahoon & Freitag, 2014). The reduction in PrsA2 could contribute to the inability to detect haemolysis by aged cells in comparison to 1 d cells (Chapter 2). Thus export is perhaps hampered for certain proteins such as LLO though not necessarily for the autolysins, which likely also use the Sec-dependent system for secretion. Other proteins related to virulence including those with key roles in host survival, immune system evasion or subversion and cell-to-cell spread were present at only low abundance and did not seem more abundant in aged cells. The overall results seem to suggest certain key invasion proteins are promoted once cells are ATP-depleted and thus could mimic in situ adaptation responses in the host that lead to cell entry. It is assumed if this is the case other elements of the virulence pathway would subsequently activate in vivo.

3.5 Conclusions

Overall, the results indicate metabolic slow down occurs in aged cells with a shift to fermentation; there is evidence of scavenging alternative substrates however by 14 d and 21 d such activities decline as they are effectively futile. The cells demonstrate possible cytokinetic dysfunction combined with evidence of autolysis, a combination that would lead to inevitably to a high level of inactivation. A survivor subpopulation hoever persists. It could be assumed that proteostasis mechanisms still are able to cope with protein aggregation in these cells. Based on Chapter 2 data transfer to fresh media results in recovery in the lag phase though as cells age this recovery takes longer and is seemingly less successful, which could suggest cells not recovering suffer possible terminal aging defects to proteostasis or to other cell metabolic systems. Other evidence points to a possibility the survivor population is more virulent due to several key invasion proteins abundant in the overall population. Specific invasion experiments were not performed though owing to the much-reduced cell viability that would make this task problematic. A modification of standard cell invasion assays could be used to determine if these cells are invasive but developing and testing this is beyond the scope of the thesis research objectives.The data suggests the tactic of invasion if induced in aged cells would likely only benefit the survivor subpopulation which by 21 d is <log 4 CFU ml^{-1}.

4 Proteomic Analysis of Listeria Monocytogenes ScottA within the Lag Phase

4.1 Abstract

The proteome dynamics of aged *L. monocytogenes* ScottA recovering during the lag phase was investigated. A quantitative analysis of ScottA proteome was based on cells first being grown at 37°C over an extended stationary growth phases (1, 7, 14 and 21 days) and then allowed to recover in fresh TSYE media over 0.5 to 4 hours. A total 459 proteins were estimated for abundance for all treatments. During the first 0.5 h of lag phase *L. monocytogenes* ScottA rapidly altered its proteome partially rebounding from the aged state but not completely reattaining the original exponential phase state; this was evident at all time points. The length of initial incubation generally did have a substantial effect on lag phase responses at the protein level. Proteins associated with carbohydrate catabolism became more abundant in the lag phase. Analysis of intermediary metabolic pathways suggests a shift to mixed acid fermentation also occurs. The data also points to activation of initial stages of biosynthetic pathways for cell components including peptidoglycan, fatty acids, and menaquinone, but not broad-scale increased abundance of whole pathways. The molecular chaperone Hsp70 complex, detoxification-associated proteins, compatible solute uptake transporters, and metal ion homoeostasis transporters were detected at higher abundances relative to aged cultures, potentially indicating processes are involved in remediation of the cytoplasmic contents. Overall, lag phase cells adjustments cover a wide range number of anabolic and remedial processes; however, the activation responses collectively do not represent a “full steam ahead” approach but is constrained possibly to ensure

precursor and energy resources can be accumulated prior to the exponential growth phase.

4.2 Introduction

The bacterial growth curve is considered to involve four phases: lag, exponential, stationary and death/decline. The lag phase is the earliest stage in the bacterial population growth cycle. It is the time that bacteria use to recover and adapt to a new environment (Rolfe et al., 2012). This process involves changes in the cell biochemistry (Monod, 1949). During the exponential phase, bacterial cells divide, and the biomass increases exponentially at definable rates over a specified period of time. In a non-continuous culture system, the exponential phase transitions to the stationary phase where bacterial metabolic activity decreases, cell numbers no longer increase, while a general stress response is manifested. Eventually, as a result of the accumulation of inhibitory metabolic products and cell component damage cells starts to inactivate and potentially even lyse thus the population is considered to decline unless cells are able to move to a new environment to start a new cell cycle. Cells in each of these phases have been optimised for the analysis of intracellular metabolites and combined transcriptome, and proteome analysis has been carried out, especially in the stationary growth phase (Kolter et al., 1993; Sonenshein, 2005; Hengge, 2011). However, significant knowledge gaps still exist in relation to the lag phase, and there is no comprehensive picture of the biochemical and molecular genetic activity of bacteria during this critical period.

Mellefont & Ross (2003) interpreted the lag phase as the amount of work required to be done by bacterial cells to adapt to a new environment and the rate at which this work can be completed. The causes of lag could be (i) change in nutrition, (ii) change in the physical environment, (iii) presence of an inhibitor, (iv) spore

germination, and/or (v) state of the inoculum (Pirt 1975). So how long is the lag phase? Many factors are influencing bacterial lag time the most important of which include the history of the cells, initial cell counts, and the past and present environment.

Predicting the lag phase duration is very important for generating process models that can be applied to such endeavours as risk assessment of food-borne pathogen growth. To date, accurate predictions are difficult to achieve as there are many factors influencing lag phase behaviour (Swinnen et al., 2004), and the associated mechanisms that determine lag time are not entirely understood. However, Robinson et al. (1998) generated an important hypothesis to determine the lag phase duration (i) the amount of work that cell has to perform to adopt to a new environment, and (ii) the rate at which it can perform that work :

<lag> . <rate> = <work>

A primary model establishes the evolution of cells number in a constant environment (over time), while a second lag phase model can be used to determine how environmental factors affect the lag time, designated as *λ.* Most primary models that have been used are deterministic or stochastic population models (Baranyi & Roberts 1994; Koseki & Nonaka 2012). One of the disadvantages of these models is that they have not been experimentally proven and thus a better understanding of the mechanism of lag phase could help develop the more predictive power of lag phase duration. The experiments carried out in this study tests the hypothesis that the *cell age* influences the rate at which cells recover and resolves the lag phase due to specific effects impacts on cell physiology. In addition, the recovery and adaption in lag phase involve fundamental metabolic changes that are common to most

bacteria. The overall aim of this study is to describe the biochemical mechanisms of recovery in model bacterial strain *Listeria monocytogenes* Scott A. The effect of cell aging was explored in chapter 2 and 3 (summarised as a schematic in Figure 36) and this study in effect studies the protein-level processes that are activated and suppressed in lag phase as Scott A recovers from these aged states. The specific aims are thus to determine i) what major metabolic pathways are activated and when in lag phase; ii) does the cell age and its associated deleterious effects have an effect on the recovery process from a protein level view; and iii) understand how the lag phase is regulated in ScottA. The latter aim is explored in depth in Chapter 5; this chapter focuses on the two former aims.

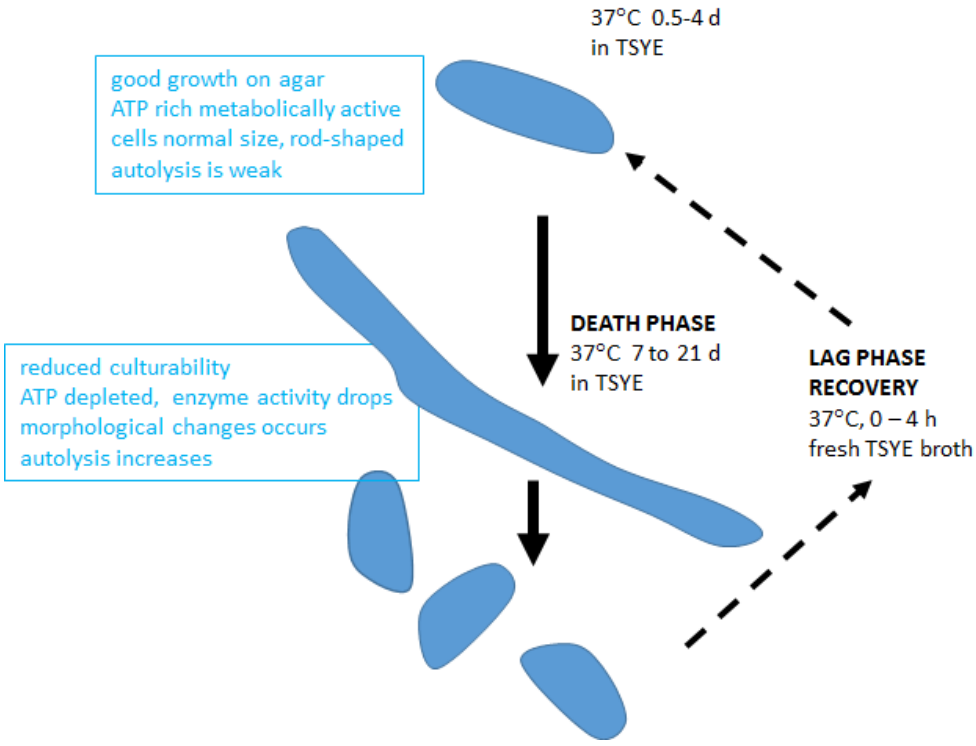

Figure 36: Experiment design for assessment of lag phase recovery of *L. monocytogenes* Scott A. Age cells (see Chapter 3) were incubated with fresh TSYE media and proteins extracted and quantified via LC/MS/MS. The time period of incubation varied based on relative duration of lag phases thus 21 d cells were incubated up to 4 h, and 1 d cells were incubated up to 0.5 h. The phenotypes indicated above for exponential, and ages cells are

based on data from Chapter 2. The protein abundances were compared to protein profiles derived from stationary growth phase (aged) and exponential phase cells.

4.3 Methods

4.3.1 Preparation of Inocula

Listeria monocytogenes ScottA serotype 4b, originally isolated from improperly pasteurised milk associated with a listeriosis outbreak in 1983 in Massachusetts USA (Fleming et al., 1985) was used in this study. A single colony of the organism was transferred into 200 ml of tryptone soya broth plus 0.6% yeast extract (Oxoid) (TSYE) and incubated at 37°C for 24 h. A 200 µl aliquot of the inocula was transferred into a current 200 ml volume of TSYE broth each day for three successive days to derive cells within the same physiological state. Cells in the exponential phase (12 h) from the passaged culture was inoculated into a current 200 ml volume of TSYE broth and incubated for 1, 7, 14 and 21 days at 37°C.

4.3.2 Proteomics Experiment

4.3.2.1 Culture Preparation

Cells were harvested on days 1, 7, 14 and 21 (20 mL each) (as done in Section 3.3.1) using centrifugation (4000 g for 10 min at 4 °C), then cell pellets were washed twice using phosphate buffered saline (PBS; Oxoid, BR0014G) with centrifugation at 4500 × *g* for 10 min at 4 °C (Microcentrifuge 5417R, Eppendorf, Germany). The resulting washed pellet was inoculated into a current 200 ml volume of TSYE. Cells were incubated for 30 min (for all time points), 1 h (7, 14, and 21 d timepoints), 2 h (14 and 21 d timepoints), 3 h (21 d time point) and 4 h (21 d time point) at 37°C. The time of incubation was calculated based on the occurrence of exponential growth from previous studies (Chapter 2; Liu, 2012) with between 1.5 to 4.5 h across

incubation times for 1 to 21 d cultures at 37°C. Immediately after incubation cells were centrifuged at 4000 × g for 10 min at 4 °C and washed twice with 5ml PBS and frozen using liquid nitrogen and stored at -80 °C until extraction of whole cell protein proceeded.

4.3.2.2 Protein Extraction

The frozen pellet was thawed on ice for ~15 min then suspended in 600 µL PBS, and 0.5 g of zircon beads (0.1 mm; Daintree Scientific, TAS, Australia) added. Cell suspensions were bead beaten for 6 min using a TissueLyser III bead beater (Qiagen) at 30 cycles/s for 6 min. The samples were centrifuged to remove the cellular debris at 14 000 rpm for 30 min at 4 °C. The protein concentration in the lysate was determined with the BCA kit (Thermo Fisher Scientific, USA) with bovine serum albumin utilised as a standard. An aliquot of each supernatant containing ~50 µg of soluble protein, as determined with the BCA kit, was then lyophilized for 2 h using a Mini Ultra Cold freeze-drier (Dynavac Australia), according to the manufacturer's instructions then subjected to tryptic digestion.

4.3.2.3 SDS-PAGE

An aliquot of the protein samples was diluted in an equal amount of sample buffer (Tris-HCl, pH7.0) and heated at 80˚C for 10 min. SDS-PAGE was performed using a 10% resolving gel and a 4% stacking gel with approximately 10 µg of protein sample added per well. The gel samples were electrophoresed at 25 mA for 1.5 h. After electrophoresis, separated proteins were visualised by silver staining using the method of (Wilson et al., 2008).

4.3.2.4 Tryptic Digestion

Protein samples were reduced with a reducing agent (50 mM dithiothreitol, 100 mM ammonium bicarbonate; incubated for 1 h at RT), alkylated with an alkylating reagent (200 mM iodoacetamide, 100 mM ammonium bicarbonate; for 1 h at RT) and reduced again with the reducing agent (for 1 h at RT). After dithiothreitol reduction and iodoacetamide alkylation of cysteine residues, all solutions were diluted to a final volume of 220 µl of digestion buffer containing (50 mM ammonium bicarbonate, 1 mM $CaCl_2$ $2H_2O$) and digested with 0.1 µg/µl Sequencing grade modified trypsin (Promega, Madison, WI; V511) at a ratio of 1:50 (trypsin/protein). After incubation at 37 °C for 18-20 h, the digested reactions were quenched by acidification with 10 µl of 10% formic acid and stored at -80 °C for further analysis.

4.3.2.5 nanoLC-LTQ-Orbitrap Tandem Mass Spectrometry

Protein samples were analysed by nanoLC-MS/MS using an LTQ-Orbitrap XL (ThermoFisher Scientific). Aliquots of tryptic peptides equivalent to 50% of the in-solution digests were loaded at 0.05 mL/min onto a C18 capillary trapping column (Peptide CapTrap, Michrom Bio- Resources) controlled by an Alliance 2690 Separations Module (Waters). Peptides were then separated on an analytical nanoHPLC column packed with 5 µm C18 media (PicoFrit Column, 15 µm i.d. pulled tip, 10 cm, New Objective) controlled using a Surveyor MS Pump Plus (ThermoFisher Scientific) at 200 nL/min over a four-step gradient of 100% buffer A (5% acetonitrile in 0.2% formic acid) to 100% buffer B (90% acetonitrile in 0.2% formic acid) using the following steps: 0− 10% B over 7.5 min; 10−25% B over 50 min; 25−55% B over 20 min; 55−100% B over 5 min; holding at 100% B for 15 min; and re-equilibration in 100% A for 15 min.

The LTQ-Orbitrap XL was controlled using Xcalibur 2.0 software (ThermoFisher Scientific) and operated in data- dependent acquisition mode, where survey scans

were acquired in the Orbitrap using a resolving power of 60 000 (at 400 m/z). MS/MS spectra were concurrently obtained in the LTQ mass analyser on the eight most intense ions from the FT survey scan. Charge state filtering, where unassigned and singly charged precursor ions were not selected for fragmentation, and dynamic exclusion (repeat count 1, repeat duration 30 s, exclusion list size 500) was used. Fragmentation conditions in the LTQ were: 35% normalised collision energy, activation q of 0.25, 30 ms activation time, and minimum ion selection intensity of 500 counts.

4.3.2.6 Peptide Identification

For peptide identification, the methods described by Bowman et al. (2011) was used. Peptide spectra were identified using the Computational Proteomics Analysis System (CPAS, LabKey Software Foundation) using a workflow, described in Porteus et al (2011), utilising X! Tandem software (http://www.thegpm.org/tandem/). Assessment of peptide and protein identifications was performed using Peptide Prophet and Protein Prophet scoring (Nesvizhskii et al., 2007). Searches were conducted against the derived proteome of Scott A (Briers et al., 2011). A subsequent reverse peptide search was conducted against all available *Listeria* proteomes to assess false positive identification error within the CPAS workflow. Filtration criteria used to ascertain reliable protein identification included the following: (i) that a given protein was represented by two or more observed unique peptides; (ii) the peptides did not match the reverse database comparisons (those that did were excluded); (iii) and that Protein Prophet scores indicated a 95% confidence value for the protein. Bioinformatically and experimentally deduced secreted, and membrane proteins were derived from previous surveys of *L. monocytogenes* genomes (Trost et al., 2005; Desvaux, 2010) while surface and cell

wall-associated proteins included those predicted by Bierne & Cossart (2007). The presence of signal peptides and transmembrane helix domains for Scott A specific protein was predicted using SignalP server v. 3.0 and TMHMM Server v. 2.0 (http://www.cbs.dtu.dk/services/TMHMM-2.0/), respectively. Scott A specific surface proteins were defined on the basis of domains and motifs determined using the NCBI Conserved Domain and Protein Classification database.

4.3.3 Data Analysis

The exponential phase control culture was compared with the lag phase cell cultures. Total spectral count normalisation was used to normalise the data. Spectral counts from these samples were thus used to determine the fold change in abundance between proteins across the time course exterminate by using the approach developed by Old et al. (2005). A pseudospectral count of 0.5 was added to each replicate data point to account for zero values.

The statistical technique of correlation analysis was used to establish if there is a statistically significant association between the average spectra count of proteins during the early part of the lag phase. For this correlation analysis was applied for the 0.5 h lag phase incubation times for the 1 d, 7 d, 14 d and 21 d culture protein profiles with the data subdivided into protein functional sets. Correlation analysis is useful in determining the strength and direction of the linear relationship between two variables. Prior to conducting the correlation analysis, the assumptions of parametric statistics were inspected. The data were examined for statistical skewness and kurtosis. The Kolmogorov-Smirnov (K-S) test was used to check the statistical significance of normal distribution of the variables at alpha = 0.001. A substantial proportion of variables were found to be normal or approximately normally distributed. Therefore, the subsequent use of the parametric statistical technique of

Pearson's correlation analysis was justified. Pearson's correlation coefficient and its statistical significance ($\alpha = 0.05$) were computed between the average spectral count readings at different days for each protein function set and for the 0.5 h time frame. A similar analysis could not be conducted for 1 h, 2 h and 4 h time frame due to a lack of sufficient data points. Significant correlations ($p<0.05$, 0.025, 0.005) as being >0.805, >0.878 and >0.959, respectively (Harris, Taylor, & Taylor, 2005). To establish if there are any statistically significant differences in the 0.5, 1, 2 and 4 h mean readings by the protein function sets, the day of observation, and the interaction between the protein function sets and day of observation while controlling for the exponential values was addressed using ANCOVA. ANCOVA is an extension of ANOVA, and it allows for controlling the linear effects of a variable which is not of direct interest in the study. The protein function set, the day of observation, and the interaction between the protein function set and day of observation have been used as independent factors; and the exponential value has been used as the covariate. The dependent variable is the spectral count reading taken on different days for the various proteins belonging to different protein function class. Four sets of ANCOVA have been conducted, once each for 0.5-hour readings, 1-hour readings, 2-hour readings and 4-hour readings. The results of this analysis are reported in sections 1.2.3.2. Quantitative analysis was conducted using IBM SPSS statistical software version 22. A paired sample *t*-test was used to establish if there are statistically significant differences between the 0.5 h average spectral count per protein (average of 1 d, 7 d 14 d, 21 d data) and the associated exponential value per protein. The same test was used for the 1 hour (average of 1 d, 7 d 14 d, 21 d) and 2 hours (average of 14 d and 21 d) data. Paired sample t-test is a useful technique to compare two means/observations drawn from the same sample. A linear trend

model (with constant) was fitted to the 0.5 hour readings time series (1 d, 7 d, 14 d, 21 d) for all proteins. The signs of the slopes of the time series were studied to establish if each time series has a general increasing or decreasing trends. To assess which proteins are lag-phase and/or exponential phase specific in terms of abundance differences k-means and unsupervised hierarchical cluster analysis was performed using CLUSTER 3.0 (de Hoon et al., 2004). The data input included log ratios of lag phase culture protein abundances relative to the equivalent aged cell cultures (1 d, 7 d 14 d, 21 d) and to exponential phase cultures (data from Chapter 3) were determined as log ratios. The k-means analysis was based on Euclidean distance calculations and 6 sets, the minimum number to yield one solution. For the hierarchical clustering log ratios were then clustered via complete linkage analysis based on uncentered correlations. The data was visualised as a heat map using JAVA TREEVIEW (Saldanha, 2004) with k-means data overlayed upon the heat map.

4.3.4 ATP analysis

From the lag phase cultures 10 ml of sample was removed and centrifuged at 4000 x g and then resuspended in Bac Titer Glo ATP assay reagent (Promega) as done in section 2.3.3. RLU units were normalised by adjusting cell density to a standard of A_{600} = 1.0 (approximately 10^8 cells ml^{-1}).

4.4 Results and Discussion

4.4.1 Overview of protein abundances in *Listeria monocytogenes* during the lag phase

A total of 459 proteins were quantified across all 4 lag phase treatments (1 d, 7, 14 d, 21 d cultures). Appendix II lists a summary of this data. A heat map with overlayed k-means groups revealed distinct groups of proteins where protein abundance changes differed in systematic ways, including proteins with enhanced abundance only within the lag phase (Figure 37). For the 0.5 h lag phase time point the effect of functional class on spectral count readings was significant ($F(36, 2247) = 6.572$, $p < 0.001$). The findings, however,

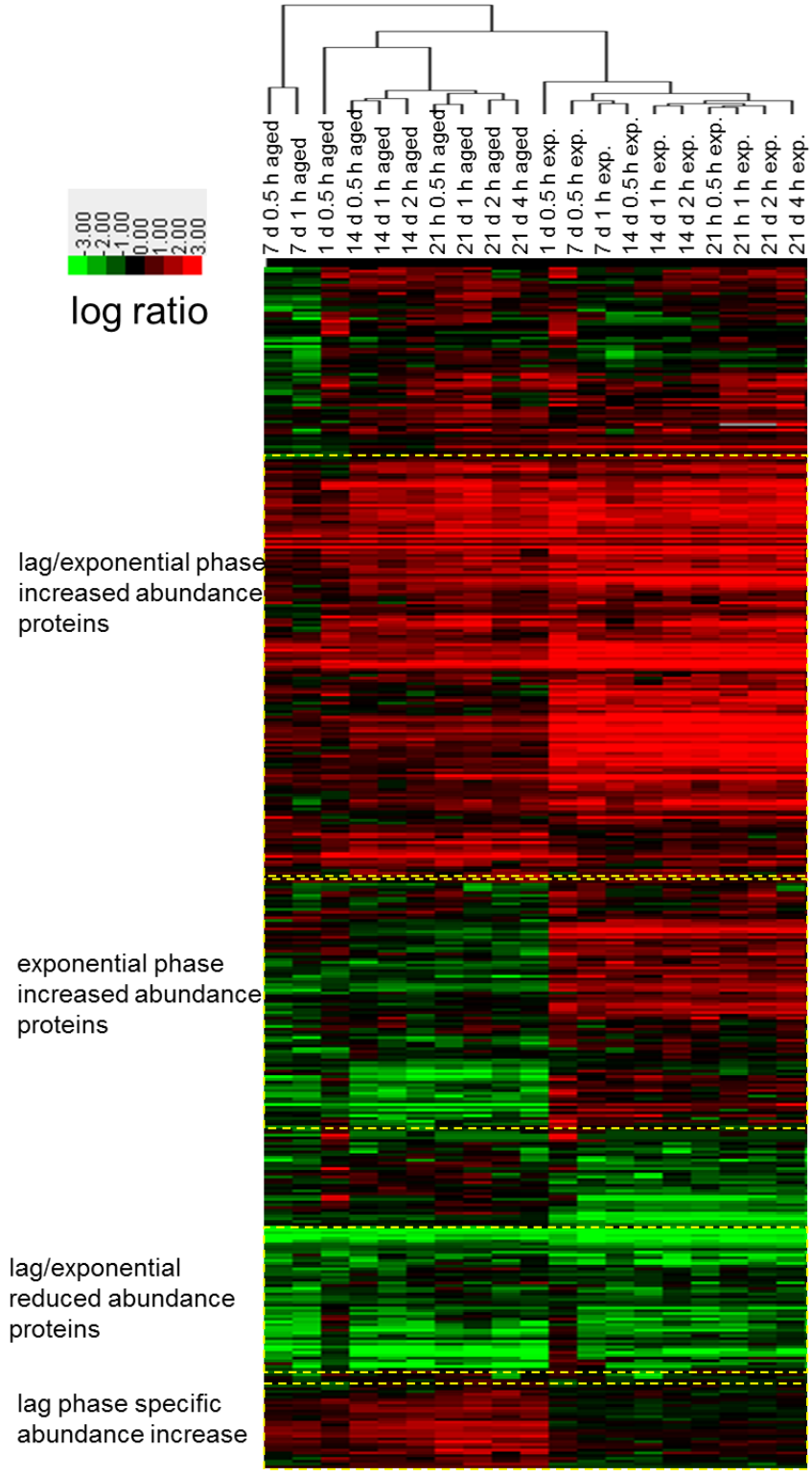

Figure 37 **:** Heat map showing protein (n=459) abundance based log ratios for lag phase treatments for *L. monocytogenes* ScottA as outlined in Figure 4.1. Comparisons of lag phase cultures (designated as initial – 1 d to 21 d then the follow up incubation – 0.5 h to 4 h) versus either aged cells (1 d to 21 d) or exponential phase (exp.) cells.

indicate that there are statistically significant differences between the mean spectral count readings by functional class (Figure 38), but not by the day of the observation nor was there an interaction between the functional class and the day of the observation. High and significant correlations (>0.959, p<0.0025) found between several functional groups are highlighted in Table 3. This suggests that early lag phase responses were relatively homogenous for the four different aged culture treatments. Furthermore, differences were greater overall between lag phase comparisons with the aged cultures and exponential cultures while the differences between lag phase time points (0.5 to 4 h) varied to a much lesser extent. Where strong measurable correlations occurred over time (e.g. 14 d, 21 d – data from 0.5 h to 4 h) only a few proteins showed >2 fold changes in actual abundance (data not shown). Thus the lag phase data of all treatments were treated collectively.

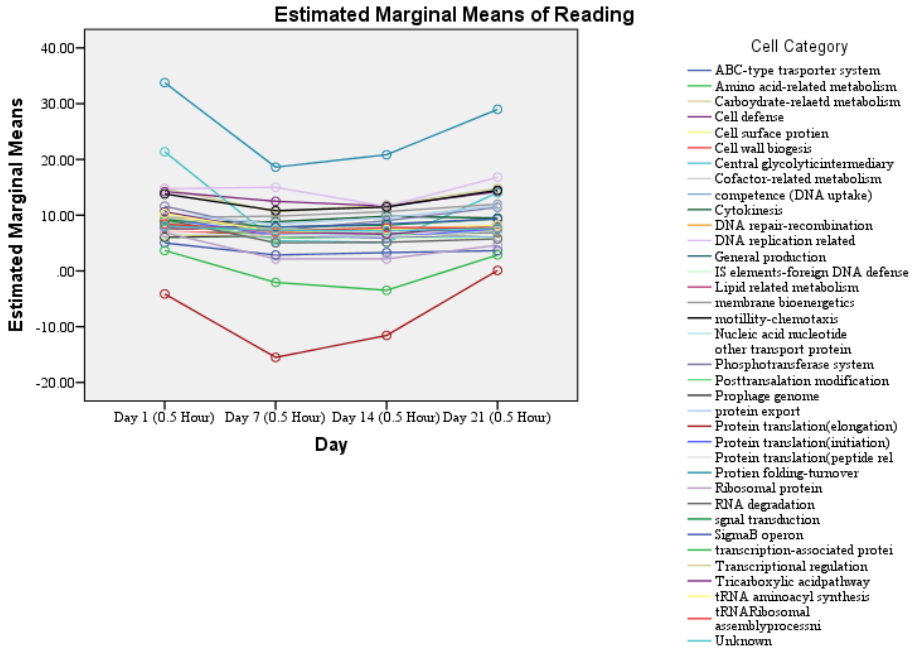

Covariates appearing in the model are evaluated at the following values: Exponential = 12.5055036856869800

Figure 38 **:** Marginal means of spectra counts for each protein function set during 5 h lag time

Table 3: *Correlation between the 0.5-hour readings on the 1st, 7th, 14th, and the 21st day for the different categories of cells*

	ABC-type transporter system	Amino acid-related metabolism	Carbohydrate-related metabolism	Cell defense	Cell surface protein	Cell wall biogenesis	Central glycolytic intermediary	Cofactor-related metabolism	DNA repair-recombination	General production	Lipid-related metabolism	membrane bioenergetics	motility-chemotaxis	Nucleic acid nucleotide	other transport protein	Phosphotransferase system	Posttranslational modification	protein export	Protein translation(elongation)	Protein translation(initiation)	Protein translation(peptide rel	Protein folding-turnover	Ribosomal protein	RNA degradation	Transcriptional regulation	transcription-associated protei	Tricarboxylic acid pathway	tRNA aminoacyl synthesis
Amino acid-related metabolism	.958*																											
Cell wall biogesis	.909	.968*	.975*	.849	.767																							
Central glycolyticintermediary	.944	.997**	.890	.891	.670	.954*																						
Cofactor-related metabolism	.992**	.975*	.799	.756	.483	.909	.970*																					
DNA repair-recombination	.965*	.980*	.800	.822	.531	.899	.984*	.990*																				
General prediction only	.977*	.971*	.775	.778	.477	.887	.972*	.996**	.997**																			
Lipid related metabolism	.984*	.956*	.745	.729	.420	.869	.954*	.996**	.989*	.997**																		
motillity-chemotaxis	.694	.846	.987*	.900	.948	.929	.839	.712	.729	.694	.653	.461																
Nucleic acid nucleotide	.979*	.959*	.746	.746	.432	.868	.959*	.995**	.992**	.999**	.999**	-.359	.659															
Phosphotransferase system	.814	.893	.991**	.807	.832	.977*	.871	.804	.786	.770	.748	.339	.962*	.745	-.735													
Posttransalation modification	.995**	.938	.735	.656	.372	.867	.927	.990**	.964*	.980*	.991**	-.359	.630	.986*	-.114	.756												
protein export	.489	.649	.913	.734	.942	.805	.630	.486	.486	.449	.408	.704	.946	.409	-.954*	.904	.406											
Protein translation(elongation)	.628	.784	.972*	.848	.957*	.896	.772	.638	.648	.612	.571	.557	.993**	.575	-.881	.954*	.555	.979*										
Protein translation(initiation)	.943	.980*	.811	.860	.574	.899	.988*	.977*	.997**	.989*	.975*	-.236	.752	.981*	-.242	.788	.940	.508	.670									
Protein translation(peptide rel	.740	.896	.859	.995**	.821	.856	.920	.805	.869	.830	.786	.092	.871	.802	-.500	.794	.714	.678	.809	.903								
Protien folding-turnover	.930	.990**	.953*	.881	.743	.992**	.983*	.942	.942	.929	.911	.055	.907	.912	-.517	.946	.897	.747	.859	.945	.896							
Ribosomal protein	.953*	.998**	.884	.877	.652	.953*	1.000**	.976*	.987*	.977*	.962*	-.114	.829	.965*	-.363	.868	.937	.618	.761	.989*	.909	.982*						
RNA degradation	.975*	.921	.675	.661	.324	.818	.919	.983*	.971*	.985*	.995**	-.451	.572	.993**	-.020	.684	.990**	.317	.486	.951*	.726	.864	.928					
sgnal transduction	.745	.878	.996**	.893	.921	.955*	.868	.758	.768	.738	.702	.408	.997**	.705	-.788	.979*	.684	.932	.985*	.786	.871	.933	.860	.626				
SigmaB operon	-.058	.132	.543	.358	.767	.352	.111	-.069	-.065	-.109	-.155	.977*	.633	-.154	-.962*	.532	-.152	.838	.718	-.033	.263	.265	.094	-.250				
Transcriptional regulation	.988*	.975*	.792	.764	.483	.903	.972*	1.000**	.993**	.998**	.997**	-.291	.707	.997**	-.192	.794	.988*	.475	.630	.982*	.814	.939	.978*	.984*				
transcription-associated protei	.786	.930	.918	.989*	.850	.914	.944	.836	.885	.850	.809	.143	.920	.821	-.564	.866	.752	.749	.867	.913	.991**	.940	.935	.747	.842			
Tricarboxylic acidpathway	.957*	.975*	.788	.826	.526	.888	.982*	.985*	.999**	.996**	.986*	-.284	.720	.991**	-.196	.771	.958*	.470	.636	.998**	.874	.935	.984*	.969*	.990*	.886		
tRNA aminoacyl synthesis	.996**	.971*	.796	.738	.471	.909	.964*	.999**	.985*	.992**	.995**	-.281	.706	.992**	-.201	.806	.993**	.484	.633	.969*	.788	.939	.971*	.983*	.998**	.823	.979*	
tRNARibosomal assemblyprocessni	.942	.854	.764	.503	.375	.869	.817	.894	.824	.849	.870	-.144	.649	.854	-.277	.824	.924	.531	.616	.785	.541	.852	.830	.863	.880	.624	.806	.908
Unknown	.933	.982*	.830	.883	.611	.908	.992**	.969*	.993**	.981*	.964*	-.194	.778	.971*	-.281	.803	.926	.540	.699	.999**	.922	.952*	.992**	.935	.974*	.931	.994**	.960*

*. Correlation is significant at the 0.05 level (2-tailed); **. Correlation is significant at the 0.01 level (2-tailed).

Very high and significant correlation (A very high correlation is defined as absolute correlation coefficient values higher than 0.8 (Harris, Taylor, & Taylor, 2005).

4.4.2 Carbon and energy metabolism reactivation during lag phase

Aged cultures were found to become metabolically inactive from about 7 d in TSYE at 37°C (see chapter 2). Since ATP is depleted at this time the assumption was that the medium D-glucose was mostly exhausted. It would be assumed that reactivation of metabolism would occur in the lag phase. From the data several phosphotransferase systems were detected perhaps reflecting the TSYE medium contains a number of growth substrates. However, PTS systems have a degree of redundancy and different substrate affinities. From Chapter 3 a number of PTS transporters were linked to transport of D-glucose and similar sugars (i.e., D-mannose). These transporters did not show significant changes in lag phase when compared to aged cultures (Figure 39). PTS phosphotransferase (PtsI) and phosphocarrier (PtsH) proteins similarly only showed slight increases in abundance during lag phase. Interestingly, FruA (fructose specific IIB PTS subunit, EGJ25855) showed a significant increase, 5-39 fold in all lag phase samples, relative to aged and exponential cells. The data could suggest this transporter and the cognate 1-fructokinase (EGJ25856) within the same operon (which is also abundant in all treatments) substrate specificity could be relatively broad and is directed at D-glucose and other unknown carbohydrate(s) present in TSYE. Further biochemical and genetic characterization is required to confirm the nature of this response.

Intermediary metabolism during recovery based on protein abundance data revealed enzymes of the glycolysis pathway remain highly abundant. The key enzyme phosphoglycerate kinase (Pgk) was significantly (3.3-fold on average) increased in abundance during the lag phase compared to aged cells (Figure 40). Phosphoglycerate mutase 1 GpmA was also more abundant. On the other hand

enolase, Eno and phosphoglycerate kinase Pgi were slightly less abundant than aged cells. YihR family predicted aldose 1-epimerase YoxA/Yih (EGJ24823) and pyruvate dikinase PspR (EGJ24993) levels were also substantially enhanced (2.7-5.8 fold) (Figure 40). The function of the former enzyme is uncertain but based on ortholog comparisons hypothetically performs the mutarotation of α and β-isomers of various hexoses, it can only be assumed this enzyme is activated for the uptake and metabolism of the aforementioned "unknown carbohydrates" in the medium. PpsR, also called PEP synthetase catalyses the reversible phosphorylation of pyruvate. Its higher abundance could suggest a greater flow of carbon units to PEP, required for PTS system activity. The enzyme was abundant in aged cells likely due to unavailability of cell energy, with ADP involved in PpsR phosphorylation activity.

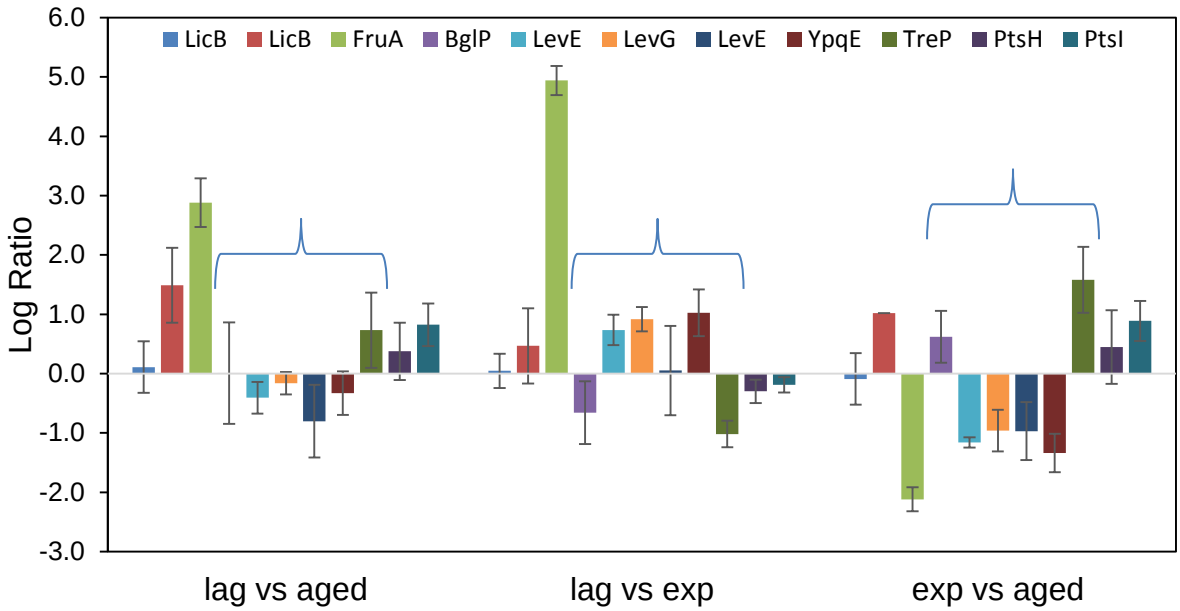

Figure 39**:** The abundance level of phosphotransferase systems in *L. monocytogenes* lag phase in relation to the control (aged and exponential) cultures in TSYE at 37°C. PTS transporters indicated by brackets represent those that most putative transport D-glucose amongst other hexoses. Standard deviations

are based on averages from multiple experiments. See Appendices I and II for details.

There was evidence most enzymes conducting mixed acid fermentation (Joseph et al., 2006) were more abundant in lag phase cultures. PdhABCD, Ldh, PflA, PflC, YdaP, AlsS and AlsD were all enhanced in comparison to aged cells (Figure 41). In comparison to exponential cells, this followed suit to even a greater degree except for the Pdh complex, which was approximately similar in abundance. The data suggests that the end products of glycolysis in the lag phase flow to mixed acid fermentation where the end-products include lactate (Ldh), formate (PlflA, PflB, PflC), ethanol (AdhE), acetate (YdaP, AckA), and acetoin (AlsS, AlsD), effectively a mix of aerobic and anaerobic-based fermentation that *L. monocytogenes* has been shown to employ in minimal media (Romick et al., 1996). The growth temperature of 37°C and static culture likely results in lower O_2 diffusion so could explain the mixed metabolism. *L. monocytogenes* typically produces acetoin as an overflow product into the growth medium when grown aerobically in the presence of glucose and during acid stress (Bowman et al., 2012), while lactate (together with acetate and other products) is the primary fermentation product under anaerobic conditions (Romick et al., 1996). Pyruvate-formate lyases are highly induced also suggesting that mixed acid fermentation is the primary mode of fermentation in *L. monocytogenes* during lag phase. Pdh converts pyruvate to acetyl-CoA; the acetyl-CoA can flow on to anabolic pathways, for example, amino acid and nucleic acid synthesis via 2-oxoglutarate in the partial TCA cycle or to fatty acid synthesis. This suggests mixed-acid fermentation is promoted in the lag phase possibly to increase available cell ATP pools and also drive anabolism. The flow of more glycolysis process carbon units to fermentation is also suggested by the lowered abundance of oxidative pentose phosphate pathway enzyme Zwf that receives glucose 6-

phosphate from glycolysis (Figure 42). The higher level of Rpe protein indicates that the pathway still contributes to anabolism by

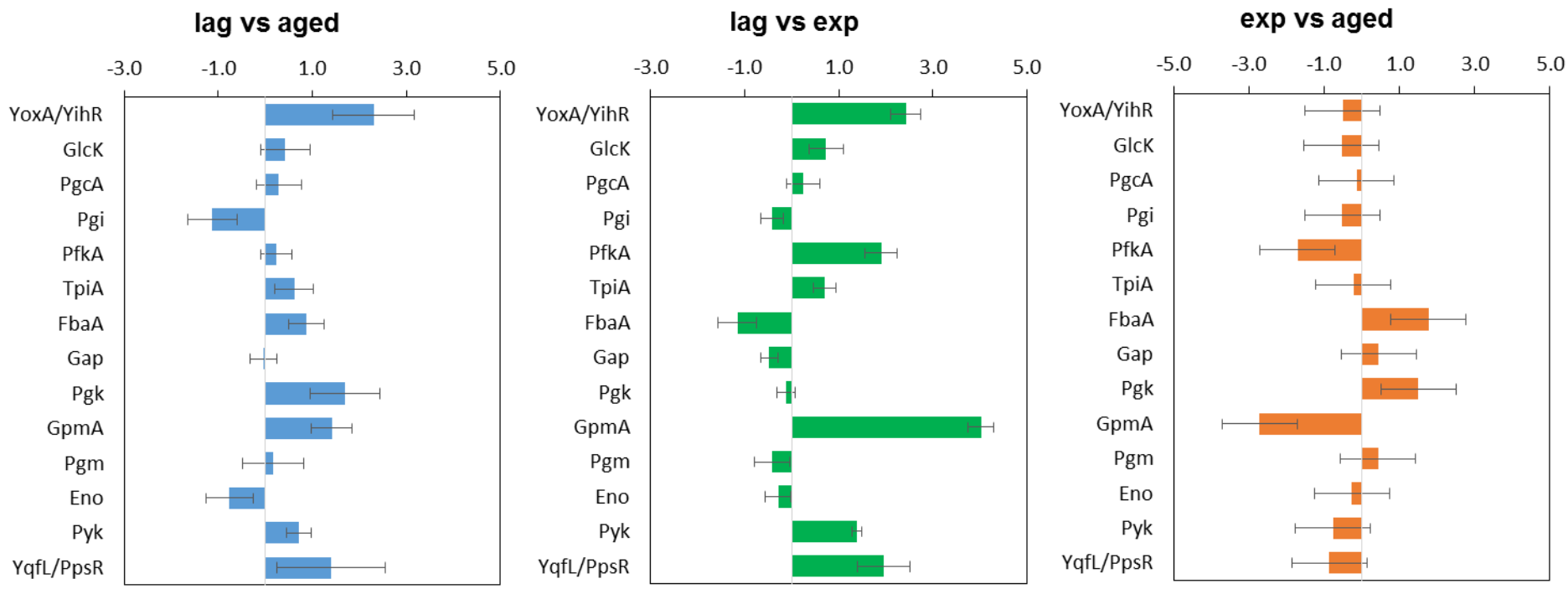

Figure 40**:** The abundance level of glycolysis associated enzymes in *L. monocytogenes* lag phase in relation to the control (aged and exponential) cultures in TSYE at 37°C. Standard deviations are based on averages from multiple experiments. See text and Appendices I and II for more details.

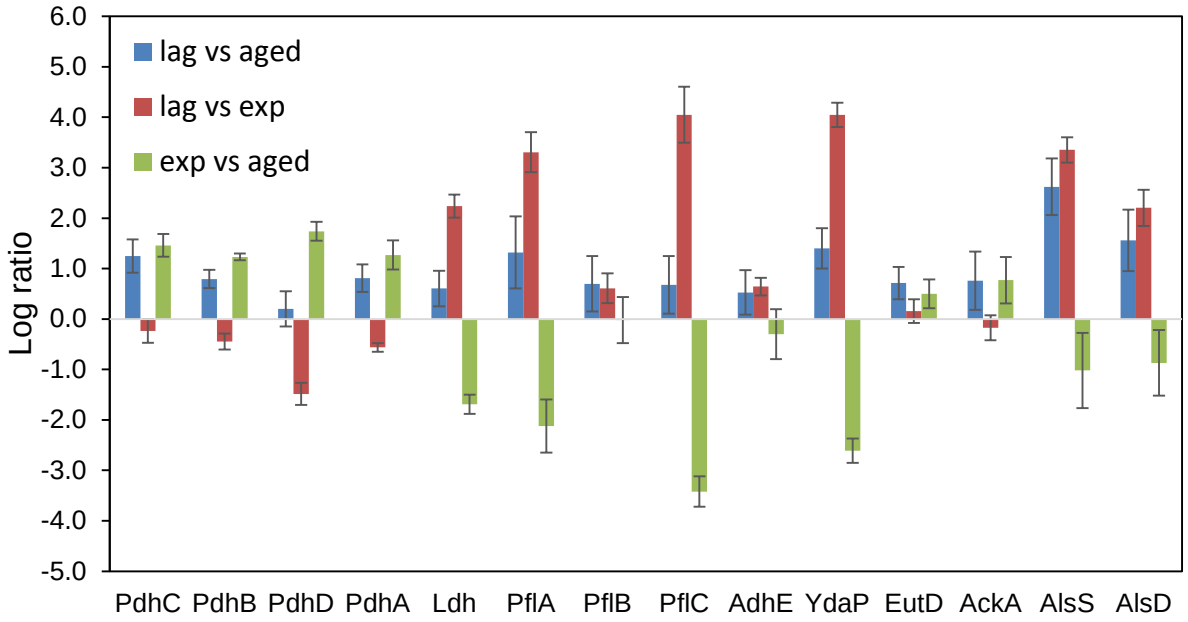

Figure 41**:** The abundance level of mixed acid fermentation associated enzymes in *L. monocytogenes* lag phase in relation to the control (aged and exponential) cultures in TSYE at 37°C. Standard deviations are based on averages from multiple experiments. See text and Appendices I and II for more details.

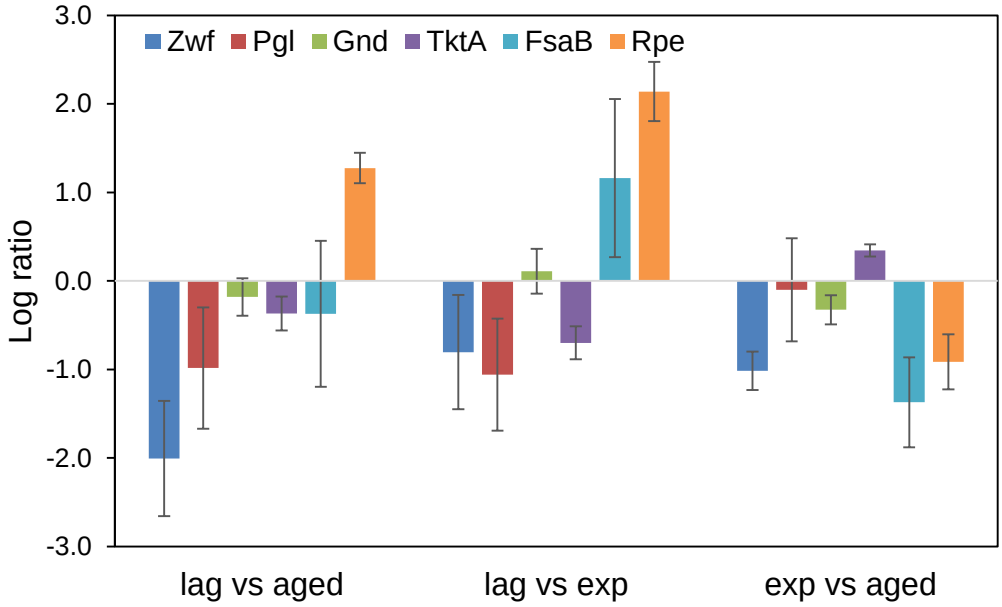

Figure 42**:** The abundance level of pentose phosphate pathway associated enzymes in *L. monocytogenes* lag phase in relation to the control (aged and exponential) cultures in TSYE at 37°C. Standard deviations are based on averages from multiple experiments. See text and Appendices I and II for more details.

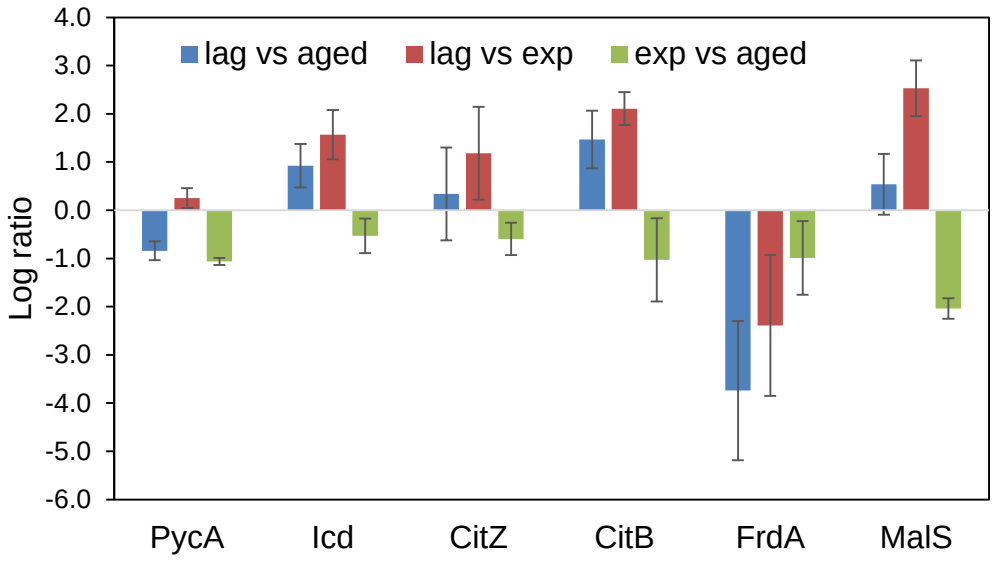

Figure 43**:** The abundance level of tricarboxylic acid pathway associated enzymes in L. monocytogenes lag phase in relation to the control (aged and exponential) cultures in TSYE at 37°C. Standard deviations are based on averages from multiple experiments. See text and Appendices I and II for more details.

adding to NAD(P)H pools (Joseph et al., 2006) and to precursors for the synthesis of nucleic acids via FbaA (transaldolase) and Rpe, both of which showed greater abundances (Figure 42).

The TCA cycle in *L. monocytogenes* is split into two sections with the pathway from pyruvate to 2-oxoglutarate directed towards anabolism (Joseph et al., 2006). Lag phase cultures had a greater abundance of citrate synthase CitB (EGJ25177), aconitate hydratase CitZ (EGJ25104), and isocitrate dehydrogenase Icd (EGJ25103), while pyruvate carboxylase PycA abundance remained high in all treatments (Figure 43). This suggests 2-oxoglutarate synthesis could be greater and thus shows an emphasis towards anabolic processes. FrdA was substantially lower in abundance (Figure 43). It was noted this enzyme was abundant in aged cells (Chapter 3). Fumarate reductase reduces fumarate to succinate and could be coupled with menaquinone reduction (in the electron transport pathway). However,

the role of FrdA remains unclear though it has been shown this enzyme plays a role, albeit minor, in anaerobic metabolism (Müller-Herbst et al., 2014). Normally fumarate reductase has multiple subunits (i.e. FrdABCD) in a membrane-anchored complex, only the FrdA flavodoxin subunit is present in *L. monocytogenes*. The greater activity of the anabolic branch of the TCA cycle putatively leads to more synthesis of L-glutamate, an essential precursor for several subsequent anabolic pathways (see Amino acid metabolism section below).

An examination of other aspects of carbohydrate metabolism in lag phase revealed several enzymes were more abundant in lag phase when compared to either aged or exponential growth phase cells. Most notably β-glucoside, glycerol and N-acetylglucosamine catabolic enzymes had increased abundance (Figure 44). The dihydroxyacetone catabolic pathway (DhaKLM) was more abundant than exponential phase but not aged cells. Trehalose catabolic enzyme trehalase levels were stable. The results suggest that several fermentable substrates are possible carbon and energy source for *L. monocytogenes* during lag phase recovery, even if they are low in the TSYE broth medium. It is possible the pathways for these substrates intersect with other stimulated biosynthetic pathway, for example, glycerophospholipid metabolism in the case of glycerol and PG synthesis in the case of N-acetylglucosamine.

In aged cultures, measurable F_1F_0 ATPase complex subunits were on average 3-fold more abundant, during lag phase the overall abundance was still elevated, 1.8-fold on average compared to the exponential growth phase cultures (Figure 45, page 163). Flavodoxin YkuP (EGJ25248), which may have a role in *L. monocytogenes* short electron transport chain had a similar response to the ATPase complex. Mn-

dependent inorganic pyrophosphatase PpaC (EGJ24984) and NADH dehydrogenase

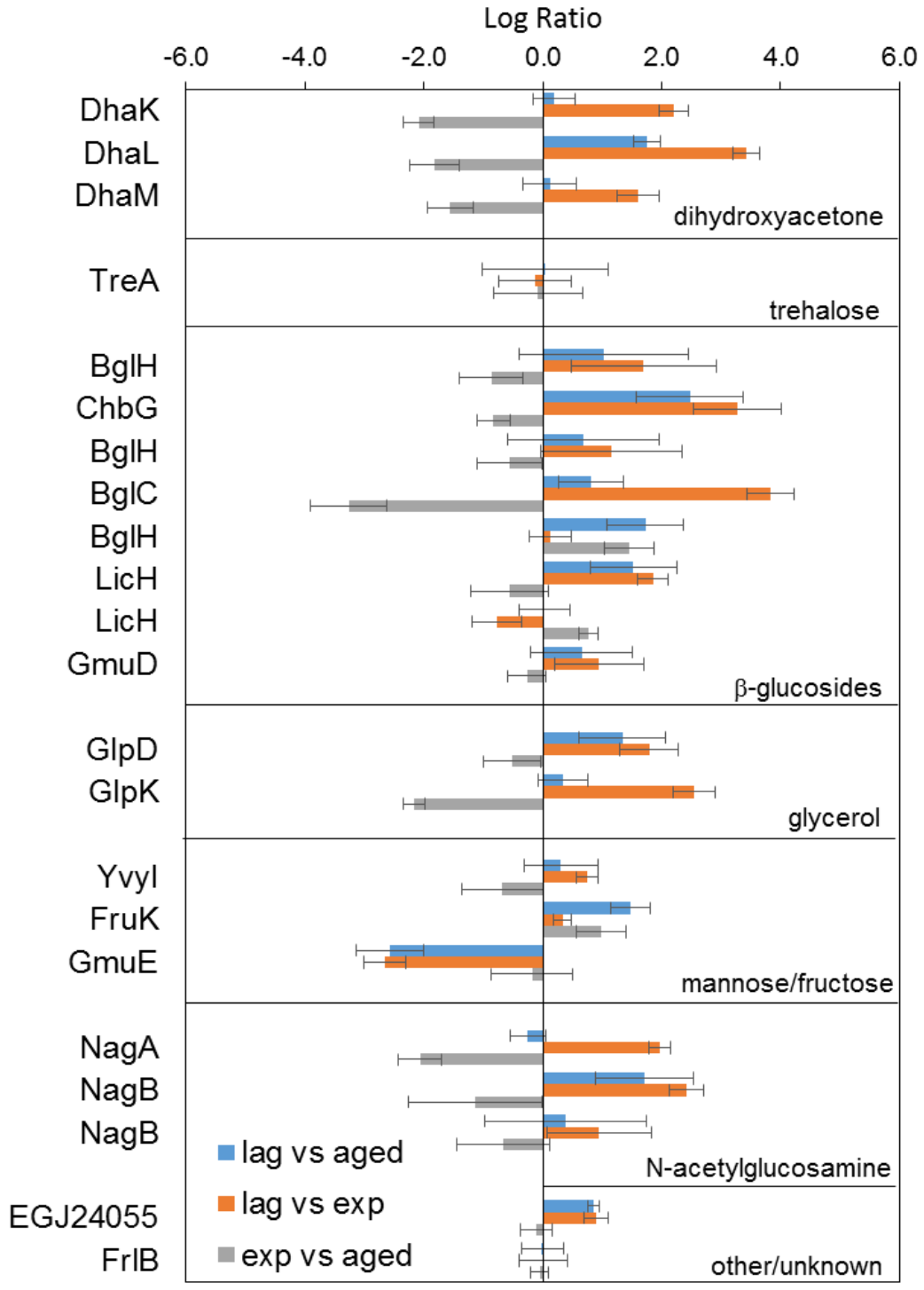

Figure 44**:** The abundance level of carbohydrate catabolic associated enzymes in *L. monocytogenes* lag phase in relation to the control (aged and exponential)

cultures in TSYE at 37°C. Standard deviations are based on averages from multiple experiments. See text and Appendices I and II for more details.

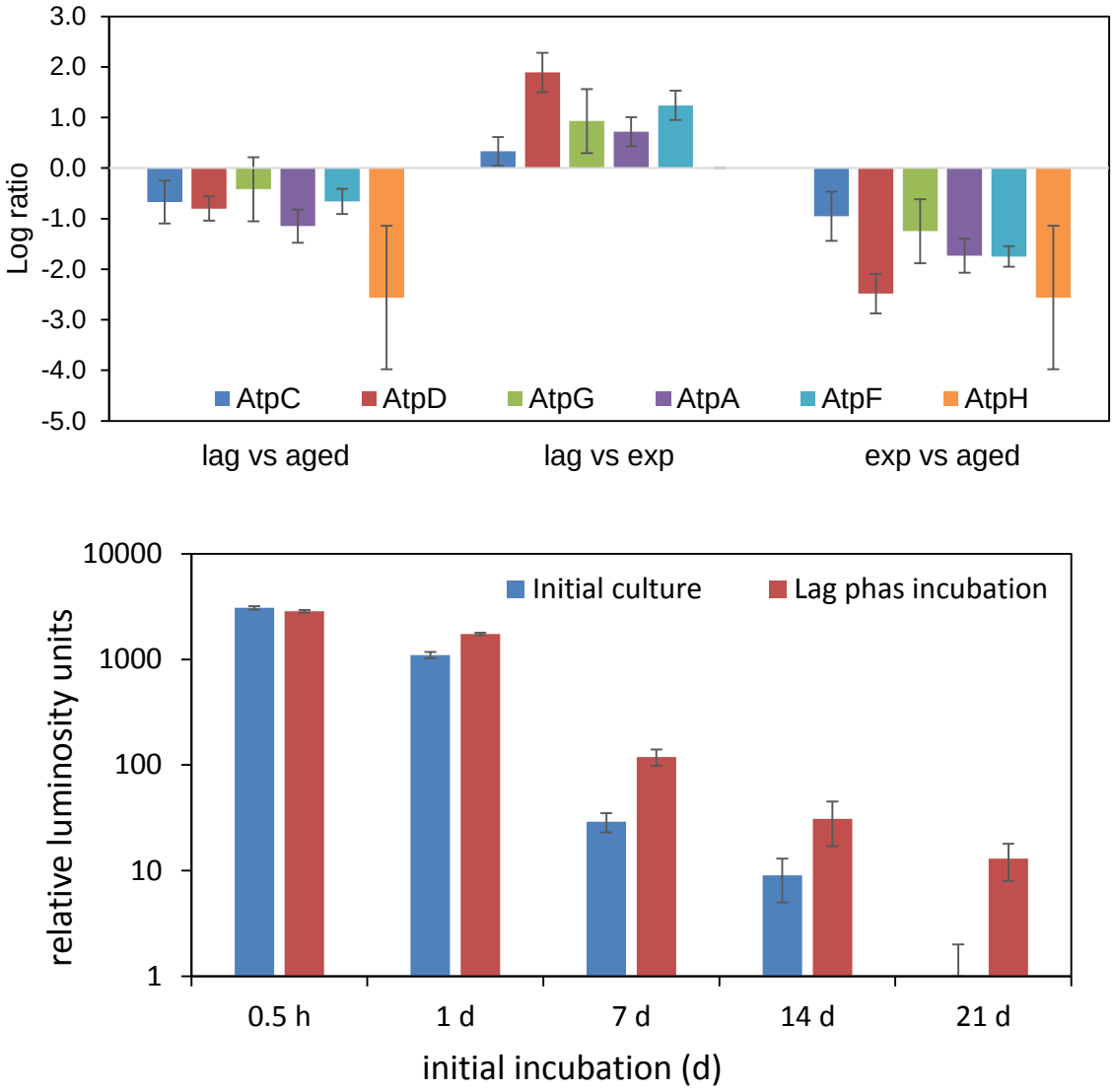

Figure 45**:** Top graph. The abundance level of F_1F_0 ATPase complex subunits in *L. monocytogenes* lag phase in relation to the control (aged and exponential) cultures in TSYE at 37°C. Standard deviations are based on averages from multiple experiments. See text and Appendices I and II for more details. Lower graph. ATP levels before and after lag phase based on luminometry. Lag phase periods match was used in the experiments indicated in this chapter and were performed in the same manner (preincubated inocula inputted to fresh TSYE at 37°C). Total RLU was normalised to a denisty of A600 (~10^8 cells ml^{-1}).

phase culture protein profiles were interrogated to determine how stress reponses occur during lag phase that could aid to remediate the cytoplasm in aged cultures.

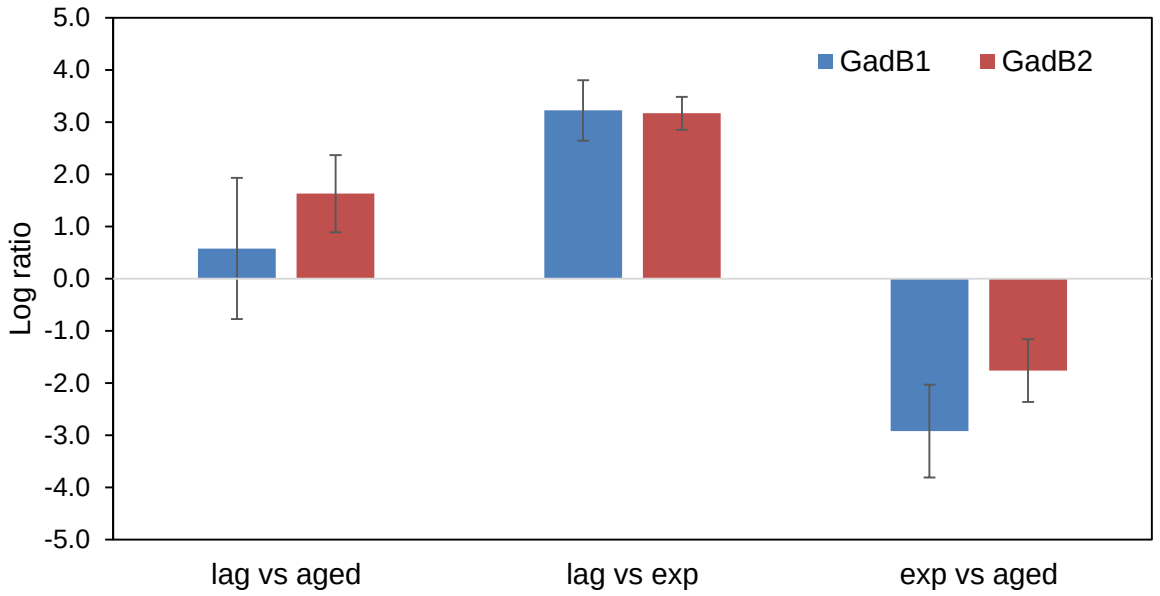

Figure 46**:** The abundance level of GAD system enzymes in *L. monocytogenes* lag phase in relation to the control (aged and exponential) cultures in TSYE at 37°C. Standard deviations are based on averages from multiple experiments. See text and Appendices I and II for more details.

Ndh (EGJ25918) stayed relatively constant across all treatment categories (see Appendix II). The data suggest that oxidative phosphorylation is not increased in lag phase and is likely not especially important for cultures grown at 37°C. ATP synthesis via F_1F_0 ATPase seems to supplement energy during aerobic growth but is essential for anaerobic growth (Muller-Herbst et al., 2014). In this role, it likely maintains the generation of the protonmotive force aiding synthesis of reducing equivalents via Ndh, which can be done by the respiratory cytochrome oxidases (only detected in exponential growth phase and aged cells at low levels). The F_1F_0

ATPase by pumping protons also contributes to cytoplasmic pH control. In lag phase cultures the SigB-independent GabB1 homologue and σ^B-dependent GabB2 homologue exhibited significantly increased abundances during that is not carried through to the exponential phase (Figure 46). The increased level of these enzymes suggests the GAD system is activated early to provide protection of cells during adaptation. ATP analysis revealed that ATP levels increased significantly after the lag phase periods used for proteomic investigation (Figure 45). The stimulation was greatest for 7 d cells (7500-fold increase) while for 14 d and 21 d cultures the ATP increase was 900-2500-fold. Overall, ATPase contributes to growth but not ATP synthesis; this seems to be done by substrate level phosphorylation reactions as part of fermentation. This appears to be effective as ATP levels rise to-three orders of magnitude from depleted levels.

4.4.3 Recovery of cell walls and cytokinesis in the lag phase

Aged ScottA cells grew poorly on agar media, became enlarged and then coccoidal and showed evidence of autolysis (Chapter 2). Proteomic data from Chapter 3 suggested this was due to extensive production of autolysins and a dysfunctional cytokinesis process driven by a lack of cell resources, including energy and precursors for cell wall synthesis. Possible protein aggregation at the “old pole” of dividing cells may also be occurring (though still to be verified) but is considered a cell age-related factor that if left unchecked could disrupt cell division (Bednarska et al., 2013). In aged cultures PG synthesis seems to be restricted in its early steps and compensated for in the endpoint steps. Proteomic data suggested the enzymes performing the first two steps of PG biosynthesis, GlmM and GlmS, become more abundant in lag phase cultures (Figure 47). These enzymes convert fructose-1,6-

biphosphate to D-glucosamine-1-phosphate leading to the synthesis of the main PG monomer N-acetylmuramic acid. MurD, which catalyses the ATP-dependent committed D-glutamate addition step to the PG amino linker was also more abundant. Otherwise, levels of other detected enzymes (GlmU, MurAA, Ddl) changed little and were abundant in all treatments. On the other hand the main autolysin present in aged cells, CwlO/Spl had substantially lowered abundance (on average 20-fold) (Figure 47).

In aged cells, the wall teichoic acid (WTA) appeared to have lowered synthesis due to the main enzymes in the preliminary steps having lower abundance than exponential phase cells. In lag phase cells the primary enzymes polymerising ribitol phosphate (TarJ) and activating it for attachment to PG via D-alanylation, performed by DltC (EGJ24474), had higher abundance than aged cells. There was also a suggestion that glucose uridylation, activating glucose for attachment to WTA via glycosylation is more active, based on increased abundance of GtaB. TagH, the teichoic acid monomer ABC-type exporter (EGJ24575) was also enhanced in lag phase. Ribitol phosphate synthesis (performed by TarI) itself stayed about the same across the treatments (Figure 48).

In lag phase, most major cell division proteins were detected and had equal or greater abundance compared to aged cells. This trend reversed slightly in exponential phase, in particular, ParB, one the main proteins involved in chromosome segregation and partitioning. Based on the data some increase was observed for Z-ring proteins FtsZ, FtsA and FtsE; cytoskeletal proteins MreB and Mbl; and proteins directing PG polymerization enzymes PpbA (EGJ24974) and PpbB (EGJ25584) both of which were not detectable) either to the Z-ring for creation of the

septum (EzrA) or to the cytoskeletal proteins for cell wall extension (GpsB) (Figure 49).

Since many cell wall, biogensis and cytokinesis proteins need to be targeted to different sites of the cell the general secretory (Sec) protein export system has an important role in cell processes. In lag phase, only some Sec proteins were detectable, probably due to extraction bias and/or relatively low abundances. Ffh and YajC were abundant while SecA1 abundance stayed stable. YajC is a membrane protein that stabilises SecA and other parts of the protein translocon in the cytoplasmic membrane. The increased abundance of Ffh, a part of the Signal Recognition Particle (SRP) protein translocation system (Figure 50), may suggest more proteins are being targeted to membranes in the lag phase.

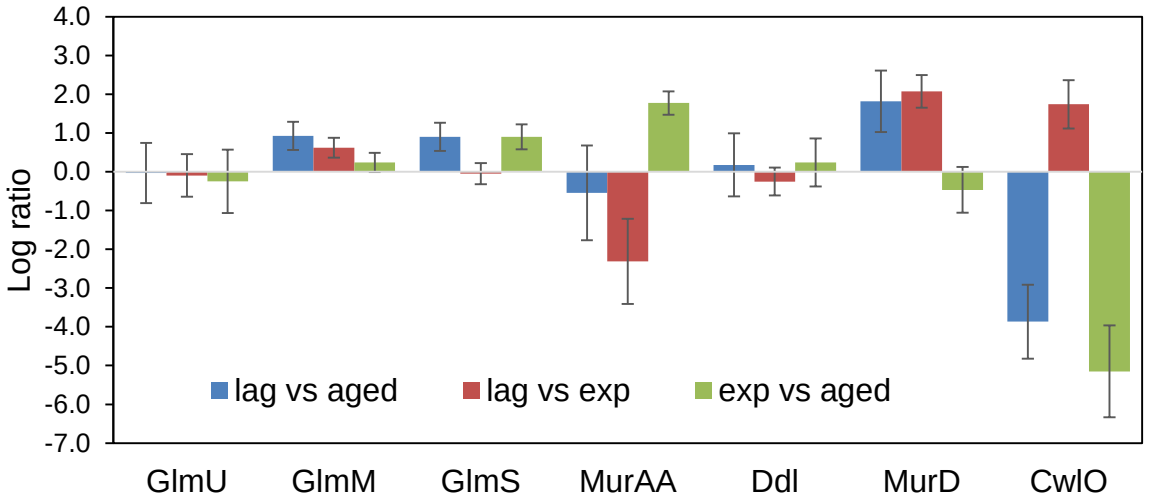

Figure 47**:** The abundance level of PG biosynthetic enzymes in *L. monocytogenes* lag phase in relation to the control (aged and exponential) cultures in TSYE at 37°C. Standard deviations are based on averages from multiple experiments. See text and Appendices I and II for more details.

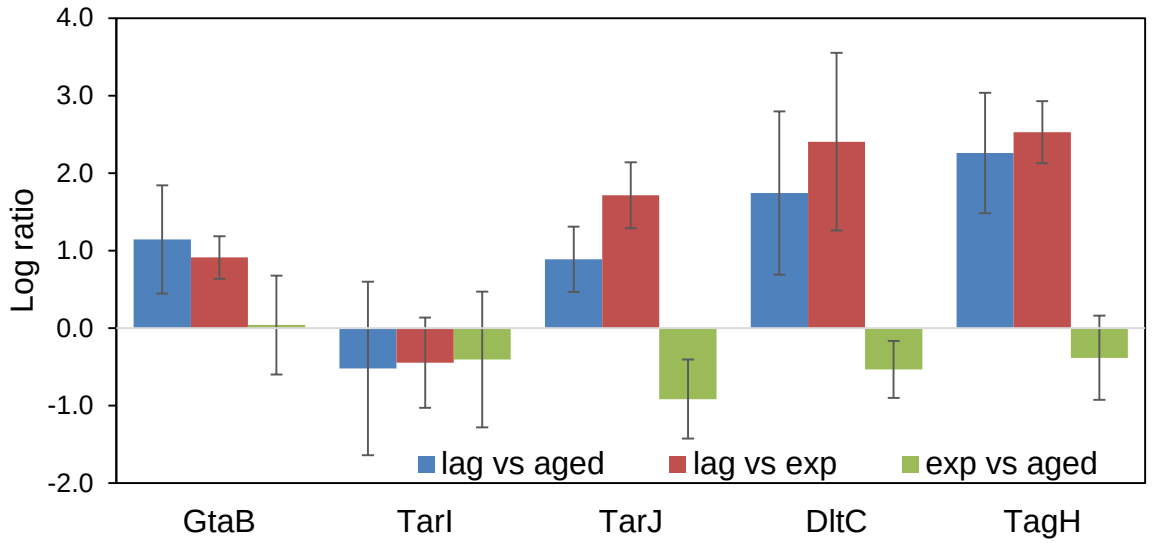

Figure 48**:** The abundance level of WTA biosynthetic enzymes in L. monocytogenes lag phase in relation to the control (aged and exponential) cultures in TSYE at 37°C. Standard deviations are based on averages from multiple experiments. See text and Appendices I and II for more details.

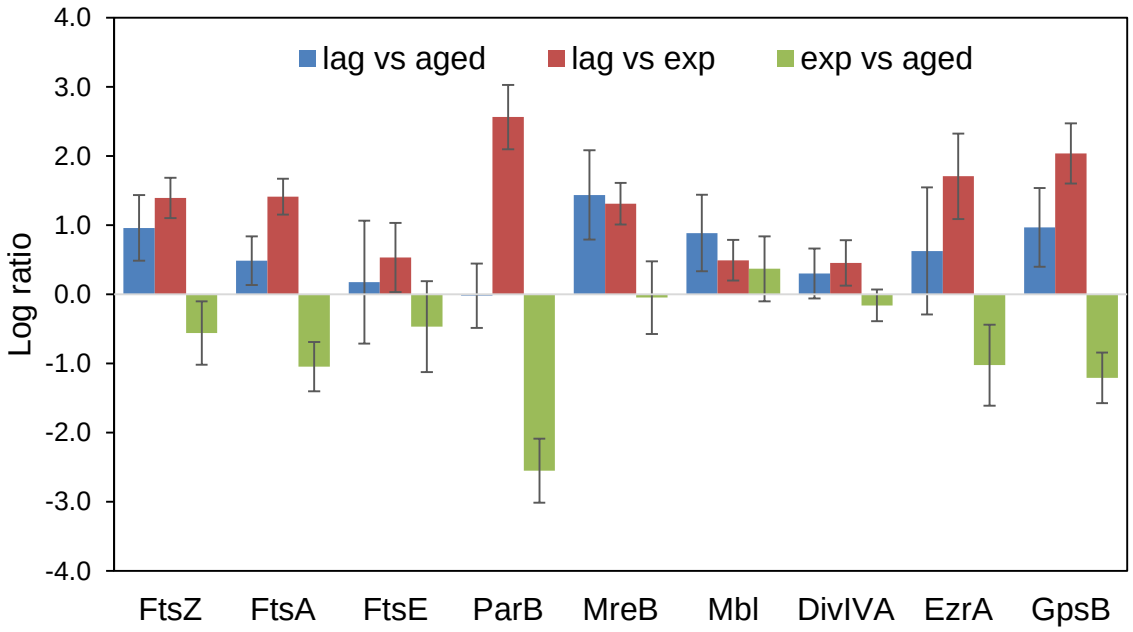

Figure 49**:** The abundance level of cytokinesis associated proteins in *L. monocytogenes* lag phase in relation to the control (aged and exponential) cultures in TSYE at 37°C. Standard deviations are based on averages from multiple experiments. See text and Appendices I and II for more details.

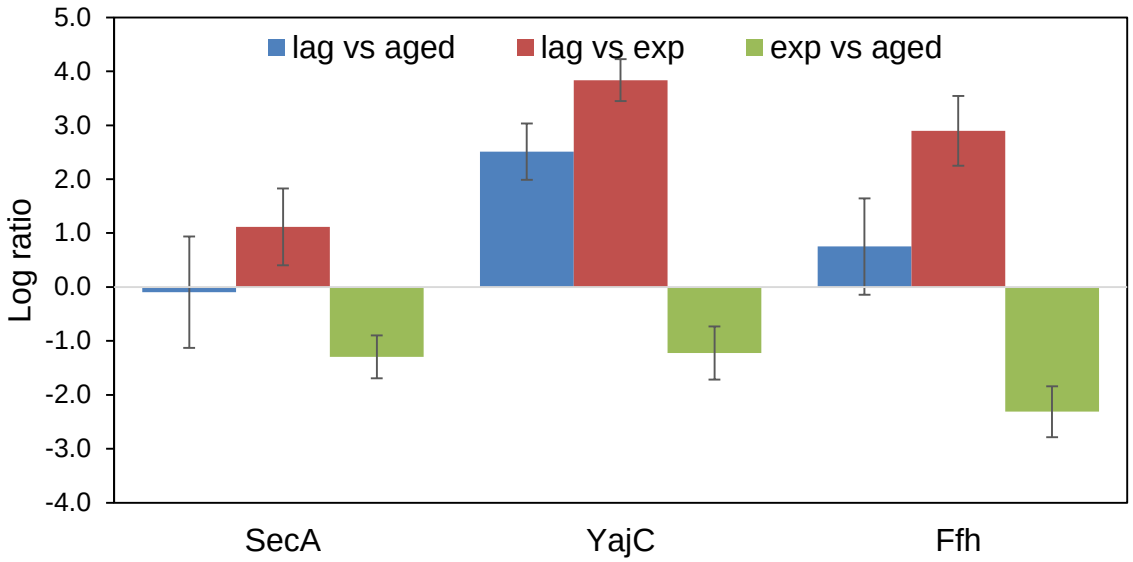

Figure 50**:** The abundance level of detected protein export associated proteins in *L. monocytogenes* lag phase in relation to the control (aged and exponential) cultures in TSYE at 37°C. Standard deviations are based on averages from multiple experiments. See text and Appendices I and II for more details.

Overall, the data points to stimulation of PG precursor synthesis, WTA ribitol phosphate polymerization, and a general increase in cytokinetic apparatus proteins. Coupled with the suggestion of greater abundance of proteins involved in membrane protein trafficking the data indicates within lag phase the scene is being set for cytokinesis being more active in exponential phase. Cell wall biogenesis is “primed” by increasing anabolic processes and accumulating pools of precursors rather than increasing the abundances of enzymes across the entire pathway, which could deplete ATP pools prematurely.

4.4.4 Protein disaggregation during lag phase

Excessive protein aggregation can potentially lead to cell toxicity. In aged cells it is possible it is one of the factors that results in aged cells’ weak growth on agar; besides autolysis. The recovery data in Chapter 2 suggests the bulk of population

seems irrecoverable by 21 d though the data here suggests homogenous responses thus it is possible that some culturability is reattained though proportionally how much is unclear. This situation is ambiguous without further targeted studies, which is unfortunately outside the scope of this thesis. For the purposes here protein responses are investigated to provide clues to the overall physiology and cell fate.

Aggregated proteins are believed to be resolubilized by AAA proteases and rescued by chaperones DnaK/DnaJ (Tyedmers et al., 2010). Aged cells showed high Clp system abundances but lower DnaK levels suggesting the disaggregation process might not be fully functional. Lag phase cultures showed somewhat lower levels of Clp proteases and higher DnaK and GrpE levels. In addition, GroEL, instrumental in protein folding to the native state was more abundant (Figure 51). The results suggest that protein turnover is more important than nascent protein folding. This makes sense given the data is collected over a short time frame indicating that lag phase cultures likely have more de novo protein synthesis and increasing protein turnover since the lag phase culture conditions should not promote misfolding or aggregation.

Lag phase cultures did not demonstrate substantially stimulated protein translation protein levels with protein elongation factors partially returning to exponential phase levels. This is shown in Figure 52 where the comparison with aged cultures indicates lag phase cultures show overall slightly greater abundances of elongation factors Ts and G and constant levels of factor Tu. Methionyl aminopeptidase Map which removes the initiating deformylated Met residues on nascent polypeptide chains was abundant. When individual lag phase time points and treatments are examined the results suggest that all three elongation factors show a greater increase for the longer aged time points, especially for 21 d cultures (Figure 53). There is also a

gradual increase in abundance in the lag phase culture incubation itself, especially Fus, which increases more than 2-fold in the 14 d and 21 d 0.5-4 h treatments (Figure 53). The overall result suggests that protein synthesis probably rebounds in the lag phase cultures from state it ws in aged cultures. However, the abundance changes do not return rapidly to exponential levels. The aged cells likely have slow protein synthesis due to lack of cell energy and certainly reduced amino acid pools. There is also a lower abundance of ribosomal proteins (see Chapter 3). tRNA aminoacyl synthetases reduced in aged cells (see Chapter 3 and Appendix I) rebound in lag phase cultures and further increase in lag phase (Figure 54). With the reactivation of anabolism and provision of more cell energy by active metabolism, translation proteins return to their nominal cell concentrations. Examination of lag phase cultures also indicates that ribosomal proteins stay at about the same level but are 30-35% lower in abundance than exponential phase cultures (Figure 54). The data also suggests the abundance of these proteins slightly subsides in exponential growth phase, which suggests the lag phase is a time of active if constrained protein synthesis.

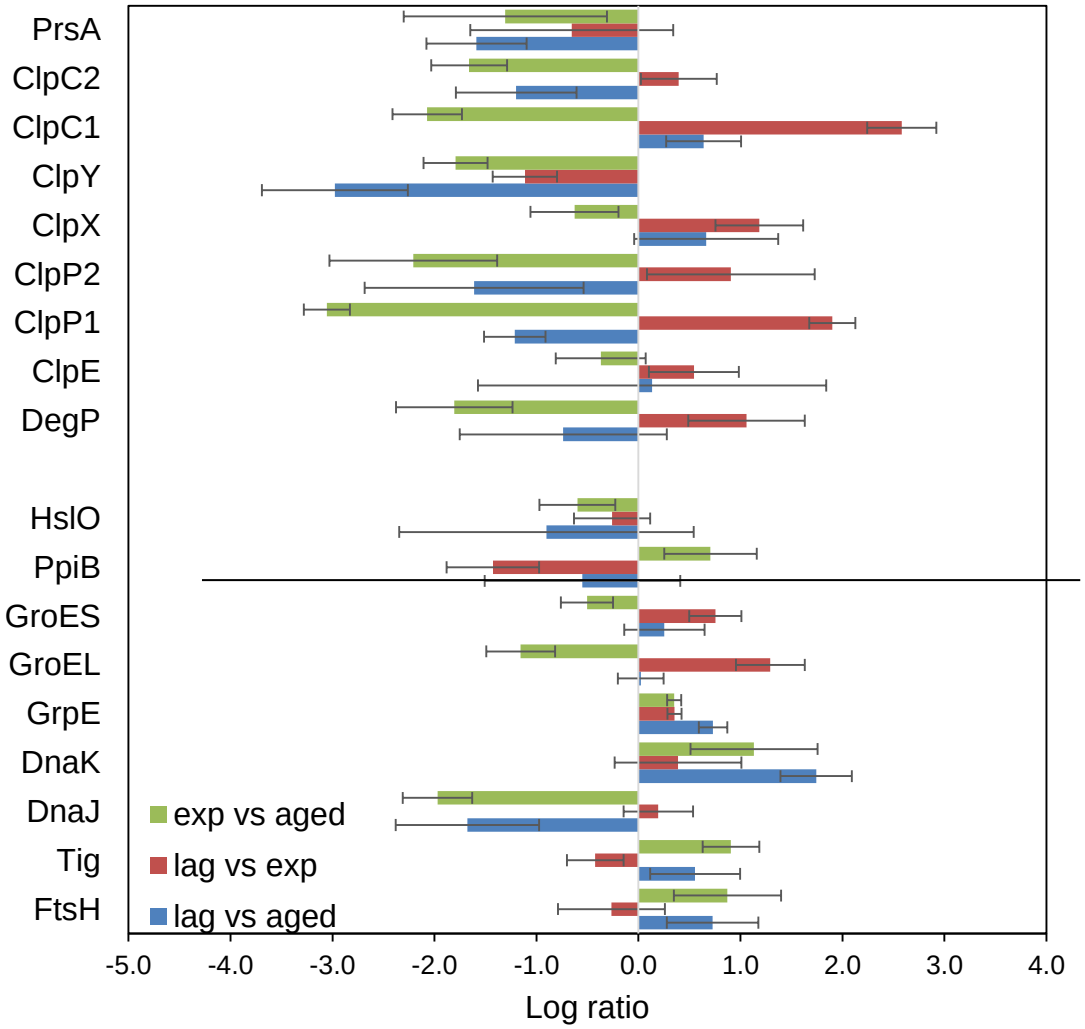

Figure 51**:** The abundance level of protein turnover and folding associated proteins in *L. monocytogenes* lag phase in relation to the control (aged and exponential) cultures in TSYE at 37°C. Standard deviations are based on averages from multiple experiments. See text and Appendices I and II for more details.

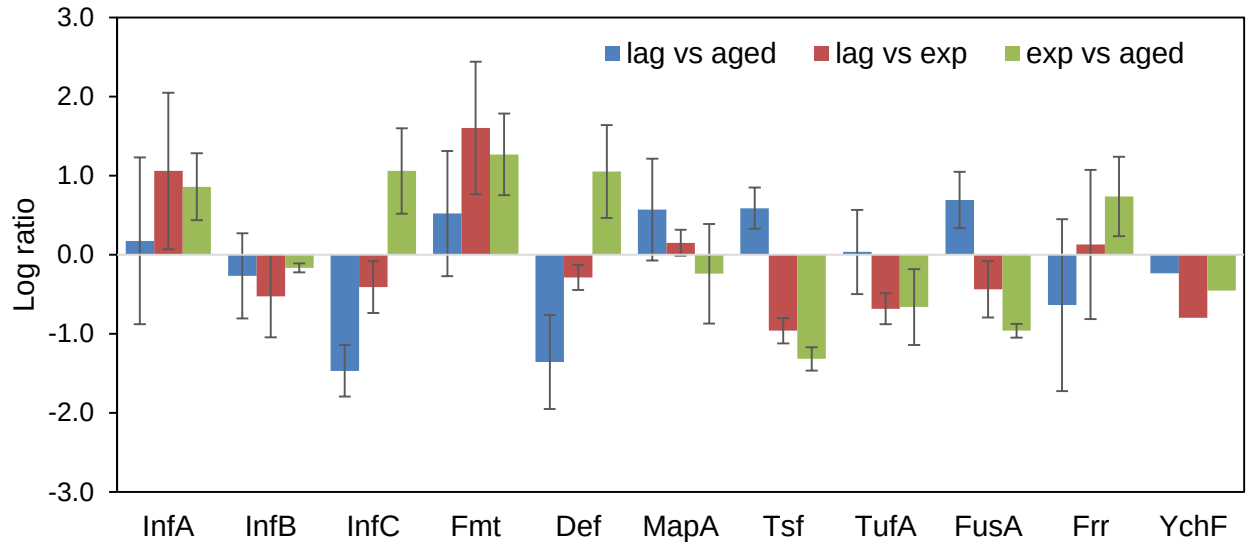

Figure 52**:** The abundance level of translation-associated proteins in *L. monocytogenes* lag phase in relation to the control (aged and exponential) cultures in TSYE at 37°C. Standard deviations are based on averages from multiple experiments. See text and Appendices I and II for more details.

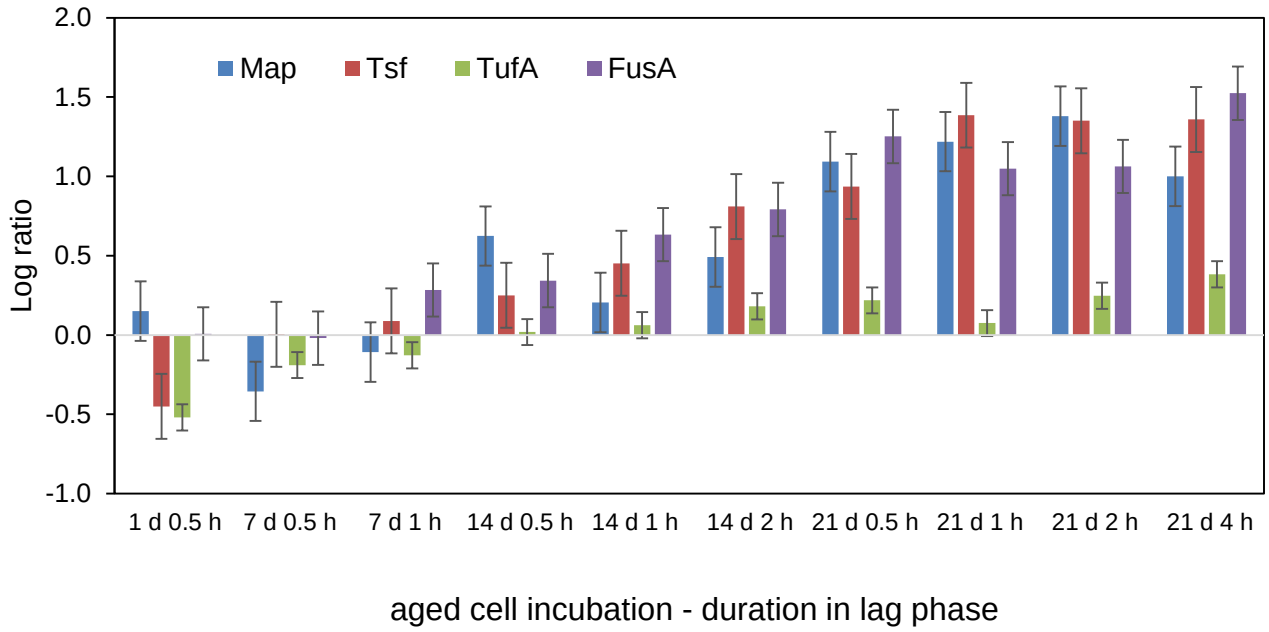

Figure 53**:** The abundance level of translation elongation factors in *L. monocytogenes* lag phase in relation to the length of lag phase incubation time in TSYE at 37°C relative to the equivalent aged cultures showing gradual increases in relative abundance over time. Standard deviations are based on averages from multiple experiments.

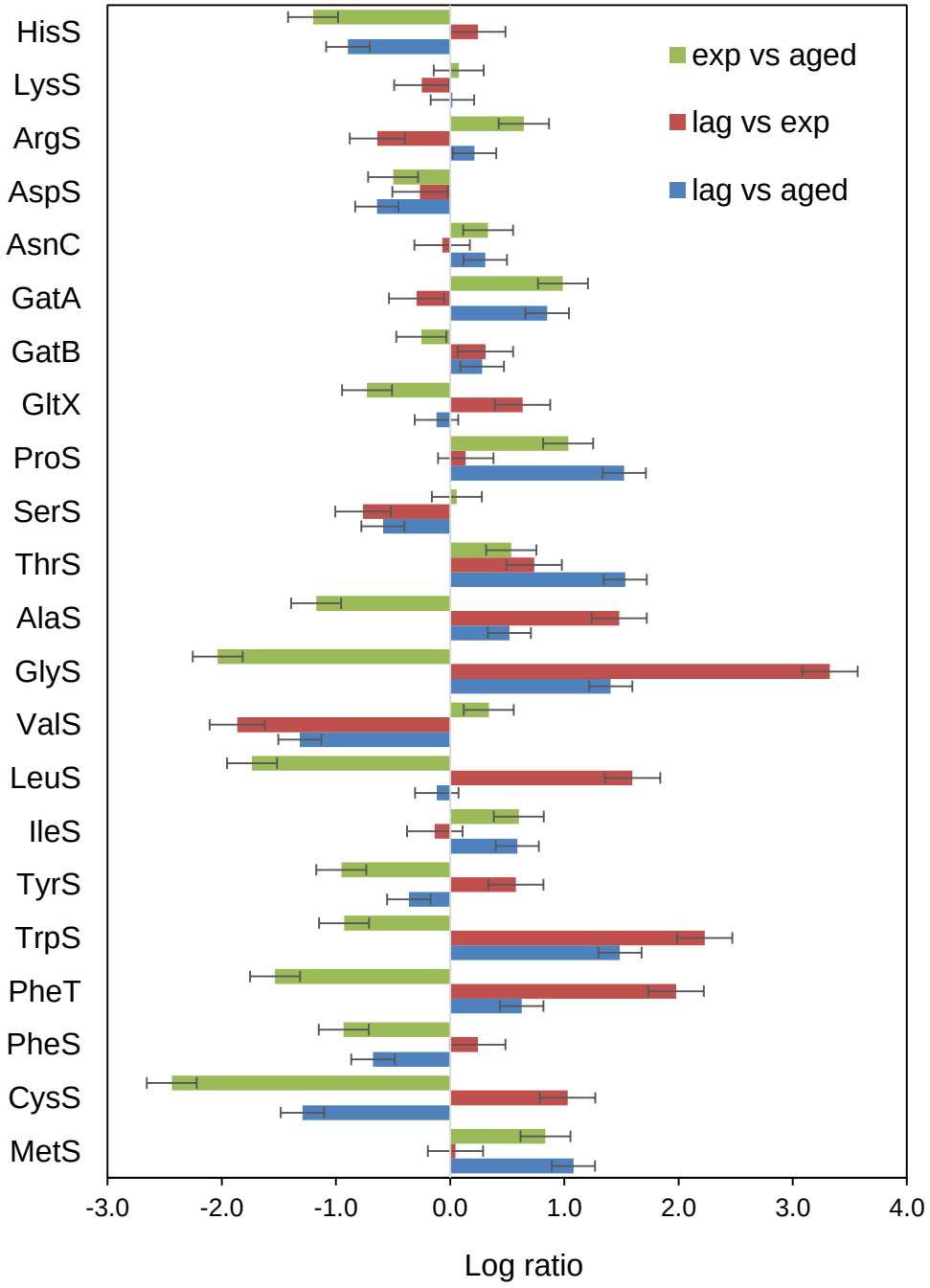

Figure 54**:** The abundance level of detected tRNA aminoacyl synthetases in *L. monocytogenes* lag phase in relation to the control (aged and exponential) cultures in TSYE at 37°C. Standard deviations are based on averages from multiple experiments. See text and Appendices I and II for more details.

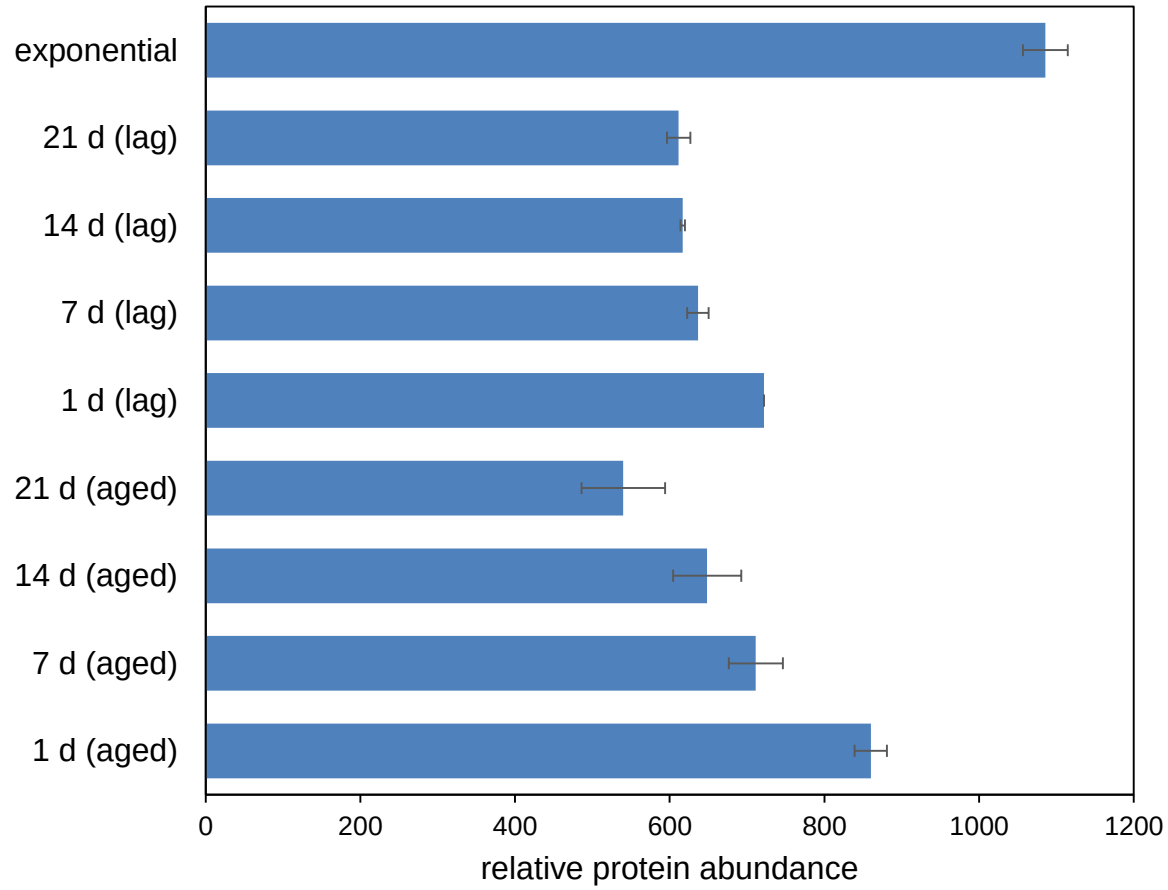

Figure 55**:** Accumulated mean ribosomal protein abundance (n=44 proteins) in *L. monocytogenes* lag phase in relation to the control (aged and exponential) cultures in TSYE at 37°C. Standard deviations are based on averages from multiple experiments. See text and Appendices II for more details.

4.4.5 Anabolic process modulation in lag phase

Lag phase is in a non-growth state suggesting certain fundamental processes such as synthesis of DNA and membrane lipids are at a lower level preventing the initiation of the series of coordinated processes involved in cell reproduction. It was noted above cytokinetic proteins rebound from aged cells that have low levels of metabolism and unable to form colonies on agar. A number of primary anabolic

processes are examined here on the protein level to determine how they respond in lag phase relative to aged and exponential phase cells.

From the proteomic data, lag phase cultures specifically have low levels of DNA topoisomerase I TopA (EGJ24815), which relaxes negative supercoils forming behind DNA replication processing (Figure 56). The result suggests DNA replication is at a low level in lag phase cells. This is supported by DNA replication complex proteins such as HolA, DnaC and PolC not being detected, besides DNA polymerase III beta subunit DnaN (EGJ23430) and other proteins that generally manage DNA and chromosomal structural integrity (SsbA, GyrA, GyrB, Hup, ParE, ParC), the abundance of which did not significantly change (Figure 56). Also DnaA, the replication initiator protein (EGJ23429) was not detected at all; it was present at low levels in exponential and aged cultures.

The SOS response seems to be invoked in lag phase cells based on the higher level of RecA accompanied by stable levels of its cognate repressor LexA (EGJ24841). In actuality of putative DNA repair proteins detected the only well-characterised protein showing greater abundance in lag phase cells was the Mfd protein (EGJ23718) (Figure 57). Mfd, also known as transcription-repair coupling factor, is responsible for the ATP-dependent displacement of stalled RNA polymerase complexes during transcription. The data suggest that the RecA regulon is not activated entirely in lag phase, possibly a process that also requires active DNA replication. Further details on the RecA regulon in lag phase and aged cells are reported in Chapter 5.

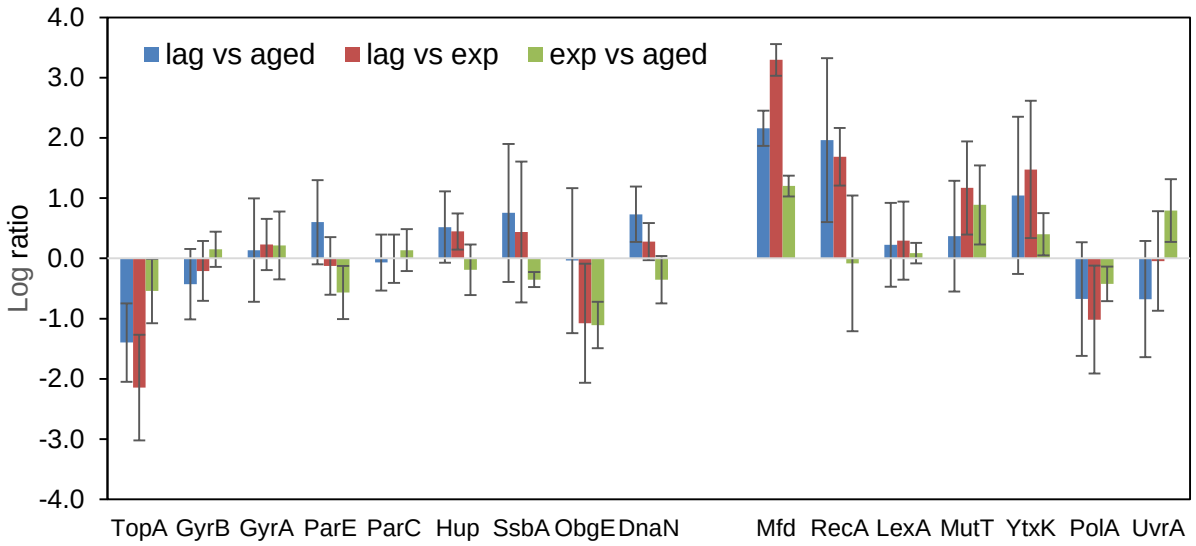

Figure 56**:** The abundance level of detected DNA replication (first group) and DNA repair (second group) proteins in *L. monocytogenes* lag phase in relation to the control (aged and exponential) cultures in TSYE at 37°C. Standard deviations are based on averages from multiple experiments. See text and Appendices II for more details.

Nucleotide acid biosynthesis is of course the prelude to DNA replication, and active de novo synthesis of purines and pyrimidine nucleotides accompanies DNA replication even if the nucleic acid building blocks are imported from the media directly. The results suggest no consistent trends in lag phase in regards to nucleotide synthesis Instead the results suggest a rebound of enzymes that were reduced in aged cells (see Chapter 3) hypothetically due to lack of precursors, back to levels found in exponential cells. This was most starkly demonstrated for GuaB1 (mean 10-fold increase), which caries out the rate-limiting step in de novo guanine nucleotide biosynthesis.

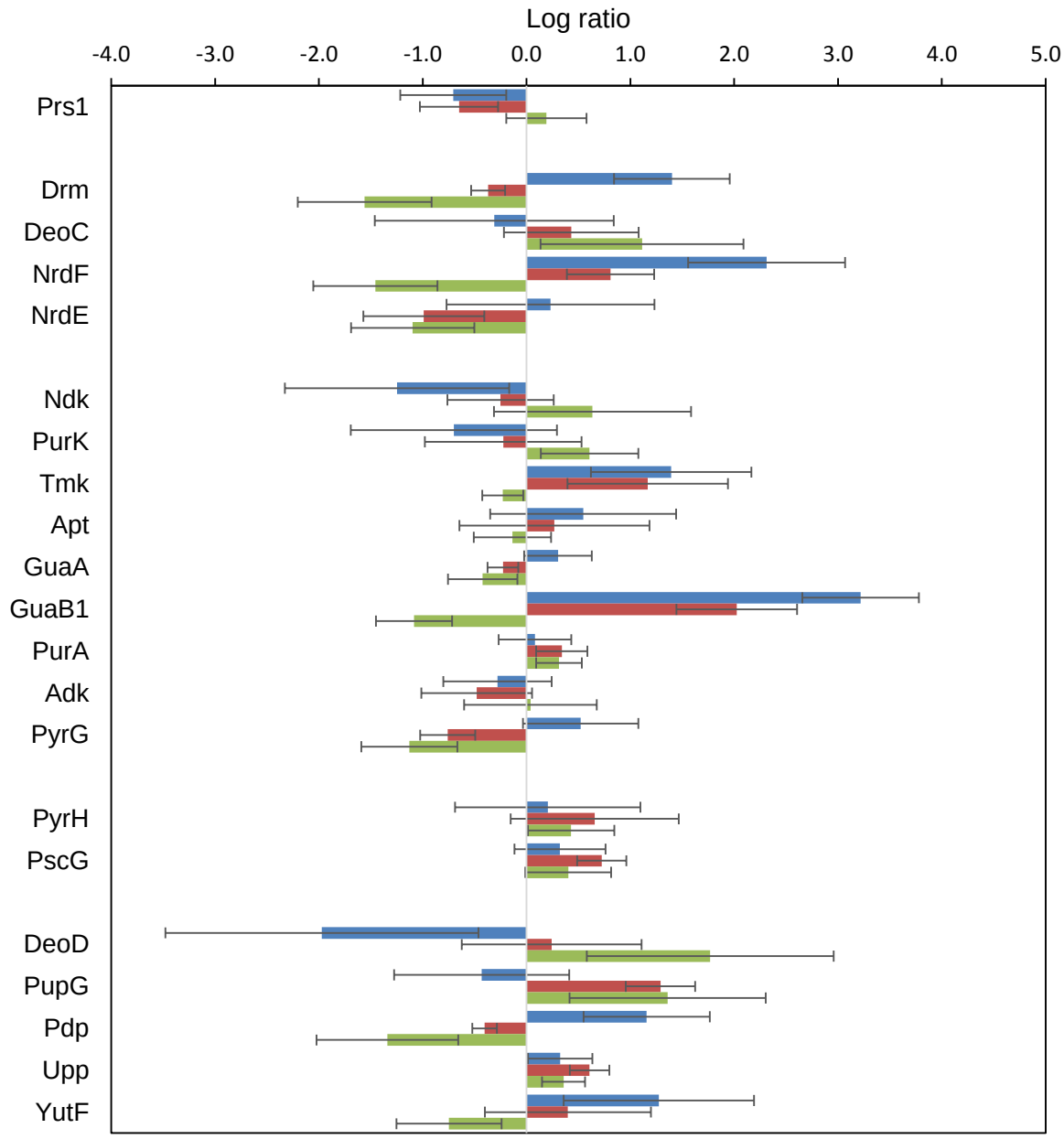

Figure 57**:** The abundance level of detected nucleotide metabolism associated enzymes in *L. monocytogenes* lag phase in relation to the control (aged and exponential) cultures in TSYE at 37°C. Standard deviations are based on averages from multiple experiments. See text and Appendices II for more details.

Transcription, on the other hand, seems to be promoted in lag phase along with apparently lower mRNA turnover. Promotion of transcription is based on the observation of increased abundance of some RNA polymerase (RNAP) complex

subunits, mainly RpoE (EGJ26084) and the primary RNA sigma (σ^{70}) factor SigA (EGJ24990) (Figure 58). Furthermore, transcription factor NusA (EGJ24860) demonstrated 3-5-fold higher abundance in lag phase relative to both exponential and aged cells. This protein is a major factor of transcription involved in coordinating transcription and translation by competing with SigA. This results in timed transcriptional elongation, pausing, termination and antitermination. Li and colleagues (2012, 2013) reported that NusA and associated transcription elongation factor GreA (EGJ25033) have chaperone activities against protein aggregation formation during thermal stress (48°C) in *E. coli*, by forming high molecular weight oligomer complexes. NusA and GreA may act to prevent aggregation of the RNAP and translation/ribosome complexes (Li et al., 2013). More work is clearly needed to determine if this purported property extends to *L. monocytogenes* and works at more normal in vivo conditions.

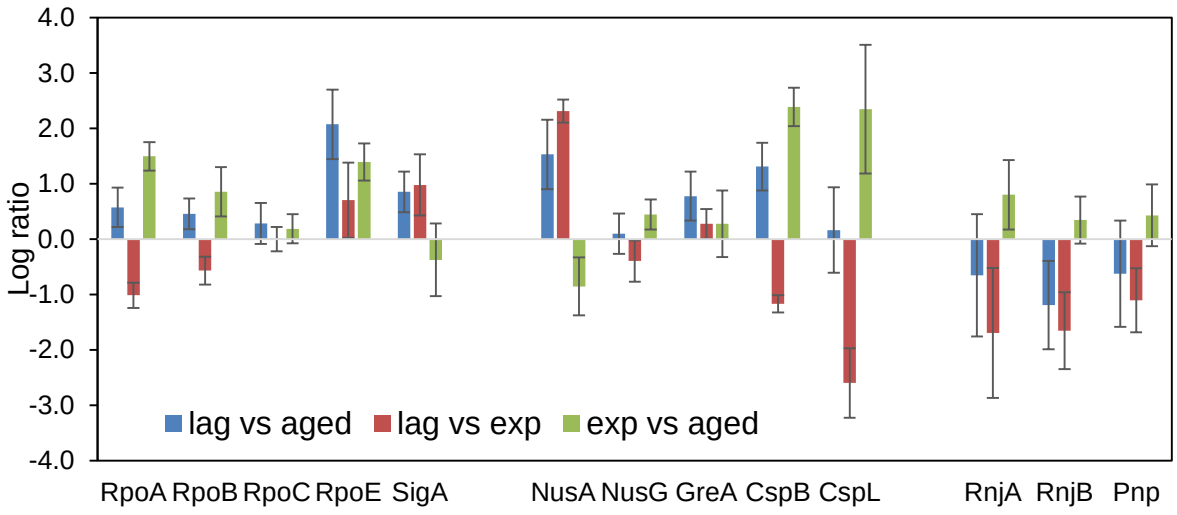

Figure 58**:** The abundance level of detected RNA polymerase subunits, transcription factors and RNA degradosome associated enzymes in *L. monocytogenes* lag phase in relation to the control (aged and exponential) cultures in TSYE at 37°C. Standard deviations are based on averages from multiple experiments. See text and Appendix II for more details.

A higher abundance was also observed for cold shock proteins CspB (EGJ25544) and CspL (EGJ24900) (Figure 58), which are thought to act as chaperones preventing formation secondary structures. Abundance reduction of ribonucleases RnjA (EGJ25431) and RnjB (EGJ24970) and polyribonucleotide nucleotidyltransferase Pnp (EGJ24869), (Figure 58) principal components of the RNA degradosome suggests mRNA could also have longer half-lives in lag phase. This would help increase the efficiency of *de novo* translation in the cells; this tendency could be a common feature of non-or poor-growth states (Zhang et al., 2010).

Fatty acids are incorporated into the component phospholipids that make up 40% of the bacterial cytoplasmic membrane. The cell membrane determines the cell's permeability in a different environment and thus is crucial for bacterial existence. *L. monocytogenes* contains mainly odd-branched straight-chain and branched chain unsaturated fatty acids when grown at 37°C , $C_{15:0}$ iso, $C_{15:0}$ anteiso, $C_{17:0}$ anteiso make ≥80% of phospholipid fatty acid (Juneja et al., 1998; Chihib et al., 2003). Fatty acids which are incorporated into polar lipids, mainly consist of phosphatidylglycerol cardiolipin (dis phosphatidylglycerol), and lysyl cardiolipin (Tatituri et al., 2015).

Key proteins involved in the initiation of straight and branched chain fatty acid and phospholipid biosynthesis were detected in lag phase (Figure 59). The first two steps of BCFA primer synthesis were modestly more abundant (2-fold) including branched chained aminotransferase IlvE (EGJ24481), and two subunits of the methyl-2-oxobutanoate dehydrogenase Bkd complex (BkdAA, BkdAB – EGJ24908-9) (Figure 59). IlvE and the Bkd complex convert BCAA to corresponding branched acid CoA primers. Coupled with this result the biotin carboxylase/acetyl-CoA carboxyltransferase complex subunits AccC (EGJ24893), AccD (EGJ25110) and

malonyl–CoA-acyl carrier protein (ACP) acyltransferase FabD (EGJ25344) were similarly overall more abundant in lag phase cells. The Acc complex creates acetoacetyl-CoA in a process that requires biotin, which *L. monocytogenes* requires as a growth factor. FabD phosphorylates acetoacetyl-CoA and with the addition of ACP synthesises malonyl-ACP the starting intermediate for straight chain saturated fatty acids. Substitution of acetoacetyl-CoA with branched acid CoA primers lead to BCFA. In the case of polar lipid synthesis glycerol-3-phosphate acyltransferase PlsX (EGJ25345) was more abundant but GpsA (EGJ25471), the start point enzyme synthesising intermediate sn-glycerol 3-phosphate, was reduced in abundance (Figure 59). The 3 to the 5-fold heightened abundance of two YerQ putative diacylglycerol kinases (EGJ24274, EGJ25288), forming 1,2-diacyl-sn-glycerol 3-phosphate derivatives and a PldB-like putative lysophospholipase YtpA (EGJ24799) could suggest polar lipid fatty groups are being recycled back to glycerol 3-phosphate. The later steps of polar lipid synthesis were howver not detected. Lipid and metabolomic analysis are needed to determine the exact situation. Overall, the data does not indicate fatty acid chain or phospholipid synthesis itself being promoted in lag phase cultures but does suggest that the scene is probably set for accelerated synthesis during active growth. This could be carried out by the accumulation of activated primers and possible “refreshing” of polar lipids that will receive new fatty acids.

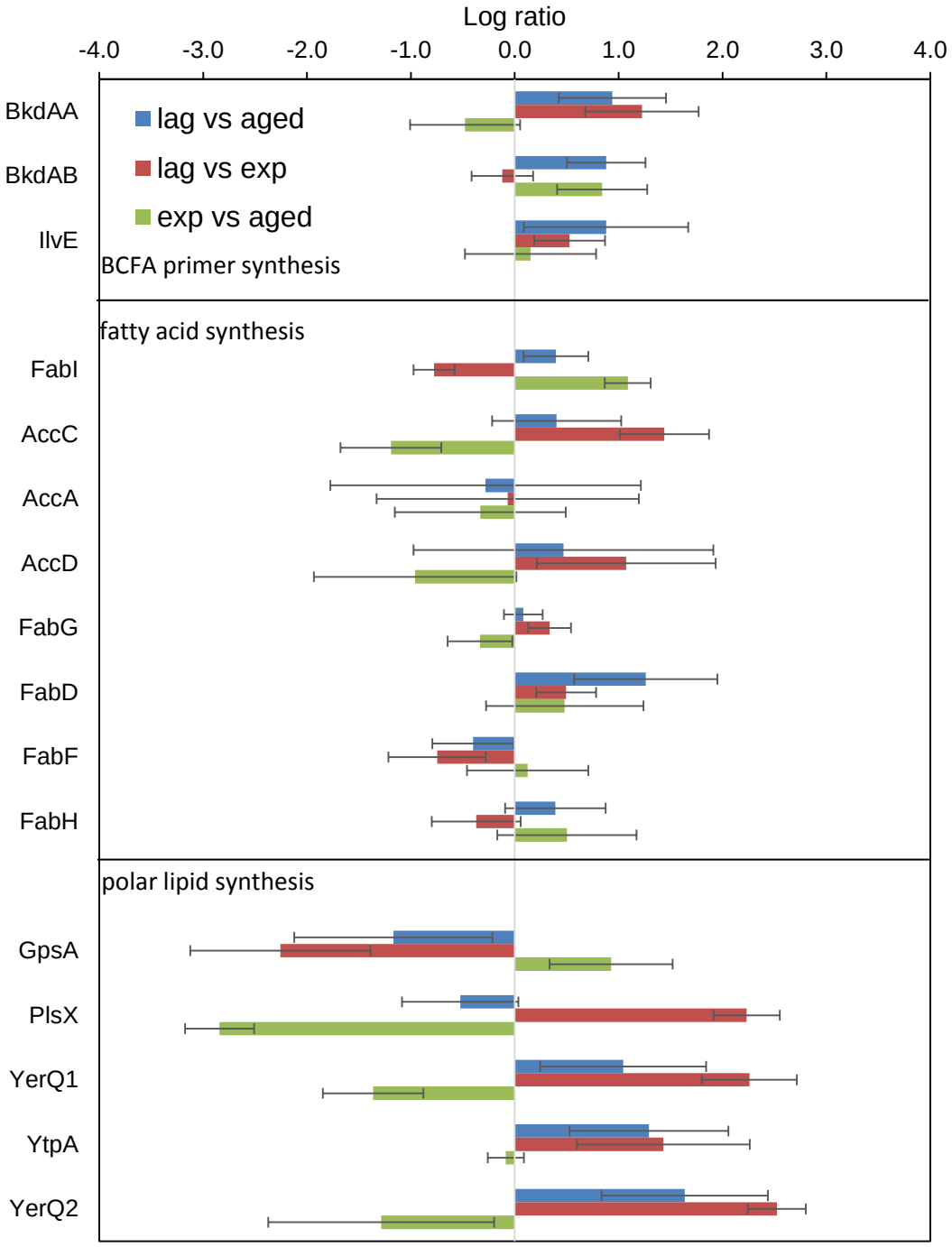

Figure 59**:** The abundance level of detected fatty acid and polar lipid synthesis enzymes in *L. monocytogenes* lag phase in relation to the control (aged and exponential) cultures in TSYE at 37°C. Standard deviations are based on averages from multiple experiments. See text and Appendices II for more details.

Overall, the data suggest that active DNA, fatty acid, and polar lipid biosynthesis is not promoted in lag phase but the activation of RecA, increased RNAP abundance, possible mRNA stabilisation and fatty acid primer synthesis could suggest the scene is set for more active synthesis in cells that can reproduce. The data also suggests an emphasis on accumulating cell resources but not the rapid consumption of these resources committed to ATP-consuming macromolecular synthesis, except perhaps RNA synthesis, effectively the start point of eventual cell growth. This is accompanied by a higher abundance of several influential metabolically constraining transcriptional regulators including CodY and catabolite control protein CcpA. Details on these proteins are given in Chapter 5.

4.4.6 Cofactor metabolism and stress protein responses occurring during the lag phase

ScottA is relatively fastidious and requires a number of vitamins, amino acids, and trace elements for growth (Schneebeli & Egli, 2103). Transport and metabolic mechanisms are present that would promote uptake of these growth factors. Furthermore, various pathways and adaptation responses are available that protect the cells from chemical stresses that would otherwise impede growth. Protein profiles in lag phase were investigated to determine if nutrient uptake and stress defences were accentuated or de-emphasised in lag phase cultures.

Owing to the substantial array of amino acids required by ScottA the primary mode of acquisition appears to be by the import of di- and oligopeptides via ABC transporters, with amino acid liberated via peptidases that have a range of different specificities. Several of these enzymes were detected as being abundant in lag phase (Figure 60). The overall consensus is that a series of specific peptidases are more abundant in lag phase and the number and degree of abundance increases

relative to the exponential phase. The most abundant of these peptidases include proline dipeptidase YtpJ (EGJ25156), Taq-like carboxypeptidase YwpA (EGJ25422) and oligo endopeptidase PepF (EGJ25735). Proline dipeptidase explicitly releases Pro residues while the other enzymes have broader specificity. Taq releases amino acids from oligopeptide terminal ends (except Pro) while PepF hydrolyses 7-17mer oligopeptides. The primary ABC transporters for oligopeptides are suppressed in lag phase cultures relative to aged cells, in particular, the OppFDCBA system (EGJ25739-43) the most abundant amino acid importer. PepF just happens to be coded adjacent to this cluster thus its increase could be just compensatory. When compared to exponential phase cultures the abundance of these transporters in lag phase cultures is more similar. The results seem to suggest uptake is constrained to conserve ATP, since this would be actively consumed by the transporters. However a greater abundance of broad specificity peptidases compensate for this. Several of these proteins are repressed by CodY as described in Chapter 5. Exponential phase cells have slightly greater CodY repression and so peptide uptake and hydrolysis is active in lag phase cultures as would be expected in cells invigorate metabolism by boosting de novo protein synthesis and anabolic pathways, however, the process is tightly regulated to allow for balanced anabolic processes throughout the cells and avoid accumulation of excessive proteins that would only lead to aggregation.

In general amino acid metabolism associated enzymes were not boosted in lag phase and thus de novo synthesis is not especially evident. Cells likely rely on importation of most amino acids. Enzymes greatly increased in aged cells had much lower abundance in lag phase cells, in particular, RocG (Figure 61). As mentioned above there was a suggestion that TCA cycle enzymes are shifted to an anabolic

mode, and the need for reductant is apparently relieved. RocG as well as threonine synthase

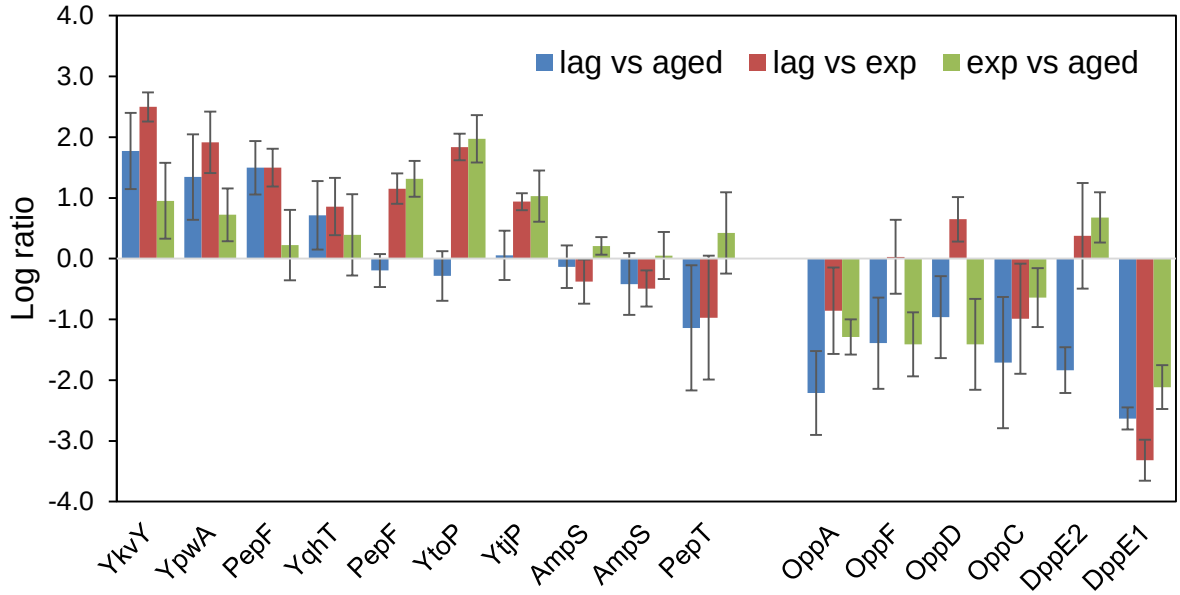

Figure 60**:** The abundance level of detected peptidases and oligopeptide transporters in *L. monocytogenes* lag phase in relation to the control (aged and exponential) cultures in TSYE at 37°C. Standard deviations are based on averages from multiple experiments. See text and Appendices II for more details.

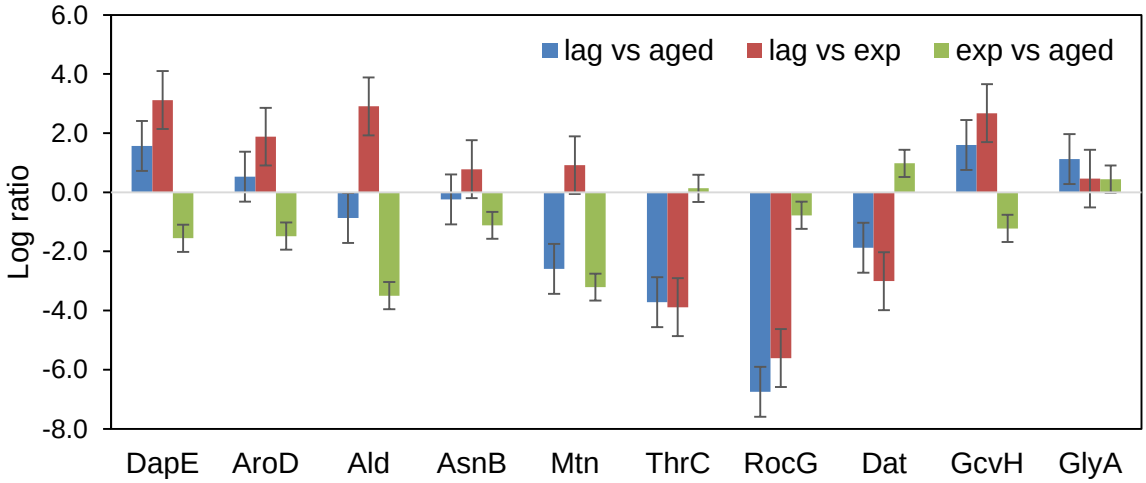

Figure 61**:** The abundance level of selected amino acid related synthesis enzymes in *L. monocytogenes* lag phase in relation to the control (aged and exponential)

cultures in TSYE at 37°C. Standard deviations are based on averages from multiple experiments. See text and Appendices II for more details.

ThrC (EGJ26071) is also subject to CodY repression (see Chapter 5). The dramatic differences in the abundance of RocG (>100-fold) is worthy of further investigation to determine how the changes in L-glutamate influences ScottA's metabolism more broadly and also to determine if the same behaviour occurs in other *L. monocytogenes* strains; there is always the possibility the tendency in ScottA is linked to its greater than normal fastidiousness.

Cofactor metabolism is essential for the creation of compounds needed for enzyme function. Based on the data some enzymes associated with cofactor synthesis seem stimulated in lag phase. However, the pattern is complicated by only some enzymes of the given pathways being detected. There seem to be suggestions that enzymes in the one carbon pool by folate pathway are more abundant including FolD (EGJ24896) and Fhs (EGJ25413) (Figure 61). These enzymes help convert precursor folate to the active methyltetrahydrofolate (methyl-THF) forms which then can donate methyl groups in single-carbon transfer reactions. THF derivatives are vital for various processes, including synthesis of lipoprotein, which is required for enzymes such as pyruvate dehydrogenase and synthesis of BCFA primers. The lipoprotein is created by cleavage of glycine. Increased abundance of GlyA (EGJ26064) and GcvH (EGJ25949) (Figure 61) may suggest a greater activity in the lipoprotein pathway consistent with the greater abundance of the Pdh and Bkd complexes. THF compounds also are required for DNA and RNA synthesis (formation of dTMP and dUMP) that also involves the participation of vitamin B12 (cobalamin).

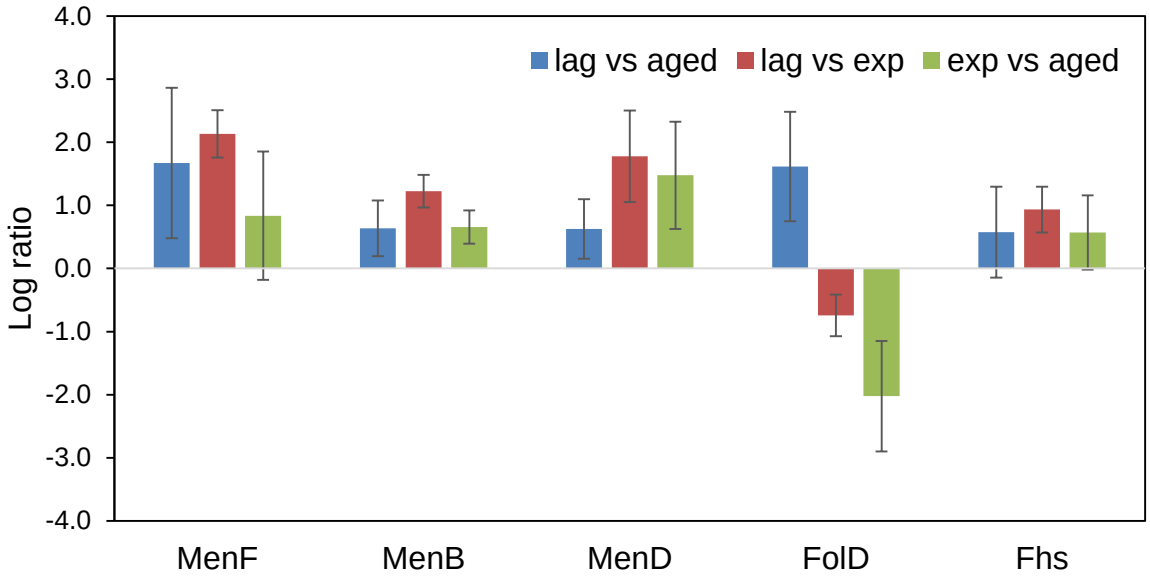

Figure 62**:** The abundance level of selected cofactor synthesis enzymes in *L. monocytogenes* lag phase in relation to the control (aged and exponential) cultures in TSYE at 37°C. Standard deviations are based on averages from multiple experiments. See text and Appendices II for more details.

Menaquinone biosynthesis proteins are also noted to be more abundant in lag phase cells including MenF (EGJ25213), MenB (EGJ25210) and MenD (EGJ25212) (Figure 62). MenF and MenB are the first two committed steps in the pathway leading to MK-8, the primary quinone in *L. monocytogenes* electron transport chain linked proteins including FrdA and glycerol 3-phosphate dehydrogenase GlpD (EGJ24832). GlpD, couples conversion of DHAP to quinone reduction, showed increased abundance (1.9-4.6-fold) unlike FrdA, which significantly declined as mentioned above. It is uncertain if MK-8 synthesis aids lag phase cells. Elevated levels could instead be a prelude to active aerobic oxidative phosphorylation in the exponential phase (see Chapter 5).

In terms of stress adaptation lag phase shows relatively speific responses. Examining stress protective related transporter proteins the data points to increased

compatible solute accumulation and copper and zinc homoeostasis in lag phase cells. Compatible solutes transported could include carnitine, choline, proline and/or glycine betaine. The carnitine Opu transporters (EGJ24962-64) were significantly more abundant while the glycine betaine/proline GbuA subunit (EGJ24518) shows some evidence of greater abundance compared to aged cells (Figure 63). Copper and zinc homeostasis protein ZosA, was notably more abundant in aged cells, and along with CopZ (EGJ25388) (Figure 62), a another putative copper homeostasis protein, likely maintain appropriate concentrations of these metal ions in cells where they can serve as enzyme cofactors, such as for metallopeptidases, which are noted as being more abundant above (Figure 60). These metal ions owing to their strong oxidising properties become toxic if they over accumulate. Several enzymes involved in detoxification are abundant in lag phase cells (Figure 64). These enzymes likely act to remediate the inputted aged cells that may have accumulated toxic intermediates. The array of toxic compounds targeted seems quite broad. However, several enzymes linked to this property remain poorly characterised. The compounds putatively include bile conjugates (Bsh), tellurite/metalloids or other toxic anions (YaaN, EGJ25503), peroxides, oxygen radicals, iron, chlorine and other reactive oxidative compounds (SodA, Dps, YqjM, YwfI, BsaA); and methylglyoxal-derived compounds and glycated amino acids emerging from glycolysis reactions (YraA, YugJ, YvgN, YqgX). Interestingly, catalase (KatX) was not detected in lag phase, this enzyme is only sufficiently abundant in exponential phase cells, likely linked to active fermentation. The enzyme pyruvate oxidase, one of the key steps in substrate phosphorylation via acetate kinase generates H_2O_2 as a consequence of its activity.

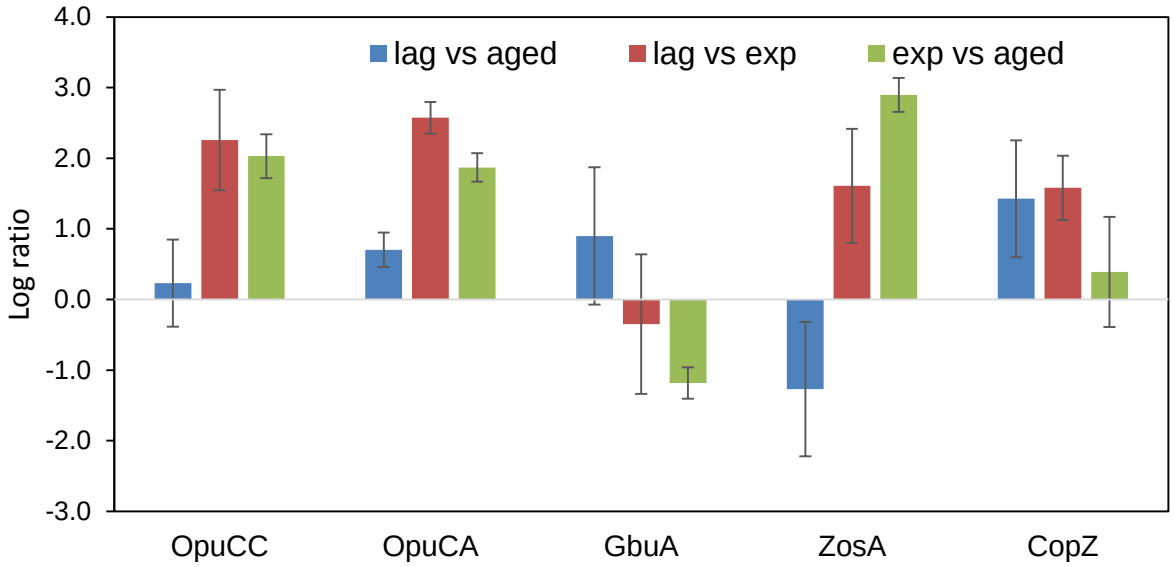

Figure 29**:** The abundance level of detected transporters involved incompatible solute uptake and metal ion homoeostasis in *L. monocytogenes* lag phase in relation to the control (aged and exponential) cultures in TSYE at 37°C. Standard deviations are based on averages from multiple experiments. See text and Appendices II for more details.

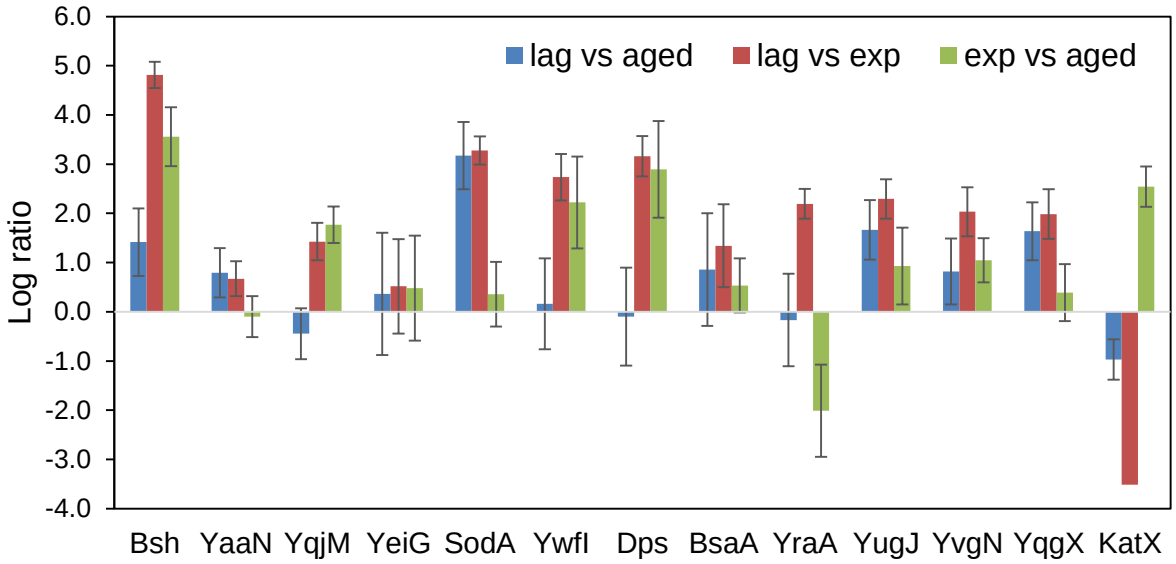

Figure 64**:** The abundance level of detected enzymes involved in detoxification processes in *L. monocytogenes* lag phase in relation to the control (aged and exponential) cultures in TSYE at 37°C. Standard deviations are based on averages from multiple experiments. See text and Appendices II for more details.

Overall, there was no compelling evidence during lag phase cultures strong activation of anabolic pathways for synthesis of amino acids occurs but stimulation of some pathways that lead to cofactors does (such as THF, MK-8). Amino acid requirements are mostly met via di- and oligopeptide uptake and peptidase activity, however, kept in balance with other processes in the cell. There was better evidence of protective responses including compatible solute uptake, toxic transition metal homoeostasis and detoxification, especially oxidising compounds. The data suggests that the cultivation conditions creates cells ready for the active growth phase. Further studies are needed to see if this overall response is similar at lower temperatures since there could be a high temperature dependency in the nature of the protein level changes.

4.5 Conclusions

Overall, lag phase cells activate a large number of processes, however, the activation is not a “full steam ahead” approach rather the changes observed in the transition from aged cells to exponential phase cells suggest: i) a reactivation of metabolism including anabolic pathways, primarily synthesis of critical precursors for downstream pathways; ii) an increase in fermentation associated proteins that would add to cell energy via substrate level phosphorylation reactions; iii) a rebound back to more exponential-like physiological state in terms of protein synthesis, folding and turnover; iv) accumulation of compatible solutes, cytoplasmic buffering via the GAD system and F_1F_0-ATPase, and RecA activation that provide subsequent protection of cells during active growth; and v) induction of tress management proteins that orimarily remediate the cell cytoplasm before active growth occurs. The data also

points to increased abundance of several regulators and regulons that lead to the lag phase transitional state. These pehomena are investigated in the next chapter,

5 Regulation within the rejuvenating aged Listeria monocytogenes Scott A

5.1 Abstract

Utilising proteomic data an original insight into the global regulation of protein production by *L. monocytogenes* ScottA during aging and lag phase processes at 37°C was performed. The data suggest that in lag phase SigB, SigH, CtsR, HrcA and AgrA regulons are more activated relative to aged and exponential cells while the PrfA and SigC regulons are strongly repressed. CodY levels were highly elevated during lag phase resulting in active repression and derepression of its regulon. The activation responses collectively link to increased fermentation and anabolic processes, protein folding and rescue, remediation of the cytoplasm from toxic compounds, and buffering of cytosolic proteins. At the same time the combined increased abundance of CodY and catabolite control protein CcpA seems to lead to constraints on the levels of enzymes that rely on expenditure of ATP, possibly allowing build-up of anabolic precursors, ATP and reducing equivalent pools prior to exponential growth. The data supports the observation that lag phase responses are rapid and that the proteomes do not rebound back to the former exponential phase state. The data also suggest that the extent of aged incubation results in largely homogenous responses throughout the lag phase though subtle differences were observed in the degree of activation of regulons. This incomplete rebound effect creates the possibility that inputted cell recovery in lag phase manifests different

outcomes for outgrowth in the exponential phase depending on the physiological nature of the inputted cells.

5.2 Introduction

A regulon is a group of genes and operons that are regulated by the same regulatory machinery, often as a unit. A bacterial regulon consists of *trans* transcription factor regulators and *cis*-regulatory binding elements in the promoters of the operons they regulate (Zhang et al., 2012). Since the term *regulon* was first proposed in 1964 by Maas and colleagues, numerous regulons have been progressively recognised in widely–studied model organisms (*E. coli*, *B. subtilis*), as well as in many other bacteria.

A number of studies have used genomic tools, including microarray analysis, to analyze transcriptomes of the food-borne pathogen *Listeria monocytogenes* during growth under normal conditions as well as under myriad stress conditions (e.g. Bayles et al., 1996; Graumann et al., 2002; Liu et al., 2002; Derré et al., 1999). The coordinated response to environmental signals is partly controlled by a genetic system under the control of the alternative RNA polymerase sigma factors (σ^B, σ^C, σ^H, and σ^L) with SigB (σ^B) the most extensively studied (Abram et al., 2008). Mutants of *L. monocytogenes* that lack the *sigB* gene have a variety of stress-sensitive phenotypes including acid and oxidative stress sensitivity, as well as being rendered virtually avirulent. In *L. monocytogenes*, the σ^B regulon broadly consists of ~150 transcriptional units encoding proteins involved in stress tolerance, carbon metabolism, transport, cell envelope-related functions, and virulence (Raengpradub et al., 2008; Kazmierczak et al., 2003). SigB has been found to be mainly responsible for acid stress adaptation but likely plays a major role in gene expression

cascades that allow *L. monocytogenes* cells to rapidly respond to a range of stresses and promote a physiological state that supports growth.

The other sigma factors of *L. monocytogenes* have defined regulons as well. SigC (σ^C), SigL (σ^L; RpoN), and SigH (σ^H) when deleted do not result in stress sensitivity or loss of virulence (Arous et al., 2004) suggesting they are involved in less critical aspects of cell function. Furthermore, the substantial overlap with other regulons (especially SigB) by SigH and SigL could render them partly redundant (Chaturongakul et al., 2011). Recently, SigH has been found to regulate competence genes (in strains that still possess this capability) and intracellular growth (Medrano Romero & Morikawa, 2016). A more recent study also has shown SigL regulon is more extensive and thus seems important in the generalized coordination of cell functions (Mattila et al., 2012). SigB also overlaps with the regulons of the transcriptional repressors CtsR and HrcA, which negatively regulate heat shock genes (e.g., *clpP*, *clpC*, *dnaK*, and *groES*) as well as genes associated with central metabolism (Hu et al., 2007a, 2007b; Chaturongakul et al., 2011).

PrfA, a Crp family regulator, activates the main pathogenicity island Lip1 (*prfA-plcA-hly-mpl-actAplcA*) in addition to other virulence genes (e.g., *inlA, inlB* and *inlC*) during host infection (Milohanic et al., 2003). PrfA is under the control of an sRNA thermoregulator (Sesto et al., 2014) and thus is only active at 37°C, however other signalling cues are required for full expression, in particular, glutathione (Reniere et al., 2015). A second essential virulence regulon in *L. monocytogenes*, after the *prfA* regulon, is controlled by VirR, which regulates virulence through cell wall component modifications (Mandin et al., 2005). It has been shown VirR controls genes that are associated with teichoic acid D-alanylation (DltABCD) as well antimicrobial efflux pump-like protein MprF (Kang et al., 2015). These proteins likely confer protection to

cells from the innate immune system as well as food preservatives (such as organic acids, nisin, chitosan and lauric alginate).

CodY, a BCAA and GTP-binding protein, was first identified in *Bacillus subtilis* as a critical factor in controlling the expression of stationary phase genes. It usually represses genes whose products are involved in adaptation to reduced nutrient growth conditions but is also involved in activation/repression of virulence genes in pathogens (Geiger & Wolz, 2014). In *L. monocytogenes* CodY controls many early stationary phase genes (Sonenshein, 2005). Other studies have demonstrated that CodY has a multifaceted role in *L. monocytogenes* being required for full *prfA* activation, linked to the stringent response, and integrating metabolism, stress management, motility and virulence (Bennett et al., 2007; Lobel & Herskovits 2016).

Iron limitation results in the regulation of a number of genes, especially those involved in iron uptake. A subset of these genes occurs in a regulon under the control of Fur (Ledal et. al, 2010). Fur represses iron uptake preventing excessive levels of iron building up in the cytoplasm since this can lead to oxidative stress via the Fenton reaction. Other regulons are involved with cell protection including PerR, which senses and regulates the removal of oxidatively damaging peroxides (Rea et al., 2004). PerR interacts with Fur and has overlaps with the SigB regulon indicating these regulators cooperate in global oxidative management (Ledala et al., 2010). Fur and PerR interact to regulate the essential iron- and DNA-binding protein Dps, which protects DNA from oxidative damage as well as store iron. Overall, the Fur and PerR regulons aid in maintaining iron and redox homoeostasis. DNA damage leads to the instigation of SOS response repair mechanism, a process regulated by recombinase RecA. The RecA regulon has been determined for *L. monocytogenes* (van der Veen

et al., 2010) and follows the conserved form in which RecA is repressed by LexA. RecA mutants tend to undergo hypermutation and have reduced fitness.

Cell adhesion in *L. monocytogenes* was found to be partly regulated by a quorum sensing autoinduction system termed the Agr system (Garmyn et al., 2009). The Agr system consists of a two-component sensor histidine/response regulator (AgrA, AgrC), a peptide processor/exporter protein (AgrB) and a quorum sensory propeptide (AgrD). The regulon controlled by AgrA was generally resolved (Garmyn et al., 2012) and found to be temperature dependent and could influence nitrogen transport, amino acid synthesis, purine and pyrimidine biosynthetic pathways and phage-related functions. The AgrA regulon also overlaps other regulons including SigB, SigH, PrfA and CodY. AgrA derepression is associated with good growth at 37°C.

Overall, *L. monocytogenes* has an extensive regulatory network that is still being unravelled, especially in terms of the roles of non-coding RNA such as sRNA elements. The fact that many regulons overlap also suggest responses to environmental challenges involve nuanced, complex responses that can result in a spectrum of adaptation states within the same cell population, situations typical of epigenetic traits (Casadesús & Low, 2013). Also, differences have been noted between *L. monocytogenes* genetic lineages such that the core genes in the SigB regulon represents a subset of only about 63 genes (Oliver et al., 2010) and the stress tolerant phenotypes attained may differ between strains (Durack et al., 2013). It is unknown how various other regulons are arranged between genetic lineages. For the purposes of this study we used the current state of knowledge to highlight the activation of regulons in *L. monocytogenes* during the aging process and during initial lag phase including an identification of the primary proteins induced under

these conditions complementing data from the previous thesis chapters. Indeed, in this study, we used the data obtained in previous chapters to test the significance of changes in overall regulons statistically. The objective was to understand better how *L. monocytogenes* generally responds during the lag phase that involves recovery responses as well as examining responses in aging cultures and in the exponential phase.

5.3 Materials and Methods

The proteomic data investigated are derived from chapters 3 and 4. All data were considered in relation to cell aging. For the lag phase investigation, only the proteomes of cells held 30 min in fresh TSYE broth were examined since other time points only subtly differed as described in Chapter 4.

The T-profiler method uses a penalised *t*-test to score the difference between the mean expression level of predefined groups of proteins and that of all other proteins within a functional set. For a given function set group G, the t-value is provided by the following formulae:

$$t_G = \frac{\mu_G - \mu_{G'}}{s\sqrt{\frac{1}{N_G} + \frac{1}{N_{G'}}}}$$

$$s = \sqrt{\frac{(N_G - 1) \times s_G^2 + (N_{G'} - 1) \times s_{G'}^2}{N_G + N_{G'} - 2}}$$

Where μ_G is the mean expression log-ratio of the N_G proteins in function set group G, $\mu_{G'}$ is the average expression log-ratio of the remaining $N_{G'}$ portion of the proteome and *s* is the pooled standard deviation, as obtained from the estimated variances for groups G and G′. The associated two-tailed P-value calculated from t using the t-distribution with $N_G - 2$ degrees of freedom and is corrected for multiple testing by multiplying it by the number of function set groups that are being tested in parallel.

The resultant *p*-values were tested for type 1 error via false discovery rate analysis (Benjamini & Hochberg 1995). All groups with a corrected P-value of ≤0.05 are considered to be significantly regulated. A *t*-value of > +3 and −3 can be considered statistically significant for all sets, regardless of size ($p < 0.01$).

A number of regulons were investigated: including; SigB (Oliver et al., 2010), SigL, SigH (Chaturongakul et al., 2011; Matilla et al., 2012; Mujahid et al., 2013), CodY (Bennett et al., 2007), PrfA (Milohanic et al., 2003), AgrA (Garmyn et al., 2012), CtsR, HrcA (Hu et al., 2007a, 2007b), Fur, PerR (Ledala et al., 2010), RecA (van der Veen et al., 2010), and VirR (Mandin et al., 2005). Though not a regulon the overall response of virulence-associated proteins was also investigated. The comprised known list of virulence factors was derived from the VFDB database (www.mgc.ac.cn/VFs/).

5.4 Results and Discussion

5.4.1 Regulon responses during the lag phase relative to aging and the exponential growth phase

Proteome data assessed using the T-profiler approach results in statistical trends (T-value scores) that can be used to ascertain whether a regulon is activated, repressed or derepressed where relevant to the particular regulon concerned. The T-value data obtained was visualised here as a heat map (Figure 65) with positive T-values indicating overall activation or derepression of the regulon while negative T-value indicate repression. Scores >+2 and <-2 are significant at the 0.05 level (+>3/-<3, $p<0.01$). It should be noted this data carries a number of caveats: i) the data involves relative comparison between cell physiological states (aged, lag phase and exponential phase) and is not examining an “on/off” response; ii) it assumes the

regulon transcriptome reflects the proteome accurately – in that sense other levels of regulation are also in essence incorporated in the trends observed; and iii) the data is an overall trend, the regulons due to their interactions include proteins behaving in contrary ways. The responses are in general complex since genetic elements are controlled at different levels and have an array of interactive molecular mechanisms that contribute to possible epigenetic heterogeneity (Guariglia-Oropeza et al., 2014).

Overall, regulons that were activated in lag phase relative to aged cells ranked in terms of the strength of the response were SigB, SigH and CtsR. Proteins of genes derepressed by CodY were also activated. When lag phase cells are compared to exponential cells, this activation is stronger with the HrcA and AgrA regulons also activated.

There were equivocal responses for the SigL, VirR, PerR and Fur regulons. The RecA regulon response also was not statistically above the signal to noise threshold. The relevant CodY and PrfA regulons were repressed in lag phase when compared with either exponential or aged cells. The overall results of the comparisons of aged versus exponential cells necessarily show that SigB, SigH, HrcA and PrfA regulons were the most activated in a relative sense while the other regulons were not statistically different. The hierarchical cluster analysis supports the strong relation of lag phase responses for the four culture age time points, which agrees with the observation of highly correlated functional set responses as shown in Chapter 4.

5.4.2 Networked regulons that contribute to lag phase recovery

Lag phase induced activation of SigB and SigH regulons and derepression of CodY, AgrA, CtsR, and HrcA regulons occurs (Figure 65); 42 and 53 proteins belonging to the aforementioned regulons were significantly activated in lag phase relative to aged cells and exponential phase cells, respectively (Table 4). For the results and

discussion of this phenomenon, CodY is treated separately due to its pleiotropic nature (section 5.4.3). The overall activation response links the involved regulated proteins in growth supporting or enacting roles. The proteins are interconnected in terms of regulation with 23% grouping in two or more regulons. Most are linked to the CodY regulon and also extend to the Fur and PerR regulons (Table 4).

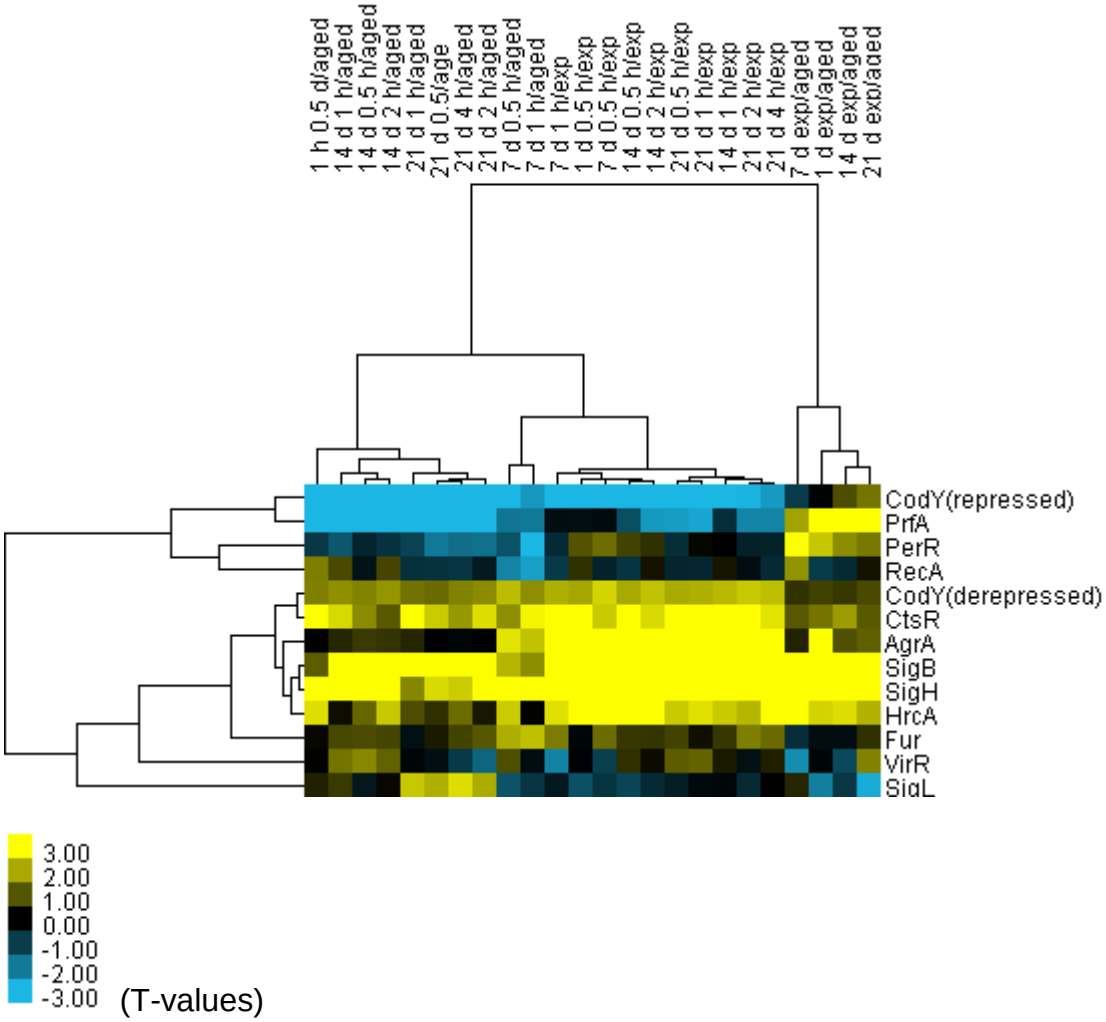

Figure 65**:** Heat map is showing statistical trends of regulons based on the proteome of *L. monocytogenes* ScottA in lag phase in TSYE at 37°C. For aged cell treatments, cells were grown for either 1 d, 7 d, 14 d or 21 d. For lag phase treatments, aged cells were resuspended in fresh TSYE at 37°C for 0.5 to 4 h (depending on the cell age). Comparisons are also made with cells from the exponential growth phase (ex) grown for approximately 12 h.

The processes the activated proteins cover is extensive, and several of the proteins listed in Table 4 have already been mentioned in Chapters 3 and 4 in relation to their involvement in aged cell and lag phase adaptation. The proteins responding in lag phase when compared between age and lag phase and aged and exponential the results are surprisingly quite consistent though some variations occur (Table 4). Amongst proteins associated with substrate uptake and subsequent catabolism, variation is observed for glucose transporters (MptC, TreP), which could have different affinities to D-glucose (Stoll & Goebel, 2010). Sugar metabolism is tightly controlled in lag phase, the putative glycolysis regulator CggR was consistently activated along with catabolite control protein (see section 5.4.4), this is not evident in aged cells. Another significant and consistent difference is that CwlO/Spl autolysin abundance is still much higher in lag phase than in exponential phase cells (but 5-40 fold lower when compared to aged cells). This protein is regulated by SigH (Chaturongakul et al., 2011). Cell autolysis could be induced if SigH levels reach a critical threshold. SigH, however, has very low abundance in cells for all treatments and was only barely detected in the 21 d cultures. It was also noted that signalling proteins activating genes relevant to cell wall stress also might influence CwlO/Spl (see section 5.4.5). Variations are also observed in terms of protein translation and folding. Aged cells have lower elongation factor G (Fus) and molecular chaperone DnaK. The rebound of these essential proteins in lag phase likely reestablishes conditions compatible for culturability. The ribosomal protein Ctc/RplY has been shown to be necessary for efficient translation under stress conditions (Schmalisch et al., 2002; Gardan et al., 2003) and damage associated with aged cells may lead to activation of Ctc in the lag phase cultures. Similarly, protein remediation also seems

an activated feature in lag phase. Removal of amino acid glycation groups from proteins by YraA was mentioned in Chapter 4. A thioredoxin family protein EGJ24563 may also have a role in redox homoeostasis though this requires specific experiments to determine the exact function of the protein. Protection of the cellular processes was also mentioned in Chapter 4 and includes removal or control of potentially toxic metabolites (formaldehyde via YeiG), metallic ions (Dps, ZosA) and general stabilisation of cytoplasmic conditions (compatible solute uptake, GAD system). The activation of cyclic-di-AMP phosphodiesterase PdeA likely aids in maximising growth rates and cell wall stability (see section 5.4.4 and 5.4.5). Several uncharacterized proteins were noted as being activated, many of which are also CodY regulated. All are relatively abundant in lag phase cells suggesting they could play significant roles in the cell. The roles these proteins play can only be speculated upon and information on these proteins are given Table 5. Of these proteins the best studied is YceI. This protein could have a possible role in PG synthesis since the lipid carrier involved in the process is a polyisoprenoid compound. Another role is in the delivery of the isoprenoid component to MK8; it was noted in Chapter 4 a number of menaquinone biosynthesis proteins were more abundant in lag phase. The YaaQ protein could also potentially have a signalling role assuming it binds cyclic-diAMP and could be linked to PdeA activity.

Table 4. *Proteins activated during the lag phase that belong to interconnected regulons (SigB, SigH, CtsR, HrcA, AgrA, CodY, PerR, Fur) in L. monocytogenes ScottA.*

Function	**Relative to stationary phase (aged cells)**	**Relative to exponential phase**
substrate uptake and catabolism	FruA, TreP	FruA, MptC
sugar metabolism	GlpD, GpmA, NagB, EGJ24055,	GlpD, GpmA, NagA, NagB, EGJ24055
fermentation	Ldh, PflA, YdaP, AlsS,	Ldh, PflA, YdaP, AlsS,

	AlsD	AlsD
regulation of central glycolysis genes	CggR	CggR
amino acid synthesis	AspB	
nucleoside biosynthesis/salvage	**GuaB1***, Pdp	**GuaB1***
ribonucleoside uptake	YufO	YufO
RNA polymerase	SigA	SigA
PG synthesis and turnover	MurD	MurD, CwlO/Spl
cell division	**MreB***, GpsB	**MreB***, GpsB
fatty acid biosynthesis		AccC
phospholipid turnover	PldB	PldB
ribosome	RplK, YvyD	RpsC, RplY/Ctc, YvyD
protein synthesis	Fus, GatA	
nascent protein folding/rescue	DnaK, GrpE	GroEL, GroES
recycling defective proteins	ClpC(ClpB)	ClpC(ClpB), ClpP1, ClpP2
protein remediation	EGJ24563	YraA, EGJ24563
iron homeostasis		**Dps****, YhgC
acid pH homoeostasis (GAD system)	GadB2	GadB2
compatible solute uptake	**OpuCA***	**OpuCA***
toxic metal ion homoeostasis		**ZosA****
detoxification of formaldehyde		YeiG
the unknown stress response	**YdaG***	**YdaG***
stress regulation	YxiE	YxiE
Signalling (improved fitness)	**PdeA***	**PdeA***
unknown function	YtxG, YceI, **YfhF***, YhfK, YjdN, YunF, EGJ24798, **EGJ24781***	YtxG, YceI, **YfhF***, YhfK, YjdN, YunF, YaaQ, **EGJ24170***, **EGJ24455***, EGJ24798, **EGJ24781***

*CodY derepressed proteins.
**Proteins regulated by Fur and/or PerR

Table 5. *Functionally unknown proteins activated in the lag phase of L. monocytogenes ScottA in TSYE broth at 37°C.*

Scott A locus		Protein features
EGJ25138	YtxG	General stress-induced membrane protein; conserved domain present is of unknown function
EGJ24296	YceI	Base induced periplasmic protein in *E. coli* (Stancik et al., 2002). Binds polyisoprenoid compounds (Handa et al., 2005).
EGJ25231, EGJ25920	YfhF, YhfK	Short chain NAD-dependent epimerase/dehydratase dehydrogenase/ REductase family protein
EGJ26249	YjdN	DNA binding 3-demethylubiquinone-9 3-methyltransferase domain-containing protein
EGJ24170 EGJ24798 EGJ24455		No conserved domain present
EGJ25932	YunF	YecE family conserved domain of unknown function
EGJ26217	YaaQ	cyclic-di-AMP receptor family protein
EGJ24781		prophage or transposon conserved domain

5.4.3 CodY contributes to adaptation during lag phase

CodY (EGJ24820) serves in a dual regulatory function that controls adaptation to low levels of specific nutrients by both directly suppressing and activating various metabolic pathways (Bennett et al., 2007; Lobel & Herskovits, 2016). CodY in *L. monocytogenes* responds to low availability of BCAAs, mainly isoleucine (Lobel et al., 2012), and within mammalian cells induces BCAA and histidine biosynthesis and virulence genes by interacting with PrfA (Lobel et al., 2015). A recent study by Lobel & Herskovits (2016) revealed under otherwise BCAA rich conditions (Brain Heart Infusion [BHI] broth, 37°C) CodY in *L. monocytogenes* strain 10403S repressed BCAA and histidine synthesis while it activated TCA cycle linked anabolism (*citZ*, *citB*, *icd, glnA, frdA*), arginine biosynthesis and motility gene expression. Purine and nitrogen metabolism (*rocG*) was repressed while virulence under low BCAA nutrient conditions (minimal medium of Phan-Thanh & Gormon, 1997; 37°C) pyruvate oxidase (*ydaP/poxB*),, stress and motility gene expression were more active. For the experiments in this study, we relied on the CodY regulon defined in strain EGD-e (Bennett et al., 2007) based on the culture conditions (BHI, 37°C) they used.

Analysis of the proteome data revealed CodY abundance was high in lag phase (abundance 6.7±1.4) but was not detected in exponential, 1 d and 7 d cells. A low level of CodY was detected in 14 d and 21 d cells (Figure 65). Lag phase incubation of ScottA, as performed here, demonstrates that CodY abundance is rapidly elevated and persists at least in the more aged cells where the data is available (Figure 65). For the extended stationary growth phase incubation experiment ScottA cells were initially passaged to achieve physiological homogeneity. The CodY levels at early stationary growth phase were similar to exponential cells. The result of this

suggests that depletion of cell ATP does not trigger the CodY regulon and that its response is restricted to amino acids and other nitrogenous compounds.

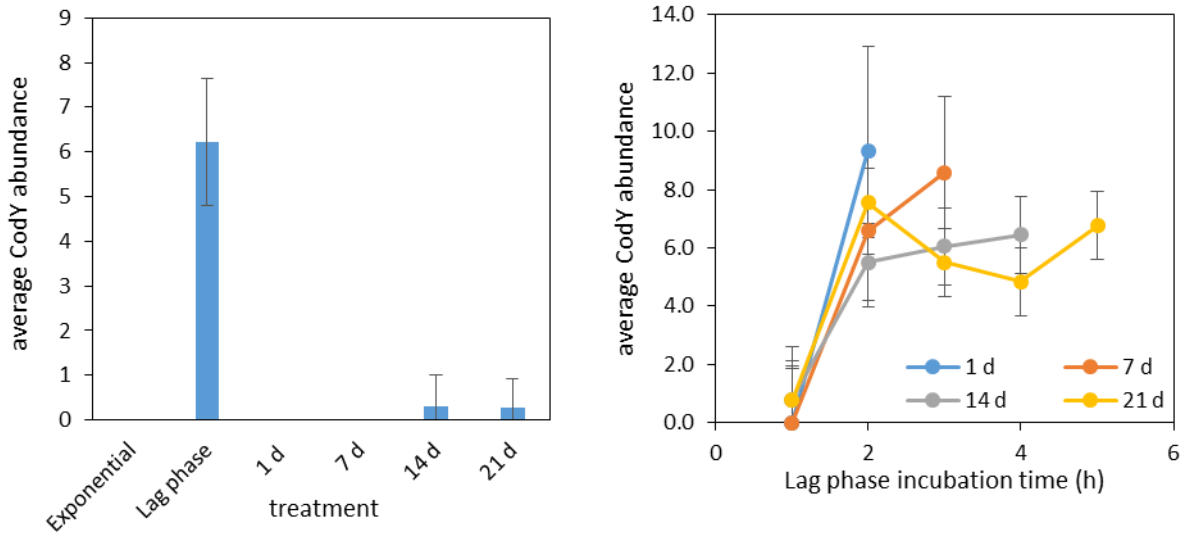

Figure 66**:** Average CodY abundance in *L. monocytogenes* grown in TSYE broth at 37°C. The right-hand graph shows CodY abundance within lag phase incubated for different times with inputted cells receiving different initial incubation durations.

Though de novo ability to synthesise BCAAs and His in ScottA is compromised enzymes of the BCAA synthesis pathway are readily detected (Figure 66); on the other hand enzymes of the histidine biosynthetic pathway are generally not identified. De novo BCAA synthesis seems most active during exponential growth. As mentioned in Chapter 3, enzymes (except LeuA) decline in overall abundance in aged cells. However, in lag phase cultures only IlvE could be detected. Lobel & Herskovits (2016) indicated *ilvC* and *ilvD*, were very strongly repressed (>50-fold) by CodY under BCAA rich conditions. The data thus suggest CodY repression is occurring in lag phase since IlvC and IlvD, relatively abundant in both exponential and aged cells are non-detectable in lag phase cells. The weak increase in CodY over the incubation time of aged cells (Figure 65) could be sufficient to detectably

reduce BCAA synthesis since the pathway draws down on pyruvate, otherwise needed for energy generation via fermentation. Since the CodY levels were rapidly achieved in lag phase (Figure 65) CodY synthesis itself could also be impeded in aged cells, possibly due to disruptions to protein translation and lack of precursors.

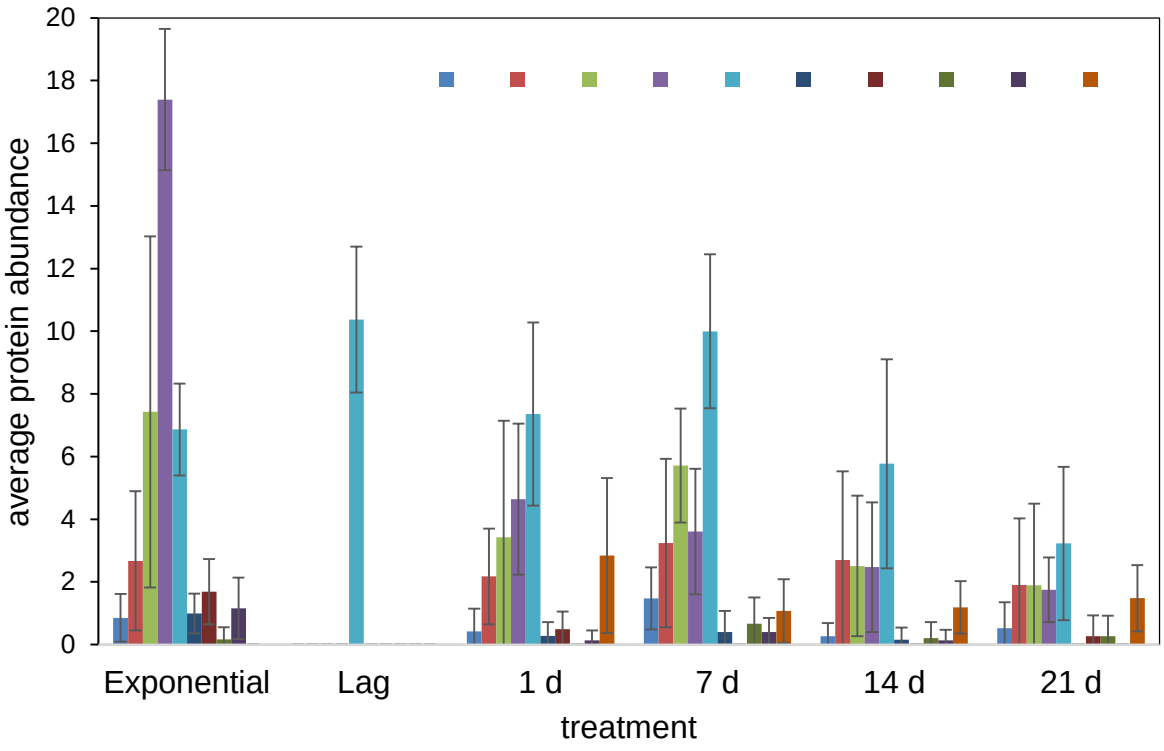

Figure 67**:** Protein abundances for enzymes of the CodY regulated BCAA synthesis pathway (excluding AlsS) showing differences between growth phases of *L. monocytogenes* grown in TSYE broth at 37°C.

Looking more broadly at the CodY regulon (based on Bennett et al., 2007 assessment) 11 proteins were significantly repressed in the lag phase while 6 to 11 proteins were derepressed (Figure 66). The proteins observed cover an extensive range processes. In lag phase controlled proteins include those involved in carbohydrate catabolism (putative fructose lysine kinase, putative alpha-1,4-glucosidase YicI, putative fructose/mannokinase GmuE); pentose phosphate pathway (transketolase Tkt); amino acid directed anabolism (glutamate

dehydrogenase RocG, D-3-phosphoglycerate dehydrogenase SerA); and motility (flagellin Fla, flagellum capping protein FliD). Three proteins included in this set only have generally predicted or unknown functions.

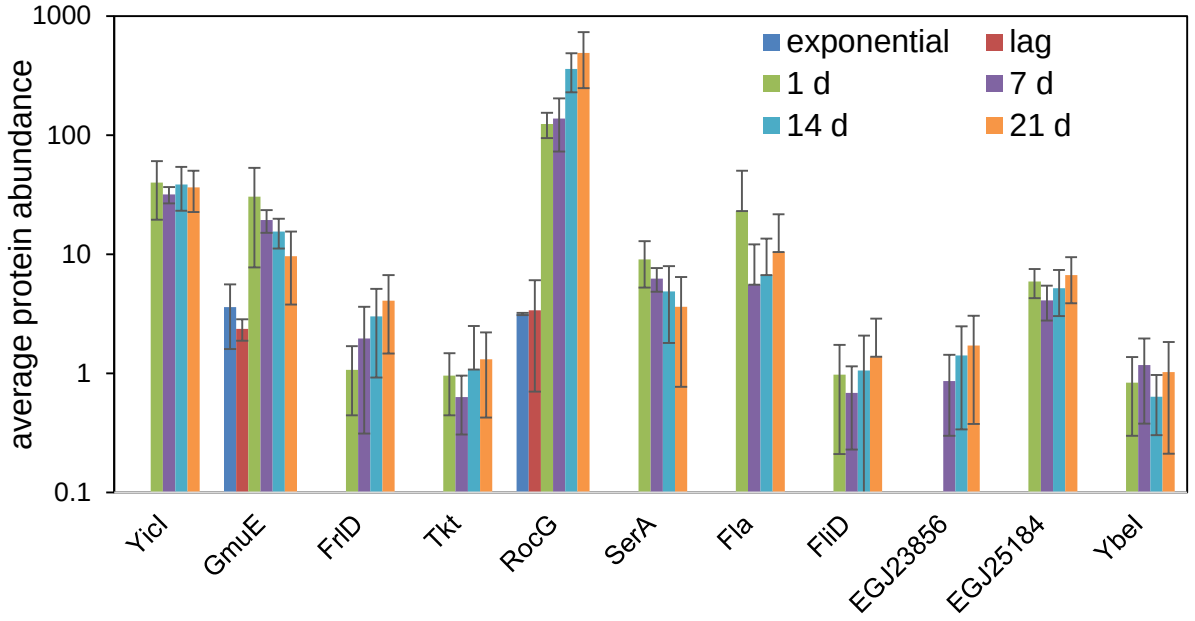

Figure 68**:** CodY repressed proteins in *L. monocytogenes* ScottA grown in TSYE at 37°C for different times and also within the lag phase.

Overall, the results generally agree with that of Lobel & Herskovits (2016) model even though they were mainly looking at an exponential culture scenario with a different strain and medium. The scenario in this study is that lag phase cells are BCAA rich due to the provision of fresh media, and this results in repression of BCAA synthesis (Figure 68). Repression also occurs for carbohydrate metabolism proteins activated in aged cells for scavenging available substrates (putatively glycated amino acids via FrlD), and hypothetically also RocG, which could be performing oxidative deamination of L-glutamate to 2-oxoglutarate.

Motility proteins, most notably Fla, however, were repressed not activated, though Fla and FliD become derepressed in aged cells where CodY levels are low (Figure

69). Other motility and chemotaxis proteins overall do not vary systematically as a group

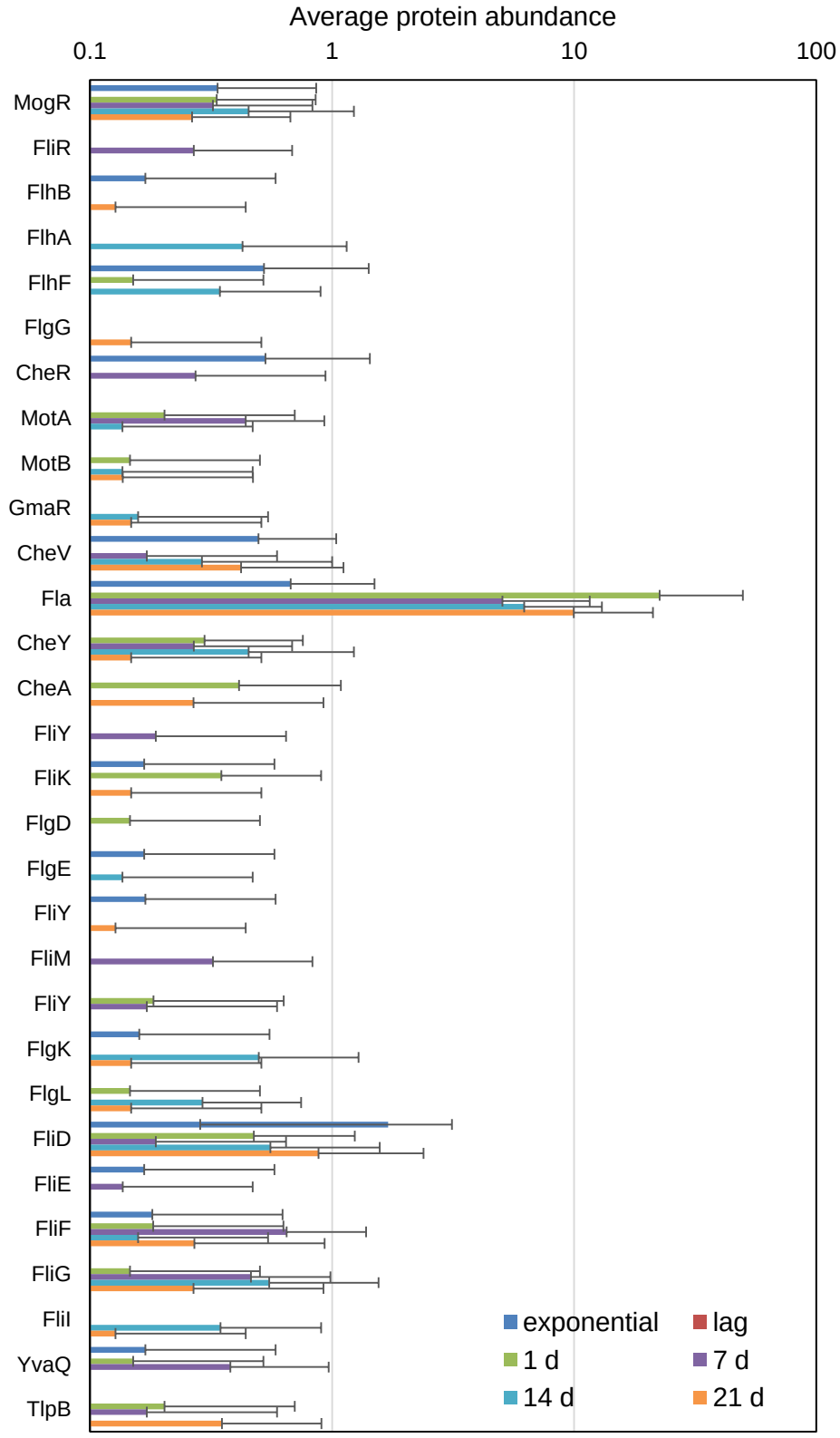

Figure 69**:** Motility and chemotaxis protein abundances in *L. monocytogenes* ScottA grown in TSYE at 37°C for different incubation times and also within the lag phase.

in terms of abundance, which is near detection limits as would be expected at 37°C. The flagella repressor MogR is detectable while the antirepressor GmaR is only detectable in 14 d and 21 d samples. The lack of motility phenotype in aged cells (Chapter 2) could suggest Fla, and FliD detected are non-secreted precursors or alternatively, a lack of ATP and an impaired chemiosmotic gradient precludes mobility activity.

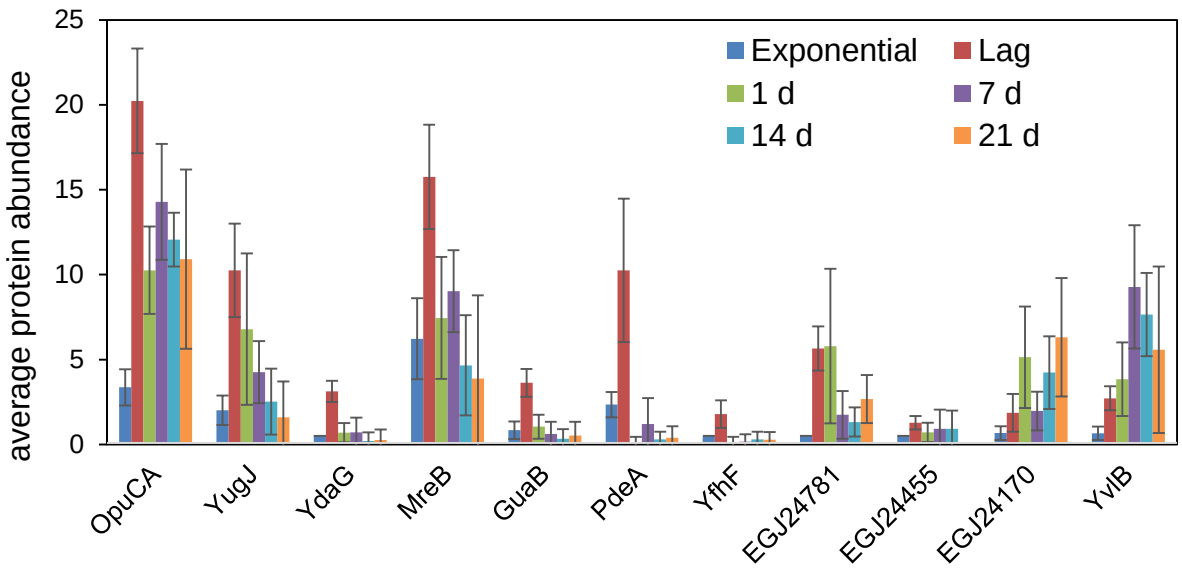

Figure 70**:** CodY derepressed proteins in *L. monocytogenes* ScottA grown in TSYE at 37°C for different times and also within the lag phase.

Several CodY regulated proteins promoting or protecting cell growth were derepressed (Figure 70) as predicted by Lobel & Herskovits (2016). Most of these proteins are interlinked within regulatory cascades. Of the 11 CodY derepressed proteins defined here, 9 are regulated by SigB and/or SigH while two are regulated by AgrA. This is consistent with the concept that CodY activation is integrated into

modulations that promote growth (or at least maintain cell viability) as well as the agr quorum sensory system, derepression of which promotes good growth at 37°C (Garmyn et al., 2012). The response incorporates proteins associated with stress response (carnitine uptake ABC transporter subunit OpuCA, putative alcohol/aldehyde dehydrogenase YugJ, general stress protein YdaG); cytokinesis (actin-like cytoskeletal protein MreB), purine biosynthesis (inosine monophosphate dehydrogenase GuaB1) and signalling related to improved fitness (cyclic-di-AMP phosphodiesterase PdeA) becoming more abundant in lag phase cells. Four other significantly derepressed proteins (YugJ, YdaG, EGJ24781, EGJ24455) have unknown functions.

Overall, CodY behaviour in lag phase and aged cells is broadly consistent with current knowledge and shows that it has a distinct role in cell recovery and adaptation in lag phase.

5.4.4 The PrfA regulon is actively repressed in lag phase cells but partially active in aged cells

PrfA and VirR regulons were assessed to determine if differential activation occurs in lag phase and/or aged cells. The proteome data was also explored to determine the landscape for possible virulence or lack of it in lag phase and in aged cultures. Lag phase cells had no detectable members of the PrfA regulon present. In exponential phase cells, only Mpl (EGJ23707) and actin mobilisation protein ActA (EGJ23708) were detected at low levels (Figure 71). This is consistent with indirect suppression of the PrfA operon by carbon catabolite repression (CCR) (Gilbreth et al., 2004). CCR is an important regulatory phenomena in bacteria, constraining catabolic metabolic rates and enabling cells to access secondary carbon sources in the presence of preferred carbon sources. The global regulation of CCR involves the

pleiotropic transcription factor CcpA (EGJ25135) in Gram-positive bacteria (Swint-Kruse & Matthews, 2009).

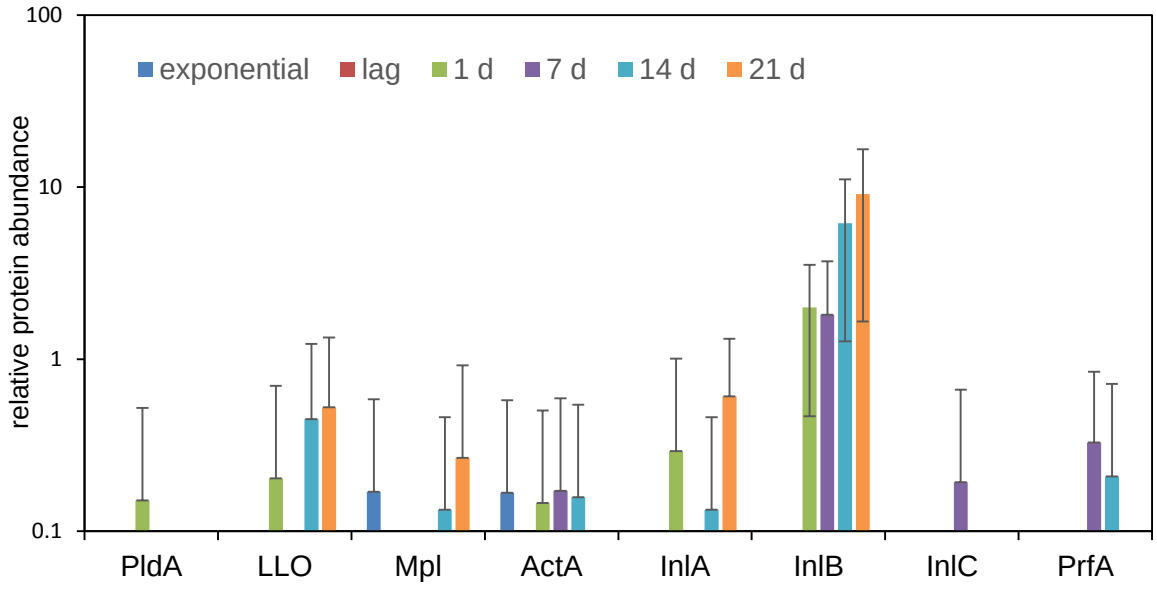

Figure 71**:** Abundance of PrfA regulated proteins detected in *L. monocytogenes* ScottA grown in TSYE at 37°C for different times and also within the lag phase.

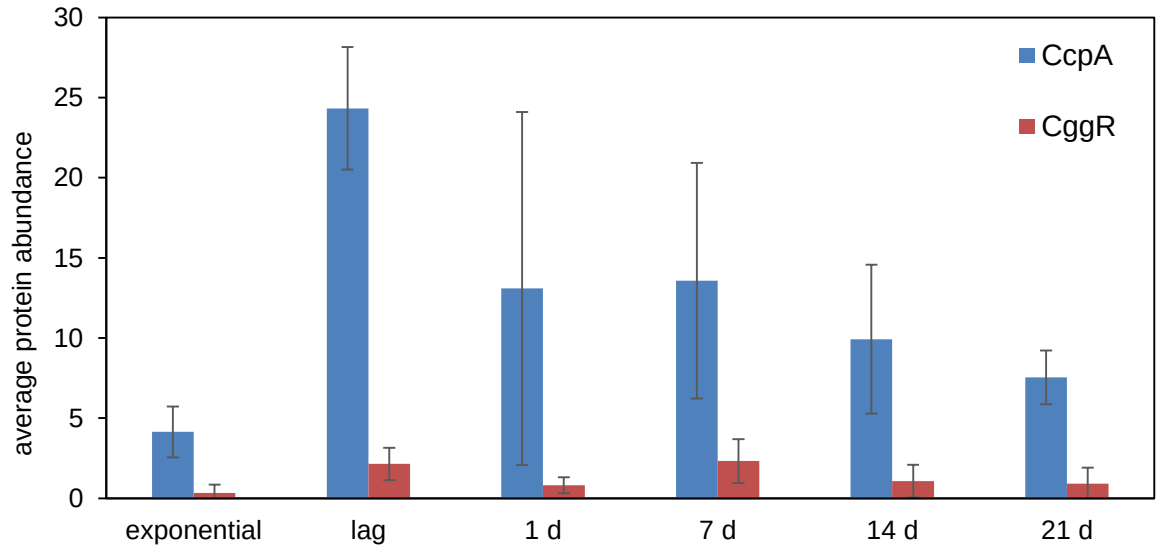

Figure 72**:** Abundance of sugar metabolism control proteins CcpA and CggR detected in *L. monocytogenes* ScottA grown in TSYE at 37°C for different times and also within the lag phase.

CcpA interacts with the phosphorylated form of PTS phosphocarrier HPr (PtsH) protein. PtsH phosphorylation increases with increasing cytoplasmic concentrations of glycolysis intermediates glucose-6-phosphate and fructose-1,6- bisphosphate (Görke & Stülke, 2008). CcpA abundance in the lag phase increased 6-fold relative to exponential phase (Figure 72). In aged cultures, CcpA levels decline approximately 40% from 1 d to 21 d. The high levels of CcpA seem to maximise the spectrum of carbon sources that can be utilised in the medium and prevents the excessive build of glycolysis intermediates such as glycerone phosphate, which can generate toxic compounds such as methylglyoxal, or excessive levels of fermentation end-products leading to acidification of the cytoplasm. The increase in CcpA couples innthe scenario studied here with increased abundance of CggR, the GapA operon repressor in lag phase. CggR putatively suppresses the expression of genes *gapA*, *pgk*, *tpi*, *pgm* and *eno* (Doan & Aymerich, 2003) in *L. monocytogenes*. CggR abundance is derepressed in lag phase consistent with overall derepression of the HrcA regulon to which it belongs. In aged cultures, CCR weakens and indirect suppression of PrfA regulon members, such as LLO, thus lessens even though many proteins still have low abundances. This could be due to protein extraction bias but also indicates another level of control on the PrfA regulon. At 14-21 d LLO, Mpl (EGJ23707), ActA, InlA and InlB were detected to varying extents. Phospholipases PldA and PldB (EGJ23705, EGJ23709) were not detected in any sample. PrfA itself was detected at 7d and 14 d. LLO-based haemolysis, however, was not detected in 7-21 d cells (Chapter 2). This could be due to lack of protein export as noted in Chapter 3 thus detection as shown in Figure 70 possibly only demonstrates unprocessed precursors, not the native secreted forms.

Cytoplasmic glutathione (GSH) levels have been shown to activate late expression of PrfA regulated genes required for cell-to-cell spread (Reniere et al., 2015, 2016). This

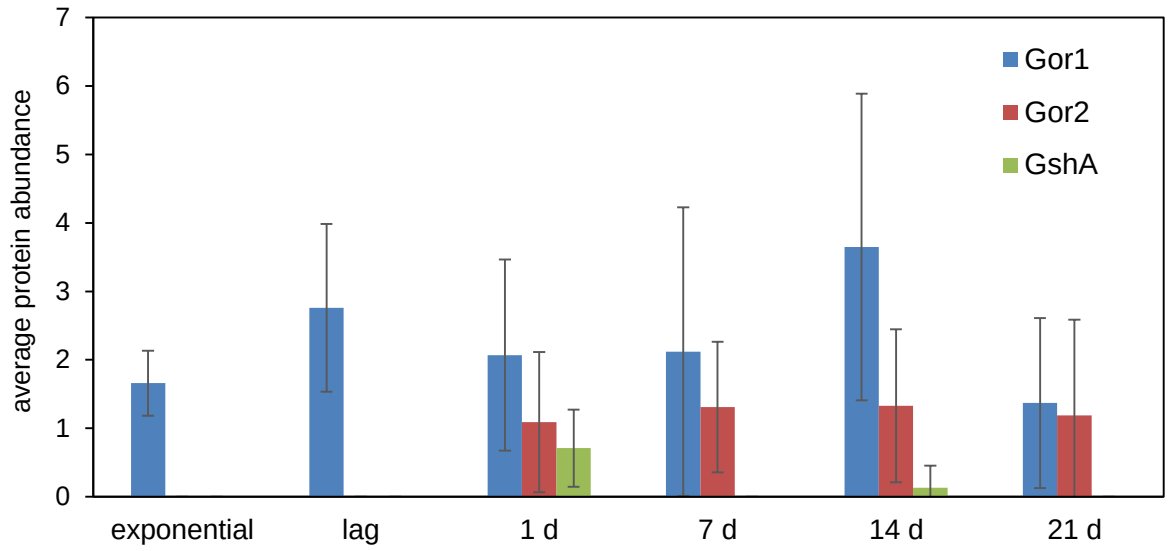

Figure 73**:** Abundance of sugar metabolism control proteins CcpA and CggR detected in *L. monocytogenes* ScottA grown in TSYE at 37°C for different times and also within the lag phase.

is achieved by GSH binding to PrfA altering the folding of the HTH domain and increasing PrfA DNA interactivity (Hall et al., 2016). GSH redox cycling has also been recently found to be essential for ActA synthesis in the host cell cytosol (Reniere et al., 2016). Low levels of glutamate-cysteine ligase/glutathione synthetase GshF (EGJ26298), which is able to de novo synthesise GSH from cysteine and glutamate, was detected maximally in 1 d cultures but barely at 14 d (Figure 73). GSH is normally most abundant in the early stationary growth phase (Sakamoto et al., 2015). However GshF levels seem to decline as cultures age. A SigB/CodY regulated GSH oxidoreductase Gor homolog (EGJ24969) was also induced in aged cells but was absent in exponential and lag phase cells. A second constitutive Gor homolog (EGJ24410) shows greater levels at 14 d, but levels decline 3-fold by 21 d

cells (Figure 72). Gor reduces GSH back to the active form. The overall results suggest that GSH is possibly elevated in early stationary growth phase but likely declines in concentration past 7 d, unless offset by active GSH transport. The likely scenario is that the level PrfA regulated virulence protein abundance is partly due to low GSH levels.

5.4.5 Signalling in lag phase and aged cells is oriented to improve cell fitness

The agr system (EGJ23488-91) is a temperature dependent, quorum sensing system in *L. monocytogenes* that influences virulence (Autret et al., 2003; Garmyn et al., 2012) and aids in cell fitness traits, such as surface attachment, metabolic optimisation and cell wall homeostasis, such that improved survival can occur in complex environments, such as soil (Vivant et al., 2014, 2015). Inactivation of the agr system affects the ability of *L. monocytogenes* to form biofilms at 25°C (Rieu et al., 2007), lowers its ability to generate infections in a murine model (Riedel et al., 2009) and overall fitness. The AgrA regulon appears to be involved in the regulation of nitrogen transport, amino acid synthesis, purine and pyrimidine biosynthetic pathways and phage-related functions (Garmyn et al., 2012). Low expression of this regulon results in a growth advantage at 37°C, but hampers salt tolerance. Though the AgrA regulon is still not fully defined our results suggest the AgrA regulon is more active in lag phase compared to exponential phase. This is indicated by CodY derepression of cyclic-di-AMP phosphodiesterase PdeA (EGJ24492) in lag phase (Figure 70) and with matching patterns of responses by the SigB, SigH and CodY regulons with which the known AgrA regulon overlaps (Figure 65). The results suggest that AgrA/AgrC signalling may integrate information on the biotic

environment around *L. monocytogenes* (Garmyn et al., 2012) with internal resource monitoring (by CodY) and may be required for rapid response to environmental change, including nutrient access. The induction of AgrA-regulated PdeA in lag phase suggests this system influences genetic changes that are relevant to growth and cell wall homeostasis processes (Witte et al., 2013)

Other proteins that act in signal transduction systems were investigated to determine which ones could also be most active in lag phase and aged cells and thus provide more perspective on the physiology of the cells as well as adaptation processes. In lag phase signalling proteins PdeA (EGJ24492), YxiE1 (EGJ24032), YxiE2 (EGJ25117), ResD (EGJ25484) and DegU (EGJ26040) are the most activated (Figure 74). YxiE1 and YxiE2 (along with YxiE3 EGJ26198) are universal stress proteins and are believed to amplify sensory sensitivity by interacting with and stabilising histidine kinase/response regulator/DNA complexes (Heermann et al., 2009). In aged cells YxiE3 is more abundant, this homolog is SigB activated. Little is known about how they actually function in *L. monocytogenes* (Seifart-Gomes et al., 2011), however their overall role is consistent with environmental adaptation and the three homologs likely play different roles depending on the scenario. ResD is the response regulator in the ResDE two component system (EGJ25453-4) that activates anaerobic respiration in *B. subtilis*. In *L. monocytogenes* ResDE activates cytochrome D ubiquinol oxidase *cydA* gene (EGJ26243) (Larsen et al., 2006), which carries out MK8 mediated electron transport respiration along with F_1F_0 ATPase. In aged cultures CydA was detectable though levels were quite low as it is a membrane protein. CydA levels were higher in exponential phase but not detected in lag phase cells. Similarly, QoxA, a transmembrane subunit of the AA3-600 quinol oxidase (QoxABCD, EGJ24346-49) was detectable in exponential phase cells but not in lag

phase cells. The data, points to possible activation of aerobic respiration, but only in the exponential phase. Further studies are needed to assess this activity, for example measuring cytochrome oxidase activity. ResDE is also involved with regulating sugar uptake by activating MptA. MptA was observed to be more abundant in aged cells (Chapter 3). The effect of ResDE needs further study especially how it relates to environmental sensing and modulation of anaerobic growth processes. The activated DegU protein on other hand is an orphan stress sensing response regulator that is associated with cell wall stability, motility and attachment. DegU mutants have low virulence, sensitivity to lysozyme and ethanol, and lack flagella and display poor attachment on surfaces (Knudsen et al., 2004; Gueriri et al., 2008; Mauder et al., 2008; Burke et al., 2014). Increased flagellin abundance (Figure 69) could be linked to DegU. DegU was also more abundant in aged cultures. The fitness inducing feature of DegU is echoed by the cyclic-di-AMP phosphodiesterase PdeA, which also influences cell wall stability. The WalRKH sensor (EGJ23800-2), response regulator LiaR, of the LiaFSR system (EGJ24524-6), and the response regulator of the LisRK (24914-5) LisR were all more abundant in aged cells and appear activated in stationary growth phase (Figure 74). These multicomponent sensor systems are associated with sensing cell wall stress and invoking stress defences. WalRKM has been demonstrated in *B. subtilis* and *B. anthracis* to coordinate cell wall metabolism (Dhiman et al., 2015) and to regulate expression of autolysins and proteins that modulate autolysin activity (Salzberg et al., 2013). The sensor system seems to ensure that PG turnover proteins such as CwlO/Spl, substantially more abundant in aged cells (Chapter 3), are promoted during growth and under stress conditions. It is possible activation by this system could push autolysin levels to the point of cell autolysis as shown in Chapter 2.

LiaFSR is a conserved sensor system found in Gram-positive bacteria and responds to cell wall stress, induced by antibiotic exposure. The version in *L. monocytogenes* influences a set of about 27 genes (Fritsch et al., 2011) that mainly includes transporters and other proteins that seem to be involved in removal of toxic substances and acquisition of sugars; some of these likely aid in antibiotic defence. In aged cultures several proteins coded by LiaRSF influenced genes showed moderate increases. The LicRK system activates oxidative stress and cell wall defences responding to ethanol, acids and hydrogen peroxide; it also protects against the lantibiotic nisin and cephalosporin family antibiotics (Cotter et al., 2002). LiaRK and another cell wall stress sensing system not detected in this study, CesRK (EGJ24956-7), contributes to global gene regulation adjusting the cells against the impacts of cell wall disturbing chemicals (Nielsen et al., 2012). Further analysis is needed to determine how these cell wall stress sensing systems are coordinated in *L. monocytogenes* including the nature of associated sensing cues and fitness adaptations. Overall, a range of sensing systems are activated in lag phase and are abundant after extended incubation, primarily focussing on cell wall integrity.

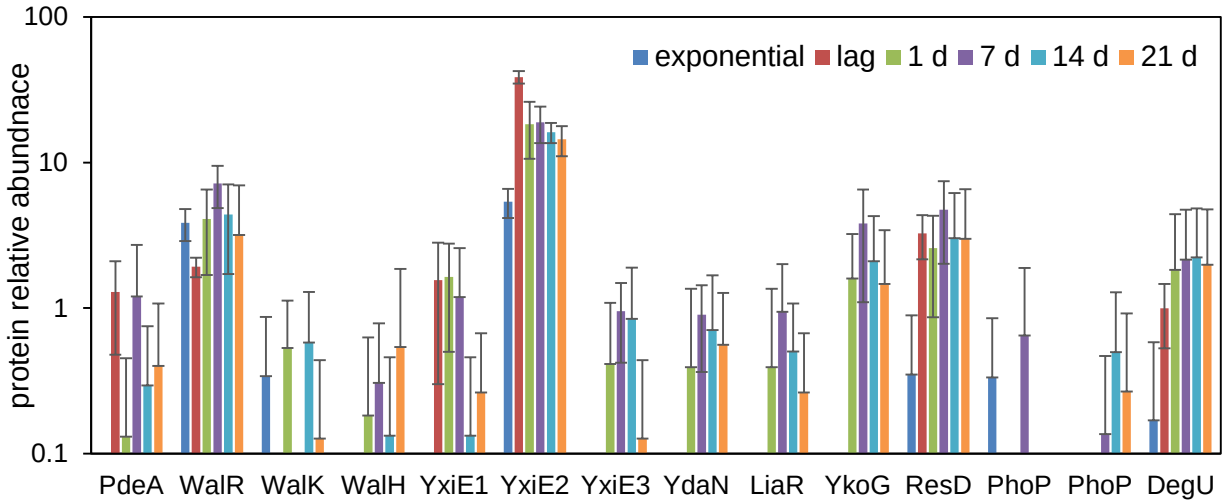

Figure 74**:** Abundance of sensor proteins detected in *L. monocytogenes* ScottA grown in TSYE at 37°C for different times and also within the lag phase. Abundances

are based on normalised spectral counts from at least 6 biological replicates and multiple experiments.

5.5 Conclusions

Overall, lag phase induced a significant response to about 60 proteins controlled by SigB, SigH, CodY, CtsR and HcrA. The interaction of these regulons likely stimulate anabolic processes, cytokinesis, improve cell wall stability and remediate the cytoplasm in preparation for exponential growth. Many of these proteins are included in networks of regulatory responses. The build up of cell precursors and energy for anabolism is however constrained by CodY as well as by the CCR presumably avoiding premature accumulation of toxic metabolites. Signalling data hinted that aerobic respiration is activated not in lag phase but in exponential phase. Thus ATP and precursor consumption seems constrained in lag phase. In addition, a generalised adaptation response occurs in both lag phase and stationary growth phase aiding fitness for a myriad of environmental or host-associated situations, for example, survival in the gastrointestinal tract, blood, and soil. Aged cultures, by comparison, did not generally have accentuated responses of this nature indeed the responses possibly due to increasingly poorer culturability that develops over time. Activated cell wall stress defences as suggested by increased abundance of a number of sensor kinase systems seems a good example of these general responses – the signalling responses did not intensify as cells aged but rather are activated as part of standard stationary growth phase survival. Cell wall stress and the subsequent overall interplay of the regulons responses could contribute to the

promotion of early PrfA regulated proteins in (such as InlB) in older cultures of *L. monocytogenes*.

6 Conclusions

This study was initiated to establish a better understanding of the processes occurring during lag phase and culture aging in *Listeria monocytogenes* ScottA mainly by using proteomics. This in effect is a “landscape” description systems-based approach. The intention was not to discover new functions but to integrate existing knowledge to try to explain complex phenomena. A large knowledge gap still exist in relation to the lag phase and culture decline in the death phase. There is no comprehensive concept of the biochemical and molecular genetic activity of bacteria during lag phase adaptation, possibly due to its temporary and/or variable nature. The growth curve death phase has also attracted less attention mechanistically though perhaps is easier to comprehend in general, but questions around how bacteria die are still relevant.

A better understanding of the processes occurring during lag phase, aging and death could provide new ideas in developing interventions against foodborne pathogens, for example chemicals able to safely interrupt their ability to adapt and recover or that enhance the death phase rate of decline. In this respect, this thesis focused on *Listeria monocytogenes*. With its comparatively streamlined genome and relatively high level of genetic characterisation there was an opportunity to use functional genomics approaches to investigate some phenotypes deeply, observe proteome-level shifts and associated regulatory responses in relation to lag phase and the death phase for the first time. The reason for this approach was the fact the alterations are broad scale and could involve long evolved core aspects of bacterial biology as opposed to specific traits and adaptations such as virulence and specialised stress defence and nutrient acquisition strategies. This follows from the

concept that bacterial growth and survival involves a complete turnover of the population and that rarely cells survive for long. This project pushed this boundary by examining *L. monocytogenes* cells that “age” and determine what their fate is. On the other side of the coin, the recovery of such cells was also observed. The overall goal was better to understand bacterial survival and develop a general mechanistic framework that can be used as a basis to better understand bacterial persistence and survival.

The thesis was able to examine the above observations in the context of *L. monocytogenes* ScottA proteomics. Proteomics offers a more of an end-point view of responses to environmental conditions as compared with gene expression studies where the coupling between mRNA and proteins may not be straight forward due to post-transcriptional regulation and disparities between mRNA and protein copy numbers per cell due to different half-lives (Maier et al., 2011; Vogel & Marcotte, 2012). Nevertheless, the data often tends to be complicated and difficult to interpret owing to the fact that protein abundances measured firstly the average of the overall population – which could be physiologically heterogeneous, and secondly, the changes could be compensatory in nature and not necessarily reflecting an overt phenotypic response. Thirdly, the entire proteome cannot be measured due to the enormous dynamic range of protein concentrations in the cell compounded with extraction biases of low solubility proteins compartmentalised in membranes. Levels of proteins in bacteria are in the range of 10^5-fold (Ishihama et al., 2008). The number of copies per cell range from 10^3-10^4 to 1 (Maier et al., 2011); and <1 if the whole population is considered. Some proteins are always low copy number in the cell and thus hard to measure reliably without using targeted approaches or more modern methods relying on fast and profound proteome peptide identification and

comparison to peptide atlases (Schubert & Aebersold, 2015). Bacteria appear to have about 3 to 4 million protein copies per μm^3 worth of cells (Milo, 2013; Maaβ et al., 2014). Typically elongation factor Tu (Tuf) is amongst the most abundant proteins at any given time in bacteria. In *B. subtilis* in the exponential growth phase, there is 190000-200000 Tuf copies/cell while by comparison D-alanine-poly(phosphoribitol) ligase DltA was present at only about 500-600 copies/cell (Maaβ et al., 2014). In the data obtained here this equates to 481.7 ± 82.1 and 1.3 ± 1.4 average spectral counts for Tuf and DltA,respectively for normalised exponential phase replicates (Appendix I). Thus the data cannot be equated accurately to a copy number per cell, at least at this stage, without further experiments. Nevertheless, the data is still useful when treatments are compared in a relative sense. With the aforementioned caveats, it was possible to still view a large proportion of the proteome at a reasonably accurate quantitative level. To supplement the proteomic analyses, orthogonal experiments were conducted that examined growth and survival, morphology, metabolism, virulence potential and the cell energy state; useful as phenotypic features that could be investigated at the proteome level.

6.1 Culture Aging and Effect on Cell Physiology

The results from Chapter 2 showed that the duration of the lag phase, in fact, depends on the culture age. The estimated lag phase duration extended up to about 5.5-6 h for the 14 d and 21 h inocula. The recovery of the inocula was initially rapid for 7-21 d cultures (0.5-1.6 log units), and the emergent outgrowth seemed to show reduced fitness at 21 d compared to 1 d cultures. (41 min versus 28 min generation time). The overall results suggest aged culture populations that were inputted into new TSYE could have differentially different levels of accumulated aging defects, for example to cytokinesis and cell wall biogenesis and impairment of cell wall integrity

and excessive protein aggregate accumulation at one or both poles as well as an altered metabolism. The results fit well with the concept that inocula physiological status is important in effect on the length of the lag phase. We can show here at least at a preliminary level it may also affect fitness consequences in the outgrowth population plus evidence of odd rebounds in culturability. Studies on *E. coli* subject to chill and water activity stress also achieved a transient reduction of viability, a rapid rebound in viability back to near the original viability, a subsequent lag adjustment period followed by exponential growth under the stress applied stress conditions that involved (Kocharunchitt et al., 2012, Mellefont et al., 2015; King et al., 2016). The gene expression and proteomic analysis revealed a complex series of transient events are invoked. It is surmised a similar process could happening with aged ScottA cells though additional data is needed to observe this. There also needs to be closer examination of the “recovery period” including the general reproducibility and the underlying physiological processes occurring. The chill/osmotic shock induced stress recovery phase is reproducible in *E. coli*, which is entirely different to this scenario but provides a basis to work upon. The loss of viability duing death phase can be connected to phenotypes defined in Chapter 2 and that were subsequently studied in depth in Chapter 3 and 4. The overall findings are logically consistent and support the known literature. Clearly the depletion of ATP and other required resources for metabolism leads to subsequent loss of control of cytokinetic and cell wall biogenic processes causing autolysis and loss of cell viability. A portion of the population does survive including a community segment that can recover back to normal or near normal fitness. For 1 d samples this is near 100% but by 21 d is less than 1 in 10000 cells. It can be assumed this subpopulation is fit enough that

recovery shifts to growth, the remaining population appear to be permanently inactivated, too damaged to ever recover.

6.2 Mechanisms of the Death Phase and Culture Aging

From the data (Chapter 3) aging in *Listeria monocytogenes* involves substantial increases in the abundance of many houses- keeping proteins, especially those involved in cell wall and protein turnover. The greater emphasis on the provision of cell wall products is a response used to maintain the integrity of the cell wall and thus provide protection against external environmental stresses. This reaction as mentioned above is likely a compensatory enhancement when cell wall biogenesis becomes dysfunctional as indicated by cell elongation. Autolysis seems to be due to mistargeting of autolysins owing to lack of export. Export proteins such as SecA2 and SppA become non-detectable in 21 d cells. SecA2 is needed for export of several vital autolysins for cell growth, namely Iap (Camejo et al., 2009). Thus accumulation of these proteins in the cytosol and near the cell wall could interfere with cytokinesis and cell wall elongation. Further analysis is needed to see if Iap and CwlO/Spl and other autolysins are being mistargeted, for example using fluorescent antibodies or GFP/YFP constructs. The increase in internalins InlA and InlB could also be “mistargeted” cytosol located precursors accumulating. Thus virulence assays should be done, but all the data at present does not show any evidence aged cultures exhibit virulence let alone enhanced virulence. In addition cell adhesion assays (Jaradat & Bhunia, 2003), would help explain if InlB and InlA are exported or not.

It is possible that nutrients released from autolysed cells are recycled by ScottA to allow survival of the remaining population, however additional experiments are needed to see if this occurs and actually provides survival benefits. There are some doubts this is occurring in the aging situation. For example, the PG esterase enzyme MurQ (EGJ25195) that allows utilisation of PG N-acetylmuramic acid residues and found to be essential for late stationary growth survival in *B. subtilis* and *S. aureus* (Borisova et al., 2016) was not activated in the aged cells significantly. Further work, for example, using mutants (such as Δ*murQ*) are needed to assess the role of proteins in aiding survival. During the aging process metabolism of the cell shows a significant down-regulation and likely affects all processes including protein translation and protein turnover. Metabolically the reactions made in aged cells seem futile. Some interesting responses are observed in any case. One of the more interesting is the possibility of oxidative deamination of alanine and glutamate to pyruvate by Ald and RocG, which would produce pyruvate, NADH and ammonia in the aged cells. At this stage, this is just a hypothesis since normally these enzymes are anabolic. Metabolomic analysis and enzyme assays would provide some clarity in this respect, for example, does 2-oxoglutarate and ammonia accumulate or not in aged cells. If there is no accumulation, this would then suggest the significant increases in the abundances of Ald and RocG is instead a futile attempt to generate alanine and glutamate. Downstream enzymes were not reflectively enhanced (for example D-alanine and D-glutamate racemases), so the possibility of oxidative deamination occurring requires confirmation. Other unusual enzymes that to date have received little study at best in bacteria let alone *Listeria monocytogenes* were enhanced in 21 d cells compared to 1 d cells. These are summarised in Table 7. Some of these have only recently determined functions. For example, a HemQ-like

protein (EGJ25658) seems to play a particular but unknown role. To date, the associated gene has been annotated as coding a heme peroxidase/chlorite O_2 lyase family protein. Recently, HemQ family proteins have been shown to act in an alternative step in the synthesis of heme b in some Gram-positive bacteria (Dailey & Gerdes, 2015). The reaction proposed is through the generation of O_2 by the enzymatic decarboxylation of coproheme to heme b. Since HemQ is only found in certain bacteria, it raises the question if the enzyme still has other roles, for example, conversion of chlorite to chloride ions via a dismutase reaction. At this stage, further study is needed of this unusual protein. Another unusual enzyme is the amino acid deglycase YraA/YhbO (Abdallah et al., 2016). How important is this enzyme during stress? The abundance of YraA/YhbO is increased in several stress scenarios (acid stress, for example, Bowman et al., 2012). Further work on its importance and specific biochemical properties would be of value. Deglycation of Maillard reaction products such as glucose lysine via FrlD (and FrlB) (Wiame et al., 2005) could allow mallaird reaction products to be used as a source of nutrients. The pathway has not been studied in *L. monocytogenes* to date and since food is often rich in Maillard reaction products the question arises are they viable sources of nutrients for survival in food? Data suggests *L. monocytogenes* resists high levels of MRPs and that they can suppress virulence without affecting growth (Sheikh-Zeinoddin, 2000; Stecchini et al., 2008). PTS transport is required in *Salmonella* for uptake of fructose lysine/glucose line (Miller et al., 2015) and the transporter in *Salmonella* is homologous to the PTS system adjacent to FrlDB (EGJ25528-30). The IIB subunit (EGJ25530) was detectable in exponential and aged cultures but not lag phase.

The reduced ATP and reductant pools seem to lead to loss of effective control of maintenance processes, for example hampering proteostasis the loss of which is

eventually lethal to the cell (Bednarska et al., 2013). Is protein aggregation a reason for the high level of inactivation observed in aged cells? Further work is clearly needed. Aggregates could be visualised by fluorescent dyes, such as thioflavin-S, shown to be an amenable way to examine protein inclusions (Pouplana et al., 2014). Such an experiment would be useful to determine how stress contributes to protein aggregation processes as well as provide insights into how it is managed.

Table 7. *Proteins with most enhanced or decreased measured abundance in aged L. monocytogenes ScottA cells (21 days versus 1 d incubated, TSYE broth, 37°C).*

Scott A Loci	Other Loci	Fold-change	Known or predicted specific function		Compartment
EGJ26016	lmo2491	15.67	putative hydrolase		cytosolic
EGJ25714	lmo2168	11.67	GloA-like lactoylglutathione lyase (glyoxylase I)	YwbC	cytosolic
EGJ26082	lmo2558	10.80	anhydrous-N-acetylmuramic-L-alanine amidase	Ami	surface
EGJ25706	lmo2160	8.33	sugar phosphate isomerase/epimerase	YfiH	cytosolic
EGJ24345	lmo0844	8.18	uncharacterised protein	YabJ	cytosolic
EGJ24098	lmo0582	8.09	γ-D-glutamate-meso-diaminopimelate muropeptidase P60	Iap	surface
EGJ26030	lmo2505	7.07	peptidoglycan DL-endopeptidase P45	CwlO	extracellular
EGJ25392	lmo1856	5.99	purine-nucleoside phosphorylase	DeoD	cytosolic
EGJ25839	lmo2256	5.11	amino acid deglycase	YraA	cytosolic
EGJ25031	lmo1494	4.96	5'-methylthioadenosine nucleosidase / S-adenosylhomocysteine nucleosidase	Mtn	cytosolic
EGJ24576	lmo1076	4.89	exoglucosaminidase/muramidase/autolysin	LytG	surface
EGJ26217	lmo2692	4.87	uncharacterised protein	YaaQ	cytosolic
EGJ25489	lmo1953	4.77	purine nucleoside phosphorylase	PupG	cytosolic
EGJ25464	lmo1929	4.68	nucleoside diphosphate kinase	Ndk	cytosolic
EGJ23959	lmo0434	4.55	internalin B	InlB	surface
EGJ25658	lmo2113	4.55	heme-containing peroxidase/chlorite O_2-lyase	HemQ	cytosolic
EGJ24445	lmo0943	3.98	non-heme iron-binding ferritin Fri	Dps	cytosolic
EGJ24076	lmo0560	3.95	NADP-specific glutamate dehydrogenase	RocG	cytosolic
EGJ25993	lmo2468	3.80	ATP-dependent Clp protease proteolytic subunit	ClpP2	cytosolic
EGJ24697	lmo1217	3.47	putative glutamyl aminopeptidase	YsdC	cytosolic
EGJ25116	lmo1579	3.36	L-alanine dehydrogenase	Ald	cytosolic
EGJ24407	lmo0903	3.20	hydroperoxidase	OhrA	cytosolic
EGJ25040	lmo1503	3.19	uncharacterised protein	YrzL	cytosolic
EGJ25938	lmo2414	3.15	FeS cluster assembly protein	SufD	cytosolic
EGJ24951	lmo1415	2.88	hydroxymethylglutaryl-CoA synthase	MvaS	cytosolic
EGJ25017	lmo1480	2.46	ribosomal protein S20	RpsT	cytosolic
EGJ26054	lmo2529	2.28	F0F1-type ATP synthase, beta subunit	AtpD	cytosolic
EGJ25980	lmo2455	2.25	enolase	Eno	cytosolic
EGJ26080	lmo2556	-2.98	fructose 1,6-bisphosphate aldolase type II	FbaA	cytosolic
EGJ24312	lmo0813	-3.28	putative fructo/mannokinase	GmuE	cytosolic

EGJ25749	lmo2202	-3.34	3-oxoacyl-[acyl-carrier-protein] synthase III	FabH	cytosolic
EGJ23784	lmo0271	-3.37	aryl-phospho-beta-glucosidase	BglC	cytosolic
EGJ24890	lmo1354	-3.48	putative PepP_like Xaa-Pro aminopeptidase	YqhT	cytosolic
EGJ26245	lmo2720	-3.64	acetyl-CoA synthetase	YtcI	cytosolic
EGJ25983	lmo2458	-3.71	phosphoglycerate kinase	Pgk	cytosolic
EGJ24563	lmo1059	-3.81	DsbG-like protein-disulfide isomerase		cytosolic
EGJ23686	lmo0182	-3.87	putative limit dextrinase		cytosolic
EGJ25333	lmo1797	-4.04	ribosomal protein S16	RpsP	cytosolic
EGJ23702	lmo0198	-4.11	glucosamine-1-phosphate N-acetyltransferase/ UDP-N-acetylglucosamine pyrophosphorylase	GlmU	cytosolic
EGJ25534	lmo2006	-4.15	alpha-acetolactate synthase	AlsS	cytosolic
EGJ24070	lmo0554	-4.25	putative Fe- and NAD(P)-dependent butanol dehydrogenase	YugJ	cytosolic
EGJ25344	lmo1808	-4.34	malonyl CoA-acyl carrier protein transacylase	FabD	cytosolic
EGJ24181	lmo0662	-4.97	pyridoxine kinase	ThiD	cytosolic
EGJ24296	lmo0796	-4.97	putative polyisoprenoid binding protein		cytosolic
EGJ24583	lmo1086	-5.78	D-ribitol-5-phosphate cytidylyltransferase	TarI	cytosolic
EGJ25212	lmo1675	-6.03	2-oxoglutarate decarboxylase / 2-succinyl-6-hydroxy-2,4-cyclohexadiene-1-carboxylate synthase	MenD	cytosolic
EGJ25523	lmo1995	-6.20	deoxyribose-phosphate aldolase	DeoC	cytosolic
EGJ25177	lmo1641	-6.65	aconitate hydratase	CitB	cytosolic
EGJ25766	lmo2219	-6.78	post-translocation molecular chaperone/foldase	PrsA2	surface
EGJ24896	lmo1360	-6.91	methylenetetrahydrofolate dehydrogenase (NADP+)/methenyltetrahydrofolate cyclohydrolase	FolD	cytosolic
EGJ24823	lmo1283	-7.81	LacX-like aldose 1-epimerase	YoxA	cytosolic
EGJ24857	lmo1319	-7.82	prolyl-tRNA synthetase	ProS	cytosolic
EGJ24900	lmo1364	-10.43	cold shock protein	CspL	cytosolic
EGJ25939	lmo2415	-12.38	Fe-S cluster assembly, ATP-binding protein	SufC	cytosolic
EGJ25879	lmo2360	-73.26	membrane protein		membrane

A metabolic map model is proposed below (Figure 75) for death phase/aging cultures. Overall, examining the decline and loss of viability of *L. monocytogenes* ScottA provides a useful perspective on survival strategies and the limitations of cell physiology. It also provides an excellent consideration of the role temperature plays in survival. Though the T_{opt} allows for the most rapid growth, it comes with a price that must be met by a continual supply of resources otherwise a tipping point into entropy occurs. Several interesting studies explore the thermodynamics of bacterial growth and its relation to proteins (e.g. Corkrey et al. 2014). likely that all bacteria

and archaea are subject to the death phase proces though how it is managed still requires further study, even in model species.

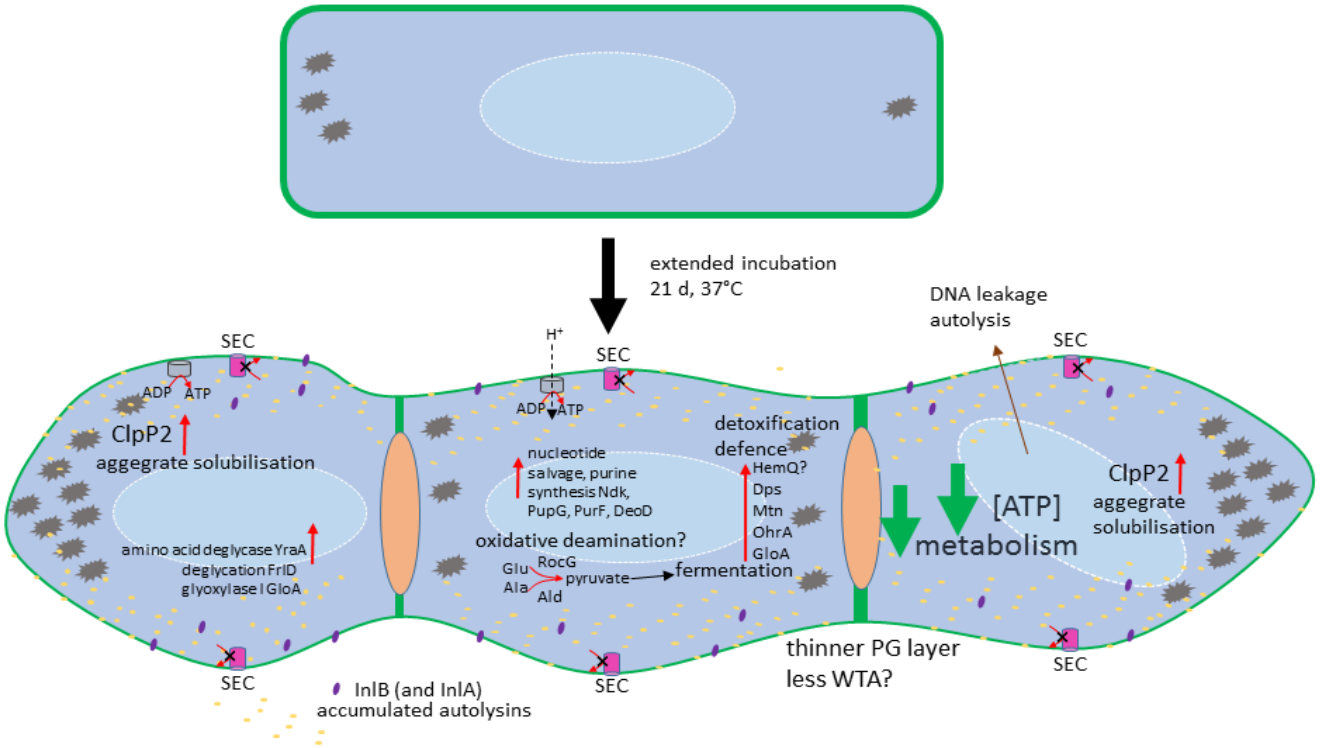

Figure 30**:** Schematic showing the protein and physiological effects of aging in *L. monocytogenes* ScottA at 37°C. Red arrows indicate more abundant proteins. Green arrows indicate a decline in abundance or activity. Items with question marks are processes for which more experimental evidence is clearly necessary.

6.3 Key Lag Phase Mechanisms Revealed by Proteomics

Analysis of the physiology and molecular biology of stationary phase *E. coli* cells revealed aging process has some fundamental similarities to that of higher organisms (Nyström, 2007). The similarities included increased oxidation of cellular constituents and associated target specificity, indicating the important role of antioxidants and oxygen tension in determining cellular life span, and an apparent trade-off between activities related to reproduction and survival (Nyström, 2004). Probably the most relevant published study to the experiments performed in this thesis is a study by Pin et al. (2009) of *E. coli* in the lag phase where gene expression was assessed. They grew strain K12 (MG1655) in Luria broth (LB) at 25°C for 2 d and 17 d, to create populations in the early ("young" cells) and late ("old cells") stationary growth phase. The cultures were then transferred to LB broth and subsamples collected for RNA analysis over time; from 0 to 1 h and 0 to 5 h for the young and old populations, respectively. The number of genes significantly differentially expressed to the time 0 start point strongly differed between the two populations. The old cell cultures differentially expressed 186 genes while young cultures differentially expressed 467 genes. An overview of the results at the level of functional sets is summarised in Table 8. Mostly both populations stimulate genes involves with the uptake of iron (and other cations), carbohydrates, alcohols and organic acids; compatible solute metabolism; and siderophore enterobactin biosynthesis. They both suppress genes associated with membrane component transporters, anaerobic respiration and fermentative metabolism, transcription factors, and acid resistance mechanisms. Young cells were more dynamic, upregulating and suppressing a wider array of functional sets than old cells. For

example, young cells activated aerobic respiration and TCA cycle genes, DNA replication, ribosomal protein and RNA processing genes as well as PG biosynthesis, flagella and several components of the chemotaxis signal transduction complex (Table 8). The result was that lag phase resolved much more quickly for the young versus the old cells (1.5 versus 5 h) (Pin et al., 2009).

Old cells specifically had greater expression of some genes encoding glycolysis proteins and strongly repressed galactose metabolism genes suggesting a metabolic realignment occurs but the general responses are that old cells do not recover as adroitly an active metabolism as younger cells and thus they not as able to get the work done quickly to achieve an exponential growth phase physiological state. The important points concluded in the Pin et al. study can be summarised:

i) Lag phase adjustments are rapid; for young cells with the lag phase transcriptome established within 15 min and staying much the same thereon;

ii) Senescent cells only partially adapt in lag phase. Compared to young cells old cells are less efficient in switching to a “rapid pace” metabolism. This was assumed to be due to accumulated age-associated defects that take longer to resolve.

iii) It was theorised that recovery continues in exponential phase (“replicative recovery”) and that loss of fitness becomes less evident as cultures are continually supplied with a non-stressful environment. Senescent cells become diluted out.

Table 8. Functional sets in E. coli K12 MG1655 in the early (young cells) and late stationary growth phases in LB broth at 25°C*.

Functional set	Young cells	Old cells
PG biosynthesis/turnover, signalling; uptake of peptides; oxidative phosphorylation; motility/ chemotaxis	↑	-
Uptake of iron and other cations	↑	↑
Uptake of carbohydrates, alcohols, organic acids	↑	↑
Aerobic respiration, TCA cycle, nucleic acid/nucleotide biosynthesis	↑	-
DNA replication/repair, RNA processing, ribosomal proteins, tRNA amino acid acylation	↑	-
Glycine betaine metabolism, enterobactin synthesis	↑	↑
Protein export	↑↓	-
Membrane component transporters	↓	↓
Glycolysis	-	↑
Fermentation, anaerobic respiration;	↓	↓
Pentose phosphate pathway; ascorbate metabolism; glycerophospholipid metabolism	-	↓
Galactose metabolism	-	↓
Fatty acid degradation	↓	-
Transcription factors	↓	↓
Protein folding and stabilisation	↓	-
Adaptation to aytipical environments;	↑↓	↑↓
GAD system/acid resistance systems	↓	↓
Trehalose metabolism	↓	-

*Data from Pin et al. (2009).

From Chapter 2 data indicated increasingly slower outgrowth of cells as they age. This result fundamentally agrees with point ii) of Pin et al. (2009) above. The thesis data also agrees with point i). The proteomic data revealed the response in lag was rapid with the proteome determined at 30 min mostly similar across all age populations and showing a substantial shift away from the aged response. Unlike the Pin study, the proteomic changes were greater for the older cultures as compared to the younger cultures. For the 21 d cultures (0.5 to 4 h) the number of proteins changing by 2-fold or more (up and down) was on average 229 (out of 459 proteins assessed), while for 1 d cultures the number of proteins significantly altered in abundance was 136. Across the whole dataset when considered as a unit the number of proteins significantly affected by lag was 148. A set of proteins were found to be selectively enhanced in lag phase only, being more or less abundant in lag phase than in aged and exponential cells. The most prominent are given in Table 9 and apply to the model developed for the lag phase shown in Figure 76.

As noted in Chapter 4, concerning translation elongation factors, over the lag phase period a slow change occurs in abundance, it does not return to a level that approximates exponential growth. In effect, there is a rapid rebound then a gradual change. This parallels the observation of a recovery phase that was noted above in *E. coli* where culturability was restored to some cells rapidly that likely is not due to growth. It seems possible that with the nutrient replenishment rapid adjustment is possible that for some cells successfully partially restore culturability but are not pushed into an active growth phase. Rapid responses may be aided by unusually stable mRNA. It was found in a non-growth state *L. monocytogenes* suppressed RNA degradation and this correlated to persistent sub-populations that were still

viable. Once the mRNA had degraded the viability of the population was permanently lost (Zhang et al., 2010).

It seems that a lag-phase viability rebound is far from a complete process and as noted by Pin and colleagues recovery in lag for senescent cells does not complete, and thus culturability is not restored for most cells, indeed based on the data it is only advantageous for a small minority within the 21 d cultures. Thus it is assumed that replicative recovery restores full fitness in the outgrowth population. This was not studied in any detail here, and careful experiments are needed to determine the influence on successive lag durations and generation times coupled with assessment of senescence traits, in particular, aggregated proteins.

Functional changes are not overviewed here again as they are complex, spread across the entire proteome. Chapter 4 provides an in-depth analysis but suffice to say they are not comparable to the Pin study indeed the nature of the experiments are different enough that contextualization of protein (and transcript) abundance is a complicated issue even when the experiments are performed with the same strain let alone a species belonging to a different phylum!

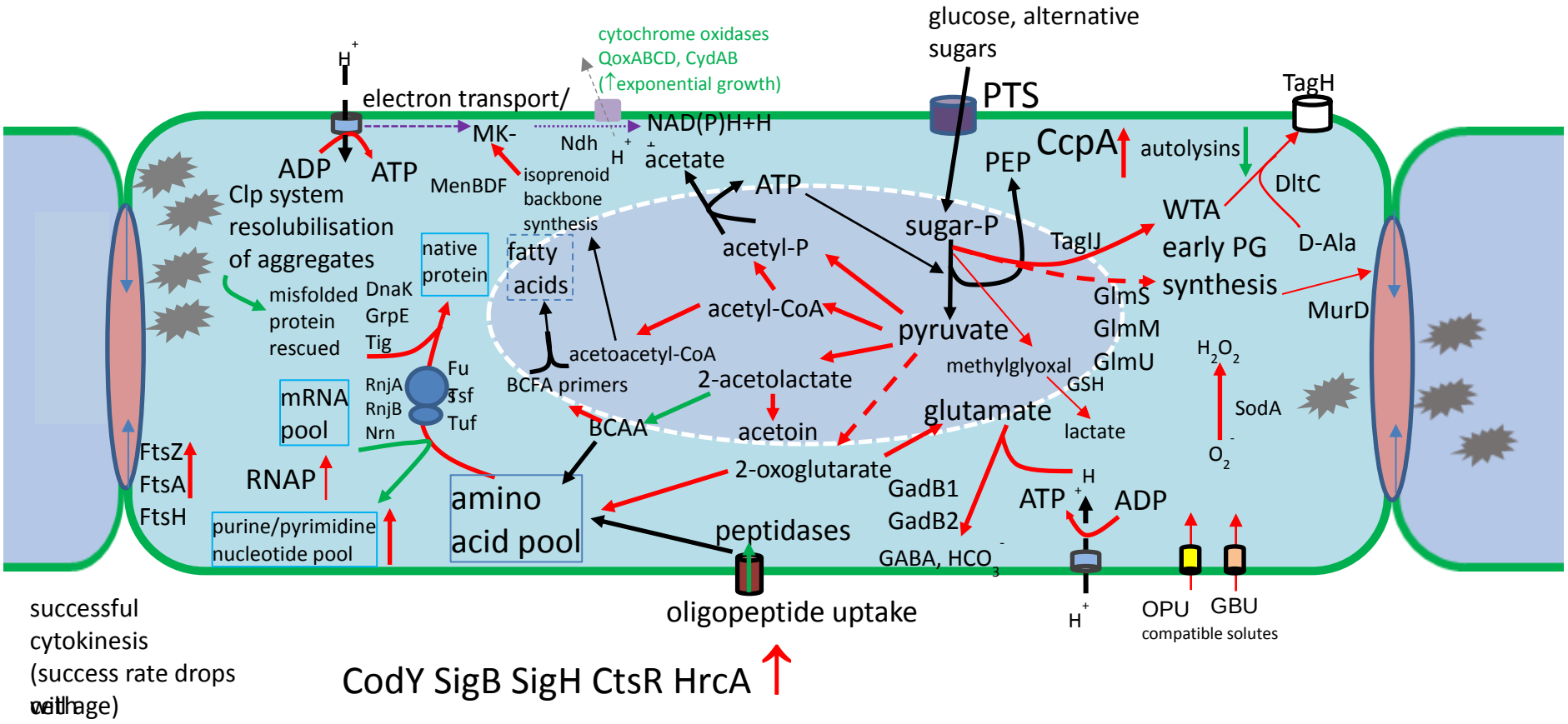

Figure 31: Schematic showing major events in lag phase recovery (duration 0.5-4 h) for stationary growth phase (aged) L. monocytogenes ScottA cells when transferred into fresh TSYE broth at 37°C. Red arrows indicate increased abundance in lag phase relative to aged cells. Green arrows indicate lower abundance (see Chapter 4 for details).

Table 9. Proteins determined to have greater or lesser abundance in L. monocytogenes relative to early to late stationary growth phase and exponential phase culture when in the lag phase in TSYE broth at 37°C.

Scott A Loci	Other Loci	Fold-change	Function		Compartment
EGJ25855	lmo2335	15.05	PTS (Fructose/Mannitol family) IIABC-6	FruA	membrane
EGJ24820	lmo1280	11.28	GTP-sensing transcriptional pleiotropic repressor	CodY	cytosolic
EGJ24975	lmo1439	9.36	superoxide dismutase	SodA	extracellular
EGJ25040	lmo1503	9.17	uncharacterised protein	YrzL	cytosolic
EGJ25066	lmo1529	9.02	preprotein translocase insertion/stabilisation protein	YajC	membrane-associated
EGJ24296	lmo0796	9.02	putative polyisoprenoid binding protein	YceI	cytosolic
EGJ25920	lmo2391	8.86	putative oxidoreductase	YhfK	cytosolic
EGJ25611	lmo2067	8.66	conjugated bile salt acid hydrolase	Bsh	cytosolic
EGJ24069	lmo0553	8.06	uncharacterised protein		cytosolic
EGJ25534	lmo2006	7.93	alpha-acetolactate synthase	AlsS	cytosolic
EGJ25633	lmo2089	7.74	putative acetyl-esterase/lipase		membrane-associated
EGJ23695	lmo0191	7.35	putative cellobiose-phosphate hydrolase	ChbG	cytosolic
EGJ23718	lmo0214	6.62	transcription-repair coupling factor	Mfd	cytosolic
EGJ24241	lmo0722	6.60	pyruvate oxidase	YdaP	cytosolic
EGJ25752	lmo2205	6.60	phosphoglycerate mutase 1	GpmA	cytosolic
EGJ26284	lmo2758	6.15	inosine monophosphate dehydrogenase	GuaB1	cytosolic
EGJ26221	lmo2696	6.01	dihydroxyacetone kinase, C-terminal domain	DhaL	cytosolic
EGJ24395	lmo0893	5.61	positive (anti-anti-sigma B) regulatory factor	RsbV	cytosolic
EGJ24391	lmo0889	5.49	positive (anti-anti-sigma B) regulatory factor	RsbR	cytosolic
EGJ25958	lmo2434	5.28	glutamate decarboxylase	GadB	cytosolic
EGJ24575	lmo1075	5.25	teichoic acid translocating ABC transporter	TagH	membrane-associated
EGJ24994	lmo1458	5.15	glycyl-tRNA synthetase, beta subunit	GlyS	cytosolic
EGJ24823	lmo1283	5.15	LacX-like aldose 1-epimerase	YoxA	cytosolic
EGJ23777	lmo0265	5.07	succinyl-diaminopimelate desuccinylase	DapE	cytosolic
EGJ25452	lmo1917	4.97	pyruvate-formate lyase	PflB	cytosolic
EGJ24781	lmo1241	4.76	uncharacterised protein		cytosolic
EGJ25423	lmo1887	4.71	putative RNA-binding methyltransferase	YpsC	cytosolic
EGJ26273	lmo2748	4.69	putative pyridoxamine/pyridoxine 5'-phosphate oxidase	YdaG	cytosolic
EGJ23891	lmo0387	4.51	uncharacterised protein	YdhG	cytosolic
EGJ25231	lmo1694	4.50	putative nucleoside-diphosphate sugar epimerase	YfhF	cytosolic
EGJ25949	lmo2425	4.40	glycine cleavage system lipoprotein	YusH	cytosolic
EGJ25115	lmo1578	4.39	putative PepP_like Xaa-Pro aminopeptidase	YkvY	cytosolic
EGJ26036	lmo2511	4.37	ribosome-associated sigma 54 modulation protein	YvyD	cytosolic
EGJ26249	lmo2724	4.30	uncharacterised protein	YjdN	cytosolic
EGJ25288	lmo1753	4.23	putative diacylglycerol kinase,	YerQ	cytosolic
EGJ24474	lmo0972	4.21	D-alanine-poly(phosphoribitol) ligase subunit 2	DltC	cytosolic
EGJ24459	lmo0957	4.16	glucosamine-6 phosphate isomerase	NagB	cytosolic
EGJ24070	lmo0554	3.94	putative butanol dehydrogenase	YugJ	cytosolic
EGJ25117	lmo1580	3.94	UspA-like universal stress protein, Usp_like family	YxiE	cytosolic

EGJ25581	lmo2036	3.85	UDP-N-acetylmuramoyl-L-alanine:D-glutamate ligase	MurD	cytosolic
EGJ24860	lmo1322	3.78	transcription elongation factor	NusA	cytosolic
EGJ25213	lmo1676	3.74	menaquinone-specific isochorismate synthase	MenF	cytosolic
EGJ25520	lmo1992	3.68	alpha-acetolactate decarboxylase	AlsD	cytosolic
EGJ25135	lmo1599	3.66	catabolite control protein A	CcpA	cytosolic
EGJ25079	lmo1542	-2.99	ribosomal protein L21	RplU	cytosolic
EGJ25089	lmo1552	-3.01	valyl-tRNA synthetase	ValS	cytosolic
EGJ25292	lmo1757	-3.02	putative sex pheromone lipoprotein	YerH	surface
EGJ23754	lmo0249	-3.04	ribosomal protein L1 RplA	RplA	cytosolic
EGJ24815	lmo1275	-3.41	topoisomerase IA	TopA	cytosolic
EGJ24819	lmo1279	-4.13	protease ATP-binding subunit	HslU	cytosolic
EGJ24568	lmo1068	-4.39	uncharacterised protein		surface
EGJ25017	lmo1480	-4.47	ribosomal protein S20	RpsT	cytosolic
EGJ25155	lmo1619	-5.43	D-alanine transaminase	Dat	cytosolic
EGJ24312	lmo0813	-6.11	putative fructo/mannokinase	GmuE	cytosolic
EGJ25077	lmo1540	-6.12	ribosomal protein L27	RpmA	cytosolic
EGJ23868	lmo0355	-7.38	fumarate reductase flavoprotein	FrdA	surface
EGJ25743	lmo2196	-7.87	oligopeptide ABC transporter	DppE	surface
EGJ26071	lmo2546	-13.93	threonine synthase	ThrC	cytosolic
EGJ24076	lmo0560	-72.43	NADP-specific glutamate dehydrogenase	RocG	cytosolic

6.4 Regulation of responses with the Death Phase and Lag Phase

In order to survive, bacteria must adapt to their environment, and to do so, they express an array of regulatory factors responsible for mounting a specific and rapid response to changes in their surroundings. The foodborne pathogen *L. monocytogenes* has the ability to adapt to diverse, complex and rapidly evolving conditions encountered in many environments such as food, soil (Vivant et al., 2015; Guldimann et al., 2016), the gastrointestinal tract, and the extra- and intracellular environment encountered in different hosts (Guariglia-Oropeza et al., 2014). The results indicate CodY regulation is important in lag phase transition processes and the results also show an increase in anabolic processes occur during the lag phase that seem linked to coordinated SigB-SigH-CtsR-HrcA-CodY multi regulon activation/derepression (Figure 76). CodY was one of the most promoted proteins during the lag phase (Table 8), indicating that it likely plays an important role in "reining" in processes enabling the return to exponential growth. It was noted that

IlvC and IlvD synthesis was strongly repressed suggesting that CodY response is both rapid and this repression occurs until CodY levels deplete. In any case, BCAA synthesis in ScottA is likely inefficient as it is auxotrophic for these amino acids, for reasons difficult to explain since all proteins could be detected (though LeuA, LeuB and LeuC were of consistently low abundance). One possibility is that one of the proteins coded is translated in a truncated form or has a mutation in its active site. Research is needed to determine what is the lesion in any case it does not seem to affect the system at a regulatory level. CcpA was also abundant, especially for 1 d samples. CcpA and CodY have been shown to compete for control of IlvE, with CcpA promoting its expression (Santiago et al., 2013). The data supports this with IlvE still prominent in lag phase. IlvE is the start point for BCFA primers and so crucial for cell survival and integrity. Based on the experimental data the levels of CodY were still quite high after 2-4 h for the 14 and 21 d samples. After lag phase completes, it is conceivable CodY depletion could be rapid in the early periods of exponential growth phase. Thus CodY could be the reason for why replicative recovery takes time. Further studies are needed to assess the role CodY plays in coordinating adaptation, recovery and growth processes.

6.5 Conclusions

The thesis work revealed the possibility that aged cells die off near the T_{opt} due to mistargeting and accumulation of autolysins owing to ATP depletion and impairment of the Sec secretion system. It is also suggested that a return to fresh media results in a rapid recovery phase. This has also been seen to occur in chill stressed *E. coli* (Mellefont et al., 2015). This is matched by a rapid proteome response in agreement with the rapid gene expression response observed in *E. coli* during lag phase (Pin et al., 2009). The subsequent recovery within lag is subsequently set a particular pace

and by the end of the lag phase is incomplete for many cells in the population. This was suggested by the proteome not rebounding back to the exponential phase cell state, even for cultures only in the early stationary growth phase. This may be due to regulatory elements such as CodY that with an associated network of regulons including SigB have created global changes that take the time to readjust. Fitness loss occurs for outgrowth of mainly aged cultures, and they show poor culturability this suggests that culture age-associated defects are only successfully remediated in part of the population supporting other conclusions of the study of Pin et al. (2009).

References

Abdallah, J., Mihoub, M., Gautier, V., & Richarme, G. (2016). The DJ-1 superfamily members YhbO and YajL from *Escherichia coli* repair proteins from glycation by methylglyoxal and glyoxal. *Biochemical and Biophysical Research Communications*, 470, 282-286.

Abram, F., Starr, E., Karatazas, K. A., Maltlawska-Wasowska, K., Boyd, A., Wiedmann, M., Boor, K.J., Conally, D., & O'Byrne, C. P. (2008). Identification of components of the sigma b Regulon in *Listeria monocytogenes* that contribute to acid and salt tolerance. *Applied and Environmental Microbiology*, 74, 6848-6858.

Ackermann, M., Stearns, S.C., & Jenal U. (2003). Senescence in a bacterium with asymmetric division, *Science*, 300,1920.

Ackermann, M., Chao, L., Bergstrom, C.T., & Doebeli, M. (2007). On the evolutionary origin of aging. *Aging Cell*, 6, 235–244.

Aguilaniu, H., Gustafsson, L., Rigoulet, M., & Nyström T. (2003). Asymmetric inheritance of oxidatively damaged proteins during cytokinesis. *Science*, 299: 1751-1753.

Akashi H., & Gojobori T. (2002). Metabolic efficiency and amino acid composition in the proteomes of *Escherichia coli* and *Bacillus subtilis*. *Proceedings of the National Academy of Sciences USA*, 99, 3695-3700.

Al-Naseri, A., Bowman, J.P., Wilson, R., Nilsson, R.E., & Britz, M.L. (2013). Impact of lactose starvation on the physiology of *Lactobacillus casei* GCRL163 in the presence or absence of Tween 80*. Journal of Proteome Research*, 12, 5313-5322.

Alonzo, F. 3rd, Xayarath, B., Whisstock, J.C., & Freitag, N.E. (2011). Functional analysis of the *Listeria monocytogenes* secretion chaperone PrsA2 and its multiple contributions to bacterial virulence. *Molecular Microbiology*, 80,1530-1548.

Arends, S. J., Kustusch, R. J., & Weiss, D. S. (2009). ATP-binding site lesions in FtsE impair cell division. *Journal of Bacteriology*, 191, 3772-3784.

Arous, S., Buchrieser, C., Folio, P., Glaser, P., Namane, A., Hébraud, M., & Héchard, Y. (2004). Global analysis of gene expression in an rpoN mutant of *Listeria monocytogenes*. *Microbiology*, 150, 1581-1590.

Asano, K., Kakizaki, I., & Nakane, A. (2012). Interaction of Listeria monocytogenes autolysin amidase with glycosaminoglycans promotes listerial adhesion to mouse hepatocytes. *Biochimie*, 94, 1291-1299.

Attaiech, L., Minnen, A., Kjos, M., Gruber, S., & Veening, J.-W. (2015). The ParB-ParS chromosome segregation system modulates competence development in *Streptococcus pneumoniae*. *mBio*, 6, e00662-15.

Augustin, J., Brouillaud-Delattre, A., Rosso, L., & Carlier, V. (2000). Significance of inoculum size in the lag time of *Listeria monocytogenes*. *Applied and Environmental Microbiology*, 66, 1706-1710.

Augustin, J., Rosso, L., & Carlier, V. (2000). A model describing the effect of temperature history on lag time for *Listeria monocytogenes*. *International Journal of Food Microbiology*, 57, 169-181.

Autret, N., Raynaud, C., Dubail, I., Berche, P., & Charbit, A. (2003). Identification of the agr locus of *Listeria monocytogenes*: role in bacterial virulence. *Infection and Immunity*, 71, 4463-4471.

Baranyi, J., & Roberts, T. (1994). A dynamic approach to predicting bacterial growth in food. *International Journal of Food Microbiology*, 23, 277-294.

Barnhart, M. M., Lynem, J., & Chapman, M. R. (2006). GlcNAc-6P levels modulate the expression of Curli fibers by *Escherichia coli*. *Journal of Bacteriology*, 188, 5212-5219.

Basan, M., Zhu, M., Dai, X., Warren, M., Sévin, D., Wang, Y.P., & Hwa, T. (2015). Inflating bacterial cells by increased protein synthesis. *Molecular Systems Biology*, 11, 836.

Baty, F., Flandrois, J., & Delignette-Muller, M. (2002). Modeling the lag time of Listeria monocytogenes from viable count enumeration and optical density data. *Applied and Environmental Microbiology*, 68, 5816-5825.

Bayles, D. O., Annous, B. A., & Wilkinson, B. J. (1996). Cold stress proteins induced in Listeria monocytogenes in response to temperature downshock and growth at low temperatures. *Applied Environmental Microbiology*, 62, 1116-1119.

Bednarska, N. G., Schymkowitz, J., Rousseau, F., & Van Eldere, J. (2013). Protein aggregation in bacteria: the thin boundary between functionality and toxicity. *Microbiology*, 159, 1795-1806.

Bellapadrona, G., Ardini, M., Ceci, P., Stefanini, S.& Chiancone E. (2010). Dps proteins prevent Fenton-mediated oxidative damage by trapping hydroxyl radicals within the protein shell. *Free Radical Biology and Medicine* 48, 292-297.

Benjamini, Y., & Hochberg, Y. (1995). Controlling the false discovery rate: a practical and powerful approach to multiple testing. *Journal of the Royal Statistical Society. Series B (Methodological)*, 57, 289-300.

Bennett, H. J., Pearce, D. M., Glenn, S., Taylor, C. M., Kuhn, M., Sonenshein, A. L., Andrew, P.W., Roberts, I. S. (2007). Characterization of *relA* and *codY* mutants of *Listeria monocytogenes*: identification of the CodY regulon and its role in virulence. *Molecular Microbiology*, 63, 1453-1467.

Bierne, H., & Cossart, P. (2007). *Listeria monocytogenes* surface proteins: from genome predictions to function. *Microbiology and Molecular Biology Reviews*, 71, 377-397.

Biswas, R., Martinez, R.E., Göhring, N., Schlag, M., Josten, M., Xia, G., Hegler, F., Gekeler, C., Gleske, A.K., Götz, F., Sahl, H.G., Kappler, A., & Peschel A. (2012). Proton-binding capacity of *Staphylococcus aureus* wall teichoic acid and its role in controlling autolysin activity. *PLoS One*, 7, e41415.

Boorsma, A., Foat, B. C., Vis, D., Klis, F., & Bussemaker, H. J. (2005). T-profiler: scoring the activity of predefined groups of genes using gene expression data. *Nucleic Acids Research*, 33, W592-W595.

Borisova, M., Gaupp, R., Duckworth, A., Schneider, A., Dalügge, D., Mühleck, M., Deubel, D., Unsleber, S., Yu, W., Muth, G., Bischoff, M., Götz, F., & Mayer, C. (2016). Peptidoglycan recycling in Gram-positive bacteria is crucial for survival in stationary phase. *Mbio*, 7, pii: e00923-16.

Bowman, J. P., Hages, E., Nilsson, R. E., Kocharunchitt, C., & Ross, T. (2012). Investigation of the *Listeria monocytogenes* Scott A acid tolerance response and associated physiological and phenotypic features via whole proteome analysis. *Journal of Proteome Research*, 11, 2409-2426.

Briers, Y., Klumpp, J., Schuppler, M., & Loessner, M. J. (2011). Genome sequence of *Listeria monocytogenes* Scott A, a clinical isolate from a food-borne listeriosis outbreak. *Journal of Bacteriology*, 193, 4284-4285.

Brown, S., Santa Maria, J.P. Jr., & Walker, S. (2013). Wall teichoic acids of gram-positive bacteria. *Annual Reviews in Microbiology*, 67, 313-336.

Buchanan, R. (1918). Life phases in a bacterial culture. *The Journal of Infectious Diseases*, 23, 109-125.

Buchanan, R., & Cygnarowicz, M. (1990). A mathematical approach toward defining and calculating the duration of the lag phase. *Food Microbiology*, 7, 237-240.

Buchanan, R., & Klawitter, L. (1991). Effect of temperature history on the growth of *Listeria monocytogenes* Scott A at refrigeration temperatures. *International Journal of Food Microbiology*, 12, 235-245.

Buchanan, R., & Solberg, M. (2006). Interaction of sodium nitrate, oxygen and pH on growth of *Staphylococcus aureus*. *Journal of Food Science*, 37, 81-85.

Budrene, E., & Berg, H. (1991). Complex patterns formed by motile cells of *Escherichia coli*. Nature, 349, 630-633.

Burke, T.P., Loukitcheva, A., Zemansky, J., Wheeler, R., Boneca, I.G., & Portnoy DA. (2014). *Listeria monocytogenes* is resistant to lysozyme through the regulation, not the acquisition, of cell wall-modifying enzymes. *Journal of Bacteriology*, 196, 3756-3767.

Cabanes, D., Dussurget, O., Dehoux, P., & Cossart, P. (2004). Auto, a surface associated autolysin of Listeria monocytogenes required for entry into eukaryotic cells and virulence. *Molecular Microbiology*, 51, 1601-1614.

Cahoon, L.A., & Freitag, N.E. (2014). *Listeria monocytogenes* virulence factor secretion: don't leave the cell without a chaperone. *Frontiers in Cellular and Infection Microbiology*, 4, 13.

Carvalho, F., Atilano, M.L., Pombinho, R., Covas, G., Gallo, R.L., Filipe, S.R., Sousa, S., & Cabanes D. (2015). L-Rhamnosylation of *Listeria monocytogenes* wall teichoic acids promotes resistance to antimicrobial peptides by delaying interaction with the membrane. *PLoS Pathogens*, 11, e1004919.

Casadesús, J., & Low, D.A. (2013). Programmed heterogeneity: epigenetic mechanisms in bacteria. *Journal of Biological Chemistry*, 288, 13929-13935.

Chakraborty, T., Leimeister-Wächter, M., Domann, E., Hartl, M., Goebel, W., Nichterlein, T., & Notermans, S. (1992). Coordinated regulation of virulence genes in *Listeria monocytogenes* requires the product of the prfA gene. *Journal of Bacteriology*, 174, 568-574.

Camejo, A., Buchrieser, C., Couvé, E., Carvalho, F., Reis, O., Ferreira, P., Sousa, S., Cossart, P., & Cabanes, D. (2009). In vivo transcriptional profiling of *Listeria*

monocytogenes and mutagenesis identify new virulence factors involved in infection. *PLoS Pathogens*, 5, e1000449.

Chan, Y. C., & Wiedmann, M. (2009). Physiology and genetics of *Listeria monocytogenes* survival and growth at cold temperatures. *Critical Reviews in Food Science and Nutrition*, 49, 237-253.

Chaturongakul, S., Raengpradub, S., Palmer, M. E., Bergholz, T. M., Orsi, R. H., Hu, Y., Ollinger, J., Weidmamm, M., & Boor, K. J. (2011). Transcriptomic and phenotypic analyses identify coregulated, overlapping regulons among PrfA, CtsR, HrcA, and the alternative sigma factors σ^B, σ^C, σ^H, and σ^L in *Listeria monocytogenes*. *Applied and Environmental Microbiology*, 77(1), 187-200.

Chesney, A. M. (1916). The latent period in the growth of bacteria. *The Journal of Experimental Medicine*, 24, 387-418.

Chien, A.C., Hill, N.S., & Levin, P.A. (2012). Cell size control in bacteria. *Current Biology*, 22, R340-349.

Chihib, N.E., Ribeiro da Silva, M., Delattre, G., Laroche, M., & Federighi, M. (2003). Different cellular fatty acid pattern behaviours of two strains of *Listeria monocytogenes* Scott A and CNL 895807 under different temperature and salinity conditions. *FEMS Microbiol Letters*, 218, 155-160.

Claessen, D., Emmins, R., Hamoen, L. W., Daniel, R. A., Errington, J., & Edwards, D. H. (2008). Control of the cell elongation-division cycle by shuttling of PBP1 protein in *Bacillus subtilis*. *Molecular Microbiology*, 68, 1029-1046.

Coelho, M., Dereli, A., Haese, A., Kühn, S., Malinovska, L., DeSantis, M.E., Shorter, J., Alberti, S., Gross, T., & Tolić-Nørrelykke, I.M. (2013). Fission yeast does not age under favorable conditions but does so after stress. *Current Biology*, 23, 1844-1852.

Cole, M.B., Jones, M.V., & Holyoak, C. (1990). The effect of pH, salt concentration and temperature on the survival and growth of *Listeria monocytogenes*. *Journal of Applied Bacteriology*, 69, 63-72.

Corkrey, R., McMeekin, T.A., Bowman, J.P., Ratkowsky, D.A., Olley, J., & Ross T. (2014). Protein thermodynamics can be predicted directly from biological growth rates. *PLoS One*, 9, e96100.

Cossart, P., & Archambaud, C. (2009). The bacterial pathogen *Listeria monocytogenes*: an emerging model in prokaryotic transcriptomics. *Journal of Biology*, 8, 107.

Costanzo, A., & Ades, S.E. (2006) Growth phase-dependent regulation of the extracytoplasmic stress factor, sigmaE, by guanosine 3',5'-bispyrophosphate (ppGpp). *Journal of Bacteriology*, 188, 4627-4634.

Cotter, P. D., & Hill, C. (2003). Surviving the acid test, response of Gram- positive bacteria to low pH. *Microbiology and Molecular Biology Reviews*, 67, 429-453.

Cotter, P.D., Guinane, C.M., & Hill, C. (2002). The LisRK signal transduction system determines the sensitivity of *Listeria monocytogenes* to nisin and cephalosporins. *Antimicrobial Agents and Chemotherapy*, 46, 2784-2790.

Craig, R., & Beavis, R. C. (2004). TANDEM: matching proteins with tandem mass spectra. *Bioinformatics*, 20, 1466-1467.

Curtis, T.D., Gram, L., & Knudsen, G.M. (2016). The small colony variant of *Listeria monocytogenes* is more tolerant to antibiotics and has altered survival in raw 264.7 murine macrophages. *Frontiers in Microbiology*, 7, 1056.

D'Arrigo, M., de Fernando , G. D., De Diego, R. V., Ordonez, J., George, S., & Pin, C. (2006). Indirect measurement of the lag time distribution of single cells of *Listeria innocua* in food. *Applied and Environmental Microbiology*, 72, 2533-2538.

Dailey, H.A., & Gerdes, S. (2015). HemQ: An iron-coproporphyrin oxidative decarboxylase for protoheme synthesis in *Firmicutes* and *Actinobacteria*. *Archives of Biochemistry and Biophysics*, 574, 27-35.

de Hoon, M.J.L., Imoto, S., Nolan, J., & Miyano, S. (2004). Open source clustering software. *Bioinformatics*, 20, 1453-1454.

Delignette-Muller, M.L., Baty, F., Cornu, M., & Bergis, H. (2005). Modelling the effect of a temperature shift on the lag phase duration of *Listeria monocytogenes*. *International Journal of Food Microbiology*, 100, 77-84.

Dell'Era, S., Buchrieser, C., Couvé, E., Schnell, B., Briers, Y., Schuppler, M., Loessner, M.J. (2009). *Listeria monocytogenes* L-forms respond to cell wall deficiency by modifying gene expression and the mode of division. *Molecular Microbiology*, 73, 306-322.

Dens, E. J., Bernaerts, K., Standaert, A. R., Kreft, J. U., & Van Impe, J. (2005). Cell division theory and individual-based modeling of microbial lag: Part II. Modeling lag phenomena induced by temperature shifts. *International Journal of Food Microbiology*, 101, 319-332.

Derré, I., Rapoport, G., & Msadek, T. (1999). CtsR, a novel regulator of stress and heat shock response, controls clp and molecular chaperone gene expression in gram-positive bacteria. *Molecular Microbiology*, 31, 117-131.

Desvaux, M., Dumas, E., Chafsey, I., Chambon, C., & Hebraud, M. (2010). Comprehensive appraisal of the extracellular proteins from a monoderm bacterium, theoretical and empirical exoproteomes of *Listeria monocytogenes* EGD-e by secretomics. *Journal of Proteome Research*, 9, 5076-5092.

Dhiman, A., Gopalani, M., & Bhatnagar, R. (2015). WalRK two component system of *Bacillus anthracis* responds to temperature and antibiotic stress. *Biochemical and Biophysical Research Communications*, 459, 623-628.

Doan, T. & Aymerich, S. (2003). Regulation of the central glycolytic genes in *Bacillus subtilis*: binding of the repressor CggR to its single DNA target sequence is modulated by fructose-1,6-bisphosphate. *Molecular Microbiology*, 47, 1709-1721.

Duffy, L., Vanderlinde, P., & Grau, F. (1994). Growth of *Listeria monocytogenes* on vacuum-packed cooked meats: effects of pH, a_w, nitrite and ascorbate. *International Journal of Food Microbiology*, 23, 377-390.

Dufrenne, J., Delfgou, E., Ritmeester, W., & Notermans, S. (1997). The effect of previous growth conditions on the lag phase time of some foodborne pathogenic micro-organisms. *International Journal of Food Microbiology*, 34, 89-94.

Dupont, C., & Augustin, J.C. (2009). Influence of stress on single-cell lag time and growth probability for *Listeria monocytogenes* in half Fraser broth. *Applied and Environmental Microbiology*, 75, 3069-3076.

Durack, J., Ross, T., & Bowman, J.P. (2013). Characterisation of the transcriptomes of genetically diverse *Listeria monocytogenes* exposed to hyperosmotic and low temperature conditions reveal global stress-adaptation mechanisms. *PLoS One*, 8, e73603.

Dussurget, O., Cabanes, D., Dehoux, P., Lecuit, M., Buchrieser, C., Glaser, P., Cossart, P., & the European Listeria Genome Consortium. (2002). *Listeria monocytogenes* bile salt hydrolase is a PrfA-regulated virulence factor involved in the intestinal and hepatic phases of listeriosis. *Molecular Microbiology*, 45, 1095-1106.

Elfwing, A., Le Marc, Y., Baranyi, J., & Ballagi, A. (2004). Observing growth and division of large numbers of individual bacteria by image analysis. *Applied and Environmental Microbiology*, 70, 675-678.

Ellis, R.J., & Minton, A.P. (2006). Protein aggregation in crowded environments. *Biological Chemistry*, 387, 485-497.

Farley, M.M., Hu, B., Margolin, W., & Liu, J. (2016). Minicells, Back in Fashion. *J Bacteriology,* 198, 1186-1195.

Fedtke, I., Mader, D., Kohler, T., Moll, H., Nicholson, G., Biswas, R., Henseler, K., Götz, F., Zähringer, U., & Peschel, A. (2007) *Staphylococcus aureus ypfP* mutant with strongly reduced lipoteichoic acid (LTA) content: LTA governs bacterial surface properties and autolysin activity. *Molecular Microbiology*, 65,1078-1091.

Feehily, C., O'Byrne, C.P., & Karatzas, K.A. (2013). Functional γ-aminobutyrate shunt in *Listeria monocytogenes*: role in acid tolerance and succinate biosynthesis. *Applied and Environmental Microbiology*, 79, 74-80.

Fischer, B., Rummel, G., Aldridge, P., & Jenal, U. (2002). The FtsH protease is involved in development, stress response and heat shock control in *Caulobacter crescentus*. *Molecular Microbiology*, 44, 461-478.

Fleming, D. W., Cochi, S. L., MacDonald, K. L., Brondum, J., Hayes, P. S., Plikaytis, B. D., Holmes, M.B., Audurier, A., Broome, C.V., & Reingold, A. L. (1985). Pasteurized milk as a vehicle of infection in an outbreak of listeriosis. *The New England Journal of Medicine*, 312, 404-407.

Francois, K., Devlieghere, F., Standaert, A., Geeraerd, A., Van Impe, J. F., & Debevere, J. (2003). Modelling the individual cell lag phase. Isolating single cells: protocol development. *Letters in Applied Microbiology*, 37, 26-37.

Francois, K., Devlieghere, F., Standaert, A.R., Geeraerd, A.H., Cools, I., Van Impe, J.F., & Debevere J. (2005a). Environmental factors influencing the relationship between optical density and cell count for *Listeria monocytogenes*. *Journal of Applied Microbiology*, 99, 1503-1515.

Francois, K., Devlieghere, F, Smet, K., Standaert, A.R., Geeraerd, A.H., Van Impe, J.F., & Debevere, J. (2005b).Modelling the individual cell lag phase: effect of temperature and pH on the individual cell lag distribution of *Listeria monocytogenes*. *International Journal of Food Microbiology*, 100, 41-53.

Francois, K., Devlieghere, F., Standaert, A., Geeraerd, A., Van Impe, J., & Debevere, J. (2006). Effect of environmental parameters (temperature, pH and a_w)

on the individual cell lag phase and generation time of *Listeria monocytogenes*. *International Journal of Food Microbiology*, 108, 326-335.

Friedman ME, Alm WL. (1962). Effect of glucose concentration on the growth medium on some metabolic activities of *Listeria monocytogenes*. *Journal of Bacteriology* 84, 375–376

Freitag, N.E., Port, G.C., & Miner, M.D. (2009). *Listeria monocytogenes* - from saprophyte to intracellular pathogen. *Nature Reviews Microbiology*, 7, 623-628.

Fritsch, F., Mauder, N., Williams, T., Weiser, J., Oberle, M., & Beier, D. (2011). The cell envelope stress response mediated by the LiaFSRLm three-component system of *Listeria monocytogenes* is controlled via the phosphatase activity of the bifunctional histidine kinase LiaSLM. *Microbiology*, 157, 373-386.

Fujii, H., Kamisango, K., Nagaoka, M., Uchikawa, K., Sekikawa, I., Yamamoto, K., & Azuma, I. (1985). Structural study on teichoic acids of *Listeria monocytogenes* types 4a and 4d. *Journal of Biochemistry*, 97, 883-891.

Gardan, R., Duché, O., Leroy-Sétrin, S., Labadie, J, & the European Listeria Genome Consortium. (2003). Role of ctc from *Listeria monocytogenes* in osmotolerance. *Applied and Environmental Microbiology*, 69, 154-161.

Garmyn, D., Augagneur, Y., Gal, L., Vivant, A. L., & Piveteau, P. (2012). Listeria monocytogenes differential transcriptome analysis reveals temperature-dependent Agr regulation and suggests overlaps with other regulons. *PLoS One*, 7, e43154.

Garmyn, D., Gal, L., Briandet, R., Guilbaud, M., Lemaître, J.P., Hartmann, A., & Piveteau, P. (2011). Evidence of autoinduction heterogeneity via expression of the Agr system of *Listeria monocytogenes* at the single-cell level. *Applied and Environmental Microbiology*, 77, 6286-6289.

Garmyn, D., Gal, L., Lemaitre, J.P., Hartmann, A., & Piveteau P. (2009). Communication and autoinduction in the species *Listeria monocytogenes*: A central role for the agr system. *Communication and Integrative Biology*, 2, 371-374.

Gay, M., Cerf, O., & Davey, K. (1996). Significance of pre-incubation temperature and inoculum concentration on subsequent growth of *Listeria monocytogenes* at 14°C. *Journal of Applied Microbiology*, 81, 433-438.

Geiger, T., & Wolz, C. (2014). Intersection of the stringent response and the CodY regulon in low GC Gram-positive bacteria. *International Journal of Medical Microbiology*, 304, 150-155.

George, S. M., & Lund, B. M. (1992). The effect of culture medium and aeration on growth of *Listeria monocytogenes* at pH 4.5. *Letters in Applied Microbiology*, 15, 49-52.

Gilbreth, S.E., Benson, A.K., & Hutkins, R.W. (2004). Catabolite repression and virulence gene expression in *Listeria monocytogenes*. *Current Microbiology* 49, 95-98.

Gokce, E., Shuford, C. M., Franck, W. L., Dean, R. A., & Muddiman, D. C. (2011). Evaluation of normalization methods on gelc - MS/MS label-free spectral counting data to correct for variation during proteomic workflows. *Journal of the American Society for Mass Spectrometry*, 22, 2199-2208.

Gomez, M. J. (2010). Aging in Bacteria, Immortality or Not - A Critical Review. *Current Aging Science*, 3, 198-218.

Goodell, E.W., & Schwarz, U. (1985). Release of cell wall peptides into culture medium by exponentially growing *Escherichia coli*. *Journal of Bacteriology*, 162, 391-397.

Görke, B., & Stülke, J. (2008). Carbon catabolite repression in bacteria: many ways to make the most out of nutrients. *Nature Reviews Microbiology*, 6, 613-624.

Graumann, P., Schroder, K., Schmid, R., & Marahiel, M. A. (1996). Cold shock stress-induced proteins in Bacillus subtilis. *Journal of Bacteriology*, 178, 4611-4619.

Guariglia-Oropeza, V., Orsi, R. H., Yu, H., Boor, K. J., Wiedmann, M., & Guldimann, C. (2014). Regulatory network features in *Listeria monocytogenes*—changing the way we talk. Frontiers in Cellular and Infection *Microbiology*, 4, 14.

Gueriri, I., Cyncynatus, C., Dubrac, S., Arana, A.T., Dussurget ,O., & Msadek, T. (2008). The DegU orphan response regulator of *Listeria monocytogenes* autorepresses its own synthesis and is required for bacterial motility, virulence and biofilm formation. *Microbiology*, 154, 2251-2264.

Guillier, L., Pardon, P., & Augustin, J. C. (2005). Influence of stress on individual lag time distributions of *Listeria monocytogenes*. *Applied and Environmental Microbiology*, 71, 2940-2948.

Guldimann, C., Boor, K. J., Wiedmann, M., & Guariglia-Oropeza, V. (2016). Resilience in the face of uncertainty: sigma B fine-tunes gene expression to support homeostasis in Gram-positive bacteria*. Applied and Environmental Microbiology*, 82, 4456–4469.

Handa, N., Terada, T., Doi-Katayama, Y., Hirota, H., Tame, J.R., Park, S.Y., Kuramitsu, S., Shirouzu, M., & Yokoyama, S. (2005). Crystal structure of a novel polyisoprenoid-binding protein from *Thermus thermophilus* HB8. *Protein Science* 14, 1004-1010.

Harris, M., Taylor, G., & Taylor, J. (2005). *Maths and Stats for the Life and Medical Sciences*. Scion, Oxfordshire.

Hausmann, C.D., & Ibba, M. (2008). Aminoacyl-tRNA synthetase complexes: molecular multitasking revealed. *FEMS Microbiology Reviews*, 32, 705-721.

Heermann, R., Weber, A., Mayer, B., Ott, M., Hauser, E., Gabriel, G., Pirch, T., & Jung, K. (2009). The universal stress protein UspC scaffolds the KdpD/KdpE signaling cascade of *Escherichia coli* under salt stress. *Journal of Molecular Biology*, 386, 134-148.

Hengge-Aronis, R. (2002). Single transduction and regulatory mechanisms involved in control of the sigma (S) (RpoS) subunit of RNA polymerase. *Microbiology and Molecular Biology Reviews*, 66, 373-395.

Hengge, R. (2011). Stationary-Phase Gene Regulation in *Escherichia coli*. *EcoSal Plus*, doi: 10.1128/ecosalplus.5.6.3.

Henke, E. & Bornscheuer, U.T. (2002). Esterases from Bacillus subtilis and B. stearothermophilus share high sequence homology but differ substantially in their properties. *Applied Microbiology and Biotechnology* 60, 320-326.

Herbert, K. C., & Foster, S. J. (2001). Starvation survival in *Listeria monocytogenes*: characterization of the response and the role of known and novel components. *Microbiology*, 147, 2275-2284.

Hershey, A. (1939). Factors limiting bacterial growth VII. respiration and growth properties of *Escherichia coli* surviving sublethal temperatures. *Journal of Bacteriology*, 38, 563-578.

Hills, B., & Wright, K. (1994). A new model for bacterial growth in heterogeneous systems. *Journal of Theoretical Biology*, 168, 31-41.

Hu, Y., Oliver, H. F., Raengpradub, S., Palmer, M. E., Orsi, R. H., Wiedmann, M., & Boor, K. J. (2007a). Transcriptomic and phenotypic analyses suggest a network between the transcriptional regulators HrcA and σ^B in *Listeria monocytogenes*. *Applied and Environmental Microbiology*, 73, 7981-7991.

Hu, Y., Raengpradub, S., Schwab, U., Loss, C., Orsi, R.H., Wiedmann, M., & Boor, K.J. (2007b). Phenotypic and transcriptomic analyses demonstrate interactions between the transcriptional regulators CtsR and σ^B in *Listeria monocytogenes*. *Applied and Environmental Microbiology*, 73, 7967-7980.

Hudson, J. (1993). Effect of pre-incubation temperature on the lag time of *Aeromonas hydrophila*. *Letters in Applied Microbiology*, 16, 274-276.

Huisman, G., Siegele, M., Zambrano, M., & Kolter, R. (1996). Morphological and physiological changes during stationary phase, p. 1672-1682. In F. C. Neidhardt et al. (ed.), *Escherichia coli and Salmonella: Cellular and Molecular Biology*. ASM Press, Washington, D.C.

Ishihama, A. (1997). Adaption of gene expression in stationary phase bacteria. *Current Opinions in Genetics and Development*, 7, 582-588.

Ishihama, Y., Schmidt, T., Rappsilber, J., Mann, M., Hartl, F.U., Kerner, M.J., & Frishman, D. 2008. Protein abundance profiling of the *Escherichia coli* cytosol. *BMC Genomics*, 9, 102.

Jacobs, C., Frère, J.M., & Normark, S. (1997). Cytosolic intermediates for cell wall biosynthesis and degradation control inducible beta-lactam resistance in Gram-negative bacteria. *Cell*, 88, 823-832.

Jaradat, Z.W., & Bhunia, A.K. (2003). Adhesion, invasion, and translocation characteristics of *Listeria monocytogenes* serotypes in Caco-2 cell and mouse models. *Applied and Environmental Microbiology*, 69, 3640-3645.

Jason, A.C. (1983). A deterministic model for monophasic growth of batch cultures of bacteria. *Antonie Van Leeuwenhoek* 49, 513-536.

Johansson, J., Mandin, P., Renzoni, A., Chiaruttini, C., Springer , M., & Cossart, P. (2002). An RNA thermosensor controls expression of virulence genes in *Listeria monocytogenes*. *Cell*, 110, 551-561.

Joseph, B., Przybilla, K., Stühler, C., Schauer, K., Slaghuis, J., Fuchs, T. M., & Goebel, W. (2006). Identification of *Listeria monocytogenes* genes contributing to intracellular replication by expression profiling and mutant screening. *Journal of Bacteriology*, 188, 556-568.

Juneja, V.K., Foglia, T.A., & Marmer, B.S. (1998). Heat resistance and fatty acid composition of *Listeria monocytogenes*: effect of pH, acidulant, and growth temperature. *Journal of Food Protection*, 61, 683-687.

Kang J, Wiedmann M, Boor KJ, & Bergholz TM. (2015). VirR-mediated resistance of *Listeria monocytogenes* against food antimicrobials and cross-protection induced by exposure to organic acid salts. *Applied and Environmental Microbiology*, 81, 4553-4562.

Kazmierczak, M. J., Mithoe, S. C., Boor, K. J., & Wiedmann, M. (2003*). Listeria monocytogenes* σ^B regulates stress response and virulence functions. *Journal of Bacteriology*, 185, 5722-5734.

King, T., Kocharunchitt, C., Gobius, K., Bowman, J.P., and Ross, T. (2016). Physiological response of *Escherichia coli* O157:H7 Sakai to dynamic changes in temperature and water activity as experienced during carcass chilling. *Molecular and Cellular Proteomics*, 15, 3331-3347.

Kirkwood, T.B. 2005. Asymmetry and the origins of aging. *Mechanisms of Aging and Development*, 126, 533–534.

Knappe, J., & Sawers, G. (1990). A Radical-Chemical Route to Acetyl-CoA: The anaerobically induced pyruvate formate-lyase system of *Escherichia coli*. *FEMS Microbiology Letters*, 75, 383-398.

Knudsen, G.M., Olsen, J.E., & Dons, L. (2004). Characterization of DegU, a response regulator in *Listeria monocytogenes*, involved in regulation of motility and contributes to virulence. *FEMS Microbiol Letters*, 240, 171-179.

Kocharunchitt, C., King, T., Gobius, K., Bowman, J. P., & Ross, T. (2012). Integrated transcriptomic and proteomic analysis of the physiological response of *Escherichia coli* O157:H7 Sakai to steady-state conditions of cold and water activity stress. *Molecular and Cellular Proteomics*, 11, M111.009019.

Komatsuzawa, H., Fujiwara, T., Nishi, H., Yamada, S., Ohara, M., McCallum, N., Berger-Bächi, B., & Sugai, M. (2004). The gate controlling cell wall synthesis in *Staphylococcus aureus*. *Molecular Microbiology*, 53, 1221-1231.

Koseki, S., & Nonaka, J. (2012). Alternative approach to modeling bacterial lag time, using logistic regression as a function of time, temperature, pH, and sodium chloride concentration. *Applied and Environmental Microbiology*, 78, 6103-6112.

Kotter, R., Siegele, D. A., & Tormo, A. (1993). The stationary phase of the bacterial life cycle. *Annual Review of Microbiology*, 47, 855-874.

Koutsoumanis, K. P., & Sofos, J. N. (2005). Effect of inoculum size on the combined temperature, pH and aw limits for growth of *Listeria monocytogenes*. *International Journal of Food Microbiology*, 104, 83-91.

Kutalik, Z., Razaz, M., Elfwing, A., Ballagi, A., & Baranyi, J. (2005). Stochastic modelling of individual cell growth using flow chamber microscopy images. *International Journal of Food Microbiology*, 105, 177-190.

Kyoui, D., Hirokawa, E., Takahashi, H., Kuda, T., & Kimura, B. (2016). Effect of glucose on Listeria monocytogenes biofilm formation, and assessment of the biofilm's sanitation tolerance. *Biofouling* 32, 815-26.

Lam, H., Oh, D., Cava, F., Takacs, C., Clardy, J., De Pedro, M., & Waldor, M. (2009). D-amino acids govern stationary phase cell wall remodeling in bacteria. *Science*, 325, 1552-1555.

Larsen, M.H., Kallipolitis, B.H., Christiansen, J.K., Olsen, J.E., & Ingmer, H. (2006). The response regulator ResD modulates virulence gene expression in response to carbohydrates in *Listeria monocytogenes*. *Molecular Microbiology*, 61, 1622-1635.

Le Marc, Y., Skandamis, P., Belessi, C., Merkouri, S., George, S., Gounadaki, A., Schvartzman, S., Jordan, K., Drosinos, E. H & Baranyi, J. (2010). Modeling the effect of abrupt acid and osmotic shifts within the growth region and across growth boundaries on adaptation and growth of *Listeria monocytogenes*. *Applied and Environmental Microbiology*, 76, 6555-6563.

Ledala, N., Sengupta, M., Muthaiyan, A., Wilkinson, B. J., & Jayaswal, R. K. (2010). Transcriptomic response of *Listeria monocytogenes* to iron limitation and fur mutation. *Applied and Environmental Microbiology*, 76, 406-416.

Lee, P.S., & Grossman, A.D. (2006). The chromosome partitioning proteins Soj (ParA) and Spo0J (ParB) contribute to accurate chromosome partitioning, separation of replicated sister origins, and regulation of replication initiation in *Bacillus subtilis*. *Molecular Microbiology*, 60, 853-869.

Leimeister-Wachter, M., Domann, E., & Chakraborty, T. (1992). The expression of virulence genes in *Listeria monocytogenes* is thermoregulated. *Journal of Bacteriology*, 174, 947-952.

Leimeister-Wächter M, Haffner C, Domann E, Goebel W, Chakraborty T. (1990). Identification of a gene that positively regulates expression of listeriolysin, the major virulence factor of *Listeria monocytogenes*. *Proceedings of the National Academy of Sciences USA*, 87, 8336-8340.

Lesniak, J., Barton, W.A., & Nikolov, D.B. (2002). Structural and functional characterization of the *Pseudomonas* hydroperoxide resistance protein Ohr, *EMBO Journal*, 21, 6649-6659.

Li, K., Jiang, T., Yu, B., Wang, L., Gao, C., Ma, C., Xu, P., and Ma, Y. (2013). *Escherichia coli* transcription termination factor NusA: heat-induced oligomerization and chaperone activity. *Science Reports*, 3, 2347.

Li, Y., Odumeru, J. A., Griffiths, M., & McKellar, R. C. (2006). Effect of environmental stresses on the mean and distribution of individual cell lag times of *Escherichia coli* O157:H7. *International Journal of Food Microbiology*, 110, 278-285.

Lim, C.J., Lee, S.Y., Kenney, L.J. & Yan, J. (2012). Nucleoprotein filament formation is the structural basis for bacterial protein H-NS gene silencing. *Scientific Reports* 2:509.

Lin, E., & Crowley, D. (2001). Duration of lag phase of *Pseudomonas fluorescens* 2-79RL starved in isolation or in the presence of soil microorganisms. *Soil Biology and Biochemistry*, 33, 2005-2010.

Lindner, A. B., Madden, R., Demarez, A., Stewart, E. J., & Taddei, F. (2008). Asymmetric segregation of protein aggregates is associated with cellular aging and recovery. *Proceedings of the National Academy of Sciences of the United States of America*, 105, 3076–3081.

Liu, S., Graham, J. E., Bigelow, L., Morse II, P. D., & Wilkinson, B. J. (2002). Identification of *Listeria monocytogenes* genes expressed in response to growth at low temperature. *Applied Environmental Microbiology*, 68, 1697-1705.

Liu, X. (2012). *Effect of Cell Age on Bacterial Lag Phase*. MAppSci Master's Thesis. School of Land and Food, University of Tasmania.

Llorens, J., Tormo, A., & Martínez-García, E. (2010). Stationary phase in Gram-negative bacteria. *FEMS Microbiology Review*, 34, 476-495.

Lobel, L., & Herskovits, A.A. (2016). Systems level analyses reveal multiple regulatory activities of CodY controlling metabolism, motility and virulence in *Listeria monocytogenes. PLoS Genetics*, 12, e1005870.

Lobel, L., Sigal, N., Borovok, I., Belitsky, B. R., Sonenshein, A. L., & Herskovits, A. A. (2015). The metabolic regulator CodY links *Listeria monocytogenes* metabolism to virulence by directly activating the virulence regulatory gene prfA. *Molecular Microbiology*, 95, 624-644.

Lobel, L., Sigal, N., Borovok, L., Ruppin, E., & Herskovits, A. A. (2012). Integrative genomic analysis identifies isoleucine and cody as regulators of *Listeria monocytogenes* virulence. *PLoS Genetics*, 8, e1002887.

Loh, E., Dussurget, O., Gripenland, J., Vaitkevicius, K., Tiensuu, T., Mandin, P., Repoila, F., Buchrieser, C., Cossart, P., & Johansson, J. (2009). A trans-acting riboswitch controls expression of the virulence regulator PrfA in *Listeria monocytogenes*. *Cell*, 139, 770-779.

Maas, W. K. (1964). Studies on the mechanism of repression of arginine biosynthesis in *Escherichia coli*. II. Dominance of repressibility in diploids. *Journal of Molecular Biology*, 8, 365-370.

Maaβ, S., Wachlin, G., Bernhardt, J., Eymann, C., Fromion, V., Riedel, K., Becher, D., & Hecker M. (2014). Highly precise quantification of protein molecules per cell during stress and starvation responses in *Bacillus subtilis*. *Molecular and Cellular Proteomics*, 13, 2260-2276.

Machata, S., Hain, T., Rohde, M., & Chakraborty, T. (2005). Simultaneous deficiency of both MurA and p60 proteins generates a rough phenotype in *Listeria monocytogenes*. *Journal of Bacteriology*, 187, 8385-8394.

Maeda, H., Jishage, M., Nomura, T., Fujita, N., & Ishihama, A. (2000). Two extracytoplasmic function sigma subunits, sigma(E) and sigma(FecI), of *Escherichia coli*: promoter selectivity and intracellular levels. *Journal of Bacteriology*, 182, 1181-1184.

Maier, T., Schmidt, A., Güell, M., Kühner, S., Gavin, A.C., Aebersold, R., & Serrano, L. (2011). Quantification of mRNA and protein and integration with protein turnover in a bacterium. *Molecular Systems Biology*, 7, 511.

Mackey, B., & Derrick, C. M. (1982). The effect of sublethal injury by heating, freezing, drying and gamma ‐ radiation on the duration of the lag phase of *Salmonella* Typhimurium. *Journal of Applied Microbiology*, 53, 243-251.

Mandin, P., Fsihi, H., Dussurget, O., Vergassola, M., Toledo-Arana, A., Lasa, I., Johansson, P., & Cossart, P. (2005). VirR, a response regulator critical for *Listeria monocytogenes* virulence. *Molecular Microbiology*, 57, 1367-80.

Mattila, M., Somervuo, P., Rattei, T., Korkeala, H., Stephan, R., & Tasara, T. (2012). Phenotypic and transcriptomic analyses of Sigma L-dependent characteristics in *Listeria monocytogenes* EGD-e. *Food Microbiology*, 32, 152-164.

Mauder, N., Williams, T., Fritsch, F., Kuhn, M., & Beier, D. (2008). Response regulator DegU of *Listeria monocytogenes* controls temperature-responsive flagellar gene expression in its unphosphorylated state. *Journal of Bacteriology*, 190, 4777-4781.

McCoy, D. R., & Ordal, Z. J. (1979). Thermal stress of *Pseudomonas fluorescens* in complex media. *Applied and Environmental Microbiology*, 37, 443-448.

McKellar , R. C., & Hawke, A. (2006). Assessment of distributions for fitting lag times of individual cells in bacterial populations. *International Journal of Food Microbiology*, 106, 169-175.

McKellar, R. C. (2007a). Effect of starvation on expression of the ribosomal RNA *rrnB* P2 promoter during the lag phase of *Pseudomonas fluorescens*. *International Journal of Food Microbiology*, 114(3), 307-315.

McKellar, R. (2007b). Effect of sub-lethal heating and growth temperature on expression of the ribosomal RNA rrnB P(2) promoter during the lag phase of *Pseudomonas fluorescens*. *International Journal of Food Microbiology*, 116(2), 248-259.

McKellar, R., & Knight, K. (2000). A combined discrete-continuous model describing the lag phase of *Listeria monocytogenes*. *International Journal of Food Microbiology*, 54, 171-180.

McKellar, R., Lu, X., & Knight, K. (2002a). Growth pH does not affect the initial physiological state parameter p0 of *Listeria monocytogenes*. *International Journal of Food Microbiology*, 73, 137-144.

McKellar, R., Lu, X., & Knight, K. (2002b). Proposal of a novel parameter to describe the influence of pH on the lag phase of *Listeria monocytogenes*. *International Journal of Food Microbiology*, 73, 127-135.

Medrano Romero, V., & Morikawa, K. (2016). *Listeria monocytogenes* σH contributes to expression of competence genes and intracellular growth. *Journal of Bacteriology*, 198, 1207-1217.

Meisner, J., Llopis, P. M., Sham, L. T., Garner, E., Bernhardt, T. G., & Rudner, D. (2013). FtsEX is required for CwlO peptidoglycan hydrolase activity during cell wall elongation in *Bacillus subtilis*. *Molecular Microbiology*, 89, 1069-1083.

Mellefont, L.A., Kocharunchitt, C., & Ross, T. (2015). Combined effect of chilling and desiccation on survival of *Escherichia coli* suggests a transient loss of culturability. *International Journal of Food Microbiology*, 208, 1-10.

Mellefont, L., & Ross, T. (2003). The effect of abrupt shifts in temperature on the lag phase duration of *Escherichia coli* and *Klebsiella oxytoca*. *International Journal of Food Microbiology*, 83, 295-305.

Membré, J. M., Ross, T., & McMeekin, T. (2002). Behaviour of *Listeria monocytogenes* under combined chilling processes. *Letter in Applied Microbiology*, 28, 216-220.

Métris, A., George, S.M., Mackey, B.M., & Baranyi, J. (2008). Modeling the variability of single-cell lag times for *Listeria innocua* populations after sublethal and lethal heat treatments. *Applied & Environmental Microbiology*, 74, 6949-6955.

Metris, A., Le Marc, Y., Elfwing, A., Ballagi, A., & Baranyi, J. (2005). Modelling the variability of lag times and the first generation times of single cells of *E. coli. International Journal of Food Microbiology*, 100, 13-19.

Miller, K.A., Phillips, R.S., Kilgore, P.B., Smith, G.L., & Hoover, T.R. (2015). A mannose family phosphotransferase system permease and associated enzymes are required for utilization of fructoselysine and glucoselysine in *Salmonella enterica* serovar Typhimurium. *Journal of Bacteriology*, 197, 2831-2839.

Milo, R. (2013). What is the total number of protein molecules per cell volume? A call to rethink some published values. *Bioessays*, 35, 1050-1055.

Milohanic, E., Glaser, P., Coppée , J. Y., Frangeul , L., Vega, Y., & Vázquez-Boland , J. A. (2003). Transcriptome analysis of *Listeria monocytogenes* identifies three groups of genes differently regulated by PrfA. *Molecular Microbiology*, 47, 1613-25.

Milohanic, E., Jonquières, R., Cossart, P., Berche, P., & Gaillard, J. L. (2001). The autolysin Ami contributes to the adhesion of Listeria monocytogenes to eukaryotic cells via its cell wall anchor. *Molecular Microbiology*, 39, 1212-1224.

Monnier, V.M. (2005). Bacterial enzymes that can deglycate glucose- and fructose-modified lysine. *Biochemical Journal*, 392, e1-3.

Monod, J. (1949). The growth of bacterial cultures. *Annual Review of Microbiology*, 3, 371-394.

Moseley, J.B. (2013). Cellular aging: symmetry evades senescence, *Current Biology*, 23, R871–R873.

Mujahid, S., Orsi, R. H., Boor, K. J., & Wiedmann, M. (2013) Protein level identification of the *Listeria monocytogenes* σ^H, σ^L, and σ^C regulons. *BMC Microbiology*, 13, 156.

Müller-Herbst, S., Wüstner, S., Mühlig, A., Eder, D., Fuchs, T., Held, C., Ehrenreich, A., & Scherer, S. (2014). Identification of genes essential for anaerobic growth of *Listeria monocytogenes*. *Microbiology*, 160, 752-765.

Muñoz-Cuevas, M., Fernández, P. S., George, S., & Pin, C. (2010). Modeling the lag period and exponential growth of *Listeria monocytogenes* under conditions of fluctuating temperature and water activity values. *Applied and Environmental Microbiology*, 76, 2908-2915.

Nelson, E. K., Piehler, B., Eckels, J., Rauch, A., Bellew, M., Hussey, P., Ramsay, S., Nathe, C., Lum, K., Krouse, K., Stearns, D., Connolly, B., Skillman, T., & Igra, M. (2011). LabKey Server: an open source platform for scientific data integration, analysis and collaboration. *BMC Bioinformatics*, 12, 71.

Nesvizhskii, A. I., Vitek, O., & Aebersold, R. (2007). Analysis and validation of proteomic data generated by tandem mass spectrometry. *Nature Methods*, 4, 787-797.

Nielsen, P.K., Andersen, A.Z., Mols, M., van der Veen, S., Abee, T., & Kallipolitis, B.H. (2012). Genome-wide transcriptional profiling of the cell envelope stress

response and the role of LisRK and CesRK in *Listeria monocytogenes*. Microbiology, 158, 963-974.

Niven, G. W., Morton, J. S., Fuks, T., & Mackey, B. M. (2008). Influence of environmental stress on distributions of times to first division in *Escherichia coli* populations, as determined by digital-image analysis of individual cells. *Applied and Environmental Microbiology*, 74, 3757-3763.

Nyström, T. (1999). Starvation, cessation of growth and bacterial aging. *Current Opinions in Microbiology*, 2, 214-219.

Nyström, T. (2004). Stationary-phase physiology. *Annual Review of Microbiology*, 58, 161-181.

Nyström T. (2007). A bacterial kind of aging. *PLoS Genetics*, 3, e224.

Old, W. M., Meyer-Arendt, K., Aveline-Wolf, L., Pierce, K. G., Mendoza, A., Sevinsky, J. R., Resing, K.A., & Ahn, N. G. (2005). Comparison of label-free methods for quantifying human proteins by shotgun proteomics. *Molecular & Cellular Proteomics*, 4, 1487-1502.

Oliver, H. F., Orsi, R. H., Wiedmann, M., & Boor, K. J. (2010). *Listeria monocytogenes* {sigma}B has a small core regulon and a conserved role in virulence but makes differential contributions to stress tolerance across a diverse collection of strains. *Applied and Environmental Microbiology*, 76, 4216-4232.

Park, S. F., & Kroll, R. G. (1993). Expression of listeriolysin and phosphatidylinositol‐specific phospholipase C is repressed by the plant‐derived molecule cellobiose in *Listeria monocytogenes*. *Molecular Microbiology*, 8, 653-661.

Pascual, C., Robinson, T., Ocio, M., Aboaba, O., & Mackey, B. (2001). The effect of inoculum size and sublethal injury on the ability of *Listeria monocytogenes* to initiate growth under suboptimal conditions. *Letters in Applied Microbiology*, 33, 357-361.

Paspaliari DK, Loose JS, Larsen MH, Vaaje-Kolstad G. (2015) Listeria monocytogenes has a functional chitinolytic system and an active lytic polysaccharide monooxygenase. *FEBS Journal* 282, 921-936.

Pham, T. V., Piersma, S. R., Warmoes, M., & Jimenez, C. R. (2010). On the beta-binomial model for analysis of spectral count data in label-free tandem mass spectrometry-based proteomics. *Bioinformatics*, 26, 363-369.

Phan-Thanh, L. & Gormon, T. (1997). A chemically defined minimal medium for the optimal culture of *Listeria*. *International Journal of Food Microbiology*, 35, 91-95.

Pilgrim, S., Kolb-Mäurer, A., Gentschev, I., Goebel, W., & Kuhn, M. (2003). Deletion of the gene encoding p60 in *Listeria monocytogenes* leads to abnormal cell division and loss of actin-based motility. *Infection and Immunity*, 71, 3473-3784.

Pinheiro, J., Reis, O., Vieira, A., Moura, I.M., Zanolli Moreno, L., Carvalho, F., Pucciarelli, M.G., García-Del Portillo, F., Sousa, S., & Cabanes D. (2016). *Listeria monocytogenes* encodes a functional ESX-1 secretion system whose expression is detrimental to in vivo infection. *Virulence*, 10, 1-12.

Pin, C., & Baranyi, J. (2008). Single-cell and population lag times as a function of cell age. *Applied and Environmental Microbiology*, 74, 2534-2536.

Pin, C., Rolfe, M. D., Muñoz-Cuevas, M., Hinton, J. C., Peck, M. W., Walton, N. J., & Baranyi, J. (2009). Network analysis of the transcriptional pattern of young and old cells of *Escherichia coli* during lag phase. *BMC Systems Biology*, 3, 108.

Pirt, S. J. (1975). *Principles of Microbe and Cell Cultivation*. Blackwell Scientific Publications.

Plata MR, Koch C, Wechselberger P, Herwig C, Lendl B. (2013) Determination of carbohydrates present in Saccharomyces cerevisiae using mid-infrared spectroscopy and partial least squares regression. *Analytical and Bioanalytic Chemistry* 405, 8241-8250.

Popowska, M. (2004). Analysis of the peptidoglycan hydrolases of *Listeria monocytogenes*: multiple enzymes with multiple functions. *Polish Journal of Microbiology*, 53, 29-34.

Popowska, M., Kłoszewska, M., Górecka, S., & Markiewicz, Z. (1999). Autolysis of *Listeria monocytogenes*. *Acta Microbiologica Polonica*, 48, 141-152.

Popowska, M., Osinska, M., & Rzeczkowska, M. (2012). N-acetylglucosamine-6-phosphate deacetylase (NagA) of *Listeria monocytogenes* EGD, an essential enzyme for the metabolism and recycling of amino sugars. *Archives of Microbiology*, 194, 255-268.

Porteus, B., Kocharunchitt, C., Nilsson, R. E., Ross, T., & Bowman, J. P. (2011). Utility of gel-free, label-free shotgun proteomics approaches to investigate microorganisms. *Applied Microbiology Biotechnology*, 90, 407-416.

Postgate, J.R., & Hunter, J.R. (1964). Accelerated death of *Aerobacter aerogenes* starved in the presence of growth-limiting substrates. *Journal of General Microbiology*, 34, 459-473.

Pouplana, S., Espargaro, A., Galdeano, C., Viayna, E., Sola, I., Ventura, S., Muñoz-Torrero, D., & Sabate, R. (2014). Thioflavin-S staining of bacterial inclusion bodies for the fast, simple, and inexpensive screening of amyloid aggregation inhibitors. *Current Medicinal Chemistry*, 21, 1152-1159.

Premaratne, R. J., Lin, W. J., & Johnson, E. A. (1991). Development of an improved chemically defined minimal medium for *Listeria monocytogenes*. *Applied and Environmental Microbiology*, 57, 3046-3048.

Raengpradub, S., Wiedmann, M., & Boor, K. J. (2008). Comparative analysis of the σB-dependent stress responses in *Listeria monocytogenes* and *Listeria innocua* strains exposed to selected stress conditions. *Applied Environmental Microbiology*, 74, 159-171.

Raimann, E., Schmid, B., Stephan, R., & Tasara, T. (2009). The alternative sigma factor sigma(L) of *L. monocytogenes* promotes growth under diverse environmental stresses. *Foodborne Pathogens and Disease*, 6, 583-591.

Rauch, A., Bellew, M., Eng, J., Fitzgibbon, M., Holzman, T., Hussey, P., Igra, M., Maclean, B., Lin, C.W., Detter, A., Fang, R., Faca, V., Gafken, P., Zhang, H., Whiteaker, J., States, D., Hanash, S., Paulovich, A., & McIntosh, M.W. (2006). Computational Proteomics Analysis System (CPAS): an extensible, open-source analytic system for evaluating and publishing proteomic data and high throughput biological experiments. *Journal of Proteome Research*, 5, 112-121.

Razavilar, V., & Genigeorgis, C. (1998). Prediction of *Listeria* spp. growth as affected by various levels of chemicals, pH, temperature and storage time in a model broth. *International Journal of Food Microbiology*, 40, 149-157.

Rea, R. B., Gahan, C. G., & Hill, C. (2004). Disruption of purative regulatory loci in *Listeria monocytogenes* demonstrates a significant role of Fur and PerR in virulence. *Infection and Immunity*, 72, 2717-2727.

Reeve, C., Bockman, A., & Matin, A. (1984). Role of protein degradation in the survival of carbon-starved *Escherichia coli* and *Salmonella* Typhimurium. *Journal of Bacteriology*, 157, 758-763.

Réglier-Poupet, H., Pellegrini, E., Charbit, A., & Berche, P. (2003). Identification of LpeA, a PsaA-like membrane protein that promotes cell entry by *Listeria monocytogenes*. *Infection and Immunity*, 71(1), 474-482.

Reniere, M.L., Whiteley, A.T., Hamilton, K. L., John, S.M., Lauer, P., Brennan, R. G., & Portnoy, D. A. (2015). Glutathione activates virulence gene expression of an intracellular pathogen. *Nature*, 517, 170-173.

Riedel, C.U., Monk, I.R., Casey, P.G., Waidmann, M.S., Gahan, C.G., & Hill,C. Reniere, M.L., Whiteley, A.T., & Portnoy, D.A. (2016). An in vivo selection identifies *Listeria monocytogenes* genes required to sense the intracellular environment and activate virulence factor expression. *PLoS Pathogens*, 12, e1005741.

Riedel C.U., Monk, I.R., Casey, P.G., Waidmann, M.S., Gahan, C.G. & Hill, C. (2009). AgrD-dependent quorum sensing affects biofilm formation, invasion, virulence and global gene expression profiles in *Listeria monocytogenes*. *Molecular Microbiology*, 71, 1177-1189.

Rieu, A., Weidmann, S., Garmyn, D., Piveteau, P., & Guzzo, J. (2007). Agr system of *Listeria monocytogenes* EGD-e: role in adherence and differential expression pattern. *Applied and Environmental Microbiology*, 73, 6125-6133.

Robinson, T. P., Aboaba, O. O., Kaloti, A., Ocio, M. J., Baranyi, J., & Mackey, B. M. (2001). The effect of inoculum size on the lag phase of *Listeria monocytogenes*. *International Journal of Food Microbiology*, 70(1), 163-173.

Robinson, T. P., Ocio, M. J., Kaloti, A., & Mackey, B. M. (1998). The effect of growth environment on the lag phase of *Listeria monocytogenes*. *International Journal of Food Microbiology*, 44, 83-92.

Rolfe, M. D., Rice, C. J., Lucchini, S., Pin, C., Thompson, A., Cameron, A. D., Alston, M., Stringer, M.F., Betts, R.P., Baranyi, J., Peck, M.W.& Baranyi, J. (2012). Lag phase is a distinct growth phase that prepares bacteria for exponential growth and involves transient metal accumulation. *Journal of Bacteriology*, 194, 686-701.

Romick, T.L., Fleming, H.P., & McFeeters, R.F. (1996). Aerobic and anaerobic metabolism of *Listeria monocytogenes* in defined glucose medium. *Applied and Environmental Microbiology*, 62, 304-307.

Rose, M.R. (1991). Evolutionary Biology of Aging. Oxford University Press, Oxford.

Ross, T., Zhang, D., & McQuestin, O. J. (2008). Temperature governs the inactivation rate of vegetative bacteria under growth-preventing conditions. *International Journal of Food Microbiology*, 128, 129-135.

Rothman, J.E., & Schekman, R. (2011). Molecular mechanism of protein folding in the cell. *Cell*, 146, 851-854.

Rouquette, C., Ripio, M.T., Pellegrini, E., Bolla, J.M., Tascon, R.I., Vázquez-Boland, J.A., & Berche, P. (1996). Identification of a ClpC ATPase required for stress tolerance and in vivo survival of *Listeria monocytogenes*. *Molecular Microbiology*, 21, 977-987.

Ruiz-González, M.X., & Marín, I. (2006). Proteasome-related HslU and HslV genes typical of eubacteria are widespread in eukaryotes. *Journal of Molecular Evolution*, 63, 504-512.

Sakamoto, A., Terui, Y., Yoshida, T., Yamamoto, T., Suzuki, H., Yamamoto, K., Ishihama, A., Igarashi, K., & Kashiwagi, K. (2015). Three members of polyamine modulon under oxidative stress conditions: two transcription factors (SoxR and EmrR) and a glutathione synthetic enzyme (GshA). *PLoS One*, 10, e0124883.

Saldanha, A.J. (2004). Java Treeview--extensible visualization of microarray data. *Bioinformatics*, 20, 3246-3248.

Salzberg, L.I., Powell, L., Hokamp, K., Botella, E., Noone, D., & Devine, K.M. (2013). The WalRK (YycFG) and σ(I) RsgI regulators cooperate to control CwlO and LytE expression in exponentially growing and stressed *Bacillus subtilis* cells. *Molecular Microbiology*, 87, 180-195.

Santiago, B., Marek, M., Faustoferri, R.C., & Quivey R.G. Jr. The *Streptococcus mutans* aminotransferase encoded by *ilvE* is regulated by CodY and CcpA. *Journal of Bacteriology*, 195, 3552-62.

Sauer, U., & Eikmanns, B.J. (2005). The PEP-pyruvate-oxaloacetate node as the switch point for carbon flux distribution in bacteria. *FEMS Microbiology Reviews*, 29, 765-794.

Schmalisch, M., Langbein, I., & Stülke, J. (2002). The general stress protein Ctc of *Bacillus subtilis* is a ribosomal protein. *Journal of Molecular Microbiology and Biotechnology*, 4, 495-501.

Schmidt, R.L., Filak, H.C., Lemon, J.D., Potter, T.A., & Lenz, L.L. (2011). A LysM and SH3-domain containing region of the *Listeria monocytogenes* p60 protein stimulates accessory cells to promote activation of host NK cells. *PLoS Pathogens*, 7, e1002368.

Schneebeli, R., & Egli, T. (2013). A defined, glucose-limited mineral medium for the cultivation of *Listeria* spp. *Applied and Environmental Microbiology*, 79, 2503-2511.

Schubert, O.T., & Aebersold, R. (2015). Microbial proteome profiling and systems biology: applications to *Mycobacterium tuberculosis*. *Advances in Experimental Medical Biology*, 883, 235-254.

Seifart Gomes, C., Izar, B., Pazan, F., Mohamed, W., Mraheil, M.A., Mukherjee, K., Billion, A., Aharonowitz, Y., Chakraborty, T., & Hain, T. (2011). Universal stress proteins are important for oxidative and acid stress resistance and growth of *Listeria monocytogenes* EGD-e in vitro and in vivo. *PLoS One*, 6, e24965.

Sesto, N., Koutero, M., & Cossart P. (2014). Bacterial and cellular RNAs at work during *Listeria* infection. *Future Microbiology*, 9, 1025-1037.

Shapiro, L., McAdams, H.H., & Losick, R. 2002. Generating and exploiting polarity in bacteria. *Science*, 298, 1942-1946.

Shapiro, L., McAdams, H.H., & Losick, R. (2009). Why and how bacteria localize proteins. *Science* 326, 1225-1228.

Sheikh-Zeinoddin, M., Perehinec, T.M., Hill, S.E., & Rees, C.E. (2000). Maillard reaction causes suppression of virulence gene expression in *Listeria monocytogenes*. *International Journal of Food Microbiology*, 61, 41-49.

Shen, A., Kamp, H.D., Gründling, A., & Higgins, D.E. (2006). A bifunctional O-GlcNAc transferase governs flagellar motility through anti-repression. *Genes and Dev.elopment* 20, 3283-3295.

Sherman, J. M., & Albus, W. R. (1924). The function of lag in bacterial cultures. *Journal of Bacteriology*, 9, 303-305.

Shinagawa, A., & Seto, H. (1990). Choline-mediated aggregation and dissociation of autolysin of *Streptococcus pneumoniae*. *Agricultural and Biological Chemistry*, 54, 1115-1119.

Siegele, D., & Kolter, R. (1992). Life after log. *Journal of Bacteriology*, 174, 345-348.

Singh, S.M., & Panda, A.K. (2005). Solubilization and refolding of bacterial inclusion body proteins. *Journal of Bioscience and Bioengineering*, 99, 303-310.

Sleator, R. D., & Hill, C. (2010). Compatible solutes, the key to *Listeria*'s success as a versatile gastrointestinal pathogen? *Gut Pathogens*, 2, 20.

Smelt, J., Otten, G., & Bos, A. (2002). Modelling the effect of sublethal injury on the distribution of the lag times of *Lactobacillus plantarum*. *International Journal of Food Microbiology*, 73, 207.

Sonenshein, A. L. (2005). CodY, a global regulator of stationary phase and virulence in Gram-positive bacteria. *Current Opinion in Microbiology*, 8, 203-207.

Srinivasan, R., Rajeswari, H., & Ajitkumar, P. (2008). Analysis of degradation of bacterial cell division protein FtsZ by the ATP-dependent zinc-metalloprotease FtsH in vitro. *Microbiological Research*, 163, 21-30.

Stancik, L.M., Stancik, D.M., Schmidt, B., Barnhart, D.M., Yoncheva, Y.N., & Slonczewski, J.L. (2002). pH-dependent expression of periplasmic proteins and amino acid catabolism in *Escherichia coli*. *Journal of Bacteriology*, 184, 4246-4258.

Stasiewicz, M. J., Wiedmann, M., & Bergholz, T. M. (2011). The transcriptional response of *Listeria monocytogenes* during adaptation to growth on lactate and diacetate includes synergistic changes that increase fermentative acetoin production. *Applied and Environmental Microbiology*, 77, 5294-5306.

Stecchini, M., Giavedoni, P., Sarais, I., & Lerici, C.R. (2008). Effect of Maillard reaction products on the growth of selected food‐poisoning micro‐organisms. *Letters in Applied Microbiology*, 13, 93-96.

Stephens, P., Joynson, J., Davies, K., Holbrook, R., Lappin-Scott, H., & Humphrey, T. (2003). The use of an automated growth analyser to measure recovery times of single heat‐injured *Salmonella* cells. *Journal of Applied Microbiology*, 83, 445-455.

Stewart, E. J.; Madden, R.; Paul, G.; Taddei, F. 2005. Aging and death in an organism that reproduces by morphologically symmetric division. *PLoS Biology*. 3, e45.

Stoll, R., & Goebel, W. (2010). The major PEP-phosphotransferase systems (PTSs) for glucose, mannose and cellobiose of *Listeria monocytogenes*, and their significance for extra- and intracellular growth. *Microbiology*, 156, 1069-1083.

Swinnen, I., Bernaerts, K., Dens, E. J., Geeraerd, A. H., & Van Impe, J. (2004). Predictive modelling of the microbial lag phase: a review. *International Journal of Food Microbiology*, 94, 137-159.

Swint-Kruse, L., & Matthews, K.S. (2009). Allostery in the LacI/GalR family: variations on a theme. *Current Opinions in Microbiology*, 12, 129-137.

Tatituri, R.V., Wolf, B.J., Brenner, M.B., Turk, J., & Hsu, F.F. (2015). Characterization of polar lipids of Listeria monocytogenes by HCD and low-energy CAD linear ion-trap mass spectrometry with electrospray ionization. *Analytical and Bioanalytical Chemistry*, 407, 2519-2528.

Trost, M., Wehmhöner, D., Kaŕst, U., Dieterich, G., Wehland, J., & Jaňsch, L. (2005). Comparative proteome analysis of secretory proteins from pathogenic and nonpathogenic *Listeria* species. *Proteomics*, 5, 1544-1557.

Tsai, H. N., & Hodgson, D. A. (2003). Development of a synthetic minimal medium for *Listeria monocytogenes*. *Applied and Environmental Microbiology*, 69, 6943-6945.

Tyedmers, J., Mogk, A., & Bukau, B. (2010). Cellular strategies for controlling protein aggregation. *Nature Reviews Molecular Cell Biology* 11, 777-788.

Tyrrell, E.A. (1973). Autolysis of *Listeria monocytogenes*. *Journal of Bacteriology* 113, 1046-1048.

van den Berg, B., Ellis, R.J., & Dobson, C.M. (1999). Effects of macromolecular crowding on protein folding and aggregation. *EMBO Journal*, 18, 6927-6933.

van der Veen, S., Hain, T., Wouters, J.A., Hossain, H., de Vos, W.M., Abee, T., Chakraborty, T., & Wells-Bennik, M.H. (2007). The heat-shock response of *Listeria monocytogenes* comprises genes involved in heat shock, cell division, cell wall synthesis, and the SOS response. *Microbiology*, 153, 3593-3607.

van der Veen, S., van Schalkwijk, S., Molenaar, D., de Vos, W. M., Abee, T., & Wells-Bennik, M. H. (2010). The SOS response of *Listeria monocytogenes* is involved in stress resistance and mutagenesis. *Microbiology*, 156, 374-84.

Van Schothorst, M., & Van Leusden, F. (1975). Comparison of several methods for the isolation of salmonellae from egg products. *Canadian Journal of Microbiology*, 21(7), 1041-1045.

Varela, C.A., Baez, M.E., & Agosin, E. (2004). Osmotic stress response: quantification of cell maintenance and metabolic fluxes in a lysine-overproducing strain of *Corynebacterium glutamicum*. *Applied and Environmental Microbiology*, 70, 4222-4229.

Vazquez, A., Beg, Q.K., Demenezes, M.A., Ernst, J., Bar-Joseph, Z., Barabási, A.-L., Boros, L.G., & Oltvai, Z.N. (2008). Impact of the solvent capacity constraint on *E. coli* metabolism. *BMC Systems Biology*, 2, 7.

Vivant, A.L., Garmyn, D., Gal, L., Hartmann, A., & Piveteau, P. (2015). Survival of *Listeria monocytogenes* in Soil Requires AgrA-Mediated Regulation. *Applied and Environmental Microbiology*, 81, 5073-5084.

Vivant, A.L., Garmyn, D., Gal, L., & Piveteau, P. 2014. The Agr communication system provides a benefit to the populations of *Listeria monocytogenes* in soil. *Frontiers in Cellular and Infection Microbiology*, 4, 160.

Vogel, C. & Marcotte, E.M. (2012). Insights into the regulation of protein abundance from proteomic and transcriptomic analyses. *Nature Review Genetics*, 13, 227-232.

Wang, P., Robert, L., Pelletier, J.; Dang, W.L., Taddei, F., Wright, A., & Jun, S. (2010). Robust growth of *E. coli*. *Current Biology*, 20, 1099–103.

Wang, C., & Shelef, L. A. (1992). Behavior of *Listeria monocytogenes* and the spoilage microflora in fresh cod fish treated with lysozyme and EDTA. *Food Microbiology*, 9, 207-213.

Watve, M., Parab, S., Jogdand, P., & Keni, S. (2006). Aging may be a conditional strategic choice and not an inevitable outcome for bacteria. *Proceedings of the National Academy of Sciences of the United States of America*, 103, 14831–14835.

Weiss, D.S. (2004). Bacterial cell division and the septal ring. *Molecular Microbiology*, 54, 588-597.

Wen, J., Deng, X., Li, Z., Dudley, E. G., Anantheswaran, R. C., Knabel, S. J., & Zhang, W. (2011). Transcriptomic response of *Listeria monocytogenes* during the transition to the long-term-survival phase. *Applied and Environmental Microbiology*, 77, 5966-5972.

Whiting, R., & Bagi, L. (2002). Modeling the lag phase of *Listeria monocytogenes*. *International Journal of Food Microbiology*, 73, 291-295.

Wiame, E., Lamosa, P., Santos, H., & Van Schaftingen, E. (2005). Identification of glucoselysine-6-phosphate deglycase, an enzyme involved in the metabolism of the fructation product glucoselysine. *Biochemical Journal*, 392, 263-269.

Wilding, E. I., Brown, J. R., Bryant, A. P., Chalker, A. F., Holmes, D. J., Ingraham, K. A., Iordanescu, S., So, C.Y., Rosenberg, M., & Gwynn, M. N. (2000). Identification, evolution, and essentiality of the mevalonate pathway for isopentenyl diphosphate biosynthesis in Gram-positive cocci. *Journal of Bacteriology*, 182, 4319-4327.

Wilson, R., Belluoccio, D., & Bateman, J. F. (2008). Proteomic analysis of cartilage proteins. *Methods*, 45, 22-31.

Witte, C.E., Whiteley, A.T., Burke, T.P., Sauer, J.D., Portnoy, D.A., & Woodward, J.J. (2013). Cyclic di-AMP is critical for Listeria monocytogenes growth, cell wall homeostasis, and establishment of infection. *Mbio*, 4, e00282-13.

Wu, Y., Griffiths, M., & McKellar, R. (2000). A comparison of the Bioscreen method and microscopy for the determination of lag times of individual cells of *Listeria monocytogenes*. *Letters in Applied Microbiology*, 30, 468.

Wuenscher, M.D., Köhler, S., Bubert, A., Gerike, U., & Goebel W. (1993). The *iap* gene of *Listeria monocytogenes* is essential for cell viability, and its gene product, p60, has bacteriolytic activity. *Journal of Bacteriology*, 175, 3491-501.

Yuste, L., Hervás, A.B., Canosa, I., Tobes, R., Jiménez, J.I., Nogales, J., Pérez-Pérez, M.M., Santero, E., Díaz, E., Ramos, J.L., de Lorenzo, V., & Rojo, F. (2006).

Growth phase-dependent expression of the *Pseudomonas putida* KT2440 transcriptional machinery analysed with a genome-wide DNA microarray. *Environmental Microbiology*, 8, 165-177.

Zhang, B., VerBerkmoes , N. C., Langston, M. A., Uberbacher, E., Hettich, R. L., & Samatova, N. F. (2006). Detecting differential and correlated protein expression in label-free shotgun proteomics. *Journal of Proteome Research*, 5, 2909-2918.

Zhang, D. L., Ross, T., & Bowman, J. P. (2010). Physiological aspects of *Listeria monocytogenes* during inactivation accelerated by mild temperatures and otherwise non-growth permissive acidic and hyperosmotic conditions. *International Journal of Food Microbiology*, 141, 177-185.

Zhang, H., Yin, Y., Olman, V., & Xu, Y. (2012). Genomic arrangement of regulons in bacterial genomes. *PLoS One*, 7, e29496.

Zwietering, M., De Wit, J., Cuppers, H., & Van't Riet, K. (1994). Modeling of bacterial growth with shifts in temperature. *Applied and Environmental Microbiology*, 60, 204-213.

Appendices I – Aged cells proteomic data summary

			Protein abundances (average)/standard deviation										Log ratios								
ScottA Loci	Other Loci		Exp	stdev	1_d	stdev	7 d	stdev	14 d	stdev	21 d	stdev	1d/Exp	p	7 d/Exp	p	14 d/Exp	p	21 d/Exp	p	k-means group
EGJ23430	lmo0002	DnaN	5.8	0.8	4.5	1.5	6.4	3.1	4.4	2.7	3.0	3.2	-0.34	0.08786	0.12	0.68252	-0.36	0.26289	-0.84	0.08732	
EGJ23434	lmo0006	GyrB	2.0	0.9	1.6	1.2	2.9	2.0	2.4	1.5	2.5	2.5	-0.26	0.50460	0.42	0.37637	0.19	0.63450	0.25	0.66774	
EGJ23435	lmo0007	GyrA	1.7	1.2	1.9	1.4	3.5	2.4	2.2	2.0	1.1	1.6	0.14	0.77478	0.89	0.13582	0.31	0.60096	-0.48	0.47847	
EGJ23451	lmo0018	BglH	0.7	0.5	2.6	2.8	2.1	2.3	1.5	1.5	0.8	1.0	1.38	0.16808	1.14	0.19302	0.76	0.25256	0.17	0.76892	2
EGJ23460	lmo0027	BglP	4.0	1.8	2.0	1.1	3.7	1.2	3.0	1.7	1.6	2.0	-0.86	0.04522	-0.13	0.68099	-0.39	0.31820	-1.09	0.05594	1
EGJ23485	lmo0044	RpsF	14.9	4.3	12.0	4.2	11.9	3.7	11.4	4.7	6.8	2.9	-0.30	0.26008	-0.32	0.21426	-0.38	0.20327	-1.07	0.00439	
EGJ23486	lmo0045	SsbA	1.7	1.2	1.0	1.6	1.3	0.8	1.2	1.2	1.3	1.1	-0.54	0.43017	-0.27	0.55421	-0.33	0.53865	-0.28	0.58034	
EGJ23487	lmo0046	RpsR	4.2	1.2	5.8	1.9	3.8	1.0	3.6	1.9	2.8	2.3	0.42	0.11379	-0.12	0.56948	-0.21	0.51677	-0.53	0.20930	
EGJ23492	lmo0051	ArgC	0.0	0.0	0.1	0.3	1.2	1.5	0.3	0.5	0.4	0.7	0.34	0.36322	1.77	0.11106	0.67	0.17615	0.85	0.20821	3
EGJ23493	lmo0052	YybT	3.3	0.8	4.4	1.2	4.1	3.1	3.2	2.9	2.5	2.3	0.36	0.10203	0.25	0.59056	-0.04	0.93076	-0.37	0.40434	
EGJ23496	lmo0055	PurA	4.7	2.5	6.5	2.3	7.2	2.3	4.9	2.0	5.6	1.3	0.42	0.22527	0.55	0.10426	0.05	0.88527	0.23	0.45636	
EGJ23521	lmo0078	GhrB	0.7	0.8	2.3	1.3	1.7	1.4	0.6	0.8	0.8	1.0	1.25	0.03149	0.92	0.15540	-0.11	0.85048	0.16	0.79770	2
EGJ23530			1.8	0.4	0.0	0.0	0.0	0.0	0.0	0.0	0.0	0.0	-2.23	0.00012	-2.23	0.00012	-2.23	0.00012	-2.23	0.00012	1
EGJ23534			0.0	0.0	0.2	0.4	0.6	0.6	1.8	2.2	1.3	1.4	0.45	0.36322	1.07	0.07607	2.17	0.10715	1.85	0.06902	4
EGJ23575	lmo2287		0.3	0.5	0.6	1.0	1.2	0.8	1.2	1.6	1.7	0.8	0.39	0.58823	1.03	0.05627	1.07	0.22689	1.40	0.00788	4
EGJ23594	lmo0086		0.2	0.4	0.4	1.0	0.1	0.3	0.6	0.9	1.1	1.9	0.44	0.60804	-0.08	0.87015	0.70	0.34143	1.24	0.29465	4
EGJ23604	lmo0096	MptA	6.5	1.1	15.3	3.3	16.4	8.5	14.2	5.0	14.8	8.6	1.17	0.00080	1.27	0.03566	1.07	0.01173	1.13	0.06359	3
EGJ23606	lmo0098	MptD	4.0	1.5	5.7	3.1	8.4	4.6	10.1	4.7	9.5	3.7	0.46	0.26362	0.99	0.06630	1.24	0.02210	1.16	0.01248	
EGJ23614	lmo0105		0.2	0.4	0.9	0.4	0.2	0.5	0.2	0.5	0.5	0.7	1.01	0.02077	0.04	0.94592	0.08	0.88879	0.62	0.28363	2
EGJ23629	lmo0120		0.2	0.4	0.6	0.7	0.8	0.8	0.4	0.7	0.5	0.7	0.78	0.19911	0.99	0.13105	0.43	0.48871	0.54	0.40995	
EGJ23639	lmo0130		0.0	0.0	1.4	0.9	0.2	0.5	0.5	0.7	0.3	0.4	1.93	0.01330	0.46	0.36322	0.97	0.17840	0.61	0.17500	2
EGJ23641	lmo0132	GuaB	0.7	0.5	0.5	0.9	0.3	0.5	0.2	0.5	0.1	0.4	-0.23	0.69324	-0.53	0.25410	-0.74	0.14348	-0.87	0.07166	
EGJ23643	lmo0134	YjdJ	0.3	0.5	0.9	1.4	0.4	0.7	0.3	0.5	0.3	0.7	0.77	0.37187	0.09	0.87982	-0.10	0.84731	-0.09	0.88971	
EGJ23644	lmo0135	OppA	8.9	2.6	22.8	2.6	16.8	5.5	24.2	8.9	27.1	9.7	1.32	0.00000	0.89	0.01467	1.40	0.00702	1.56	0.00475	4
EGJ23659	lmo0152	DppE	0.0	0.0	2.3	1.8	1.4	0.5	2.2	1.0	1.0	1.0	2.49	0.02788	1.92	0.00064	2.43	0.00272	1.62	0.05466	3
EGJ23666	lmo0159		0.3	0.5	0.3	0.5	0.1	0.3	0.4	0.7	0.7	1.3	-0.02	0.97000	-0.41	0.44130	0.14	0.82557	0.56	0.51104	
EGJ23667	lmo0160		0.2	0.4	0.1	0.4	0.3	0.7	0.2	0.4	0.7	1.0	-0.05	0.91923	0.20	0.76605	-0.03	0.96126	0.83	0.25996	
EGJ23668	lmo0161	RsbRD	0.3	0.5	1.7	1.3	1.0	1.1	0.3	0.4	0.5	0.9	1.38	0.05470	0.85	0.22410	-0.14	0.78375	0.26	0.70775	2
EGJ23677	lmo0170		2.4	0.6	2.1	1.3	3.4	2.2	2.2	1.4	1.4	1.6	-0.15	0.65628	0.43	0.32486	-0.09	0.78429	-0.58	0.21369	
EGJ23680	lmo0177	MetS	8.8	3.5	9.0	8.6	3.9	2.6	4.4	2.5	3.1	2.0	0.03	0.96314	-1.07	0.02160	-0.93	0.03159	-1.35	0.00879	5
EGJ23685	lmo0181	YesO	31.6	2.7	54.8	19.6	36.9	15.8	54.6	28.0	64.4	33.7	0.78	0.03359	0.22	0.45120	0.78	0.10028	1.02	0.06261	4
EGJ23686	lmo0182		30.3	1.4	16.5	10.3	13.8	4.6	6.7	3.3	4.3	5.1	-0.86	0.02124	-1.10	0.00016	-2.10	0.00000	-2.69	0.00003	5
EGJ23687	lmo0183		32.5	1.5	39.6	20.6	31.3	5.0	38.1	15.4	36.0	13.9	0.28	0.43604	-0.05	0.59604	0.23	0.40989	0.15	0.55600	
EGJ23688	lmo0184	TreA	47.8	13.6	12.1	5.7	24.9	8.3	17.0	7.5	7.3	9.8	-1.94	0.00068	-0.93	0.00747	-1.46	0.00136	-2.63	0.00022	1

ScottA Loci	Other Loci		Exp	stdev	1_d	stdev	7 d	stdev	14 d	stdev	21 d	stdev	1d/Exp	p	7 d/Exp	p	14 d/Exp	p	21 d/Exp	p	k-means group
EGJ23689	lmo0185	YabD	0.8	0.8	0.2	0.5	0.1	0.3	0.2	0.5	0.4	0.7	-0.91	0.12776	-1.06	0.08088	-0.90	0.13466	-0.56	0.32150	1
EGJ23692	lmo0188	KsgA	0.2	0.4	0.5	0.9	0.7	0.5	0.2	0.5	0.3	0.7	0.62	0.40292	0.80	0.09853	0.11	0.85258	0.22	0.73439	
EGJ23699	lmo0195	YknZ	0.0	0.0	1.0	1.7	0.1	0.3	0.0	0.0	0.0	0.0	1.63	0.19319	0.34	0.36322	0.00		0.00		2
EGJ23700	lmo0196	SpoVG	4.7	1.4	8.7	5.5	8.6	7.1	5.7	3.5	4.2	3.7	0.82	0.13756	0.81	0.24176	0.26	0.51853	-0.13	0.78880	
EGJ23701	lmo0197	SpoVG	23.0	14.2	16.2	11.0	22.3	17.7	16.1	11.1	16.1	14.6	-0.49	0.37679	-0.04	0.94359	-0.50	0.37537	-0.50	0.42695	
EGJ23702	lmo0198	GlmU	3.0	1.7	6.5	3.0	5.7	2.9	2.8	2.0	1.6	2.2	1.01	0.03517	0.82	0.08255	-0.09	0.83955	-0.74	0.24775	2
EGJ23703	lmo0199	Prs1	4.6	1.4	6.4	2.7	6.6	5.1	5.1	3.8	3.5	4.1	0.46	0.16949	0.50	0.37770	0.15	0.74502	-0.34	0.57210	
EGJ23712	lmo0208	YbjQ	0.2	0.4	2.5	3.0	3.7	3.4	2.9	2.2	2.6	2.8	2.17	0.11321	2.66	0.05017	2.35	0.02929	2.21	0.09151	3
EGJ23714	lmo0210	Ldh	7.2	2.0	28.4	11.4	25.2	5.7	20.6	2.7	23.5	7.8	1.91	0.00559	1.74	0.00029	1.46	0.00000	1.64	0.00298	3
EGJ23715	lmo0211	Ctc	5.9	1.0	23.3	6.6	18.8	9.0	19.9	7.2	17.8	4.9	1.90	0.00120	1.60	0.01695	1.68	0.00468	1.53	0.00159	3
EGJ23718	lmo0214	Mfd	0.2	0.4	1.2	1.3	1.1	1.0	1.0	0.8	0.8	1.0	1.40	0.09752	1.23	0.08257	1.19	0.05531	0.98	0.19155	3
EGJ23719	lmo0215	MurJ	0.3	0.8	0.3	0.5	0.3	0.5	0.7	0.7	0.5	1.0	0.02	0.97756	-0.03	0.96433	0.57	0.36878	0.33	0.69041	
EGJ23722	lmo0218	YabR	3.0	2.2	2.4	2.1	4.0	2.4	2.7	1.0	1.6	2.0	-0.31	0.60322	0.34	0.49288	-0.16	0.72308	-0.75	0.26349	
EGJ23723	lmo0219	TilS	6.7	0.7	2.5	1.7	3.5	2.5	2.0	1.4	2.0	2.4	-1.28	0.00077	-0.83	0.02716	-1.51	0.00016	-1.50	0.00439	1
EGJ23724	lmo0220	FtsH	10.4	2.7	6.1	3.1	8.8	4.0	3.5	2.0	4.6	4.2	-0.72	0.03061	-0.23	0.44360	-1.45	0.00071	-1.10	0.01972	5
EGJ23726	lmo0222	HslO	0.3	0.5	0.4	0.7	1.3	1.3	0.7	0.8	0.8	1.0	0.16	0.79519	1.07	0.15940	0.56	0.35065	0.62	0.35164	3
EGJ23727	lmo0223	CysK	13.5	4.2	31.2	22.6	25.3	9.8	22.8	6.8	15.0	9.9	1.18	0.11420	0.88	0.03003	0.74	0.02026	0.15	0.74296	2
EGJ23730	lmo0224	Sul	0.0	0.0	0.0	0.0	0.7	0.9	1.0	1.2	1.1	1.0	0.00		1.31	0.10783	1.61	0.09210	1.66	0.04159	4
EGJ23733	lmo0227	DusB	1.2	1.0	0.5	0.5	0.1	0.3	0.3	0.7	0.5	0.7	-0.80	0.16450	-1.42	0.05060	-1.11	0.10602	-0.81	0.18794	1
EGJ23734	lmo0228	LysS	7.1	1.5	7.9	3.8	10.1	1.9	7.4	2.3	3.3	3.8	0.15	0.64061	0.49	0.01035	0.05	0.80111	-1.00	0.06028	
EGJ23738	lmo0232	ClpC	2.2	0.7	7.3	6.3	11.6	8.8	7.7	7.7	6.0	8.2	1.55	0.10305	2.18	0.04788	1.62	0.13849	1.29	0.30250	3
EGJ23739	lmo0233	RadA	0.2	0.4	0.2	0.4	0.1	0.3	0.3	0.7	0.3	0.5	-0.04	0.94220	-0.07	0.88813	0.24	0.72404	0.33	0.54977	
EGJ23743	lmo0237	GltX	15.5	3.5	26.9	6.0	23.5	6.1	23.9	3.4	30.3	8.8	0.78	0.00358	0.59	0.02299	0.61	0.00177	0.95	0.00726	
EGJ23745	lmo0239	CysS	0.2	0.4	4.3	3.1	3.2	0.8	2.8	2.0	2.4	1.0	2.84	0.02205	2.47	0.00006	2.33	0.01922	2.11	0.00193	3
EGJ23747	lmo0241	RlmB	0.5	0.8	0.3	0.4	0.8	0.7	0.3	0.5	0.1	0.3	-0.38	0.56731	0.32	0.58233	-0.36	0.58503	-0.67	0.34573	
EGJ23751	lmo0246	NusG	3.5	0.6	2.6	1.3	3.1	2.3	1.8	1.3	2.4	2.1	-0.36	0.16553	-0.16	0.68312	-0.81	0.01857	-0.46	0.26925	
EGJ23753	lmo0248	RplK	33.9	13.3	17.1	5.3	10.7	2.2	7.4	2.4	8.4	3.8	-0.97	0.02548	-1.62	0.00738	-2.13	0.00407	-1.95	0.00432	1
EGJ23754	lmo0249	RplA	72.6	12.1	41.3	21.8	33.0	13.4	29.3	12.9	21.7	14.8	-0.81	0.01562	-1.13	0.00032	-1.29	0.00014	-1.72	0.00008	5
EGJ23755	lmo0250	RplJ	38.6	3.7	16.3	4.8	18.1	4.7	10.2	5.7	18.5	11.1	-1.22	0.00001	-1.07	0.00001	-1.86	0.00000	-1.04	0.00542	1
EGJ23756	lmo0251	RplL	10.6	5.0	37.9	24.2	31.3	23.2	32.4	23.2	30.8	21.4	1.79	0.03875	1.52	0.08120	1.57	0.06927	1.50	0.06852	3
EGJ23757	lmo0256	YbxB	0.5	0.5	0.7	0.5	0.8	0.7	0.2	0.5	0.1	0.3	0.24	0.58106	0.37	0.42129	-0.48	0.37215	-0.66	0.19027	
EGJ23765	lmo0258	RpoB	50.3	13.8	37.3	14.3	33.4	6.9	25.1	10.9	18.5	16.5	-0.43	0.14065	-0.59	0.02998	-0.99	0.00609	-1.42	0.00489	5
EGJ23766	lmo0259	RpoC	30.8	4.5	30.9	10.3	31.7	7.8	25.6	11.0	21.2	14.9	0.00	0.99284	0.04	0.81935	-0.26	0.32267	-0.53	0.18145	
EGJ23768	lmo0261	BglH	0.2	0.4	0.7	1.3	0.3	0.5	1.0	0.6	0.1	0.4	0.82	0.39839	0.28	0.59785	1.17	0.01883	-0.04	0.93205	
EGJ23774	lmo0263	InlH	0.2	0.4	0.2	0.4	0.3	0.5	0.1	0.3	0.4	0.7	-0.04	0.93610	0.27	0.60811	-0.08	0.87064	0.46	0.46781	
EGJ23777	lmo0265	DapE	0.0	0.0	0.6	0.7	2.0	1.9	0.8	1.3	0.8	0.9	1.11	0.10909	2.32	0.04889	1.38	0.20163	1.40	0.07637	3
EGJ23784	lmo0271	BglC	2.4	1.3	7.6	5.4	4.6	2.1	4.0	2.3	2.3	1.3	1.50	0.06323	0.84	0.05595	0.66	0.16275	-0.06	0.87818	2
EGJ23791	lmo0278	MsmX	3.0	1.8	5.9	3.2	11.3	7.8	8.0	3.8	8.5	3.7	0.88	0.08382	1.76	0.04784	1.29	0.02120	1.36	0.01266	3

ScottA Loci	Other Loci		Exp	stdev	1_d	stdev	7 d	stdev	14 d	stdev	21 d	stdev	1d/Exp	p	7 d/Exp	p	14 d/Exp	p	21 d/Exp	p	k-means group
EGJ23792	lmo0279	NrdD	0.8	0.8	0.3	0.7	0.1	0.3	0.1	0.3	0.1	0.3	-0.74	0.23810	-1.06	0.08175	-1.06	0.08165	-1.08	0.07757	1
EGJ23797	lmo0284	MetQ	0.2	0.4	0.5	0.5	1.4	0.6	0.3	0.6	0.6	0.7	0.52	0.30269	1.55	0.00249	0.34	0.54094	0.73	0.22523	
EGJ23798	lmo0285	MetN	1.0	0.6	2.4	1.4	1.3	1.1	1.3	0.5	1.3	0.7	0.93	0.05897	0.23	0.62708	0.25	0.39889	0.25	0.46254	
EGJ23800	lmo0287	WalR	3.8	1.0	4.1	2.4	7.2	2.3	4.4	2.7	3.2	3.8	0.08	0.81458	0.82	0.01463	0.17	0.65486	-0.24	0.69371	
EGJ23805	lmo0292	HtrC	0.8	0.7	5.8	4.0	2.2	2.4	5.7	3.7	4.1	1.0	2.23	0.02962	1.01	0.23527	2.22	0.02127	1.77	0.00010	3
EGJ23818		HsdR	0.2	0.4	0.2	0.4	0.2	0.5	0.2	0.5	0.1	0.4	-0.02	0.96313	0.07	0.90342	0.10	0.86288	-0.03	0.95225	
EGJ23834	lmo0319	BglH	4.6	2.3	1.7	1.5	1.9	0.9	1.2	1.3	0.8	1.3	-1.19	0.03429	-1.06	0.03856	-1.56	0.01547	-1.99	0.00838	1
EGJ23837	lmo0322		0.2	0.4	0.8	0.9	2.8	2.1	2.9	2.3	1.7	1.3	0.91	0.20299	2.30	0.02750	2.32	0.03381	1.70	0.03342	3
EGJ23845			0.2	0.4	0.3	0.4	0.4	0.7	1.2	1.3	1.1	2.0	0.22	0.66814	0.50	0.43838	1.33	0.12870	1.26	0.30261	4
EGJ23846	lmo0333	InlI	0.8	0.8	1.0	0.6	0.5	0.7	0.3	0.7	0.8	0.7	0.17	0.67796	-0.37	0.47035	-0.80	0.19575	-0.04	0.94085	
EGJ23854	lmo0342	Tkt	0.2	0.4	0.3	0.5	0.6	0.5	0.3	0.7	0.3	0.7	0.30	0.56936	0.77	0.10519	0.22	0.73462	0.22	0.73823	
EGJ23856	lmo0344		0.0	0.0	0.0	0.0	0.4	0.6	0.9	1.1	1.2	1.3	0.00		0.79	0.17554	1.50	0.09185	1.77	0.07706	4
EGJ23867	lmo0354	YtcI	0.3	0.5	0.3	0.4	1.9	1.0	0.5	0.7	0.6	0.9	-0.08	0.87141	1.56	0.01083	0.24	0.69442	0.34	0.59778	0
EGJ23868	lmo0355	FrdA	4.6	3.6	15.2	7.0	4.5	4.2	8.8	5.5	14.0	8.8	1.63	0.01195	-0.04	0.95264	0.86	0.15636	1.50	0.04848	4
EGJ23871	lmo0358	FruA	0.5	0.6	0.2	0.5	0.0	0.0	0.0	0.0	1.1	1.2	-0.52	0.34160	-1.01	0.07615	-1.01	0.07615	0.70	0.28480	1
EGJ23877	lmo0369	YeeI	1.5	0.6	1.6	0.4	2.0	1.2	1.3	1.0	1.1	0.9	0.07	0.75272	0.34	0.37176	-0.18	0.63559	-0.36	0.35485	
EGJ23878	lmo0370		1.0	0.9	1.5	1.7	0.2	0.4	0.5	0.8	0.0	0.0	0.41	0.54829	-1.18	0.08385	-0.60	0.32354	-1.60	0.04484	5
EGJ23887	lmo0383	MmsA	0.2	0.4	0.1	0.3	0.4	0.6	0.3	0.7	0.3	0.5	-0.08	0.86821	0.36	0.51411	0.24	0.72354	0.32	0.56568	
EGJ23891	lmo0387	YdhG	0.3	0.5	1.9	1.5	1.8	1.6	1.3	1.2	0.7	1.0	1.51	0.04977	1.49	0.06791	1.10	0.12305	0.47	0.51914	3
EGJ23896	lmo0392	YqfA	7.4	2.1	20.9	9.7	28.9	12.7	21.8	7.7	19.0	17.1	1.44	0.01821	1.90	0.00824	1.51	0.00488	1.31	0.15733	3
EGJ23912	lmo0401		0.0	0.0	1.9	1.8	3.7	3.8	1.6	2.4	0.1	0.3	2.29	0.04322	3.08	0.06183	2.07	0.15819	0.35	0.36322	3
EGJ23917	lmo0406	YyaH	0.0	0.0	1.0	0.7	0.9	0.9	0.0	0.0	0.2	0.5	1.62	0.01627	1.46	0.05361	0.00		0.49	0.36322	2
EGJ23926	lmo0415	YjeA	0.2	0.4	0.5	0.8	0.2	0.4	0.2	0.5	0.4	0.7	0.55	0.41191	0.01	0.98594	0.09	0.87704	0.44	0.48316	
EGJ23935	lmo0427	FruA	0.2	0.4	0.7	1.0	0.3	0.8	0.6	0.6	0.4	1.0	0.89	0.22535	0.34	0.65803	0.66	0.24177	0.44	0.60430	
EGJ23936	lmo0428	ManP	0.5	0.6	0.2	0.4	0.3	0.4	0.1	0.3	0.1	0.3	-0.63	0.22365	-0.39	0.42120	-0.67	0.19253	-0.67	0.19769	
EGJ23942			0.3	0.5	0.9	1.0	0.2	0.5	0.4	0.7	0.3	0.4	0.75	0.24332	-0.28	0.60889	0.14	0.80889	-0.11	0.82784	
EGJ23959	lmo0434	InlB	0.0	0.0	2.0	1.5	1.8	1.9	6.2	4.9	9.1	7.5	2.32	0.02417	2.21	0.06610	3.74	0.02734	4.27	0.03038	4
EGJ23967	lmo0443	LytR	0.3	0.8	1.1	0.8	0.0	0.0	0.4	0.6	0.8	2.0	0.97	0.10905	-0.72	0.36322	0.16	0.82327	0.67	0.59374	
EGJ23971	lmo0451		0.0	0.0	0.0	0.0	1.1	1.5	0.4	0.6	0.0	0.0	0.00		1.70	0.11649	0.88	0.17470	0.00		0
EGJ23978	lmo0458		0.0	0.0	0.0	0.0	0.2	0.5	0.0	0.0	1.2	1.2	0.00		0.46	0.36322	0.00		1.73	0.06454	4
EGJ23996	lmo0481		0.2	0.4	1.1	1.2	1.1	1.3	0.3	0.5	0.7	1.0	1.31	0.11787	1.25	0.14581	0.35	0.52488	0.80	0.31576	3
EGJ23999	lmo0484	YetG	1.2	0.7	0.0	0.0	0.0	0.0	0.0	0.0	0.0	0.0	-1.74	0.01189	-1.74	0.01189	-1.74	0.01189	-1.74	0.01189	1
EGJ24005	lmo0487		0.0	0.0	2.5	3.1	0.9	1.7	0.6	0.5	0.3	0.6	2.61	0.10311	1.53	0.22228	1.19	0.03016	0.59	0.36322	2
EGJ24008	lmo0490	AroE	0.5	0.6	0.8	0.6	0.7	0.6	0.6	0.7	0.3	0.4	0.34	0.45481	0.26	0.56779	0.07	0.89133	-0.40	0.40908	
EGJ24009	lmo0491	AroD	0.0	0.0	1.6	1.6	0.7	0.6	0.8	0.7	0.7	0.8	2.09	0.05043	1.27	0.03788	1.34	0.04091	1.22	0.09470	3
EGJ24012	lmo0494		0.3	0.5	0.4	0.7	0.5	1.0	0.3	0.5	0.1	0.3	0.13	0.82187	0.33	0.65159	-0.06	0.90353	-0.40	0.43210	
EGJ24026	lmo0509	Prs2	2.2	0.7	0.7	0.8	0.3	0.4	0.4	0.5	0.3	0.4	-1.10	0.01129	-1.80	0.00062	-1.53	0.00105	-1.81	0.00062	1
EGJ24029	lmo0512		0.2	0.4	1.8	1.3	0.7	0.5	0.7	0.8	0.6	0.7	1.77	0.02498	0.84	0.08738	0.87	0.17341	0.73	0.22375	2

ScottA Loci	Other Loci		Exp	stdev	1_d	stdev	7 d	stdev	14 d	stdev	21 d	stdev	1d/Exp	p	7 d/Exp	p	14 d/Exp	p	21 d/Exp	p	k-means group
EGJ24032	lmo0515	YxiE	0.0	0.0	1.6	1.1	1.2	1.4	0.1	0.3	0.3	0.4	2.10	0.01682	1.76	0.08959	0.34	0.36322	0.61	0.17500	2
EGJ24038	lmo0521	LicH	1.9	1.1	4.9	3.9	4.4	1.9	2.0	1.1	1.7	1.6	1.20	0.11476	1.06	0.01901	0.10	0.80163	-0.08	0.87520	2
EGJ24050	lmo0534		1.2	0.7	2.2	1.1	3.9	3.6	1.5	1.7	2.1	0.7	0.68	0.10505	1.40	0.12875	0.25	0.68369	0.66	0.05053	
EGJ24052	lmo0536	LicH	5.9	1.9	3.2	2.5	3.9	2.3	3.0	1.8	2.9	2.0	-0.78	0.06526	-0.53	0.14143	-0.85	0.02357	-0.91	0.02449	
EGJ24055	lmo0539		30.7	7.6	43.7	8.5	30.3	9.1	29.9	6.3	30.6	5.7	0.51	0.01898	-0.02	0.93498	-0.03	0.85898	0.00	0.99250	
EGJ24057	lmo0541	FhuD	3.6	5.5	0.0	0.0	0.0	0.0	0.1	0.3	0.1	0.3	-3.04	0.16853	-3.04	0.16853	-2.70	0.18218	-2.71	0.18153	1
EGJ24069	lmo0553		1.2	1.0	3.1	1.2	5.8	2.2	3.7	4.0	3.6	3.3	1.12	0.01332	1.93	0.00199	1.35	0.17878	1.31	0.13047	3
EGJ24070	lmo0554	YugJ	1.5	0.9	6.8	4.5	4.3	1.8	2.5	1.9	1.6	2.1	1.85	0.03325	1.24	0.01237	0.58	0.28353	0.05	0.93861	2
EGJ24074	lmo0558	Pgl	7.9	1.2	13.4	5.2	10.8	6.2	6.6	5.3	5.3	5.9	0.73	0.04833	0.43	0.30549	-0.23	0.60136	-0.53	0.33714	
EGJ24076	lmo0560	RocG	136.4	37.5	124.2	30.0	137.9	65.5	358.9	130.2	490.4	241.7	-0.14	0.54662	0.02	0.96313	1.39	0.00739	1.84	0.01524	4
EGJ24098	lmo0582	Iap	0.9	1.4	2.3	2.0	3.6	3.3	12.7	7.1	18.8	12.5	1.05	0.17393	1.57	0.10924	3.28	0.00861	3.82	0.01702	4
EGJ24108	lmo0592		1.9	0.4	3.7	1.7	8.1	2.6	5.6	1.6	4.2	1.1	0.84	0.04286	1.87	0.00162	1.39	0.00163	1.00	0.00251	3
EGJ24125	lmo0609	YtwF	2.0	1.1	0.0	0.0	0.0	0.0	0.0	0.0	0.1	0.3	-2.33	0.00667	-2.33	0.00667	-2.33	0.00667	-1.98	0.00755	1
EGJ24129	lmo0613	YogA	2.2	2.0	1.7	1.1	1.6	1.0	1.4	1.5	0.6	0.9	-0.28	0.61823	-0.39	0.49200	-0.49	0.45581	-1.35	0.10156	5
EGJ24156	lmo0640	YcsN	1.4	0.6	5.4	2.8	4.8	2.2	4.8	3.5	6.3	4.7	1.68	0.01474	1.51	0.01023	1.52	0.06121	1.87	0.05047	3
EGJ24157	lmo0641	ZosA	0.0	0.0	3.5	1.9	3.5	2.9	2.4	2.6	3.6	2.4	3.01	0.00674	3.01	0.02957	2.54	0.07563	3.03	0.01469	3
EGJ24169	lmo0653		1.0	0.0	1.4	0.3	0.7	0.8	1.4	0.7	0.4	0.7	0.35	0.02552	-0.36	0.34921	0.30	0.27771	-0.71	0.09351	
EGJ24170	lmo0654		0.2	0.4	5.1	3.0	2.0	1.1	4.2	2.1	6.3	3.5	3.08	0.00916	1.89	0.01022	2.83	0.00506	3.35	0.00737	3
EGJ24181	lmo0662	ThiD	5.2	1.9	6.6	4.9	4.9	2.0	2.1	2.0	1.3	1.4	0.31	0.54642	-0.10	0.75412	-1.13	0.01999	-1.65	0.00313	5
EGJ24182	lmo0663	YwpJ	0.0	0.0	1.0	1.2	0.9	1.3	0.3	0.4	0.3	0.4	1.60	0.09523	1.53	0.13288	0.62	0.17472	0.61	0.17500	2
EGJ24189	lmo0669	YhxD	0.4	0.5	0.6	0.8	0.3	0.4	0.8	1.0	0.6	0.5	0.42	0.47636	-0.15	0.77473	0.58	0.38472	0.39	0.40157	
EGJ24193	lmo0673		0.0	0.0	0.2	0.4	0.0	0.0	1.0	0.6	1.2	0.4	0.38	0.36322	0.00		1.58	0.00871	1.72	0.00079	4
EGJ24194	lmo0674		0.3	0.5	0.3	0.5	0.3	0.5	0.5	0.8	0.3	0.4	-0.01	0.99147	-0.03	0.96036	0.19	0.77094	-0.13	0.79282	
EGJ24210	lmo0690	Hag	0.7	0.8	22.6	27.2	5.1	6.6	6.2	6.8	10.0	11.2	4.30	0.10530	2.24	0.16308	2.51	0.10320	3.16	0.09755	3
EGJ24227	lmo0707	FliD	1.7	1.4	0.5	0.8	0.2	0.5	0.6	1.0	0.9	1.5	-1.18	0.10013	-1.68	0.04679	-1.06	0.14128	-0.68	0.35120	1
EGJ24232	lmo0713	FliF	0.2	0.4	0.2	0.4	0.6	0.7	0.2	0.4	0.3	0.7	0.00	0.99453	0.75	0.21603	-0.05	0.92575	0.18	0.79021	
EGJ24241	lmo0722	YdaP	0.8	0.8	6.1	2.2	9.4	4.7	7.9	2.6	7.6	4.4	2.31	0.00137	2.89	0.00597	2.65	0.00069	2.60	0.01294	3
EGJ24245	lmo0727	GlmS	9.3	1.5	4.4	3.2	5.8	2.7	5.8	3.3	3.5	4.3	-1.02	0.00976	-0.64	0.02476	-0.65	0.04851	-1.31	0.01816	1
EGJ24273	lmo0773	YhfP	0.8	0.4	0.2	0.4	1.1	1.7	0.3	0.5	0.4	0.7	-0.96	0.02643	0.25	0.74647	-0.65	0.11780	-0.57	0.21235	
EGJ24274	lmo0774	YerQ	0.7	1.2	3.0	1.0	4.0	1.1	2.0	1.2	1.6	1.5	1.56	0.00527	1.94	0.00055	1.11	0.08327	0.84	0.26029	3
EGJ24280	lmo0781	MpoA	0.0	0.0	0.4	0.6	0.9	0.9	1.1	1.0	0.1	0.4	0.79	0.17469	1.46	0.05425	1.65	0.04387	0.37	0.36322	3
EGJ24282	lmo0783	MpoC	1.0	0.0	2.6	1.7	4.2	2.7	1.8	1.2	1.8	2.0	1.04	0.07218	1.64	0.03668	0.63	0.15609	0.58	0.40627	3
EGJ24285	lmo0786	YvaB	0.8	0.8	2.0	2.1	3.9	2.7	2.3	2.2	2.2	2.9	0.93	0.23569	1.71	0.04073	1.10	0.15711	1.04	0.29897	3
EGJ24287	lmo0788		0.5	0.5	1.1	1.3	0.8	1.0	0.7	0.8	0.9	1.3	0.66	0.36505	0.40	0.50687	0.26	0.63811	0.53	0.46133	
EGJ24291	lmo0791		2.5	0.8	1.7	1.1	1.1	0.6	1.7	1.0	2.3	1.6	-0.45	0.19008	-0.87	0.01019	-0.46	0.16399	-0.11	0.78219	
EGJ24296	lmo0796	YceI	0.2	0.4	7.8	6.0	5.4	3.7	4.4	4.5	1.6	0.9	3.60	0.02678	3.12	0.01727	2.86	0.06930	1.60	0.01055	3
EGJ24310	lmo0811	Cah	2.7	1.1	0.3	0.5	0.5	0.7	0.2	0.4	0.0	0.0	-1.94	0.00238	-1.63	0.00382	-2.29	0.00193	-2.68	0.00214	1
EGJ24312	lmo0813	GmuE	14.7	2.4	30.0	22.8	18.9	4.2	15.1	4.4	9.2	5.9	1.01	0.16045	0.35	0.07003	0.03	0.86235	-0.65	0.07216	2

ScottA Loci	Other Loci		Exp	stdev	1_d	stdev	7 d	stdev	14 d	stdev	21 d	stdev	1d/Exp	p	7 d/Exp	p	14 d/Exp	p	21 d/Exp	p	k-means group
EGJ24313	lmo0814		0.3	0.8	2.1	2.1	1.9	0.5	1.1	0.6	0.8	1.0	1.66	0.10201	1.52	0.00340	0.99	0.07716	0.67	0.37593	3
EGJ24325	lmo0823	YvgN	0.2	0.4	0.9	0.8	0.3	0.5	0.4	0.6	0.3	0.7	1.05	0.09971	0.29	0.58560	0.37	0.51421	0.20	0.76008	2
EGJ24329	lmo0829	YdbK	0.0	0.0	0.7	0.6	0.0	0.0	0.2	0.5	1.2	0.9	1.31	0.03376	0.00		0.50	0.36322	1.77	0.01798	4
EGJ24330	lmo0830	Fbp	0.0	0.0	0.2	0.4	0.1	0.3	0.0	0.0	1.3	1.3	0.45	0.36322	0.35	0.36322	0.00		1.88	0.05545	4
EGJ24342	lmo0841	YloB	0.2	0.4	0.5	0.6	0.5	0.8	0.9	1.4	0.3	0.4	0.60	0.25838	0.55	0.43953	1.10	0.23874	0.19	0.69259	3
EGJ24345	lmo0844	YabJ	0.0	0.0	0.6	1.0	1.3	1.3	3.2	3.5	4.8	3.9	1.12	0.21099	1.81	0.07090	2.89	0.07511	3.41	0.03014	4
EGJ24357	lmo0855	Ddl	1.5	0.8	1.5	1.4	1.9	0.8	1.4	1.2	0.4	0.5	-0.01	0.97697	0.28	0.39289	-0.09	0.83965	-1.14	0.02398	5
EGJ24368	lmo0866	CshA	31.6	3.5	14.9	6.4	20.0	10.6	13.2	11.8	9.5	12.4	-1.06	0.00056	-0.65	0.04323	-1.23	0.01063	-1.68	0.00617	1
EGJ24382	lmo0880		1.0	1.5	0.6	1.1	0.4	0.7	0.3	0.7	0.4	0.6	-0.47	0.59547	-0.65	0.45359	-0.94	0.32512	-0.80	0.36902	
EGJ24391	lmo0889	RsbR	0.0	0.0	2.2	1.5	2.7	1.9	2.5	2.1	1.3	0.4	2.46	0.01477	2.67	0.01659	2.59	0.03090	1.84	0.00048	3
EGJ24396	lmo0894	RsbW	2.7	0.5	3.3	1.6	5.0	1.5	3.7	2.2	2.7	3.3	0.26	0.38958	0.79	0.01124	0.42	0.28664	0.00	0.99886	
EGJ24400	lmo0898	YdcI	0.7	0.8	1.0	1.3	2.1	2.0	1.8	1.1	0.9	1.0	0.35	0.62045	1.11	0.16889	0.94	0.07728	0.19	0.75483	3
EGJ24407	lmo0903	OhrB	2.2	0.8	4.0	4.7	5.3	6.7	12.7	15.0	13.0	17.5	0.75	0.38368	1.09	0.31616	2.29	0.14889	2.32	0.19226	4
EGJ24410	lmo0906		1.7	0.5	2.1	1.4	2.1	2.1	3.7	2.2	1.4	1.2	0.25	0.52555	0.28	0.62159	0.94	0.08156	-0.21	0.60668	
EGJ24411	lmo0907		1.5	0.6	4.6	2.7	3.0	2.1	3.8	1.5	3.2	1.0	1.34	0.03809	0.81	0.13580	1.11	0.00942	0.87	0.00617	3
EGJ24417	lmo0913	GabD	0.3	0.5	0.3	0.5	0.6	1.0	0.9	0.8	1.2	1.4	-0.01	0.98003	0.33	0.64275	0.78	0.16830	0.99	0.21761	
EGJ24430	lmo0927	LtaSA	0.2	0.4	0.2	0.5	0.1	0.3	1.9	1.2	1.5	1.2	0.07	0.89536	-0.07	0.88224	1.83	0.01589	1.55	0.04457	4
EGJ24432	lmo0929	SrtA	0.3	0.5	0.6	0.7	1.3	1.2	1.0	0.9	0.7	0.7	0.40	0.46814	1.09	0.13614	0.81	0.18342	0.59	0.24674	3
EGJ24433	lmo0930	YhfI	0.2	0.4	0.8	0.7	0.6	0.5	0.5	0.8	0.2	0.5	1.01	0.06669	0.77	0.10591	0.59	0.37859	0.09	0.87500	2
EGJ24434	lmo0931	YhfJ	4.0	1.0	2.4	3.6	3.4	2.5	1.4	2.2	1.2	1.6	-0.61	0.35479	-0.21	0.59700	-1.23	0.03299	-1.40	0.00543	5
EGJ24438	lmo0935	CspR	0.2	0.4	1.1	1.4	0.7	0.9	0.2	0.5	0.3	0.7	1.31	0.15926	0.91	0.19782	0.11	0.85258	0.22	0.73439	2
EGJ24445	lmo0943	Dps	8.3	3.7	36.0	6.9	37.2	16.6	93.3	34.1	143.2	78.9	2.05	0.00003	2.09	0.00719	3.41	0.00161	4.03	0.00856	4
EGJ24457	lmo0955	LiaH	0.5	0.5	1.9	1.5	5.2	1.8	5.4	1.1	3.5	1.3	1.29	0.06895	2.54	0.00094	2.57	0.00002	2.02	0.00128	3
EGJ24458	lmo0956	NagA	2.4	1.7	8.5	4.9	10.1	7.1	13.9	8.8	15.1	9.2	1.64	0.02645	1.88	0.04369	2.31	0.02291	2.43	0.01899	4
EGJ24459	lmo0957	NagB	0.0	0.0	2.6	3.2	0.7	0.5	0.3	0.7	0.0	0.0	2.63	0.10529	1.25	0.02722	0.66	0.36322	0.00		2
EGJ24462	lmo0960	YrrN	0.2	0.4	0.5	0.5	0.4	0.7	0.4	0.7	0.4	0.7	0.52	0.30235	0.44	0.48560	0.47	0.46718	0.43	0.49401	
EGJ24464	lmo0962		0.8	0.4	2.3	2.9	4.9	4.3	2.3	2.2	2.7	3.2	1.06	0.27040	2.02	0.06727	1.09	0.15265	1.25	0.22114	3
EGJ24472	lmo0970	FabI	21.1	4.3	11.6	2.2	10.5	2.2	8.9	3.0	8.1	3.3	-0.84	0.00169	-0.98	0.00090	-1.20	0.00032	-1.33	0.00021	1
EGJ24476	lmo0974	DltA	1.3	1.4	0.0	0.0	0.2	0.4	0.0	0.0	0.0	0.0	-1.87	0.06525	-1.45	0.09817	-1.87	0.06525	-1.87	0.06525	1
EGJ24481	lmo0978	YwaA	6.9	1.5	7.4	2.9	10.0	2.5	5.8	3.3	3.2	2.4	0.09	0.72319	0.51	0.02742	-0.23	0.48623	-0.98	0.01375	
EGJ24485	lmo0982	YhfE	1.9	1.0	1.7	1.4	1.4	1.7	1.1	1.2	1.0	1.1	-0.10	0.82351	-0.35	0.54653	-0.54	0.29031	-0.69	0.17063	
EGJ24486	lmo0983	BsaA	0.2	0.4	0.3	0.4	1.2	1.0	0.3	0.5	0.3	0.4	0.22	0.66814	1.35	0.05827	0.33	0.54967	0.23	0.65230	
EGJ24505	lmo1002	PtsH	164.0	36.4	221.2	45.7	118.0	29.1	95.1	35.5	83.6	72.6	0.43	0.03875	-0.47	0.03747	-0.78	0.00784	-0.97	0.04412	
EGJ24506	lmo1003	PtsI	64.4	20.1	42.6	11.4	41.1	10.1	31.9	13.4	25.6	17.4	-0.59	0.04987	-0.64	0.03681	-1.00	0.00969	-1.31	0.00519	5
EGJ24511	lmo1008	YkuJ	0.2	0.4	0.7	1.0	1.3	0.7	0.9	0.9	0.7	0.8	0.87	0.23896	1.46	0.00866	1.02	0.14639	0.82	0.19916	3
EGJ24514	lmo1011	DapH	7.6	2.3	6.6	2.3	4.5	2.3	2.7	1.7	2.5	2.8	-0.20	0.45669	-0.70	0.04392	-1.35	0.00233	-1.44	0.00697	5
EGJ24515	lmo1012	DapL	2.7	0.6	0.7	0.5	0.7	0.8	1.1	0.6	0.9	1.0	-1.45	0.00009	-1.44	0.00068	-1.03	0.00090	-1.16	0.00696	1
ScottA	Other		Exp	stdev	1_d	stdev	7 d	stdev	14 d	stdev	21 d	stdev	1d/Exp	p	7	p	14	p	21	p	k-

Loci	Loci														d/Exp		d/Exp		d/Exp		means group
EGJ24518	lmo1014	GbuA	2.0	1.3	0.8	0.7	0.8	0.7	0.4	0.5	0.5	0.8	-1.00	0.06971	-0.99	0.07141	-1.44	0.02872	-1.29	0.04295	1
EGJ24521	lmo1017	YpqE	0.0	0.0	0.6	0.7	1.2	1.3	0.6	0.7	0.8	0.9	1.11	0.10909	1.78	0.07561	1.08	0.09533	1.40	0.07637	3
EGJ24531	lmo1027	RnjA	3.0	1.0	2.6	2.1	2.1	1.3	1.3	1.1	0.7	1.0	-0.18	0.67346	-0.47	0.16164	-0.95	0.01819	-1.61	0.00204	5
EGJ24532	lmo1028	YkzG	2.4	1.1	3.1	1.4	5.3	2.4	2.5	1.6	0.9	1.4	0.32	0.35859	1.02	0.02753	0.08	0.83837	-1.01	0.08043	0
EGJ24533	lmo1029	YkrA	0.0	0.0	0.9	0.8	1.3	1.5	0.4	0.5	0.7	1.1	1.47	0.03433	1.89	0.08037	0.89	0.07685	1.22	0.18884	3
EGJ24555	lmo1051	Def	0.8	0.7	3.2	1.4	1.4	0.8	1.7	1.1	3.2	2.2	1.48	0.00649	0.49	0.24420	0.73	0.13855	1.50	0.04162	4
EGJ24556	lmo1052	PdhA	54.0	6.5	26.0	2.9	26.1	6.7	20.7	5.8	17.1	3.9	-1.04	0.00003	-1.03	0.00003	-1.36	0.00000	-1.63	0.00000	1
EGJ24557	lmo1053	PdhB	54.7	10.5	23.1	5.1	24.1	6.2	23.6	4.2	21.6	4.3	-1.22	0.00025	-1.17	0.00025	-1.19	0.00036	-1.32	0.00024	1
EGJ24558	lmo1054	PdhC	49.4	19.5	16.0	6.5	22.0	7.0	17.9	7.3	15.4	8.5	-1.59	0.00699	-1.15	0.01642	-1.44	0.00889	-1.65	0.00597	1
EGJ24559	lmo1055	PdhD	85.9	4.9	23.4	7.4	22.0	4.3	28.8	11.6	27.8	7.6	-1.86	0.00000	-1.94	0.00000	-1.56	0.00001	-1.61	0.00000	1
EGJ24563	lmo1059		4.9	1.1	6.1	2.2	4.0	1.7	2.7	1.4	1.6	1.0	0.31	0.24163	-0.27	0.31234	-0.76	0.01365	-1.34	0.00030	5
EGJ24565	lmo1065	YktB	0.3	0.5	0.9	1.3	0.5	0.5	0.1	0.3	0.3	0.6	0.73	0.36373	0.22	0.66054	-0.39	0.45043	-0.13	0.82668	
EGJ24567	lmo1067	BipA	7.5	3.7	1.4	1.5	3.4	1.3	2.7	1.8	1.3	1.8	-2.10	0.00819	-1.02	0.04497	-1.32	0.02450	-2.12	0.00789	1
EGJ24568	lmo1068		1.7	1.2	4.2	1.2	1.2	1.2	2.8	1.7	3.4	2.3	1.13	0.00372	-0.35	0.51698	0.62	0.19487	0.84	0.14759	4
EGJ24571	lmo1072	PycA	10.6	3.1	21.8	8.3	21.8	5.5	24.2	4.7	23.3	8.5	1.00	0.01959	1.00	0.00259	1.15	0.00025	1.09	0.01347	3
EGJ24573	lmo1073	YvrC	0.0	0.0	1.1	1.7	0.2	0.4	0.4	1.0	0.5	1.3	1.69	0.16825	0.43	0.36322	0.87	0.36322	1.06	0.36322	3
EGJ24576	lmo1076	LytG	0.3	0.5	2.0	2.4	3.6	2.6	11.6	10.5	9.8	7.8	1.59	0.15265	2.28	0.02845	3.85	0.04612	3.63	0.03108	4
EGJ24582	lmo1078	GtaB	8.0	1.8	9.0	5.0	12.8	3.0	7.5	2.5	4.1	5.5	0.16	0.66231	0.65	0.00862	-0.09	0.68336	-0.88	0.15231	
EGJ24583	lmo1086	TarI	1.9	0.8	5.0	4.0	3.8	0.8	2.5	1.7	0.9	1.0	1.21	0.11926	0.85	0.00227	0.35	0.42732	-0.80	0.08942	2
EGJ24584	lmo1087	TarJ	0.8	0.7	1.8	1.7	3.6	1.1	1.8	1.5	1.3	2.1	0.77	0.25414	1.64	0.00051	0.80	0.18273	0.45	0.60937	3
EGJ24589	lmo1092	YueK	0.3	0.5	2.0	1.7	1.3	0.9	0.7	1.1	0.8	1.2	1.62	0.05165	1.15	0.04185	0.50	0.49795	0.64	0.42168	2
EGJ24590	lmo1093	NadE	2.7	0.8	3.0	2.8	3.6	3.5	1.3	0.8	2.3	2.4	0.15	0.77302	0.35	0.57326	-0.80	0.01695	-0.16	0.76208	
EGJ24591	lmo1094		0.0	0.0	0.0	0.0	0.4	0.6	1.0	1.2	1.1	1.5	0.00		0.79	0.17554	1.56	0.11090	1.72	0.11260	4
EGJ24593	lmo1096	GuaA	33.9	1.9	29.1	5.6	28.2	11.1	27.4	9.7	17.7	6.3	-0.21	0.09605	-0.26	0.27337	-0.30	0.16640	-0.92	0.00103	
EGJ24594		YeeA	0.2	0.4	0.2	0.4	0.3	0.5	0.3	0.5	0.4	0.6	-0.02	0.96313	0.31	0.55564	0.35	0.52488	0.36	0.51158	
EGJ24620	lmo1138	ClpP	1.7	0.9	14.7	3.6	17.2	2.5	21.8	6.1	18.1	5.1	2.79	0.00019	3.01	0.00001	3.34	0.00041	3.08	0.00042	3
EGJ24637	lmo1156	PduG	0.3	0.5	0.9	0.8	1.3	1.1	0.5	0.8	0.9	0.8	0.76	0.17421	1.07	0.10267	0.30	0.63841	0.78	0.15349	
EGJ24697	lmo1217	YsdC	8.5	3.0	6.1	3.4	10.0	6.3	12.4	5.3	21.3	21.7	-0.44	0.22810	0.23	0.60665	0.52	0.15449	1.27	0.21094	4
EGJ24698	lmo1218	YsgA	0.3	0.5	0.4	0.6	0.5	0.6	0.1	0.3	0.1	0.4	0.07	0.90454	0.27	0.58908	-0.38	0.46099	-0.35	0.49821	
EGJ24701	lmo1221	PheS	0.7	0.8	1.9	1.4	1.9	1.2	1.3	0.4	1.9	0.9	1.03	0.09803	1.04	0.06322	0.60	0.14670	1.07	0.03188	3
EGJ24702	lmo1222	PheT	1.0	1.2	4.7	4.5	5.8	2.3	3.4	2.5	2.2	0.8	1.82	0.09717	2.09	0.00229	1.39	0.07308	0.84	0.08433	3
EGJ24706	lmo1226	YdhG	0.2	0.4	0.5	0.9	0.3	0.5	0.4	1.0	0.3	0.7	0.55	0.46047	0.25	0.64406	0.40	0.63295	0.22	0.74873	
EGJ24712	lmo1232	MutSB	0.2	0.4	0.2	0.4	0.5	0.7	0.3	0.5	0.1	0.3	0.03	0.95259	0.64	0.27397	0.34	0.54393	-0.09	0.85279	
EGJ24713	lmo1233	TrxA	2.7	0.6	5.5	3.1	3.0	1.1	2.7	1.8	4.2	2.3	0.90	0.07879	0.14	0.54509	0.02	0.96473	0.56	0.17623	
EGJ24716	lmo1236	YslB	0.7	0.5	1.1	1.8	0.7	0.8	0.7	1.1	1.0	1.1	0.48	0.55907	0.06	0.90431	0.06	0.92323	0.32	0.57284	
EGJ24718	lmo1237	RacE	0.2	0.4	0.6	0.5	0.1	0.3	0.3	0.7	0.4	0.7	0.78	0.10858	-0.08	0.87636	0.21	0.75632	0.43	0.49681	
EGJ24719	lmo1238	Rph	0.0	0.0	0.5	0.6	1.3	1.1	0.7	0.6	0.1	0.3	1.02	0.08215	1.86	0.03259	1.25	0.03148	0.33	0.36322	3
EGJ24721	lmo1240	YsnB	0.3	0.5	1.6	1.3	1.8	0.8	0.4	0.7	0.0	0.0	1.30	0.07784	1.46	0.00398	0.09	0.88022	-0.76	0.17508	2
ScottA	**Other**		**Exp**	**stdev**	**1_d**	**stdev**	**7 d**	**stdev**	**14 d**	**stdev**	**21 d**	**stdev**	**1d/Exp**	**p**	**7**	**p**	**14**	**p**	**21**	**p**	**k-**

Loci	Loci														d/Exp		d/Exp		d/Exp		means group
EGJ24725			0.0	0.0	0.2	0.5	1.1	1.2	0.6	1.1	0.1	0.4	0.49	0.36322	1.68	0.07607	1.17	0.20392	0.37	0.36322	3
EGJ24765			0.2	0.4	1.5	1.7	0.9	0.9	0.9	0.9	0.4	0.5	1.56	0.11797	1.03	0.11917	1.05	0.12109	0.42	0.39305	2
EGJ24781	lmo1241		0.0	0.0	5.8	4.6	1.7	1.4	1.3	0.9	2.7	1.4	3.65	0.02643	2.17	0.02898	1.86	0.01292	2.67	0.00565	3
EGJ24795	lmo1254	TreA	6.9	1.7	10.3	7.2	12.2	3.5	6.4	3.3	3.5	3.0	0.55	0.30512	0.78	0.01131	-0.10	0.75217	-0.89	0.04338	
EGJ24796	lmo1255	TreP	9.2	1.9	3.4	2.6	3.8	0.6	3.1	2.1	1.4	1.6	-1.32	0.00170	-1.16	0.00066	-1.44	0.00037	-2.39	0.00002	5
EGJ24798	lmo1257		1.5	1.2	4.2	2.8	4.1	1.6	3.5	2.0	3.4	3.0	1.24	0.06545	1.22	0.01049	1.01	0.06306	0.98	0.18678	3
EGJ24800	lmo1259	ProA	1.7	0.8	2.9	2.6	4.5	2.5	3.3	2.4	3.0	3.0	0.64	0.31763	1.20	0.03773	0.82	0.15945	0.68	0.34123	3
EGJ24801	lmo1260	ProJ	0.2	0.4	0.7	0.6	0.7	0.5	0.1	0.3	0.3	0.4	0.85	0.09254	0.83	0.09426	-0.08	0.87712	0.19	0.69181	
EGJ24802	lmo1261		0.0	0.0	0.3	0.5	1.3	0.8	0.8	1.0	0.8	0.7	0.73	0.17796	1.83	0.00911	1.40	0.11236	1.40	0.04044	3
EGJ24807	lmo1267	Tig	46.9	9.4	25.5	18.2	29.4	18.6	26.8	13.6	18.7	16.7	-0.86	0.03586	-0.67	0.07710	-0.79	0.01587	-1.31	0.00712	1
EGJ24808	lmo1268	ClpX	2.0	0.9	3.3	2.9	5.1	2.8	3.3	1.6	2.2	2.6	0.63	0.32156	1.17	0.03962	0.60	0.13017	0.12	0.85456	3
EGJ24815	lmo1275	TopA	2.4	0.9	2.6	2.0	1.7	1.6	1.2	1.2	0.8	0.9	0.13	0.76927	-0.40	0.37569	-0.78	0.07961	-1.12	0.01375	5
EGJ24816	lmo1276	Gid	1.0	1.1	4.2	2.6	4.2	2.3	1.9	1.6	1.8	0.8	1.64	0.03038	1.65	0.01891	0.66	0.30315	0.63	0.17751	2
EGJ24818	lmo1278	ClpQ	12.7	3.8	2.6	2.4	4.8	2.0	2.4	2.6	1.4	1.5	-2.08	0.00051	-1.31	0.00244	-2.16	0.00045	-2.82	0.00037	1
EGJ24819	lmo1279	ClpY	8.7	0.9	23.1	8.8	35.2	7.7	38.3	9.4	31.2	5.8	1.36	0.01030	1.96	0.00035	2.08	0.00056	1.78	0.00018	3
EGJ24823	lmo1283	YoxA	2.0	2.1	7.4	8.9	4.1	1.6	2.7	2.6	1.0	1.2	1.65	0.20319	0.86	0.08939	0.35	0.62820	-0.80	0.30923	2
EGJ24825	lmo1285	YneT	0.3	0.5	0.7	0.8	0.8	0.7	0.5	0.8	0.3	0.6	0.53	0.38597	0.68	0.20208	0.18	0.77893	-0.16	0.80246	
EGJ24826	lmo1286	ParE	1.3	0.8	1.1	0.8	1.1	0.3	0.6	0.5	0.3	0.5	-0.23	0.55045	-0.20	0.50565	-0.69	0.10192	-1.14	0.02869	5
EGJ24827	lmo1287	ParC	1.3	0.5	1.9	1.9	1.9	0.6	0.9	1.7	1.5	2.0	0.40	0.49878	0.37	0.11779	-0.35	0.59884	0.13	0.84331	
EGJ24828	lmo1288	LuxS	0.0	0.0	1.0	1.1	1.2	1.7	0.7	0.9	0.7	1.1	1.56	0.08308	1.78	0.13800	1.26	0.13091	1.22	0.18884	3
EGJ24830	lmo1291	OatA	0.2	0.4	0.1	0.4	0.5	0.6	0.1	0.3	0.1	0.3	-0.05	0.91923	0.60	0.26587	-0.08	0.87064	-0.07	0.88256	
EGJ24832	lmo1293	GlpD	1.9	1.9	2.5	1.8	4.9	1.8	2.8	1.8	2.0	2.8	0.33	0.57673	1.20	0.01733	0.50	0.38629	0.07	0.93353	0
EGJ24838	lmo1299	GlnA	32.4	4.0	12.5	4.9	16.1	3.9	11.9	3.1	13.4	4.8	-1.34	0.00002	-0.98	0.00003	-1.41	0.00000	-1.24	0.00003	1
EGJ24844	lmo1305	Tkt	30.5	10.1	25.1	6.7	24.6	3.1	22.5	2.4	23.8	4.1	-0.28	0.29503	-0.31	0.21569	-0.44	0.10759	-0.36	0.17197	
EGJ24845	lmo1306	YneF	0.2	0.4	0.9	0.8	3.1	1.3	1.3	1.2	1.0	1.1	1.08	0.07356	2.43	0.00201	1.42	0.07665	1.14	0.15279	3
EGJ24852	lmo1314	Frr	6.1	3.2	9.6	4.3	10.7	4.3	10.4	2.0	11.1	6.6	0.62	0.13888	0.77	0.06043	0.73	0.02095	0.82	0.13146	
EGJ24857	lmo1319	ProS	5.9	2.0	5.2	5.2	3.6	1.8	3.0	2.6	0.7	0.9	-0.17	0.76316	-0.64	0.06604	-0.86	0.06038	-2.46	0.00074	5
EGJ24858	lmo1320	PolC	0.7	0.8	0.9	0.5	0.4	0.7	2.0	1.3	0.8	1.0	0.30	0.50865	-0.35	0.57023	1.09	0.06170	0.15	0.80811	4
EGJ24860	lmo1322	NusA	2.8	1.5	4.6	2.4	8.6	4.1	6.7	4.1	3.5	4.5	0.62	0.15215	1.44	0.01702	1.10	0.07111	0.25	0.75304	3
EGJ24863	lmo1325	InfB	7.3	2.4	6.2	3.2	9.8	3.7	6.3	3.8	4.6	5.7	-0.22	0.50855	0.40	0.20047	-0.21	0.56906	-0.63	0.31204	
EGJ24868	lmo1330	RpsO	2.7	2.0	5.3	2.7	4.8	2.0	5.6	2.5	2.6	1.8	0.85	0.09148	0.72	0.10401	0.92	0.05231	-0.05	0.92368	
EGJ24869	lmo1331	PnpA	12.1	3.4	6.8	4.8	15.2	4.9	9.7	7.7	6.2	7.4	-0.80	0.05090	0.31	0.24083	-0.32	0.49388	-0.92	0.11517	
EGJ24872	lmo1334	YqzD	0.7	0.5	0.8	1.6	1.8	0.7	0.7	0.9	0.6	1.0	0.17	0.83860	0.97	0.01377	0.08	0.88134	-0.13	0.83100	
EGJ24876	lmo1339	GlcK	2.9	1.8	7.0	1.6	5.5	2.9	4.1	1.7	2.4	1.8	1.15	0.00200	0.83	0.09278	0.43	0.27509	-0.24	0.62564	2
EGJ24884	lmo1348	GcvT	0.2	0.4	0.1	0.3	0.3	0.4	0.3	0.7	0.1	0.3	-0.09	0.86178	0.20	0.68197	0.21	0.75632	-0.07	0.88256	
EGJ24886	lmo1350	GcvPB	0.0	0.0	1.4	1.0	0.6	0.7	0.7	0.9	0.4	0.7	1.94	0.01757	1.18	0.08399	1.29	0.09769	0.84	0.20669	3
EGJ24887	lmo1351	YqhL	1.2	0.4	0.8	1.0	3.1	2.7	1.0	0.9	1.9	2.4	-0.36	0.42367	1.12	0.14162	-0.12	0.76429	0.52	0.50174	0
EGJ24890	lmo1354	YqhT	3.4	1.7	9.0	6.7	4.5	2.4	4.2	3.4	2.6	3.2	1.29	0.09681	0.36	0.38634	0.26	0.63870	-0.33	0.60657	2
ScottA	**Other**		**Exp**	**stdev**	**1_d**	**stdev**	**7 d**	**stdev**	**14 d**	**stdev**	**21 d**	**stdev**	**1d/Exp**	**p**	**7**	**p**	**14**	**p**	**21**	**p**	**k-**

Loci	Loci														d/Exp		d/Exp		d/Exp		means group
EGJ24891	lmo1355	Efp	0.7	0.5	0.1	0.3	1.1	0.7	0.8	0.7	0.1	0.3	-0.90	0.06067	0.42	0.30697	0.11	0.80429	-0.89	0.06436	
EGJ24893	lmo1357	AccC	1.2	1.0	3.9	1.2	4.6	2.6	3.3	1.8	1.9	2.0	1.41	0.00158	1.64	0.01866	1.21	0.03324	0.51	0.46282	3
EGJ24895	lmo1359	NusB	1.7	0.8	0.1	0.3	0.5	0.8	0.0	0.0	0.3	0.6	-1.78	0.00369	-1.15	0.03034	-2.12	0.00365	-1.53	0.00696	1
EGJ24896	lmo1360	FolD	8.3	1.7	3.7	2.1	2.3	1.2	1.3	0.9	0.5	0.6	-1.06	0.00215	-1.63	0.00007	-2.32	0.00003	-3.09	0.00003	5
EGJ24900	lmo1364	CspC	14.2	20.3	8.4	5.2	1.9	0.6	2.0	1.9	0.8	1.0	-0.73	0.52092	-2.60	0.19832	-2.57	0.20027	-3.50	0.16640	5
EGJ24901	lmo1365	Dxs	0.2	0.4	0.2	0.4	0.4	0.7	0.2	0.4	0.5	1.3	0.05	0.92621	0.45	0.46763	0.00	0.99335	0.65	0.52716	
EGJ24904	lmo1368	RecN	0.8	0.4	0.8	0.7	1.4	1.6	1.0	1.2	1.3	2.0	-0.02	0.96033	0.51	0.43154	0.15	0.79409	0.48	0.55264	
EGJ24907	lmo1371	LpdV	0.2	0.4	0.3	0.6	0.9	1.2	0.9	0.7	0.6	0.7	0.20	0.75105	1.12	0.17610	1.09	0.06441	0.68	0.26517	3
EGJ24908	lmo1372	BkdAA	0.5	0.9	1.6	1.3	1.3	1.1	0.6	1.0	0.5	0.7	1.05	0.13426	0.81	0.20415	0.04	0.95886	0.01	0.98576	2
EGJ24909	lmo1373	BkdAB	5.9	1.4	4.2	0.7	4.0	2.4	2.4	2.2	2.2	2.8	-0.43	0.03823	-0.51	0.14091	-1.15	0.00931	-1.27	0.02095	5
EGJ24913	lmo1376	Gnd	39.6	13.5	59.2	10.7	46.7	13.1	47.1	12.0	47.2	12.1	0.57	0.02018	0.23	0.37770	0.25	0.33180	0.25	0.33134	
EGJ24914	lmo1377	LicR	0.0	0.0	1.6	1.6	3.8	2.7	2.1	2.2	1.5	2.0	2.07	0.06185	3.11	0.01853	2.38	0.06512	1.98	0.12643	3
EGJ24924	lmo1388	YufN	14.5	0.5	20.2	4.6	16.2	3.9	20.6	7.0	20.3	4.3	0.46	0.02876	0.15	0.34721	0.49	0.08748	0.46	0.02285	
EGJ24925	lmo1389	YufO	1.8	1.0	0.6	0.7	3.7	2.3	1.5	1.8	1.2	1.8	-1.09	0.03059	0.85	0.11020	-0.20	0.72600	-0.47	0.46528	0
EGJ24929	lmo1393	YmfH	1.0	0.0	0.3	0.6	0.5	0.8	0.3	0.5	0.1	0.4	-0.98	0.03624	-0.62	0.18640	-0.92	0.01224	-1.22	0.00200	1
EGJ24931	lmo1395	YmfM	0.7	0.5	1.6	1.3	1.3	1.3	0.4	0.5	1.1	1.4	0.81	0.15634	0.63	0.29225	-0.34	0.40637	0.41	0.53752	
EGJ24934	lmo1398	RecA	1.7	0.9	1.1	1.6	5.2	1.9	1.7	1.4	0.4	0.6	-0.45	0.44339	1.39	0.00435	0.03	0.94922	-1.30	0.01759	0
EGJ24935	lmo1399	YmdA	1.7	1.0	2.7	3.1	3.3	2.4	2.8	2.7	2.0	2.4	0.55	0.47854	0.81	0.16897	0.60	0.38071	0.22	0.74913	
EGJ24937	lmo1401	YmdB	0.8	0.8	2.5	2.4	1.4	1.1	1.3	0.7	1.3	2.0	1.16	0.15973	0.46	0.38371	0.45	0.25666	0.45	0.58294	2
EGJ24939	lmo1403	MutS	0.5	0.8	0.6	0.7	0.8	0.7	0.9	1.2	0.5	0.8	0.17	0.78990	0.43	0.46483	0.46	0.53568	0.06	0.93570	
EGJ24940	lmo1404	MutL	0.5	0.5	0.3	0.4	1.0	0.9	1.1	1.4	0.8	1.0	-0.35	0.47257	0.60	0.28794	0.69	0.36090	0.39	0.52167	
EGJ24942	lmo1406	PflB	43.6	17.3	42.9	26.7	65.8	22.3	44.7	27.7	30.0	34.0	-0.02	0.95573	0.59	0.08458	0.04	0.93558	-0.53	0.40915	
EGJ24943	lmo1407	PflA	0.0	0.0	4.4	2.9	6.7	4.2	4.6	4.0	4.0	5.3	3.30	0.01367	3.85	0.01071	3.35	0.03619	3.16	0.12728	3
EGJ24950	lmo1414	MmgA	1.3	1.2	0.3	0.5	0.3	0.4	0.5	1.0	0.7	0.8	-1.16	0.09794	-1.25	0.08410	-0.80	0.25126	-0.65	0.28308	1
EGJ24951	lmo1415	MvaS	0.7	0.5	4.2	2.6	7.8	7.1	11.3	7.2	12.1	8.0	2.00	0.02156	2.82	0.05759	3.33	0.01517	3.42	0.01712	4
EGJ24956	lmo1420	MurB	1.0	0.6	0.4	0.7	0.0	0.0	0.0	0.0	0.6	0.7	-0.68	0.18330	-1.60	0.01145	-1.60	0.01145	-0.45	0.31523	1
EGJ24958	lmo1422	BileB	0.3	0.5	0.2	0.4	0.2	0.4	0.2	0.4	0.3	0.5	-0.29	0.59516	-0.32	0.56086	-0.35	0.51645	0.00	0.99286	
EGJ24959	lmo1423		0.0	0.0	1.9	0.9	1.2	0.9	1.1	1.2	0.8	1.0	2.25	0.00462	1.77	0.02203	1.70	0.07823	1.38	0.10257	3
EGJ24960	lmo1424	MntH	0.2	0.4	0.6	0.9	0.4	0.4	0.7	0.8	0.6	0.7	0.69	0.33949	0.45	0.33960	0.86	0.18383	0.68	0.26517	
EGJ24962	lmo1426	OpuCC	0.2	0.4	1.9	1.1	2.7	2.4	3.0	3.6	1.8	1.3	1.80	0.01339	2.22	0.05154	2.37	0.11294	1.73	0.02880	3
EGJ24964	lmo1428	OpuCA	2.9	1.1	10.3	2.6	14.3	3.4	12.1	1.6	10.9	5.3	1.68	0.00041	2.14	0.00024	1.90	0.00000	1.76	0.01274	3
EGJ24967	lmo1431	YkpA	1.4	1.5	0.4	0.6	0.3	0.5	0.0	0.0	0.3	0.7	-1.07	0.19463	-1.20	0.16026	-1.89	0.08196	-1.27	0.15456	1
EGJ24969	lmo1433	Gor	0.0	0.0	1.1	1.0	1.3	1.0	1.3	1.1	1.2	1.4	1.67	0.04742	1.85	0.02024	1.87	0.03298	1.76	0.09112	3
EGJ24970	lmo1434	RnjB	5.5	3.0	4.4	2.8	6.3	3.3	3.8	1.6	2.9	2.4	-0.28	0.54453	0.19	0.65439	-0.46	0.26873	-0.83	0.12683	
EGJ24971	lmo1435	DapA	2.2	0.7	7.0	3.5	6.4	1.4	7.3	2.7	4.9	2.3	1.49	0.01956	1.38	0.00018	1.55	0.00460	1.02	0.03180	3
EGJ24972	lmo1436	DapG	0.7	0.5	1.7	1.0	2.1	0.5	1.5	1.3	1.3	1.8	0.92	0.06570	1.18	0.00056	0.76	0.20395	0.67	0.40673	3
EGJ24973	lmo1437	Asd	3.2	0.7	6.1	2.0	5.5	3.0	2.9	2.1	2.5	2.7	0.84	0.01625	0.72	0.11498	-0.11	0.76962	-0.28	0.60079	
EGJ24975	lmo1439	SodA	10.3	4.6	25.0	15.7	14.1	3.5	10.6	2.1	8.4	4.0	1.24	0.07153	0.43	0.14354	0.04	0.89997	-0.28	0.45710	2
ScottA	**Other**		**Exp**	**stdev**	**1_d**	**stdev**	**7 d**	**stdev**	**14 d**	**stdev**	**21 d**	**stdev**	**1d/Exp**	**p**	**7**	**p**	**14**	**p**	**21**	**p**	**k-**

Loci	Loci														d/Exp		d/Exp		d/Exp		means group
EGJ24984	lmo1448	PpaC	6.2	1.4	8.0	2.4	9.8	4.1	6.3	3.3	4.7	5.3	0.33	0.15906	0.62	0.08829	0.03	0.92750	-0.37	0.52589	
EGJ24985	lmo1449	YqfS	0.2	0.4	0.3	0.4	1.0	0.8	0.6	0.7	0.1	0.3	0.23	0.65094	1.15	0.05840	0.74	0.22513	-0.09	0.85279	0
EGJ24986	lmo1450	CshB	0.0	0.0	0.3	0.6	2.1	2.0	0.8	1.1	0.8	0.7	0.61	0.36322	2.37	0.05225	1.41	0.11024	1.39	0.03742	3
EGJ24988	lmo1452	YqfO	0.7	0.5	0.5	0.6	0.7	0.8	1.2	1.1	0.5	1.0	-0.20	0.63934	0.00	0.99778	0.52	0.34131	-0.18	0.77586	
EGJ24989	lmo1453	TrmK	1.2	0.4	0.7	0.6	0.8	0.6	0.3	0.5	0.1	0.3	-0.48	0.12875	-0.41	0.22306	-1.08	0.00580	-1.42	0.00070	5
EGJ24990	lmo1454	SigA	1.8	0.7	4.3	3.2	3.1	1.6	2.4	1.3	1.2	1.2	1.05	0.11538	0.64	0.11502	0.30	0.40040	-0.49	0.27318	2
EGJ24993	lmo1457	YqfL	0.2	0.4	1.7	1.6	1.4	2.1	0.3	0.5	0.1	0.3	1.69	0.07535	1.49	0.21216	0.34	0.54393	-0.07	0.88848	2
EGJ24994	lmo1458	GlyS	0.8	0.8	8.1	6.4	4.3	2.0	3.5	1.5	4.8	1.1	2.70	0.03849	1.85	0.00702	1.59	0.00518	2.01	0.00005	3
EGJ24995	lmo1459	GlyQ	0.0	0.0	0.8	0.8	2.0	1.1	1.1	0.6	1.2	1.2	1.41	0.05472	2.34	0.00552	1.69	0.00767	1.77	0.05905	3
EGJ24998	lmo1462	Era	0.3	0.5	1.8	1.4	1.5	1.0	0.6	0.7	0.3	0.4	1.49	0.04082	1.27	0.03549	0.44	0.43723	-0.09	0.85445	2
EGJ25003	lmo1467	PhoH	0.5	0.8	1.3	0.5	0.7	0.5	0.6	0.7	0.6	0.7	0.86	0.07366	0.25	0.65026	0.10	0.87914	0.14	0.82670	
EGJ25005	lmo1468	YqeY	1.4	1.1	4.6	2.5	2.9	1.9	3.3	1.7	2.3	3.3	1.45	0.02226	0.89	0.11532	1.01	0.05151	0.57	0.54721	3
EGJ25006	lmo1469	RpsU	1.5	0.6	1.0	1.0	4.1	1.8	3.4	0.9	3.9	1.2	-0.40	0.31745	1.20	0.01503	0.94	0.00323	1.14	0.00269	
EGJ25008	lmo1471	PrmA	0.2	0.4	0.4	1.0	1.1	1.2	0.1	0.3	0.3	0.4	0.42	0.61776	1.24	0.13307	-0.07	0.88143	0.19	0.69989	
EGJ25009	lmo1472	DnaJ	0.8	0.4	5.0	2.1	6.2	3.0	4.7	4.8	3.3	3.4	2.05	0.00382	2.34	0.00649	1.97	0.10386	1.52	0.13973	3
EGJ25010	lmo1473	DnaK	188.8	41.7	158.8	50.7	79.0	18.0	75.2	23.6	57.4	29.2	-0.25	0.28998	-1.25	0.00065	-1.32	0.00042	-1.71	0.00014	5
EGJ25011	lmo1474	GrpE	12.4	4.8	10.2	2.9	9.9	1.7	9.3	2.1	9.2	1.3	-0.27	0.35456	-0.31	0.26572	-0.41	0.18045	-0.41	0.16349	
EGJ25016	lmo1479	LepA	0.0	0.0	0.5	0.5	1.0	0.7	0.9	0.8	0.0	0.0	0.95	0.07962	1.60	0.02114	1.49	0.03477	0.00		3
EGJ25017	lmo1480	RpsT	2.7	0.8	2.1	1.3	4.9	2.5	5.4	2.8	5.1	3.6	-0.30	0.37340	0.77	0.07919	0.89	0.06284	0.83	0.15592	
EGJ25026	lmo1489	YqeI	0.2	0.4	0.3	0.4	0.1	0.3	0.3	0.5	0.1	0.3	0.20	0.69962	-0.10	0.83674	0.22	0.67253	-0.10	0.84876	
EGJ25028	lmo1491	YqeH	0.2	0.4	0.5	0.6	1.2	1.7	0.0	0.0	0.5	0.5	0.58	0.27214	1.36	0.19334	-0.42	0.36322	0.55	0.29184	0
EGJ25030	lmo1493	PepF	4.8	1.7	9.9	6.9	14.7	11.9	15.5	11.3	11.5	5.3	0.96	0.13763	1.52	0.09724	1.59	0.06685	1.18	0.02565	3
EGJ25031	lmo1494	Mtn	0.0	0.0	1.5	0.7	4.6	5.0	4.9	3.6	7.6	4.9	2.02	0.00318	3.34	0.07467	3.44	0.01962	4.02	0.01215	4
EGJ25033	lmo1496	GreA	5.0	1.6	6.4	2.3	5.1	2.1	3.9	1.3	2.1	1.5	0.31	0.27414	0.01	0.98410	-0.33	0.19935	-1.09	0.00711	5
EGJ25036	lmo1499	YrrL	1.5	1.0	1.3	0.6	0.1	0.3	0.0	0.0	0.4	0.7	-0.12	0.75477	-1.64	0.02216	-1.99	0.01667	-1.11	0.06489	5
EGJ25040	lmo1503	YrzL	0.0	0.0	0.9	1.1	1.1	1.7	1.8	2.6	3.0	3.3	1.52	0.08840	1.66	0.17516	2.20	0.15269	2.80	0.07536	4
EGJ25041	lmo1504	AlaS	3.5	1.7	13.3	5.3	11.6	7.6	6.0	3.4	5.9	7.0	1.76	0.00498	1.58	0.04914	0.69	0.15287	0.66	0.46070	2
EGJ25056	lmo1519	AspS	3.9	1.6	7.5	3.1	6.0	2.5	5.5	3.0	4.2	3.0	0.87	0.03596	0.57	0.11756	0.46	0.27195	0.10	0.83529	
EGJ25057	lmo1520	HisS	2.0	0.7	6.7	5.0	5.6	4.5	3.8	3.7	5.5	4.3	1.50	0.07194	1.27	0.11431	0.78	0.29132	1.25	0.10198	3
EGJ25058	lmo1521	YrvJ	0.2	0.4	0.3	0.5	0.4	0.9	1.2	1.0	2.4	1.8	0.32	0.55306	0.41	0.62046	1.38	0.05454	2.10	0.02751	4
EGJ25059	lmo1522	YrzB	0.2	0.4	0.5	0.5	0.7	1.4	0.6	1.0	0.4	1.0	0.55	0.28730	0.90	0.36683	0.75	0.35534	0.44	0.60794	
EGJ25061	lmo1524	Apt	2.4	0.8	3.1	2.2	2.2	1.9	1.8	1.5	1.5	1.7	0.35	0.45416	-0.06	0.89394	-0.31	0.45563	-0.52	0.29723	
EGJ25062	lmo1525	RecJ	0.3	0.5	0.4	0.7	0.6	0.7	0.5	0.8	0.7	1.1	0.18	0.76482	0.36	0.50864	0.26	0.68202	0.53	0.48584	
EGJ25064	lmo1527	SecDF	0.8	0.7	2.2	1.1	4.3	1.5	4.9	1.8	3.7	2.4	1.02	0.02824	1.85	0.00141	2.03	0.00152	1.64	0.03422	3
EGJ25066	lmo1529	YajC	1.4	1.1	2.2	0.9	5.4	4.6	4.6	4.7	4.0	3.4	0.52	0.19068	1.65	0.08542	1.44	0.16172	1.28	0.12147	3
EGJ25067	lmo1530	Tgt	2.0	0.9	2.4	2.4	2.3	0.9	1.0	1.0	1.3	1.3	0.21	0.71553	0.15	0.62868	-0.71	0.10134	-0.45	0.33540	
EGJ25071	lmo1534	Ldh	1.3	1.0	1.4	1.0	1.9	0.8	0.6	0.9	0.6	0.7	0.07	0.87650	0.42	0.26977	-0.78	0.20008	-0.72	0.19412	
EGJ25074	lmo1537	ObgE	1.0	0.0	0.0	0.0	0.4	0.5	0.2	0.4	0.3	0.7	-1.59	0.00000	-0.68	0.03760	-1.19	0.00286	-0.96	0.04333	1
ScottA	**Other**		**Exp**	**stdev**	**1_d**	**stdev**	**7 d**	**stdev**	**14 d**	**stdev**	**21 d**	**stdev**	**1d/Exp**	**p**	**7**	**p**	**14**	**p**	**21**	**p**	**k-**

Loci	Loci														d/Exp		d/Exp		d/Exp		means group
EGJ25075	lmo1538	GlpK	1.7	0.8	7.8	4.6	10.4	3.4	9.3	5.7	9.9	5.7	1.92	0.02298	2.32	0.00105	2.16	0.02148	2.25	0.01616	3
EGJ25077	lmo1540	RpmA	3.7	1.1	7.7	5.3	7.1	3.0	7.2	3.2	9.1	4.2	0.98	0.12195	0.87	0.03715	0.89	0.04362	1.21	0.02218	3
EGJ25079	lmo1542	RplU	34.8	6.4	17.9	12.5	19.5	13.5	20.0	12.5	14.4	10.3	-0.94	0.02030	-0.82	0.03972	-0.79	0.03472	-1.24	0.00314	1
EGJ25081	lmo1544	MinD	0.8	0.8	1.0	0.6	1.4	1.4	1.0	1.1	1.1	1.4	0.18	0.66904	0.54	0.37434	0.14	0.80611	0.29	0.65675	
EGJ25082	lmo1545	MinC	0.0	0.0	0.0	0.0	1.2	1.0	0.0	0.0	0.0	0.0	0.00		1.73	0.03973	0.00		0.00		
EGJ25084	lmo1547	MreC	0.2	0.4	0.5	0.6	1.8	1.9	1.8	1.5	1.3	0.8	0.62	0.24165	1.80	0.08680	1.83	0.03732	1.48	0.01690	3
EGJ25085	lmo1548	MreB	5.7	2.4	7.4	3.6	9.0	2.4	4.7	3.0	3.9	4.9	0.35	0.35496	0.61	0.03819	-0.27	0.50882	-0.51	0.43343	
EGJ25089	lmo1552	ValS	8.6	1.1	11.0	6.0	7.3	4.8	5.7	5.7	4.2	4.8	0.34	0.37584	-0.21	0.57245	-0.53	0.29042	-0.95	0.07634	
EGJ25090	lmo1553	HemL	0.3	0.5	2.8	1.0	3.1	3.5	1.9	1.7	1.6	1.7	1.98	0.00072	2.13	0.10821	1.53	0.07901	1.34	0.12389	3
EGJ25091	lmo1554	HemB	1.2	0.4	5.7	5.5	4.2	4.1	3.4	3.2	2.0	1.8	1.89	0.09900	1.50	0.12667	1.22	0.15174	0.59	0.29998	3
EGJ25093	lmo1556	HemC	0.3	0.5	0.7	0.5	0.4	0.6	0.4	0.7	0.1	0.3	0.49	0.29812	0.08	0.88123	0.16	0.78520	-0.40	0.42995	
EGJ25096	lmo1559	ThrS	3.6	1.2	3.8	0.9	3.9	1.5	1.5	1.3	1.2	1.0	0.07	0.74509	0.11	0.69895	-1.03	0.01641	-1.29	0.00379	5
EGJ25102	lmo1565	PolA	2.0	1.3	1.1	1.3	1.4	1.2	1.1	1.4	1.9	1.5	-0.64	0.26304	-0.39	0.42888	-0.63	0.28105	-0.03	0.95383	
EGJ25103	lmo1566	Icd	0.7	0.5	1.5	0.8	0.9	0.8	0.8	1.1	1.6	1.4	0.79	0.06504	0.23	0.61402	0.22	0.70647	0.89	0.15674	
EGJ25107	lmo1570	Pyk	75.0	9.2	160.8	48.5	142.2	84.0	109.5	52.6	108.5	41.6	1.09	0.00690	0.92	0.10770	0.54	0.17033	0.53	0.10747	3
EGJ25108	lmo1571	PfkA	12.2	1.3	38.6	10.0	54.0	18.5	42.0	20.4	32.9	15.0	1.62	0.00124	2.10	0.00261	1.74	0.01572	1.39	0.01940	3
EGJ25109	lmo1572	AccA	0.8	0.4	0.8	1.0	3.3	1.6	1.0	1.2	0.5	0.8	-0.02	0.97277	1.52	0.01178	0.19	0.72294	-0.37	0.44952	0
EGJ25110	lmo1573	AccD	0.2	0.4	1.8	2.1	1.3	0.7	0.8	1.1	0.0	0.0	1.81	0.10603	1.45	0.00747	1.00	0.19604	-0.42	0.36322	2
EGJ25111	lmo1574	DnaE	0.2	0.4	0.4	0.7	0.1	0.3	0.3	0.7	0.7	1.5	0.48	0.45612	-0.06	0.90094	0.26	0.70468	0.92	0.38157	
EGJ25114	lmo1577	YtkL	0.3	0.5	0.5	0.9	1.0	0.8	0.5	0.7	0.7	0.8	0.34	0.62332	0.84	0.13716	0.23	0.70228	0.50	0.40263	
EGJ25115	lmo1578	YkvY	3.5	1.5	11.1	6.4	10.5	2.8	5.1	3.1	4.6	2.8	1.53	0.03202	1.45	0.00068	0.48	0.29181	0.35	0.41927	2
EGJ25116	lmo1579	Ald	3.7	0.9	24.3	5.7	43.0	31.9	56.9	32.4	81.6	46.3	2.56	0.00026	3.37	0.02956	3.77	0.01014	4.29	0.00917	4
EGJ25117	lmo1580	YxiE	5.4	1.2	18.4	7.7	18.9	5.3	16.1	2.5	14.4	3.4	1.68	0.00881	1.72	0.00125	1.50	0.00003	1.34	0.00070	3
EGJ25118	lmo1581	AckA	27.0	3.2	20.7	7.0	17.4	7.6	16.9	9.2	9.6	10.1	-0.38	0.08369	-0.62	0.02685	-0.66	0.04374	-1.44	0.00697	5
EGJ25120	lmo1583	Tpx	3.0	0.6	2.0	1.6	1.2	1.4	0.6	0.7	1.2	1.2	-0.51	0.17580	-1.04	0.02517	-1.73	0.00007	-1.05	0.01049	1
EGJ25123	lmo1586	PpnK	0.8	0.8	5.5	2.7	5.4	2.9	7.3	4.4	5.1	3.3	2.15	0.00774	2.14	0.01110	2.55	0.01445	2.07	0.02455	3
EGJ25129	lmo1592	YtbJ	0.2	0.4	0.8	1.0	1.1	1.1	0.3	0.5	0.9	1.0	1.01	0.16009	1.30	0.08539	0.27	0.59726	1.11	0.14070	3
EGJ25131	lmo1594	EzrA	0.5	0.5	0.8	1.0	2.9	1.5	1.2	1.4	1.7	1.8	0.43	0.49492	1.78	0.00987	0.73	0.32610	1.16	0.16417	3
EGJ25133	lmo1596	RpsD	17.7	2.9	47.8	22.3	33.3	12.8	27.3	10.8	18.9	9.1	1.41	0.02099	0.89	0.03039	0.61	0.08285	0.09	0.77557	2
EGJ25134	lmo1598	TyrS	2.8	0.9	7.6	5.0	4.8	1.9	5.0	1.0	6.9	3.4	1.27	0.06735	0.66	0.05700	0.73	0.00305	1.15	0.03125	3
EGJ25135	lmo1599	CcpA	4.1	1.6	12.6	11.0	13.1	7.4	9.4	4.6	7.0	1.7	1.50	0.11965	1.55	0.02999	1.10	0.03781	0.70	0.01181	3
EGJ25136	lmo1600	AroG	1.9	0.4	0.4	0.7	1.9	0.9	1.3	1.7	0.3	0.6	-1.36	0.00198	0.00	0.99775	-0.39	0.45827	-1.64	0.00063	1
EGJ25137	lmo1601	YtxH	2.0	0.9	13.2	6.5	20.6	5.5	26.7	7.3	25.8	6.6	2.46	0.00771	3.08	0.00034	3.45	0.00037	3.40	0.00028	3
EGJ25138	lmo1602	YtxG	5.6	2.5	7.4	5.0	8.1	4.2	5.9	3.6	5.3	5.4	0.36	0.46907	0.49	0.24965	0.05	0.90895	-0.09	0.88350	
EGJ25139	lmo1603	AmpS	10.6	2.1	10.4	4.4	8.2	2.5	9.3	3.1	8.6	4.3	-0.02	0.95099	-0.35	0.11039	-0.18	0.41803	-0.29	0.33661	
EGJ25140	lmo1604	YkuU	3.2	1.3	1.5	0.8	3.3	1.2	1.1	1.1	0.4	1.0	-0.90	0.02570	0.06	0.82945	-1.19	0.01604	-2.02	0.00257	5
EGJ25141	lmo1605	MurC	1.3	0.5	1.6	1.6	1.9	1.4	1.2	1.1	1.0	0.8	0.18	0.72300	0.40	0.38238	-0.13	0.75164	-0.32	0.37615	
EGJ25143	lmo1607	YtpR	5.2	1.3	3.0	2.2	1.6	1.1	1.3	0.7	0.7	1.1	-0.70	0.06725	-1.44	0.00053	-1.63	0.00035	-2.25	0.00011	5
ScottA	**Other**		**Exp**	**stdev**	**1_d**	**stdev**	**7 d**	**stdev**	**14 d**	**stdev**	**21 d**	**stdev**	**1d/Exp**	**p**	**7**	**p**	**14**	**p**	**21**	**p**	**k-**

Loci	Loci													d/Exp		d/Exp		d/Exp		means group
EGJ25145	lmo1609	YtpP	0.3	0.5	0.4	0.7	0.6	0.5	0.3	0.6	0.3	0.4	0.18	0.76960	0.38	0.39772	0.02	0.97640	-0.13	0.79282	
EGJ25147	lmo1611	YtoP	6.7	1.5	20.9	9.0	24.2	12.5	29.8	16.8	39.5	22.1	1.57	0.01117	1.78	0.01822	2.07	0.01964	2.47	0.01490	4
EGJ25151	lmo1615	TrmB	0.7	0.5	0.3	0.6	0.1	0.3	0.3	0.4	0.3	0.4	-0.60	0.26586	-0.87	0.06574	-0.59	0.18059	-0.60	0.17197	
EGJ25155	lmo1619	Dat	18.9	5.2	11.7	3.6	11.3	3.0	9.6	5.0	6.0	7.6	-0.67	0.02057	-0.72	0.01377	-0.95	0.00954	-1.57	0.00762	5
EGJ25156	lmo1620	YtjP	7.2	1.7	18.7	3.8	19.1	5.6	15.3	7.0	10.0	10.0	1.31	0.00029	1.34	0.00273	1.03	0.03613	0.43	0.54039	3
EGJ25157	lmo1621		0.2	0.4	0.5	0.6	1.9	1.7	0.6	0.7	0.4	0.6	0.61	0.26088	1.86	0.05446	0.67	0.25353	0.42	0.49349	0
EGJ25171	lmo1634		149.5	82.2	264.3	37.6	227.5	5.0	153.0	42.4	126.4	53.4	0.82	0.01708	0.60	0.06785	0.03	0.92943	-0.24	0.57924	
EGJ25177	lmo1641	CitB	0.5	0.9	3.5	3.2	2.3	1.5	1.2	1.1	0.5	0.7	1.97	0.07054	1.45	0.03633	0.70	0.29217	0.00	0.99981	2
EGJ25179	lmo1643		0.5	0.5	0.6	0.9	0.7	0.5	1.3	1.4	0.7	0.6	0.20	0.73704	0.25	0.56649	0.84	0.24401	0.24	0.59582	
EGJ25180	lmo1644	YwqA	0.3	0.5	0.1	0.4	0.5	0.6	0.7	0.6	0.3	0.4	-0.36	0.49077	0.26	0.60201	0.52	0.27673	-0.12	0.81272	
EGJ25184	lmo1649		2.2	0.9	5.4	1.6	3.6	1.3	4.7	2.2	6.2	2.8	1.16	0.00277	0.63	0.05630	0.97	0.03393	1.33	0.01503	4
EGJ25187	lmo1652	YbeI	1.3	1.0	0.3	0.5	0.7	0.8	0.1	0.3	0.5	0.8	-1.13	0.06271	-0.64	0.23395	-1.53	0.03017	-0.84	0.15462	1
EGJ25188	lmo1653		1.0	1.1	0.4	0.8	0.2	0.5	0.5	1.0	0.3	0.7	-0.65	0.33251	-1.11	0.13623	-0.51	0.47553	-0.96	0.19111	
EGJ25192	lmo1657	Tsf	110.8	10.5	67.4	6.9	52.7	19.1	44.8	15.5	23.9	16.8	-0.71	0.00002	-1.06	0.00021	-1.30	0.00001	-2.19	0.00000	5
EGJ25193	lmo1658	RpsB	32.1	5.7	41.2	9.8	35.3	12.5	35.7	16.0	26.6	16.1	0.35	0.08573	0.14	0.58362	0.15	0.62175	-0.27	0.45788	
EGJ25197	lmo1660	LeuS	2.2	0.8	9.3	7.7	8.4	2.3	7.9	4.0	8.5	6.8	1.86	0.07362	1.71	0.00071	1.64	0.01602	1.73	0.07235	3
EGJ25200	lmo1663	AsnB	1.7	1.0	4.3	2.4	5.8	3.0	4.2	2.5	2.9	2.0	1.15	0.04786	1.55	0.01879	1.13	0.05697	0.64	0.22407	3
EGJ25201	lmo1664	MetK	1.0	0.0	2.8	2.0	2.9	1.9	2.0	1.2	1.8	1.8	1.13	0.08373	1.18	0.06204	0.72	0.09411	0.60	0.34811	3
EGJ25203	lmo1666		0.5	0.5	1.2	1.0	0.3	0.5	1.8	2.2	1.7	2.6	0.75	0.19842	-0.27	0.58479	1.19	0.21882	1.18	0.29678	4
EGJ25204	lmo1667	Ldh	0.5	0.6	0.5	1.0	0.8	1.0	0.6	0.8	0.7	0.8	0.04	0.95130	0.37	0.54712	0.11	0.84487	0.22	0.68008	
EGJ25205	lmo1668	YtmB	0.7	0.5	0.9	1.0	0.4	0.4	0.5	0.8	0.8	0.7	0.21	0.70971	-0.37	0.36538	-0.23	0.66750	0.17	0.69360	
EGJ25210	lmo1673	MenB	7.2	1.2	12.0	5.7	15.1	3.7	10.5	4.4	9.8	4.2	0.69	0.09571	1.01	0.00275	0.51	0.13559	0.41	0.20133	
EGJ25212	lmo1675	MenD	0.2	0.4	3.4	2.9	1.8	1.9	0.8	0.7	0.6	0.7	2.54	0.04152	1.78	0.08599	0.93	0.09108	0.67	0.27558	2
EGJ25213	lmo1676	MenF	0.7	0.8	3.3	1.6	3.2	3.0	1.0	1.6	0.4	0.6	1.68	0.00949	1.66	0.09017	0.40	0.62156	-0.40	0.51987	2
EGJ25222	lmo1685	GsaB	2.2	0.8	0.7	0.5	2.7	2.3	1.0	1.6	1.4	2.3	-1.20	0.00351	0.24	0.63881	-0.82	0.14909	-0.47	0.47981	1
EGJ25225	lmo1688	FabL	0.3	0.5	0.3	0.4	0.1	0.3	0.3	0.5	0.3	0.4	-0.08	0.87192	-0.38	0.46189	-0.06	0.89973	-0.11	0.81679	
EGJ25228	lmo1691	YncF	0.0	0.0	1.1	1.0	0.3	0.5	0.0	0.0	0.3	0.6	1.67	0.03930	0.69	0.17856	0.00		0.59	0.36322	2
EGJ25231	lmo1694	YfhF	0.3	0.5	0.1	0.3	0.2	0.4	0.3	0.5	0.3	0.4	-0.41	0.43360	-0.32	0.56054	-0.08	0.87464	-0.09	0.85395	
EGJ25246	lmo1709	MapA	3.7	1.0	3.6	2.5	5.1	2.9	2.8	2.0	1.6	1.9	-0.04	0.92279	0.41	0.31511	-0.35	0.36079	-0.98	0.04999	
EGJ25247	lmo1710	YkuP	2.5	0.6	2.2	1.4	2.3	1.2	1.8	1.6	1.2	1.0	-0.15	0.64967	-0.09	0.75037	-0.40	0.33605	-0.80	0.02648	
EGJ25248	lmo1711	AmpS	9.2	1.9	10.8	2.2	12.5	3.7	9.7	4.1	6.4	6.4	0.21	0.22036	0.41	0.09455	0.07	0.81334	-0.49	0.34486	
EGJ25254	lmo1718		0.3	0.5	0.7	1.3	2.6	3.3	1.4	1.0	1.4	1.7	0.48	0.58764	1.87	0.15446	1.16	0.05917	1.18	0.19195	3
EGJ25257	lmo1721	LevR	0.3	0.5	0.3	0.4	1.7	1.7	0.0	0.0	0.3	0.4	-0.09	0.85232	1.40	0.11329	-0.74	0.17469	-0.13	0.79782	0
EGJ25262	lmo1726	YulF	1.3	0.5	3.8	1.9	3.1	1.2	1.4	1.5	1.2	1.9	1.23	0.02454	0.97	0.01393	0.08	0.87190	-0.12	0.86098	2
EGJ25264	lmo1728		0.2	0.4	0.3	0.5	0.4	0.7	0.4	0.7	0.7	1.3	0.29	0.59661	0.41	0.51377	0.44	0.50145	0.78	0.41011	
EGJ25270	lmo1734	GltA	0.2	0.4	0.7	0.9	0.2	0.5	0.3	0.7	0.4	0.7	0.89	0.22122	0.06	0.91907	0.26	0.70827	0.44	0.48119	
EGJ25277	lmo1742	AdeC	0.2	0.4	0.4	0.6	0.3	0.4	0.6	0.8	0.3	0.5	0.43	0.45963	0.22	0.65222	0.72	0.25695	0.35	0.52599	
EGJ25279	lmo1744		1.2	0.8	0.0	0.0	0.3	0.4	0.0	0.0	0.0	0.0	-1.76	0.01438	-1.14	0.03721	-1.76	0.01438	-1.76	0.01438	1
ScottA	**Other**		**Exp**	**stdev**	**1_d**	**stdev**	**7 d**	**stdev**	**14 d**	**stdev**	**21 d**	**stdev**	**1d/Exp**	**p**	**7**	**p**	**14**	**p**	**21**	**p**	**k-**

Loci	Loci														d/Exp		d/Exp		d/Exp		means group
EGJ25285	lmo1750		0.0	0.0	0.4	0.7	1.5	1.7	0.5	0.7	0.4	0.7	0.90	0.21374	1.97	0.09324	0.97	0.17840	0.85	0.19303	3
EGJ25288	lmo1753	YerQ	0.0	0.0	2.3	1.6	1.4	1.1	0.2	0.4	0.1	0.3	2.47	0.01857	1.95	0.02660	0.40	0.36322	0.33	0.36322	2
EGJ25289	lmo1754	GatB	8.3	3.5	14.3	6.4	13.1	5.1	9.9	7.0	5.2	6.4	0.75	0.08036	0.63	0.09067	0.25	0.62382	-0.62	0.33576	
EGJ25290	lmo1755	GatA	11.9	3.6	7.3	3.8	7.7	3.2	4.8	2.2	3.9	2.3	-0.66	0.06074	-0.59	0.06070	-1.22	0.00313	-1.49	0.00150	5
EGJ25292	lmo1757	YerH	1.2	0.7	2.6	1.7	2.1	1.0	2.2	2.6	1.0	1.2	0.89	0.10050	0.67	0.07842	0.73	0.36802	-0.13	0.80414	
EGJ25293	lmo1758	LigA	0.3	0.8	1.0	1.2	1.9	2.0	1.5	1.0	0.8	0.7	0.88	0.25239	1.50	0.12181	1.28	0.04316	0.66	0.30694	3
EGJ25294	lmo1759	PcrA	0.2	0.4	0.6	0.7	1.4	1.1	0.4	0.7	0.8	1.2	0.66	0.25463	1.54	0.03205	0.47	0.45524	0.95	0.28320	
EGJ25299	lmo1764	PurD	0.2	0.4	0.2	0.4	0.3	0.4	0.3	0.8	0.4	0.6	-0.04	0.93610	0.20	0.68941	0.29	0.69416	0.41	0.49829	
EGJ25300	lmo1765	PurH	0.8	0.4	0.8	1.0	2.2	1.5	2.1	1.6	1.0	1.1	0.00	0.99290	1.00	0.07697	0.95	0.11211	0.13	0.80494	0
EGJ25302	lmo1767	PurM	0.0	0.0	0.2	0.4	1.1	1.2	0.5	0.8	0.0	0.0	0.45	0.36322	1.68	0.07607	1.00	0.18141	0.00		0
EGJ25303	lmo1768	PurF	0.0	0.0	0.2	0.5	1.3	1.9	1.4	1.0	2.1	2.1	0.49	0.36322	1.83	0.15179	1.92	0.02053	2.37	0.05748	4
EGJ25304	lmo1769	PurL	0.0	0.0	0.9	0.9	1.6	1.2	0.4	0.6	0.4	0.7	1.49	0.05148	2.08	0.02034	0.79	0.17965	0.85	0.19303	3
EGJ25306	lmo1771	PurS	0.0	0.0	1.2	0.9	2.1	2.1	2.4	2.6	2.3	1.5	1.80	0.02156	2.40	0.05469	2.56	0.06799	2.46	0.01442	3
EGJ25308	lmo1773	PurB	0.2	0.4	0.4	0.7	0.7	0.6	0.3	0.4	0.3	0.4	0.48	0.47139	0.87	0.10749	0.20	0.68597	0.19	0.69989	
EGJ25309	lmo1774	PurK	0.5	0.6	1.3	0.5	1.7	1.2	0.6	0.7	0.7	0.6	0.84	0.02623	1.15	0.05784	0.14	0.79054	0.30	0.51398	2
EGJ25310	lmo1775	PurE	0.3	0.5	0.4	0.6	0.5	0.6	0.2	0.5	0.4	0.5	0.07	0.89589	0.27	0.59939	-0.25	0.67185	0.11	0.81225	
EGJ25315	lmo1780	PepT	1.7	0.9	4.3	2.5	3.4	2.0	1.9	1.8	1.2	1.4	1.12	0.05256	0.82	0.10569	0.12	0.83138	-0.35	0.49364	2
EGJ25318	lmo1783	RplT	28.0	7.9	9.9	6.5	7.8	7.3	4.2	1.2	4.0	1.7	-1.45	0.00170	-1.77	0.00105	-2.59	0.00066	-2.65	0.00055	1
EGJ25319	lmo1784	RpmI	3.8	0.7	5.2	3.6	6.2	2.5	5.8	2.9	5.7	3.9	0.40	0.40105	0.62	0.06642	0.54	0.15799	0.51	0.30598	
EGJ25320	lmo1785	InfC	4.9	1.5	10.4	1.9	10.8	1.3	11.2	2.6	10.2	2.2	1.03	0.00030	1.08	0.00003	1.13	0.00089	1.00	0.00084	3
EGJ25323	lmo1787	RplS	54.9	7.8	17.8	7.1	15.5	8.8	17.2	12.8	13.1	7.1	-1.60	0.00001	-1.79	0.00001	-1.64	0.00024	-2.03	0.00000	1
EGJ25327	lmo1791		0.0	0.0	0.4	0.6	2.0	1.4	2.2	2.1	2.7	2.5	0.77	0.18047	2.34	0.01678	2.46	0.05045	2.69	0.04124	4
EGJ25329	lmo1793	RimM	0.8	0.4	0.8	0.9	0.7	0.8	0.8	0.9	0.4	0.6	-0.08	0.85890	-0.19	0.66112	-0.01	0.98178	-0.59	0.18877	
EGJ25333	lmo1797	RpsP	4.2	1.6	12.6	6.9	13.1	10.1	6.9	4.3	3.1	2.6	1.49	0.02918	1.55	0.08060	0.66	0.19400	-0.37	0.41847	2
EGJ25337	lmo1801	Ffh	0.2	0.4	3.6	2.4	4.0	2.9	2.3	2.3	1.7	1.9	2.64	0.01674	2.76	0.02181	2.10	0.06909	1.75	0.09502	3
EGJ25339	lmo1803	FtsY	0.2	0.4	1.0	1.0	1.6	2.0	1.1	1.4	0.6	1.2	1.20	0.08813	1.68	0.13338	1.28	0.17004	0.79	0.39197	3
EGJ25340	lmo1804	Smc	0.3	0.5	0.3	0.7	0.3	0.5	0.3	0.5	1.1	1.0	-0.06	0.92610	-0.03	0.95662	-0.08	0.87514	0.94	0.14006	
EGJ25341	lmo1805	Rnc	0.0	0.0	0.2	0.4	0.9	0.8	1.2	0.9	0.1	0.3	0.45	0.36322	1.44	0.04374	1.75	0.01994	0.35	0.36322	3
EGJ25343	lmo1807	FabG	6.2	3.5	11.0	2.9	7.0	1.2	6.7	2.8	7.5	0.8	0.79	0.02634	0.17	0.59046	0.11	0.78732	0.27	0.38712	
EGJ25344	lmo1808	FabD	5.5	1.3	7.5	3.6	4.1	2.3	3.6	1.8	1.7	2.5	0.43	0.23265	-0.38	0.22989	-0.55	0.06325	-1.42	0.01155	5
EGJ25345	lmo1809	PlsX	0.0	0.0	3.2	1.5	4.1	2.0	3.2	1.4	2.1	2.0	2.87	0.00366	3.20	0.00431	2.90	0.00233	2.40	0.05074	3
EGJ25350	lmo1814	YloV	1.8	1.1	0.1	0.3	0.6	0.5	0.1	0.3	0.2	0.5	-1.88	0.01384	-1.02	0.05567	-1.88	0.01388	-1.73	0.01601	1
EGJ25352	lmo1816	RpmB	1.0	0.0	0.0	0.0	0.1	0.3	0.3	0.5	0.0	0.0	-1.59	0.00000	-1.25	0.00120	-0.93	0.01166	-1.59	0.00000	1
EGJ25354	lmo1818	Rpe	1.5	0.6	3.8	2.7	4.3	2.2	2.5	2.0	2.8	1.2	1.08	0.09777	1.26	0.02334	0.58	0.28865	0.73	0.04538	3
EGJ25356	lmo1820	PrkC	0.2	0.4	1.6	1.6	1.6	1.3	1.5	1.8	2.3	1.8	1.67	0.07494	1.64	0.04795	1.62	0.12586	2.08	0.03577	3
EGJ25357	lmo1821	PrpC	0.2	0.4	1.7	2.2	1.2	1.1	1.2	1.4	0.7	0.8	1.69	0.15260	1.31	0.07266	1.33	0.13921	0.81	0.20140	3
EGJ25359	lmo1823	Fmt	0.3	0.5	2.2	1.0	2.3	1.7	1.0	0.8	0.9	0.8	1.72	0.00378	1.75	0.03517	0.81	0.15540	0.80	0.14408	3
EGJ25361	lmo1825	CoaBC	0.2	0.4	1.4	1.0	1.8	1.4	0.4	0.7	0.5	0.9	1.48	0.03484	1.77	0.03270	0.41	0.51597	0.58	0.44731	2
ScottA	**Other**		**Exp**	**stdev**	**1_d**	**stdev**	**7 d**	**stdev**	**14 d**	**stdev**	**21 d**	**stdev**	**1d/Exp**	**p**	**7**	**p**	**14**	**p**	**21**	**p**	**k-**

Loci	Loci													d/Exp		d/Exp		d/Exp		means group
EGJ25362	lmo1826	RpoZ	0.0	0.0	1.1	1.4	0.5	0.6	0.0	0.0	0.0	0.0	1.69	0.10583	0.99	0.07910	0.00		0.00		2
EGJ25364	lmo1828	YloC	0.0	0.0	0.0	0.0	0.0	0.0	0.6	1.0	1.1	1.0	0.00		0.00		1.08	0.23950	1.68	0.04381	4
EGJ25366	lmo1830		0.3	0.5	2.6	0.7	2.5	1.7	4.1	1.4	4.5	3.5	1.91	0.00011	1.84	0.02968	2.47	0.00072	2.59	0.03158	4
EGJ25383	lmo1847	LpeA	0.2	0.4	9.1	5.5	8.8	3.4	7.3	1.9	5.9	4.7	3.84	0.01048	3.79	0.00144	3.53	0.00017	3.27	0.03057	3
EGJ25385	lmo1849	LpeC	0.0	0.0	3.5	3.3	3.9	3.6	3.7	4.0	3.0	3.5	3.01	0.04789	3.12	0.04669	3.06	0.07426	2.79	0.09291	3
EGJ25386	lmo1850	YpoP	1.0	0.0	0.4	0.6	0.1	0.3	0.0	0.0	0.0	0.0	-0.80	0.03919	-1.25	0.00120	-1.59	0.00000	-1.59	0.00000	1
EGJ25392	lmo1856	DeoD	2.4	0.9	3.9	1.4	4.8	4.6	15.3	7.3	23.7	15.6	0.64	0.04173	0.89	0.25320	2.47	0.00717	3.08	0.02041	4
EGJ25394	lmo1858		0.0	0.0	0.2	0.4	0.3	0.5	0.9	1.1	1.8	0.9	0.38	0.36322	0.72	0.18342	1.50	0.09288	2.17	0.00590	4
EGJ25395	lmo1859	YppQ	0.0	0.0	1.1	1.0	0.3	0.4	0.2	0.4	0.0	0.0	1.68	0.04667	0.62	0.17472	0.40	0.36322	0.00		2
EGJ25404	lmo1868	YetH	1.0	0.0	0.6	0.6	0.2	0.4	0.1	0.3	0.0	0.0	-0.50	0.14700	-1.16	0.00449	-1.25	0.00113	-1.59	0.00000	5
EGJ25407			0.0	0.0	0.4	0.9	0.2	0.4	1.5	1.5	2.0	2.2	0.79	0.36322	0.43	0.36322	1.98	0.06160	2.29	0.08233	4
EGJ25408	lmo1871		0.2	0.4	0.4	0.9	1.4	1.1	0.1	0.3	0.3	0.6	0.37	0.64097	1.51	0.04425	-0.08	0.87064	0.17	0.78681	
EGJ25411	lmo1874	ThyA	1.0	1.6	1.0	1.1	2.6	1.2	0.5	1.0	0.5	0.8	-0.03	0.96474	1.04	0.08162	-0.52	0.56106	-0.54	0.53251	0
EGJ25413	lmo1877		7.6	1.6	15.9	6.7	16.8	4.9	9.1	6.2	7.1	6.4	1.03	0.02803	1.10	0.00428	0.24	0.58773	-0.09	0.86045	2
EGJ25416	lmo1880	YpdQ	0.2	0.4	0.4	0.6	0.1	0.3	0.2	0.5	0.1	0.3	0.38	0.50470	-0.07	0.88287	0.09	0.88224	-0.07	0.88911	
EGJ25422	lmo1886	YpwA	0.2	0.4	0.8	0.8	1.0	0.7	0.5	0.8	0.3	0.4	0.99	0.11745	1.16	0.03282	0.55	0.40290	0.19	0.69989	2
EGJ25423	lmo1887	YpsC	0.0	0.0	0.6	0.6	1.2	1.2	0.1	0.3	0.3	0.7	1.10	0.07613	1.74	0.05592	0.35	0.36322	0.62	0.36322	3
EGJ25424	lmo1888	GpsB	1.2	0.4	4.6	3.9	3.9	1.2	2.9	1.3	2.4	1.9	1.61	0.08345	1.40	0.00203	1.01	0.02094	0.81	0.17297	3
EGJ25432	lmo1896	AsnC	4.7	1.2	4.2	1.9	3.4	1.6	4.0	2.7	3.1	3.8	-0.16	0.57645	-0.42	0.14716	-0.22	0.56236	-0.52	0.37124	
EGJ25433	lmo1897	AspB	1.9	0.8	1.6	1.4	2.4	1.9	1.1	1.2	1.3	1.4	-0.20	0.64654	0.27	0.57036	-0.57	0.23338	-0.42	0.39264	
EGJ25438	lmo1902	PanB	0.2	0.4	1.6	0.8	1.4	0.6	1.3	0.4	0.9	0.5	1.60	0.00559	1.45	0.00342	1.38	0.00101	1.02	0.03369	3
EGJ25442	lmo1906	MgsA	0.0	0.0	0.6	0.9	1.5	2.0	1.5	1.7	1.4	2.2	1.10	0.19584	1.98	0.12475	2.03	0.07276	1.89	0.18536	3
EGJ25443	lmo1907	DapB	0.5	0.9	1.4	1.0	1.6	1.8	1.8	1.1	1.8	1.2	0.87	0.14825	1.05	0.21610	1.14	0.05853	1.16	0.06165	3
EGJ25450	lmo1915	MalS	0.2	0.4	2.5	2.0	2.0	2.6	2.7	3.3	1.8	1.2	2.17	0.03699	1.92	0.14387	2.26	0.12021	1.81	0.01874	3
EGJ25452	lmo1917		8.7	5.9	39.4	10.8	61.0	13.8	39.8	17.3	24.6	27.1	2.12	0.00032	2.75	0.00007	2.14	0.00557	1.46	0.21205	3
EGJ25454	lmo1919	YugP	1.2	1.3	1.9	1.2	3.3	1.4	3.4	0.9	1.9	1.2	0.46	0.38491	1.16	0.01984	1.20	0.00642	0.46	0.38779	3
EGJ25458	lmo1923	AroA	1.2	0.8	0.4	0.6	0.3	0.4	0.0	0.0	0.0	0.0	-0.98	0.06615	-1.13	0.03977	-1.76	0.01511	-1.76	0.01511	1
EGJ25463	lmo1928	AroF	0.7	0.5	0.6	0.7	1.6	1.2	0.6	1.0	0.6	1.2	-0.04	0.93417	0.87	0.11553	-0.11	0.86073	-0.02	0.98292	
EGJ25464	lmo1929	Ndk	4.7	1.6	3.3	3.5	5.4	5.1	11.6	8.6	15.3	11.6	-0.46	0.39196	0.18	0.76399	1.22	0.10615	1.60	0.07659	4
EGJ25469	lmo1934	Hbs	260.6	49.8	217.9	100.8	165.5	66.6	225.4	134.1	335.5	247.3	-0.26	0.38190	-0.65	0.02014	-0.21	0.56762	0.36	0.49751	
EGJ25470	lmo1935		1.5	1.2	2.0	2.6	1.7	1.6	1.2	1.1	1.3	2.1	0.36	0.64773	0.12	0.84363	-0.20	0.70331	-0.12	0.87969	
EGJ25471	lmo1936	GpsA	5.9	0.9	3.0	1.9	5.0	1.0	2.7	2.1	1.5	1.8	-0.86	0.01147	-0.21	0.14788	-0.99	0.01108	-1.66	0.00080	5
EGJ25472	lmo1937	EngA	1.2	0.8	1.3	1.2	2.8	2.5	2.4	1.2	2.1	2.2	0.10	0.84033	0.97	0.18334	0.81	0.06213	0.65	0.36257	
EGJ25473	lmo1938	RpsA	6.3	1.1	16.3	7.6	25.2	13.6	16.5	9.1	10.4	11.3	1.30	0.02325	1.91	0.01902	1.31	0.03984	0.67	0.42193	3
EGJ25474	lmo1939	Cmk	0.5	0.6	0.8	0.9	0.7	0.8	1.1	1.3	0.9	1.2	0.34	0.56491	0.22	0.68861	0.66	0.35097	0.51	0.44150	
EGJ25475	lmo1940	AsnZ	0.3	0.5	0.3	0.4	0.1	0.3	0.3	0.4	0.3	0.7	-0.09	0.85263	-0.39	0.44958	-0.11	0.82898	-0.10	0.87303	
EGJ25480			0.3	0.5	0.6	0.7	1.1	0.9	1.0	1.0	0.3	0.4	0.44	0.42329	0.92	0.11064	0.81	0.23155	-0.10	0.84771	
EGJ25484	lmo1948	ResD	0.4	0.5	2.6	1.7	4.7	2.7	3.0	3.2	3.0	3.6	1.86	0.02288	2.62	0.01012	2.05	0.09354	2.04	0.12856	3
ScottA	**Other**		**Exp**	**stdev**	**1_d**	**stdev**	**7 d**	**stdev**	**14 d**	**stdev**	**21 d**	**stdev**	**1d/Exp**	**p**	**7**	**p**	**14**	**p**	**21**	**p**	**k-**

Loci	Loci														d/Exp		d/Exp		d/Exp		means group
EGJ25489	lmo1953	PupG	8.9	1.0	10.0	5.5	19.7	19.6	31.9	22.0	47.8	38.1	0.17	0.63033	1.11	0.23466	1.79	0.05034	2.37	0.05431	4
EGJ25490	lmo1954	Drm	22.3	4.8	9.3	3.8	12.1	5.0	5.8	3.6	4.1	4.6	-1.22	0.00044	-0.86	0.00451	-1.85	0.00007	-2.31	0.00005	5
EGJ25492	lmo1956	Fur	0.0	0.0	0.4	0.7	1.1	1.8	0.3	0.7	0.3	0.6	0.87	0.19358	1.66	0.19237	0.62	0.36322	0.59	0.36322	3
EGJ25503	lmo1967	YaaN	3.3	2.6	2.3	2.7	4.8	3.7	3.1	3.6	2.4	2.9	-0.43	0.54231	0.48	0.44126	-0.08	0.91477	-0.37	0.59913	
EGJ25505	lmo1976	YqjQ	0.0	0.0	0.3	0.4	1.2	1.2	0.7	0.8	0.5	0.7	0.64	0.17599	1.75	0.05658	1.26	0.08648	1.07	0.10171	3
EGJ25507	lmo1978	Zwf	7.6	3.0	16.2	10.7	14.0	4.7	14.5	8.1	19.7	13.4	1.04	0.10915	0.83	0.02229	0.88	0.09630	1.31	0.07912	4
EGJ25511	lmo1983	IlvD	17.4	2.3	4.6	2.4	3.6	2.0	2.5	2.1	1.8	1.0	-1.80	0.00000	-2.12	0.00000	-2.59	0.00000	-2.99	0.00000	1
EGJ25512	lmo1984	IlvI	2.7	2.2	2.2	1.5	3.2	2.7	2.7	2.8	1.9	2.1	-0.25	0.66287	0.24	0.69674	0.01	0.98281	-0.40	0.55367	
EGJ25513	lmo1985	IlvH	0.9	0.8	0.4	0.7	1.5	1.0	0.3	0.4	0.5	0.8	-0.55	0.34046	0.55	0.25256	-0.81	0.13973	-0.40	0.49255	
EGJ25514	lmo1986	IlvC	7.4	5.6	3.4	3.7	5.7	1.8	2.5	2.2	1.9	2.6	-1.01	0.18079	-0.35	0.50291	-1.40	0.08911	-1.73	0.06425	5
EGJ25515	lmo1987	LeuA	0.0	0.0	2.8	2.5	1.1	1.0	1.2	0.8	1.5	1.1	2.74	0.03712	1.65	0.04954	1.75	0.01768	1.99	0.01858	3
EGJ25516	lmo1988	LeuB	1.7	1.0	0.5	0.6	0.0	0.0	0.0	0.0	0.3	0.7	-1.13	0.04029	-2.13	0.01074	-2.13	0.01074	-1.51	0.02162	1
EGJ25518	lmo1990	LeuD	1.2	1.0	0.1	0.3	0.4	0.4	0.1	0.3	0.0	0.0	-1.39	0.05068	-0.87	0.13127	-1.38	0.05163	-1.73	0.03438	1
EGJ25519	lmo1991	IlvA	1.0	0.6	0.3	0.4	0.4	0.7	0.2	0.4	0.0	0.0	-0.93	0.05104	-0.73	0.14917	-1.18	0.02445	-1.58	0.01234	1
EGJ25520	lmo1992	AlsD	0.2	0.4	1.7	1.5	0.5	0.7	0.7	0.6	0.3	0.7	1.76	0.05177	0.65	0.26265	0.84	0.09583	0.21	0.74238	2
EGJ25521	lmo1993	Pdp	13.6	1.5	7.1	2.6	8.6	3.3	3.2	2.5	3.3	3.7	-0.89	0.00076	-0.63	0.01260	-1.94	0.00002	-1.91	0.00054	5
EGJ25523	lmo1995	DeoC	1.2	1.9	6.6	3.6	5.1	1.9	2.6	2.1	1.1	1.4	2.04	0.01339	1.71	0.00512	0.84	0.26850	-0.14	0.87365	2
EGJ25526	lmo1998	FrlB	3.5	2.8	4.3	2.2	3.4	1.9	3.4	1.6	3.5	0.5	0.27	0.57739	-0.02	0.97092	-0.04	0.93081	0.00	0.99929	
EGJ25527	lmo1999		0.0	0.0	0.6	0.6	1.5	1.7	2.5	2.1	3.6	2.6	1.10	0.07613	1.98	0.08203	2.59	0.03195	3.03	0.02012	4
EGJ25530	lmo2002	LevE	0.7	0.5	0.7	0.6	0.5	0.5	0.1	0.3	0.1	0.3	0.07	0.84759	-0.28	0.50707	-0.86	0.06676	-0.88	0.06035	
EGJ25533	lmo2005	YrpG	0.0	0.0	0.0	0.0	0.7	1.4	1.5	2.3	0.4	0.6	0.00		1.28	0.26305	1.97	0.18051	0.77	0.18126	4
EGJ25534	lmo2006	AlsS	1.3	1.2	6.2	4.3	4.0	1.2	2.6	2.3	1.5	0.8	1.87	0.03722	1.31	0.00272	0.77	0.26993	0.13	0.78458	2
EGJ25535	lmo2007	LplA	0.2	0.4	0.7	1.3	0.1	0.3	0.2	0.4	0.1	0.3	0.85	0.36042	-0.10	0.83674	-0.05	0.92575	-0.12	0.81447	
EGJ25543	lmo2015		0.2	0.4	0.1	0.4	0.3	0.4	0.3	0.5	0.4	0.7	-0.05	0.92593	0.21	0.67401	0.25	0.62445	0.46	0.46686	
EGJ25544	lmo2016	CspB	182.5	46.2	45.0	23.2	30.0	19.0	39.6	21.9	26.5	30.1	-2.01	0.00027	-2.58	0.00018	-2.19	0.00022	-2.76	0.00009	1
EGJ25546	lmo2018	DapF	1.2	0.7	0.5	0.5	1.5	0.8	1.2	1.5	0.7	1.0	-0.80	0.08573	0.24	0.52979	0.00	0.99475	-0.54	0.34236	
EGJ25547	lmo2019	IleS	11.7	1.8	7.9	4.7	11.1	3.7	7.4	4.5	4.9	5.2	-0.54	0.10922	-0.08	0.71339	-0.62	0.07188	-1.17	0.02185	5
EGJ25548	lmo2020	DivIVA	7.2	1.2	7.1	2.8	10.4	4.0	7.9	5.5	7.5	6.8	-0.03	0.90685	0.49	0.11955	0.12	0.78190	0.05	0.92740	
EGJ25577	lmo2032	FtsZ	4.2	0.8	7.0	2.4	10.0	2.6	5.2	3.9	4.7	4.5	0.67	0.03798	1.16	0.00210	0.27	0.58036	0.14	0.81014	0
EGJ25578	lmo2033	FtsA	2.4	0.6	6.6	2.4	6.0	2.7	5.9	4.4	3.6	4.3	1.31	0.00681	1.18	0.02227	1.16	0.10639	0.52	0.51693	3
EGJ25580	lmo2035	MurG	0.0	0.0	1.7	1.6	1.4	1.5	2.2	1.7	1.0	1.1	2.13	0.05074	1.91	0.07065	2.43	0.02663	1.54	0.08027	3
EGJ25581	lmo2036	MurD	1.2	1.3	2.6	1.8	2.6	0.8	1.7	0.6	0.8	1.0	0.91	0.14571	0.91	0.05043	0.39	0.42040	-0.34	0.62231	
EGJ25586	lmo2041	RsmH	0.3	0.5	0.5	0.5	0.4	0.7	0.8	1.0	0.3	0.7	0.23	0.65313	0.16	0.78614	0.66	0.32877	-0.12	0.84964	
EGJ25611	lmo2067	YxeI	0.0	0.0	6.2	3.2	9.5	8.0	3.7	1.1	3.8	3.1	3.74	0.00503	4.32	0.03297	3.06	0.00053	3.10	0.02910	3
EGJ25612	lmo2068	GroEL	192.8	23.8	308.6	100.0	432.5	43.1	517.8	53.4	495.3	101.7	0.68	0.03562	1.16	0.00000	1.42	0.00000	1.36	0.00056	4
EGJ25613	lmo2069	GroES	49.1	13.2	60.6	11.9	81.2	18.9	81.9	20.6	59.2	12.5	0.30	0.14428	0.72	0.00790	0.73	0.01011	0.27	0.20490	
EGJ25616	lmo2072	YdiH	4.0	0.9	2.2	1.8	3.7	1.8	2.3	2.1	1.5	1.7	-0.73	0.06664	-0.09	0.74635	-0.71	0.10721	-1.18	0.01295	5
EGJ25619	lmo2075	Gcp	0.0	0.0	0.1	0.3	1.0	0.6	0.0	0.0	0.4	0.7	0.34	0.36322	1.62	0.00844	0.00		0.84	0.20741	
ScottA	**Other**		**Exp**	**stdev**	**1_d**	**stdev**	**7 d**	**stdev**	**14 d**	**stdev**	**21 d**	**stdev**	**1d/Exp**	**p**	**7**	**p**	**14**	**p**	**21**	**p**	**k-**

Loci	Loci														d/Exp		d/Exp		d/Exp		means group
EGJ25633	lmo2089		0.7	0.5	5.2	3.5	9.1	5.0	5.3	3.1	3.2	4.3	2.26	0.02505	3.03	0.00860	2.29	0.01469	1.65	0.21524	3
EGJ25638	lmo2094		0.0	0.0	0.0	0.0	0.6	0.6	1.1	1.5	0.9	1.5	0.00		1.07	0.07607	1.70	0.12481	1.46	0.21301	4
EGJ25645	lmo2101	PdxS	0.0	0.0	3.3	2.4	2.4	1.2	2.2	0.7	2.4	1.1	2.92	0.02135	2.51	0.00442	2.42	0.00064	2.53	0.00378	3
EGJ25647	lmo2103	EutD	25.1	5.1	23.2	7.6	14.2	3.8	16.7	6.0	17.2	7.3	-0.11	0.62204	-0.80	0.00224	-0.57	0.02619	-0.54	0.05662	
EGJ25655	lmo2110	YvyI	3.1	1.9	7.0	2.5	8.4	2.8	4.7	3.6	2.5	3.1	1.08	0.01269	1.32	0.00412	0.55	0.34857	-0.24	0.72304	2
EGJ25656	lmo2111	YcnD	0.3	0.5	0.2	0.4	0.1	0.3	0.1	0.3	0.3	0.6	-0.35	0.50780	-0.39	0.45189	-0.39	0.45228	-0.13	0.82970	
EGJ25658	lmo2113	YwfI	1.0	0.6	2.8	1.0	4.6	4.3	10.3	7.6	12.9	8.8	1.14	0.00496	1.76	0.09668	2.84	0.03082	3.15	0.02114	4
EGJ25659	lmo2114	YxdL	2.7	0.9	1.5	1.0	3.0	1.0	3.0	1.9	1.5	1.1	-0.69	0.04937	0.15	0.54705	0.14	0.70984	-0.65	0.07279	
EGJ25663	lmo2118	GlmM	6.3	1.0	6.7	3.3	4.6	3.9	5.6	5.4	4.5	5.0	0.07	0.80582	-0.43	0.33322	-0.16	0.76387	-0.46	0.41443	
EGJ25679	lmo2133	IolJ	0.0	0.0	0.0	0.0	0.2	0.5	0.5	0.8	1.0	1.3	0.00		0.47	0.36322	1.00	0.18186	1.59	0.11492	4
EGJ25700	lmo2154	NrdF	1.3	1.0	0.0	0.0	0.7	1.3	0.1	0.3	0.0	0.0	-1.86	0.02511	-0.59	0.37553	-1.51	0.03561	-1.86	0.02511	1
EGJ25701	lmo2155	NrdE	4.9	2.2	1.8	1.8	3.6	1.3	2.2	0.6	1.0	0.9	-1.19	0.02806	-0.38	0.27187	-0.99	0.03266	-1.82	0.00666	5
EGJ25704	lmo2158	CsbD	0.0	0.0	9.1	11.3	2.8	4.3	8.2	16.0	12.7	10.7	4.26	0.10749	2.73	0.16678	4.12	0.26491	4.72	0.03377	4
EGJ25706	lmo2160	YfiH	0.0	0.0	0.4	0.9	2.0	2.3	1.7	3.1	3.0	5.2	0.79	0.36322	2.34	0.08170	2.12	0.23630	2.82	0.21433	4
EGJ25714	lmo2168	GloA	0.0	0.0	0.0	0.0	1.1	1.4	1.0	2.0	2.0	3.3	0.00		1.68	0.11144	1.63	0.25949	2.31	0.20211	4
EGJ25716	lmo2170		0.8	1.3	0.3	0.5	0.4	1.0	1.9	2.5	2.9	1.5	-0.76	0.37559	-0.57	0.53073	0.86	0.37504	1.34	0.03105	4
EGJ25725	lmo2179		0.5	0.6	0.2	0.5	0.3	0.5	1.0	1.3	0.4	1.0	-0.52	0.33951	-0.30	0.55578	0.58	0.41363	-0.16	0.82953	
EGJ25726			0.0	0.0	0.7	0.6	1.1	0.7	0.7	0.8	0.7	0.8	1.26	0.02817	1.70	0.01135	1.30	0.08455	1.22	0.09112	3
EGJ25735	lmo2188	PepF	3.6	2.1	7.5	6.6	4.5	1.9	3.6	2.2	2.6	1.3	0.98	0.21380	0.30	0.42975	0.02	0.96561	-0.41	0.35032	
EGJ25739	lmo2192	OppF	2.2	0.7	4.4	1.8	10.3	1.3	8.1	2.6	5.1	2.5	0.89	0.02793	2.01	0.00000	1.69	0.00205	1.06	0.03542	3
EGJ25740	lmo2193	OppD	1.8	0.9	2.5	2.1	6.8	1.6	9.5	2.8	6.2	2.8	0.35	0.51730	1.65	0.00018	2.11	0.00063	1.54	0.00993	4
EGJ25741	lmo2194	OppC	2.2	0.4	2.2	1.6	4.6	3.2	5.3	1.9	3.3	1.2	0.03	0.93652	0.93	0.12894	1.12	0.00819	0.49	0.07168	4
EGJ25742	lmo2195	OppB	3.5	2.4	0.8	0.9	2.9	2.4	2.0	1.3	1.9	1.6	-1.66	0.03598	-0.21	0.69675	-0.70	0.20136	-0.72	0.20833	1
EGJ25743	lmo2196	DppE	203.2	21.0	162.5	62.6	89.7	8.4	127.3	27.2	139.5	48.6	-0.32	0.18135	-1.18	0.00001	-0.67	0.00037	-0.54	0.02219	1
EGJ25745	lmo2198	TrpS	1.0	0.9	4.0	4.5	2.5	2.3	1.9	1.5	1.5	1.7	1.60	0.15895	0.98	0.18868	0.70	0.22811	0.44	0.51283	2
EGJ25748	lmo2201	FabF	11.4	2.2	15.5	3.4	13.4	3.3	9.2	4.0	6.0	5.3	0.43	0.03380	0.23	0.22921	-0.30	0.27143	-0.87	0.05716	
EGJ25749	lmo2202	FabH	7.3	2.8	8.9	4.5	6.0	2.7	4.2	2.4	2.7	3.3	0.28	0.46220	-0.25	0.44342	-0.74	0.06498	-1.29	0.02669	5
EGJ25752	lmo2205	GpmA	2.5	0.8	22.5	5.8	24.7	5.2	16.9	5.2	15.0	5.5	2.94	0.00032	3.07	0.00011	2.53	0.00094	2.36	0.00241	3
EGJ25753	lmo2206	ClpC	7.6	2.9	42.2	17.7	39.3	5.7	31.4	7.5	24.9	15.8	2.39	0.00453	2.29	0.00000	1.97	0.00026	1.64	0.04336	3
EGJ25758	lmo2211	HemH	5.2	1.2	2.2	2.3	4.2	2.4	2.1	1.9	1.7	2.7	-1.07	0.02259	-0.29	0.38258	-1.16	0.00773	-1.37	0.02193	1
EGJ25759	lmo2212	HemE	1.2	0.5	0.8	0.7	1.3	0.9	0.7	0.6	0.4	0.7	-0.36	0.32327	0.13	0.70941	-0.51	0.13281	-0.90	0.04204	
EGJ25760	lmo2213	YhgC	0.2	0.4	4.1	1.3	4.7	3.2	4.0	3.1	3.5	3.9	2.78	0.00040	2.96	0.01856	2.74	0.02877	2.58	0.09207	3
EGJ25762	lmo2215	EcsA	0.0	0.0	0.3	0.4	1.2	0.8	0.9	0.8	0.3	0.4	0.64	0.17599	1.74	0.01674	1.51	0.03682	0.63	0.17615	3
EGJ25763	lmo2216	HinT	1.2	1.1	1.1	1.0	0.9	0.9	0.7	0.8	0.7	0.8	-0.08	0.87982	-0.30	0.58121	-0.49	0.39207	-0.45	0.42789	
EGJ25764	lmo2217	YhaH	0.7	0.8	1.3	0.5	3.4	2.7	4.2	1.6	5.2	0.9	0.64	0.13009	1.75	0.05172	2.01	0.00144	2.29	0.00000	4
EGJ25766	lmo2219	PrsA2	1.0	1.3	6.5	2.7	5.0	2.1	3.0	2.3	1.0	1.0	2.21	0.00264	1.85	0.00422	1.22	0.09544	-0.06	0.93235	2
EGJ25771	lmo2223	YheA	2.7	0.8	9.0	6.5	7.1	3.7	3.9	2.7	4.5	5.0	1.58	0.06321	1.27	0.03006	0.47	0.33105	0.65	0.42377	2
EGJ25784			0.2	0.4	0.5	0.6	0.2	0.4	0.1	0.3	0.1	0.4	0.61	0.26047	0.01	0.98528	-0.07	0.88797	-0.04	0.93205	
ScottA	**Other**		**Exp**	**stdev**	**1_d**	**stdev**	**7 d**	**stdev**	**14 d**	**stdev**	**21 d**	**stdev**	**1d/Exp**	**p**	**7**	**p**	**14**	**p**	**21**	**p**	**k-**

Loci	Loci														d/Exp		d/Exp		d/Exp		means group
EGJ25831	lmo2248	YkaA	14.3	3.6	9.0	6.2	9.4	7.3	7.6	2.6	4.9	1.8	-0.65	0.10521	-0.58	0.17898	-0.88	0.00487	-1.47	0.00060	5
EGJ25839	lmo2256	YraA	4.1	2.5	8.1	5.8	16.2	16.9	19.1	15.7	41.2	39.6	0.90	0.16934	1.86	0.14010	2.09	0.06655	3.18	0.07034	4
EGJ25851	lmo2268	AddB	0.2	0.4	0.1	0.4	0.1	0.3	0.3	0.7	0.3	0.5	-0.05	0.92528	-0.07	0.88813	0.21	0.75132	0.32	0.56631	
EGJ25855	lmo2335	FruA	2.5	0.9	13.7	15.8	15.0	16.1	11.3	12.8	11.1	12.3	2.22	0.14559	2.35	0.11594	1.97	0.15333	1.94	0.14841	3
EGJ25856	lmo2336	FruK	29.3	3.9	21.5	7.7	15.4	5.5	12.2	3.3	11.1	3.0	-0.44	0.06040	-0.90	0.00070	-1.23	0.00001	-1.36	0.00001	5
EGJ25857	lmo2337	FruR	0.5	0.6	0.4	1.0	0.1	0.3	0.6	0.7	0.3	0.4	-0.17	0.80677	-0.66	0.19820	0.14	0.78326	-0.40	0.40908	
EGJ25858	lmo2338		0.0	0.0	1.0	1.1	3.0	2.5	0.9	0.9	0.5	0.5	1.58	0.08018	2.80	0.03129	1.48	0.06583	0.97	0.08413	3
EGJ25859	lmo2340	PscG	2.6	1.6	2.8	2.3	4.6	1.0	5.0	2.6	2.7	1.7	0.06	0.91089	0.71	0.02868	0.81	0.09045	0.03	0.94170	
EGJ25877	lmo2358	NagB	0.2	0.4	0.7	1.1	1.3	1.3	0.0	0.0	0.7	0.8	0.85	0.27993	1.40	0.08412	-0.45	0.36322	0.82	0.21547	
EGJ25879	lmo2360		1.2	0.8	39.5	23.3	0.1	0.3	0.4	0.6	0.5	0.6	4.56	0.01014	-1.42	0.02086	-0.96	0.06975	-0.70	0.14913	2
EGJ25880	lmo2361	IscR	0.0	0.0	2.5	1.4	2.5	0.9	2.5	1.5	1.9	1.7	2.60	0.00672	2.60	0.00125	2.57	0.00958	2.27	0.03841	3
EGJ25883	lmo2363	GadB1	0.0	0.0	4.2	2.3	6.4	3.2	3.5	2.7	1.1	1.2	3.22	0.00648	3.78	0.00458	2.99	0.02733	1.68	0.08346	3
EGJ25886	lmo2367	Pgi	64.6	5.0	66.0	19.0	73.8	41.4	122.5	51.1	128.8	48.6	0.03	0.86475	0.19	0.60813	0.92	0.03875	0.99	0.02272	
EGJ25888	lmo2369	YugI	0.7	0.5	1.0	0.9	0.1	0.3	0.9	1.0	0.3	0.6	0.38	0.45114	-0.86	0.06603	0.26	0.64411	-0.61	0.25131	
EGJ25890	lmo2371		0.2	0.4	1.3	1.6	2.2	1.2	1.1	1.0	0.4	0.5	1.39	0.15625	2.02	0.00660	1.27	0.07493	0.45	0.35044	3
EGJ25891	lmo2372		0.3	0.5	0.9	0.9	0.6	0.8	0.8	0.7	0.4	0.9	0.69	0.27801	0.40	0.51192	0.59	0.24496	0.07	0.92960	
EGJ25892	lmo2373	LicB	3.9	1.2	6.7	1.0	3.8	1.5	3.5	1.3	3.2	2.6	0.72	0.00159	-0.01	0.98412	-0.13	0.62552	-0.24	0.59367	
EGJ25904	lmo2376	PpiB	4.4	1.3	3.8	2.7	2.7	2.2	2.4	1.4	1.5	1.7	-0.19	0.64475	-0.60	0.14203	-0.75	0.02793	-1.28	0.00774	5
EGJ25918	lmo2389	YumB	6.9	2.2	7.2	3.8	11.3	9.6	6.1	4.6	4.7	5.4	0.06	0.86919	0.67	0.32229	-0.15	0.73608	-0.50	0.39779	
EGJ25920	lmo2391	YhfK	0.0	0.0	3.8	1.6	4.5	2.5	2.6	1.5	2.4	2.1	3.12	0.00177	3.32	0.00655	2.62	0.00796	2.52	0.03675	3
EGJ25932	lmo2406	YunF	0.2	0.4	0.2	0.4	0.8	0.4	0.8	0.7	0.7	0.8	0.03	0.95187	0.98	0.02277	0.92	0.10280	0.81	0.21080	
EGJ25935	lmo2411	SufB	6.4	1.8	4.1	2.8	6.8	4.2	6.9	4.0	6.1	1.5	-0.59	0.12500	0.09	0.81890	0.10	0.78834	-0.06	0.75436	
EGJ25937	lmo2413	SufS	2.2	2.1	0.0	0.0	0.4	0.9	0.2	0.5	0.3	0.5	-2.45	0.04678	-1.62	0.08871	-1.94	0.06319	-1.71	0.07628	1
EGJ25938	lmo2414	SufD	6.9	2.1	2.4	1.0	8.0	6.6	8.4	7.8	7.4	5.5	-1.37	0.00187	0.21	0.69900	0.26	0.66806	0.10	0.83668	1
EGJ25939	lmo2415	SufC	5.4	2.7	5.9	4.3	4.9	2.4	1.8	2.3	0.5	0.5	0.11	0.82050	-0.13	0.72774	-1.39	0.03041	-2.60	0.00571	5
EGJ25941	lmo2417	MetN	1.4	1.5	4.5	1.5	3.0	2.8	4.5	2.6	3.6	2.0	1.42	0.00493	0.92	0.23675	1.44	0.03337	1.13	0.06109	3
EGJ25949	lmo2425	YusH	0.8	0.8	3.3	3.1	3.2	1.0	3.0	2.2	1.4	1.3	1.49	0.11366	1.46	0.00121	1.40	0.06265	0.54	0.36344	3
EGJ25950	lmo2426	YusI	1.8	1.2	2.5	2.8	0.7	1.1	0.6	1.0	0.0	0.0	0.35	0.61619	-0.95	0.11498	-1.16	0.06543	-2.23	0.01113	5
EGJ25957	lmo2433	YeiG	0.2	0.4	0.9	1.5	1.6	2.2	0.0	0.0	0.0	0.0	1.08	0.27440	1.68	0.15732	-0.42	0.36322	-0.42	0.36322	0
EGJ25958	lmo2434	GadB2	0.2	0.4	2.9	2.1	2.5	1.0	1.2	0.8	0.9	1.4	2.35	0.02606	2.20	0.00124	1.41	0.01833	1.10	0.26018	3
EGJ25971	lmo2446		0.2	0.4	0.3	0.5	0.3	0.5	0.3	0.7	0.5	0.7	0.33	0.54144	0.32	0.54757	0.26	0.70827	0.55	0.39354	
EGJ25974	lmo2449	Rnr	1.5	1.1	0.8	0.8	0.3	0.7	0.8	0.7	0.9	0.7	-0.59	0.26420	-1.39	0.04603	-0.67	0.19330	-0.56	0.26497	1
EGJ25976	lmo2451	SecG	1.0	0.6	0.2	0.4	0.1	0.3	0.3	0.5	0.0	0.0	-1.13	0.03201	-1.24	0.02104	-0.91	0.05762	-1.58	0.01280	1
EGJ25980	lmo2455	Eno	587.5	37.8	460.0	33.6	589.2	315.8	887.9	303.9	1035.2	273.3	-0.35	0.00011	0.00	0.98999	0.60	0.05988	0.82	0.00981	
EGJ25981	lmo2456	Pgm	28.5	5.5	26.9	14.5	26.4	4.4	20.5	10.6	13.4	13.2	-0.08	0.80648	-0.11	0.48835	-0.47	0.14173	-1.06	0.03810	5
EGJ25982	lmo2457	TpiA	30.0	5.7	52.8	31.5	33.4	17.0	26.8	6.1	31.3	3.6	0.81	0.13708	0.15	0.65998	-0.16	0.36507	0.06	0.63204	
EGJ25983	lmo2458	Pgk	180.4	21.7	126.8	29.2	76.7	10.5	49.2	8.6	34.2	22.8	-0.51	0.00547	-1.23	0.00001	-1.86	0.00000	-2.38	0.00000	5
EGJ25984	lmo2459	Gap	526.8	29.9	345.2	79.3	468.8	215.5	339.8	85.1	409.8	178.3	-0.61	0.00158	-0.17	0.54169	-0.63	0.00205	-0.36	0.17067	
ScottA	**Other**		**Exp**	**stdev**	**1_d**	**stdev**	**7 d**	**stdev**	**14 d**	**stdev**	**21 d**	**stdev**	**1d/Exp**	**p**	**7**	**p**	**14**	**p**	**21**	**p**	**k-**

Loci	Loci														d/Exp		d/Exp		d/Exp		means group
EGJ25985	lmo2460	CggR	0.3	0.5	0.3	0.5	1.8	1.4	0.6	1.0	0.4	1.0	-0.03	0.95544	1.48	0.04514	0.37	0.61574	0.13	0.86877	0
EGJ25987	lmo2462		0.0	0.0	1.8	1.8	1.6	1.3	0.7	1.0	0.7	0.8	2.21	0.05970	2.07	0.02831	1.24	0.14443	1.23	0.08831	3
EGJ25993	lmo2468	ClpP	7.3	2.5	16.2	5.5	32.8	24.4	47.4	36.1	61.7	55.4	1.11	0.00841	2.10	0.05018	2.63	0.04125	3.00	0.06116	4
EGJ25996	lmo2471	YqjM	1.5	1.0	4.2	2.4	7.0	4.2	8.0	4.6	6.8	1.9	1.23	0.03944	1.89	0.02397	2.08	0.01724	1.87	0.00037	3
EGJ25999	lmo2474	YvcJ	0.0	0.0	1.5	1.6	2.0	1.3	1.1	1.3	1.7	2.2	1.97	0.07235	2.33	0.01144	1.72	0.08565	2.16	0.11310	3
EGJ26000	lmo2475	PgcA	6.4	2.6	10.2	4.0	8.6	4.3	6.6	4.4	4.5	5.1	0.62	0.09209	0.40	0.31824	0.04	0.92378	-0.48	0.42838	
EGJ26002	lmo2477	GalE	3.0	1.5	2.6	1.9	2.4	1.6	1.7	1.6	1.2	0.9	-0.21	0.63464	-0.30	0.48545	-0.66	0.17769	-1.04	0.03625	5
EGJ26003	lmo2478	TrxB	2.0	1.0	2.1	1.1	1.9	1.3	1.7	2.1	1.4	1.7	0.04	0.90355	-0.08	0.84612	-0.23	0.69965	-0.45	0.41550	
EGJ26006	lmo2481	HprP	0.4	0.5	0.1	0.3	1.1	1.5	0.3	0.7	0.0	0.0	-0.43	0.41919	0.95	0.27402	-0.14	0.82883	-0.77	0.17497	
EGJ26008	lmo2483	HprK	0.2	0.4	1.2	1.2	1.3	1.1	0.6	0.7	0.7	0.8	1.38	0.08433	1.45	0.04720	0.75	0.21434	0.82	0.20174	3
EGJ26012	lmo2487	YvlB	0.2	0.4	3.8	2.2	9.3	3.6	7.7	2.5	5.6	4.9	2.71	0.00830	3.89	0.00156	3.62	0.00057	3.20	0.04215	3
EGJ26013	lmo2488	UvrA	0.5	0.8	1.5	1.2	2.2	1.3	1.0	1.0	0.7	0.8	1.01	0.11434	1.40	0.03031	0.55	0.38913	0.21	0.74177	3
EGJ26016	lmo2491		0.0	0.0	0.3	0.5	0.9	1.1	4.2	2.2	5.2	2.3	0.74	0.17715	1.45	0.10656	3.24	0.00497	3.52	0.00267	4
EGJ26024	lmo2499	PstS	0.0	0.0	1.9	3.3	0.7	0.8	0.4	0.7	0.7	1.0	2.27	0.20959	1.30	0.08045	0.89	0.19178	1.27	0.15426	3
EGJ26027	lmo2502	MinJ	0.2	0.4	0.9	1.0	0.5	0.7	0.3	0.4	0.1	0.3	1.05	0.15331	0.54	0.40064	0.22	0.64890	-0.05	0.91364	2
EGJ26029	lmo2504	EnvC	0.2	0.4	0.1	0.4	0.1	0.3	1.1	1.5	0.2	0.5	-0.05	0.91923	-0.07	0.88222	1.29	0.18304	0.07	0.90115	4
EGJ26030	lmo2505	Spl	0.0	0.0	6.2	2.5	12.5	8.2	25.2	18.9	43.9	38.9	3.75	0.00165	4.70	0.01358	5.68	0.02237	6.47	0.03973	4
EGJ26032	lmo2507	FtsE	0.7	0.5	1.0	1.2	2.6	2.3	0.6	1.0	0.8	1.2	0.38	0.53939	1.41	0.09110	-0.07	0.91008	0.14	0.83191	0
EGJ26035	lmo2510	SecA	1.3	1.0	3.7	3.3	5.9	2.7	3.8	2.9	2.8	3.6	1.22	0.13924	1.83	0.00639	1.25	0.09386	0.87	0.36238	3
EGJ26036	lmo2511	YvyD	7.3	2.5	21.5	4.7	26.1	4.9	21.7	7.5	17.9	10.7	1.50	0.00023	1.77	0.00005	1.51	0.00408	1.24	0.05874	3
EGJ26040	lmo2515	DegU	0.2	0.4	1.8	2.6	2.2	2.6	2.2	2.6	2.0	2.8	1.80	0.17864	1.99	0.11952	2.03	0.11208	1.89	0.17189	3
EGJ26049	lmo2524	FabZ	0.2	0.4	0.2	0.4	0.5	1.0	1.2	2.0	1.4	2.8	0.05	0.93174	0.65	0.41268	1.35	0.26473	1.56	0.31356	4
EGJ26050	lmo2525	Mbl	8.0	1.3	4.6	3.0	10.0	3.0	6.0	4.2	4.9	5.7	-0.74	0.03816	0.30	0.18862	-0.39	0.30246	-0.65	0.24569	
EGJ26051	lmo2526	MurAA	3.1	1.6	0.4	0.6	0.9	1.1	0.5	0.7	0.5	0.8	-2.04	0.00732	-1.34	0.02368	-1.90	0.00828	-1.82	0.00909	1
EGJ26053	lmo2528	AtpC	2.4	0.9	1.7	0.7	5.4	2.0	6.2	2.9	5.8	2.0	-0.37	0.18736	1.05	0.01147	1.24	0.02111	1.14	0.00606	4
EGJ26054	lmo2529	AtpD	16.1	2.5	55.2	26.8	88.2	22.9	121.6	20.1	125.7	29.2	1.75	0.01585	2.42	0.00054	2.88	0.00004	2.93	0.00024	4
EGJ26055	lmo2530	AtpG	2.2	0.4	3.6	1.1	6.2	1.3	6.6	1.4	7.0	1.6	0.60	0.02835	1.32	0.00045	1.41	0.00038	1.50	0.00055	
EGJ26056	lmo2531	AtpA	14.3	2.8	35.8	14.2	39.5	7.7	61.2	6.5	62.5	10.5	1.29	0.01303	1.44	0.00022	2.06	0.00000	2.09	0.00005	4
EGJ26057	lmo2532	AtpH	0.0	0.0	0.2	0.4	4.0	3.2	5.2	3.7	3.9	2.4	0.45	0.36322	3.17	0.02910	3.50	0.01824	3.14	0.01043	4
EGJ26058	lmo2533	AtpF	1.4	0.9	5.9	4.2	6.9	2.1	7.7	3.0	5.6	3.2	1.78	0.04500	2.00	0.00059	2.15	0.00269	1.71	0.02140	3
EGJ26063	lmo2538	Upp	9.0	2.1	13.1	5.1	13.3	5.0	10.9	5.0	9.8	2.6	0.52	0.11138	0.54	0.09475	0.26	0.41511	0.11	0.59616	
EGJ26064	lmo2539	GlyA	2.2	0.7	2.4	2.3	2.2	1.7	1.0	1.1	0.8	1.4	0.11	0.84015	0.01	0.97633	-0.87	0.04993	-1.03	0.06235	5
EGJ26068	lmo2543	PrfA	0.8	0.4	0.6	0.5	2.3	1.5	0.6	0.8	0.3	0.6	-0.22	0.49894	1.09	0.05219	-0.24	0.57438	-0.82	0.09030	0
EGJ26070	lmo2545	ThrB	0.2	0.4	0.8	1.0	0.8	1.0	0.3	0.6	0.5	0.8	0.93	0.20003	0.99	0.19493	0.36	0.52206	0.64	0.35519	
EGJ26071	lmo2546	ThrC	13.9	2.0	14.0	7.2	12.0	5.2	13.3	7.9	11.4	3.5	0.01	0.98220	-0.20	0.43567	-0.07	0.85082	-0.28	0.16835	
EGJ26072	lmo2547	Hom	1.8	1.5	5.1	2.5	4.3	2.6	3.4	2.3	3.3	3.0	1.29	0.02263	1.07	0.07811	0.76	0.18989	0.73	0.30861	3
EGJ26073	lmo2548	RpmE	7.2	1.3	13.2	5.2	9.9	4.0	10.0	6.5	8.7	8.4	0.83	0.03456	0.43	0.16849	0.44	0.35180	0.25	0.69143	
EGJ26080	lmo2556	FbaA	219.4	19.1	117.9	51.0	71.4	17.9	50.0	18.0	39.6	7.3	-0.89	0.00327	-1.61	0.00000	-2.12	0.00000	-2.46	0.00000	5
ScottA	**Other**		**Exp**	**stdev**	**1_d**	**stdev**	**7 d**	**stdev**	**14 d**	**stdev**	**21 d**	**stdev**	**1d/Exp**	**p**	**7**	**p**	**14**	**p**	**21**	**p**	**k-**

Loci	Loci														d/Exp		d/Exp		d/Exp		means group
EGJ26082	lmo2558	Ami	0.0	0.0	0.5	1.0	1.6	1.2	4.8	4.1	5.9	4.4	1.06	0.22386	2.10	0.02291	3.42	0.03434	3.67	0.02180	4
EGJ26083	lmo2559	PyrG	16.1	2.6	8.5	1.8	10.3	3.2	5.9	4.3	4.8	4.6	-0.88	0.00025	-0.62	0.00650	-1.38	0.00093	-1.63	0.00079	5
EGJ26084	lmo2560	RpoE	4.7	1.3	1.0	0.7	1.9	2.0	1.9	1.1	1.2	1.0	-1.76	0.00043	-1.10	0.02237	-1.11	0.00300	-1.61	0.00057	1
EGJ26085	lmo2561	ArgS	6.7	1.7	7.0	5.8	4.5	1.5	3.5	1.6	2.6	1.5	0.05	0.91513	-0.55	0.03269	-0.87	0.00644	-1.21	0.00138	5
EGJ26088	lmo2564	YwhB	0.0	0.0	0.0	0.0	0.2	0.5	1.2	1.9	1.6	2.5	0.00		0.46	0.36322	1.77	0.17516	2.09	0.17469	4
EGJ26121	lmo2596	RpsI	39.6	5.3	18.0	7.7	15.8	10.4	11.9	5.8	12.4	4.5	-1.12	0.00033	-1.29	0.00135	-1.69	0.00001	-1.63	0.00000	1
EGJ26122	lmo2597	RplM	7.1	2.3	9.2	4.2	12.9	3.4	10.1	2.9	5.7	1.9	0.35	0.31503	0.82	0.00731	0.48	0.07277	-0.28	0.29218	
EGJ26130	lmo2605	RplQ	21.0	9.1	10.6	4.9	9.1	2.6	11.5	4.0	9.2	4.1	-0.96	0.04026	-1.16	0.02287	-0.84	0.05256	-1.15	0.02357	1
EGJ26131	lmo2606	RpoA	37.4	3.7	15.1	3.4	15.2	7.0	11.6	4.9	10.6	7.4	-1.28	0.00000	-1.27	0.00017	-1.65	0.00000	-1.78	0.00008	1
EGJ26132	lmo2607	RpsK	8.7	2.9	11.5	4.0	12.0	6.5	9.8	5.5	8.8	5.5	0.38	0.20620	0.44	0.29843	0.16	0.67298	0.01	0.97800	
EGJ26133	lmo2608	RpsM	3.0	1.0	12.2	6.4	9.1	2.7	9.5	4.1	8.2	4.4	1.84	0.01646	1.44	0.00170	1.50	0.01058	1.30	0.03239	3
EGJ26134	lmo2609	RpmJ	2.8	1.1	1.7	1.2	3.8	1.9	2.5	1.8	2.2	1.0	-0.58	0.12377	0.36	0.31892	-0.15	0.70107	-0.31	0.31108	
EGJ26135	lmo2610	InfA	1.2	1.4	2.5	2.2	2.4	1.6	2.6	2.5	2.8	2.3	0.83	0.24235	0.76	0.20388	0.88	0.26163	0.97	0.17476	
EGJ26136	lmo2611	Adk	8.9	1.7	16.3	4.3	10.7	4.0	6.6	2.5	6.0	4.2	0.84	0.00673	0.25	0.34888	-0.41	0.08942	-0.53	0.16152	
EGJ26138	lmo2613	RplO	35.0	10.4	18.5	5.7	11.0	2.8	12.8	4.5	9.4	1.3	-0.90	0.00986	-1.62	0.00188	-1.42	0.00215	-1.84	0.00169	1
EGJ26139	lmo2614	RpmD	1.3	0.8	5.1	4.3	1.9	1.3	4.0	2.6	3.6	1.6	1.62	0.08521	0.41	0.35996	1.29	0.05488	1.15	0.01754	3
EGJ26140	lmo2615	RpsE	13.5	2.9	12.4	9.3	14.3	8.9	10.4	4.7	11.0	5.5	-0.12	0.78421	0.07	0.85331	-0.37	0.19708	-0.29	0.34565	
EGJ26141	lmo2616	RplR	12.6	4.0	5.9	3.5	5.7	2.9	5.0	2.0	3.2	2.0	-1.04	0.01141	-1.09	0.00718	-1.25	0.00373	-1.84	0.00110	1
EGJ26142	lmo2617	RplF	26.6	9.5	37.8	6.1	25.4	4.4	26.9	5.1	21.6	3.1	0.50	0.04004	-0.07	0.78746	0.01	0.96229	-0.29	0.26522	
EGJ26143	lmo2618	RpsH	49.7	17.8	17.1	8.4	17.6	14.8	13.9	10.0	11.4	9.1	-1.51	0.00464	-1.47	0.00718	-1.80	0.00272	-2.08	0.00189	1
EGJ26144	lmo2619	RpsN	3.2	0.8	1.6	0.8	2.2	1.9	1.4	0.9	1.0	0.8	-0.79	0.00745	-0.47	0.27445	-0.97	0.00543	-1.34	0.00085	
EGJ26145	lmo2620	RplE	53.5	3.4	48.0	19.7	22.9	7.2	17.2	4.4	16.0	4.3	-0.16	0.52557	-1.20	0.00003	-1.61	0.00000	-1.71	0.00000	5
EGJ26146	lmo2621	RplX	2.7	1.1	3.6	2.7	5.2	2.0	6.5	1.5	5.5	2.8	0.39	0.43775	0.87	0.02478	1.15	0.00057	0.92	0.05896	4
EGJ26147	lmo2622	RplN	3.0	0.9	7.9	4.8	5.6	2.3	5.2	2.3	5.7	2.4	1.26	0.05250	0.78	0.04168	0.69	0.06948	0.81	0.04295	3
EGJ26148	lmo2623	RpsQ	4.8	1.0	9.4	7.6	7.4	1.8	7.5	2.8	3.6	2.3	0.90	0.20353	0.57	0.01751	0.59	0.06836	-0.37	0.29085	
EGJ26149	lmo2624	RpmC	1.3	0.5	2.7	2.0	1.7	0.6	1.9	0.6	1.6	0.9	0.78	0.17150	0.24	0.30791	0.35	0.16328	0.17	0.61804	
EGJ26150	lmo2625	RplP	9.6	0.9	15.4	5.2	12.9	5.2	11.0	6.4	9.7	7.1	0.66	0.03907	0.41	0.17971	0.20	0.59996	0.02	0.96778	
EGJ26151	lmo2626	RpsC	8.0	0.9	19.8	8.8	20.9	8.6	19.7	6.8	12.9	5.5	1.25	0.02193	1.32	0.01446	1.24	0.00811	0.66	0.08120	3
EGJ26152	lmo2627	RplV	3.0	1.3	9.3	6.2	6.8	2.6	4.5	2.5	3.3	1.9	1.49	0.05592	1.07	0.01364	0.53	0.21417	0.14	0.71712	2
EGJ26153	lmo2628	RpsS	25.4	3.6	21.6	6.6	13.3	2.7	13.7	5.6	8.1	3.0	-0.23	0.25595	-0.91	0.00009	-0.87	0.00234	-1.60	0.00001	5
EGJ26154	lmo2629	RplB	58.1	22.8	57.1	29.6	40.4	18.9	33.9	13.7	32.5	15.4	-0.03	0.94867	-0.52	0.17476	-0.77	0.05606	-0.83	0.04999	
EGJ26155	lmo2630	RplW	11.0	2.5	19.3	6.9	9.6	5.0	12.1	4.8	9.9	3.1	0.78	0.03187	-0.19	0.55310	0.13	0.63092	-0.14	0.51885	
EGJ26156	lmo2631	RplD	93.3	4.2	40.5	10.6	35.0	11.7	35.5	10.6	31.1	9.7	-1.19	0.00002	-1.40	0.00002	-1.38	0.00001	-1.57	0.00000	1
EGJ26157	lmo2632	RplC	162.2	10.7	44.5	4.9	34.7	21.6	32.2	20.5	25.7	15.3	-1.86	0.00000	-2.21	0.00000	-2.31	0.00000	-2.64	0.00000	1
EGJ26158	lmo2633	RpsJ	21.6	5.5	8.3	2.2	11.3	7.8	7.4	4.7	6.6	3.9	-1.34	0.00112	-0.91	0.02554	-1.48	0.00079	-1.65	0.00040	1
EGJ26161	lmo2636	ApbE	0.0	0.0	0.2	0.4	0.5	1.3	1.7	1.5	0.3	0.5	0.45	0.36322	1.02	0.36322	2.14	0.04182	0.73	0.18843	4
EGJ26162	lmo2637		25.6	6.0	1.4	1.6	1.4	1.3	3.5	2.2	3.3	1.9	-3.80	0.00010	-3.78	0.00012	-2.72	0.00011	-2.77	0.00013	1
EGJ26163	lmo2638	YumB	36.2	7.5	34.8	13.0	46.2	11.3	36.6	2.1	26.9	8.0	-0.06	0.82429	0.35	0.10483	0.02	0.90424	-0.42	0.06458	
ScottA	**Other**		**Exp**	**stdev**	**1_d**	**stdev**	**7 d**	**stdev**	**14 d**	**stdev**	**21 d**	**stdev**	**1d/Exp**	**p**	**7**	**p**	**14**	**p**	**21**	**p**	**k-**

Loci	Loci														d/Exp		d/Exp		d/Exp		means group
EGJ26177	lmo2653	TufA	481.7	82.1	334.0	131.3	325.8	173.4	296.2	163.0	266.5	189.3	-0.53	0.04623	-0.56	0.08609	-0.70	0.03992	-0.85	0.03871	
EGJ26178	lmo2654	FusA	150.1	39.3	96.3	22.0	99.0	29.3	76.4	36.8	48.0	51.0	-0.64	0.01955	-0.60	0.03043	-0.97	0.00744	-1.64	0.00341	
EGJ26179	lmo2655	RpsG	10.4	2.1	19.2	11.0	15.5	9.5	15.2	9.6	11.9	7.3	0.85	0.10755	0.55	0.24930	0.53	0.27747	0.19	0.64448	
EGJ26180	lmo2656	RpsL	4.4	0.7	11.0	8.2	6.4	1.2	6.5	0.9	5.0	1.8	1.24	0.10554	0.51	0.00719	0.51	0.00157	0.17	0.44588	2
EGJ26181	lmo2657	Dgt	0.0	0.0	0.7	0.9	2.2	2.4	1.8	1.7	2.2	1.7	1.26	0.11027	2.42	0.07747	2.23	0.04401	2.42	0.02448	3
EGJ26199	lmo2674	YwlF	1.0	0.0	1.1	0.6	0.5	0.7	0.3	0.7	0.8	0.7	0.12	0.64186	-0.54	0.14030	-0.97	0.03915	-0.21	0.51754	
EGJ26202	lmo2677	YugF	0.0	0.0	1.6	1.6	2.2	1.5	0.6	1.1	0.5	0.7	2.07	0.05604	2.43	0.01685	1.17	0.20392	1.06	0.10019	3
EGJ26215	lmo2690	YvkB	0.0	0.0	0.3	0.5	1.1	1.6	1.8	1.7	1.3	1.1	0.70	0.18187	1.65	0.16299	2.18	0.05363	1.83	0.03404	4
EGJ26216	lmo2691	LytF	0.0	0.0	5.0	3.5	1.4	1.4	3.9	1.7	2.6	1.8	3.45	0.01764	1.95	0.05333	3.14	0.00263	2.62	0.01732	3
EGJ26217	lmo2692	YaaQ	0.7	0.5	1.1	1.2	1.3	1.5	3.5	4.2	5.2	5.2	0.42	0.48608	0.62	0.36999	1.79	0.15401	2.28	0.08487	4
EGJ26220	lmo2695	DhaK	1.7	1.5	11.0	4.6	8.0	1.5	8.9	1.9	7.2	2.3	2.42	0.00300	1.98	0.00002	2.12	0.00004	1.83	0.00088	3
EGJ26221	lmo2696	DhaL	1.7	0.5	10.4	2.3	8.2	2.5	6.0	1.4	5.2	3.5	2.33	0.00020	2.01	0.00118	1.59	0.00032	1.40	0.05847	3
EGJ26222	lmo2697	DhaM	0.5	0.6	3.6	2.2	1.8	1.1	3.0	1.8	2.0	1.2	2.00	0.01881	1.15	0.04589	1.76	0.01814	1.31	0.02602	3
EGJ26226	lmo2700	YvgN	0.0	0.0	0.6	1.0	1.0	0.9	0.3	0.7	0.1	0.3	1.17	0.18187	1.62	0.04280	0.63	0.36322	0.33	0.36322	3
EGJ26229	lmo2703	YaaK	1.5	0.9	2.9	1.7	2.6	2.1	2.7	1.0	2.5	1.2	0.76	0.11551	0.61	0.29480	0.67	0.05641	0.58	0.12343	
EGJ26233	lmo2707		0.0	0.0	1.5	1.9	1.4	1.9	0.0	0.0	0.0	0.0	1.99	0.11667	1.91	0.14031	0.00		0.00		2
EGJ26243	lmo2718	CydA	1.8	0.8	0.2	0.4	0.9	1.1	0.6	0.7	0.3	0.7	-1.78	0.00165	-0.75	0.12015	-1.11	0.01417	-1.61	0.00333	1
EGJ26245	lmo2720	YtcI	9.8	1.4	8.4	6.4	7.8	4.9	3.5	2.6	2.3	2.6	-0.22	0.60166	-0.31	0.37476	-1.37	0.00078	-1.88	0.00028	5
EGJ26249	lmo2724		0.7	0.5	3.4	2.2	1.5	0.9	1.8	2.0	1.9	1.2	1.72	0.03098	0.78	0.09038	1.00	0.21909	1.06	0.05774	3
EGJ26268	lmo2743	YwjH	0.7	0.9	1.5	1.1	2.2	1.8	3.8	2.0	3.4	0.8	0.74	0.19183	1.19	0.10536	1.86	0.01021	1.70	0.00025	4
EGJ26272	lmo2747	SerS	4.1	2.1	5.6	3.0	4.2	1.5	2.8	1.3	3.5	0.3	0.41	0.34211	0.03	0.93971	-0.46	0.25906	-0.21	0.50936	
EGJ26279		CsbC	0.5	0.6	0.3	0.6	0.5	0.8	0.9	0.7	0.4	0.5	-0.40	0.50020	0.05	0.92833	0.49	0.31479	-0.14	0.75736	
EGJ26280	lmo2754	DacA	0.3	0.5	0.3	0.5	0.7	0.9	1.5	1.3	2.2	1.9	-0.03	0.96037	0.53	0.41927	1.27	0.07621	1.71	0.06391	4
EGJ26281	lmo2755		0.2	0.4	0.2	0.4	0.2	0.5	0.2	0.5	0.3	0.7	0.05	0.93174	0.06	0.91907	0.10	0.85716	0.21	0.74238	
EGJ26282	lmo2756	TopB	0.2	0.4	0.1	0.3	0.7	1.1	0.2	0.4	0.7	1.0	-0.08	0.86759	0.82	0.32067	-0.02	0.96740	0.79	0.32180	
EGJ26284	lmo2758	GuaB	1.8	0.7	1.0	0.7	0.6	0.7	0.3	0.6	0.5	0.8	-0.60	0.08597	-1.06	0.01580	-1.48	0.00311	-1.20	0.01468	1
EGJ26295	lmo2767		0.0	0.0	0.6	0.8	1.2	0.6	0.9	0.8	0.7	0.8	1.16	0.10113	1.74	0.00622	1.51	0.03682	1.23	0.08831	3
EGJ26299	lmo2771	BglA	0.3	0.5	0.2	0.4	1.2	1.3	0.7	0.6	0.1	0.3	-0.28	0.60929	1.04	0.16655	0.55	0.25200	-0.40	0.43168	0
EGJ26307	lmo2779	YchF	1.8	0.8	1.2	1.3	2.3	1.8	0.9	0.7	0.8	1.3	-0.45	0.34579	0.25	0.60099	-0.74	0.05698	-0.87	0.12080	
EGJ26313	lmo2785	KatX	5.2	1.5	0.1	0.4	0.6	0.7	0.7	0.8	0.6	0.7	-3.14	0.00026	-2.39	0.00021	-2.27	0.00021	-2.35	0.00021	1
EGJ26315	lmo2790	ParB	0.0	0.0	1.5	1.1	3.8	2.2	2.8	1.9	2.1	2.5	2.01	0.01977	3.09	0.00799	2.72	0.01453	2.37	0.09739	3
EGJ26316	lmo2791	ParA	0.0	0.0	1.1	1.0	1.6	0.8	0.8	1.3	0.3	0.6	1.67	0.04828	2.05	0.00509	1.42	0.16694	0.59	0.36322	3
EGJ26317	lmo2792		1.3	1.2	7.6	4.0	10.1	2.6	9.1	2.0	6.3	2.8	2.15	0.01070	2.53	0.00015	2.40	0.00004	1.90	0.00517	3
EGJ26335	lmo2810	GidA	1.3	1.5	2.1	1.3	2.0	1.5	1.0	1.3	1.4	1.3	0.48	0.39643	0.42	0.49545	-0.33	0.66019	0.06	0.92693	
EGJ26346	lmo2821	InlJ	0.2	0.4	0.1	0.3	0.6	0.5	0.2	0.5	0.3	0.5	-0.08	0.86759	0.76	0.11272	0.09	0.87704	0.32	0.56631	
EGJ26348	lmo2823		3.4	0.6	2.7	1.6	4.2	2.7	2.2	1.4	1.5	1.7	-0.28	0.36599	0.28	0.50516	-0.49	0.11062	-0.95	0.03930	
EGJ26349	lmo2824	SerA	2.6	2.0	8.6	3.8	5.8	1.4	4.4	3.1	3.1	2.8	1.53	0.01062	1.00	0.01314	0.64	0.27633	0.21	0.74192	2
ScottA Loci	**Other Loci**		**Exp**	**stdev**	**1_d**	**stdev**	**7 d**	**stdev**	**14 d**	**stdev**	**21 d**	**stdev**	**1d/Exp**	**p**	**7 d/Exp**	**p**	**14 d/Exp**	**p**	**21 d/Exp**	**p**	**k-means**

																				group
EGJ26350	lmo2825	SerC	9.8	3.2	8.3	5.9	7.1	6.6	14.6	10.8	16.2	12.5	-0.23	0.59988	-0.43	0.39889	0.55	0.33610	0.70	0.27347	
EGJ26354	lmo2829		3.3	1.0	5.4	2.5	5.3	2.7	4.4	1.1	3.6	1.6	0.62	0.10982	0.59	0.14252	0.35	0.12021	0.10	0.71737	
EGJ26356	lmo2831	PgcM	1.0	0.0	0.0	0.0	0.4	0.9	0.0	0.0	0.5	0.9	-1.59	0.00000	-0.77	0.16774	-1.59	0.00000	-0.56	0.25506	1
EGJ26364	lmo2839	YcjN	0.2	0.4	0.4	0.7	0.7	0.9	0.5	0.6	0.1	0.4	0.52	0.41238	0.85	0.23305	0.60	0.25795	-0.03	0.95712	
EGJ26377	lmo2853	Jag	1.2	0.7	1.5	1.3	1.5	1.4	1.3	1.2	1.0	1.2	0.23	0.64414	0.23	0.66816	0.07	0.88669	-0.19	0.73265	
EGJ26381	lmo2857	YnaF	0.4	0.9	0.3	0.4	0.1	0.3	0.8	1.0	0.3	0.7	-0.15	0.83945	-0.44	0.57696	0.62	0.42369	-0.16	0.84876	

Appendices II – Lag phase proteome data summary

ScottA loci	Other Loci		Mean abundance lag phase	STDEV	Lag vs aged	STDEV	p	Lag vs exponential	STDEV	p	Exponential vs aged	STDEV	p
EGJ23430	lmo0002	DnaN	7.85	1.61	0.73	0.46	0.00021	0.28	0.31	0.00496	0.35	0.39	0.06859
EGJ23434	lmo0006	GyrB	2.29	0.72	-0.43	0.58	0.92027	-0.21	0.50	0.53476	-0.15	0.29	0.54437
EGJ23435	lmo0007	GyrA	2.64	0.77	0.14	0.86	0.31604	0.23	0.42	0.11681	-0.21	0.56	0.45473
EGJ23451	lmo0018	BglH	4.73	2.58	1.03	1.42	0.00553	1.69	1.22	0.00067	-0.86	0.53	0.02917
EGJ23460	lmo0027	BglP	3.03	0.89	0.01	0.85	0.29952	-0.66	0.53	0.24642	0.62	0.44	0.11086
EGJ23485	lmo0044	RpsF	13.12	2.43	0.38	0.40	0.03309	-0.25	0.24	0.37632	0.52	0.37	0.05693
EGJ23486	lmo0045	SsbA	3.79	2.48	0.76	1.15	0.00951	0.44	1.17	0.03890	0.35	0.13	0.41983
EGJ23492	lmo0051		1.79	0.81	0.81	0.81	0.00070	1.74	0.55	0.00006	-0.90	0.61	0.01298
EGJ23493	lmo0052	YybT	2.42	0.72	-0.67	0.50	0.04400	-0.74	0.50	0.04303	-0.05	0.33	0.72450
EGJ23496	lmo0055	PurA	6.70	1.07	0.08	0.35	0.23721	0.34	0.25	0.11083	-0.31	0.22	0.26484
EGJ23604	lmo0096	LevE	11.83	1.86	-0.41	0.27	0.02489	0.74	0.26	0.00000	-1.16	0.08	0.00000
EGJ23606	lmo0098	LevG	8.57	1.16	-0.16	0.19	0.88800	0.92	0.21	0.00013	-0.96	0.35	0.00027
EGJ23644	lmo0135	OppA	5.88	3.83	-2.21	0.69	0.00000	-0.86	0.71	0.08514	-1.29	0.29	0.00000
EGJ23659	lmo0152	DppE	0.82	0.83	-1.64	0.73	0.01929	0.37	0.87	0.01257	-2.11	0.41	0.00000
EGJ23680	lmo0177	MetS	9.81	1.97	1.08	0.43	0.00044	0.05	0.30	0.54766	0.83	0.60	0.05892
EGJ23695	lmo0191	ChbG	5.36	2.21	2.47	0.90	0.00005	3.28	0.74	0.00003	-0.83	0.28	0.00856
EGJ23696	lmo0192	PurR	1.98	0.65	1.63	0.87	0.00000	1.92	0.45	0.00000	-0.36	0.73	0.06392
EGJ23700	lmo0196	SpoVG	9.93	4.86	0.53	0.74	0.10995	0.80	0.65	0.00820	-0.44	0.46	0.08760
EGJ23701	lmo0197	SpoVG	37.66	14.67	0.96	0.71	0.00195	0.55	0.70	0.07388	0.38	0.23	0.43334
EGJ23702	lmo0198	GlmU	3.49	1.39	-0.03	0.78	0.41375	-0.09	0.55	0.54880	-0.25	0.82	0.23730
EGJ23703	lmo0199	Prs1	3.32	0.85	-0.71	0.51	0.02051	-0.65	0.38	0.08725	-0.19	0.39	0.39012
EGJ23712	lmo0208	YbjQ	5.49	1.33	0.66	0.26	0.00099	3.00	0.33	0.00000	-2.35	0.22	0.00007
EGJ23714	lmo0210	Ldh	36.67	5.82	0.61	0.35	0.00004	2.24	0.23	0.00000	-1.69	0.19	0.00000
EGJ23715	lmo0211	Ctc	14.07	2.41	-0.50	0.36	0.00094	1.12	0.28	0.00000	-1.68	0.16	0.00000
EGJ23718	lmo0214	Mfd	6.58	1.15	2.16	0.29	0.00000	3.29	0.26	0.00000	-1.20	0.17	0.00288
EGJ23722	lmo0218	YabR	2.77	1.40	-0.20	0.73	0.84583	-0.51	0.72	0.79936	0.22	0.45	0.70998
EGJ23723	lmo0219	TilS	2.87	0.79	-0.03	0.56	0.46878	-1.37	0.40	0.00000	1.28	0.32	0.00000
EGJ23724	lmo0220	FtsH	9.32	2.40	0.73	0.45	0.00274	-0.26	0.37	0.45568	0.87	0.52	0.00624
EGJ23726	lmo0222	HslO	1.27	2.24	-0.90	1.44	0.55131	-0.26	1.25	0.24026	-0.60	0.37	0.13526
EGJ23727	lmo0223	CysK	29.25	4.27	0.48	0.42	0.08366	1.05	0.21	0.00002	-0.74	0.43	0.00545
EGJ23734	lmo0228	LysS	6.49	1.35	0.02	0.57	0.45001	-0.25	0.30	0.44829	0.08	0.64	0.91682
EGJ23735	lmo0229	CtsR	0.63	0.42	0.05	0.42	0.00353	0.19	0.59	0.00104	-0.26	0.34	0.08717
EGJ23738	lmo0232	ClpC	3.69	1.15	-1.20	0.59	0.00959	0.40	0.51	0.00642	-1.66	0.37	0.00086
EGJ23743	lmo0237	GltX	25.03	3.25	-0.12	0.28	0.50757	0.63	0.18	0.00029	-0.73	0.17	0.00007
EGJ23745	lmo0239	CysS	1.58	0.83	-1.29	0.83	0.00207	1.03	0.89	0.00050	-2.44	0.31	0.00000

ScottA loci	Other Loci		Mean abundance lag phase	STDEV	Lag vs aged	STDEV	p	Lag vs exponential	STDEV	p	Exponential vs aged	STDEV	p
EGJ23751	lmo0246	NusG	3.15	0.83	0.10	0.36	0.14624	-0.40	0.37	0.32224	0.45	0.27	0.02587
EGJ23753	lmo0248	RplK	31.81	3.11	1.72	0.43	0.00000	-0.12	0.14	0.71717	1.67	0.51	0.00747
EGJ23754	lmo0249	RplA	16.30	7.88	-0.92	0.71	0.00119	-2.30	0.63	0.00001	1.24	0.38	0.00003
EGJ23755	lmo0250	RplJ	20.78	3.71	0.38	0.36	0.01357	-0.93	0.24	0.00000	1.30	0.38	0.00000
EGJ23756	lmo0251	RplL	60.31	4.75	0.89	0.17	0.00000	2.44	0.11	0.00000	-1.60	0.14	0.00008
EGJ23765	lmo0258	RpoB	34.76	6.74	0.46	0.28	0.09124	-0.57	0.25	0.03938	0.86	0.44	0.00924
EGJ23766	lmo0259	RpoC	31.67	4.78	0.28	0.37	0.12890	0.00	0.22	0.72831	0.19	0.26	0.25634
EGJ23768	lmo0261	BglH	1.94	1.33	0.68	1.27	0.00900	1.16	1.20	0.00218	-0.56	0.54	0.13671
EGJ23777	lmo0265	DapE	4.59	1.36	1.57	0.64	0.00000	3.12	0.55	0.00000	-1.55	0.53	0.00080
EGJ23784	lmo0271	BglC	7.37	2.12	0.82	0.55	0.01024	1.31	0.39	0.00005	-0.73	0.64	0.02022
EGJ23800	lmo0287	WalR	2.43	0.30	-0.98	0.49	0.00140	-0.85	0.17	0.01355	-0.21	0.44	0.25010
EGJ23805	lmo0292	HtrC	3.61	3.58	-0.74	1.01	0.53350	1.06	0.97	0.03915	-1.81	0.57	0.00003
EGJ23834	lmo0319	BglH	5.70	1.26	1.72	0.64	0.00000	0.13	0.36	0.31406	1.45	0.42	0.01930
EGJ23868	lmo0355		2.03	3.83	-3.39	1.44	0.00013	-2.38	1.46	0.20442	-0.99	0.76	0.01197
EGJ23877	lmo0369	YeeI	2.59	0.58	0.45	0.39	0.00036	0.33	0.33	0.00409	0.03	0.30	0.96803
EGJ23891	lmo0387	YdhG	5.54	1.96	1.69	0.77	0.00004	2.66	0.47	0.00001	-1.14	0.49	0.00501
EGJ23896	lmo0392	YqfA	15.42	2.48	-0.55	0.38	0.00952	0.96	0.22	0.00002	-1.54	0.25	0.00000
EGJ23961	lmo0437	YtfG	0.88	0.84	0.37	0.61	0.02265	-0.25	0.89	0.12536	0.45	0.55	0.43126
EGJ23967	lmo0443	LytR	1.03	1.68	-0.63	1.03	0.45392	-0.36	1.12	0.27370	-0.27	0.74	0.52130
EGJ23998	lmo0483	YdeE	1.49	0.62	0.72	0.66	0.00013	1.44	0.70	0.00003	-0.74	0.25	0.00448
EGJ24009	lmo0491	AroD	1.93	0.60	0.52	0.48	0.00145	1.88	0.50	0.00000	-1.48	0.41	0.00013
EGJ24029	lmo0512		0.84	0.56	-0.77	0.56	0.70195	0.13	0.76	0.01432	-1.05	0.48	0.00566
EGJ24032	lmo0515	YxiE	2.05	1.25	0.81	1.41	0.01497	1.71	1.11	0.00058	-1.20	0.86	0.00135
EGJ24038	lmo0521	LicH	8.68	1.41	1.53	0.72	0.00000	1.85	0.25	0.00000	-0.57	0.65	0.05325
EGJ24052	lmo0536	LicH	3.85	1.10	0.02	0.42	0.28828	-0.78	0.41	0.04733	0.77	0.17	0.01685
EGJ24055	lmo0539		58.62	9.65	0.86	0.10	0.00000	0.90	0.21	0.00003	-0.11	0.26	0.43455
EGJ24069	lmo0553		22.15	3.57	2.30	0.51	0.00000	3.72	0.26	0.00000	-1.43	0.35	0.00040
EGJ24070	lmo0554	YugJ	10.25	2.76	1.66	0.61	0.00001	2.29	0.40	0.00000	-0.93	0.78	0.00590
EGJ24074	lmo0558	YkgB	4.42	2.27	-0.94	0.68	0.00354	-1.06	0.63	0.00141	-0.10	0.58	0.40161
EGJ24076	lmo0560	RocG	3.36	2.53	-6.75	1.18	0.00000	-5.61	0.84	0.00033	-0.78	0.99	0.00378
EGJ24090	lmo0574	GmuD	1.08	0.55	0.65	0.86	0.00023	0.95	0.74	0.00016	-0.27	0.32	0.16974
EGJ24108	lmo0592		8.01	1.12	0.48	0.35	0.00019	1.75	0.20	0.00000	-1.28	0.46	0.00000
EGJ24156	lmo0640	YcsN	4.95	1.95	-0.36	0.68	0.67205	1.32	0.55	0.00018	-1.65	0.17	0.00001
EGJ24157	lmo0641	ZosA	1.73	0.83	-1.27	0.95	0.00907	1.61	0.81	0.00010	-2.90	0.24	0.00000
EGJ24170	lmo0654		1.86	1.12	-1.67	1.23	0.00083	1.21	1.00	0.00090	-2.79	0.64	0.00000
EGJ24181	lmo0662	ThiD	3.69	1.14	0.29	0.54	0.96290	-0.69	0.42	0.11973	0.64	0.90	0.17876
EGJ24189	lmo0669	YhxD	0.81	0.46	-0.58	0.77	0.23839	-0.24	0.72	0.11311	-0.31	0.32	0.41820

ScottA loci	Other Loci		Mean abundance lag phase	STDEV	Lag vs aged	STDEV	p	Lag vs exponential	STDEV	p	Exponential vs aged	STDEV	p
EGJ24241	lmo0722	YdaP	22.33	3.55	1.40	0.40	0.00000	4.04	0.24	0.00000	-2.61	0.24	0.00000
EGJ24245	lmo0727	GlmS	9.70	1.90	0.90	0.36	0.00001	-0.05	0.27	0.68998	0.90	0.32	0.00011
EGJ24274	lmo0774	YerQ	5.86	1.57	1.04	0.80	0.00005	2.26	0.46	0.00001	-1.36	0.48	0.00808
EGJ24282	lmo0783	LevE	1.73	0.76	-0.80	0.61	0.09249	0.05	0.75	0.01430	-0.97	0.49	0.00127
EGJ24285	lmo0786	YvaB	2.45	0.97	-0.42	0.72	0.76924	0.76	0.64	0.00269	-1.19	0.35	0.00527
EGJ24296	lmo0796	YceI	14.94	4.07	1.93	0.79	0.00000	4.41	0.36	0.00000	-2.79	0.86	0.00005
EGJ24310	lmo0811		1.04	1.53	0.05	1.11	0.14360	-2.23	1.10	0.02767	2.13	0.45	0.00285
EGJ24312	lmo0813	GmuE	2.48	0.60	-2.57	0.57	0.00001	-2.65	0.35	0.00004	-0.18	0.69	0.23945
EGJ24325	lmo0823	YvgN	1.26	0.83	0.30	0.79	0.01665	0.66	0.90	0.00364	-0.48	0.38	0.20439
EGJ24349	lmo0848	ArtR	0.92	0.49	0.18	0.82	0.00073	-0.03	0.77	0.04393	0.32	0.30	0.50279
EGJ24357	lmo0855	Ddl	1.73	0.48	0.18	0.81	0.12544	-0.25	0.36	0.56427	0.24	0.62	0.63359
EGJ24368	lmo0866	CshA	15.73	6.29	0.17	0.64	0.65426	-1.11	0.46	0.00001	1.16	0.43	0.00000
EGJ24391	lmo0889	RsbR	6.20	1.33	1.31	0.61	0.00000	3.60	0.31	0.00000	-2.39	0.38	0.00000
EGJ24395	lmo0893	RsbV	4.28	2.21	2.09	1.02	0.00030	2.89	0.88	0.00017	-0.73	0.59	0.01416
EGJ24396	lmo0894	RsbW	7.24	2.08	0.82	0.50	0.00030	1.13	0.47	0.00005	-0.37	0.33	0.05633
EGJ24407	lmo0903	OhrB	1.47	1.05	-3.15	1.49	0.00784	-1.24	1.10	0.14652	-1.61	0.81	0.01542
EGJ24410	lmo0906	Gor	3.26	1.22	0.20	0.77	0.09244	0.48	0.65	0.00288	-0.31	0.47	0.14739
EGJ24411	lmo0907		5.40	1.54	0.40	0.37	0.01082	1.38	0.38	0.00001	-1.03	0.24	0.00006
EGJ24434	lmo0931	YhfJ	1.64	0.93	-0.71	1.22	0.42923	-1.74	1.04	0.00073	0.86	0.55	0.00902
EGJ24438	lmo0935	CspR	0.98	0.91	-0.25	0.93	0.27692	0.18	1.00	0.02687	-0.64	0.57	0.10481
EGJ24445	lmo0943	Dps	81.84	23.51	-0.10	0.99	0.76296	3.16	0.41	0.00000	-2.89	0.98	0.00001
EGJ24455	lmo0953		1.28	0.39	0.40	0.67	0.00552	1.28	0.54	0.00000	-1.08	0.72	0.00139
EGJ24457	lmo0955	LiaH	5.21	1.55	0.12	0.82	0.07085	2.33	0.48	0.00000	-2.10	0.60	0.00000
EGJ24458	lmo0956	NagA	11.32	1.41	-0.25	0.30	0.71426	1.96	0.18	0.00000	-2.07	0.37	0.00001
EGJ24459	lmo0957	NagB	2.71	0.59	1.70	0.82	0.00017	2.41	0.29	0.00000	-1.13	1.12	0.02838
EGJ24464	lmo0962		3.52	1.22	-0.02	0.62	0.54575	1.32	0.49	0.00003	-1.35	0.45	0.00294
EGJ24472	lmo0970	FabI	12.71	1.67	0.40	0.31	0.00083	-0.78	0.20	0.00409	1.09	0.22	0.00083
EGJ24474	lmo0972	DltC	3.33	1.99	1.74	1.05	0.00081	2.41	1.15	0.00051	-0.53	0.37	0.01588
EGJ24481	lmo0978	YwaA	10.87	2.33	0.88	0.79	0.00036	0.53	0.34	0.00087	0.15	0.63	0.77383
EGJ24485	lmo0982	YhfE	1.66	0.83	-0.22	0.95	0.32640	-0.73	0.93	0.69411	0.42	0.25	0.27015
EGJ24486	lmo0983	BsaA	1.93	0.90	0.86	1.15	0.00064	1.34	0.84	0.00013	-0.53	0.55	0.13447
EGJ24500	lmo0997	ClpE	2.63	6.72	0.13	1.71	0.27796	0.54	1.72	0.24803	-0.37	0.44	0.09279
EGJ24505	lmo1002	PtsH	135.01	19.19	0.38	0.48	0.72914	-0.30	0.20	0.11630	0.45	0.62	0.11767
EGJ24506	lmo1003	PtsI	57.20	5.27	0.82	0.36	0.00000	-0.19	0.13	0.42375	0.89	0.34	0.01433
EGJ24514	lmo1011	DapH	4.46	1.77	0.17	0.80	0.61180	-0.97	0.62	0.02059	0.92	0.58	0.01097
EGJ24515	lmo1012	DapL	1.92	0.81	0.33	0.73	0.00231	-0.88	0.75	0.04375	1.27	0.21	0.00006
EGJ24518	lmo1014	OpuAA	2.54	2.29	0.90	0.97	0.02693	-0.35	0.99	0.57142	1.18	0.22	0.04537

ScottA loci	Other Loci		Mean abundance lag phase	STDEV	Lag vs aged	STDEV	p	Lag vs exponential	STDEV	p	Exponential vs aged	STDEV	p
EGJ24521	lmo1017	YpqE	1.05	0.24	-0.33	0.37	0.22048	1.02	0.39	0.00000	-1.34	0.32	0.00032
EGJ24531	lmo1027	RnjA	1.66	2.27	-0.65	1.10	0.98855	-1.69	1.17	0.11575	0.80	0.63	0.01759
EGJ24532	lmo1028	YkzG	3.87	1.60	0.44	1.16	0.19115	0.30	0.73	0.04056	-0.10	0.84	0.36863
EGJ24555	lmo1051	Def	1.24	0.63	-1.36	0.79	0.00622	-0.29	0.84	0.27098	-1.05	0.52	0.00257
EGJ24556	lmo1052	PdhA	36.97	2.22	0.81	0.27	0.00000	-0.56	0.09	0.00099	1.27	0.29	0.00001
EGJ24557	lmo1053	PdhB	40.69	4.47	0.79	0.18	0.00000	-0.45	0.16	0.02044	1.23	0.07	0.00052
EGJ24558	lmo1054	PdhC	42.93	7.64	1.25	0.33	0.00000	-0.24	0.24	0.46498	1.46	0.22	0.00988
EGJ24559	lmo1055	PdhD	31.22	4.79	0.20	0.35	0.01659	-1.48	0.22	0.00000	1.74	0.18	0.00000
EGJ24563	lmo1059		8.66	2.79	1.42	0.52	0.00016	0.63	0.44	0.00217	0.52	0.70	0.06681
EGJ24567	lmo1067	BipA	3.38	1.45	0.27	0.88	0.05604	-1.39	0.75	0.04253	1.64	0.56	0.01676
EGJ24568	lmo1068		0.77	0.84	-2.42	0.79	0.00007	-1.85	0.84	0.14617	-0.56	0.64	0.06969
EGJ24571	lmo1072	PycA	13.39	1.95	-0.83	0.20	0.00000	0.25	0.21	0.09203	-1.06	0.07	0.00000
EGJ24575	lmo1075	TagH	2.98	0.72	2.26	0.78	0.00000	2.53	0.40	0.00000	-0.38	0.54	0.06854
EGJ24582	lmo1078	GtaB	16.19	2.66	1.14	0.70	0.00000	0.91	0.27	0.00000	0.04	0.64	0.77780
EGJ24583	lmo1086	TarI	1.87	0.73	-0.52	1.12	0.05613	-0.44	0.58	0.99506	-0.40	0.88	0.07943
EGJ24584	lmo1087	TarJ	4.51	1.19	0.89	0.42	0.00012	1.71	0.42	0.00000	-0.91	0.51	0.01132
EGJ24589	lmo1092	YueK	1.32	0.59	-0.28	0.69	0.73317	0.52	0.76	0.00378	-0.98	0.51	0.01472
EGJ24593	lmo1096	GuaA	29.49	2.96	0.30	0.33	0.07479	-0.23	0.15	0.00280	0.42	0.33	0.00036
EGJ24620	lmo1138	ClpP	8.30	1.13	-1.21	0.30	0.00000	1.90	0.20	0.00000	-3.05	0.23	0.00000
EGJ24697	lmo1217	YsdC	9.34	2.19	-0.65	0.47	0.24257	0.02	0.36	0.56475	-0.40	0.71	0.16758
EGJ24701	lmo1221	PheS	1.52	0.70	-0.68	0.76	0.46443	0.24	0.70	0.06200	-0.93	0.22	0.02253
EGJ24702	lmo1222	PheT	5.95	1.16	0.63	0.75	0.01035	1.98	0.32	0.00001	-1.53	0.54	0.00100
EGJ24713	lmo1233	TrxA	4.39	1.18	0.07	0.41	0.37850	0.42	0.36	0.00199	-0.40	0.40	0.03938
EGJ24781	lmo1241		5.66	1.30	1.04	0.58	0.00061	3.46	0.36	0.00000	-2.59	0.78	0.00008
EGJ24795	lmo1254	TreA	7.31	3.19	0.04	1.06	0.60384	-0.13	0.61	0.74262	-0.08	0.75	0.37048
EGJ24796	lmo1255	TreP	4.84	0.73	0.73	0.63	0.00026	-1.02	0.22	0.00195	1.58	0.56	0.00011
EGJ24798	lmo1257		6.55	1.55	0.61	0.36	0.00043	1.68	0.39	0.00001	-1.11	0.14	0.00380
EGJ24799	lmo1258	YtpA	1.57	0.93	1.29	0.77	0.00055	1.43	0.83	0.00049	-0.09	0.17	0.32772
EGJ24807	lmo1267	Tig	36.01	7.61	0.56	0.44	0.01211	-0.42	0.30	0.04103	0.91	0.28	0.00082
EGJ24808	lmo1268	ClpX	5.98	2.05	0.66	0.71	0.00683	1.19	0.51	0.00012	-0.63	0.43	0.02662
EGJ24815	lmo1275	TopA	0.82	0.85	-1.40	0.65	0.07965	-2.14	0.88	0.00632	0.54	0.53	0.12251
EGJ24816	lmo1276	Gid	4.17	1.58	0.44	0.55	0.09495	1.39	0.57	0.00036	-1.14	0.58	0.00583
EGJ24819	lmo1279	ClpY	4.53	1.79	-2.98	0.72	0.00000	-1.11	0.53	0.00003	-1.79	0.31	0.00000
EGJ24820	lmo1280	CodY	6.71	1.42	3.27	0.56	0.00000	3.72	0.30	0.00000	-0.32	0.37	0.16195
EGJ24823	lmo1283	YoxA	13.89	3.35	2.30	0.86	0.00000	2.43	0.32	0.00000	-0.51	1.03	0.20263
EGJ24826	lmo1286	ParE	1.77	0.62	0.60	0.70	0.00055	-0.12	0.48	0.26849	0.57	0.44	0.15033
EGJ24827	lmo1287	ParC	1.90	0.52	-0.07	0.46	0.37279	-0.01	0.40	0.06632	-0.14	0.35	0.56537

ScottA loci	Other Loci		Mean abundance lag phase	STDEV	Lag vs aged	STDEV	p	Lag vs exponential	STDEV	p	Exponential vs aged	STDEV	p
EGJ24832	lmo1293	GlpD	8.60	3.05	1.34	0.72	0.00016	1.79	0.48	0.00008	-0.52	0.48	0.21662
EGJ24838	lmo1299	GlnA	16.51	4.56	0.22	0.39	0.09104	-1.03	0.34	0.00001	1.24	0.19	0.00001
EGJ24841	lmo1302	LexA	0.69	0.44	0.23	0.70	0.00096	0.29	0.65	0.00076	-0.09	0.17	0.32772
EGJ24844	lmo1305	Tkt	19.25	2.50	-0.34	0.19	0.00038	-0.70	0.19	0.03965	0.34	0.07	0.17282
EGJ24851	lmo1313	PyrH	0.93	0.68	0.20	0.89	0.00765	0.66	0.81	0.00185	-0.43	0.42	0.02344
EGJ24852	lmo1314	Frr	7.39	1.89	-0.64	0.36	0.00689	0.13	0.36	0.38426	-0.74	0.09	0.01827
EGJ24857	lmo1319	ProS	7.29	2.03	1.52	0.91	0.00013	0.14	0.38	0.22317	1.03	0.99	0.02281
EGJ24860	lmo1322	NusA	16.72	2.40	1.53	0.63	0.00000	2.31	0.21	0.00000	-0.85	0.53	0.00757
EGJ24863	lmo1325	InfB	6.43	3.28	-0.27	1.05	0.83318	-0.52	0.99	0.53156	0.17	0.42	0.64537
EGJ24868	lmo1330	RpsO	8.79	4.07	0.81	0.89	0.01019	1.29	0.73	0.00141	-0.61	0.45	0.08258
EGJ24869	lmo1331	PnpA	6.39	3.11	-0.62	0.96	0.08495	-1.10	0.58	0.00661	0.43	0.56	0.19004
EGJ24872	lmo1334	YqzD	1.65	0.83	0.15	1.09	0.05862	0.33	0.79	0.01000	-0.27	0.48	0.34069
EGJ24876	lmo1339	GlcK	5.81	1.57	0.42	0.53	0.15489	0.73	0.37	0.00982	-0.54	0.60	0.06985
EGJ24887	lmo1351	YqhL	1.10	0.61	-1.15	0.89	0.19464	-0.78	0.78	0.79842	-0.29	0.67	0.23063
EGJ24890	lmo1354	YqhT	7.38	2.19	0.71	0.56	0.05795	0.86	0.47	0.00158	-0.39	0.67	0.17437
EGJ24893	lmo1357	AccC	4.67	1.34	0.40	0.62	0.05052	1.44	0.43	0.00004	-1.19	0.48	0.00108
EGJ24896	lmo1360	FolD	5.38	1.15	1.62	0.87	0.00000	-0.75	0.33	0.00614	2.02	0.87	0.00005
EGJ24900	lmo1364	CspC	2.65	1.20	0.16	0.77	0.49719	-2.60	0.63	0.22147	2.35	1.16	0.24452
EGJ24908	lmo1372	BkdAA	2.53	0.83	0.94	0.52	0.00020	1.22	0.54	0.00120	-0.48	0.53	0.29445
EGJ24909	lmo1373	BkdAB	6.00	1.23	0.88	0.38	0.00006	-0.12	0.30	0.88691	0.84	0.43	0.00355
EGJ24913	lmo1376	YqjI	43.84	7.44	-0.17	0.21	0.08365	0.11	0.25	0.50396	-0.33	0.16	0.12694
EGJ24924	lmo1388	YufN	16.91	4.28	-0.28	0.31	0.17104	0.13	0.37	0.11791	-0.39	0.16	0.00014
EGJ24925	lmo1389	YufO	3.64	1.27	0.74	0.95	0.00301	0.55	0.54	0.00694	0.23	0.81	0.88634
EGJ24934	lmo1398	RecA	7.41	2.58	1.96	1.36	0.00004	1.69	0.48	0.00003	0.08	1.13	0.48238
EGJ24937	lmo1401	YmdB	1.76	0.90	-0.34	0.84	0.78971	0.19	0.83	0.05088	-0.63	0.35	0.10148
EGJ24942	lmo1406	PflB	68.56	12.71	0.70	0.55	0.00348	0.61	0.30	0.01476	-0.02	0.46	0.81241
EGJ24943	lmo1407	PflA	8.75	2.66	0.68	0.57	0.00332	4.05	0.55	0.00000	-3.42	0.30	0.00000
EGJ24951	lmo1415		2.78	1.47	-2.13	1.22	0.00035	1.00	0.99	0.00139	-2.89	0.65	0.00001
EGJ24962	lmo1426	OpuCC	3.57	1.41	0.23	0.62	0.06136	2.26	0.71	0.00002	-2.03	0.31	0.00016
EGJ24964	lmo1428	OpuCA	20.23	3.08	0.70	0.24	0.00000	2.57	0.22	0.00000	-1.87	0.20	0.00000
EGJ24970	lmo1434	RnjB	2.11	1.02	-1.19	0.80	0.00141	-1.65	0.70	0.03735	0.34	0.42	0.42828
EGJ24971	lmo1435	DapA	3.42	1.21	-1.02	0.51	0.00007	0.28	0.52	0.02104	-1.36	0.24	0.00000
EGJ24972	lmo1436	DapG	1.42	0.61	-0.69	0.88	0.45689	0.13	0.78	0.01964	-0.88	0.22	0.00574
EGJ24973	lmo1437	Asd	4.44	1.33	0.13	0.70	0.80519	0.21	0.44	0.02704	-0.29	0.57	0.10415
EGJ24975	lmo1439	SodA	107.15	22.76	3.17	0.68	0.00000	3.28	0.29	0.00000	-0.36	0.66	0.15149
EGJ24984	lmo1448	PpaC	6.57	1.39	-0.08	0.58	0.51360	-0.06	0.30	0.62928	-0.15	0.42	0.34200
EGJ24988	lmo1452	YqfO	2.09	0.53	0.73	0.53	0.00001	0.80	0.35	0.00030	-0.03	0.33	0.84933

ScottA loci	Other Loci		Mean abundance lag phase	STDEV	Lag vs aged	STDEV	p	Lag vs exponential	STDEV	p	Exponential vs aged	STDEV	p
EGJ24989	lmo1453	TrmK	1.78	0.87	0.93	1.00	0.00085	-0.09	0.80	0.08260	0.84	0.48	0.00589
EGJ24990	lmo1454	SigA	4.87	1.65	0.85	0.37	0.00527	0.98	0.55	0.00019	-0.38	0.66	0.09795
EGJ24993	lmo1457	YqfL	2.74	0.92	1.41	1.15	0.00011	1.95	0.56	0.00000	-0.86	0.86	0.04306
EGJ24994	lmo1458	GlyS	13.49	2.63	1.41	0.54	0.00000	3.33	0.26	0.00000	-2.04	0.48	0.00001
EGJ24998	lmo1462	Era	2.01	0.70	0.67	1.09	0.00618	1.17	0.57	0.00011	-0.77	0.73	0.02934
EGJ25003	lmo1467	PhoH	1.94	0.69	0.62	0.78	0.00037	0.84	0.72	0.00600	-0.34	0.36	0.45009
EGJ25005	lmo1468	YqeY	3.92	1.33	0.15	0.56	0.32339	1.00	0.49	0.00132	-0.98	0.36	0.01079
EGJ25009	lmo1472	DnaJ	1.69	0.83	-1.68	0.70	0.00024	0.19	0.75	0.01421	-1.97	0.34	0.00001
EGJ25010	lmo1473	DnaK	248.86	26.83	1.74	0.35	0.00000	0.39	0.14	0.01449	1.13	0.62	0.00091
EGJ25011	lmo1474	GrpE	16.62	1.68	0.73	0.14	0.00000	0.35	0.14	0.08610	0.35	0.07	0.21531
EGJ25017	lmo1480	RpsT	1.26	1.36	-2.52	1.41	0.00015	-1.80	1.10	0.01982	-0.55	0.57	0.01554
EGJ25024	lmo1487	YqeK	1.10	0.72	0.74	1.01	0.00140	0.45	0.95	0.00466	0.20	0.23	0.64755
EGJ25030	lmo1493	PepF	11.98	1.93	-0.19	0.27	0.63445	1.15	0.25	0.00001	-1.31	0.30	0.00031
EGJ25031	lmo1494	Mtn	1.05	0.53	-2.59	0.98	0.00043	0.92	0.72	0.00014	-3.21	0.84	0.00002
EGJ25033	lmo1496	GreA	6.82	1.23	0.78	0.44	0.00041	0.28	0.27	0.04220	0.28	0.60	0.40957
EGJ25040	lmo1503	YrzL	10.44	3.07	2.06	0.73	0.00000	4.33	0.43	0.00000	-2.04	0.58	0.00152
EGJ25041	lmo1504	AlaS	11.47	2.16	0.52	0.69	0.14066	1.48	0.27	0.00000	-1.17	0.58	0.00091
EGJ25047	lmo1510	YrrB	2.22	1.19	1.03	0.96	0.00089	1.91	0.94	0.00023	-0.90	0.07	0.00419
EGJ25052	lmo1515	CymR	2.52	0.78	1.79	0.53	0.00000	1.88	0.39	0.00000	-0.26	0.59	0.40101
EGJ25056	lmo1519	AspS	3.86	1.43	-0.64	0.46	0.01558	-0.26	0.51	0.98751	-0.50	0.32	0.04713
EGJ25057	lmo1520	HisS	3.57	2.23	-0.90	0.94	0.11106	0.24	0.95	0.06740	-1.20	0.31	0.00100
EGJ25061	lmo1524	Apt	4.04	2.26	0.55	0.90	0.03574	0.27	0.92	0.05440	0.14	0.37	0.71386
EGJ25066	lmo1529	YajC	27.54	7.30	2.51	0.52	0.00000	3.84	0.39	0.00000	-1.22	0.49	0.00536
EGJ25067	lmo1530	Tgt	1.94	0.82	-0.18	0.69	0.67371	-0.52	0.75	0.87759	0.20	0.45	0.62054
EGJ25074	lmo1537	ObgE	0.97	1.12	-0.04	1.20	0.06662	-1.07	0.99	0.91471	1.11	0.39	0.00000
EGJ25075	lmo1538	GlpK	13.08	2.89	0.34	0.42	0.00920	2.54	0.36	0.00000	-2.16	0.18	0.00000
EGJ25077	lmo1540	RpmA	1.39	1.53	-3.13	1.21	0.00000	-2.10	1.19	0.00428	-0.99	0.16	0.00010
EGJ25079	lmo1542	RplU	8.43	1.16	-1.09	0.28	0.00060	-2.08	0.20	0.00014	0.95	0.21	0.00029
EGJ25085	lmo1548	MreB	15.75	3.07	1.44	0.65	0.00000	1.31	0.30	0.00001	-0.05	0.52	0.68331
EGJ25089	lmo1552	ValS	2.70	0.98	-1.32	0.59	0.00111	-1.87	0.67	0.00000	0.34	0.55	0.23734
EGJ25091	lmo1554	HemB	4.62	2.02	0.22	0.81	0.43881	1.31	0.77	0.00037	-1.30	0.55	0.00285
EGJ25096	lmo1559	ThrS	6.87	1.34	1.53	0.70	0.00000	0.74	0.28	0.00030	0.54	0.73	0.13333
EGJ25102	lmo1565	PolA	1.45	0.89	-0.67	0.94	0.85654	-1.02	0.90	0.39189	0.42	0.29	0.32978
EGJ25103	lmo1566	Icd	3.65	1.54	1.02	0.45	0.00055	1.57	0.51	0.00011	-0.53	0.36	0.08070
EGJ25104	lmo1567	CitZ	1.39	0.96	0.53	0.96	0.00498	1.18	0.96	0.00134	-0.59	0.33	0.00824
EGJ25107	lmo1570	Pyk	197.72	15.04	0.72	0.26	0.00002	1.38	0.11	0.00000	-0.77	0.28	0.00018
EGJ25108	lmo1571	PfkA	48.62	11.34	0.24	0.33	0.19088	1.90	0.33	0.00000	-1.71	0.29	0.00000

ScottA loci	Other Loci		Mean abundance lag phase	STDEV	Lag vs aged	STDEV	p	Lag vs exponential	STDEV	p	Exponential vs aged	STDEV	p
EGJ25109	lmo1572	AccA	1.74	1.33	-0.28	1.49	0.54701	-0.07	1.26	0.06788	-0.33	0.82	0.11539
EGJ25110	lmo1573	AccD	1.60	0.75	0.47	1.44	0.10310	1.07	0.86	0.00022	-0.96	0.97	0.01465
EGJ25114	lmo1577	YtkL	2.49	0.90	1.02	0.63	0.00005	1.49	0.55	0.00003	-0.48	0.27	0.22083
EGJ25115	lmo1578	YkvY	23.06	3.75	1.77	0.63	0.00000	2.50	0.24	0.00000	-0.95	0.62	0.00108
EGJ25116	lmo1579	Ald	32.06	6.00	-0.87	0.69	0.02004	2.91	0.28	0.00000	-3.50	0.73	0.00000
EGJ25117	lmo1580	YxiE	39.11	3.78	1.23	0.24	0.00000	2.73	0.14	0.00000	-1.56	0.17	0.00000
EGJ25118	lmo1581	AckA	24.70	3.87	0.76	0.58	0.00051	-0.17	0.25	0.22226	0.77	0.46	0.00007
EGJ25119	lmo1582	YtxK	1.77	1.13	1.05	1.30	0.00146	1.48	1.14	0.00080	-0.40	0.35	0.05442
EGJ25120	lmo1583	Tpx	0.88	0.62	-1.04	0.89	0.28251	-2.24	0.81	0.00004	1.08	0.50	0.00013
EGJ25123	lmo1586	PpnK	5.59	1.18	-0.21	0.34	0.75478	2.03	0.35	0.00000	-2.23	0.22	0.00000
EGJ25129	lmo1592	YtbJ	1.44	1.01	-0.07	1.16	0.10039	0.82	1.01	0.00350	-0.92	0.45	0.01801
EGJ25131	lmo1594	EzrA	3.52	1.31	0.63	0.92	0.00210	1.71	0.62	0.00002	-1.02	0.59	0.00693
EGJ25133	lmo1596	RpsD	30.12	4.24	0.18	0.43	0.66101	0.72	0.19	0.00001	-0.75	0.55	0.00083
EGJ25134	lmo1598	TyrS	5.17	1.45	-0.36	0.54	0.27489	0.58	0.44	0.00163	-0.95	0.30	0.00023
EGJ25135	lmo1599	CcpA	24.83	3.83	1.34	0.37	0.00000	2.41	0.21	0.00000	-1.21	0.40	0.00037
EGJ25137	lmo1601	YtxH	9.67	1.78	-1.32	0.34	0.00000	1.94	0.25	0.00000	-3.10	0.45	0.00000
EGJ25138	lmo1602	YtxG	14.96	1.32	1.17	0.29	0.00000	1.28	0.13	0.00007	-0.20	0.27	0.46825
EGJ25139	lmo1603	AmpS	8.78	2.26	-0.14	0.35	0.74216	-0.38	0.36	0.13853	0.21	0.15	0.21898
EGJ25140	lmo1604	YkuU	2.55	0.56	0.67	0.95	0.00909	-0.57	0.36	0.30988	1.01	0.86	0.03152
EGJ25143	lmo1607	YtpR	6.72	1.16	1.96	0.48	0.00000	0.22	0.26	0.04520	1.50	0.64	0.00040
EGJ25147	lmo1611	YtoP	26.03	3.76	-0.28	0.41	0.47582	1.84	0.22	0.00000	-1.97	0.39	0.00000
EGJ25155	lmo1619	Dat	2.58	0.88	-1.88	0.77	0.00000	-3.00	0.57	0.00051	0.98	0.41	0.00460
EGJ25156	lmo1620	YtjP	14.87	1.45	0.06	0.41	0.58362	0.94	0.14	0.00000	-1.03	0.42	0.00002
EGJ25157	lmo1621	MutT	1.68	0.76	0.37	0.92	0.01966	1.17	0.77	0.00014	-0.89	0.66	0.02656
EGJ25171	lmo1634	AdhE	235.88	29.42	0.53	0.44	0.01414	0.64	0.18	0.04936	-0.30	0.49	0.27289
EGJ25177	lmo1641	CitB	4.57	1.22	1.41	0.60	0.00007	2.11	0.34	0.00000	-1.03	0.86	0.02612
EGJ25192	lmo1657	Tsf	57.54	6.34	0.59	0.64	0.04037	-0.96	0.16	0.00001	1.32	0.63	0.00000
EGJ25193	lmo1658	RpsB	28.02	3.57	-0.23	0.30	0.03757	-0.23	0.18	0.15167	-0.09	0.26	0.48942
EGJ25197	lmo1660	LeuS	8.42	2.26	-0.12	0.35	0.94626	1.60	0.37	0.00000	-1.74	0.09	0.00001
EGJ25200	lmo1663	AsnB	3.94	1.42	-0.24	0.69	0.61392	0.78	0.54	0.00261	-1.12	0.37	0.00081
EGJ25201	lmo1664	MetK	2.02	1.11	-0.59	0.78	0.48671	0.21	0.86	0.01805	-0.91	0.29	0.00082
EGJ25210	lmo1673	MenB	18.33	3.28	0.64	0.44	0.00012	1.23	0.26	0.00000	-0.66	0.26	0.00020
EGJ25212	lmo1675	MenD	2.61	1.70	0.63	0.47	0.15932	1.78	0.72	0.00128	-1.48	0.85	0.00281
EGJ25213	lmo1676	MenF	5.30	1.34	1.67	1.19	0.00001	2.13	0.38	0.00000	-0.84	1.02	0.02775
EGJ25220	lmo1683	PerR	2.05	0.57	1.21	0.51	0.00000	1.98	0.43	0.00000	-0.92	0.53	0.00015
EGJ25222	lmo1685	GsaB	2.32	0.86	0.20	0.93	0.07111	-0.31	0.56	0.75455	0.56	0.61	0.15163
EGJ25231	lmo1694	YfhF	3.63	0.82	2.25	0.30	0.00000	2.09	0.32	0.00000	0.22	0.16	0.62323

ScottA loci	Other Loci		Mean abundance lag phase	STDEV	Lag vs aged	STDEV	p	Lag vs exponential	STDEV	p	Exponential vs aged	STDEV	p
EGJ25246	lmo1709	MapA	4.66	0.51	0.57	0.59	0.01631	0.15	0.16	0.06159	0.24	0.59	0.53092
EGJ25247	lmo1710	YkuP	1.36	0.56	-0.82	0.77	0.10704	-1.30	0.76	0.00309	0.36	0.33	0.09976
EGJ25248	lmo1711	AmpS	7.06	1.52	-0.42	0.51	0.01398	-0.49	0.30	0.04059	-0.05	0.39	0.62413
EGJ25254	lmo1718		2.48	1.87	0.02	0.93	0.20292	1.26	0.91	0.00600	-1.17	0.57	0.01793
EGJ25262	lmo1726	YulF	2.02	0.99	-0.34	0.82	0.46370	-0.04	0.81	0.09107	-0.54	0.66	0.02414
EGJ25288	lmo1753	YerQ	2.92	0.60	1.64	0.80	0.00000	2.52	0.28	0.00000	-1.29	1.09	0.00122
EGJ25289	lmo1754	GatB	11.01	1.82	0.28	0.51	0.80241	0.31	0.24	0.12332	-0.25	0.62	0.25886
EGJ25290	lmo1755	GatA	10.30	2.02	0.85	0.50	0.00007	-0.29	0.32	0.35557	0.99	0.44	0.00733
EGJ25292	lmo1757	YerH	0.74	0.57	-1.79	0.80	0.00348	-1.40	0.74	0.25232	-0.54	0.46	0.08390
EGJ25309	lmo1774	PurK	0.98	0.54	-0.70	0.99	0.63388	-0.22	0.76	0.12939	-0.61	0.47	0.06480
EGJ25315	lmo1780	PepT	1.41	1.07	-1.14	1.03	0.03181	-0.97	1.02	0.57244	-0.42	0.67	0.09678
EGJ25318	lmo1783	RplT	13.03	4.25	1.15	0.19	0.00111	-1.19	0.43	0.00411	2.11	0.60	0.00069
EGJ25319	lmo1784	RpmI	2.69	1.26	-1.35	0.65	0.00027	-0.82	0.61	0.03387	-0.52	0.09	0.01074
EGJ25320	lmo1785	InfC	4.29	1.73	-1.47	0.54	0.00000	-0.41	0.52	0.50266	-1.06	0.06	0.00001
EGJ25323	lmo1787	RplS	9.48	0.83	-0.73	0.26	0.00166	-2.55	0.13	0.00003	1.76	0.19	0.00000
EGJ25333	lmo1797	RpsP	5.89	5.60	-0.49	0.80	0.20673	0.02	0.86	0.38234	-0.83	0.90	0.00790
EGJ25337	lmo1801	Ffh	5.28	1.68	0.75	0.89	0.00327	2.89	0.65	0.00000	-2.31	0.47	0.00001
EGJ25343	lmo1807	FabG	8.49	1.22	0.08	0.19	0.53230	0.34	0.21	0.16926	-0.34	0.31	0.25609
EGJ25344	lmo1808	FabD	8.59	1.71	1.26	0.69	0.00002	0.50	0.29	0.00135	0.48	0.76	0.15931
EGJ25345	lmo1809	PlsX	2.40	0.49	-0.52	0.56	0.06645	2.23	0.32	0.00000	-2.84	0.33	0.00000
EGJ25354	lmo1818	Rpe	9.11	2.32	1.31	0.17	0.00001	2.14	0.33	0.00000	-0.91	0.31	0.00074
EGJ25357	lmo1821	PrpC	1.04	0.65	-0.77	0.84	0.71836	0.38	0.90	0.00572	-1.29	0.36	0.00544
EGJ25359	lmo1823	Fmt	2.58	0.57	0.52	0.33	0.00398	1.60	0.33	0.00000	-1.27	0.54	0.00091
EGJ25361	lmo1825	CoaBC	2.19	0.93	0.66	1.02	0.00579	1.52	0.82	0.00005	-1.06	0.66	0.00843
EGJ25366	lmo1830		6.09	5.08	0.26	1.01	0.13736	2.59	0.88	0.00585	-2.20	0.38	0.00000
EGJ25388	lmo1852	CopZ	1.56	0.47	1.43	0.83	0.00000	1.58	0.46	0.00000	-0.39	0.78	0.14419
EGJ25392	lmo1856	DeoD	3.96	2.35	-1.97	1.51	0.00373	0.24	0.87	0.07675	-1.77	1.19	0.00061
EGJ25413	lmo1877		15.87	3.89	0.58	0.72	0.06576	0.94	0.36	0.00005	-0.57	0.59	0.00673
EGJ25422	lmo1886	YpwA	2.66	0.87	1.34	0.70	0.00001	1.92	0.51	0.00000	-0.72	0.44	0.05242
EGJ25423	lmo1887	YpsC	3.21	0.89	1.83	0.33	0.00000	2.64	0.35	0.00000	-0.95	0.61	0.00366
EGJ25424	lmo1888	GpsB	7.10	1.91	0.97	0.57	0.00011	2.04	0.43	0.00000	-1.21	0.36	0.00011
EGJ25432	lmo1896	AsnC	5.15	1.54	0.31	0.44	0.04293	-0.07	0.43	0.52673	0.33	0.17	0.16472
EGJ25433	lmo1897	AspB	3.00	1.26	0.51	0.90	0.00970	0.21	0.69	0.04341	0.23	0.37	0.51422
EGJ25443	lmo1907	DapB	1.82	0.52	-0.33	0.45	0.53252	0.78	0.43	0.01402	-1.06	0.13	0.03014
EGJ25450	lmo1915	MalS	4.12	1.76	0.53	0.63	0.01684	2.53	0.58	0.00004	-2.04	0.21	0.00023
EGJ25452	lmo1917		93.38	21.83	1.32	0.71	0.00001	3.31	0.40	0.00000	-2.12	0.53	0.00000
EGJ25463	lmo1928	AroF	1.73	0.56	0.38	0.49	0.00449	0.51	0.46	0.00218	-0.18	0.46	0.50430

ScottA loci	Other Loci		Mean abundance lag phase	STDEV	Lag vs aged	STDEV	p	Lag vs exponential	STDEV	p	Exponential vs aged	STDEV	p
EGJ25464	lmo1929	Ndk	4.61	1.59	-1.25	1.08	0.03069	-0.25	0.51	0.92202	-0.64	0.95	0.03694
EGJ25469	lmo1934	Hbs	362.95	76.67	0.52	0.59	0.00344	0.45	0.30	0.00609	0.19	0.42	0.52210
EGJ25470	lmo1935		2.25	0.84	0.09	0.90	0.14404	0.04	0.78	0.21330	-0.04	0.25	0.90359
EGJ25471	lmo1936	GpsA	1.54	0.77	-1.17	0.96	0.00344	-2.26	0.87	0.00000	0.93	0.59	0.00007
EGJ25472	lmo1937	EngA	1.99	0.58	-0.52	0.62	0.68532	0.19	0.46	0.05516	-0.63	0.38	0.05870
EGJ25473	lmo1938	RpsA	26.87	5.46	0.77	0.67	0.00198	1.94	0.30	0.00000	-1.30	0.51	0.00011
EGJ25484	lmo1948	ResD	3.76	1.10	-0.07	0.68	0.52786	2.08	0.50	0.00000	-2.14	0.33	0.00004
EGJ25489	lmo1953	PupG	23.41	4.59	-0.43	0.84	0.49154	1.29	0.33	0.00000	-1.36	0.95	0.00263
EGJ25490	lmo1954	Drm	17.76	2.01	1.40	0.56	0.00000	-0.37	0.16	0.06535	1.56	0.64	0.00016
EGJ25503	lmo1967	YaaN	6.19	1.52	0.79	0.50	0.00070	0.67	0.35	0.04083	0.10	0.42	0.91488
EGJ25507	lmo1978	Zwf	5.11	2.47	-1.86	0.65	0.00001	-0.80	0.65	0.11591	-1.02	0.22	0.00097
EGJ25520	lmo1992	AlsD	3.13	0.79	1.56	0.61	0.00000	2.20	0.36	0.00000	-0.87	0.65	0.02379
EGJ25521	lmo1993	Pdp	10.69	0.86	1.16	0.61	0.00000	-0.40	0.12	0.00297	1.34	0.68	0.00000
EGJ25523	lmo1995	DeoC	2.55	1.21	-0.31	1.15	0.09088	0.43	0.65	0.17314	-1.11	0.98	0.02361
EGJ25526	lmo1998	FrlB	4.14	1.21	-0.01	0.36	0.33822	0.00	0.41	0.59943	-0.05	0.15	0.89316
EGJ25531	lmo2003	FrlR	1.63	0.77	1.27	0.76	0.00012	1.09	0.88	0.00021	0.09	0.40	0.92103
EGJ25534	lmo2006	AlsS	18.85	3.10	2.62	0.56	0.00000	3.35	0.25	0.00000	-1.02	0.75	0.00890
EGJ25544	lmo2016	CspD	81.86	8.57	1.31	0.43	0.00000	-1.17	0.16	0.00289	2.39	0.35	0.00037
EGJ25546	lmo2018	DapF	1.31	0.51	-0.22	0.87	0.17876	-0.46	0.62	0.69709	0.27	0.48	0.54357
EGJ25547	lmo2019	IleS	11.46	2.77	0.59	0.66	0.01031	-0.14	0.38	0.81874	0.60	0.45	0.00434
EGJ25548	lmo2020	DivIVA	10.80	2.29	0.30	0.36	0.04154	0.45	0.33	0.00111	-0.16	0.23	0.38378
EGJ25577	lmo2032	FtsZ	12.56	2.42	0.96	0.47	0.00001	1.39	0.29	0.00000	-0.56	0.46	0.00674
EGJ25578	lmo2033	FtsA	7.71	1.53	0.49	0.35	0.01637	1.41	0.26	0.00000	-1.04	0.36	0.00029
EGJ25581	lmo2036	MurD	7.23	1.91	1.82	0.79	0.00000	2.07	0.42	0.00000	-0.47	0.59	0.23973
EGJ25611	lmo2067	YxeI	14.25	2.36	1.42	0.69	0.00000	4.81	0.27	0.00000	-3.56	0.60	0.00001
EGJ25612	lmo2068	GroEL	478.60	70.59	0.02	0.22	0.21933	1.29	0.22	0.00000	-1.16	0.34	0.00000
EGJ25613	lmo2069	GroES	85.97	19.27	0.25	0.39	0.04976	0.75	0.37	0.00050	-0.50	0.26	0.00771
EGJ25616	lmo2072	YdiH	4.32	1.90	0.60	0.81	0.01761	-0.17	0.58	0.67338	0.68	0.45	0.00763
EGJ25623	lmo2079		0.74	0.50	-0.31	0.68	0.09280	-0.07	0.74	0.02920	-0.33	0.50	0.35647
EGJ25633	lmo2089		19.84	4.20	1.86	0.77	0.00000	4.04	0.32	0.00000	-2.31	0.57	0.00001
EGJ25645	lmo2101	PdxS	1.41	0.84	-1.21	0.71	0.00822	1.32	0.72	0.00049	-2.60	0.22	0.00000
EGJ25647	lmo2103	EutD	28.87	4.80	0.71	0.32	0.00002	0.16	0.23	0.17538	0.50	0.29	0.01558
EGJ25655	lmo2110	YvyI	5.99	0.77	0.30	0.62	0.67129	0.74	0.19	0.00999	-0.68	0.69	0.02623
EGJ25658	lmo2113	YwfI	10.53	3.35	0.16	0.92	0.11961	2.74	0.47	0.00001	-2.22	0.93	0.00015
EGJ25659	lmo2114	YxdL	2.91	0.79	0.07	0.48	0.11550	-0.19	0.40	0.64151	0.26	0.47	0.38252
EGJ25663	lmo2118	GlmM	10.65	1.87	0.93	0.36	0.00002	0.62	0.26	0.00004	0.24	0.25	0.31708
EGJ25700	lmo2154	NrdF	3.31	1.07	2.31	0.76	0.00000	0.81	0.42	0.00333	1.46	0.60	0.04432

ScottA loci	Other Loci		Mean abundance lag phase	STDEV	Lag vs aged	STDEV	p	Lag vs exponential	STDEV	p	Exponential vs aged	STDEV	p
EGJ25701	lmo2155	NrdE	2.87	0.96	0.23	1.00	0.11173	-0.99	0.58	0.08441	1.10	0.59	0.03082
EGJ25706	lmo2160	YfiH	3.28	1.10	0.30	0.98	0.05202	2.62	0.60	0.00001	-2.02	0.87	0.01220
EGJ25713	lmo2167	YgqX	2.09	0.72	1.64	0.59	0.00000	1.98	0.50	0.00001	-0.39	0.58	0.06448
EGJ25735	lmo2188	PepF	11.78	2.65	1.50	0.44	0.00000	1.50	0.31	0.00001	-0.22	0.58	0.41340
EGJ25739	lmo2192	OppF	2.95	1.22	-1.39	0.75	0.00001	0.03	0.61	0.13239	-1.41	0.53	0.00000
EGJ25740	lmo2193	OppD	3.75	0.97	-0.96	0.67	0.00248	0.65	0.37	0.00245	-1.41	0.75	0.00001
EGJ25741	lmo2194	OppC	1.58	0.84	-1.71	1.08	0.00021	-0.99	0.91	0.08252	-0.64	0.48	0.00263
EGJ25743	lmo2196	DppE	20.94	5.18	-2.63	0.18	0.00000	-3.32	0.34	0.00000	0.68	0.36	0.00002
EGJ25745	lmo2198	TrpS	7.36	2.05	1.49	0.62	0.00001	2.23	0.47	0.00000	-0.93	0.50	0.03359
EGJ25748	lmo2201	FabF	7.38	2.18	-0.40	0.39	0.00811	-0.75	0.47	0.00502	0.12	0.58	0.81581
EGJ25749	lmo2202	FabH	6.27	2.06	0.39	0.48	0.42910	-0.37	0.43	0.46635	0.50	0.67	0.21742
EGJ25752	lmo2205	GpmA	49.78	8.55	1.42	0.43	0.00000	4.03	0.27	0.00000	-2.72	0.33	0.00000
EGJ25753	lmo2206	ClpC	49.09	5.74	0.64	0.37	0.00012	2.58	0.17	0.00000	-2.07	0.34	0.00000
EGJ25758	lmo2211	HemH	4.00	1.38	0.43	0.98	0.03324	-0.63	0.70	0.09425	0.97	0.47	0.00142
EGJ25759	lmo2212	HemE	1.73	0.96	0.32	1.02	0.01765	-0.20	0.94	0.15579	0.41	0.43	0.16108
EGJ25760	lmo2213	YhgC	5.33	2.02	0.17	0.58	0.15381	2.90	0.57	0.00001	-2.76	0.16	0.00000
EGJ25764	lmo2217	YhaH	7.22	1.06	0.68	0.53	0.00000	2.62	0.21	0.00000	-1.68	0.72	0.00002
EGJ25766	lmo2219	PrsA	1.27	1.04	-1.59	0.49	0.00054	-0.65	1.10	0.70129	-1.31	1.00	0.00192
EGJ25771	lmo2223	YheA	11.77	2.41	1.05	0.56	0.00009	1.86	0.31	0.00000	-0.99	0.52	0.00276
EGJ25831	lmo2248	YkaA	10.89	1.43	0.58	0.46	0.00800	-0.46	0.18	0.06853	0.89	0.40	0.00395
EGJ25839	lmo2256	YraA	21.43	4.32	-0.17	0.94	0.95531	2.19	0.30	0.00000	-2.01	0.94	0.00305
EGJ25855	lmo2335	FruA	94.29	15.82	2.88	0.41	0.00000	4.94	0.25	0.00000	-2.12	0.20	0.00116
EGJ25856	lmo2336	FruK	37.78	3.91	1.47	0.33	0.00000	0.34	0.15	0.00148	0.98	0.41	0.00001
EGJ25859	lmo2340	PscG	5.26	0.90	0.32	0.44	0.00797	0.72	0.24	0.00721	-0.40	0.41	0.17134
EGJ25872	lmo2354	YtcJ	0.98	0.61	0.19	1.11	0.00907	0.74	0.84	0.00066	-0.53	0.71	0.03798
EGJ25877	lmo2358	NagB	1.52	0.76	0.39	1.36	0.01414	0.95	0.87	0.00056	-0.66	0.78	0.07844
EGJ25880	lmo2361	YwgB	4.15	0.79	0.57	0.44	0.00004	3.02	0.34	0.00000	-2.51	0.16	0.00000
EGJ25883	lmo2363	GadB	5.01	1.82	0.58	1.35	0.15256	3.23	0.58	0.00001	-2.92	0.89	0.00000
EGJ25886	lmo2367	Pgi	49.47	8.47	-1.13	0.53	0.00007	-0.41	0.24	0.00052	-0.53	0.49	0.00303
EGJ25890	lmo2371		3.67	1.20	1.25	0.67	0.00005	2.36	0.64	0.00000	-1.28	0.64	0.00152
EGJ25892	lmo2373	LicB	4.59	0.95	0.11	0.43	0.60347	0.05	0.29	0.24816	-0.09	0.43	0.51305
EGJ25904	lmo2376	PpiB	2.16	1.06	-0.55	0.96	0.43011	-1.43	1.04	0.00560	0.71	0.45	0.01987
EGJ25918	lmo2389	YumB	7.28	1.45	0.06	0.54	0.97642	-0.04	0.28	0.69573	-0.02	0.49	0.77685
EGJ25920	lmo2391	YhfK	11.73	1.90	1.76	0.51	0.00000	4.53	0.25	0.00000	-2.90	0.39	0.00000
EGJ25928	lmo2401	YutF	1.97	0.82	1.27	0.92	0.00007	0.40	0.80	0.00267	0.75	0.51	0.03222
EGJ25932	lmo2406	YunF	2.53	0.49	1.10	0.31	0.00000	1.90	0.30	0.00000	-0.69	0.44	0.05843
EGJ25935	lmo2411	SufB	3.79	1.02	-0.88	0.57	0.00629	-0.91	0.41	0.01298	0.12	0.32	0.67738

ScottA loci	Other Loci		Mean abundance lag phase	STDEV	Lag vs aged	STDEV	p	Lag vs exponential	STDEV	p	Exponential vs aged	STDEV	p
EGJ25938	lmo2414	SufD	2.89	1.40	-1.53	0.99	0.00838	-1.51	0.71	0.00347	0.20	0.78	0.81496
EGJ25939	lmo2415	SufC	10.71	2.44	2.29	1.13	0.00000	0.81	0.36	0.00293	1.00	1.25	0.12807
EGJ25949	lmo2425	YusH	8.59	0.99	1.60	0.46	0.00000	2.68	0.17	0.00000	-1.22	0.46	0.00148
EGJ25950	lmo2426	YusI	3.04	1.23	1.63	0.88	0.00057	0.23	0.74	0.07538	1.00	1.06	0.15252
EGJ25957	lmo2433	YeiG	1.19	0.95	0.36	1.24	0.19830	0.52	0.96	0.01090	-0.48	1.07	0.16683
EGJ25958	lmo2434	GadB	6.07	1.39	1.63	0.74	0.00000	3.17	0.32	0.00000	-1.76	0.60	0.00005
EGJ25980	lmo2455	Eno	488.79	96.74	-0.76	0.50	0.00200	-0.29	0.27	0.01317	-0.27	0.54	0.03628
EGJ25981	lmo2456	Pgm	22.16	4.82	0.17	0.65	0.89709	-0.43	0.38	0.04350	0.43	0.46	0.05880
EGJ25982	lmo2457	TpiA	50.13	8.23	0.61	0.42	0.00635	0.70	0.23	0.00005	-0.22	0.42	0.20190
EGJ25983	lmo2458	Pgk	168.33	23.30	1.69	0.75	0.00000	-0.12	0.20	0.31662	1.50	0.81	0.00000
EGJ25984	lmo2459	Gap	382.25	50.59	-0.05	0.29	0.80517	-0.48	0.19	0.00000	0.44	0.22	0.00033
EGJ25985	lmo2460	CggR	2.64	1.01	1.10	1.04	0.00015	1.56	0.63	0.00003	-0.49	0.68	0.16732
EGJ25993	lmo2468	ClpP	16.42	9.78	-1.61	1.07	0.00856	0.91	0.70	0.01706	-2.21	0.82	0.00031
EGJ25996	lmo2471	YqjM	5.58	1.48	-0.45	0.52	0.29066	1.43	0.38	0.00002	-1.77	0.37	0.00000
EGJ25999	lmo2474	YvcJ	2.21	1.27	-0.14	1.03	0.23635	1.91	0.93	0.00037	-2.04	0.26	0.00005
EGJ26000	lmo2475	PgcA	8.51	2.31	0.29	0.47	0.39904	0.25	0.35	0.13881	-0.14	0.48	0.47976
EGJ26003	lmo2478	TrxB	2.91	2.28	0.25	0.61	0.16744	-0.01	0.69	0.30885	0.18	0.21	0.59015
EGJ26012	lmo2487	YvlB	2.72	0.70	-1.42	0.68	0.00006	1.99	0.38	0.00000	-3.36	0.51	0.00000
EGJ26013	lmo2488	UvrA	1.15	0.73	-0.68	0.97	0.55309	-0.04	0.83	0.16105	-0.79	0.52	0.07481
EGJ26030	lmo2505	CwlO	1.84	0.98	-3.87	0.95	0.00073	1.74	0.62	0.00022	-5.15	1.18	0.00030
EGJ26032	lmo2507	FtsE	1.79	0.67	0.18	0.89	0.19000	0.53	0.50	0.00257	-0.47	0.66	0.14735
EGJ26035	lmo2510	SecA	4.32	1.80	-0.10	1.04	0.76687	1.12	0.71	0.00069	-1.29	0.40	0.00119
EGJ26036	lmo2511	YvyD	58.51	16.44	1.40	0.56	0.00004	2.85	0.44	0.00000	-1.51	0.22	0.00000
EGJ26040	lmo2515	DegU	1.50	0.47	-0.84	0.46	0.30443	1.10	0.44	0.00008	-1.93	0.10	0.00149
EGJ26050	lmo2525	Mbl	12.22	2.56	0.89	0.55	0.00004	0.49	0.29	0.00074	0.37	0.47	0.13150
EGJ26051	lmo2526	MurAA	1.09	1.52	-0.54	1.22	0.33729	-2.31	1.10	0.03161	1.77	0.30	0.01091
EGJ26053	lmo2528	AtpC	3.66	0.75	-0.67	0.42	0.06693	0.33	0.28	0.01210	-0.76	0.76	0.00086
EGJ26054	lmo2529	AtpD	63.36	13.80	-0.80	0.24	0.00046	1.89	0.39	0.00000	-2.49	0.55	0.00000
EGJ26055	lmo2530	AtpG	5.18	1.05	-0.42	0.36	0.20034	0.93	0.29	0.00000	-1.21	0.41	0.00000
EGJ26056	lmo2531	AtpA	24.76	3.99	-1.15	0.33	0.00000	0.72	0.29	0.00003	-1.72	0.41	0.00000
EGJ26058	lmo2533	AtpF	4.49	0.87	-0.66	0.25	0.00595	1.24	0.29	0.00002	-1.91	0.20	0.00000
EGJ26063	lmo2538	Upp	14.63	1.85	0.32	0.31	0.01415	0.61	0.19	0.00038	-0.36	0.21	0.04155
EGJ26064	lmo2539	GlyA	3.81	1.04	1.13	0.70	0.00008	0.46	0.41	0.00208	0.45	0.59	0.20937
EGJ26071	lmo2546	ThrC	1.26	0.94	-3.71	1.09	0.00000	-3.89	1.08	0.00000	0.14	0.13	0.39998
EGJ26073	lmo2548	RpmE	9.37	2.14	-0.16	0.30	0.44715	0.25	0.33	0.02570	-0.49	0.25	0.02340
EGJ26080	lmo2556	FbaA	103.17	37.72	0.88	0.38	0.03353	-1.16	0.42	0.00000	1.77	0.68	0.00000
EGJ26083	lmo2559	PyrG	9.95	1.82	0.52	0.56	0.01543	-0.76	0.26	0.00095	1.13	0.46	0.00003

ScottA loci	Other Loci		Mean abundance lag phase	STDEV	Lag vs aged	STDEV	p	Lag vs exponential	STDEV	p	Exponential vs aged	STDEV	p
EGJ26084	lmo2560	RpoE	9.24	3.93	2.07	0.63	0.00013	0.70	0.68	0.00558	1.39	0.34	0.00096
EGJ26085	lmo2561	ArgS	5.00	2.06	0.21	0.59	0.52489	-0.64	0.58	0.09203	0.65	0.54	0.02909
EGJ26117	lmo2592	YvgN	2.16	0.74	0.82	0.67	0.00003	2.03	0.50	0.00001	-1.05	0.45	0.00081
EGJ26121	lmo2596	RpsI	27.15	7.51	0.92	0.33	0.00034	-0.61	0.40	0.00182	1.43	0.27	0.00000
EGJ26122	lmo2597	RplM	5.82	1.15	-0.64	0.55	0.00027	-0.41	0.29	0.24440	-0.34	0.46	0.07283
EGJ26130	lmo2605	RplQ	10.32	2.24	-0.05	0.37	0.82039	-1.09	0.31	0.03461	1.03	0.15	0.03186
EGJ26131	lmo2606	RpoA	18.99	2.95	0.58	0.35	0.00055	-1.01	0.23	0.00000	1.50	0.26	0.00000
EGJ26132	lmo2607	RpsK	8.60	2.03	-0.31	0.39	0.13264	-0.13	0.32	0.93063	-0.25	0.20	0.27956
EGJ26133	lmo2608	RpsM	4.25	1.37	-1.24	0.39	0.00001	0.20	0.47	0.05671	-1.52	0.23	0.00000
EGJ26135	lmo2610	InfA	3.66	0.84	0.18	0.44	0.03624	1.06	0.43	0.00537	-0.86	0.08	0.07443
EGJ26136	lmo2611	Adk	7.10	2.27	-0.28	0.52	0.04540	-0.48	0.53	0.09614	-0.04	0.64	0.45391
EGJ26138	lmo2613	RplO	16.42	2.21	0.45	0.33	0.00895	-1.12	0.19	0.00678	1.44	0.40	0.00286
EGJ26139	lmo2614	RpmD	1.31	1.30	-2.09	1.33	0.00231	-1.00	1.22	0.97504	-1.12	0.51	0.00148
EGJ26140	lmo2615	RpsE	16.80	3.10	0.46	0.36	0.00956	0.24	0.26	0.05803	0.18	0.20	0.42161
EGJ26141	lmo2616	RplR	5.45	2.24	0.09	0.44	0.57760	-1.35	0.45	0.00505	1.30	0.37	0.00392
EGJ26142	lmo2617	RplF	16.22	1.75	-0.67	0.27	0.00000	-0.75	0.15	0.04301	-0.04	0.33	0.76665
EGJ26143	lmo2618	RpsH	12.12	1.87	-0.25	0.33	0.20330	-2.07	0.23	0.00346	1.72	0.28	0.00394
EGJ26145	lmo2620	RplE	28.85	3.06	0.51	0.46	0.43449	-0.91	0.16	0.00000	1.17	0.71	0.00000
EGJ26146	lmo2621	RplX	2.21	0.50	-1.47	0.50	0.00000	-0.55	0.33	0.38718	-0.83	0.32	0.00117
EGJ26147	lmo2622	RplN	5.72	1.44	-0.15	0.27	0.64394	0.66	0.34	0.00037	-0.89	0.26	0.00026
EGJ26148	lmo2623	RpsQ	5.79	1.79	-0.18	0.62	0.27844	0.05	0.49	0.19462	-0.42	0.55	0.04374
EGJ26150	lmo2625	RplP	8.14	1.15	-0.53	0.18	0.00354	-0.32	0.20	0.01672	-0.32	0.28	0.04556
EGJ26151	lmo2626	RpsC	18.38	2.83	0.07	0.45	0.97712	1.09	0.23	0.00000	-1.12	0.31	0.00000
EGJ26152	lmo2627	RplV	4.30	2.06	-0.41	0.98	0.12397	0.17	0.65	0.14718	-0.81	0.59	0.00642
EGJ26153	lmo2628	RpsS	16.61	5.55	0.41	0.36	0.28646	-0.70	0.39	0.00188	0.90	0.56	0.00006
EGJ26154	lmo2629	RplB	19.55	3.90	-0.94	0.18	0.00007	-1.61	0.29	0.00868	0.53	0.36	0.13829
EGJ26155	lmo2630	RplW	9.36	1.09	-0.33	0.34	0.01691	-0.31	0.17	0.17067	-0.14	0.45	0.30302
EGJ26156	lmo2631	RplD	32.89	4.79	-0.08	0.14	0.32497	-1.52	0.19	0.00000	1.39	0.15	0.00000
EGJ26157	lmo2632	RplC	20.87	6.81	-0.65	0.39	0.00270	-3.02	0.43	0.00000	2.25	0.32	0.00000
EGJ26158	lmo2633	RpsJ	10.97	5.42	0.27	0.72	0.21396	-1.15	0.65	0.00338	1.34	0.32	0.00096
EGJ26163	lmo2638	YumB	50.78	7.57	0.55	0.42	0.00017	0.45	0.22	0.00320	0.03	0.32	0.98809
EGJ26177	lmo2653	TufA	302.16	31.78	0.03	0.26	0.91840	-0.68	0.16	0.00225	0.66	0.15	0.00166
EGJ26178	lmo2654	FusA	112.26	15.70	0.69	0.53	0.00184	-0.44	0.20	0.06562	0.96	0.48	0.00481
EGJ26179	lmo2655	RpsG	12.68	3.60	-0.25	0.42	0.21235	0.18	0.34	0.13008	-0.53	0.27	0.02008
EGJ26180	lmo2656	RpsL	6.65	0.71	-0.01	0.34	0.56691	0.44	0.16	0.00005	-0.61	0.45	0.00739
EGJ26202	lmo2677	YugF	2.92	1.17	0.95	1.08	0.00178	2.42	0.66	0.00003	-1.68	0.67	0.00019
EGJ26208	lmo2683	LicB	1.51	0.52	1.49	0.63	0.00001	0.47	0.63	0.00571	1.02	0.00	0.07587

ScottA loci	Other Loci		Mean abundance lag phase	STDEV	Lag vs aged	STDEV	p	Lag vs exponential	STDEV	p	Exponential vs aged	STDEV	p
EGJ26217	lmo2692	YaaQ	3.10	0.99	-0.28	1.02	0.68805	1.33	0.51	0.00002	-1.28	0.90	0.01180
EGJ26218	lmo2693	Tmk	1.67	0.84	1.39	0.77	0.00017	1.17	0.77	0.00027	0.23	0.20	0.59712
EGJ26219	lmo2694	YaaO	1.02	0.64	0.50	1.00	0.00176	0.79	0.88	0.00066	-0.37	0.28	0.04725
EGJ26220	lmo2695	DhaK	10.04	1.80	0.19	0.35	0.14534	2.20	0.25	0.00000	-2.09	0.25	0.00000
EGJ26221	lmo2696	DhaL	23.50	4.36	1.75	0.23	0.00000	3.42	0.23	0.00000	-1.83	0.42	0.00000
EGJ26222	lmo2697	DhaM	3.17	0.76	0.12	0.45	0.16555	1.60	0.35	0.00000	-1.56	0.39	0.00004
EGJ26229	lmo2703	YaaK	2.71	0.95	-0.28	0.50	0.94158	0.35	0.51	0.02480	-0.65	0.08	0.02553
EGJ26240	lmo2715	CydD	1.38	0.83	0.90	0.88	0.00079	0.80	0.95	0.00144	0.12	0.33	0.82327
EGJ26249	lmo2724	YjdN	7.29	1.06	1.58	0.40	0.00000	2.63	0.20	0.00000	-1.14	0.41	0.00126
EGJ26268	lmo2743	YwjH	3.12	1.62	-0.39	0.83	0.54659	1.16	0.89	0.00165	-1.37	0.51	0.00085
EGJ26272	lmo2747	SerS	2.82	0.88	-0.59	0.60	0.02101	-0.76	0.44	0.21702	0.06	0.37	0.94605
EGJ26273	lmo2748	YdaG	3.12	0.62	1.84	0.47	0.00000	2.62	0.29	0.00000	-0.91	0.42	0.00185
EGJ26284	lmo2758	GuaB1	10.25	4.23	3.22	0.56	0.00005	2.02	0.58	0.00012	1.08	0.37	0.00796
EGJ26307	lmo2779	YchF	1.61	0.96	-0.23	1.09	0.46531	-0.80	0.94	0.59633	0.45	0.50	0.21867
EGJ26315	lmo2790	ParB	3.09	0.89	-0.02	0.47	0.28161	2.57	0.46	0.00000	-2.55	0.46	0.00000
EGJ26317	lmo2792		16.25	2.75	0.93	0.35	0.00000	3.14	0.25	0.00000	-2.24	0.28	0.00000
EGJ26354	lmo2829		2.05	1.12	0.41	0.29	0.00016	2.25	2.92	0.04166	-0.41	0.24	0.03436